

TRADITIONAL MEDICINE AND RHEUMATOLOGY

EDITED BY: Runyue Huang, Per-Johan Jakobsson and Xiaojuan He
PUBLISHED IN: Frontiers in Pharmacology





frontiers

Frontiers eBook Copyright Statement

The copyright in the text of individual articles in this eBook is the property of their respective authors or their respective institutions or funders. The copyright in graphics and images within each article may be subject to copyright of other parties. In both cases this is subject to a license granted to Frontiers.

The compilation of articles constituting this eBook is the property of Frontiers.

Each article within this eBook, and the eBook itself, are published under the most recent version of the Creative Commons CC-BY licence.

The version current at the date of publication of this eBook is CC-BY 4.0. If the CC-BY licence is updated, the licence granted by Frontiers is automatically updated to the new version.

When exercising any right under the CC-BY licence, Frontiers must be attributed as the original publisher of the article or eBook, as applicable.

Authors have the responsibility of ensuring that any graphics or other materials which are the property of others may be included in the CC-BY licence, but this should be checked before relying on the CC-BY licence to reproduce those materials. Any copyright notices relating to those materials must be complied with.

Copyright and source acknowledgement notices may not be removed and must be displayed in any copy, derivative work or partial copy which includes the elements in question.

All copyright, and all rights therein, are protected by national and international copyright laws. The above represents a summary only. For further information please read Frontiers' Conditions for Website Use and Copyright Statement, and the applicable CC-BY licence.

ISSN 1664-8714

ISBN 978-2-88971-226-7

DOI 10.3389/978-2-88971-226-7

About Frontiers

Frontiers is more than just an open-access publisher of scholarly articles: it is a pioneering approach to the world of academia, radically improving the way scholarly research is managed. The grand vision of Frontiers is a world where all people have an equal opportunity to seek, share and generate knowledge. Frontiers provides immediate and permanent online open access to all its publications, but this alone is not enough to realize our grand goals.

Frontiers Journal Series

The Frontiers Journal Series is a multi-tier and interdisciplinary set of open-access, online journals, promising a paradigm shift from the current review, selection and dissemination processes in academic publishing. All Frontiers journals are driven by researchers for researchers; therefore, they constitute a service to the scholarly community. At the same time, the Frontiers Journal Series operates on a revolutionary invention, the tiered publishing system, initially addressing specific communities of scholars, and gradually climbing up to broader public understanding, thus serving the interests of the lay society, too.

Dedication to Quality

Each Frontiers article is a landmark of the highest quality, thanks to genuinely collaborative interactions between authors and review editors, who include some of the world's best academicians. Research must be certified by peers before entering a stream of knowledge that may eventually reach the public - and shape society; therefore, Frontiers only applies the most rigorous and unbiased reviews.

Frontiers revolutionizes research publishing by freely delivering the most outstanding research, evaluated with no bias from both the academic and social point of view. By applying the most advanced information technologies, Frontiers is catapulting scholarly publishing into a new generation.

What are Frontiers Research Topics?

Frontiers Research Topics are very popular trademarks of the Frontiers Journals Series: they are collections of at least ten articles, all centered on a particular subject. With their unique mix of varied contributions from Original Research to Review Articles, Frontiers Research Topics unify the most influential researchers, the latest key findings and historical advances in a hot research area! Find out more on how to host your own Frontiers Research Topic or contribute to one as an author by contacting the Frontiers Editorial Office: frontiersin.org/about/contact

TRADITIONAL MEDICINE AND RHEUMATOLOGY

Topic Editors:

Runyue Huang, Guangdong Provincial Hospital of Chinese Medicine, China

Per-Johan Jakobsson, Karolinska Institutet (KI), Sweden

Xiaojuan He, China Academy of Chinese Medical Sciences, China

Citation: Huang, R., Jakobsson, P.-J., He, X., eds. (2021). Traditional Medicine and Rheumatology. Lausanne: Frontiers Media SA. doi: 10.3389/978-2-88971-226-7

Table of Contents

- 05 Editorial: Traditional Medicine and Rheumatology**
Zhihua Yang, Xuan Tang, Huasheng Liang, Kaixin Gao, Maojie Wang, Xiaojuan He, Per-Johan Jakobsson and Runyue Huang
- 07 Identification of Characteristic Autoantibodies Associated With Deficiency Pattern in Traditional Chinese Medicine of Rheumatoid Arthritis Using Protein Chips**
Heru Zhao, Yin Zhang, Bin Liu, Li Li, Lulu Zhang, Mei Bao, Hongtao Guo, Haiyu Xu, Hui Feng, Lianbo Xiao, Wenjun Yi, Jianfeng Yi, Peng Chen, Cheng Lu and Aiping Lu
- 16 Deciphering the Pharmacological Mechanisms of the Huayu-Qiangshen-Tongbi Formula Through Integrating Network Pharmacology and In Vitro Pharmacological Investigation**
Zihao Wang, Ke-Gang Linghu, Yuanjia Hu, Huali Zuo, Hao Yi, Shi-Hang Xiong, Jinjian Lu, Ging Chan, Hua Yu and Run-Yue Huang
- 27 Application and Mechanisms of Triptolide in the Treatment of Inflammatory Diseases—A Review**
Kai Yuan, Xiaohong Li, Qingyi Lu, Qingqing Zhu, Haixu Jiang, Ting Wang, Guangrui Huang and Anlong Xu
- 39 Alleviation of Synovial Inflammation of Juanbi-Tang on Collagen-Induced Arthritis and TNF-Tg Mice Model**
Tengteng Wang, Qingyun Jia, Tao Chen, Hao Yin, Xiaoting Tian, Xi Lin, Yang Liu, Yongjian Zhao, Yongjun Wang, Qi Shi, Chenggang Huang, Hao Xu and Qianqian Liang
- 56 Adjunctive Chinese Herbal Products Therapy Reduces the Risk of Ischemic Stroke Among Patients With Rheumatoid Arthritis**
Hsuan-Shu Shen, Jen-Huai Chiang and Nai-Huan Hsiung
- 68 Synergistic Effects of Erzhi Pill Combined With Methotrexate on Osteoblasts Mediated via the Wnt1/LRP5/ β -Catenin Signaling Pathway in Collagen-Induced Arthritis Rats**
Xiaoya Li, Xiangcheng Lu, Danping Fan, Li Li, Cheng Lu, Yong Tan, Ya Xia, Hongyan Zhao, Miaoxuan Fan and Cheng Xiao
- 78 Quercetin Combined With Human Umbilical Cord Mesenchymal Stem Cells Regulated Tumour Necrosis Factor- α /Interferon- γ -Stimulated Peripheral Blood Mononuclear Cells via Activation of Toll-Like Receptor 3 Signalling**
Guiling Chen, Yang Ye, Ming Cheng, Yi Tao, Kejun Zhang, Qiong Huang, Jingwen Deng, Danni Yao, Chuanjian Lu and Yu Huang
- 88 Tanshinone IIA Suppresses Proliferation and Inflammatory Cytokine Production of Synovial Fibroblasts From Rheumatoid Arthritis Patients Induced by TNF- α and Attenuates the Inflammatory Response in AIA Mice**
Hongyan Du, Yuechun Wang, Yongchang Zeng, Xiaoming Huang, Dingfei Liu, Lvlan Ye, Yang Li, Xiaochen Chen, Tiancai Liu, Hongwei Li, Jing Wu, Qinghong Yu, Yingsong Wu and Ligang Jie

- 103** *Uncovering the Complexity Mechanism of Different Formulas Treatment for Rheumatoid Arthritis Based on a Novel Network Pharmacology Model*
Ke-xin Wang, Yao Gao, Cheng Lu, Yao Li, Bo-ya Zhou, Xue-mei Qin, Guan-hua Du, Li Gao, Dao-gang Guan and Ai-ping Lu
- 127** *Potential Advantages of Bioactive Compounds Extracted From Traditional Chinese Medicine to Inhibit Bone Destructions in Rheumatoid Arthritis*
Yingjie Shi, Haiyang Shu, Xinyu Wang, Hanxiao Zhao, Cheng Lu, Aiping Lu and Xiaojuan He
- 143** *Computational Prediction of Antiangiogenesis Synergistic Mechanisms of Total Saponins of Panax japonicus Against Rheumatoid Arthritis*
Xiang Guo, Jinyu Ji, Goutham Sanker Jose Kumar Sreena, Xiaoqiang Hou, Yanan Luo, Xianyun Fu, Zhigang Mei and Zhitao Feng
- 153** *Chinese Medicine Formula PSORI-CM02 Alleviates Psoriatic Dermatitis via M-MDSCs and Th17 Crosstalk*
Jingwen Deng, Siyi Tan, Ruonan Liu, Wanlin Yu, Haiming Chen, Nan Tang, Ling Han and Chuanjian Lu



Editorial: Traditional Medicine and Rheumatology

Zhihua Yang¹, Xuan Tang¹, Huasheng Liang¹, Kaixin Gao¹, Maojie Wang^{1,2,3,4,5}, Xiaojuan He⁶, Per-Johan Jakobsson⁷ and Runyue Huang^{1,2,3,4*}

¹Guangzhou University of Chinese Medicine, Guangzhou, China, ²Guangdong-Hong Kong-Macau Joint Lab on Chinese Medicine and Immune Disease Research, Guangzhou University of Chinese Medicine, Guangzhou, China, ³State Key Laboratory of Dampness Syndrome of Chinese Medicine, The Second Affiliated Hospital of Guangzhou University of Chinese Medicine, Guangzhou, China, ⁴Guangdong Provincial Key Laboratory of Clinical Research on Traditional Chinese Medicine Syndrome, Guangzhou, China, ⁵Center for Molecular Medicine, University Medical Center Utrecht, Utrecht, Netherlands, ⁶China Academy of Chinese Medical Sciences, Beijing, China, ⁷Karolinska Institutet (KI), Solna, Sweden

Keywords: disease-modifying antirheumatic drug (DMARD), traditional Chinese medicine, mechanism study, rheumatology, rheumatoid arthritis

Editorial on the Research Topic

Traditional Medicine and Rheumatology

Disease-modifying antirheumatic drugs (DMARDs) are often used in the treatment of several rheumatic diseases, such as Rheumatoid Arthritis (RA), Systemic Lupus Erythematosus (SLE) and Psoriasis. Methotrexate (MTX), the most common DMARD, even stands as the first-line therapy for RA (Smolen et al., 2020). However, due to the adverse events of synthetic DMARDs and high cost of biological DMARDs, the attainment rate of standardized therapies is not ideal. An increasing number of patients afflicted by rheumatic diseases are searching for help from Traditional Chinese Medicine (TCM). TCM has long been prescribed to prevent and treat rheumatic diseases with a good efficacy and little adverse reactions, but the mechanisms still remain largely ambiguous. On the one hand, we need robust evidence from high-quality clinical researches (including well-designed trials and meta-analysis). On the other hand, in-depth studies (such as multi-omics studies and network pharmacology) are needed to demonstrate the complex mechanisms of TCM. The aim of this editorial is to help understanding disease-modifying antirheumatic effects of TCM in rheumatic diseases.

Rheumatoid Arthritis (RA) is a systemic, autoimmune-related diseases, causing damage to bone and cartilage. Several studies have revealed the efficacy and safety of TCM in treating RA. It is found that most TCM compounds have good DMARD-likeness properties through literature screening (Li and Zhang, 2020). A meta-analysis (Daily et al., 2017) of randomized controlled trials on TCM compound GSZD (Guizhi-Shaoyao-Zhimu Decotion) showed that GSZD may have equal or superior effectiveness and safety when compared with conventional treatment. Clinical evidence from a monocenter, open-label, randomized controlled trial (Wu et al.) shows that HQT (a TCM formula) with MTX is a good therapeutic option in MTX-based treatment for RA. No statistical difference was observed between TCM formula-HQT with MTX group and Leflunomide with MTX group in terms of ACR20, ACR50, ACR70 and frequency of adverse events. The encouraging evidence has led to TCM treatments being increasingly favored by clinicians.

However, the unspecific mechanism hinders the widespread and standardization of TCM. To explore the mechanisms of TCM treatment for RA, researchers (Wang et al.) performed a network pharmacology analysis and a Key gene Network Motif with Significant (KNMS) detection to figure out the most important components in three independent TCM formulas (Wang et al.). They found that three TCM formulas treat RA via VEGF signaling pathway, HIF-1 signaling pathway, PI3K-Akt

OPEN ACCESS

Edited and reviewed by:

Michael Heinrich,
UCL School of Pharmacy,
United Kingdom

*Correspondence:

Runyue Huang
ryhuang@gzucm.edu.cn

Specialty section:

This article was submitted to
Ethnopharmacology,
a section of the journal
Frontiers in Pharmacology

Received: 10 May 2021

Accepted: 11 June 2021

Published: 24 June 2021

Citation:

Yang Z, Tang X, Liang H, Gao K,
Wang M, He X, Jakobsson P-J and
Huang R (2021) Editorial: Traditional
Medicine and Rheumatology.
Front. Pharmacol. 12:707811.
doi: 10.3389/fphar.2021.707811

signaling pathway, etc., which were further verified by *in vitro* cell experiments. The mechanisms of disease-modifying antirheumatic effects of TCM is also observed in animal experiments. For example, differentially expressed genes analysis, computational prediction and verification on collagen-induced arthritis (CIA) mice were utilized to reveal the mechanisms of TSPJ (a TCM formula) against RA. Led by a variety of bioinformatic cues, (Guo et al.) found that SRC and STAT3 may be the key targets of TSPJ through the VEGF and HIF-1 signaling pathways, thus suppressing inflammation and angiogenesis of RA. Moreover, (Du et al.) discovered that Tanshinone IIA, an isolated active ingredient in TCM, appears to act on MAPK, Akt/mTOR, HIF-1 pathways. In this study, Tanshinone IIA attenuated the inflammatory response (especially in terms of several inflammatory cytokines) in Avridine Induced Arthritis (AIA) mice and suppressed the activation of RA-FLSs induced by TNF- α . Above studies from the cellular level to the animal experiments convincingly demonstrate the antirheumatic effects of TCM in the treatment of RA. Most of them applied network pharmacology before verification. The work of Wang, et al. shed light on the antioxidant, and anti-inflammatory activities of TCM *via* examining the NO (nitric oxide) levels in different groups. Animal experiments by Guo et al. and Du et al. mimic the inflammatory status in RA patients. Compared to control intervention, TCM is not inferior in controlling inflammatory response and joint manifestations.

Bone destruction/erosion, an inevitable progress of RA, is a big challenge in RA treatments. (Cai et al.) addressed this challenge *via* a systematic review and meta-analysis, which provided literature evidence on bone-protecting efficiency of TCM in the treatment of RA. Bioactive compounds such as Triptolide and Celastrol extracted from TCM shows bone-protecting efficacy, and they have achieved good results from different aspects according to another meta-analysis study (Shi et al.).

Notably, the advantages of TCM treatment are also effective in other rheumatic diseases, such as Psoriatic Dermatitis and

Osteoarthritis. Through flow cytometric analysis, CD4⁺ T cells and MDSCs (myeloid-derived suppressor cells) co-culture and a series of verification methods, (Deng et al.) revealed the complex mechanisms that TCM preparation PSORI-CM02 alleviated IMQ-induced psoriatic dermatitis and inhibited cell proliferation of Th17 by targeting M-MDSCs-induced (monocytic myeloid-derived suppressor cells) arginase-1.

The use of TCM in rheumatic diseases dates back to thousands of years ago. Compared with standardized treatment, TCM has the advantages of low cost, low side effects, and flexible medication. Multi-component, multi-target and multi-pathway allows TCM to modify rheumatic diseases in different ways, which also makes it difficult to assess efficacy and figure out the specific mechanisms. Current studies on TCM in rheumatic diseases varied in study design and research findings. Most of them merely focused on the relationship “drug-gene-protein-disease,” but they seldomly illustrate the specific pharmacological actions. Weak foundation in prior work results in this situation. TCM researches is dwarfed by conventional DMARDs researches in pharmacology, toxicity and pharmacokinetics. Since there were plenty of literature studies, we need to form hypotheses or generate specific research directions according to former findings.

With the help of new and high-tech methods, current mechanism researches of TCM against rheumatic diseases has been developing. We believed that current findings are only a tip of the iceberg, but the unknown mechanisms and unspecific efficacy holds a great potential in Rheumatology.

AUTHOR CONTRIBUTIONS

ZY, XT, HL and KG finished the writing of this editorial. MW and RH provided support and mentoring of this editorial. XH and P-JJ provided specific suggestions and comments in this process.

REFERENCES

- Daily, J. W., Zhang, T., Cao, S., and Park, S. (2017). Efficacy and Safety of GuiZhi-ShaoYao-ZhiMu Decoction for Treating Rheumatoid Arthritis: A Systematic Review and Meta-Analysis of Randomized Clinical Trials. *J. Altern. Complement. Med.* 23 (10), 756–770. doi:10.1089/acm.2017.0098
- Li, X. Z., and Zhang, S. N. (2020). Herbal Compounds for Rheumatoid Arthritis: Literatures Review and Cheminformatics Prediction. *Phytotherapy Res.* 34 (1), 51–66. doi:10.1002/ptr.6509
- Smolen, J. S., Landewé, R. B. M., Bijlsma, J. W. J., Burmester, G. R., Dougados, M., Kerschbaumer, A., et al. (2020). EULAR Recommendations for the Management of Rheumatoid Arthritis with Synthetic and Biological

Disease-Modifying Antirheumatic Drugs: 2019 Update. *Ann. Rheum. Dis.* 79 (6), 685–699. doi:10.1136/annrheumdis-2019-216655

Conflict of Interest: The authors declare that the research was conducted in the absence of any commercial or financial relationships that could be construed as a potential conflict of interest.

Copyright © 2021 Yang, Tang, Liang, Gao, Wang, He, Jakobsson and Huang. This is an open-access article distributed under the terms of the Creative Commons Attribution License (CC BY). The use, distribution or reproduction in other forums is permitted, provided the original author(s) and the copyright owner(s) are credited and that the original publication in this journal is cited, in accordance with accepted academic practice. No use, distribution or reproduction is permitted which does not comply with these terms.



Identification of Characteristic Autoantibodies Associated With Deficiency Pattern in Traditional Chinese Medicine of Rheumatoid Arthritis Using Protein Chips

OPEN ACCESS

Edited by:

Runyue Huang,
Guangzhou University of
Chinese Medicine, China

Reviewed by:

Baosheng Boris Guo,
Nanjing University, China
Deng Mingjing,
Peking University, China
Yuanjia Hu,
University of Macau, China

Correspondence:

Aiping Lu
aipinglu@hkbu.edu.hk
Cheng Lu
lv_cheng0816@163.com
Peng Chen
sdzpcchenpeng@qq.com
Jianfeng Yi
ycxyyjf@163.com

Specialty section:

This article was submitted to
Ethnopharmacology,
a section of the journal
Frontiers in Pharmacology

Received: 07 March 2019

Accepted: 11 June 2019

Published: 10 July 2019

Citation:

Zhao H, Zhang Y, Liu B, Li L,
Zhang L, Bao M, Guo H, Xu H,
Feng H, Xiao L, Yi W, Yi J,
Chen P, Lu C and Lu A (2019)
Identification of Characteristic
Autoantibodies Associated With
Deficiency Pattern in Traditional
Chinese Medicine of Rheumatoid
Arthritis Using Protein Chips.
Front. Pharmacol. 10:755.
doi: 10.3389/fphar.2019.00755

Heru Zhao^{1,2}, **Yin Zhang**^{1,2}, **Bin Liu**², **Li Li**², **Lulu Zhang**^{1,2}, **Mei Bao**^{1,2}, **Hongtao Guo**³,
Haiyu Xu⁴, **Hui Feng**⁵, **Lianbo Xiao**⁵, **Wenjun Yi**⁶, **Jianfeng Yi**^{1*}, **Peng Chen**^{7*}, **Cheng Lu**^{2*}
and **Aiping Lu**^{8*}

¹ Key Laboratory for Research on Active Ingredients in Natural Medicine of Jiangxi Province, Yichun University, Yichun, China, ² Institute of Basic Research in Clinical Medicine, China Academy of Chinese Medical Sciences, Beijing, China, ³ Department of Rheumatology, First Affiliated Hospital of Henan University of TCM, Zhengzhou, China, ⁴ Institute of Chinese Materia Medica, China Academy of Chinese Medical Sciences, Beijing, China, ⁵ Shanghai Guanghua Hospital of Integrated Traditional Chinese and Western Medicine, Shanghai, China, ⁶ China Association of Acupuncture and Moxibustion, Beijing, China, ⁷ Beijing Key Laboratory of Traditional Chinese Medicine Basic Research on Prevention and Treatment for Major Diseases, Experimental Research Center, China Academy of Chinese Medical Sciences, Beijing, China, ⁸ Law Sau Fai Institute for Advancing Translational Medicine in Bone & Joint Diseases, School of Chinese Medicine, Hong Kong Baptist University, Kowloon Tong, Hong Kong

Background: Rheumatoid arthritis (RA) is an autoimmune disease. Based on traditional Chinese medicine (TCM) theory, deficiency pattern (DP) which leads to specific treatment principles in clinical management is a crucial pattern diagnosis among RA patients, and autoantibodies have potential implications in TCM pattern classification. The purpose of this study was to identify specific RA DP-associated autoantibodies.

Methods: RA DP patients, RA nondeficiency pattern (NDP) patients and healthy controls (HCs) were recruited for this study. Then, clinical data and sera from all subjects were collected. After that, the sera were probed with protein chips, which were constructed by known RA related autoantigens, to screen for DP-associated candidate autoantibodies. Lastly, candidate autoantibodies were validated *via* enzyme-linked immunosorbent assay (ELISA) and function was evaluated by network analysis.

Results: Protein chips results showed that RA patients have higher levels of anti-vascular endothelial growth factor (VEGF) A165 antibodies than HC ($P < 0.005$); anti-VEGFA165 antibodies levels of patients with RA DP were lower than patients with RA NDP ($P < 0.05$). The results of the ELISA also showed statistically significant differences in anti-VEGFA165 antibodies between the RA and HC group ($P < 0.0001$); and there were statistically significant differences in anti-VEGFA165 antibodies between the RA DP and RA NDP group ($P < 0.05$). Network analysis results suggested IL-6 signaling pathway has a significant effect on VEGFA165 in RA patients.

Conclusion: Autoantibodies identification in RA using protein chips help in understanding DP in TCM. Discovery of anti-VEGFA165 antibodies may provide the possibility for clinical precision treatment.

Keywords: autoimmune disease, rheumatoid arthritis, deficiency pattern, autoantibody, protein chips, vascular endothelial growth factor A165

INTRODUCTION

Rheumatoid arthritis (RA) is a common autoimmune disease, accounting for more than 1% of the world's population (Uhlig et al., 2014). Although the exact cause of RA is still unclear, immunity disorder and chronic inflammation are generally considered as contribution to RA (Okada et al., 2010). In the later stages, other parts/organs of the RA patients may be affected, resulting in disability, declined quality of life, decreased ability to work (de Hair et al., 2013), and improved health care utilization (Boonen and Severens, 2011). In recent years, research has focused on the disease in the field of RA, leading to the discovery that autoantibodies can precede the clinical onset of the disease by many years (van Boekel et al., 2002).

Traditional Chinese medicine (TCM) techniques have shown therapeutic promise in treating RA (Goldbach-Mansky et al., 2009). In TCM theory, RA is considered an impediment disease ("Bi" pattern in Mandarin) and is caused by the invasion of heat pathogens, wind, or dampness into the human body (Li, 2002). According to RA patients symptoms further stratified, a pattern diagnosis can be determined for a subgroup of the patients, and then will prescribe specific therapy based on these pattern classifications, the special treatment principle can improve clinical efficacy (Lu et al., 2012). Deficiency pattern (DP) as key pattern diagnosis among RA patients can lead to a specific treatment principle of "tonifying the DP" in clinical management (Wang et al., 2013). In the practice of TCM, it has been found that Tripterygium glycosides and qingluo tongbi granules are safe and effective in the treatment of RA DP (Zhou et al., 2004), thus the treatment of RA DP has a good efficacy.

Autoantibodies can distinguish subgroups of the autoimmunity disease. Such as adult latent autoimmune diabetes and phenotypic type 2 diabetes can be distinguished by autoantibodies against zinc transporter 8, insulin, insulinoma antigen-2 and glutamic acid decarboxylase (Sorgjerd, 2018). There are two types of autoimmune hepatitis: type 1 (smooth muscle antibodies and antinuclear antibodies) and type 2 (liver cytosol antibodies and/or antibodies to liver and kidney microsomes type 1 and/or antibodies to liver and kidney microsomes type 3), which

can be classified based on autoantibodies (Zhang et al., 2014). Some scholars found that the positive rates of anti-U1 RNP antibodies were significantly different between the systemic lupus erythematosus DP and systemic lupus erythematosus TCM excess pattern groups (Dai et al., 2016). It was discovered that a significant difference exists between antinuclear antibodies in the kidney DP and kidney excess pattern groups (Guo et al., 2013). Autoantibodies have potential implications in TCM RA pattern classification.

The advent of protein chip technology has enabled a large-scale analysis of proteins to recognize biomarkers of RA subtypes, and identify the mechanisms underlying these subtypes (Hueber et al., 2005). We applied contain panels of RA autoantigens arrays to profile autoantibodies in sera derived from RA DP patients, identified autoantibodies associated with RA DP, and further validated protein chip results by ELISA. Finally, we analyzed the possible network of the association between RA DP and autoantibodies.

METHODS

Serum Samples

All the samples were collected from female RA patients (patients with RA include RA DP and non-deficiency RA) in Henan Province Hospital of TCM, included 20 sera from RA DP, 40 sera from RA NDP (nondeficiency pattern), and 40 HC matched by age and gender. Of which 15 sera of RA DP, 15 sera of RA NDP, and 15 sera of HC were used for screening of protein chips, and all the samples were used for ELISA validation. RA patients were eligible to participate if they had met the American College of Rheumatology criteria for RA for at least one year, with functional classes of I, II, or III (Arnett et al., 1988). Weakness in the waist, fatigue, dizziness, heavy limbs, nocturia, and numb limbs (Zhang et al., 2012), inhibited stretching and bending in limbs, pain occurring or worsening during moodiness, pain occurring or worsening at night, and deformity were categorized in TCM RA DP (Wang et al., 2013). NDP means that there is no typical DP in the RA. Patients with RA DP were recorded with whole clinical manifestations according to TCM theory using a questionnaire, a tongue examination, and pulse diagnosis by 3 appointed TCM practitioners. Patients were included in the study only if the 3 practitioners reported consistent results. This study was approved by the Ethics Committee at the Institute of Basic Research in Clinical Medicine, China Academy of Chinese Medical Sciences, and was conducted according to the standards of the Declaration of Helsinki. Written informed consent was obtained from the participants.

Abbreviations: RA, Rheumatoid arthritis; TCM, Traditional Chinese medicine; DP, Deficiency pattern; HC, Healthy controls; VEGF 165, Vascular endothelial growth factor 165; ELISA, Enzyme-linked immunosorbent assay; IL-6, Interleukin 6; IgG, Immunoglobulin G; PBS, Phosphate buffered saline; PBST, Phosphate buffered saline with Tween 20; Cy3, Cyanine dye 3; ESR, Erythrocyte sedimentation rate; CRP, C reactive protein; RF-IgG, Rheumatoid factor immunoglobulin G; RF-IgA, Rheumatoid factor immunoglobulin A; RF IgM, Rheumatoid factor immunoglobulin M; Anti-dsDNA, Anti-dsDNA antibody; Anti-CCP, Anti-cyclic citrullinated peptide.

Gene Cloning, Expression, Purification, and Mass Spectrometry

We expressed and purified seven proteins. Extraction of RNA from cells was carried out as per TRIzol reagent kit instructions (Invitrogen, CA; Lot No. 291946AX). Then amplification of genes was performed by RT-PCR using kit instructions (Biomake, Shanghai, China; Lot No: 20). The PCR product of the gene was sequenced by Sangon Biology (Shanghai, China). Proteins were over expressed in pET28a and then purified the recombinant protein by Ni-NTA kit (CWBI, Beijing, China; Lot No.01376/20302). Purified recombinant proteins were confirmed by proteomics analyzer AB 4700 mass spectrometry (Applied Biosystems, Foster City, CA).

Fabrication of the Protein Chips

Thirty autoantibodies associated with RA were found by reading the literature, and then designed a protein matrix using these autoantibodies. Printed autoantigens included 22 purchased, 7 expressed proteins (SinoBiological, Beijing, China; Diarect AG, Freiburg, Germany; Arotec, São Paulo, Brazil), and 1 protein extract that was derived from human stratum corneum whole protein. A 12-hole rubber gasket (CapitalBio, Beijing, China; Lot No.0011016) was applied to each chip to form 12 individual chambers. All the proteins were printed in duplicate within chamber, and identical probe areas were fabricated in 12 chambers. Each chamber included positive spots (human IgG) and blank spots. The printed chips were allowed to remain at room temperature for 1 h before storage at 4°C.

Serum Assays on Protein Chips

Blocked 1 h with PBS containing 5% fetal calf serum (Lot No. 18040502), incubated 2 h with 40 µl of 1:50 dilutions of RA DP patients, RA NDP patients and HC sera, and washed three times with PBST. Then incubated with a 1:400 dilution of Cy3-conjugated goat anti-human IgG secondary antibody (Lot No. AA03187869) and followed by PBST washing three times. The chips were scanned using a microarray scanner (CapitalBio, Beijing, China).

ELISA

The candidate proteins were coated onto 96-well plates and overnight at 4°C. The CB coating solution was prepared as follows: 0.795 g of Na₂CO₃ and 1.465 g of NaHCO₃ were dissolved in 500 ml of water and stored at 4°C. 200 µl of 5% fetal calf serum (Lot No. 18040502) was added to each well for blocked nonspecific binding. 100 µl human serum (1:50) was added to each well and incubated for 75 min at 37°C, then the plates were washed three times with PBST. 100 µl of horseradish peroxidase-labeled mouse anti-human IgG monoclonal antibody was added (1:10,000; Beijing Protein Innovation Co. Ltd; 130499) to each well for 45 min and then we washed the plates three times with PBST. 50 µl of tetramethylbenzidine substrate solution was added (makewoderbio, Beijing, China; Lot No.20180813). After this the plates were kept in a dark, room-temperature place for 8 min. The reaction was stopped after 50 µl H₂SO₄ entry and the immunoreactivity was measured by reading A450 (BioTek, Winooski, Vermont).

Statistical Analysis and Network Analysis

Chemiluminescent signals were acquired using microarray scanner, and the intensity value (signal intensity – background) was normalized using the mean of positive point signals. Each protein is in duplicate print, the average of each replicate is used as the final signal intensity for a given protein. Using a value of two times the standard deviation above mean_{healthy} as a cutoff value. SAS version 9.4 (SAS Institute Inc, *LICENSE = SAS 000062456227) was used to perform means, standard deviation and the t-test, *P*-value (*P* < 0.05) was taken as significant. Network analysis was conducted using the Ingenuity Pathway Analysis system (IPA, Ingenuity® Systems, <http://www.ingenuity.com>).

RESULTS

Baseline Characteristics of Study Subjects

The characteristics of the enrolled subjects, including age, ESR, CRP, RF-IgG, RF-IgA, RF-IgM, complement C3, complement C4, anti-dsDNA, anti-CCP were shown in **Table 1**. The age of the

TABLE 1 | Characteristics among the groups of enrolled subjects.

Indicators/Groups	DP (protein chip)	NDP (protein chip)	DP (ELISA)	NDP (ELISA)
Number of subjects	15	15	20	40
Age (years)	59.8 ± 8.94*	49.33 ± 9.66	62.32 ± 10.00**	49.72 ± 12.36
Duration of RA (month)	151.45 ± 144.11	120.14 ± 112.21	160.10 ± 160.80	96.72 ± 112.00
ESR (mm/h)	45.53 ± 28.02	57.4 ± 29.35	50.05 ± 29.34	48.21 ± 29.77
CRP (mg/L)	34.04 ± 38.61	39.31 ± 42.45	35.89 ± 37.29	28.78 ± 33.69
RF-IgG (RU/ml)	32.8 ± 73.53	16.92 ± 20.94	28.29 ± 67.53	15.99 ± 23.63
RF-IgA (RU/ml)	112.92 ± 109.71	132.11 ± 114.61	131.43 ± 110.52	124.39 ± 105.95
RF-IgM (RU/ml)	230.93 ± 134.67	301.16 ± 171.55	260.02 ± 140.76	296.92 ± 134.08
Complement C3 (g/L)	1.28 ± 0.24	1.26 ± 0.19	1.27 ± 0.22	1.24 ± 0.17
Complement C4 (g/L)	0.28 ± 0.13	0.26 ± 0.08	0.29 ± 0.12	0.26 ± 0.07
Anti-dsDNA (IU/ml)	3.53 ± 0.80	3.88 ± 0.69	3.34 ± 0.89	3.88 ± 0.76
Anti-CCP (RU/ml)	65.58 ± 42.71	78.09 ± 51.55	71.91 ± 41.50	85.43 ± 46.56

ESR indicates erythrocyte sedimentation rate; CRP, C reactive protein; RF-IgG, rheumatoid factor immunoglobulin G; RF-IgA, rheumatoid factor immunoglobulin A; RF IgM, rheumatoid factor immunoglobulin M; Anti-dsDNA, anti-distrand-DNA antibody; Anti-CCP, anti-cyclic citrullinated peptide.

The comparisons of clinical indicators between DP and NDP. Unpaired t-test was applied to continuous variables analysis, and the data are expressed as the mean ± SD when appropriate (95% CI). The DP (protein chip) groups age vs NDP (protein chip) groups age **P* < 0.05, DP (ELISA) groups age vs NDP groups age (ELISA) ***P* < 0.01.

RA DP patients was older than that of the RA NDP patients ($P < 0.0005$). There was no significant difference in other indicators between the RA DP and RA NDP patients. Two groups used for protein chips technology or ELISA showed the above results.

Gene Cloning, Expression, and Purification of Proteins

Seven proteins were expressed and purified for fabrication of protein chips. First, synthetic gene was cloned into pET28a (Figure 1A). Second, coomassie brilliant blue staining of expressed proteins on SDS-PAGE, purified proteins were separated with 10% SDS-PAGE and then stained with coomassie brilliant blue. Visible proteins migrated at their expected molecular weights (Figure 1B). Last, proteins from Ni-NTA resin were reassured by mass spectrometry, and the results show that putative proteins have a highly homologous identity ($P < 0.05$).

Construction of RA-associated Protein Chips

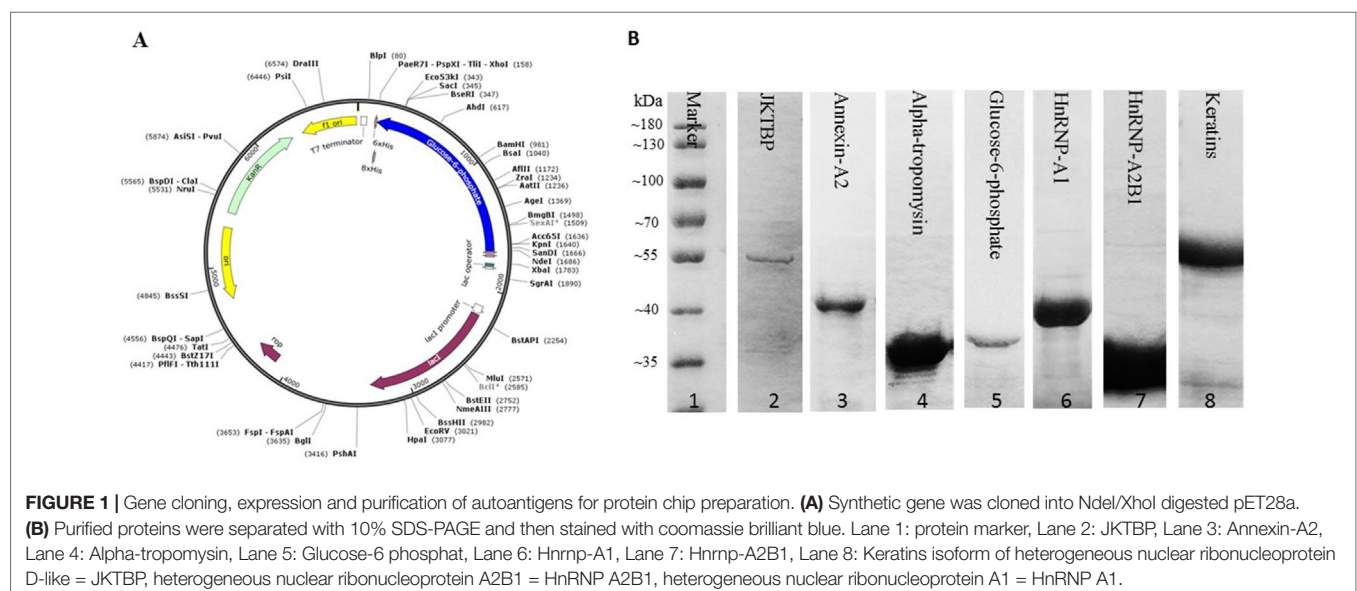
In order to optimize the serum profiling assay, we tested a variety of different conditions in a pilot assay. And polymer-slide H was chosen for chips fabrication, 20-fold dilution was chosen as the most appropriate serum concentration, 400-fold dilution was chosen as the most appropriate Cy3-conjugated anti-human IgG antibody. Finally, we employed the protein chips containing 30 RA-associated autoantigens to perform serum profiling of samples collected from 15 DP, 15 NDP, and 15 HC subjects (Figure 2A). Human IgG at a known concentration was printed at each chamber on the chips to serve as a control and landmark. Anti-vimentin antibodies and anti-heat shock protein 60 antibodies were incubated in 1 individual chambers for checkout the protein's activity (Figure 2B). The results showed protein chips had a high correlation coefficient (0.978) between duplicate spots, which suggested that it was of high quality (Figure 2C).

Probing Results of the Protein Chips

We observed that autoantigens could be readily recognized by sera from DP and NDP groups, and the serum profiles also showed obvious individual-to-individual variation within among groups (Figure 3A). To identify potential RA DP-associated autoantigens, we used microarray scanner to acquire the resultant signal intensities of all protein spots in each assay and identified the positives within each chip (see details under Methods). Protein chips results showed that RA have higher levels of anti-vascular endothelial growth factor (VEGF) A165 (P15692) antibodies than HC ($P < 0.005$); anti-VEGFA165 antibodies levels of patients with RA DP were lower than patients with RA NDP ($P < 0.05$); patients with RA DP have higher levels of anti-VEGFA165 antibodies than HC ($P < 0.01$). There was no statistical difference between RA DP and RA NDP groups for other autoantibodies. Using a value of two times the standard deviation above mean_{healthy} as a cutoff value, an anti-IgG antibody reaction against VEGFA165 was observed in 2 out of 15 RA DP patients (13%), 6 out of 15 RA NDP patients (40%), 0 out of 15 HC patients (0%). Finally, to visualize the range of signal intensities, we conducted box-whisker plot analysis for anti-VEGFA165 antibodies across the various groups of sera (Figure 3B).

Verification by ELISA

In order to validate the candidate autoantibodies identified using protein chips technology, ELISA of anti-VEGFA165 antibodies were carried out with 20 RA DP, 40 RA NDP, and 40 HC subject sera to verification. The results showed reactivity of RA serum IgG antibodies against were higher than HC ($P < 0.0001$); the reactivity of RA DP serum IgG antibodies against were lower than NDP ($P < 0.05$), and the reactivity of RA DP serum IgG antibodies against were higher than HC ($P < 0.05$) (Figure 4). Therefore, the anti-VEGFA165 antibodies were confirmed as being able to distinguish between RA DP and RA NDP.



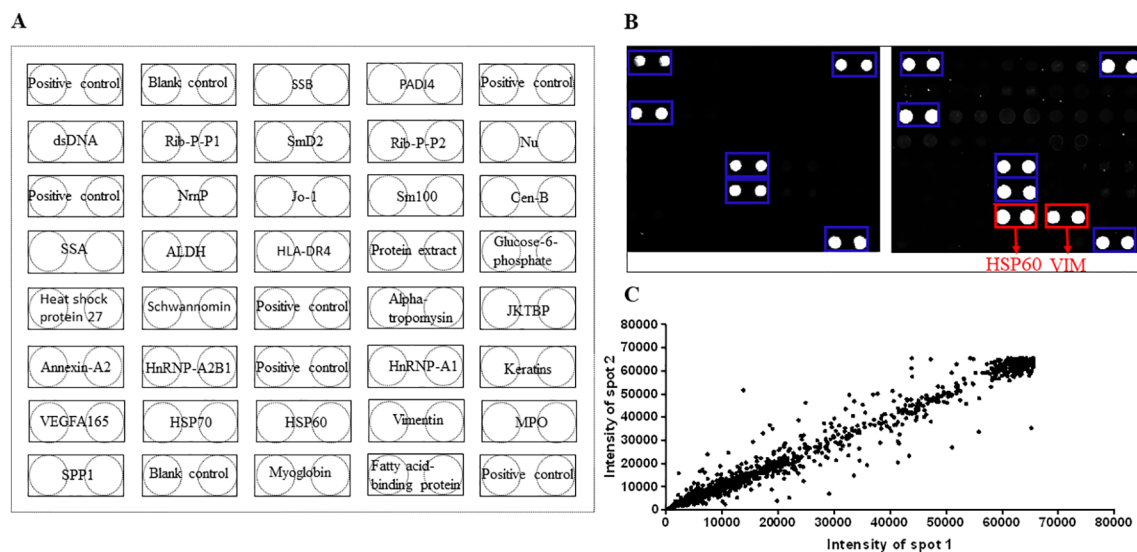


FIGURE 2 | Construction RA associated protein chip. **(A)** Human proteins were purified and printed in duplicate on poly-L-lysine coated microscope slides. **(B)** Correlation of spot intensities of all the duplicate pairs. The signal intensities of duplicate spots (Spot 1 versus its corresponding Spot 2) were plotted against each other. The resulting correlation coefficient was 0.97, indicating high reproducibility of the protein spotting. **(C)** To monitor the quality and relative quantity of the printed proteins on glass slides, the human protein chips were probed with anti-His antibody, followed by Cy3-labeled secondary antibody to visualize the signals, red boxes indicate His-tag group. Blue boxes indicate human IgG (the positive control), red boxes indicate HSP60 and VIM antibody. Sjogren syndrome antigen B = SSB, peptidyl arginine deiminase 4 = PAD4, double-stranded DNA = dsDNA, ribosomal protein P1 = Rib-P-P1, smithD2 = SmD2, ribosomal protein P2 = Rib-P-P2, nucleosome = Nu, nuclear ribonucleoprotein = NrnP, smith100 = Sm100, centromere protein b = Cen-B, sjogren syndrome antigen A = SSA, aldehyde dehydrogenase = ALDH, human leukocyte antigen-DR4 = HLA-DR4, isoform of heterogeneous nuclear ribonucleoprotein D-like = JKTBP, heterogeneous nuclear ribonucleoprotein A2B1 = HnRNP A2B1, heterogeneous nuclear ribonucleoprotein A1 = HnRNP A1, vascular endothelial growth factor A165 = VEGFA165, Heat shock protein 70 = HSP70, heat shock protein 60 = HSP60, myeloperoxidase = MPO, osteopontin = SPP1.

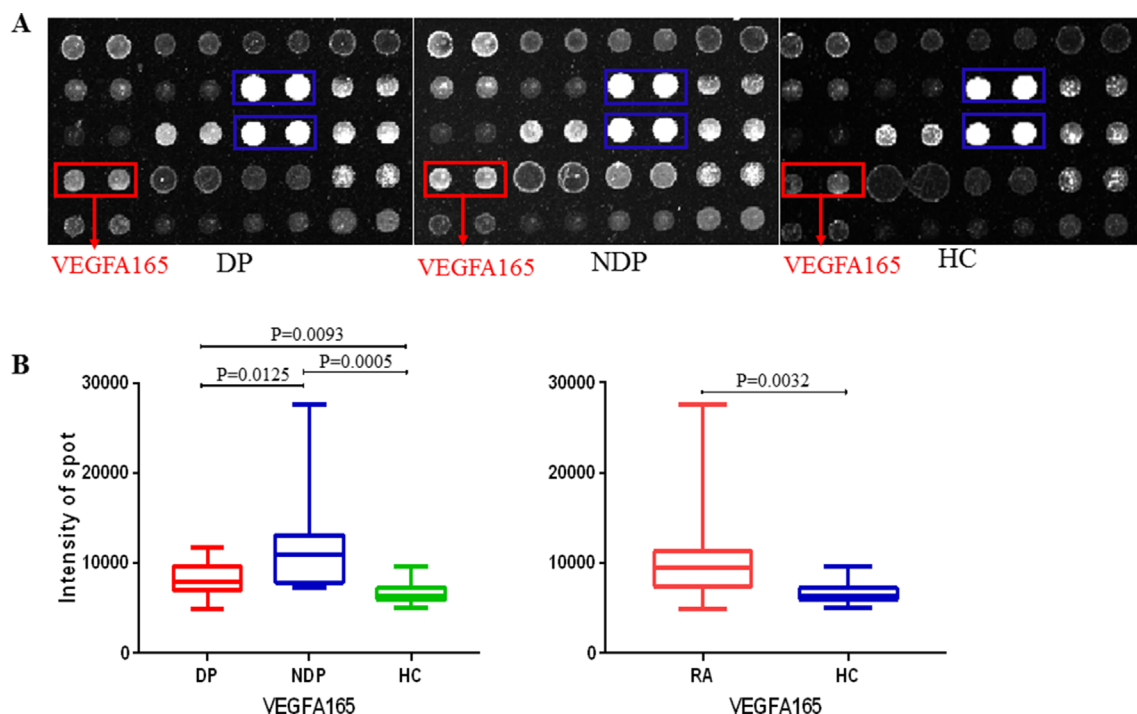


FIGURE 3 | Probing results of the human protein chip with DP and NDP sera. **(A)** Fifteen DP, 15 NDP, and 15 HC serum samples were diluted 1:20 and individually incubated with the human protein chip, followed by the addition of the anti-human IgG antibody (Cy3-conjugated). Chips were dried and scanned to acquire the images. Representative areas of the images are illustrated. Red boxes indicate the positive candidate autoantigens, and blue boxes indicate human IgG (the positive control). **(B)** Fifteen DP, NDP, and 15 HC. The signal distributions of VEGFA165 reacting with the serum samples is displayed. The bar within the rectangle indicates the median value.

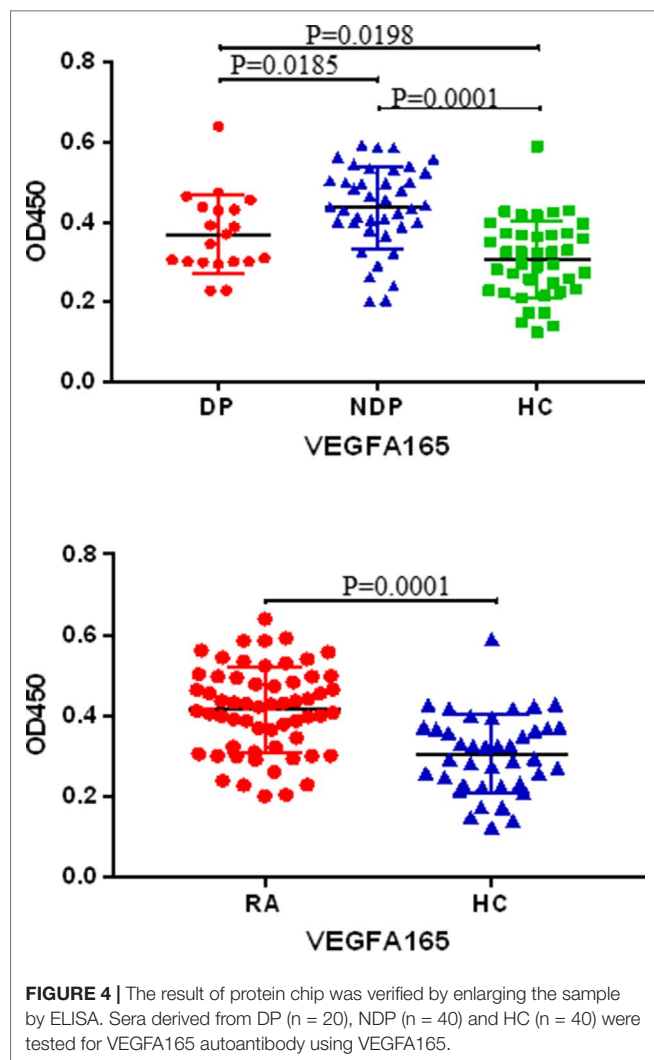


FIGURE 4 | The result of protein chip was verified by enlarging the sample by ELISA. Sera derived from DP (n = 20), NDP (n = 40) and HC (n = 40) were tested for VEGFA165 autoantibody using VEGFA165.

DISCUSSION

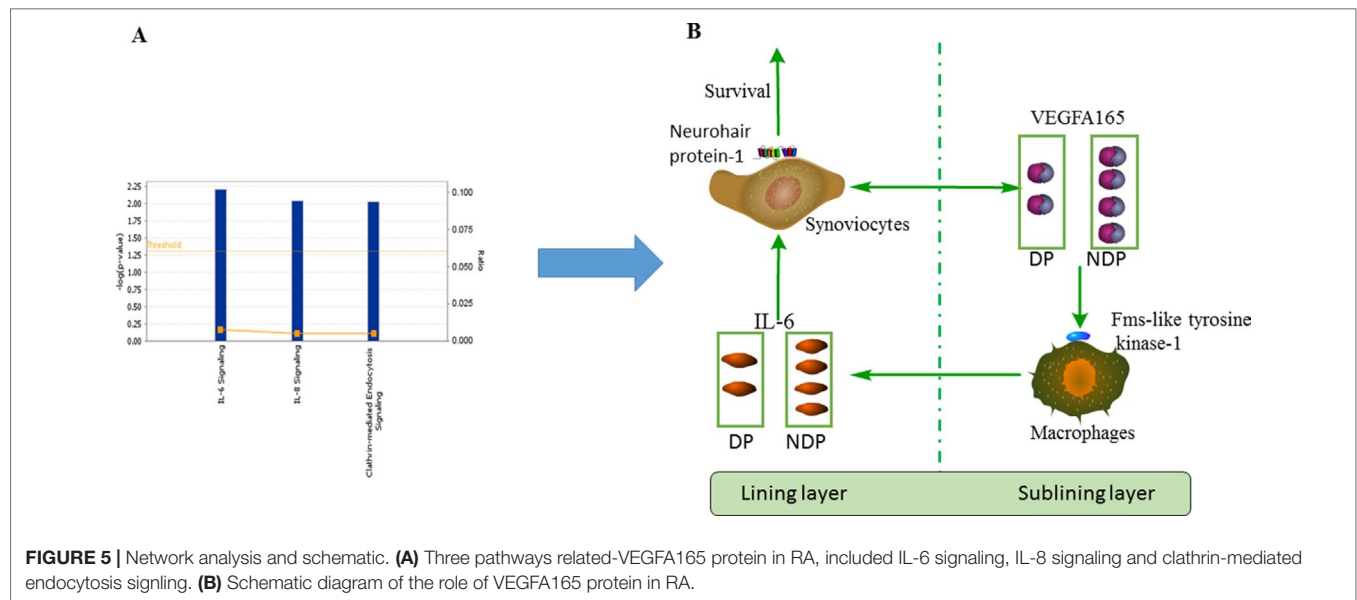
TCM pattern classification analysis was carried out through data collected by four combined diagnostic methods, including WANG (inspection), WEN (falling-rising tone, auscultation, and olfaction), WEN (falling tone, inquiry), and QIE (palpation) (Tao et al., 2017). The “Cold,” “Heat,” “Deficiency,” and “Excess” were four basic patterns in TCM (Jiang, 2005). Pattern classification was the advantage of TCM, which can guide herbal prescriptions (Chai et al., 2011). Some TCM herbal formulae have been reported for the treatment of DP, such as WuziYanzong Pill, which protected the impaired spermatogenesis possibly by mediating mitochondrial energy metabolism in DP rats (Liu, 2014). Both crude and bran-processed rhizome of *Atractylodes lancea* have alleviated the symptoms of spleen DP in rats (Xue et al., 2018). *Radix Astragali* and its split components can promote water metabolism in rats with the syndrome of dampness stagnancy due to spleen deficiency by regulating the expression of AQP (Zhao et al.,

2017). Xiaoyaosan intervention may effectively adjust the gut dysbacteriosis in functional dyspepsia (Qiu et al., 2017). TCM has a good effect in treating DP.

In TCM practice, an experiential diagnosis approach has been frequently used in pattern classification in RA patients (Mo et al., 2016). In order to promote the traditional experiential diagnosis, the scientific evidence for pattern classification is essential, and it would be beneficial to understand essence of the pattern classification. The study suggested that statistical-based clinical data classification had a similar TCM pattern differentiation in RA patients (He et al., 2008). We had previous used integrating liquid chromatography/mass spectrometry and gas chromatography/mass spectrometry platforms in conjunction with the Ingenuity Pathway Analysis software identified the biomarkers in RA patients with typical TCM cold or heat patterns (Gu et al., 2012; Guo et al., 2016). And we identified the network-based gene expression biomarkers for both cold- and heat-patterns of RA by obtained gene expression profilings of CD₄ + T cells from cold-pattern RA patients and heat-pattern RA patients using microarray (Lu et al., 2012). In this study, we explored the autoantibody of sera in RA patients with typical TCM DP and NDP by protein chips technology, and anti-VEGFA165 antibodies which DP-associated in RA was identified.

Our previous study of the TCM DP-related genes network study found TCM DP is probably related to immune response (Wang et al., 2013). Mo, Na et al. found that the age of disease onset exhibited significant differences between DP and NDP, which is consistent with our research. The RA DP patients were older than the RA NDP, this finding is in agreement with the TCM theory that Qi, Xue, Yin, and Yang are more insufficient in older than in younger people (Wu et al., 2012). (Yin, things associated with the physical form of an object; Yang, things associated with energetic qualities; Qi, life force that animates the forms of the world; Xue, dense form of body fluids that have been acted upon and energized by Qi) (Wang et al., 2012). Anti-cyclic citrullinated peptides antibodies levels of patients with RA DP were higher than the RA NDP (Mo et al., 2016), and our experiments show that the level of anti VEGFA165 antibodies in patients with RA DP is lower than that in patients with RA NDP. We also found RA DP patients have higher levels of anti-VEGFA165 antibodies than HC, and confirmed RA have higher levels of anti-VEGFA165 antibodies than HC. Autoantibodies are associated with RA DP, and it may be used to classify TCM pattern.

VEGF is a dimeric glycoprotein, VEGFA, B, C, D and placenta growth factor consisted the VEGF family in mammals. VEGFA included five isoforms: VEGFA121, VEGFA145, VEGFA165, VEGFA189, and VEGFA206 (Olsson et al., 2006), and VEGFA165 was the most abundant factor in most cells and tissues (Neufeld et al., 1996). VEGFA165 can promote the formation of new blood vessels and increased vascular permeability. Inflammation and angiogenesis were interdependent processes, and angiogenesis have significant effects on inflammatory mediators (Oura et al., 2003). VEGF165 has a direct pro-inflammatory effect in the pathogenesis of RA (Yoo et al., 2005). Research has discovered



the VEGFA165 levels in sera synovial fluid from RA patients are significantly higher than in synovial fluid from osteoarthritis patients (Lee et al., 2001; Yoo et al., 2005).

Our research found there were statistically significant differences in anti-VEGFA165 antibodies between the RA and HC groups. We also found that anti-VEGFA165 antibodies levels of subjects with RA DP were lower than subjects with RA NDP. No statistical differences were found between RA DP and RA NDP groups and other autoantibodies. Through the analysis of the VEGF165-related pathway, we found three pathways related to autoimmunity, including IL-6 signaling, IL-8 signaling and clathrin-mediated endocytosis signaling, the IL-6 signaling pathway is most relevant compared to the other two pathways (**Figure 5A**). VEGFA165 protein is expressed by synovial fibroblasts and synovial macrophages in the synovial tissues of RA patients. A study found that cultured synovial cells are able to secrete VEGFA165 when stimulated with IL-6 (Yoo et al., 2005). The serum levels of IL-6 in RA patients were significantly higher than subjects in HC (Diaz-Torne et al., 2018), and the DP was significantly lower than that in NDP (Peng et al., 2008). VEGFA165 plays a biological role by binding to its receptor subtypes, namely fms-like tyrosine kinase and neurohair protein-1 (Ferrara et al., 2003). VEGFA165 may recruit monocytes around endothelial cells in synovial membranes, where newly employed macrophages can produce IL-6 when stimulated by VEGFA165/fms-like tyrosine kinase-1 binding or *via* cell contact with activated endothelial cells (Yoo et al., 2005). Thus, this creates a self-perpetuating cycle of inflammation. Short interfering RNA down-regulates neurohair protein-1 transcript products and induces spontaneous apoptosis of synovial cells, which is related to the decrease of Bcl-2 expression and the increase of Bax transport to mitochondria (Yoo et al., 2008), which leads to synovial hyperplasia. And in the RA DP, swollen feet joints

are more common than in RA NDP (Yuan-Wei and Lou, 2017) (**Figure 5B**). Some of the above findings may partly explain the statistically significant differences in VEGFA165 antibodies between the RA DP and RA NDP groups.

Limitations of this study include the fact that it is the limited sample size with the participants recruited. Due to the fact that RA patients with a single DP are not easy to obtain, since patients usually present with multiple-patterns, larger sample size study is needed in the future.

CONCLUSION

In this study, a protein chip containing RA associated autoantigens was successfully constructed. Using this chip, the anti-VEGF 165 antibody was found to be related to the TCM DP of RA, a finding further validated with the ELISA method. This study may promote the development of precise diagnosis and treatment of RA in TCM clinical, provide some clues for understanding the causes of DP of RA.

DATA AVAILABILITY

The raw data supporting the conclusions of this manuscript will be made available by the authors, without undue reservation, to any qualified researcher.

ETHICS STATEMENT

This study was approved by the Ethics Committee at the Institute of Basic Research in Clinical Medicine, China Academy of Chinese Medical Sciences, and was conducted according to

the standards of the Declaration of Helsinki. Written informed consent was obtained from the participants.

AUTHOR CONTRIBUTIONS

CL, PC, HZ, AL, JY, and YZ conceived the project. PC, HZ, and CL designed the experiments. HG collected the sera. HZ, PC, and YZ carried out the research. HZ conducted the data analysis and wrote the paper. HZ, YZ, BL, LL, LZ, MB, HG, HX,

HF, LX, WY, JY, PC, CL and AL have read and approved the final manuscript.

FUNDING

This study was supported by grants from the Fundamental Research Funds for the Central public welfare research institutes (ZZ11-113, ZZ11-056) and National Natural Science Foundation of China (grant no. 81403209).

REFERENCES

- Arnett, F. C., Edworthy, S. M., Bloch, D. A., McShane, D. J., Fries, J. F., Cooper, N. S., et al. (1988). The american rheumatism association 1987 revised criteria for the classification of rheumatoid arthritis. *Arthritis Rheum.* 31 (3), 315–324. doi: 10.1002/art.1780310302
- Boonen, A., and Severens, J. L. (2011). The burden of illness of rheumatoid arthritis. *Clin. Rheumatol.* 30 Suppl 1, S3–8. doi: 10.1007/s10067-010-1634-9
- Chai, C., Kou, J., Zhu, D., Yan, Y., and Yu, B. (2011). Mice exposed to chronic intermittent hypoxia simulate clinical features of deficiency of both qi and yin syndrome in traditional chinese medicine. *Evid. Based Complement. Alternat. Med.* 2011, 356252. doi: 10.1093/ecam/nep226
- Dai, R. Q., Pan, L., and Yang, L. J. (2016). Correlation of autoantibodies and TCM syndrome differentiation in the patients of systemic lupus erythematosus. *World J. Integr. Tradit. West. Med.* 11 (6), 808–811. doi: 10.13935/j.cnki.sjzx.160618
- de Hair, M. J., Landewe, R. B., van de Sande, M. G., van Schaardenburg, D., van Baarsen, L. G., Gerlag, D. M., et al. (2013). Smoking and overweight determine the likelihood of developing rheumatoid arthritis. *Ann. Rheum. Dis.* 72 (10), 1654–1658. doi: 10.1136/annrheumdis-2012-202254
- Diaz-Torne, C., Ortiz, M. D. A., Moya, P., Hernandez, M. V., Reina, D., Castellvi, I., et al. (2018). The combination of IL-6 and its soluble receptor is associated with the response of rheumatoid arthritis patients to tocilizumab. *Semin. Arthritis Rheum.* 47 (6), 757–764. doi: 10.1016/j.semarthrit.2017.10.022
- Ferrara, N., Gerber, H. P., and LeCouter, J. (2003). The biology of VEGF and its receptors. *Nat. Med.* 9 (6), 669–676. doi: 10.1038/nm0603-669
- Goldbach-Mansky, R., Wilson, M., Fleischmann, R., Olsen, N., Silverfield, J., Kempf, P., et al. (2009). Comparison of Tripterygium wilfordii Hook F versus sulfasalazine in the treatment of rheumatoid arthritis: a randomized trial. *Ann. Intern. Med.* 151 (4), 229–240, w249–251. doi: 10.7326/0003-4819-151-4-200908180-00005
- Gu, Y., Lu, C., Zha, Q., Kong, H., Lu, X., Lu, A., et al. (2012). Plasma metabolomics study of rheumatoid arthritis and its Chinese medicine subtypes by using liquid chromatography and gas chromatography coupled with mass spectrometry. *Mol. Biosyst.* 8 (5), 1535–1543. doi: 10.1039/c2mb25022e
- Guo, H., Niu, X., Gu, Y., Lu, C., Xiao, C., Yue, K., et al. (2016). Differential amino acid, carbohydrate and lipid metabolism perpetuations involved in a subtype of rheumatoid arthritis with chinese medicine cold pattern. *Int. J. Mol. Sci.* 17 (10), 1757. doi: 10.3390/ijms17101757
- Guo, L. K., Luo, S. Z., Liao, Q. H., Lai, R. G., Liu, X. L., Liu, L. J., et al. (2013). Correlation study of auto-immune antibodies and rheumatoid arthritis patients of Shen deficiency syndrome. *Zhongguo Zhong Xi Yi Jie He Za Zhi* 33 (5), 619–622. doi: 10.7661/CJIM.2013.05.0619
- He, Y., Lu, A., Zha, Y., and Tsang, I. (2008). Differential effect on symptoms treated with traditional Chinese medicine and western combination therapy in RA patients. *Complement. Ther. Med.* 16 (4), 206–211. doi: 10.1016/j.ctim.2007.08.005
- Hueber, W., Kidd, B. A., Tomooka, B. H., Lee, B. J., Bruce, B., Fries, J. F., et al. (2005). Antigen microarray profiling of autoantibodies in rheumatoid arthritis. *Arthritis Rheum.* 52 (9), 2645–2655. doi: 10.1002/art.21269
- Jiang, W. Y. (2005). Therapeutic wisdom in traditional Chinese medicine: a perspective from modern science. *Discov. Med.* 5 (29), 455–461. doi: 10.1016/j.tips.2005.09.006
- Lee, S. S., Joo, Y. S., Kim, W. U., Min, D. J., Min, J. K., Park, S. H., et al. (2001). Vascular endothelial growth factor levels in the serum and synovial fluid of patients with rheumatoid arthritis. *Clin. Exp. Rheumatol.* 19 (3), 321–324. doi: 10.1002/1529-0131(200105)44:5<1229::AID-ANR209>3.0.CO;2-E
- Li, S. (2002). Advances in TCM symptomatology of rheumatoid arthritis. *J. Tradit. Chin. Med.* 22 (2), 137–142. doi: 10.3969/j.issn.0255-2922.2002.02.018
- Liu, B. (2014). AB60. Effect of WuziYanzong Pill on Cox7a2 gene and Claudin-11 expression in Rats with kidney essence deficiency syndrome. *Transl. Androl. Urol.* 3 (Suppl 1), AB60. doi: 10.3978/j.issn.2223-4683.2014.s060
- Lu, C., Niu, X., Xiao, C., Chen, G., Zha, Q., Guo, H., et al. (2012). Network-based gene expression biomarkers for cold and heat patterns of rheumatoid arthritis in traditional chinese medicine. *Evid. Based Complement. Alternat. Med.* 2012, 203043. doi: 10.1155/2012/203043
- Mo, N., Lai, R., Luo, S., Xie, J., Wang, X., Liu, L., et al. (2016). A Transmembrane Polymorphism of Fcγ Receptor IIb Is associated with kidney deficiency syndrome in rheumatoid arthritis. *Evid. Based Complement. Alternat. Med.* 2016, 3214657. doi: 10.1155/2016/3214657
- Neufeld, G., Cohen, T., Gitay-Goren, H., Poltorak, Z., Tessler, S., Sharon, R., et al. (1996). Similarities and differences between the vascular endothelial growth factor (VEGF) splice variants. *Cancer Metastasis Rev.* 15 (2), 153–158. doi: 10.1007/BF00437467
- Okada, T., Tsukano, H., Endo, M., Tabata, M., Miyata, K., Kadomatsu, T., et al. (2010). Synovial cell-derived angiopoietin-like protein 2 contributes to synovial chronic inflammation in rheumatoid arthritis. *Am. J. Pathol.* 176 (5), 2309–2319. doi: 10.2353/ajpath.2010.090865
- Olsson, A. K., Dimberg, A., Kreuger, J., and Claesson-Welsh, L. (2006). VEGF receptor signalling - in control of vascular function. *Nat. Rev. Mol. Cell Biol.* 7 (5), 359–371. doi: 10.1038/nrm1911
- Oura, H., Bertoncini, J., Velasco, P., Brown, L. F., Carmeliet, P., and Detmar, M. (2003). A critical role of placental growth factor in the induction of inflammation and edema formation. *Blood* 101 (2), 560–567. doi: 10.1182/blood-2002-05-1516
- Peng, Y. L., Ren, Y. G., Zhuang, J. H., Ding, H. M., Pan, W. Y., and Deng, Z. Z. J. o. P. M. (2008). Relationship between syndrome patterns of rheumatoid arthritis and interleukin-6 and interleukin-18 levels in serum. *J. Prac. Med.* 24 (12), 2061–2063. http://en.cnki.com.cn/Article_en/CJFDTotat-SYYZ200812023.htm
- Qiu, J. J., Liu, Z., Zhao, P., Wang, X. J., Li, Y. C., Sui, H., et al. (2017). Gut microbial diversity analysis using Illumina sequencing for functional dyspepsia with liver depression-spleen deficiency syndrome and the interventional Xiaoyaosan in a rat model. *World. J. Gastroenterol.* 23 (5), 810–816. doi: 10.3748/wjg.v23.i5.810
- Sorgjerd, E. P. (2018). Type 1 diabetes-related autoantibodies in different forms of diabetes. *Curr. Diabetes Rev.* 15 (3), 199–204. doi: 10.2174/1573399814666180730105351
- Tao, F., Lu, P., Xu, C., Zheng, M., Liu, W., Shen, M., et al. (2017). Metabolomics analysis for defining serum biochemical markers in colorectal cancer patients with qi deficiency syndrome or yin deficiency syndrome. *Evid. Based Complement. Alternat. Med.* 2017, 7382752. doi: 10.1155/2017/7382752
- Uhlig, T., Moe, R. H., and Kvien, T. K. J. P. (2014). The burden of disease in rheumatoid arthritis. *Pharmacoeconomics* 32 (3), 841–851. doi: 10.1007/s40273-014-0174-6
- van Boekel, M. A., Vossenaar, E. R., van den Hoogen, F. H., and van Venrooij, W. J. (2002). Autoantibody systems in rheumatoid arthritis: specificity, sensitivity and diagnostic value. *Arthritis Res.* 4 (2), 87–93. doi: 10.1186/ar395

- Wang, L. M., Zhao, X., Wu, X. L., Li, Y., Yi, D. H., Cui, H. T. et al. (2012). Diagnosis analysis of 4 TCM patterns in suboptimal health status: a structural equation modelling approach. *Evid. Based Complement. Alternat. Med.* 2012(3), 970985. doi: 10.1155/2012/970985
- Wang, M., Chen, G., Lu, C., Xiao, C., Li, L., Niu, X., et al. (2013). Rheumatoid arthritis with deficiency pattern in traditional chinese medicine shows correlation with cold and hot patterns in gene expression profiles. *Evid. Based Complement. Alternat. Med.* 2013, 248650. doi: 10.1155/2013/248650
- Wu, T., Yang, M., Wei, H. F., He, S. H., Wang, S. C., and Ji, G. (2012). Application of metabolomics in traditional chinese medicine differentiation of deficiency and excess syndromes in patients with diabetes mellitus. *Evid. Based Complement. Alternat. Med.* 2012, 968083. doi: 10.1155/2012/968083
- Xue, D. H., Liu, Y. Q., Cai, Q., Liang, K., Zheng, B. Y., Li, F. X., et al. (2018). Comparison of Bran-Processed and Crude Atractylodes Lancea Effects on Spleen Deficiency Syndrome in Rats. *Pharmacogn. Mag.* 14 (54), 214–219. doi: 10.4103/pm.pm_126_17
- Yoo, S. A., Bae, D. G., Ryoo, J. W., Kim, H. R., Park, G. S., Cho, C. S., et al. (2005). Arginine-rich anti-vascular endothelial growth factor (anti-VEGF) hexapeptide inhibits collagen-induced arthritis and VEGF-stimulated productions of TNF- α and IL-6 by human monocytes. *J. Immunol.* 174 (9), 5846–5855. doi: 10.4049/jimmunol.174.9.5846
- Yoo, S. A., Kwok, S. K., and Kim, W. U. (2008). Proinflammatory role of vascular endothelial growth factor in the pathogenesis of rheumatoid arthritis: prospects for therapeutic intervention. *Mediators Inflamm.* 2008, 129873. doi: 10.1155/2008/129873
- Yuan-Wei, L. I., and Lou, Y. Q. (2017). Clinical study on the similarities and differences of TCM syndromes of rheumatoid arthritis with and without swollen foot joint. *Rheum. Arthritis.* 6 (4), 17–21. http://en.cnki.com.cn/Article_en/CJFDTotal-FSBG201708006.htm
- Zhang, C., Jiang, M., Chen, G., and Lu, A.J.E.J.o.I.M. (2012). Incorporation of traditional Chinese medicine pattern diagnosis in the management of rheumatoid arthritis. *Eur. J. Integr. Med.* 4 (3), e245–e254. doi: 10.1016/j.eujim.2012.02.004
- Zhang, W. C., Zhao, F. R., Chen, J., and Chen, W. X. (2014). Meta-analysis: diagnostic accuracy of antinuclear antibodies, smooth muscle antibodies and antibodies to a soluble liver antigen/liver pancreas in autoimmune hepatitis. *PLoS One* 9 (3), e92267. doi: 10.1371/journal.pone.0092267
- Zhao, W. X., Cui, N., Jiang, H. Q., Ji, X. M., Han, X. C., Han, B. B., et al. (2017). Effects of radix astragali and its split components on gene expression profiles related to water metabolism in Rats with the Dampness Stagnancy due to Spleen Deficiency Syndrome. *Evid. Based Complement. Alternat. Med.* 2017, 4946031. doi: 10.1155/2017/4946031
- Zhou, X., Zhou, Z., Jin, M., Wang, H., Wu, M., Song, Y., et al. (2004). Clinical study of qingluo tongbi granules in treating 63 patients with rheumatoid arthritis of the type of yin-deficiency and heat in collaterals. *J. Tradit. Chin. Med.* 24 (2), 83–87. doi: 10.3969/j.issn.0255-2922.2004.02.001

Conflict of Interest Statement: The authors declare that the research was conducted in the absence of any commercial or financial relationships that could be construed as a potential conflict of interest.

Copyright © 2019 Zhao, Zhang, Liu, Li, Zhang, Bao, Guo, Xu, Feng, Xiao, Yi, Yi, Chen, Lu and Lu. This is an open-access article distributed under the terms of the Creative Commons Attribution License (CC BY). The use, distribution or reproduction in other forums is permitted, provided the original author(s) and the copyright owner(s) are credited and that the original publication in this journal is cited, in accordance with accepted academic practice. No use, distribution or reproduction is permitted which does not comply with these terms.



Deciphering the Pharmacological Mechanisms of the Huayu-Qiangshen-Tongbi Formula Through Integrating Network Pharmacology and *In Vitro* Pharmacological Investigation

OPEN ACCESS

Edited by:

Min Ye,
Peking University,
China

Reviewed by:

Hanne Merete Lindegaard,
Odense University Hospital,
Denmark
Shivaprasad Venkatesha,
Uniformed Services University
of the Health Sciences,
United States

*Correspondence:

Hua Yu
yuhuayu@vip.sina.com
Ging Chan
GChan@um.edu.mo

[†]These authors have contributed
equally to this work

Specialty section:

This article was submitted to
Ethnopharmacology,
a section of the journal
Frontiers in Pharmacology

Received: 19 March 2019

Accepted: 21 August 2019

Published: 23 September 2019

Citation:

Wang Z, Linghu K-G, Hu Y, Zuo H,
Yi H, Xiong S-H, Lu J, Chan G, Yu H
and Huang R-Y (2019) Deciphering
the Pharmacological Mechanisms
of the Huayu-Qiangshen-Tongbi
Formula Through Integrating
Network Pharmacology and *In Vitro*
Pharmacological Investigation.
Front. Pharmacol. 10:1065.
doi: 10.3389/fphar.2019.01065

Zihao Wang^{1†}, Ke-Gang Linghu^{1†}, Yuanjia Hu¹, Huali Zuo¹, Hao Yi², Shi-Hang Xiong¹,
Jinjian Lu¹, Ging Chan^{1*}, Hua Yu^{1,3,4*} and Run-Yue Huang^{2,5}

¹ State Key Laboratory of Quality Research in Chinese Medicine, Institute of Chinese Medical Sciences, University of Macau, Macau, China, ² Department of Rheumatology and Immunology, The Second Affiliated Hospital of Guangzhou University of Chinese Medicine, Guangdong Provincial Hospital of Chinese Medicine, Guangzhou, China, ³ HKBU Shenzhen Research Center, Shenzhen, China, ⁴ School of Chinese Medicine, Hong Kong Baptist University, Hong Kong, Hong Kong,

⁵ Guangdong Provincial Key Laboratory of Clinical Research on Traditional Chinese Medicine Syndrome, Guangzhou, China

Rheumatoid arthritis is a chronic inflammatory autoimmune disease, causing articular and extra-articular dysfunctions among patients, and it could result in irreversible joint damages or disability if untreated. A traditional Chinese medicine formula, Huayu-Qiangshen-Tongbi (HT) formula, has been observed successful in controlling rheumatoid arthritis progression in traditional Chinese medicine clinics. In this study, we conducted a systematic analysis of the HT formula with a purpose of proposing for its potential mechanism of action using network pharmacological methods. The potential targets of the formula were collected and screened according to the topological features of their protein-protein interaction network, and we subsequently validated our prediction results through *in vitro* experiments. We proposed that the HT formula could interfere with the bone metabolism and the inflammatory pathways of the body. The experimental validation results indicated that HT formula could exhibit anti-inflammatory effects by regulating several signaling pathways specifically the Toll-like receptor signaling pathway, phosphoinositide-3-kinase-Akt signaling pathway, hypoxia-inducible factor 1 signaling pathway, mitogen-activated protein kinase signaling pathway and activator protein 1 signaling pathway.

Keywords: rheumatoid arthritis, network pharmacology, traditional Chinese medicine, Huayu-Qiangshen-Tongbi formula, *in vitro* validation

INTRODUCTION

Rheumatoid arthritis (RA) has been regarded as one of the most common autoimmune inflammatory diseases, and effective treatments for RA require the use of disease-modifying antirheumatic drugs (DMARDs). Although DMARDs have been frequently prescribed in clinic, patients often suffered from unwanted side effects from the treatment, such as the myelosuppression and the injuries of liver and kidney (Obiri et al., 2014). Traditional Chinese medicine (TCM) herbal formula has

gained attention as an alternative remedy practiced for over a thousand years due to their observed efficacy with reduced side effects (Venkatesha et al., 2011; He et al., 2014).

Huayu-Qiangshen-Tongbi (HT) formula, a TCM herbal formula for treating RA, was developed by the Department of Rheumatology and Immunology from the Guangdong Provincial Hospital of Chinese Medicine, and its clinical efficacy was based on more than 20 years of clinical observation and clinical practice. The composition of the formula reflects the academic thoughts regarding the RA treatment by Liang-Chun Zhu, the well-known TCM Master in Rheumatology, and Liang Liu. The formula is composed of these 10 herbs: *Salvia miltiorrhiza* Bge. (Danshen), *Dioscorea nipponica* Makino (Chuanshanlong), *Astragalus mongholicus* Bge. (Huangqi), *Paeonia lactiflora* Pall. (Baishao), *Saussurea involucreata* (Kar. & Kir.) Sch.Bip. (Xuelian), *Eucommia ulmoides* Oliv. (Duzhong), *Drynaria roosii* Nakaike (Gusuibu), *Dipsacus inermis* Wall. (Chuanxuduan), *Rehmannia glutinosa* (Gaertn.) DC. (Dihuang), and *Glycyrrhiza uralensis* Fisch. (Gancao). Lu et al. observed the treatment for a total of 77 patients with RA, and they concluded that a combination of HT formula with methotrexate (MTX) could achieve an equivalent efficacy to that of leflunomide with MTX after 12 weeks of treatment, and the patients went through a combination therapy of using HT formula and MTX experienced less adverse effect than that of the other treatment (Lu et al., 2019). Although the HT formula is commonly used in clinic in China, there is a lack of pharmacological researches to elucidate the mechanisms of action (MOA) on the HT formula treating RA largely due to the complex composition of the formula, limiting further development of the prescription.

In order to overcome the technical barriers for deciphering the MOA for TCM prescriptions, recently, network pharmacological methods were developed by integrating dry and wet lab techniques. In this way, the individual chemical ingredients contained in the herbal formula could be analyzed for their therapeutic effects without jeopardizing the completeness of the treatment (Li and Zhang, 2013). Through systematically studying the information revealed in a network, the network analysis method could provide the prediction results regarding the MOA of the herbal formulae. In addition, the preliminary results from the network analysis could also offer a direction for the following pharmacological verification, facilitating the holistic examinations of the TCM formulae. Inspired by this promising method, various researchers in the field of rheumatology had applied network pharmacological methods to study and explore the anti-RA effects of the TCM formulae. Zhang et al. proposed the potential rationale behind the interactions among the herbs in the Wu Tou Tang decoction (WTD) when treating RA. They predicted the potential MOA of the WTD by analyzing the RA protein-protein interaction (PPI) network and identified the candidate effector molecules of the WTD (Zhang et al., 2013). Li et al. collected and analyzed 871 anti-RA herbal prescriptions from a clinic using an herb-compound-target-disease coherent network, and they proposed the synergistic effects underlying the core herbs of these prescriptions as well as the pharmacological mechanisms underlying these prescriptions combating RA (Li et al., 2015).

By integrating network analysis, *in vivo* as well as *in vitro* experiments, Guo et al. concluded that WTD could act on RA progression by inhibiting inflammatory responses through modulating the C-C chemokine receptor type 5 signaling pathway in macrophages (Guo et al., 2017).

In this study, we aim to explore active compounds and action mechanisms of the HT formula by combining computational predictions based on network pharmacology, chemical analysis, and *in vitro* investigations. As illustrated in **Figure 1**, we collected and analyzed the potential targets of the HT formula for a systematic study of the formula. The obtained targets were compared to the RA-related targets for deducing the potential clinical indications of the HT formula in treating RA. In order to study the RA-related interactions involved by the human body after consuming the HT formula, the PPI data among the potential targets of the HT formula and the RA-related targets were visualized in a network, and the potential MOA was proposed by studying the major hubs of the PPI network. Finally, the *in vitro* experiments were integrated to validate the anti-inflammatory properties of the HT formula. This work may provide a valuable reference to the further quality control, product development, as well as clinical applications of the HT formula.

MATERIAL AND METHODS

Network Pharmacology Analysis of the HT Formula

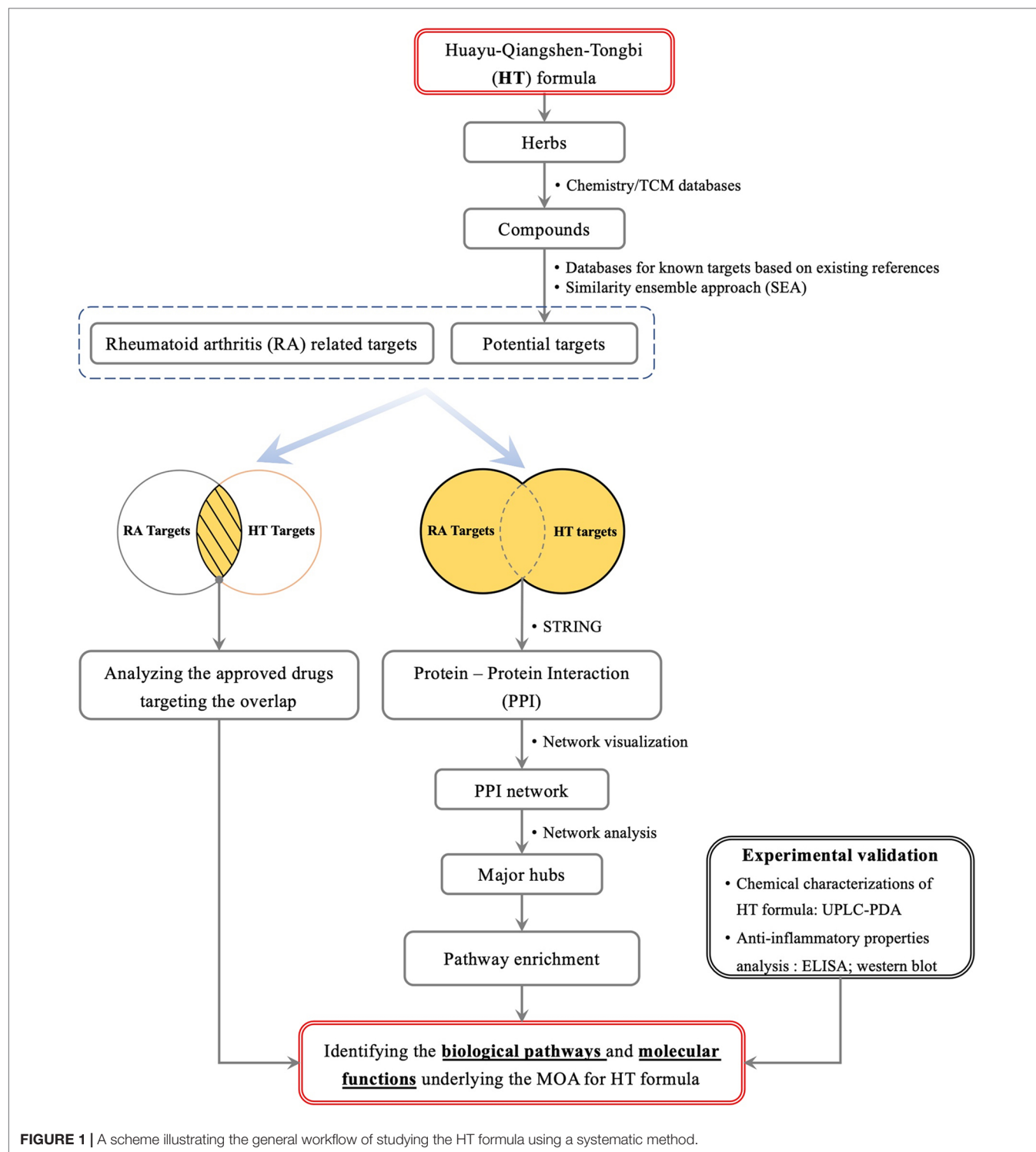
Data Preparation

The chemical information of the herbs contained in the HT formula was manually curated from an integration of three databases, including the Shanghai Institute of Organic Chemistry of Chinese Academy of Sciences, Chemistry Database (last updated on June 17th, 2016) (Shanghai Institute of Organic Chemistry), TCM Database @ Taiwan (last updated on March 25th, 2014) (Chen, 2011), as well as SciFinder database. The existent compound-target interaction (CTI) information for the HT formula was acquired from the current literatures using ChEMBL database (version 23) (Gaulton et al., 2017), and only the human targets were retained for further studying.

The phytochemicals obtained were submitted to the Similarity Ensemble Approach (Keiser et al., 2007) for predicting potential CTIs, and the human targets with high confidence ($T_c \geq 0.57$) were selected from the prediction results as the potential targets of the phytochemicals.

The RA-related targets were collected from DrugBank database (version 5.0) (Wishart et al., 2018), Online Mendelian Inheritance in Man (last updated in May, 2018) (Amberger and Hamosh, 2017), the Genetic Association Database (last updated in August, 2014) (Becker et al., 2004), and Kyoto Encyclopedia of Genes and Genomes (KEGG) pathway database (last updated in May, 2018) (Kanehisa et al., 2017).

The PPI data for the acquired targets were obtained from the STRING database (V10.5) (Szklarczyk et al., 2016). PPIs with medium confidence based on the confident scores defined by the STRING developers were retained for network analysis.



Network Construction and Analysis

The PPIs of the HT targets in addition to the RA-related targets were visualized using Cytoscape (version 3.6.1) (Shannon et al., 2003). A hub in the HT targets–RA targets PPI network was defined as the node having a degree of more than twofold of the median degree of all the nodes (Li et al., 2007). The major hubs in the

PPI network of the hubs were identified for the sake of screening the important hubs, and the major hubs were calculated based on four topological features, that is “Degree,” “Node betweenness,” “Closeness,” and “K-core value” (Zhang et al., 2017).

Pathway enrichment analysis for the major hubs was performed using the data from KEGG in the Database for

Annotation, Visualization and Integrated Discovery (V6.8) (Huang et al., 2008; Huang et al., 2009).

Experimental Investigations of the HT Formula

Herbal Extraction

The herbs were soaked in 600 ml of deionized water (five times water of the total weight of TCM) for 30 min. Then, the mixture was heated to boiling before being decocted for 30 min. The filtrate of the first decoction was collected, while the remaining herbs were treated with another 500 ml of deionized water for the second decoction at the boiling point for 60 min. The filtrate of the second decoction was combined with the filtrate from the first decoction and was centrifuged at 2,500 rpm for 10 min. The supernatant was subsequently concentrated using rotary evaporator, and the concentrate was frozen at -80°C for 24 h before acquiring its lyophilized powder.

Chemical Analysis

Danshensu sodium salt, 3-caffeoylquinic acid, caffeic acid, paeoniflorin, rutin, quercetin, rosmarinic acid, salvigenin, calycosin, and glycyrrhizic acid (the purities of all standards were higher than 98% by high-performance liquid chromatography analysis) were purchased from Chengdu Pufeide Biotech Co., Ltd. (Chengdu, China). Acetonitrile and methanol as high-performance liquid chromatography grade were purchased from RCI Labscan Limited (Thailand). Phosphoric acid as analytical grade was purchased from Sigma Chemicals Ltd. (St. Louis, MO, USA). Milli-Q water was prepared using a Milli-Q system (Millipore, MA, USA).

The quantifications of 10 compounds in the HT extract were performed by a Waters ACQUITY- Ultraperformance Liquid Chromatography (UPLC) Class system (Waters Corp., Milford, USA) coupled with an ACQUITY UPLC HSS T3 column (150 mm \times 2.1 mm, 1.8 μm) maintained at 40°C . Elution was performed with a mobile phase of A (0.2% phosphoric acid in water) and B (0.2% phosphoric acid in acetonitrile) under a gradient program: 0–2 min, 2% B; 2–4 min, 2–8% B; 4–12 min, 8–12% B; 12–14 min, 12–20% B; 14–18 min, 20–25% B; 18–25 min, 25–40% B; 25–30 min, 40–60% B. The flowrate was 0.4 ml/min, and the injection volume was 2 μl . The analytes were monitored at the UV wavelength of 215 nm. Between the two injections, the column was washed with 100% B for 2 min and equilibrated with the initial mobile phase for 5 min.

Anti-Inflammatory Properties

RAW264.7 cells were obtained from the American Type Culture Collection (ATCC; Manassas, VA, USA). Cells were cultured in Dulbecco's modified Eagle medium supplemented with 10% heat-inactivated fetal bovine serum and 1% P/S in an incubator with 95% humidity and 5% CO_2 at 37°C . Cells were subcultured after scraping away from the flask (25 cm^2 ; Thermo Fisher Scientific, MA, USA) when the cells reached 80% confluence. The cells were cotreated with the extracts in 96-well plates at the indicated concentrations for 24 h, and then, the cell viability was detected by 3-(4,5-dimethylthiazol-2-yl)

-2,5-diphenyltetrazolium bromide (MTT) assay. The cells were pretreated with the extracts at the concentrations of 100, 200, and 400 $\mu\text{g/ml}$ in 24-well plates for 1 h before they were stimulated with lipopolysaccharides (LPS, 1 $\mu\text{g/ml}$) for 24 h, and the supernatants were collected to determine NO release using Griess reagent, and the cytokines secretion was determined using ELISA kits (Neobioscience Technology Co., Ltd., Shenzhen, China). In addition, the cells were pretreated with the extracts at the concentrations of 100, 200, 400 $\mu\text{g/ml}$ in six-well plates for 1 h first, and then, they were stimulated with LPS (1 $\mu\text{g/ml}$) for 1 or 12 h, respectively. The total proteins were extracted from the harvested cells using radioimmunoprecipitation assay buffer containing 1 mM phenylmethanesulfonyl fluoride and protease inhibitor cocktail. Relevant proteins from the network analysis were detected by western blotting analysis as previously described (Sang et al., 2018). Immunofluorescence staining was used to detect the expression of inducible nitric oxide synthase (iNOS) and the translocation of nuclear factor kappa B (NF- κB) p65 (Li et al., 2018).

Statistical Analysis

Each experiment was performed in triplicate and was repeated for at least thrice. The Student's *t* test was used to compare the two groups. ANOVA followed by Dunnett's test were used to compare three or more groups. $P < 0.05$ was considered having statistically significant difference.

RESULTS

Computational Predictions

Putative Targets and the Major Hubs of the HT Formula

A total of 800 unique compounds were identified from the 10 herbs of the HT formula. Using the data from ChEMBL (Gaulton et al., 2017), we collected 560 targets for the compounds in the HT formula. The experimentally validated CTI information and the predicted CTIs using the Similarity Ensemble Approach were combined to give a total of 739 unique targets responsible for the compounds contained in the HT formula.

Based on the databases selected, 287 human targets were collected as being related to the pathological mechanism of RA (Table S1), and 35 of them were found to be potentially targeted by the chemical constituents of the HT formula. In order to deduce the possible MOA from clinically prescribed drugs that were sharing the same targets with the HT formula, we compared the targets of the HT formula to the targets of the currently approved drugs recorded in the DrugBank database (Wishart et al., 2018) for RA treatment, and a total of 23 drugs were detected having overlapping targets with the HT formula (Table 1), including four kinds of DMARDs. These approved drugs have been frequently prescribed to RA patients due to their anti-inflammatory and analgesic effects (Wishart et al., 2018), indicating that the HT formula may function through a similar MOA when treating RA.

The interactions among the targets of the HT formula and the RA targets were determined using PPI data. Using the PPI

TABLE 1 | List of the approved disease-modifying antirheumatic drugs (DMARDs) and nonsteroidal anti-inflammatory drugs (NSAIDs) sharing common targets with the Huayu-Qiangshen-Tongbi (HT) formula.

Approved Drugs	DrugBank ID	Shared targets	Type
Ibuprofen	DB01050	25	NSAID
Indomethacin	DB00328	21	NSAID
Diclofenac	DB00586	20	NSAID
Acetylsalicylic acid	DB00945	15	NSAID
Celecoxib	DB00482	10	NSAID
Flurbiprofen	DB00712	10	NSAID
Ketoprofen	DB01009	10	NSAID
Sulindac	DB00605	10	NSAID
Etodolac	DB00749	9	NSAID
Naproxen	DB00788	9	NSAID
Sulfasalazine	DB00795	9	DMARD
Meloxicam	DB00814	7	NSAID
Piroxicam	DB00554	7	NSAID
Diflunisal	DB00861	6	NSAID
Tolmetin	DB00500	6	NSAID
Fenoprofen	DB00573	5	NSAID
Leflunomide	DB01097	4	DMARD
Meclofenamic acid	DB00939	4	NSAID
Nabumetone	DB00461	4	NSAID
Tenoxicam	DB00469	4	NSAID
Azathioprine	DB00993	3	DMARD
Oxaprozin	DB00991	3	NSAID
Hydroxychloroquine	DB01611	2	DMARD

data among the HT and RA targets, a PPI network for the targets of the HT formula and the RA targets was constructed. Since a node could be identified as a hub if its degree was more than twofold of the median degree of all the nodes in a network (Li et al., 2007), 150 hubs were identified in the HT-RA PPI network. To screen out the nodes playing critical roles in the network, we determined the major hubs of the hubs interaction network by calculating four topological indicators, including “Degree,” “Node betweenness,” “Closeness,” and “K-core value” (Zhang et al., 2017). The median values of the four indicators were 42.5, 0.00397, 0.634, and 34, respectively. The hubs showing values higher than the medians of the four indicators were determined as the major hubs of the network. Among the 41 major hubs identified (Table S2), 29 of them were the potential targets of the HT formula.

Potential Pathways Involved and Possible MOA for the HT Formula

The major hubs identified were submitted to the Database for Annotation, Visualization and Integrated Discovery (Huang et al., 2008; Huang et al., 2009) for pathway enrichment analysis based on the data from KEGG pathway database. As shown in Figure 2, the major hubs were mainly associated with the function of bone metabolism and the inflammatory pathways (Table 2).

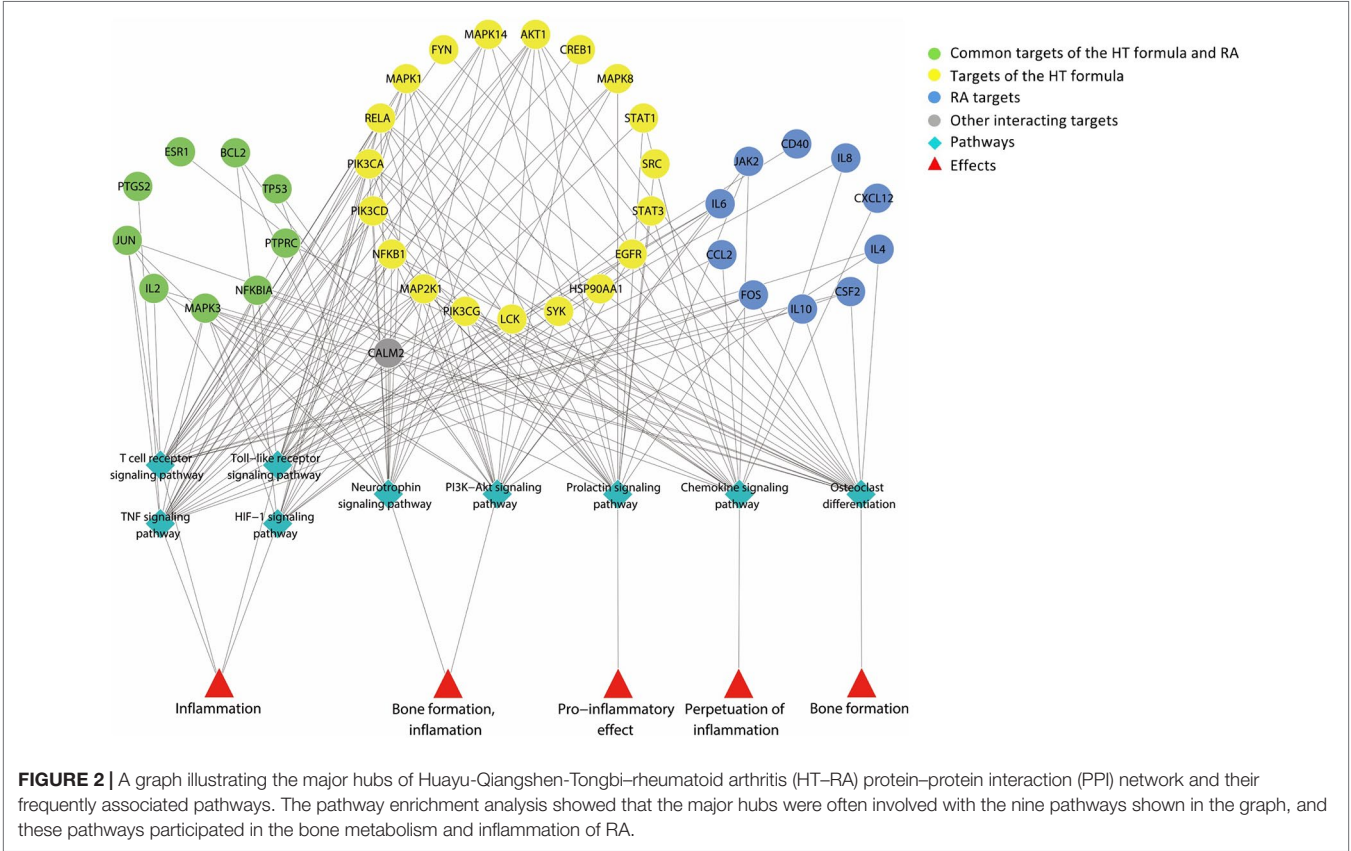


TABLE 2 | The major hubs of the Huayu-Qiangshen-Tongbi-rheumatoid arthritis (HT-RA) protein-protein interaction (PPI) network and their frequently associated pathways.

Term	Nodes	Gene IDs
Osteoclast differentiation	20	LCK, PTPRC, NFKBIA, PIK3CG, MAP2K1, MAPK3, NFKB1, IL2, JUN, IL4, PIK3CD, CSF2, PIK3CA, IL10, RELA, MAPK1, FYN, MAPK14, FOS, AKT1
T cell receptor signaling pathway	20	LCK, PTPRC, NFKBIA, PIK3CG, MAP2K1, MAPK3, NFKB1, IL2, JUN, IL4, PIK3CD, CSF2, PIK3CA, IL10, RELA, MAPK1, FYN, MAPK14, FOS, AKT1
TNF signaling pathway	19	CCL2, NFKBIA, PTGS2, PIK3CG, MAP2K1, MAPK3, NFKB1, IL6, CREB1, JUN, PIK3CD, CSF2, PIK3CA, RELA, MAPK1, MAPK14, FOS, AKT1, MAPK8
Prolactin signaling pathway	17	STAT1, SRC, PIK3CG, MAP2K1, MAPK3, NFKB1, ESR1, PIK3CD, JAK2, PIK3CA, RELA, MAPK1, MAPK14, FOS, AKT1, STAT3, MAPK8
Toll-like receptor signaling pathway	18	STAT1, CD40, NFKBIA, PIK3CG, MAP2K1, MAPK3, NFKB1, IL6, JUN, PIK3CD, PIK3CA, RELA, MAPK1, MAPK14, FOS, IL8, AKT1, MAPK8
HIF-1 signaling pathway	13	PIK3CD, PIK3CA, MAPK1, RELA, PIK3CG, MAPK3, MAP2K1, NFKB1, IL6, EGFR, STAT3, AKT1, BCL2
PI3K-Akt signaling pathway	19	PIK3CG, MAPK3, MAP2K1, NFKB1, IL6, CREB1, TP53, IL2, HSP90AA1, IL4, PIK3CD, JAK2, SYK, PIK3CA, RELA, MAPK1, EGFR, AKT1, BCL2
Chemokine signaling pathway	17	STAT1, SRC, CCL2, NFKBIA, PIK3CG, MAP2K1, MAPK3, NFKB1, CXCL12, PIK3CD, JAK2, PIK3CA, RELA, MAPK1, IL8, AKT1, STAT3
Neurotrophin signaling pathway	16	NFKBIA, PIK3CG, MAPK3, MAP2K1, NFKB1, TP53, JUN, PIK3CD, CALM2, PIK3CA, RELA, MAPK1, MAPK14, AKT1, MAPK8, BCL2

Experimental Investigations

Characterization of the HT Formula

Chemical Constituents

A total of 10 compounds contained in the extract of the HT formula were quantitatively determined using the UPLC-photodiode array (UPLC-PDA) method. As illustrated in **Figure 3**, all of the compounds detected could be chromatographically separated without interferences. Moreover, the contents of the 10 compounds in the HT extract were quantified to be $0.143 \pm 0.001\%$ (danshensu), $0.083 \pm 0.001\%$ (3-caffeoylquinic acid), $0.061 \pm 0.001\%$ (caffeic acid), $0.611 \pm 0.011\%$ (paeoniflorin), $0.232 \pm 0.001\%$ (rutin), $0.202 \pm 0.001\%$ (quercetin), $0.052 \pm 0.001\%$ (rosmarinic acid), $0.104 \pm 0.002\%$ (salvigenin), $0.009 \pm 0.001\%$ (calycosin), and $0.131 \pm 0.004\%$ (glycyrrhizic acid), respectively.

Anti-Inflammatory Properties

Results from MTT assay showed that the HT extract ($\leq 400 \mu\text{g/ml}$) was noncytotoxic to the RAW264.7 macrophages (**Figure 4A**). Under the safety dosages, the HT extract inhibited the interleukin 6 (IL-6) secretion (**Figure 4B**) and the NO

production (**Figure 4C**) in a dose-dependent manner. The HT extract also reduced the excessive expression of iNOS (**Figure 5**). The HT extract blocked the activation of NF- κ B (**Figures 6A, B**). In addition, the HT extract activated the phosphoinositide-3-kinase/AKT signaling pathway and inhibited the expression of hypoxia-inducible factor 1- α (**Figure 6C**). **Figure 6D** shows that the HT extract suppressed the expression of the mitogen-activated protein kinase (MAPK) family proteins including the p-p38 and p-JNK, and the HT extract also inhibited the activation of activator protein 1 (AP-1) through c-Fos and c-Jun.

DISCUSSION

RA is a chronic inflammatory systemic disease mainly affecting the joints, which is characterized by synovial hyperplasia and inflammatory cells infiltration, leading to the tissue destruction and functional disability (Scott and Wolfe F, 2010). RA treatment in TCM has a long history in China, and there have been several herbal formulae created by the famous TCM doctors based on their clinical experiences as well as the TCM theories considered effective, and the HT formula has been regarded as one of such. In this study, we aim to provide a comprehensive analysis of the HT formula integrating computational predictions and *in vitro* experimental methods, contributing to the quality control, product development, as well as the clinical applications of the formula.

According to the results from the pathway enrichment analysis, the major hubs of the HT formula were frequently involved with the chemokine signaling pathway, prolactin signaling pathway, T cell receptor signaling pathway, tumor necrosis factor (TNF) signaling pathway, Toll-like receptor signaling pathway, as well as HIF-1 signaling pathway. These interactions were associated with the pathological mechanisms of RA. Chemokine signaling pathway had been found to be a contributor for chronic inflammation among RA patients (Zhang et al., 2015). Prolactin signaling pathway perplexed with the progression of RA in a way through the incorporation between prolactin and other proinflammatory stimuli to activate macrophages (Tang et al., 2016). T cell receptor signaling pathway had been detected to participate in the initiation and progression of RA (Lundy et al., 2007). TNF signaling pathway was regarded as being related to inflammation, and the inhibitors targeting TNF receptors had been used to treat systemic inflammatory disorders since the 1990s (Scheinecker et al., 2012). Toll-like receptors were key mediators of inflammation in RA, and its signaling pathway was considered linked to the progression of the disease (Monaco et al., 2011). Studies had found out that HIF-1 signaling pathway could interact with Toll-like receptor signaling pathway to induce inflammation in RA (Hu et al., 2014). As deduced from the pathway enrichment results, HT formula mainly regulated the bone metabolism and inflammatory pathways when treating RA, indicating that the formula may play an important role in regulating the bone density among RA patients, as well as the progression of RA. There were 20 major hubs identified as being involved with the osteoclast differentiation. In addition, 19 major hubs considered

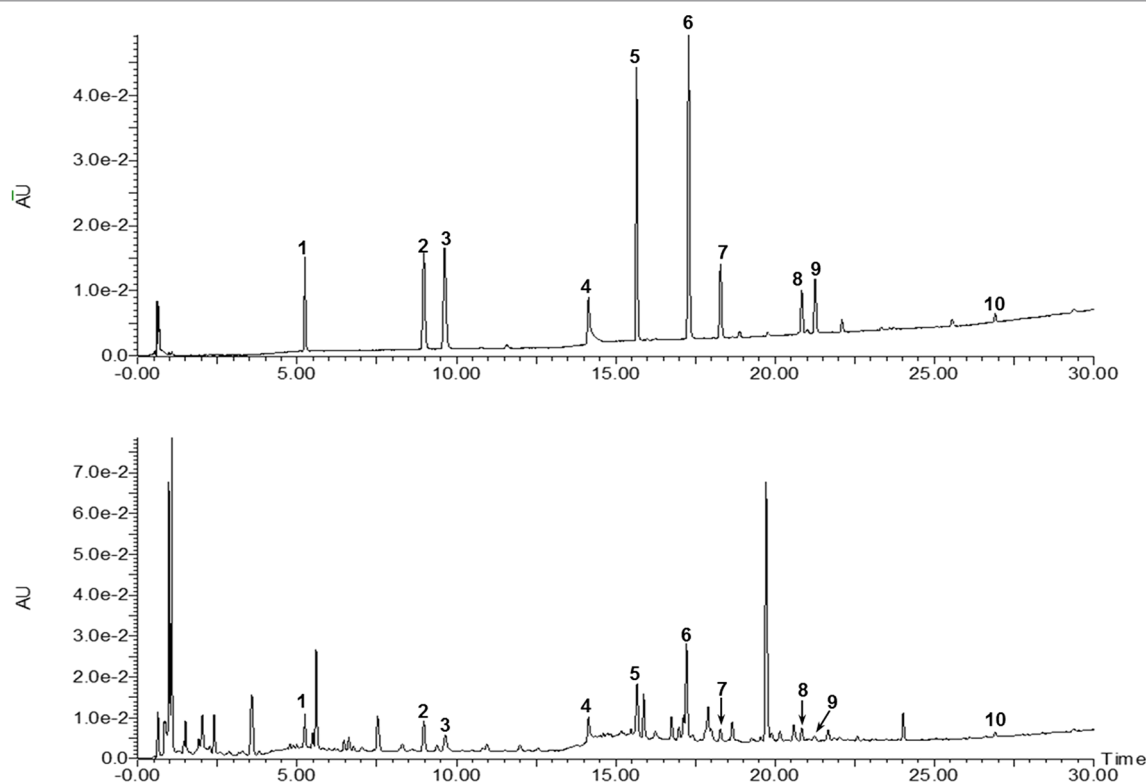


FIGURE 3 | Ultraperformance liquid chromatography-photodiode array (UPLC-PDA) chromatograms of the mixed standards and HT. **1:** Danshensu, **2:** 3-caffeoylquinic acid, **3:** caffeic acid, **4:** paeoniflorin, **5:** rutin, **6:** quercetrin, **7:** rosmarinic acid, **8:** salvigenin, **9:** calycosin, and **10:** glyrrhizic acid.

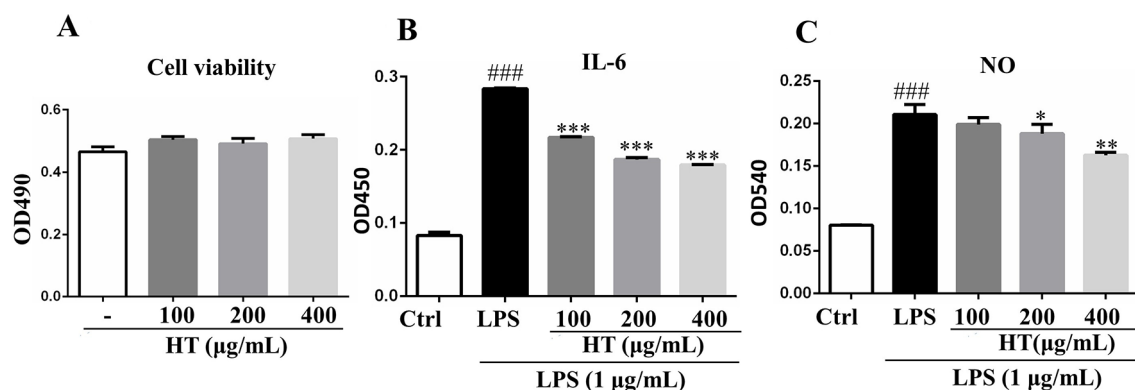
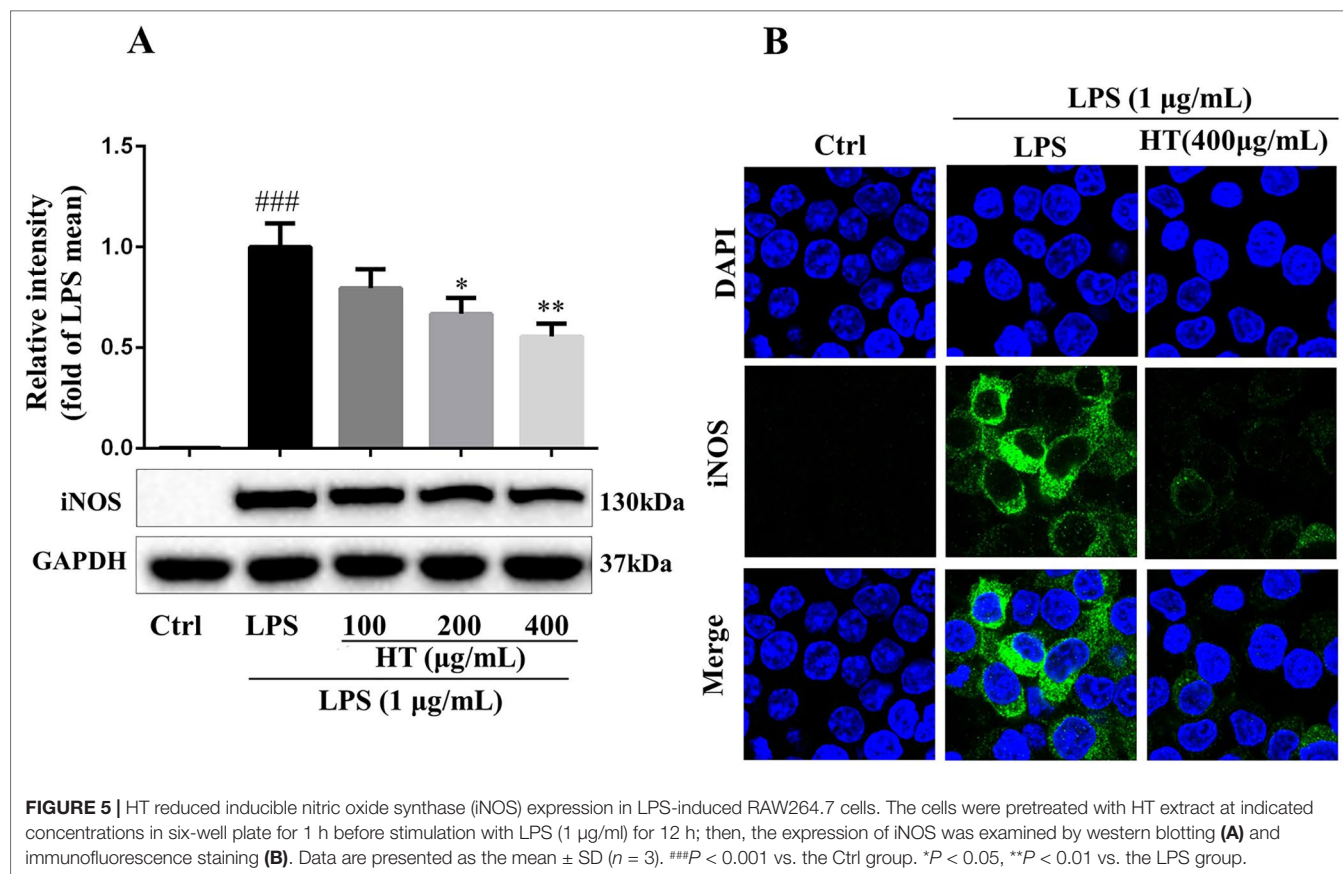


FIGURE 4 | Effects of HT on RAW264.7 cells in the presence or absence of lipopolysaccharide (LPS). The cells were cotreated with the extracts in 96-well plate at indicated concentrations for 24 h; then, the cell viability was detected by 3-(4,5-dimethylthiazol-2-yl)-2,5-diphenyltetrazolium bromide (MTT) assay **(A)**. The cells were pretreated with the extracts at the concentrations of 100, 200, and 400 µg/ml in 24-well plate for 1 h, then stimulated with LPS (1 µg/ml) for 24 h; the supernatants were collected to determine cytokines secretion with ELISA kit **(B)** and NO release with Griess reagent **(C)**. Data are presented as the mean \pm SD ($n = 3$). $###P < 0.001$ vs. the Ctrl group. $*P < 0.05$, $**P < 0.01$, $***P < 0.001$ vs. the LPS group.

belonging to the phosphatidylinositol 3'-kinase (PI3K)-Akt signaling pathway, and the PI3K-Akt signaling pathway had been considered important in regulating the differentiation and the formation of the osteoblasts (Xi et al., 2015). Besides, 16 major hubs were determined as belonging to the neurotrophin

signaling pathway, which had been linked to osteogenesis (Su et al., 2016). Bone erosion had been regarded as one of the main features among patients suffering from chronic RA (Schett and Gravallese, 2012), and the results from the enrichment analysis of the major hubs of the HT formula shed light on its potential



MOA in combating RA by regulating the biological pathways related to bone metabolism.

The computational predictions showed us that the HT formula could ameliorate RA through several signaling pathways by targeting different genes. Thus, we evaluated the results from the prediction with *in vitro* investigations. As illustrated in **Figure 3**, the 11 compounds contained in the HT formula were quantitatively determined using the UPLC-PDA methods, and these data provided us with the guidance for the quality control of the HT formula. As shown in **Figure 4**, the HT extract significantly reduced the secretion of IL-6 and NO under the nontoxic dosages, which indicated that the HT formula would be a potential anti-inflammatory formula in accordance with the prediction results. Furthermore, our experimental results suggested that the HT extract could decrease the LPS-induced excessive expression of the iNOS (**Figure 5**), which has been reported to promote the production of IL-6 and NO during the development of RA (Li et al., 2017; Liu et al., 2018). As well known, iNOS is the downstream signal in the network of inflammatory cascade reaction, and several signaling pathways including the Toll-like receptor signaling pathway (Li et al., 2019), PI3K-Akt signaling pathway (Cao et al., 2019), HIF-1 signaling pathway (Lee et al., 2018), and TNF signaling pathway (Pooladanda et al., 2019) from our prediction results have been reported to regulate

inflammation by mediating the expression of iNOS. To further examine the underlying mechanism of the HT formula in regulating the signaling pathways and potentially ameliorating inflammation, it was first observed that the HT extract could block the activation of NF-κB (**Figures 6A, B**), which was the downstream of TLR4. As **Figure 6C** shows, the HT extract also activated the PI3K/AKT signaling pathway and inhibited the hypoxia-inducible factor 1-α expression. Besides, **Figure 6D** shows that the HT extract suppressed the MAPK family by interfering with p-p38 and p-JNK (**Figure 6D**), which was in accordance with our predication results as shown in **Table 2**. JNK has been reported to mediate the expression of AP-1, which was involved in the progression of RA (Hannemann et al., 2017; Yang et al., 2017; Kim et al., 2018). As is shown in **Figure 6D**, the HT extract could inhibit the activation of AP-1 composed with c-Fos and c-Jun.

In summary, we made a systematic analysis for the HT formula using computational prediction as well as *in vitro* investigational methods. Our experimental results were in good accordance with the results predicted from the network analysis of the HT formula, especially the anti-inflammatory properties of the formula. This study not only evaluated the anti-inflammatory effects of the HT formula when treating RA but also proposed the potentiality of the HT formula on regulating the bone metabolism in the body, which deserves future examination.

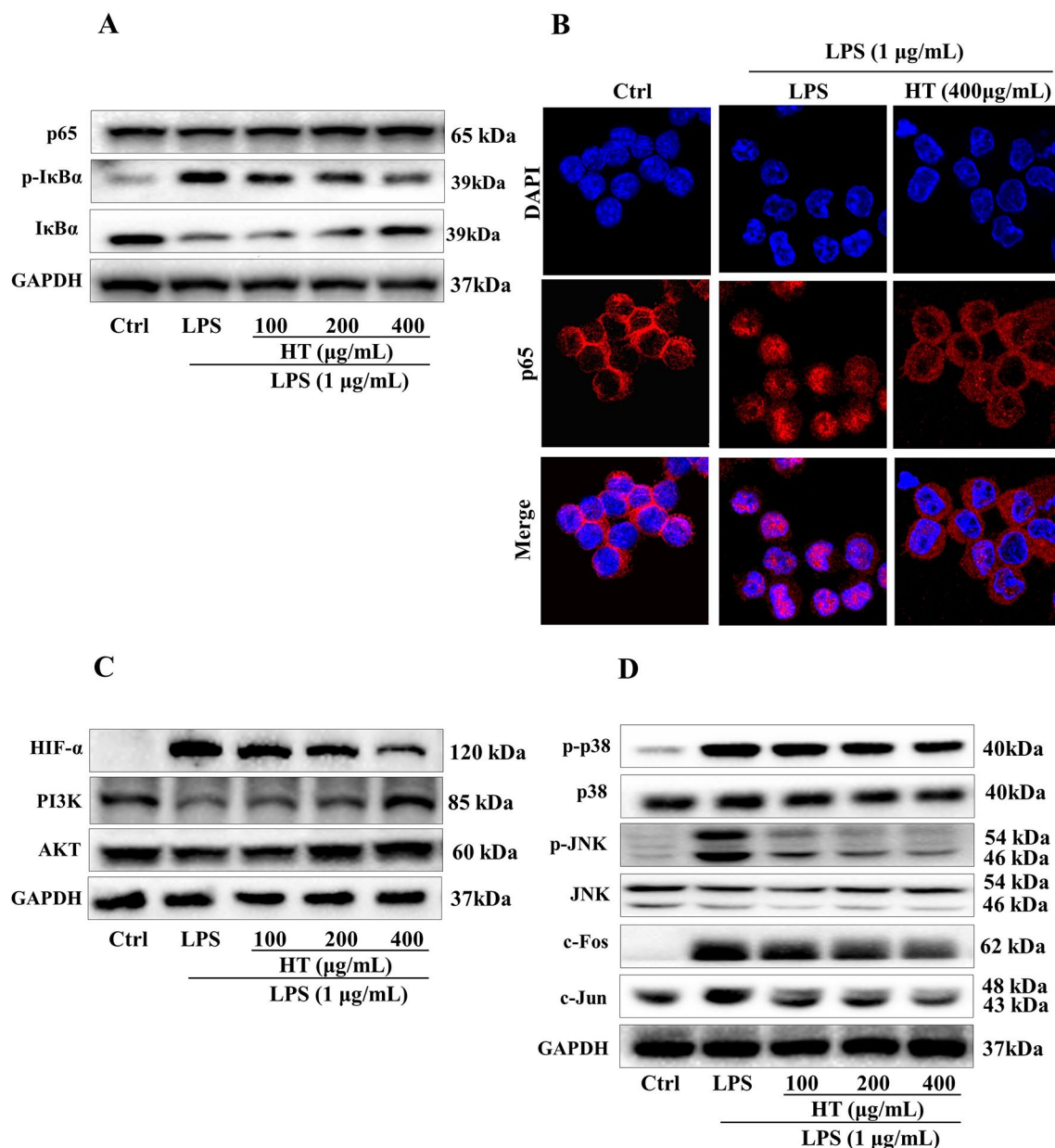


FIGURE 6 | Effects of the HT extract on the relevant proteins in the LPS-induced RAW264.7 cells. Cells were pre-treated with the extract at the concentrations of 100, 200, 400 μg/mL in the 6-well plates for 1 h prior to the stimulation with LPS (1 μg/mL) for 12 h or 1 h, and the relevant proteins deduced from the computational predictions were analyzed by western blotting (**A**, **C** and **D**) and immunofluorescence staining (**B**) subsequently.

DATA AVAILABILITY

All datasets generated for this study are included in the manuscript and the **Supplementary Files**.

AUTHOR CONTRIBUTIONS

ZW and K-GL designed and conducted the study with equal contribution. YH, GC, and HuY supervised the study. R-YH, HaY, S-HX, JL, and HZ provided the technical support and

advice for the study. All authors contributed to the review and the approval of the final manuscript.

FUNDING

We appreciate the financial support received from the National Natural Science Foundation of China (NSFC, No. 81470170), Macau Science and Technology Development Fund (013/2015/A1), University of Macau (MYRG2016-00144-ICMS-QRCM, MYRG2017-00178-ICMS, MYRG2018-00043-ICMS),

Guangdong-Macao Traditional Chinese Medicine Technology Industrial Park (D-Pro-0274-2017), Natural Science Foundation of China (No.81774218), Guangdong Provincial Hospital of Chinese Medicine (No. YN2018ML08, YN2018ZD06), the Science and Technology Project of Guangdong Province (No. 2016A020226041), the 1010 Project of Guangdong Provincial Hospital of Chinese Medicine (No. YN10101906), Guangzhou Municipal Science and Technology Innovation Committee (No.

201710010076), and Science and Technology Planning Project of Guangdong Province (No. 2017B030314166) for this research.

SUPPLEMENTARY MATERIAL

The Supplementary Material for this article can be found online at: <https://www.frontiersin.org/articles/10.3389/fphar.2019.01065/full#supplementary-material>

REFERENCES

- Amberger, J. S., and Hamosh, A. (2017). Searching Online Mendelian Inheritance in Man (OMIM): a knowledgebase of human genes and genetic phenotypes. *Curr. Protoc. Bioinforma.* 58, 1.2.1–1.2.12. doi: 10.1002/cpbi.27
- Becker, K. G., Barnes, K. C., Bright, T. J., and Wang, S. A. (2004). The genetic association database. *Nat. Genet.* 36, 431. doi: 10.1038/ng0504-431
- Cao, Y., Li, F., Luo, Y., Zhang, L., Lu, S., Xing, R., et al. (2019). 20-Hydroxy-3-oxolupan-28-oic acid attenuates inflammatory responses by regulating PI3K-Akt and MAPKs signaling pathways in LPS-stimulated RAW264.7 macrophages. *Mol.* 24, 386. doi: 10.3390/molecules24030386
- Chen, C. Y.-C. (2011). TCM Database@Taiwan: the world's largest traditional Chinese medicine database for drug screening in silico. *PLoS One* 6, e15939–e15939. doi: 10.1371/journal.pone.0015939
- Gaulton, A., Hersey, A., Nowotka, M., Bento, A. P., Chambers, J., Mendez, D., et al. (2017). The ChEMBL database in 2017. *Nucleic Acids Res.* 45, D945–D954. doi: 10.1093/nar/gkw1074
- Guo, Q., Zheng, K., Fan, D., Zhao, Y., Li, L., Bian, Y., et al. (2017). Wu-Tou decoction in rheumatoid arthritis: integrating network pharmacology and in vivo pharmacological evaluation. *Front. Pharmacol.* 8, 230. doi: 10.3389/fphar.2017.00230
- Hannemann, N., Jordan, J., Paul, S., Reid, S., Baenkler, H.-W., Sonnewald, S., et al. (2017). The AP-1 transcription factor c-Jun promotes arthritis by regulating cyclooxygenase-2 and arginase-1 expression in macrophages. *J. Immunol.* 198, 3605 LP–3614. doi: 10.4049/jimmunol.1601330
- He, Y., Ou, A., Yang, X., Chen, W., Fu, L., Lu, A., et al. (2014). Traditional Chinese medicine versus western medicine as used in China in the management of rheumatoid arthritis: a randomized, single-blind, 24-week study. *Rheumatol. Int.* 34, 1647–1655. doi: 10.1007/s00296-014-3010-6
- Hu, F., Mu, R., Zhu, J., Shi, L., Li, Y., Liu, X., et al. (2014). Hypoxia and hypoxia-inducible factor-1 α provoke toll-like receptor signalling-induced inflammation in rheumatoid arthritis. *Ann. Rheum. Dis.* 73, 928 LP–928936. doi: 10.1136/annrheumdis-2012-202444
- Huang, D. W., Sherman, B. T., and Lempicki, R. A. (2008). Systematic and integrative analysis of large gene lists using DAVID bioinformatics resources. *Nat. Protoc.* 4, 44. doi: 10.1038/nprot.2008.211
- Huang, D. W., Sherman, B. T., and Lempicki, R. A. (2009). Bioinformatics enrichment tools: paths toward the comprehensive functional analysis of large gene lists. *Nucleic Acids Res.* 37, 1–13. doi: 10.1093/nar/gkn923
- Kanehisa, M., Furumichi, M., Tanabe, M., Sato, Y., and Morishima, K. (2017). KEGG: new perspectives on genomes, pathways, diseases and drugs. *Nucleic Acids Res.* 45, D353–D361. doi: 10.1093/nar/gkw1092
- Keiser, M. J., Roth, B. L., Armbruster, B. N., Ernsberger, P., Irwin, J. J., and Shoichet, B. K. (2007). Relating protein pharmacology by ligand chemistry. *Nat. Biotechnol.* 25, 197. doi: 10.1038/nbt1284
- Kim, S.-J., Song, Y.-S., Pham, T.-H., Bak, Y., Lee, H., Hong, J.-T. et al., (2018). (E)-2-Methoxy-4-(3-(4-methoxyphenyl) prop-1-en-1-yl) phenol attenuates PMA-induced inflammatory responses in human monocytic cells through PKC δ /JNK/AP-1 pathways. *Eur. J. Pharmacol.* 825, 19–27. doi: 10.1016/j.ejphar.2018.01.024
- Lee, M., Wang, C., Jin, S., Labrecque, M., Beischlag, T., Brockman, M. et al., (2018). Expression of human inducible nitric oxide synthase in response to cytokines is regulated by hypoxia-inducible factor-1. *Free Radic. Biol. Med.* 130, 278–287. doi: 10.1016/j.freeradbiomed.2018.10.441
- Li, D., Liu, Q., Sun, W., Chen, X., Wang, Y., Sun, Y., et al. (2018). 1,3,6,7-Tetrahydroxy-8-prenylxanthone ameliorates inflammatory responses resulting from the paracrine interaction of adipocytes and macrophages. *Br. J. Pharmacol.* 175, 1590–1606. doi: 10.1111/bph.14162
- Li, Q., Ye T., Long, T., and Peng, X. (2019). Ginkgetin exerts anti-inflammatory effects on cerebral ischemia/reperfusion-induced injury in a rat model via the TLR4/NF- κ B signaling pathway. *AU - Li, Qin. Biosci. Biotechnol. Biochem.* 83, 1–9. doi: 10.1080/09168451.2018.1553608
- Li, S., and Zhang, B. (2013). c. *Chin. J. Nat. Med.* 11, 110–120. doi: 10.1016/S1875-5364(13)60037-0
- Li, S., Zhang, Z. Q., Wu, L. J., Zhang, X. G., Li, Y. D., and Wang, Y. Y. (2007). Understanding ZHENG in traditional Chinese medicine in the context of neuroendocrine-immune network. *IET Syst. Biol.* 1, 51–60. doi: 10.1049/iet-syb:20060032
- Li, X., Jiang, C., and Zhu, W. (2017). Crocin reduces the inflammation response in rheumatoid arthritis AU- Li, Xiang. *Biosci. Biotechnol. Biochem.* 81, 891–898. doi: 10.1080/09168451.2016.1263145
- Li, Y., Li, R., Ouyang, Z., and Li, S. (2015). Herb network analysis for a famous TCM doctor's prescriptions on treatment of rheumatoid arthritis. *Evid. Based. Complement. Alternat. Med.* 2015, 451319. doi: 10.1155/2015/451319
- Liu, H., Wei, S.-P., Zhi, L.-Q., Liu, L.-P., Cao, T.-P., Wang, S.-Z., et al. (2018). Synovial GATA1 mediates rheumatoid arthritis progression via transcriptional activation of NOS2 signaling. *Microbiol. Immunol.* 62, 594–606. doi: 10.1111/1348-0421.12637
- Lu, Y., Chen, X., Huang, R., Zhao, Y., Wu, J., Chen, X., et al. (2019). Huayu Qiangshen Tongbi recipe combined with methotrexate for treatment of patients with rheumatoid arthritis: a retrospective study. *Zhongguo Zhong Xi Yi Jie He Za Zhi* 39, 547–552. [Article in Chinese]. doi: 10.7661/j.cjmm.20190329.110
- Lundy, S. K., Sarkar, S., Tesmer, L. A., and Fox, D. A. (2007). Cells of the synovium in rheumatoid arthritis. T lymphocytes. *Arthritis Res. Ther.* 9, 202. doi: 10.1186/ar2107
- Monaco, C., Terrando, N., and Midwood, K. S. (2011). Toll-like receptor signaling: Common pathways that drive cardiovascular disease and rheumatoid arthritis. *Arthritis Care Res. (Hoboken)* 63, 500–511. doi: 10.1002/acr.20382
- Obiri, D. D., Osafo, N., Ayande, P. G., and Antwi, A. O. (2014). Xylopia aethiopica (Annonaceae) fruit extract suppresses Freund's adjuvant-induced arthritis in Sprague-Dawley rats. *J. Ethnopharmacol.* 152, 522–531. doi: 10.1016/j.jep.2014.01.035
- Pooladanda, V., Thatikonda, S., Bale, S., Pattnaik, B., Sigalapati, D. K., Bathini, N. B., et al. (2019). Nimbolide protects against endotoxin-induced acute respiratory distress syndrome by inhibiting TNF- α mediated NF- κ B and HDAC-3 nuclear translocation. *Cell Death Dis.* 10, 81. doi: 10.1038/s41419-018-1247-9
- Sang, W., Zhong, Z., Linghu, K., Xiong, W., Tse, A. K. W., Cheang, W. S., et al. (2018). Siegesbeckia pubescens Makino inhibits Pam(3)CSK(4)-induced inflammation in RAW 264.7 macrophages through suppressing TLR1/TLR2-mediated NF- κ B activation. *Chin. Med.* 13, 37. doi: 10.1186/s13020-018-0193-x
- Scheinecker, C., Smolen, J. S., Redlich, K., and Blüml, S. (2012). Targeting TNF receptors in rheumatoid arthritis. *Int. Immunol.* 24, 275–281. doi: 10.1093/intimm/dxs047
- Schett, G., and Gravallese, E. (2012). Bone erosion in rheumatoid arthritis: mechanisms, diagnosis and treatment. *Nat. Rev. Rheumatol.* 8, 656. doi: 10.1038/nrrheum.2012.153
- Scott, D. L., and Wolfe F. H. T. (2010). Rheumatoid arthritis. *Lancet* 376, 1094–1108. doi: 10.1016/S0140-6736(10)60826-4
- Shanghai Institute of Organic Chemistry, C. A. @ of S. S. I. @ of O. C. @ of C. C. D. www.organchem.csdb.c. Shanghai Institute of Organic Chemistry, Chinese Academy of Sciences. Shanghai Institute of Organic Chemistry of CAS. Chemistry Database[DB/OL]. www.organchem.csdb.cn.

- Shannon, P., Markiel, A., Ozier, O., Baliga, N. S., Wang, J. T., Ramage, D., et al. (2003). Cytoscape: a software environment for integrated models of biomolecular interaction networks. *Genome Res.* 13, 2498–2504. doi: 10.1101/gr.1239303
- Su, Y.-W., Chung, R., Ruan, C.-S., Chim, S. M., Kuek, V., Dwivedi, P. P., et al. (2016). Neurotrophin-3 induces BMP-2 and VEGF activities and promotes the bony repair of injured growth plate cartilage and bone in rats. *J. Bone Miner. Res.* 31, 1258–1274. doi: 10.1002/jbmr.2786
- Szklarczyk, D., Morris, J., Cook, H., Kuhn, M., Wyder, S., Simonovic, M. et al., (2016). The STRING database in 2017: quality-controlled protein-protein association networks, made broadly accessible. *Nucleic Acids Res.* 45 (D1), D362–D368 doi: 10.1093/nar/gkw937
- Tang, M. W., Reedquist, K. A., Garcia, S., Fernandez, B. M., Codullo, V., Vieira-Sousa, E., et al. (2016). The prolactin receptor is expressed in rheumatoid arthritis and psoriatic arthritis synovial tissue and contributes to macrophage activation. *Rheumatology (Oxford)*. 55, 2248–2259. doi: 10.1093/rheumatology/kew316
- Venkatesha, S. H., Berman, B. M., and Moudgil, K. D. (2011). Herbal medicinal products target defined biochemical and molecular mediators of inflammatory autoimmune arthritis. *Bioorg. Med. Chem.* 19, 21–29. doi: 10.1016/j.bmc.2010.10.053
- Wishart, D. S., Feunang, Y. D., Guo, A. C., Lo, E. J., Marcu, A., Grant, J. R., et al. (2018). DrugBank 5.0: a major update to the DrugBank database for 2018. *Nucleic Acids Res.* 46, D1074–D1082. doi: 10.1093/nar/gkx1037
- Xi, J. C., Zang, H.-Y., Guo, L.-X., Xue, H.-B., Liu, X.-D., Bai, Y.-B., and Ma, Y.-Z. (2015). The PI3K/AKT cell signaling pathway is involved in regulation of osteoporosis. *AU - Xi, Jian-Cheng. J. Recept. Signal Transduct.* 35, 640–645. doi: 10.3109/10799893.2015.1041647
- Yang, C.-M., Chen, Y.-W., Chi, P.-L., Lin, C.-C., and Hsiao, L.-D. (2017). Resveratrol inhibits BK-induced COX-2 transcription by suppressing acetylation of AP-1 and NF- κ B in human rheumatoid arthritis synovial fibroblasts. *Biochem. Pharmacol.* 132, 77–91. doi: 10.1016/j.bcp.2017.03.003
- Zhang, L., Yu, M., Deng, J., Lv, X., Liu, J., Xiao, Y., et al. (2015). Chemokine signaling pathway involved in CC12 expression in patients with rheumatoid arthritis. *Yonsie Med. J.* 56, 1134–1142. doi: 10.3349/ymj2015.1134
- Zhang, Y., Guo, Q., Li, Q., Ren, W., Tang, S., Wang, S., et al. (2017). Main active constituent identification in Guanxinjing capsule, a traditional Chinese medicine, for the treatment of coronary heart disease complicated with depression. *Acta Pharmacol. Sin.* 39, 975. doi: 10.1038/aps.2017.117
- Zhang, Y., Wang, D., Tan, S., Xu, H., Liu, C., and Lin, N. (2013). A systems biology-based investigation into the pharmacological mechanisms of wu tou tang acting on rheumatoid arthritis by integrating network analysis. *Evid. Based. Complement. Alternat. Med.* 2013, 548498. doi: 10.1155/2013/548498

Conflict of Interest Statement: The authors declare that the research was conducted in the absence of any commercial or financial relationships that could be construed as a potential conflict of interest.

Copyright © 2019 Wang, Linghu, Hu, Zuo, Yi, Xiong, Lu, Chan, Yu and Huang. This is an open-access article distributed under the terms of the Creative Commons Attribution License (CC BY). The use, distribution or reproduction in other forums is permitted, provided the original author(s) and the copyright owner(s) are credited and that the original publication in this journal is cited, in accordance with accepted academic practice. No use, distribution or reproduction is permitted which does not comply with these terms.



Application and Mechanisms of Triptolide in the Treatment of Inflammatory Diseases—A Review

Kai Yuan^{1†}, Xiaohong Li^{1†}, Qingyi Lu¹, Qingqing Zhu¹, Haixu Jiang¹, Ting Wang^{2*}, Guangrui Huang^{1*} and Anlong Xu^{1,3*}

¹ School of Life Sciences, Beijing University of Chinese Medicine, Beijing, China, ² Beijing Research Institute of Chinese Medicine, Beijing University of Chinese Medicine, Beijing, China, ³ State Key Laboratory of Biocatalysis, Department of Biochemistry, School of Life Sciences, Sun Yat-Sen (Zhongshan) University, Guangzhou, China

OPEN ACCESS

Edited by:

Xiaojuan He,
China Academy of Chinese Medical
Sciences, China

Reviewed by:

Zhenzhou Jiang,
Jiangsu Key Laboratory of Drug
Screening and Jiangsu Center for
Pharmacodynamics Research
and Evaluation, China
Johanna Mahwahwate Bapela,
University of Pretoria,
South Africa

*Correspondence:

Ting Wang
wangting1973@sina.com
Guangrui Huang
hgr@bucm.edu.cn
Anlong Xu
xuanlong@bucm.edu.cn

[†]These authors have contributed
equally to this work

Specialty section:

This article was submitted to
Ethnopharmacology,
a section of the journal
Frontiers in Pharmacology

Received: 27 July 2019

Accepted: 13 November 2019

Published: 06 December 2019

Citation:

Yuan K, Li X, Lu Q, Zhu Q, Jiang H,
Wang T, Huang G and Xu A (2019)
Application and Mechanisms
of Triptolide in the Treatment of
Inflammatory Diseases—A Review.
Front. Pharmacol. 10:1469.
doi: 10.3389/fphar.2019.01469

Bioactive compounds from medicinal plants with anti-inflammatory and immunosuppressive effects have been emerging as important sources of drugs for the treatment of inflammatory disorders. Triptolide, a diterpene triepoxide, is a pharmacologically active compound isolated from *Tripterygium wilfordii* Hook F (TwHF) that is used as a remedy for inflammatory and autoimmune diseases. As the most promising bioactive compound obtained from TwHF, triptolide has attracted considerable interest recently, especially for its potent anti-inflammatory and immunosuppressive activities. Over the past few years, an increasing number of studies have been published emphasizing the value of triptolide in the treatment of diverse inflammatory disorders. Here, we systematically review the mechanism of action and the therapeutic properties of triptolide in various inflammatory diseases according to different systematic organs, including lupus nephritis, inflammatory bowel disease, asthma, and rheumatoid arthritis with pubmed and Embase. Based on this review, potential research strategies might contribute to the clinical application of triptolide in the future.

Keywords: triptolide, inflammatory disorders, anti-inflammation, immunosuppression, pubmed, Embase

INTRODUCTION

Complementary and alternative medications, including traditional Chinese medicines (TCMs), have long been used to treat inflammatory disorders, and they are generally well tolerated by patients (Goldrosen and Straus, 2004). The use of TCMs has necessitated urgent research into the mechanisms of action of natural products. One TCM, *Tripterygium wilfordii* Hook F (TwHF), has been used in folk medicine for the treatment of a variety of inflammatory disorders for many centuries (Tao et al., 1991; Goldbach-Mansky et al., 2009; Lv et al., 2015). TwHF belongs to Celastraceae family and *Tripterygium* genus. It has been collected in Southern China and its roots have been used in various preparations to “relieve stasis and internal warmth,” among many other conditions diagnosed by TCM practitioners. TwHF was used to deal with rheumatoid arthritis and psoriasis in ancient China. In addition, TwHF was also used as a method of birth control in men. Previous studies demonstrated TwHF exhibited multiple pharmacological activities including antitumor, immune modulation, anti-inflammatory, and antifertility effects. Especially in RA, TwHF was found to have anti-inflammatory and cartilage protective effects (Zhou et al., 2018). However, TwHF might have significant side effects and severe toxicity, which limits the clinical application.

Triptolide is a major bioactive compound derived from *T. wilfordii* Hook F (Kupchan et al., 1972). It is a diterpene triepoxide containing three epoxy groups, a C-14-hydroxyl group and a lactone ring (Figure 1).

With pubmed and Embase, we systematically review the therapeutic properties of triptolide in inflammatory diseases according to different systematic organs and illustrate its potential clinical applications.

POTENTIAL EFFECTS OF TRIPTOLIDE ON INFLAMMATORY DISEASES

The therapeutic potential of triptolide has been tested in various inflammatory and autoimmune disorder models, including nephritis, asthma, arthritis, and neurodegenerative disorders, and triptolide has been found to modulate a wide variety of inflammatory mediators. These disorders and their inflammatory mediators will be discussed in brief below.

Renal Diseases

Membranous Nephropathy

Membranous nephropathy (MN) is one of the major causes of nephrotic syndrome in adults and is characterized by subepithelial deposition of immune complexes (Cattran and Brenchley, 2017). Globally, the overall incidence of membranous nephropathy (MN) is estimated as 1/100,000. Immune-mediated podocyte injury is considered to underlie the proteinuria in MN. Asymptomatic proteinuria and generalized edema are clinical presentations of MN. Researchers found that triptolide could reduce podocyte injuries in MN to reduce proteinuria and alleviate inflammatory response in animal model of MN.

Chen et al. (2010) demonstrated that 200 $\mu\text{g/kg/day}$ triptolide could effectively reduce proteinuria and inhibit

immune-mediated injuries in an experimental rat model of MN. The recovery of podocyte injuries was promoted after triptolide treatment, accompanied by a reduction in glomerular complement component 5b-9 (C5b-9) deposits. In addition, Triptolide also suppressed reactive oxygen species (ROS) generation and p38 mitogen-activated protein kinase (MAPK) activation in the podocytes induced by C5b-9.

Later, Zhou et al. (2016) showed that 200 $\mu\text{g/kg/day}$ triptolide attenuated the inflammatory response in MN rats *via* suppression of the nuclear factor-kappa B (NF- κB) signaling pathway. Interestingly, they also found that triptolide treatment could significantly decrease malondialdehyde (MDA) levels while enhancing superoxide dismutase (SOD) activity in the serum to reduce oxidative stress and inflammatory responses.

More recently, Chen et al. (2017) revealed that 100 and 200 $\mu\text{g/kg/day}$ triptolide reduces podocyte injury by inhibiting podocyte apoptosis in an experimental rat model of MN. Cleaved caspase-3 and cleaved poly ADP-ribose polymerase (PARP) were markedly decreased after triptolide treatment. Triptolide inhibited C5b-9-induced MAPK activation in podocytes by decreasing p-JNK and p-ERK expression.

So, triptolide could alleviate membranous nephropathy by inhibiting inflammatory signaling pathways including NF- κB and MAPK pathways. Oxidative stress and apoptosis were also involved in the mechanism of triptolide against MN. However, the researchers have not investigated the triptolide cytotoxicity in the organ of animal model of MN. Only Chen et al. (2017) studied aminotransferase in the serum.

Lupus Nephritis

Lupus nephritis is inflammation of the kidney caused by systemic lupus erythematosus and is characterized by increased production of cytokines and autoantibodies, deposition of immune complexes, and infiltration of leukocytes (Lech and Anders, 2013). Lupus nephritis (LN) influences almost 40% of patients with systemic lupus erythematosus (SLE).

Tao et al. (2008) discovered that triptolide with 15 weeks administration could increase the survival rate, reduce disease severity and decrease cytokine production in mice with lupus nephritis (LN). They indicated that the survival rate of mice was significantly higher in the triptolide group (87.5%) than in the vehicle group (35.7%). Triptolide could decrease proteinuria and blood urea nitrogen levels were significantly reduced in the triptolide-treated mice compared with the control mice throughout the treatment period. Histopathologic analysis showed that triptolide-treated mice had less severe kidney disease, with significantly diminished glomerular and interstitial disease. In this study, the NZB/NZWf1 mice were used as the animal model of LN. There are some shortcomings of NZB/NZWf1 mice. These mice do not possess some clinical manifestations of lupus such as arthritis and rash. Another drawback of this strain is the long disease incubation time almost 6 months which is the long disease incubation time.

Kidney Transplantation

Due to allograft rejection, the fate of long-term grafts has not changed significantly over the past decades. Allograft rejection,

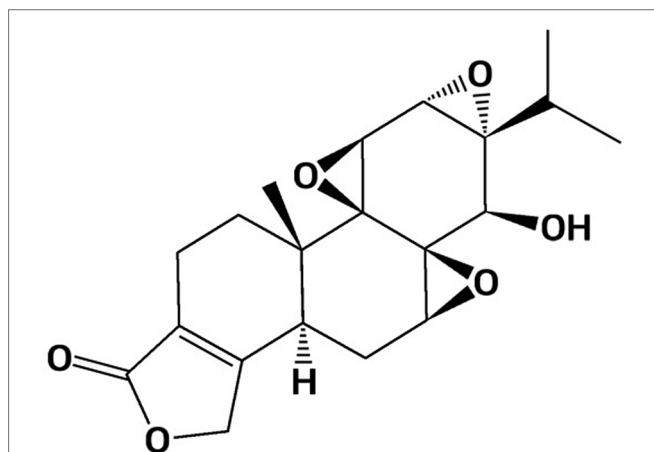


FIGURE 1 | Chemical structure of triptolide. Triptolide has been shown to possess a broad spectrum of anti-inflammatory and immunosuppressive properties in treating various inflammatory disorder models. Based on potent anti-inflammatory biological activities, triptolide has increasingly drawn attention worldwide in recent decades.

characterized by the activation of various inflammatory cells, cytokines, chemokines, and adhesion molecules, is one of the leading causes of graft loss in clinical transplantation (Ingulli, 2010). Triptolide could prolong the survival of kidney transplantation by inhibiting inflammatory activities.

In 2009, an experimental study demonstrated that triptolide with 250 and 500 µg/kg/day treatment effectively prolongs allograft survival (Zhang et al., 2009). Brown Norway rat kidneys were transplanted into Lewis recipients to generate allograft groups, and graft recipients were treated with 0.25 and 0.5 mg/kg/day triptolide for 14 days. The average median survival time (MST) was 18 and 19.8 days in the 0.25 and 0.5 mg/kg/day triptolide treatment groups, respectively. There had some flaws in this study. The researchers have not evaluated the cytotoxicity of triptolide in the healthy organs of kidney transplantation animal model.

Later, Zhang et al. (2013) demonstrated that complex phenotypic and allostimulatory functional changes induced in rat bone marrow-derived dendritic cells (DCs) by 1–10 nM triptolide may account for the prolonged allograft survival. They also found that triptolide-conditioned DCs could induce allospecific T-cell regulation and prolong renal graft survival.

Crews et al. (2005) demonstrated that downregulation of vascular cell adhesion molecule 1 (VCAM-1) and transforming growth factor beta (TGF-β) are associated with successful 500 µg/kg/day triptolide with 10 days treatment of chronic allograft rejection in rats. The gene expression levels of VCAM-1 and TGF-β exhibited significant associations with the CADI scores of the experimental groups.

Importantly, Hong et al. (2002) showed triptolide is a potent suppressant of C3, CD40 and B7h expression in activated human proximal tubular epithelial cells (PTECs). Triptolide exerts inhibitory effects on C3, CD40, and B7h expression in TNF-α-stimulated PTECs.

Therefore, triptolide might have a beneficial effect on kidney transplantation by inhibiting inflammatory molecules such as VCAM-1, TGF-β, C3, and CD40.

Renal Fibrosis

Renal fibrosis is associated with a decline in renal excretory function, and unresolved inflammation promotes progressive renal fibrosis, which can culminate in end-stage renal disease (Zhou et al., 2016). It has been found that 0.6 mg/kg per day triptolide attenuates renal interstitial fibrosis by decreasing α-SMA and TGF-β1 expression and interstitial collagen deposition in the kidney (Yuan et al., 2011). Triptolide could also inhibit macrophage and myofibroblast infiltration.

Gastrointestinal Disease Inflammatory Bowel Disease

Inflammatory bowel disease (IBD) includes ulcerative colitis and Crohn's disease (CD) and is characterized by chronic inflammation of the gastrointestinal tract (Abraham and Cho, 2009). An estimated 1.6 million Americans are affected by IBD, and approximately 2.5–3 million people in Europe currently have IBD. Previous studies found that triptolide could deal with IBD in mouse model and patients.

Two kinds of inflammatory bowel disease animal models including dextran sulfate sodium (DSS) induced colitis mice and interleukin-10 gene-deficient (IL-10^{-/-}) mice were adopted in these studies. 0.07 mg/kg/day Triptolide with 8 weeks treatment alleviated diarrhea, edema, hyperemia, and inflammatory cells infiltration in the animal models (Wei et al., 2008). In addition, researchers also investigated the mechanism of triptolide in the treatment of IBD. Li et al. (2010) found that triptolide ameliorates colitis by suppressing the IL-6/signal transducer and activator of transcription 3 (STAT3) signaling pathway and downregulating IL-17. Zhang et al. (2014) found that 0.6 mg/kg/day triptolide administration ameliorates intestinal injury by inhibiting the expression of secondary lymphoid tissue chemokine chemokine (C-C motif) ligand 21 (CCL21), which has chemotactic effects on T cells, B cells, NK cells, and DCs. However, they only investigated the expression of CCL21, which is not sufficient to demonstrate triptolide influence the chemotactic effects of T cells, B cells, NK cells, and DCs.

Inflammatory bowel disease is associated with an increased risk of developing colorectal cancer. Wang et al. demonstrated that triptolide with 0.1, 0.3, or 1 mg/kg/day for 20 weeks inhibited colitis-related colon cancer progression *in vivo* via downregulating Rac1 and the Janus kinase (JAK)/STAT3 pathway (Wang et al., 2009). *In vitro* cell cycle analysis revealed that triptolide inhibits the proliferation, migration and colony formation of colon cancer cells. Triptolide could reduce the secretion of IL6 and levels of JAK1 and IL6R by interrupting the IL6R-JAK/STAT pathway. The shortcoming in this study was that the high dose group was 1 mg/kg/day which might lead to organ damage. However, Wang et al. have not investigated the organ damage in this group.

Intestinal Fibrosis

Intestinal fibrosis is a common complication of inflammatory bowel disease that is characterized by abnormal deposition of extracellular matrix proteins produced by activated myofibroblasts in the intestine (Rieder and Fiocchi, 2008). Tao et al. (2015) discovered that 45 mg/kg per day triptolide ameliorates colonic fibrosis in an experimental rat model. Triptolide could reduce collagen production and extracellular matrix deposition in the colon. Collagen I protein and collagen Iα1 transcript expression were also inhibited after treatment in the isolated subepithelial myofibroblasts of rats with colonic fibrosis.

Liver Fibrosis

Liver fibrosis is the excessive accumulation of extracellular matrix that occurs in most types of chronic liver diseases (Bataller and Brenner, 2005). Chong et al. (2011) found that 20 µg/kg triptolide exerts antihepatofibrotic effects in animal model of liver fibrosis. Triptolide inhibited the NF-κB signaling pathway in hepatic stellate cells. In addition, triptolide treatment reduced hepatic fibrosis scores *in vivo*.

Respiratory Disease Asthma

Asthma is a common long-term inflammatory airway disorder. Airway smooth muscle cells, goblet cells and eosinophils

contribute to asthmatic airway inflammation (Cohn et al., 2004). Approximately 8% of the adult population in worldwide are diagnosed asthma. Triptolide could inhibit asthma airway remodeling by suppressing the inflammatory signaling pathway, interfering with the production of pro-inflammatory chemokines and cytokines.

In the ovalbumin (OVA)—sensitized asthma mice model, Chen et al. showed that 40 µg/kg/day triptolide treatment may function as an inhibitor of asthma airway remodeling (Chen et al., 2011; Chen et al., 2015b). Triptolide could inhibit mucous gland hypertrophy, goblet cell hyperplasia and collagen deposition through the suppression of TGF-β1/Smad and NF-κB signaling pathways in airways. However, they only tested p-P65 protein in NF-κB signaling pathway which was not sufficient to demonstrate NF-κB signaling pathway was involved in the mechanism of triptolide. Furthermore, they revealed that triptolide inhibits the proliferation and migration of rat ASMCS (Chen et al., 2015a). Triptolide exerts a time- and dose-dependent inhibition of TGF-β1-induced ASMC proliferation by blocking S and G2/M phases without apparent cytotoxic effects.

Apart from signaling pathways, researchers also focused on the inflammatory cells in asthma. Ji et al. (2015) have shown that triptolide modulates the CD4⁺ T cell balance in an asthmatic animal model. Triptolide could regulate Th1/Th2 balance and Th17/Treg equilibrium. Inflammatory cytokines in the bronchoalveolar lavage fluid (BALF), such as IL-10, IL-13, IL-17, TNF-α, and TGF-β, are downregulated after treatment. Mao et al. (2008) found that 2 weeks of 40 µg/kg/day triptolide treatment alleviated eosinophil recruitment in BALF by inhibiting bone marrow eosinophilopoiesis. The number of eosinophils in the peripheral blood and bone marrow were significantly reduced after triptolide treatment

Acute Lung Injury

Acute lung injury (ALI) is a disorder of acute inflammation consisting of acute hypoxemic respiratory failure (Rubinfeld et al., 2005). Triptolide was found to alleviate ALI in LPS-induced mouse model and chlorine exposure mouse model.

In mouse models of chlorine gas-induced acute lung injury, triptolide ranged 100–1,000 µg/kg/day administration showed anti-inflammatory effects by decreasing neutrophils infiltration to the lung lavage fluid and lung tissue (Hoyle et al., 2010). In the LPS-induced ALI mouse model, 1–50 µg/kg/day triptolide ameliorated ALI by inhibiting the NF-κB signaling pathway (Wang et al., 2014). Triptolide inhibited chemokines such as macrophage inflammatory protein alpha (MIP-1α), MIP-1β, regulated upon activation normal T cell express sequence (RANTES) in the lung tissue and inflammatory cytokines such as TNF-α, IL-1β, IL-6 in the BALF of mice with ALI. Suppressed expression of p-IκB-α and p-NF-κB p65 showed that triptolide inhibits the NF-κB signaling pathway. Moreover, in the same animal model, Wei et al. found that triptolide with 5, 10, and 15 µg/kg treatment attenuated the LPS-induced inflammatory response by inhibiting the MAPK signaling pathway (Wei and Huang, 2014). Triptolide inhibits the phosphorylation of p38, JNK, and ERK. However, there have some significant disadvantages in LPS-induced ALI mouse model. LPS preparations might be contaminated with

bacterial materials and other bacterial lipoproteins. LPS does not induce injury of epithelial and endothelial cells occurring in acute respiratory distress syndrome of humans.

Pulmonary Arterial Hypertension

Pulmonary arterial hypertension (PAH) is an incurable disease characterized by increased blood pressure in the arteries of the lungs (Farber and Loscalzo, 2004). There is an increasing appreciation of inflammation in the pathogenesis of PAH with an accumulation of inflammatory cells and elevated cytokines. Triptolide could attenuate the development of pulmonary hypertension by down-regulating expression of functionally related genes.

In a rat experimental pulmonary arterial hypertension model, it has been shown that 0.25 mg/kg/day triptolide can effectively attenuate the development of pulmonary hypertension (Faul et al., 2000). By Day 35, the mean pulmonary arterial pressure was diminished in triptolide-treated rats compared with vehicle-treated rats. Triptolide-treated rats also showed significantly less pulmonary arterial neointimal formation and right ventricular hypertrophy. Another study analyzed longitudinal transcriptional expression in pulmonary hypertension rats administered 0.25 mg/kg/day triptolide treatment for 30 days (Vaszar et al., 2004). Transcriptional analysis with total lung RNA was performed for every experimental time point. They found that a group of functionally related genes, such as matrix metalloproteinase (MMP) and mast cell chymases, were significantly coexpressed with the development of PAH. The global gene expression pattern also resembled that seen in intermediate stages of severity. Functionally related genes were downregulated in response to triptolide treatment. Monocrotaline (MCT)-induced pulmonary hypertension (MCTP) was used as animal model in these two studies. Compared with chronic hypoxia PAH animal model, MCTP is easily to be therapeutically improved owing to the acute nature, which is not alike the characteristics of PAH in human.

Pulmonary Fibrosis

Pulmonary fibrosis is a chronic, debilitating and lethal lung disorder. Pulmonary fibrosis is estimated to have prevalence of 13 to 20 per 100,000 people worldwide. It has been demonstrated that 0.25 mg/kg triptolide effectively reduced radiation-induced lung fibrosis (Yang et al., 2015; Chen et al., 2016). Triptolide improved the pulmonary function by inhibiting myofibroblast activation, collagen deposition and ROS production in lung tissues. Triptolide also mitigated pulmonary fibrosis partly by downregulating nicotinamide adenine dinucleotide phosphate-oxidase 2 (NOX2) through the NF-κB pathway.

Endocrine Diseases

Diabetic Nephropathy

Diabetic nephropathy (DN) is a serious complication in those with diabetes mellitus. Podocyte injuries, such as decreased density of podocytes due to chronic inflammation and oxidative stress, are observed in the development of diabetic glomerular injury (Navarro-González and Mora-Fernández, 2008). Triptolide exerted protective effects on DN of DN animal model.

In an *in vitro* model of db/db diabetic mice with increased albuminuria, it has been revealed that triptolide markedly attenuates albuminuria. It has been shown that 50 µg/kg/day triptolide with 12 weeks treatment attenuates inflammation in the kidneys accompanied by alleviated podocyte injury. Triptolide could reduce the expression of desmin protein, MCP-1 protein and CD68-positive macrophages in db/db diabetic mouse kidneys (Gao et al., 2010).

Apart from db/db diabetic animal model, investigators also used streptozocin-induced DN model to reveal the mechanism of triptolide against DN. db/db diabetic animal model was used to be type 2 diabetes model, while streptozocin-induced DN model was used to be type 1 diabetes model.

Ma et al. demonstrated that 8 weeks of 100 µg/kg/day triptolide administration significantly reduces the expression of TGF-β1 and osteopontin to alleviate inflammation in the kidney. (Ma et al., 2013). Later, Guo et al. discovered that 4 weeks of 6, 12, or 24 mg/kg/day triptolide improves DN by regulating Th cell balance and macrophage infiltration (Guo et al., 2016). Triptolide could inhibit proinflammatory cytokines and increase anti-inflammatory cytokines by regulating the Th1/Th2 cell balance. Triptolide also inhibits macrophage infiltration and macrophage-mediated inflammation in the kidneys. Han et al. (2017) confirmed that triptolide significantly inhibits mesangial cell proliferation by suppressing the PDK1/Akt/mTOR pathway. More recently, Dong et al. (2017) reported that triptolide alleviates oxidative stress in the kidneys of DN. Renal homogenate SOD and MDA were significantly downregulated after treatment.

So, Th cell balance, macrophage, oxidative stress might be involved in the mechanism of triptolide in treating DN.

Diabetic Cardiomyopathy

Diabetic cardiomyopathy is one of the leading cardiovascular complications in diabetic patients. Chronic inflammation plays an important role in diabetic cardiomyopathy (Frati et al., 2017).

Studies have suggested that triptolide ranged 100, 200, or 400 µg/kg/day improves cardiac diastolic and systolic function in diabetic rats (Wen et al., 2013; Guo et al., 2016). Triptolide treatment prevents myocardial fibrosis and collagen accumulation in diabetic myocardium by decreasing the expression of cardiac inflammatory mediators including TGF-β1, α-SMA, TNF-α, IL-1β, and vimentin. Triptolide treatment also inhibits the recruitment of macrophages and T lymphocytes in diabetic rat hearts. The inhibitory effect of triptolide on diabetic cardiomyopathy might be mediated by the suppression of the NF-κB immune pathway. More recently, Liang et al. (2015) detected that 100, 200, or 400 µg/kg/day triptolide improves cardiac function and increases cardiac energy metabolism by activating the MAPK signaling pathway.

Thus, triptolide could inhibit inflammatory cells recruitment and cytokines expression to reduce myocardial fibrosis, apoptosis and necrosis in diabetic cardiomyopathy. The shortcomings of these studies were that the researchers only tested NF-κB p65 in NF-κB signaling pathway and p38 MAPK protein in MAPK signaling pathway when they studied the related pathways. Only one protein in the inflammatory signaling pathway was not

persuasive to demonstrate the related pathways were involved in the mechanism.

Rheumatic Diseases

Rheumatoid Arthritis

Rheumatoid arthritis (RA) is a systemic inflammatory autoimmune disorder in which genetic and environmental risk factors contribute to disease development (Collison, 2016). Descriptive epidemiology studies of RA showed a population prevalence of 0.5–1% in worldwide. The disease is characterized by inflammation of synovial joints leading to the destruction of articular cartilage and erosion of the bone. Fibroblast-like synoviocytes (FLS), T cells, macrophages, DCs, osteoclasts, and chondrocytes play important roles in the pathogenesis of RA. Previous studies have observed antirheumatic properties of triptolide. In an animal model of RA, triptolide ameliorates the severity of arthritis (Gu and Brandwein, 1998). The anti-inflammatory effects of triptolide in dealing with RA have thus far been attributed to the aspects described in Figure 2.

Fibroblast-Like Synoviocytes

Fibroblast-like synoviocytes, also known as synovial fibroblasts, are special cells that play a crucial role in the pathogenesis of RA (Bartok and Firestein, 2010). In RA, FLSs are the most common cell type at the cartilage-pannus junction and perpetrate inflammation through their massive production of inflammatory cytokines, chemokines, and matrix-degrading molecules and through immigration and invasion of joint cartilage (Bustamante et al., 2017).

Triptolide has been found to inhibit inflammation of fibroblast-like synoviocytes in several studies. Triptolide with

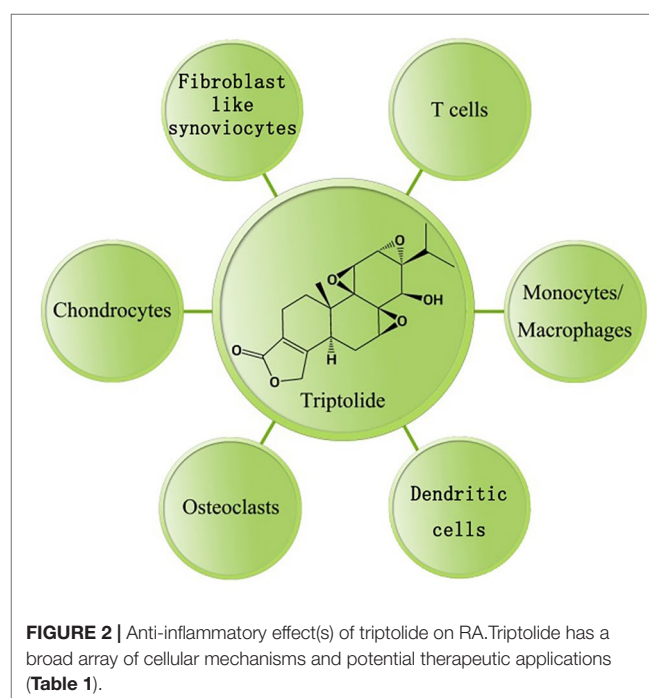


TABLE 1 | Cellular target(s) modulated by triptolide in rheumatoid arthritis.

Type of cells	Mechanism(s) of action
Fibroblast-like synoviocytes	Inhibits viability, proliferation, migration and invasive capacities. Affects cytoskeletal rearrangement. Arrests the cell cycle. Induces apoptosis. Reduces inflammatory mediators, including IL-18, prostaglandin E2 (PGE-2), cyclooxygenase-2 (COX-2), pro-MMP1 and 3. Inhibits the NF- κ B and MAPK pathways.
T cells	Inhibits proliferation and differentiation. Induces apoptosis. Reduces inflammatory cytokines, including IL-2, IL-13, IL-17 and IFN- γ . Inhibits the NF- κ B and MAPK pathways.
Monocytes/Macrophages	Reduces inflammatory cytokines, including IL-1 β , IL-6, IL-8, IL-12, IL-37, TNF- α and IFN- γ . Reduces inflammatory chemokines, including CCL-1, 2, 5, 7, and 12 as well as chemokine (C-X-C motif) ligand (CXCL)-10 and 11. Reduces the expression of costimulatory molecules CD80 and CD86. Reduces production of nitric oxide (NO), superoxide anion and ROS. Induces apoptosis. Inhibits the NF- κ B pathway and TAK1 kinase activity.
Dendritic cells	Inhibits differentiation, maturation, allostimulatory capacities, chemotactic responses and migration. Induces apoptosis. Reduces inflammatory mediators, including MIP-1 α , MIP-1 β , MCP-1, PGE-2 and COX-2. Reduces the expression of costimulatory molecules CD1a, CD40, CD80 and CD86. Inhibits the PI3-K/Akt and NF- κ B pathways.
Osteoclasts	Inhibits differentiation and osteoclastogenesis. Regulates the RANKL/RANK/osteoprotegerin signaling pathway. Inhibits NF- κ B activation.
Chondrocytes	Reduces inflammatory mediators, including TNF- α , IL-6, PGE-2, COX-2, MMP-3 and MMP-13. Inhibits aggrecanase-1 expression. Inhibits NF- κ B activation.

100 ng/ml concentration could inhibit inflammatory cytokine production of FLS and inhibit invasive capacities of FLS. Lu et al. (2008) demonstrated that triptolide inhibits the expression of IL-18 and its receptor in PMA-stimulated FLSs in a dose-dependent manner by suppressing NF- κ B activity. However, Lu et al. (2008) only analyzed one inflammatory cytokine produced by FLS. Lin et al. (2001) demonstrated that 28–140 nM triptolide suppresses the production of proMMP1 and 3 in IL-1 α -induced FLSs. In addition, triptolide downregulates the expression of PGE-2 in activated FLSs by selectively suppressing the production of COX-2. Kusunoki et al. (2004) revealed that 100nM triptolide decreases viability, inhibits proliferation, and induces apoptosis of FLSs in a concentration-dependent manner at very low concentrations. Later, Yang et al. (2016) discovered that 10–50 nM triptolide reduces the migratory and invasive capacities of FLSs by affecting the cytoskeletal rearrangement of FLSs. They also indicated that triptolide blocks the activation of the JNK MAPK pathway in FLSs. Thus, triptolide suppresses the inflammatory mediators including IL-18, COX-2, proMMP1 and 3 in activated FLS. NF- κ B and MAPK pathways might be involved in the mechanism of inhibiting FLS inflammatory activities.

T Cells

T cells take center stage in the pathogenesis of rheumatoid arthritis (Cope et al., 2007). The predominance of T cells in lymphocytic infiltrates in the tissue of patients with RA has been defined.

Previous studies have demonstrated the immunosuppressive effects of triptolide in regulating T cell function. Inflammatory cytokine production, apoptosis, cell proliferation, and inflammatory pathways were involved in the effects of 10–500 nmol triptolide on T cells. Inflammatory cytokines production of T cells including IL-2, IFN- γ , IL-13, IL-17 were inhibited by triptolide (Chan et al., 1999; Dai et al., 2013). Qiu et al. (1999) reported that triptolide inhibits IL-2 expression in T cells at the level of purine-box/nuclear factor of activated T cells and NF- κ B transcriptional activation triggered by all stimuli examined. Dai et al. (2013) demonstrated that triptolide inhibits IL-13 expression by inhibiting GATA3 and nuclear factor of activated T cells 1 (NFAT1) nuclear translocation and their binding rates to the IL-13 gene promoter region. However, Dai et al. have not revealed the relationship between IL-13 and GATA3 in T cells clearly. They only examined the expression of IL-13 and GATA3 after triptolide administration.

In the aspects of apoptosis and signaling pathways, Yang et al. (1998) discovered that 10–100 ng/ml triptolide induces T cell apoptosis accompanied by increased caspase activity and degradation of the caspase substrate PARP. Liu et al. (2000) showed that 2–10 μ g/L triptolide attenuates T cell NF- κ B activation by upregulating I κ B α mRNA expression. In addition, Ho et al. (2013) discovered that 50–200 ng/ml triptolide attenuates both the NF- κ B and MAPK signaling pathways.

Monocytes/Macrophages

Monocytes/macrophages play an important role in the pathogenesis of rheumatoid arthritis (Davignon et al., 2013). A number of monocytes/macrophages infiltrate into the rheumatoid synovium. They are a potent source of cytokines, chemokines and ROS that participate in the initiation, maintenance, and resolution of inflammation. The number of macrophages in the inflamed synovial membrane and cartilage-pannus junction are correlated with cartilage and bone destruction in RA (Kinne et al., 2007). As such, monocytes and macrophages are viewed as relevant therapeutic targets in treating RA.

Triptolide has been found to inhibit inflammation of monocytes and macrophages. Triptolide inhibited inflammatory cytokines and costimulatory molecules in monocytes. Triptolide suppressed the production of IL-12 in the THP-1 human monocytic leukemia cell line at dosage of 2.5–0.625 μ g/L (Liu et al., 2005). Triptolide also suppressed expression of the costimulatory molecules CD80 and CD86 on LPS-activated THP-1 cells. In addition, 5–25 nM triptolide prompted THP-1 apoptosis by inhibiting the NF- κ B pathway and activating the MAPK pathway (Park and Kim, 2013). Interestingly, MAPK pathway was activated in this study, which is different with other studies. Activated MAPK pathway might contribute to the apoptosis of monocytes induced by triptolide.

Apart from monocytes, triptolide inhibits the inflammatory activities of macrophages through multiple mechanisms. First, 5–40 ng/ml triptolide inhibits some key inflammation-related cytokines in LPS-activated macrophages, including TNF- α , IL-1 β , IL-6, IL-8, and IFN- γ (Wu et al., 2006; Yang et al., 2010). Some proinflammatory chemokines, including CCL-1, 2, 5, 7, and 12, as well as CXCL-10 and 11, are attenuated after triptolide

administration with concentrations as low as 10–50 nM (Matta et al., 2009). Second, several studies have revealed that 5–25 ng/ml triptolide suppresses nitric oxide (NO) and ROS production in activated macrophages (Wang et al., 2004; Bao et al., 2007). Kim et al. (2004) discovered that triptolide abrogates inducible NO synthase (iNOS) gene expression and inhibits NO production in a dose-dependent manner. Wu et al. (2006) found that triptolide inhibits superoxide anion and ROS production in murine peritoneal macrophages. Third, triptolide down-regulates NF- κ B activation and JNK phosphorylation. Kim et al. (2004) revealed that triptolide significantly inhibits the DNA binding activity of NF- κ B, whereas Premkumar et al. (2010) showed that myeloid differentiation primary response 88 (MyD88)-dependent and independent pathways of toll-like receptors (TLRs) are engaged in the biological activity of triptolide. So, triptolide could influence the inflammatory cytokines production, oxidative stress, and related inflammatory signaling pathways in the macrophages to alleviate inflammation.

Dendritic Cells

Dendritic cells play important roles in the induction of immunity and in mediating immune tolerance as professional antigen-presenting cells (Khan et al., 2009). In the synovial fluid of RA joints, DCs amplify immune responses by ingesting and presenting antigens to T cells (Bell et al., 2017).

It has been found that triptolide could suppress the migration and differentiation of dendritic cells DCs. Chen et al. (2005) found that triptolide is a potent suppressor of DCs maturation and trafficking. The allostimulatory capacities and chemotactic responses of DCs are inhibited by 2.5–10 nM triptolide over a pharmacologic concentration range. Zhu et al. (2005) discovered that 20 ng/ml triptolide prevents the differentiation of immature DCs by inhibiting CD1a, CD40, CD80, CD86 and HLA-DR expression. Thus, triptolide could inhibit the trafficking, maturation, and differentiation of DCs and. In another article, triptolide inhibits DC-mediated chemoattraction of neutrophils and T cells by inhibiting DC production of CC and CXC chemokines, including MIP-1 α , MIP-1 β , and MCP-1, in response to LPS (Liu et al., 2006). However, they have not revealed the mechanisms of triptolide inhibiting DC-mediated chemoattraction of other inflammatory cells. Later, Liu et al. (2007) revealed that 10–100 ng/ml triptolide impairs DC migration by inhibiting the phosphatidylinositol-3 kinase (PI3-K)/Akt and NF- κ B pathways. Triptolide-mediated suppression of the NF- κ B pathway, STAT3 phosphorylation and an increase in suppressor of cytokine signaling 1 (SOCS1) expression in DCs may be involved in the inhibitory effect of triptolide. (Liu et al., 2004).

Osteoclasts

Extensive bone destruction is a feature of patients with rheumatoid arthritis, leading to severe deformity of the affected joints. As a result, ameliorating bone destruction is a very important issue in the treatment of RA.

Triptolide has been shown to efficiently ameliorate the progression of bone destruction in rheumatoid arthritis by inhibiting osteoclast activities. The related signaling pathways

might include receptor activator of the nuclear factor kappa-B ligand (RANKL)/RANK/osteoprotegerin (OPG) and NF- κ B signaling pathways. Liu et al. (2013) showed that 8–32 μ g/kg/day triptolide prevents bone destruction and inhibits osteoclast formation in an animal model of RA by regulating the RANKL/RANK/OPG signaling pathway. Later, Huang et al. (2015) reported that 1.25 nM triptolide inhibits osteoclastogenesis and osteoclastic bone resorption by suppressing RANKL-induced activation of NF- κ B and p65 nuclear translocation in osteoclast-like cells. More recently, Xu et al. (2016) found that triptolide inhibits osteoclast differentiation and bone resorption by increasing expression of the immunosuppressive cytokines IL-10 and TGF- β 1 by Tregs. Therefore, these data show that triptolide is effective in treating bone destruction by regulating osteoclast inflammatory activities, which is a hallmark of RA pathophysiology.

Chondrocytes

Rheumatoid arthritis is characterized by synovitis in joints and destruction of cartilage. Cartilage is destroyed by enzymatic and mechanical processes. The chondrocytes themselves also synthesize cytokines and MMPs or respond to local cytokine release to accelerate articular cartilage destruction (Otero and Goldring, 2007).

Triptolide could reduce the expression of inflammatory mediators including TNF- α , IL-6, COX-2, and MMPs in chondrocytes to prevent cartilage damage. In 2005, Liacini et al. (2005) showed that triptolide at 125–250 nM concentrations possesses cartilage-protective effects by suppressing MMP expression in chondrocytes *in vitro*. 100 nM triptolide inhibits proinflammatory cytokine-induced MMP-3 and MMP-13 expression in chondrocytes in a dose-dependent manner. Later, Lin et al. (2007) discovered that triptolide suppresses inflammation and cartilage destruction in RA mice. In 2009, Xiao et al. (2009) demonstrated that triptolide reduces the expression of the proinflammatory cytokines COX-2 and NF- κ B in paw cartilage in arthritic rats. Immunohistochemistry staining revealed that triptolide inhibits the expression of TNF- α , IL-6, COX-2 and NF- κ B in superficial cartilage. The flaw of this study was that they only test NF- κ B protein in the tissue. Other proteins in the NF- κ B signaling pathway have not been investigated.

Neurologic Diseases

In the last decade, many studies have demonstrated that triptolide is a promising neuroprotective agent and alleviates neuroinflammation in animal models of neurodegenerative diseases.

Alzheimer's Disease

Alzheimer's disease (AD) is a chronic neurodegenerative disease that devastates later decades of life. Increasing evidence suggests that the pathogenesis of AD is not restricted to the neuronal compartment but includes strong interactions with neuroinflammation in the brain (Heneka et al., 2015). The prevalence of AD worldwide is approximately as high as 24 million. Triptolide could alleviate the immune-inflammatory

pathology including A β deposition, cytokines expression, and oxidative stress in the treatment of AD.

Triptolide treatment with 0.4 mg/kg/day administration of 18 days could reduce A β deposition and neuroinflammation in the hippocampal and cortical areas by upregulating the degradation pathway of A β in a transgenic Alzheimer's disease model (Cheng et al., 2014). Another study found that 20 μ g/kg/day triptolide for 8 weeks exerted anti-inflammatory and antioxidative effects on the transgenic mouse brain (Wang et al., 2014). Triptolide inhibited the expression of proinflammatory markers TNF α and IL-1 β in the hippocampus in the hippocampus. Recently, Li et al. (2016) demonstrated that 5 μ g/kg/day triptolide treatment for 45 days inhibits the activation and proliferation of microglial cells and astrocytes in the hippocampus in a transgenic AD mouse model, reducing neuroinflammation in the brain. Additionally, Cui et al. (2016) found that triptolide with 20 μ g/kg/day for 15 weeks alleviates neuroinflammation by suppressing MAPK activity. In the previous studies, APP transgenic mice were used as animal models. The brain of APP transgenic mice is similar to the brain pathology of AD patients with A β deposition and neuroinflammation.

Similar to what is observed in animal models of Alzheimer's disease, the protective effect of triptolide has been found *in vitro*. Xu et al. demonstrated that triptolide has a protective effect in PC12 cells against A β_{25-35} -induced cytotoxicity by inhibiting the autophagy pathway (Xu et al., 2015). Furthermore, they found that triptolide protects PC12 cells by reducing oxidative stress. Triptolide downregulated the expression of ROS, hydrogen peroxide and MDA induced by A β_{25-35} (Xu et al., 2016). PC12 cell line was used to mimic AD *in vitro* model in these studies. Apart from PC12 cell line, human neuroblastoma and human induced pluripotent stem cells are also used as *in vitro* model for AD research. However, these cell lines are not really satisfactory *in vitro* model in order to mimic the features of AD.

Parkinson's Disease

Parkinson's disease (PD) is a chronic and progressive disorder. Chronic inflammation is a major characteristic of PD (Herrero et al., 2015). There were 6.1 million prevalent cases of PD globally. The worldwide the burden of Parkinson's disease has more than 6.1 million patients. Triptolide shows anti-inflammatory and neuroprotective effects *in vivo* and *in vitro*. Triptolide protected dopaminergic cells and reduced inflammatory cytokines expression in the brain of PD.

It has been demonstrated that triptolide protects dopaminergic neurons from inflammation-mediated damage. Moreover, 1–10 nM triptolide has been found to suppress LPS-induced activation of microglia and excessive production of TNF α and NO (Li et al., 2004). The administration of triptolide 1 or 5 μ g/kg for 24 days also attenuated the depletion of dopamine in the striatum and protected dopaminergic neurons from the injury induced by intranigral LPS injection (Zhou et al., 2005). Hu and colleagues have shown that 50 nM triptolide promotes the clearance of pathogenic proteins in neuronal cells using *in vitro* models of PD (Hu et al., 2017).

In addition, using an *in vitro* Parkinson's disease model of lipopolysaccharides -stimulated PC12 cells, it has been shown

that 10–100 ng/ml triptolide downregulates inflammatory mediators such as COX-2 and PGE-2 by inhibiting the NF- κ B and MAPK signaling pathways in LPS-stimulated PC12 cells (Geng et al., 2012). Triptolide with concentration more than 200ng/ml showed cytotoxicity effects on PC12 cells. PC12 cells were also used to mimic AD as *in vitro* model. So, this cell lines are not really satisfactory *in vitro* model in order to mimic the features of PD.

Multiple Sclerosis

Multiple sclerosis (MS) is a chronic inflammatory autoimmune disease, and experimental autoimmune encephalomyelitis (EAE) is considered an animal model for MS (Constantinescu et al., 2011). MS affects more than 2 million individuals in the worldwide. Triptolide alleviate MS in animal models by reducing inflammation and demyelination pathology.

Kizelsztejn et al. (2009) discovered that 100 μ g/kg/day triptolide for 2 weeks reduces cellular infiltration and tissue damage in experimental autoimmune encephalomyelitis mice. EAE-promoting cytokines, including IL-2, IL-6 and TNF- α , were reduced in inflamed brains. Molecular analysis revealed that triptolide suppressed NF- κ B signaling pathway. Another study conducted by Wang et al. (2008) found that 100 μ g/kg/day triptolide for 4 weeks modulates T-cell inflammatory responses and ameliorates EAE. Triptolide inhibited the mRNA expression of both Th1/Th(IL-17) and Th2 cytokines in spleen mononuclear cells and in spinal cord tissues. The levels of IFN- γ , TNF- α , IL-12, IL-6, IL-17 and IL-23 were significantly reduced in both spleen MNCs and spinal cord tissues after triptolide administration. EAE animal model was used to mimic MS in these studies. However, there are some limitations of EAE animal model. Firstly, EAE model offer little information on the progression of MS. EAE is an infectious disorder affecting white matter of spinal cord, whereas MS affects cerebral and cerebellar cortex.

CONCLUSION

With an increasing worldwide rate of inflammatory disorders, there is an urgent need for the improvement of the therapeutic activity of anti-inflammatory agents. The anti-inflammatory and immunosuppressive properties of triptolide make it a promising agent to treat inflammatory disorders. In this review, we systemically discussed the potential effects and mechanisms of triptolide in the treatment of different inflammatory diseases including MN, lupus nephritis, kidney transplantation, IBD, asthma, ALI, PAH, etc. Firstly, triptolide could reduce the production of inflammatory mediators such as TNF- α , IL-6, IL-17. Secondly, triptolide alleviated oxidative stress of damaged organs in animal model and related cell lines. Thirdly, triptolide could inhibit the activities of inflammatory cells such as T cells and macrophages. The most related signaling pathway involved in the mechanisms of triptolide was NF- κ B and MAPK signaling pathways. Despite the great therapeutic potential of triptolide, there are still some shortcomings in the process of developing it as a new drug. The most studies were focused on the studies of animal models and cell lines. The successful track records of

real patients in randomized controlled trials seem very poor. The triptolide cytotoxicity in other healthy organs have not been investigated clearly, either. Hopefully, future stringent preclinical studies on triptolide will provide crucial information regarding its pharmacokinetics and dosage, allowing for further optimization of this compound.

AUTHOR CONTRIBUTIONS

KY, XL, QL, QZ, and HJ summarized the literature and drafted the manuscript. KY, XL, TW, GH, and AX revised and edited the

manuscript. AX, TW, and GH supervised the work. KY, XL, TW, GH, and AX initiated, finalized, and submitted the manuscript.

FUNDING

This work was supported by the National Natural Science Foundation of China (grant numbers 81430099 and 31500704), Projects of International Cooperation and Exchanges (grant number 2014DFA32950) and research program from Beijing University of Chinese Medicine (grant numbers BUCM-2019-JCRC006 and 2019-JYB-TD013).

REFERENCES

- Abraham, C., and Cho, J. H. (2009). Inflammatory bowel disease. *N. Engl. J. Med.* 361, 2066–2078. doi: 10.1056/NEJMra0804647
- Bao, X., Cui, J., Wu, Y., Han, X., Gao, C., Hua, Z., et al. (2007). The roles of endogenous reactive oxygen species and nitric oxide in triptolide-induced apoptotic cell death in macrophages. *J. Mol. Med. (Berl)*. 85, 85–98. doi: 10.1007/s00109-006-0113-x
- Bartok, B., and Firestein, G. S. (2010). Fibroblast-like synoviocytes: key effector cells in rheumatoid arthritis. *Immunol. Rev.* 233, 233–255. doi: 10.1111/j.0105-2896.2009.00859.x
- Bataller, R., and Brenner, D. A. (2005). Liver fibrosis. *J. Clin. Invest.* 115, 209–218. doi: 10.1172/JCI24282
- Bell, G. M., Anderson, A. E., Diboll, J., Reece, R., Eltherington, O., Harry, R. A., et al. (2017). Autologous tolerogenic dendritic cells for rheumatoid and inflammatory arthritis. *Ann. Rheumatol. Dis.* 76, 227–234. doi: 10.1136/annrheumdis-2015-208456
- Bustamante, M. F., Garcia-Carbonell, R., Whisenant, K. D., and Guma, M. (2017). Fibroblast-like synovocyte metabolism in the pathogenesis of rheumatoid arthritis. *Arthritis Res. Ther.* 19, 110. doi: 10.1186/s13075-017-1303-3
- Cattran, D. C., and Brenchley, P. E. (2017). Membranous nephropathy: integrating basic science into improved clinical management. *Kidney Int.* 91, 566–574. doi: 10.1016/j.kint.2016.09.048
- Chan, M. A., Kohlmeier, J. E., Branden, M., Jung, M., and Benedict, S. H. (1999). Triptolide is more effective in preventing T cell proliferation and interferon-gamma production than is FK506. *Phytother. Res.* 13, 464–467. doi: 10.1002/(sici)1099-1573(199909)13:6<464::aid-ptr483>3.0.co;2-4
- Chen, X., Murakami, T., Oppenheim, J. J., and Howard, O. M. (2005). Triptolide, a constituent of immunosuppressive Chinese herbal medicine, is a potent suppressor of dendritic-cell maturation and trafficking. *Blood* 106, 2409–2416. doi: 10.1182/blood-2005-03-0854
- Chen, Z. H., Qin, W. S., Zeng, C. H., Zheng, C. X., Hong, Y. M., Lu, Y. Z., et al. (2010). Triptolide reduces proteinuria in experimental membranous nephropathy and protects against C5b-9-induced podocyte injury *in vitro*. *Kidney Int.* 77, 974–988. doi: 10.1038/ki.2010.41
- Chen, M., Lv, Z., and Jiang, S. (2011). The effects of triptolide on airway remodelling and transforming growth factor- β_1 /Smad signalling pathway in ovalbumin-sensitized mice. *Immunology* 132, 376–384. doi: 10.1111/j.1365-2567.2010.03392.x
- Chen, M., Lv, Z., Huang, L., Zhang, W., Lin, X., Shi, J., et al. (2015a). Triptolide inhibits TGF- β_1 -induced cell proliferation in rat airway smooth muscle cells by suppressing Smad signaling. *Exp. Cell Res.* 331, 362–368. doi: 10.1016/j.yexcr.2014.10.016
- Chen, M., Lv, Z., Zhang, W., Huang, L., Lin, X., Shi, J., et al. (2015b). Triptolide suppresses airway goblet cell hyperplasia and Muc5ac expression *via* NF- κ B in a murine model of asthma. *Mol. Immunol.* 64, 99–105. doi: 10.1016/j.molimm.2014.11.001
- Chen, C., Yang, S., Zhang, M., Zhang, Z., Hong, J., Han, D., et al. (2016). Triptolide mitigates radiation-induced pulmonary fibrosis *via* inhibition of axis of alveolar macrophages-NOXes-ROS-myofibroblasts. *Cancer Biol. Ther.* 17, 381–389. doi: 10.1080/15384047.2016.1139229
- Chen, Y., Song, R., and Zhang, Y. (2017). Triptolide reduces podocytes injury through blocking ERK and JNK pathways in passive Heymann nephritis (PHN) model. *Int. J. Clin. Exp. Med.* 10, 692–699.
- Cheng, S., LeBlanc, K. J., and Li, L. (2014). Triptolide preserves cognitive function and reduces neuropathology in a mouse model of Alzheimer's disease. *PLoS One* 9, e108845. doi: 10.1371/journal.pone.0108845
- Chong, L. W., Hsu, Y. C., Chiu, Y. T., Yang, K. C., and Huang, Y. T. (2011). Antifibrotic effects of triptolide on hepatic stellate cells and dimethylnitrosamine-intoxicated rats. *Phytother. Res.* 25, 990–999. doi: 10.1002/ptr.3381
- Cohn, L., Elias, J. A., and Chupp, G. L. (2004). Asthma: mechanisms of disease persistence and progression. *Annu. Rev. Immunol.* 22, 789–815. doi: 10.1146/annurev.immunol.22.012703.104716
- Collison, J. (2016). Rheumatoid arthritis: Tipping the balance towards resolution. *Nat. Rev. Rheumatol.* 12, 622. doi: 10.1038/nrrheum.2016.159
- Constantinescu, C. S., Farooqi, N., O'Brien, K., and Gran, B. (2011). Experimental autoimmune encephalomyelitis (EAE) as a model for multiple sclerosis (MS). *Br. J. Pharmacol.* 164, 1079–1106. doi: 10.1111/j.1476-5381.2011.01302.x
- Cope, A. P., Schulze-Koops, H., and Aringer, M. (2007). The central role of T cells in rheumatoid arthritis. *Clin. Exp. Rheumatol.* 25, S4–11.
- Crews, G. M., Erickson, L., Pan, F., Fisniku, O., Jang, M. S., Wynn, C., et al. (2005). Down-regulation of TGF- β and VCAM-1 is associated with successful treatment of chronic rejection in rats. *Transplant. Proc.* 37, 1926–1928. doi: 10.1016/j.transproceed.2005.02.096
- Cui, Y. Q., Wang, Q., Zhang, D. M., Wang, J. Y., Xiao, B., Zheng, Y., et al. (2016). Triptolide rescues spatial memory deficits and amyloid- β aggregation accompanied by inhibition of inflammatory responses and MAPKs activity in APP/PS1 transgenic mice. *Curr. Alzheimer Res.* 13, 288–296. doi: 10.2174/156720501303160217122803
- Dai, S., Yin, K., Yao, X., and Zhou, L. (2013). Inhibition of interleukin-13 gene expression by triptolide in activated T lymphocytes. *Respirology* 18, 1249–1255. doi: 10.1111/resp.12145
- Davignon, J. L., Hayder, M., Baron, M., Boyer, J. F., Constantin, A., Apparailly, F., et al. (2013). Targeting monocytes/macrophages in the treatment of rheumatoid arthritis. *Rheumatol. (Oxford)* 52, 590–598. doi: 10.1093/rheumatology/kes304
- Dong, X. G., An, Z. M., Guo, Y., Zhou, J. L., and Qin, T. (2017). Effect of triptolide on expression of oxidative carbonyl protein in renal cortex of rats with diabetic nephropathy. *J. Huazhong Univ. Sci. Technol. Med. Sci.* 37, 25–29. doi: 10.1007/s11596-017-1689-9
- Farber, H. W., and Loscalzo, J. (2004). Pulmonary arterial hypertension. *N. Engl. J. Med.* 351, 1655–1665. doi: 10.1056/NEJMra035488
- Faul, J. L., Nishimura, T., Berry, G. J., Benson, G. V., Pearl, R. G., and Kao, P. N. (2000). Triptolide attenuates pulmonary arterial hypertension and neointimal formation in rats. *Am. J. Respir. Crit. Care Med.* 162, 2252–2258. doi: 10.1164/ajrccm.162.6.2002018
- Fрати, G., Schirone, L., Chimenti, I., Yee, D., Biondi-Zoccai, G., Volpe, M., et al. (2017). An overview of the inflammatory signalling mechanisms in the myocardium underlying the development of diabetic cardiomyopathy. *Cardiovasc. Res.* 113, 378–388. doi: 10.1093/cvr/cvx011

- Gao, Q., Shen, W., Qin, W., Zheng, C., Zhang, M., Zeng, C., et al. (2010). Treatment of db/db diabetic mice with triptolide: a novel therapy for diabetic nephropathy. *Nephrol. Dial. Transplant.* 25, 3539–3547. doi: 10.1093/ndt/gfq245
- Geng, Y., Fang, M., Wang, J., Yu, H., Hu, Z., Yew, D. T., et al. (2012). Triptolide down-regulates COX-2 expression and PGE2 release by suppressing the activity of NF- κ B and MAP kinases in lipopolysaccharide-treated PC12 cells. *Phytother. Res.* 26, 337–343. doi: 10.1002/ptr.3538
- Goldbach-Mansky, R., Wilson, M., Fleischmann, R., Olsen, N., Silverfield, J., Kempf, P., et al. (2009). Comparison of Tripterygium wilfordii Hook F versus sulfasalazine in the treatment of rheumatoid arthritis: a randomized trial. *Ann. Intern. Med.* 151, 229–240. doi: 10.7326/0003-4819-151-4-200908180-00005
- W49–51.
- Goldrosen, M. H., and Straus, S. E. (2004). Complementary and alternative medicine: assessing the evidence for immunological benefits. *Nat. Rev. Immunol.* 4, 912–921. doi: 10.1038/nri1486
- Gu, W. Z., and Brandwein, S. R. (1998). Inhibition of type II collagen-induced arthritis in rats by triptolide. *Int. J. Immunopharmacol.* 20, 389–400. doi: 10.1016/s0192-0561(98)00035-6
- Guo, H., Pan, C., Chang, B., Wu, X., Guo, J., Zhou, Y., et al. (2016). Triptolide improves diabetic nephropathy by regulating Th cell balance and macrophage infiltration in rat models of diabetic nephropathy. *Exp. Clin. Endocrinol. Diabetes* 124, 389–398. doi: 10.1055/s-0042-106083
- Guo, X., Xue, M., Li, C. J., Yang, W., Wang, S. S., Ma, Z. J., et al. (2016). Protective effects of triptolide on TLR4 mediated autoimmune and inflammatory response induced myocardial fibrosis in diabetic cardiomyopathy. *J. Ethnopharmacol.* 193, 333–344. doi: 10.1016/j.jep.2016.08.029
- Han, F., Xue, M., Chang, Y., Li, X., Yang, Y., Sun, B., et al. (2017). Triptolide suppresses glomerular mesangial cell proliferation in diabetic nephropathy is associated with inhibition of PDK1/Akt/mTOR pathway. *Int. J. Biol. Sci.* 13, 1266–1275. doi: 10.7150/ijbs.20485
- Heneka, M. T., Carson, M. J., El Khoury, J., Landreth, G. E., Brosseron, F., Feinstein, D. L., et al. (2015). Neuroinflammation in Alzheimer's disease. *Lancet Neurol.* 14, 388–405. doi: 10.1016/S1474-4422(15)70016-5
- Herrero, M. T., Estrada, C., Maatouk, L., and Vyas, S. (2015). Inflammation in Parkinson's disease: role of glucocorticoids. *Front. Neuroanat.* 9, 32. doi: 10.3389/fnana.2015.00032
- Ho, L. J., Chang, W. L., Chen, A., Chao, P., and Lai, J. H. (2013). Differential immunomodulatory effects by Tripterygium wilfordii Hook f-derived refined extract PG27 and its purified component PG490 (triptolide) in human peripheral blood T cells: potential therapeutics for arthritis and possible mechanisms explaining in part Chinese herbal theory Junn-Chenn-Zuou-SS. *J. Transl. Med.* 11, 294. doi: 10.1186/1479-5876-11-294
- Hong, Y., Zhou, W., Li, K., and Sacks, S. H. (2002). Triptolide is a potent suppressant of C3, CD40 and B7h expression in activated human proximal tubular epithelial cells. *Kidney Int.* 62, 1291–1300. doi: 10.1111/j.1523-1755.2002.kid586.x
- Hoyle, G. W., Hoyle, C. I., Chen, J., Chang, W., Williams, R. W., and Rando, R. J. (2010). Identification of triptolide, a natural diterpenoid compound, as an inhibitor of lung inflammation. *Am. J. Physiol. Lung Cell Mol. Physiol.* 298, L830–L836. doi: 10.1152/ajplung.00014.2010
- Hu, G., Gong, X., Wang, L., Liu, M., Liu, Y., Fu, X., et al. (2017). Triptolide promotes the clearance of α -synuclein by enhancing autophagy in neuronal cells. *Mol. Neurobiol.* 54, 2361–2372. doi: 10.1007/s12035-016-9808-3
- Huang, J., Zhou, L., Wu, H., Pavlos, N., Chim, S. M., Liu, Q., et al. (2015). Triptolide inhibits osteoclast formation, bone resorption, RANKL-mediated NF- κ B activation and titanium particle-induced osteolysis in a mouse model. *Mol. Cell Endocrinol.* 399, 346–353. doi: 10.1016/j.mce.2014.10.016
- Inguili, E. (2010). Mechanism of cellular rejection in transplantation. *Pediatr. Nephrol.* 25, 61–74. doi: 10.1007/s00467-008-1020-x
- Ji, N. F., Wang, W. J., Zhang, M. S., and Huang, M. (2015). Triptolide modulates the CD4⁺ T cells balance in an allergic asthmatic mouse model. *Eur. Respir. J.* 46, PA4371. doi: 10.1183/13993003.congress-2015.PA4371
- Khan, S., Greenberg, J. D., and Bhardwaj, N. (2009). Dendritic cells as targets for therapy in rheumatoid arthritis. *Nat. Rev. Rheumatol.* 5, 566–571. doi: 10.1038/nrrheum.2009.185
- Kim, Y. H., Lee, S. H., Lee, J. Y., Choi, S. W., Park, J. W., and Kwon, T. K. (2004). Triptolide inhibits murine-inducible nitric oxide synthase expression by down-regulating lipopolysaccharide-induced activity of nuclear factor- κ B and c-Jun NH2-terminal kinase. *Eur. J. Pharmacol.* 494, 1–9. doi: 10.1016/j.ejphar.2004.04.040
- Kinne, R. W., Stuhlmueller, B., and Burmester, G. R. (2007). Cells of the synovium in rheumatoid arthritis. Macrophages. *Arthritis Res. Ther.* 9, 224. doi: 10.1186/ar2333
- Kizelsztejn, P., Komarnitsky, S., and Raskin, I. (2009). Oral administration of triptolide ameliorates the clinical signs of experimental autoimmune encephalomyelitis (EAE) by induction of HSP70 and stabilization of NF- κ B/I κ Ba transcriptional complex. *J. Neuroimmunol.* 217, 28–37. doi: 10.1016/j.jneuroim.2009.08.017
- Kupchan, S. M., Court, W. A., Dailey, R. G. Jr., Gilmore, C. J., and Bryan, R. F. (1972). Triptolide and triptolide: novel antileukemic diterpenoid triepoxides from Tripterygium wilfordii. *J. Am. Chem. Soc.* 94, 7194–7195. doi: 10.1021/ja00775a078
- Kusunoki, N., Yamazaki, R., Kitasato, H., Beppu, M., Aoki, H., and Kawai, S. (2004). Triptolide, an active compound identified in a traditional Chinese herb, induces apoptosis of rheumatoid synovial fibroblasts. *BMC Pharmacol.* 4, 2. doi: 10.1186/1471-2210-4-2
- Lech, M., and Anders, H. J. (2013). The pathogenesis of lupus nephritis. *J. Am. Soc. Nephrol.* 24, 1357–1366. doi: 10.1681/ASN.2013010026
- Li, F. Q., Lu, X. Z., Liang, X. B., Zhou, H. F., Xue, B., Liu, X. Y., et al. (2004). Triptolide, a Chinese herbal extract, protects dopaminergic neurons from inflammation-mediated damage through inhibition of microglial activation. *J. Neuroimmunol.* 148, 24–31. doi: 10.1016/j.jneuroim.2003.10.054
- Li, Y., Yu, C., Zhu, W. M., Xie, Y., Qi, X., Li, N., et al. (2010). Triptolide ameliorates IL-10-deficient mice colitis by mechanisms involving suppression of IL-6/STAT3 signaling pathway and down-regulation of IL-17. *Mol. Immunol.* 47, 2467–2474. doi: 10.1016/j.molimm.2010.06.007
- Li, J. M., Zhang, Y., Tang, L., Chen, Y. H., Gao, Q., Bao, M. H., et al. (2016). Effects of triptolide on hippocampal microglial cells and astrocytes in the APP/PS1 double transgenic mouse model of Alzheimer's disease. *Neural. Regen. Res.* 11, 1492–1498. doi: 10.4103/1673-5374.191224
- Liacini, A., Sylvester, J., and Zafarullah, M. (2005). Triptolide suppresses proinflammatory cytokine-induced matrix metalloproteinase and aggrecanase-1 gene expression in chondrocytes. *Biochem. Biophys. Res. Commun.* 327, 320–327. doi: 10.1016/j.bbrc.2004.12.020
- Liang, Z., Leo, S., Wen, H., Ouyang, M., Jiang, W., and Yang, K. (2015). Triptolide improves systolic function and myocardial energy metabolism of diabetic cardiomyopathy in streptozotocin-induced diabetic rats. *BMC Cardiovasc. Disord.* 15, 42. doi: 10.1186/s12872-015-0030-4
- Lin, N., Sato, T., and Ito, A. (2001). Triptolide, a novel diterpenoid triepoxide from Tripterygium wilfordii Hook. f., suppresses the production and gene expression of pro-matrix metalloproteinases 1 and 3 and augments those of tissue inhibitors of metalloproteinases 1 and 2 in human synovial fibroblasts. *Arthritis Rheumatol.* 44, 2193–2200. doi: 10.1002/1529-0131(200109)44:9<2193::aid-art373>3.0.co;2-5
- Lin, N., Liu, C., Xiao, C., Jia, H., Imada, K., Wu, H., et al. (2007). Triptolide, a diterpenoid triepoxide, suppresses inflammation and cartilage destruction in collagen-induced arthritis mice. *Biochem. Pharmacol.* 73, 136–146. doi: 10.1016/j.bcp.2006.08.027
- Liu, H., Liu, Z. H., Chen, Z. H., Yang, J. W., and Li, L. S. (2000). Triptolide: a potent inhibitor of NF- κ B in T-lymphocytes. *Acta Pharmacol. Sin.* 21, 782–786.
- Liu, Q., Chen, T., Chen, H., Zhang, M., Li, N., Lu, Z., et al. (2004). Triptolide (PG-490) induces apoptosis of dendritic cells through sequential p38 MAP kinase phosphorylation and caspase 3 activation. *Biochem. Biophys. Res. Commun.* 319, 980–986. doi: 10.1016/j.bbrc.2004.04.201
- Liu, J., Wu, Q. L., Feng, Y. H., Wang, Y. F., Li, X. Y., and Zuo, J. P. (2005). Triptolide suppresses CD80 and CD86 expressions and IL-12 production in THP-1 cells. *Acta Pharmacol. Sin.* 26, 223–227. doi: 10.1111/j.1745-7254.2005.00035.x
- Liu, Q., Chen, T., Chen, G., Li, N., Wang, J., Ma, P., et al. (2006). Immunosuppressant triptolide inhibits dendritic cell-mediated chemoattraction of neutrophils and T cells through inhibiting Stat3 phosphorylation and NF- κ B activation. *Biochem. Biophys. Res. Commun.* 345, 1122–1130. doi: 10.1016/j.bbrc.2006.05.024
- Liu, Q., Chen, T., Chen, G., Shu, X., Sun, A., Ma, P., et al. (2007). Triptolide impairs dendritic cell migration by inhibiting CCR7 and COX-2 expression through PI3-K/Akt and NF- κ B pathways. *Mol. Immunol.* 44, 2686–2696. doi: 10.1016/j.molimm.2006.12.003

- Liu, C., Zhang, Y., Kong, X., Zhu, L., Pang, J., Xu, Y., et al. (2013). Triptolide prevents bone destruction in the collagen-induced arthritis model of rheumatoid arthritis by targeting RANKL/RANK/OPG signal pathway. *Evid. Based Complement Alternat. Med.* 2013, 626038. doi: 10.1155/2013/626038
- Lu, Y., Wang, W. J., Leng, J. H., Cheng, L. F., Feng, L., and Yao, H. P. (2008). Inhibitory effect of triptolide on interleukin-18 and its receptor in rheumatoid arthritis synovial fibroblasts. *Inflamm. Res.* 57, 260–265. doi: 10.1007/s00011-007-7128-9
- Lv, Q. W., Zhang, W., Shi, Q., Zheng, W. J., Li, X., Chen, H., et al. (2015). Comparison of Tripterygium wilfordii Hook F with methotrexate in the treatment of active rheumatoid arthritis (TRIFRA): a randomised, controlled clinical trial. *Ann. Rheumatol. Dis.* 74, 1078–1086. doi: 10.1136/annrheumdis-2013-204807
- Ma, R., Liu, L., Liu, X., Wang, Y., Jiang, W., and Xu, L. (2013). Triptolide markedly attenuates albuminuria and podocyte injury in an animal model of diabetic nephropathy. *Exp. Ther. Med.* 6, 649–656. doi: 10.3892/etm.2013.1226
- Mao, H., Chen, X. R., Yi, Q., Li, S. Y., Wang, Z. L., and Li, F. Y. (2008). Mycophenolate mofetil and triptolide alleviating airway inflammation in asthmatic model mice partly by inhibiting bone marrow eosinophilopoiesis. *Int. Immunopharmacol.* 8, 1039–1048. doi: 10.1016/j.intimp.2008.03.009
- Matta, R., Wang, X., Ge, H., Ray, W., Nelin, L. D., and Liu, Y. (2009). Triptolide induces anti-inflammatory cellular responses. *Am. J. Transl. Res.* 1, 267–282.
- Navarro-González, J. F., and Mora-Fernández, C. (2008). The role of inflammatory cytokines in diabetic nephropathy. *J. Am. Soc. Nephrol.* 19, 433–442. doi: 10.1681/ASN.2007091048
- Otero, M., and Goldring, M. B. (2007). Cells of the synovium in rheumatoid arthritis. Chondrocytes. *Arthritis Res. Ther.* 9, 220. doi: 10.1186/ar2292
- Park, S. W., and Kim, Y. I. (2013). Triptolide induces apoptosis of PMA-treated THP-1 cells through activation of caspases, inhibition of NF- κ B and activation of MAPKs. *Int. J. Oncol.* 43, 1169–1175. doi: 10.3892/ijo.2013.2033
- Premkumar, V., Dey, M., Dorn, R., and Raskin, I. (2010). MyD88-dependent and independent pathways of Toll-Like Receptors are engaged in biological activity of Triptolide in ligand-stimulated macrophages. *BMC Chem. Biol.* 10, 3. doi: 10.1186/1472-6769-10-3
- Qiu, D., Zhao, G., Aoki, Y., Shi, L., Uyei, A., Nazarian, S., et al. (1999). Immunosuppressant PG490 (triptolide) inhibits T-cell interleukin-2 expression at the level of purine-box/nuclear factor of activated T-cells and NF- κ B transcriptional activation. *J. Biol. Chem.* 274, 13443–13450. doi: 10.1074/jbc.274.19.13443
- Rieder, F., and Fiocchi, C. (2008). Intestinal fibrosis in inflammatory bowel disease - Current knowledge and future perspectives. *J. Crohns Colitis* 2, 279–290. doi: 10.1016/j.crohns.2008.05.009
- Rubinfeld, G. D., Caldwell, E., Peabody, E., Weaver, J., Martin, D. P., Neff, M., et al. (2005). Incidence and outcomes of acute lung injury. *N. Engl. J. Med.* 353, 1685–1693. doi: 10.1056/NEJMoa050333
- Tao, X., Davis, L. S., and Lipsky, P. E. (1991). Effect of an extract of the Chinese herbal remedy Tripterygium wilfordii Hook F on human immune responsiveness. *Arthritis Rheumatol.* 34, 1274–1281. doi: 10.1002/art.1780341011
- Tao, X., Fan, F., Hoffmann, V., Gao, C. Y., Longo, N. S., Zervas, P., et al. (2008). Effective therapy for nephritis in (NZB x NZW)F1 mice with triptolide and triptolide, the principal active components of the Chinese herbal remedy Tripterygium wilfordii Hook F. *Arthritis Rheumatol.* 58, 1774–1783. doi: 10.1002/art.23513
- Tao, Q., Wang, B., Zheng, Y., Li, G., and Ren, J. (2015). Triptolide ameliorates colonic fibrosis in an experimental rat model. *Mol. Med. Rep.* 12, 1891–1897. doi: 10.3892/mmr.2015.3582
- Vaszar, L. T., Nishimura, T., Storey, J. D., Zhao, G., Qiu, D., Faul, J. L., et al. (2004). Longitudinal transcriptional analysis of developing neointimal vascular occlusion and pulmonary hypertension in rats. *Physiol. Genomics* 17, 150–156. doi: 10.1152/physiolgenomics.00198.2003
- Wang, B., Ma, L., Tao, X., and Lipsky, P. E. (2004). Triptolide, an active component of the Chinese herbal remedy Tripterygium wilfordii Hook F, inhibits production of nitric oxide by decreasing inducible nitric oxide synthase gene transcription. *Arthritis Rheumatol.* 50, 2995–2303. doi: 10.1002/art.20459
- Wang, Y., Mei, Y., Feng, D., and Xu, L. (2008). Triptolide modulates T-cell inflammatory responses and ameliorates experimental autoimmune encephalomyelitis. *J. Neurosci. Res.* 86, 2441–2449. doi: 10.1002/jnr.21683
- Wang, Z., Jin, H., Xu, R., Mei, Q., and Fan, D. (2009). Triptolide downregulates Rac1 and the JAK/STAT3 pathway and inhibits colitis-related colon cancer progression. *Exp. Mol. Med.* 41, 717–727. doi: 10.3858/emmm.2009.41.10.078
- Wang, Q., Xiao, B., Cui, S., Song, H., Qian, Y., Dong, L., et al. (2014). Triptolide treatment reduces Alzheimer's disease (AD)-like pathology through inhibition of BACE1 in a transgenic mouse model of AD. *Dis. Model Mech.* 7, 1385–1395. doi: 10.1242/dmm.018218
- Wang, X., Zhang, L., Duan, W., Liu, B., Gong, P., Ding, Y., et al. (2014). Anti-inflammatory effects of triptolide by inhibiting the NF- κ B signalling pathway in LPS-induced acute lung injury in a murine model. *Mol. Med. Rep.* 10, 447–452. doi: 10.3892/mmr.2014.2191
- Wei, D., and Huang, Z. (2014). Anti-inflammatory effects of triptolide in LPS-induced acute lung injury in mice. *Inflammation* 37, 1307–1316. doi: 10.1007/s10753-014-9858-5
- Wei, X., Gong, J., Zhu, J., Wang, P., Li, N., Zhu, W., et al. (2008). The suppressive effect of triptolide on chronic colitis and TNF- α /TNFR2 signal pathway in interleukin-10 deficient mice. *Clin. Immunol.* 129, 211–218. doi: 10.1016/j.clim.2008.07.018
- Wen, H. L., Liang, Z. S., Zhang, R., and Yang, K. (2013). Anti-inflammatory effects of triptolide improve left ventricular function in a rat model of diabetic cardiomyopathy. *Cardiovasc. Diabetol.* 12, 50. doi: 10.1186/1475-2840-12-50
- Wu, Y., Cui, J., Bao, X., Chan, S., Young, D. O., Liu, D., et al. (2006). Triptolide attenuates oxidative stress, NF- κ B activation and multiple cytokine gene expression in murine peritoneal macrophage. *Int. J. Mol. Med.* 17, 141–150.
- Xiao, C., Zhou, J., He, Y., Jia, H., Zhao, L., Zhao, N., et al. (2009). Effects of triptolide from Radix Tripterygium wilfordii (Leigongteng) on cartilage cytokines and transcription factor NF- κ B: a study on induced arthritis in rats. *Chin. Med.* 4, 13. doi: 10.1186/1749-8546-4-13
- Xu, P., Li, Z., Wang, H., Zhang, X., and Yang, Z. (2015). Triptolide inhibited cytotoxicity of differentiated PC12 cells induced by Amyloid-Beta₂₅₋₃₅ via the autophagy pathway. *PloS One* 10, e0142719. doi: 10.1371/journal.pone.0142719
- Xu, H., Zhao, H., Lu, C., Qiu, Q., Wang, G., Huang, J., et al. (2016). Triptolide inhibits osteoclast differentiation and bone resorption *in vitro* via enhancing the production of IL-10 and TGF- β 1 by regulatory T cells. *Mediators Inflammation*, 2016, 8048170. doi: 10.1155/2016/8048170
- Xu, P., Wang, H., Li, Z., and Yang, Z. (2016). Triptolide attenuated injury via inhibiting oxidative stress in Amyloid-Beta₂₅₋₃₅-treated differentiated PC12 cells. *Life Sci.* 145, 19–26. doi: 10.1016/j.lfs.2015.12.018
- Yang, Y., Liu, Z., Tolosa, E., Yang, J., and Li, L. (1998). Triptolide induces apoptotic death of T lymphocyte. *Immunopharmacology* 40, 139–149. doi: 10.1016/s0162-3109(98)00036-8
- Yang, F., Bai, X. J., Hu, D., Li, Z. F., and Liu, K. J. (2010). Effect of triptolide on secretion of inflammatory cellular factors TNF- α and IL-8 in peritoneal macrophages of mice activated by lipopolysaccharide. *World J. Emerg. Med.* 1, 70–74.
- Yang, S., Zhang, M., Chen, C., Cao, Y., Tian, Y., Guo, Y., et al. (2015). Triptolide mitigates radiation-induced pulmonary fibrosis. *Radiat. Res.* 184, 509–517. doi: 10.1667/RR13831.1
- Yang, Y., Ye, Y., Qiu, Q., Xiao, Y., Huang, M., Shi, M., et al. (2016). Triptolide inhibits the migration and invasion of rheumatoid fibroblast-like synoviocytes by blocking the activation of the JNK MAPK pathway. *Int. Immunopharmacol.* 41, 8–16. doi: 10.1016/j.intimp.2016.10.005
- Yuan, X. P., He, X. S., Wang, C. X., Liu, L. S., and Fu, Q. (2011). Triptolide attenuates renal interstitial fibrosis in rats with unilateral ureteral obstruction. *Nephrol. (Carlton)* 16, 200–210. doi: 10.1111/j.1440-1797.2010.01359.x
- Zhang, G., Liu, Y., Guo, H., Sun, Z., and Zhou, Y. H. (2009). Triptolide promotes generation of FoxP3+ T regulatory cells in rats. *J. Ethnopharmacol.* 125, 41–46. doi: 10.1016/j.jep.2009.06.020
- Zhang, G., Chen, J., Liu, Y., Yang, R., Guo, H., and Sun, Z. (2013). Triptolide-conditioned dendritic cells induce allo-specific T-cell regulation and prolong renal graft survival. *J. Invest. Surg.* 26, 191–199. doi: 10.3109/08941939.2012.737408
- Zhang, H., Zhang, X., Ding, X., Cao, W., Qu, L., and Zhou, G. (2014). Effect of secondary lymphoid tissue chemokine suppression on experimental ulcerative colitis in mice. *Genet. Mol. Res.* 13, 3337–3345. doi: 10.4238/2014.April.29.12
- Zhang, H., Gong, C., Qu, L., Ding, X., Cao, W., Chen, H., et al. (2016). Therapeutic effects of triptolide via the inhibition of IL-1 β expression in a mouse model of ulcerative colitis. *Exp. Ther. Med.* 12, 1279–1286. doi: 10.3892/etm.2016.3490
- Zhou, D., and Liu, Y. (2016). Renal fibrosis in 2015: Understanding the mechanisms of kidney fibrosis. *Nat. Rev. Nephrol.* 12, 68–70. doi: 10.1038/nrneph.2015.215

- Zhou, H. F., Liu, X. Y., Niu, D. B., Li, F. Q., He, Q. H., and Wang, X. M. (2005). Triptolide protects dopaminergic neurons from inflammation-mediated damage induced by lipopolysaccharide intranigral injection. *Neurobiol. Dis.* 18, 441–449. doi: 10.1016/j.nbd.2004.12.005
- Zhou, Y., Hong, Y., and Huang, H. (2016). Triptolide attenuates inflammatory response in membranous glomerulo-nephritis rat *via* downregulation of NF- κ B signaling pathway. *Kidney Blood Press Res.* 41, 901–910. doi: 10.1159/000452591
- Zhou, Y. Y., Xia, X., Peng, W. K., Wang, Q. H., Peng, J. H., Li, Y. L., et al. (2018). The Effectiveness and Safety of Tripterygium wilfordii Hook. F Extracts in Rheumatoid Arthritis: A Systematic Review and Meta-Analysis. *Front. Pharmacol.* 9, 356. doi: 10.3389/fphar.2018.00356
- Zhu, K. J., Shen, Q. Y., Cheng, H., Mao, X. H., Lao, L. M., and Hao, G. L. (2005). Triptolide affects the differentiation, maturation and function of human dendritic cells. *Int. Immunopharmacol.* 5, 1415–1426. doi: 10.1016/j.intimp.2005.03.020
- Conflict of Interest:** The authors declare that the research was conducted in the absence of any commercial or financial relationships that could be construed as a potential conflict of interest.
- Copyright © 2019 Yuan, Li, Lu, Zhu, Jiang, Wang, Huang and Xu. This is an open-access article distributed under the terms of the Creative Commons Attribution License (CC BY). The use, distribution or reproduction in other forums is permitted, provided the original author(s) and the copyright owner(s) are credited and that the original publication in this journal is cited, in accordance with accepted academic practice. No use, distribution or reproduction is permitted which does not comply with these terms.



Alleviation of Synovial Inflammation of Juanbi-Tang on Collagen-Induced Arthritis and TNF-Tg Mice Model

Tengteng Wang^{1,2†}, Qingyun Jia^{3†}, Tao Chen^{1,2,4†}, Hao Yin⁵, Xiaoting Tian⁵, Xi Lin⁶, Yang Liu^{1,2,4}, Yongjian Zhao^{1,2,4}, Yongjun Wang^{1,2,4}, Qi Shi^{1,2,4}, Chenggang Huang⁵, Hao Xu^{1,2,4*} and Qianqian Liang^{1,2,4*}

OPEN ACCESS

Edited by:

Xiaojuan He,
China Academy of Chinese Medical
Sciences, China

Reviewed by:

Youhua Wang,
Nantong University, China
Fang Liu,
University of New South Wales,
Australia

*Correspondence:

Qianqian Liang
liangqianqiantcm@126.com
Hao Xu
hoxu@163.com

[†]These authors have contributed
equally to this work

Specialty section:

This article was submitted to
Ethnopharmacology,
a section of the journal
Frontiers in Pharmacology

Received: 01 July 2019

Accepted: 14 January 2020

Published: 14 February 2020

Citation:

Wang T, Jia Q, Chen T, Yin H, Tian X,
Lin X, Liu Y, Zhao Y, Wang Y, Shi Q,
Huang C, Xu H and Liang Q (2020)
Alleviation of Synovial Inflammation of
Juanbi-Tang on Collagen-Induced
Arthritis and TNF-Tg Mice Model.
Front. Pharmacol. 11:45.
doi: 10.3389/fphar.2020.00045

¹ Longhua Hospital, Shanghai University of Traditional Chinese Medicine, Shanghai, China, ² Institute of Spine, Shanghai University of Traditional Chinese Medicine, Shanghai, China, ³ Second Ward of Trauma Surgery Department, Linyi People's Hospital, Linyi, China, ⁴ Key Laboratory of Theory and Therapy of Muscles and Bones, Ministry of Education, Shanghai University of Traditional Chinese Medicine, Shanghai, China, ⁵ Shanghai Institute of Materia Medica, Chinese Academy of Sciences, Shanghai, China, ⁶ Department of Pathology and Laboratory Medicine, University of Rochester, Rochester, NY, United States

Rheumatoid arthritis (RA) is a chronic autoimmune disease that is primarily characterized by synovial inflammation. In this study, we found that a traditional Chinese decoction, Juanbi-Tang (JBT), JBT attenuated the symptoms of collagen-induced arthritis (CIA) mice and in tumor necrosis factor transgenic (TNF-Tg) mice by attenuating the arthritis index and hind paw thickness. According to histopathological staining of ankle sections, JBT significantly decreased the area of inflammation and reduced bone destruction of ankle joints in both these two types of mice. Moreover, decreased tartaric acid phosphatase-positive osteoclasts were observed in the JBT group compared with those found in the control group. We also revealed that JBT suppressed monocytes and T cells as well as the production of CCL2, CCR6, and CXCR3 ligands. We next used high-performance liquid chromatography to investigate the components and pharmacological properties of this classical herbal medicine in traditional Chinese medicine. Based on network pharmacology, we performed computational prediction simulation of the potential targets of JBT, which indicated the NF-kappa B pathway as its target, which was confirmed in vitro. JBT suppressed the production of pro-inflammatory cytokines including interleukin-6 (IL-6) and IL-8, and inhibited the expression of matrix metalloproteinase 1 in fibroblast-like synoviocytes derived from RA patients (MH7A cells). Furthermore, JBT also suppressed the phosphorylation of p38, JNK, and p65 in TNF- α -treated MH7A cells. In summary, this study proved that JBT could inhibit synovial inflammation and bone destruction, possibly by blocking the phosphorylation of NF-kappa B pathway-mediated production of proinflammatory effectors.

Keywords: Juanbi-Tang, rheumatoid arthritis, collagen-induced arthritis, synoviocyte, tumor necrosis factor

BACKGROUND

Rheumatoid arthritis (RA), one of the major contributors to disability globally (Vos et al., 2017), is characterized by synovitis, pannus formation, adjacent bone erosion, and joint destruction (Rana et al., 2018), although its etiology remains largely unclear. Among the potential cellular participants in RA, fibroblast-like synoviocytes (FLSs) play a critical role by regulating the secretion of inflammatory mediators and expression of matrix metalloproteinases (MMPs), which cause changes in chondrocyte metabolism and matrix degradation (Korb-Pap et al., 2016). Treatment targeting RA-FLSs has been recognized as a novel approach with the potential to improve clinical outcomes while having limited impact on systemic immunity (Wangyang et al., 2018; Zhang and Zhou, 2018). Tumor necrosis factor- α (TNF- α) acts as a primary cytokine in the pathology of RA. TNF- α can rapidly induce MMP gene expression in cultured FLSs. Its inhibitors provide other options for RA patients in whom treatment with conventional disease-modifying anti-rheumatic drugs (DMARDs) has failed (Luchetti et al., 2017; Ornbjerg, 2018). Given its immunogenicity and high cost, an increasing number of alternatives to DMARDs are being explored (Sun et al., 2018).

Juanbi-Tang (JBT), traditional Chinese herbal compounds, has been widely used for the treatment of RA in China. It has proven to relieve the symptoms of arthritis and activate joint function of patients (Li, 2011; Li and Niu, 2011; Ni and Fu, 2014). In addition, JBT has been reported to reduce serum TNF- α and IL-1 levels in rats with RA (Yu et al., 2015), downregulate IgG in serum (Cheng et al., 2018) and prostaglandin E receptor 4 in synovial tissue (Xu et al., 2017), and relieve acute and chronic ear inflammation in rats (Niu et al., 2018a). It was also demonstrated that JBT could regulate immune balance by reducing nature killer cells and promoting T-reg cells of CIA rats (Niu et al., 2018b), and reduce the cAMP level in T lymphocytes in rats with adjuvant arthritis (Xu et al., 2018). However, the mechanism by which JBT reduces inflammatory cytokines and chemokines warrants further research.

With the increasing investment in research on traditional Chinese herbal medicine, it has become increasingly important to determine the efficacy, toxicology, and therapeutic targets of such medicine, for which network pharmacology is a useful approach (Jiang et al., 2015).

Our study involved a search for as many as 44 active components of JBT by high-performance liquid chromatography–quadrupole time-of-flight mass spectrometry (HPLC–Q-TOF). By applying a network pharmacology method, we also enumerated the possible targets of the herbal components to look for their pharmacological effects. We further performed experiments to verify these predictions.

MATERIALS AND METHODS

Preparation of JBT

Herbs in JBT (Table 1) were authenticated by a pharmacognosist of Longhua Hospital affiliated to Shanghai University of Traditional Chinese Medicine, in accordance with standard protocols. In line with standard methods of Chinese Pharmacopoeia, all crude drugs except *Cinnamomi cortex* were soaked in 12 volumes of water for 40 min and boiled for 40 min (*C. cassia* was added at 35 min). The extracts were filtered, and the filter residue was boiled in eight volumes of water for another 40 min and the solution was filtered again. Both batches of the filtrate of the drugs were mixed and concentrated to 0.557 kg/L, which were prepared for intragastric administration. The filtrate was vacuum-freeze-dehydrated, prepared to treat cells after high-speed centrifugation three times, and stored at -80°C overnight.

Other Agents

Methotrexate (MTX, cat. #100138) was purchased from Shanghai Oriental Medicine Science and Technology Industry Co., Ltd. (Shanghai, China); bovine type II collagen (cat. #20021), Freund's complete adjuvant (CFA, cat. #7001), and Freund's incomplete adjuvant (IFA, cat. #7002) were from Chondrex (Redmond, WA, USA); eosin (Sigma, cat. #E4009-5G), hematoxylin (Sigma, cat. #H-3136), Alcian Blue (Sigma, cat. #A5268), orange G (Sigma, cat. #1936-15-8), phloxine B (Sigma, cat. #18472-87-2), ammonium aluminum sulfate (Sigma, cat. #A-2140), sodium iodate (Sigma, cat. #S-4007), tartaric acid (Sigma-vetec, cat. #87-69-4), phenol AS-BI phosphate (Sigma, cat. #1919-91-1), phosphate buffered saline (PBS) (Medicago, cat. #09-2052-100), MCP-1 polyclonal antibody (CCL2) (ABclonal, cat. #A7277), CXCR3 polyclonal antibody (ABclonal, A2939), p44/42 MAPK (Erk1/2) (137F5) (rabbit

TABLE 1 | Prescription of Juanbi-Tang (JBT).

Latin name	Amount (g)	Lot No.	Place of origin	Company
Radix angelicae pubescentis	3 g	140421-1	Hubei, China	Shanghai WanShiCheng Chinese Medicine Co. Ltd.
Notopterygium incisum	3 g	140529	Sichuan, China	Shanghai Hongqiao traditional Chinese medicine decoction pieces Co., Ltd.
Cinnamomum cassia Presl	1.5 g	140326-1	Guangxi, China	Shanghai WanShiCheng Chinese Medicine Co. Ltd.
Gentiana macrophylla Pall.	3 g	140620	Gansu, China	Shanghai Hongqiao traditional Chinese medicine decoction pieces Co., Ltd.
Angelica sinensis (Oliv.) Diels	9 g	140627	Gansu, China	Shanghai Kangqiao Chinese Herbal Medicine Co. Ltd.
Ligusticum chuanxiong Hort.	2.1 g	140518	Sichuan, China	Shanghai Kangqiao Chinese Herbal Medicine Co. Ltd.
Glycyrrhiza uralensis Fisch.	1.5 g	140616	Xinjiang, China	Shanghai Kangqiao Chinese Herbal Medicine Co. Ltd.
Caulis Piperis Kadsurae	6 g	131106-1	Yunnan, China	Shanghai WanShiCheng Chinese Medicine Co. Ltd.
Morus alba L.	9 g	140624	Zhejiang, China	Shanghai Hongqiao traditional Chinese medicine decoction pieces Co., Ltd.
Olibanum	2.4 g	LY1303120	Ethiopia	Shanghai Hua Yu Pharmaceutical Co., Ltd.
Radix Aucklandiae	2.4 g	2014061004	Yunnan, China	Shanghai Hua Pu Chinese medicine decoction pieces Co., Ltd.

mAb, CST, cat. #4695s), recombinant anti-CD3 antibody [SP162] (Abcam, cat. #ab135372), anti-CCR6 (Abcam, cat. #ab78429), F4/80 antibody (GeneTex, cat. #GTX26640), iNOS polyclonal antibody (Thermo Fisher Scientific, cat. #PA1-036), Diaminobenzidine (DAB) Histochemistry Kit (Thermo Fisher Scientific, cat. #D22187), DAB Peroxidase (HRP) Substrate Kit (with nickel) (VECTOR, cat. #SK-4100), VECTASTAIN® Elite® ABC HRP Kit (VECTOR, cat. #PK-6100), goat anti-rat IgG (H+L) antibody (KPL, cat. #072-03-16-06), and goat anti-rabbit IgG (H+L) antibody (KPL, cat. #03-15-06) were also obtained. In addition, MMP-1 antibodies (cat. #ab137332) and ELISA kit (cat. #ab215083), TNF α (cat. #EMC102a), IL-1 β (cat. #EMC001b), IL-6 (cat. #EMC004), IL-8 (cat. #EMC104), and ELISA kit were purchased from Neobioscience (Shanghai, China); recombinant human tumor necrosis factor (TNF- α ; PeproTech, cat. #300-1A), anti-phospho-p38 (CST, cat. #4511), anti-phospho-ERK (cat. #4370), anti-phospho-JNK (CST, cat. #4255), anti-phospho-p65 (CST, cat. #3033), β -actin (CST, cat. #8457), NF-kappa B p65 (D14E12) XP® Rabbit mAb (CST, cat. #8242s), ERK1/ERK2 polyclonal antibody (ABclonal, cat. #A16686), JNK1 polyclonal antibody (ABclonal, cat. #A0288), and SAPK/JNK antibody (CST, cat. #9252s); trypsin digestion solution (Leagene, cat. #IH0310), goat anti-rabbit IgG H&L (Alexa FluorR488, Abcam, cat. #ab150077), actinomycin D (Sigma, cat. #A1410), 4',6-diamidino-2-phenylindole (DAPI, Sigma, cat. #D9564), cell culture medium, fetal bovine serum, and trypsin were obtained from Gibco (Grand Island, NE, USA).

Model Establishment and Evaluation of Collagen-Induced Arthritis

Specific pathogen-free, DBA/1J male mice (7–8-week-old) were purchased from Vital River (Beijing, China). The CIA model was established in accordance with a previously reported protocol (Brand et al., 2007). Briefly, the mice were immunized intradermally with 100 mg of bovine type II collagen emulsified in complete Freund's adjuvant. To ensure a high incidence of RA induction in the CIA model, a booster immunization of bovine type II collagen emulsified in incomplete Freund's adjuvant was used at 21 d after the primary immunization. Typically, the first signs of arthritis appeared in this model at 21–28 d after immunization. CIA was considered to have successfully developed when swelling was observed in at least one paw.

TNF-Tg Mice

The 3647 line of TNF-Tg mice in a C57BL/6 background was originally obtained from Dr. G. Kollias's lab (Keffer et al., 1991) (Institute of Immunology, Alexander Fleming Biomedical Sciences Research Center, Vari, Greece) and was maintained as heterozygotes by backcrossing with C57BL/6 mice. Non-transgenic littermates were used as aged-matched wild-type (WT) controls. This line of TNF-Tg mice carries one copy of the human TNF transgene, overexpresses human TNF- α , and develops erosive polyarthritis with many characteristics also observed in RA patients (Jiang et al., 2015). TNF-Tg mice develop mild ankle joint inflammation and bone erosion at

3 months old, which become more severe with aging (Li et al., 2004; Guo et al., 2009; Chen et al., 2016). Therefore, in this study, we chose 3-month-old TNF-Tg mice and WT littermates.

Experimental Groups

Forty DBA/1J mice were randomly divided into four groups (10 mice/group): group 1, control (normal, nonimmunized and untreated); group 2, CIA-Veh [positive control, PBS, 0.2 ml/day, intraperitoneally]; group 3, CIA-MTX (MTX, 0.1 mg/kg/3 d, intraperitoneally); and group 4, CIA-JBT (JBT, 12 g/kg/day, orally). All of the mice from these groups received additional treatments between day 22 and day 50.

Seven 3-month-old TNF-Tg mice were orally administered JBT (12 g/kg) or the same volume of physiological saline once every day for 12 weeks. Seven 3-month-old WT littermates were treated with the same volume of physiological saline as a negative control. Twelve weeks later, all mice were sacrificed and their ankle joints were harvested for histological staining and data analysis.

All animal procedures were approved by Longhua Hospital Animal Ethics Committee and were performed in accordance with the Guiding Principles for the Care and Use of Laboratory Animals approved by the Animal Regulations of National Science and Technology Committee of China.

Arthritis Assessment

After the CIA model had been successfully established, we measured the arthritis index and hind paw thickness every 5 d in a blinded manner. Each paw was scored on a scale of 0–4 by visual evaluation as follows: 0, no evidence of erythema and swelling; 1, erythema and mild swelling confined to the tarsals or ankle joint; 2, erythema and mild swelling extending from the ankle to the tarsals; 3, erythema and moderate swelling extending from ankle to metatarsal joints; and 4, erythema and severe swelling encompassing the ankle, foot, and digits, or ankylosis of the limb. The final score for each mouse was the sum of the scale score from four paws. TNF-Tg mice were measured the deformity score every week in a blinded manner for 12 weeks. Each paw was scored on a scale of 0–4 by visual evaluation as follows: 0, no deformity; 1, mild deformity; 2, obvious deformity; 3, moderate deformity; 4, severe deformity. The final score for each mouse was the sum of the scale score from four paws. Thickness of the ankle was measured separately by two individuals with digital calipers placed across the ankle joint at its widest point.

Histopathological Examination

After final treatment, the mice were sacrificed. Ankle joints were carefully dissected and cleared of adjacent muscle, followed by being fixed in 4% paraformaldehyde at room temperature for 48 h, decalcified in 10% EDTA for 20 d, dehydrated through a series of ethanol, and embedded in paraffin. A total of 30 4- μ m-thick consecutive sections from one ankle joint in the sagittal position were collected and mounted on common slides, and were divided into three levels. Each level was 40 μ m from the previous level. One section from each of the three levels was subjected to hematoxylin and eosin (H&E) staining, Alcian Blue/

Orange G (ABOG) staining, tartrate-resistant acid phosphatase (TRAP) staining, and immunofluorescence and immunohistochemical staining. After the full-length scan by Olympus VS120-SL, the target area of the ankle talus was analyzed with Olympus VS120 image analysis software. We traced the area of interest, which was then measured by the software (in mm²). The inflammatory area (multinuclear dark zone) and bone area (astragalus bone zone) were analyzed on HE-stained sections. Cartilage area (blue zone) at astragalus bone was measured on ABOG-stained sections, and TRAP-positive area was evaluated on TRAP-stained sections. The data are presented as the mean from three levels from each ankle joint sample.

Micro-Computed Tomography (Micro-CT) Analysis

After excision from DBA/1J mice, right legs were fixed in 4% paraformaldehyde for 24 h, washed in PBS for 2 h, and then immersed in 75% ethanol, until a micro-CT (Scanco VIVA CT80, SCANCO Medical AG, Bassersdorf, Zurich, Switzerland) scan. The X-ray tube voltage was 55 kV and tube current was 72 μ A, with a pixel size of 9 μ m and 200 ms integration time. The cross-sectional images were then reconstructed and realigned in 3D. A density threshold was set from 370 to 1,000 as bone using the μ CT Evaluation program V6.6 (Scanco Medical AG). A stack of 340–441 cross sections was reconstructed, with an interslice distance of 1 pixel (15.6 μ m), corresponding to a reconstructed height of 5.3–6.9 mm, recreating the ankle joint.

HPLC–Q-TOF of JBT

Characterization of the components of JBT was performed by a 1260 series HPLC instrument (Agilent, Waldbronn, Germany) connected to an Agilent 6530 Q-TOF mass spectrometer (Agilent Corp., USA) equipped with Dual Agilent Jet Stream Electrospray Ionization (Dual AJS ESI). The operating parameters were optimized in both positive and negative modes, as follows: capillary voltage, 3,500 V for ESI mode and 4000 V for ESI+ mode; nozzle voltage, 500 V; fragmentor, 110 V; nebulizer, 45 psi; drying gas temperature, 300°C; drying gas flow rate, 6 L/min; sheath gas temperature, 320°C; and sheath gas flow rate, 12 L/min. Separation of compounds in JBT was carried out on an ACE Excel 3 Super C18 column (100 mm \times 2.1 mm; Advanced Chromatography Technologies Ltd., Aberdeen, Scotland). The mobile phase was composed of solvent A (water containing 0.1% formic acid) and solvent B (acetonitrile containing 0.1% formic acid), with a flow rate of 0.35 ml/min. Gradient elution was performed as follows: 0–30 min, 95%–23% A; 30–40 min, 23%–15% A; 40–45 min, 15%–10% A; 45–50 min, 10%–5% A; 50–55 min, 5% A; 55–56 min, 5%–95% A; and 56–66 min, 95% A. The column temperature was maintained at 40°C. System operations and data analysis were conducted on Masshunter Workstation software (Agilent Technologies, USA).

Network Pharmacological Analysis of JBT

The 44 active chemical components deriving from 11 components of JBT were collected by HPLC–MS. The Chinese

Medicine System Pharmacology Database and Analysis Platform and Swiss Target Prediction databases were used to screen the targets of these 44 compounds. The DisGeNET database was used to find the targets related to RA. Cytoscape 3.6.0 was used to analyze the targets of JBT in the treatment of RA, and the DAVID database was used to analyze the specific mechanism of action of JBT in the treatment of RA. Twenty-four of the pharmacological components (see **Figure 3** for the chemical formulas) that satisfied the above conditions were selected. Then, we used Drug Bank, TCMID, Gene Cards, and STITCH databases to validate 194 RA targets to construct a compound target network using Cytoscape 3.3.0 software. To explain the participation of targets in the progression of RA, we established a network between target and function using Cytoscape 3.3.0. Multiple targets presaged an integral function of JBT in RA and shared the synergistic targets of the different compounds.

Cell Culture

MH7A, a human RA-FLS cell line (Miyazawa et al., 1998; Jia et al., 2019), was a gift from the Chinese Academy of Sciences, Shenzhen, which had been purchased from the Riken Cell Bank (Tsukuba, Japan). Cells were maintained in Roswell Park Memorial Institute 1640 medium (Hyclone, USA), supplemented with 10% fetal bovine serum (Gibco, USA) and penicillin/streptomycin (1:100; Sigma, St. Louis, MO), in a humidified atmosphere of 95% air and 5% CO₂ in an incubator at 37°C.

Cell Viability Assay

Cell viability was determined using the CCK-8 assay. Briefly, MH7A cells were seeded in 96-well culture plates at 5000 cells/well for 72 h and then treated with various concentrations of JBT (0, 0.25, 0.5, 1, and 2 mg/ml) for 24 h. Then, CCK-8 (Dojindo, Japan) was added and incubated at 37°C for 1.5 h. The optical density was detected at 450 nm with a microplate reader (BioTek Synergy 3).

Quantitative Real-Time PCR Analysis

MH7A cells were pretreated with various concentrations of JBT lyophilized powder (0, 0.5, 1, and 1.5 mg/ml) for 2 h, and then incubated for another 24 h with or without stimulation by 10 ng/ml TNF- α . Total RNA was extracted using Trizol reagent, in accordance with the manufacturer's instructions, and each sample was reverse-transcribed using the cDNA synthesis kit, in accordance with the manufacturer's protocol. Real-time PCR analysis was performed using SYBR Green PCR Premix Ex Taq II reagents on a CFX96 real-time system (Thermo, USA). Relative gene expression was calculated by the $^{-\Delta\Delta C_t}$ method. The sequence of primers (forward and reverse) was as follows: actin, 5'-CGTTGACATCCGTAAAGACC-3' and 5'-TAGGAGCCAGAGCAGTAATC-3'; IL-6, 5'-TGTATGAACAACGATGATGCACTT-3' and 5'-ACTCTGGCTTTGTCTTTCTTGTATCT-3'; IL-8, 5'-GGTGCAAGTTTTGCCAAGGAG-3' and 5'-TTCCTTGGGGTCCAGACAGA-3'; and MMP-1, 5'-CTCAATTTCACTTCTGTTTTCTG-3' and 5'-CATCTCTGTCCGCAATTCGT-3'. The efficiencies of the

primers were 90%-95%. The PCR reaction system was 20 μ l: SYBR 10 μ l, water 7 μ l, cDNA 1 μ l, front and rear primers 1 μ l. The thermocycling condition: 95°C for 5 min, 95°C for 30 sec \rightarrow 60°C for 30 sec \rightarrow 72°C for 40 sec, 30 cycles, 72°C for 7 min, and stored at 4°C.

Enzyme-Linked Immunosorbent Assay

MH7A cells were seeded in six-well plates (1×10^6 cells/well) for 24 h, and then pretreated or left untreated with the indicated concentrations of JBT for 2 h, followed by incubation for another 24 h with or without TNF- α (10 ng/ml). Cell culture supernatants were collected and stored at -80°C until analysis. The concentrations of the cytokines in culture supernatants were determined by ELISA using a commercial kit, in accordance with the manufacturer's instructions.

Western Blot Analysis

MH7A cells were treated with or without TNF- α (10 ng/ml) in the presence or absence of JBT (0.5, 1, and 1.5 mg/ml) for 24 or 0.5 h. The protein was collected, and 30 μ g of it from each sample was separated by 10% SDS-PAGE and transferred to a polyvinylidene fluoride membrane. After blocking with 5% bovine serum albumin in TBST at room temperature for 1 h, the membranes were incubated with the corresponding primary antibodies overnight at 4°C. After washing with TBST three times, the membranes were incubated with the secondary antibodies. Proteins were scanned and analyzed by the chemiluminescence system and autoradiography.

Statistical Analysis

The data are presented as mean \pm standard deviation (SD) from at least three separate experiments. Statistical analysis was performed using GraphPad Prism 7.0 software (GraphPad, La Jolla, CA, USA). One-way ANOVA followed by Dunnett's t-test was used to determine the significance of differences between groups. In cases of three groups treated at different times points, we applied two-way ANOVA for comparison. We used Fisher's test in the analysis of categorical data. $P < 0.05$ was considered statistically significant.

RESULTS

JBT Clearly Attenuated Symptoms, Synovitis, Cartilage, and Bone Damage of CIA Mice

To investigate the therapeutic effects of JBT on RA *in vivo*, we established a CIA mouse model. Compared with the WT group, CIA mice showed higher scores for the arthritis index and greater hind paw thickness. JBT treatment had improved the function of ankle by attenuating the arthritis index (Figure 1A) and hind paw thickness (Figure 1B). HE, ABOG, and TRAP staining at ankle joints was scanned using an Olympus VS120-SL (Figure 1C). Treatment of mice with JBT was initiated at 22 d after the primary immunization. Both JBT and MTX treatments had positive effects on attenuating the inflammatory area

(Figure 1D) and restoring bone (Figure 1E) and cartilage area (Figure 1F) of CIA mice. JBT treatment significantly reduced the number of osteoclasts with TRAP-positive staining (Figure 1G). Micro-CT showed that the JBT group, as well as the MTX group, suffered less bone damage in their ankle joints than the control group (Figure 1H). These results indicated that JBT effectively inhibited the development of arthritis in CIA mice.

JBT Attenuated Symptoms, Inflammatory Synovial Volume and Bone Erosion at Ankle Joint of TNF-Tg Mice

To investigate the effect of JBT on arthritis, TNF-Tg mice were orally administered JBT once a day for 12 weeks. Compared with the WT group, TNF-Tg mice showed higher deformity score and greater hind paw thickness. JBT treatment had improved the function of ankle by attenuating the deformity score (Figure 2A) and hind paw thickness (Figure 2B). HE, ABOG, and TRAP staining at the ankle joints indicated normal integrity of the ankle joint without synovial inflammation and bone erosion in WT mice (Figure 2C). In TNF-Tg mice, there was a large amount of synovial inflammation in the ankle joint, with the presence of a large number of TRAP-positive osteoclasts, and severe bone erosion was observed at the ankle joint, while cartilage with Alcian Blue-positive staining almost disappeared. JBT treatment significantly reduced the inflammatory synovial volume, bone erosion (Figures 2D, E), and osteoclasts positively stained for TRAP (Figure 2F), while increasing cartilage area at the ankle joints (Figure 2G). Micro-CT showed that the JBT group suffered less bone damage in the ankle joints (Figure 2H). These results indicated that JBT effectively inhibited the development of arthritis in TNF-Tg mice.

JBT Suppressed Inflammatory Cell Infiltration and the Production of CCL2, CXCR3, and CCR6

To further investigate the effect of JBT on inflammatory cell infiltration, immunofluorescence staining was performed to mark macrophages with F4/80/iNOS and T cells with CD3. Immunohistochemical staining was performed to label CCL2, CXCR3 and CCR6. The results showed that JBT inhibited F4/80/iNOS+ macrophages (Figures 3A, B and Supplementary 5A, B) and CD3+ T cells (Figures 3C, D) in the ankle joints of CIA and TNF-Tg mice, and reduced the expression of CCL2, CXCR3, and CCR6 (Figures 3E, F and Supplementary 5C, D).

HPLC-Q-TOF Detected 44 Compounds in JBT Decoction

With the aid of accurate masses measured by HPLC-Q-TOF, a total of 44 detected peaks were identified in the JBT decoction, as shown in Table 2. Among them, there were 24 compounds (Figure 4 and Supplementary 4) definitively identified by comparison with the standard compounds, while the remaining 20 compounds were tentatively characterized according to their formula, retention time, and fragmentation patterns.

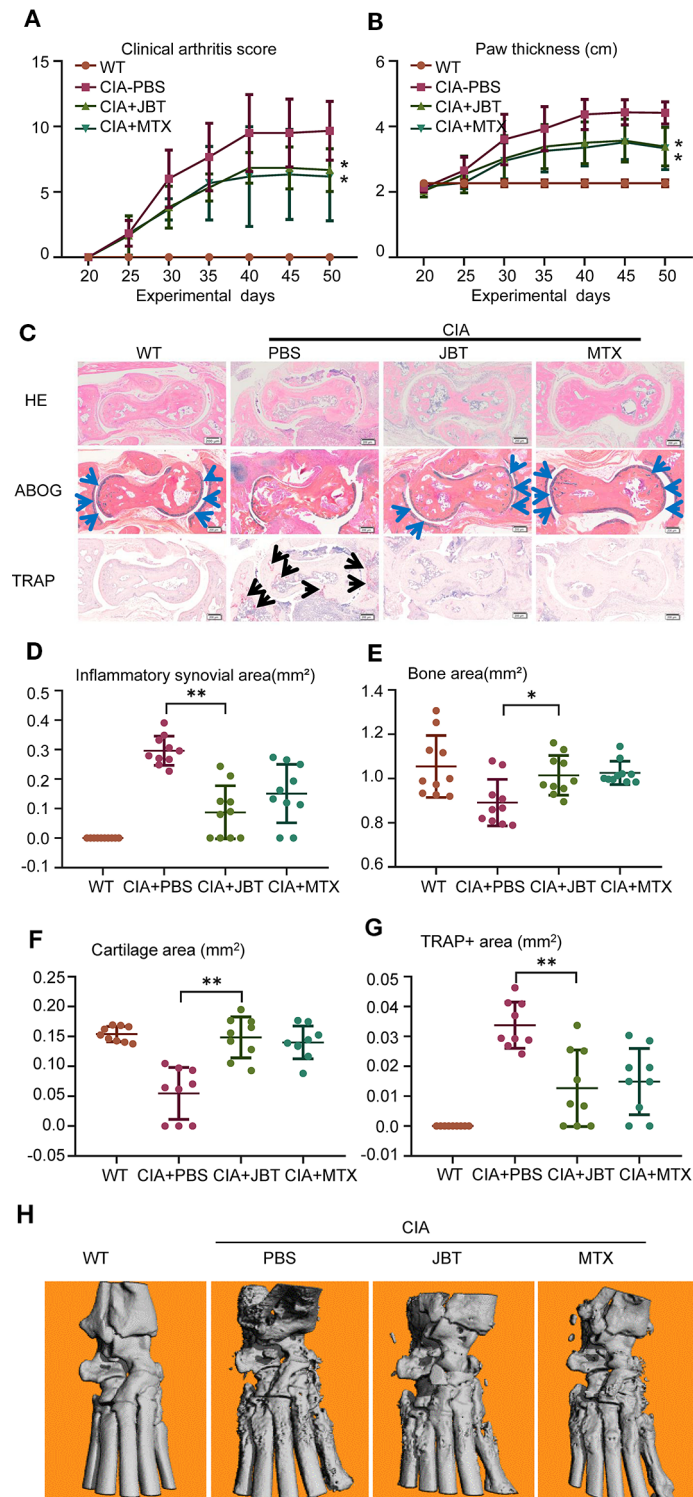


FIGURE 1 | Juanbi-Tang (JBT) clearly attenuated symptoms, synovitis, cartilage, and bone damage of collagen-induced arthritis (CIA) mice. The arthritis index **(A)** and hind paw thickness **(B)** of CIA mice were scored and recorded every 5 d in a blinded manner. **(C)** Hematoxylin–eosin staining, ABOG staining, and TRAP staining were used to analyze the ankle joints of WT and CIA mice after treatment for 12 weeks. Bar, 200 μ m. **(D)** Histomorphometric assessment of inflammatory synovial volume area. **(E)** Histomorphometric assessment of bone area. **(F)** Histomorphometric assessment of cartilage area. **(G)** Histomorphometric assessment of TRAP+ osteoclast area. **(H)** Micro-CT of ankle joints. Results are shown as mean \pm SEM ($n = 10$). * $p < 0.05$, ** $p < 0.01$ versus CIA+PBS group.

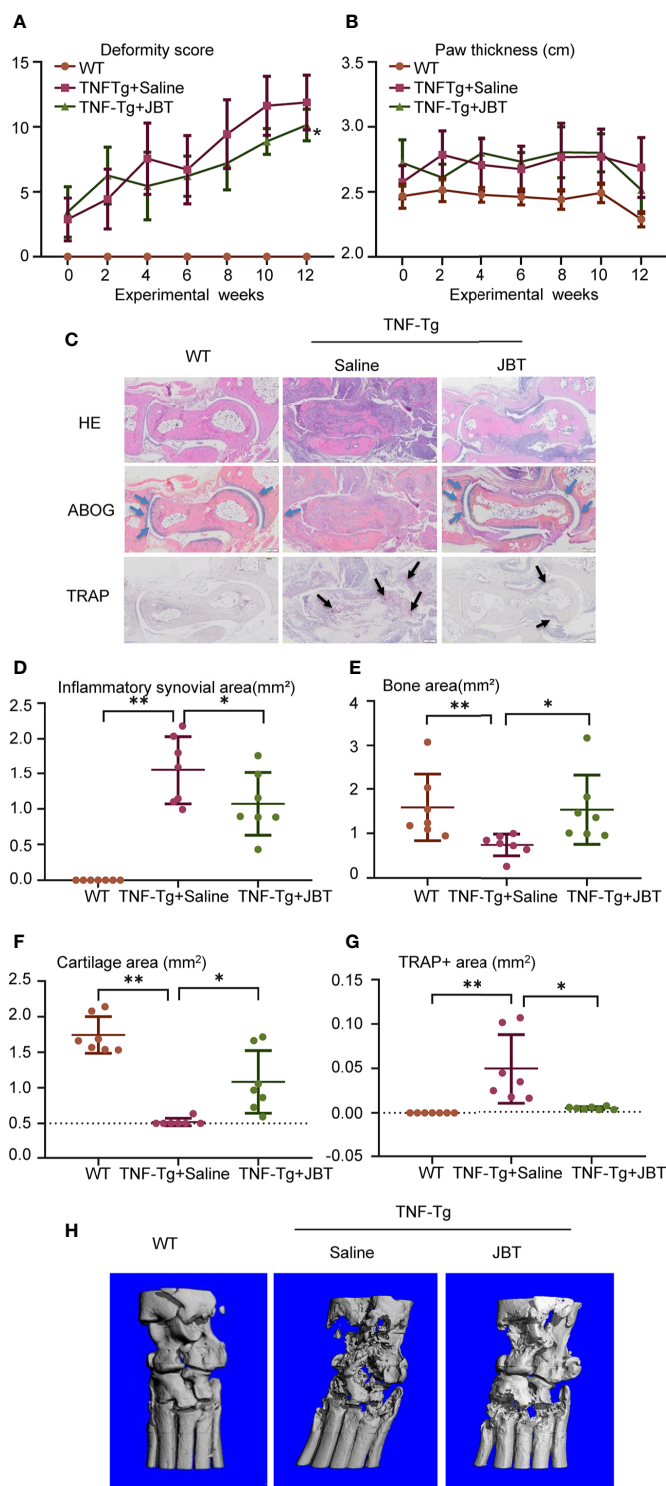


FIGURE 2 | Juanbi-Tang (JBT) attenuated symptoms, inflammatory synovial volume and bone erosion at ankle joint of tumor necrosis factor transgenic (TNF-Tg) mice. The deformity score **(A)** and hind paw thickness **(B)** of TNF-Tg mice and WT littermates were scored and recorded every week in a blinded manner. **(C)** Hematoxylin–eosin staining, ABOG staining, and TRAP staining were used to analyze the ankle joints of WT and TNF-Tg mice, which were treated with saline or JBT for 12 weeks. Bar, 200 μ m. **(D)** Histomorphometric assessment of inflammatory synovial volume area. **(E)** Histomorphometric assessment of bone area. **(F)** Histomorphometric assessment of cartilage area. **(G)** Histomorphometric assessment of TRAP+ osteoclast area. **(H)** Micro-CT of ankle joints. Results are shown as mean \pm SEM, for 6–8 legs per group. Three sections per mice were analyzed. ** $p < 0.01$ versus TNF-Tg + saline, * $p < 0.05$ versus TNF-Tg + saline.

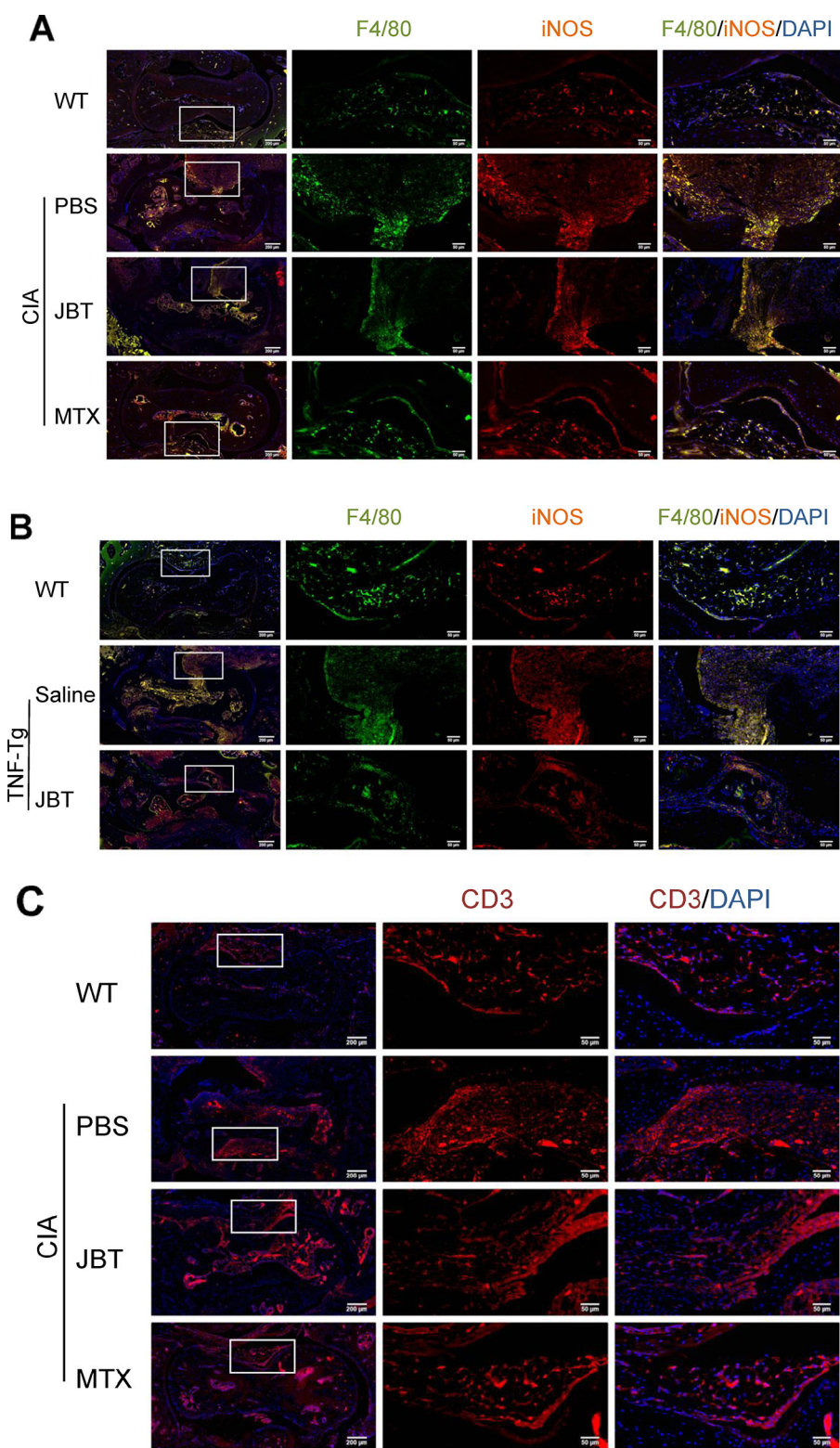


FIGURE 3 | Continued

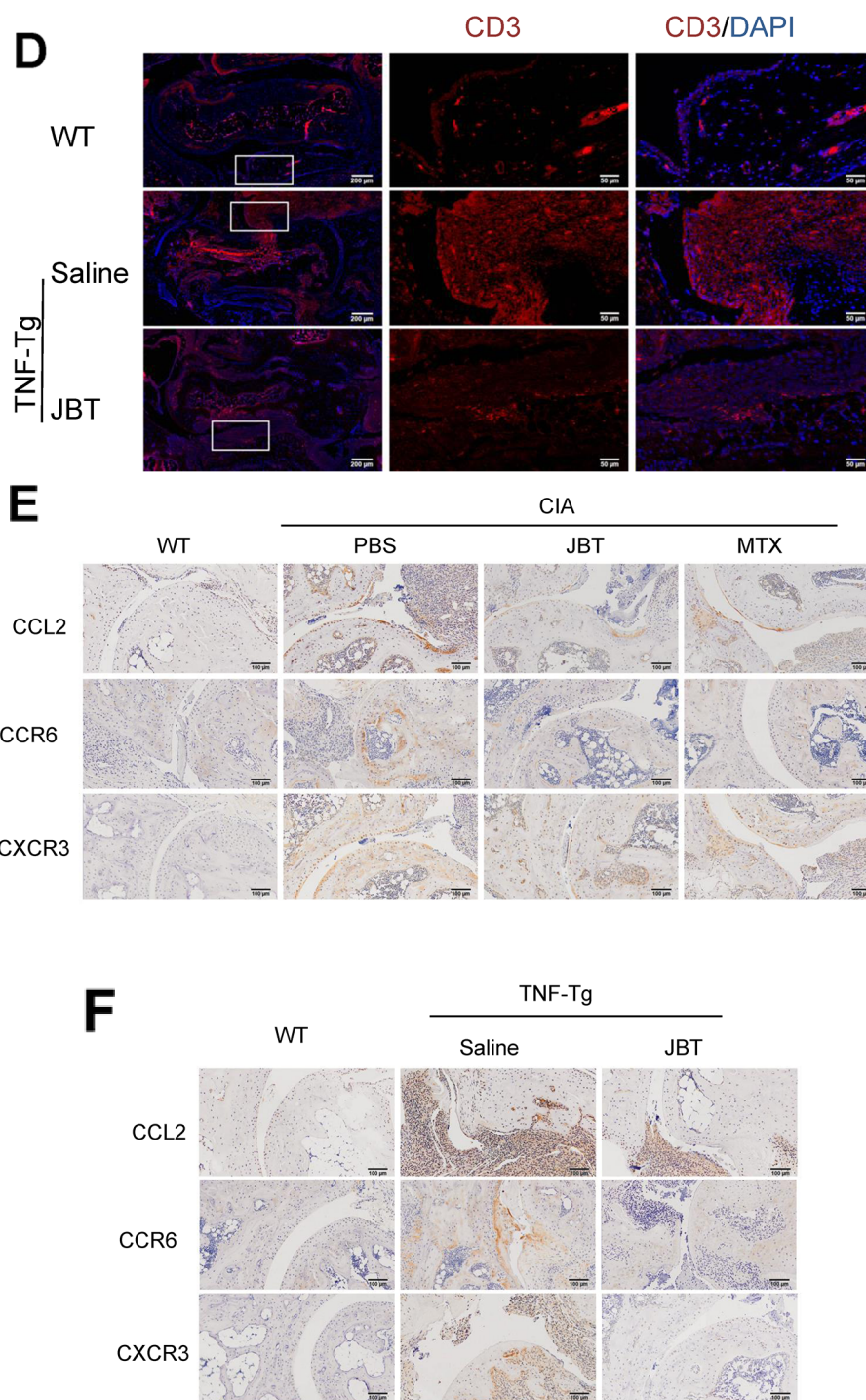


FIGURE 3 | Juanbi-Tang (JBT) suppressed inflammatory cells and production of CCL2, CXCR3, and CCR6. **(A)** Immunofluorescence staining with F4/80/iNOS marking macrophages of collagen-induced arthritis (CIA) mice. **(B)** Immunofluorescence staining with F4/80/iNOS marking macrophages of tumor necrosis factor transgenic (TNF-Tg) mice and WT littermates. **(C)** Immunofluorescence staining with CD3 labeling T cells of CIA mice. **(D)** Immunofluorescence staining with CD3 labeling T cells of TNF-Tg mice and WT littermates. **(E)** Immunohistochemical staining with CCL2, CXCR3, and CCR6 of CIA mice. **(F)** Immunohistochemical staining with CCL2, CXCR3, and CCR6 of TNF-Tg mice and WT littermates.

TABLE 2 | The mass information and source of identified compounds in Juanbi-Tang (JBT) by high-performance liquid chromatography quadrupole time-of-flight mass spectrometry (HPLC-Q-TOF).

No	Rt (min)	Identification	Formula	Mass	[M+H] ⁺	[M-H] ⁻	Error (ppm)	Source
1	5.62	Protocatechuic aldehyde	C ₇ H ₆ O ₃	138.031		137.0242	-1.8	CNM
2	6.23	Loganic acid*	C ₁₆ H ₂₄ O ₁₀	376.163		375.1291	-1.6	RGM
3	6.93	Mulberroside A	C ₂₆ H ₃₂ O ₁₄	568.1792	569.1865		2.3	MBT
4	7.03	Chlorogenic acid*	C ₁₆ H ₁₈ O ₉	354.095	355.1025		0.4	NRR, APR
5	7.23	6'-O-β-D-Glucopyransylgentiopicoside	C ₂₂ H ₃₀ O ₁₄	518.164	519.1703		1.3	RGM
6	7.33	Vanillic acid	C ₈ H ₈ O ₄	168.042	169.0492		-1.4	NRR, ALS
7	7.53	Caffeic acid*	C ₉ H ₈ O ₄	180.042	181.0498		0.9	ALS
8	8.04	Gentiopicroside*	C ₁₆ H ₂₀ O ₉	356.109	357.1166		-3.6	RGM
9	8.24	Sweroside*	C ₁₆ H ₂₂ O ₉	358.123	359.134		0.8	RGM, CNM
10	8.75	3,4-Dicaffeoylquinic acid	C ₂₅ H ₂₄ O ₁₂	516.1268		515.119	-1.0	NRR
11	10.06	Scopoletin*	C ₁₀ H ₈ O ₄	192.042	193.0495		-0.4	APR, CNM
12	10.26	Ferulic acid*	C ₁₀ H ₁₀ O ₄	194.058	195.0652		0.2	NRR, RGM ALS, LTW APR
13	10.36	Liquiritin*	C ₂₁ H ₂₂ O ₉	418.128	419.1353		5.0	GRR
14	10.57	Isoquercitrin*	C ₂₁ H ₂₀ O ₁₂	464.095	465.105		-1.9	MBT
15	10.97	Nodakenin*	C ₂₀ H ₂₄ O ₉	408.144	409.1506		3.8	NRR
16	11.57	Columbianetin	C ₁₄ H ₁₄ O ₄	246.089	247.0964		-0.9	APR
17	11.58	3,5-Dicaffeoylquinic acid	C ₂₅ H ₂₄ O ₁₂	516.1268		515.1188	-1.4	NRR
18	12.18	4,5-Dicaffeoylquinic acid	C ₂₅ H ₂₄ O ₁₂	516.1268		515.1184	-2.1	NRR
19	12.69	Senkyunolide I*	C ₁₂ H ₁₆ O ₄	224.105	225.1124		1.7	LTW
20	13.09	Isoliquiritin	C ₂₁ H ₂₂ O ₉	418.127	419.1334		1.4	GRR
21	13.60	Senkyunolide H	C ₁₂ H ₁₆ O ₄	224.107	225.1118		-1.3	LTW
22	13.90	Liquiritigenin*	C ₁₅ H ₁₂ O ₄	256.074	257.0809		1.1	GRR
23	16.52	Xanthotoxin*	C ₁₂ H ₈ O ₄	216.042	217.0495		-0.2	NRR, APR
24	17.84	Isoliquiritigenin*	C ₁₅ H ₁₂ O ₄	256.073	257.0805		-2.2	GRR
25	17.94	Bergapten/ Isobergapten	C ₁₂ H ₈ O ₄	216.042	217.0495		-0.2	NRR, APR
26	18.75	Glycyrrhizic acid*	C ₄₂ H ₆₂ O ₁₆	822.405	823.411		0.9	GRR
27	20.16	Columbianetin acetate*	C ₁₆ H ₁₆ O ₅	288.1	289.1071		0.2	APR
28	21.68	Imperatorin	C ₁₆ H ₁₄ O ₄	270.089	271.0967		0.6	NRR, APR
29	21.98	Butylphthalide*	C ₁₂ H ₁₄ O ₂	190.099	191.1064		0.2	LTW
30	22.99	Licochalcone A*	C ₂₁ H ₂₂ O ₄	338.152	339.1595		1.9	GRR
31	23.80	Phenethyl ferulate	C ₁₈ H ₁₈ O ₄	298.121	299.1281		2.1	NRR
32	23.90	Z-ligustilide	C ₁₂ H ₁₄ O ₂	190.099	191.1066		-0.5	ALS
33	24.10	Notopterol*	C ₂₁ H ₂₂ O ₅	354.147	355.1543		1.1	NRR
34	24.30	Costunolide*	C ₁₅ H ₂₀ O ₂	232.146	233.1536		0.1	ALR
35	24.40	Osthole*	C ₁₅ H ₁₆ O ₃	244.111	245.1177		2.7	NRR, APR
36	25.01	Isoimperatorin*	C ₁₆ H ₁₄ O ₄	270.089	271.0965		0.1	NRR, APR
37	25.31	Kadsurenone	C ₂₁ H ₂₄ O ₅	356.1623	357.1701		1.0	PKC
38	27.43	E-ligustilide	C ₁₂ H ₁₄ O ₂	190.099	191.1066		-2.7	ALS
39	29.86	Levistilide A*	C ₂₄ H ₂₈ O ₄	380.199	381.206		0.6	ALS
40	31.40	Glycyrrhetic acid	C ₃₀ H ₄₆ O ₄	470.337		469.3303	-4.6	GRR
41	36.22	11-Keto-β-acetyl-boswellic acid*	C ₃₂ H ₄₈ O ₅	512.353	513.358		2.4	FKC
42	37.53	Ursolic acid	C ₃₀ H ₄₈ O ₃	456.361	457.3679		1.8	RGM
43	41.52	α-boswellic acid	C ₃₀ H ₄₈ O ₃	456.359		455.3515	-3.3	FKC
44	46.55	β-boswellic acid	C ₃₀ H ₄₈ O ₃	456.359		455.3515	-3.3	FKC

*Identified with the reference compounds.

Herb medicine. NRR, *Notopterygii Rhizoma et Radix*; APR, *Angelicae Pubescentis Radix*; RGM, *Radix Gentianae Macrophyllae*; LTW, *Ligusticum wallichii*; ALS, *Angelica sinensis*; PKC, *Piperis Kadsurae Caulis*; MBT, *Mulberry twig*; ALR, *Aucklandiae radix*; FKC, *Piperis Kadsurae Caulis*; GRR, *Glycyrrhizae radix et rhizome*; CNM, *Cinnamon*.

Network of 44 Potential Compounds Predicted to Have 194 Potential Targets

We obtained the SMILE number of 44 compounds through the PubChem database (<https://pubchem.ncbi.nlm.nih.gov/>); then, we used the Swisst Target Prediction database (<http://swisstargetprediction.ch/>) to query the target sites of the 44 compounds. After removing the duplicates, a total of 194 targets were obtained. After querying the JBT target in the Swiss Target Prediction database, the protein interaction network related to JBT

was constructed with the STRING database. Using DisGeNET (<http://www.disgenet.org/>) database, we found 1,848 genes related to RA. Network of compounds in JBT and their potential targets. JBT (yellow rectangle), JBT 11 herbs (H, red diamond), and network of 44 potential compounds (C, blue ellipse) predicted to have 194 potential targets (green triangle). It comprised 252 nodes and 702 edges, as shown in **Figure 5A**. We use the DAVID database to analyze the GO enrichment and KEGG pathways of JBT genes in RA. To make the research more targeted, we used the JBT targets

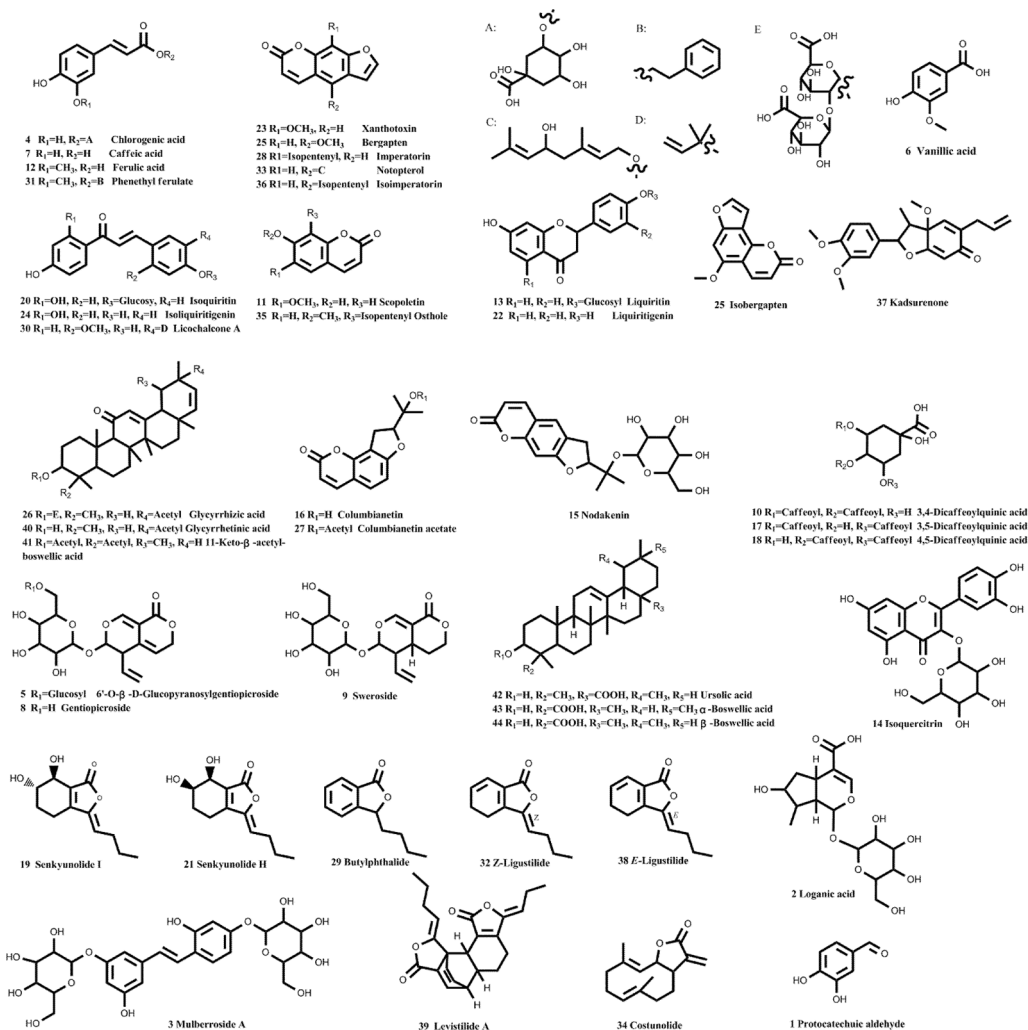


FIGURE 4 | Chemical structures of 44 identified components in JBT. With the aid of accurate masses measured by HPLC-Q-TOF, a total of 44 detected peaks were identified in Juanbi-Tang (JBT) decoction, as shown in **Table 2** and **Figure 4**. Among them, 24 compounds were definitively identified by comparison with the standard compounds, while the remaining 20 compounds were tentatively characterized according to their formula, retention time, and fragmentation patterns.

applied as queries in DisGeNET to map the RA genes, and constructed the common genes through the STRING database to obtain the *in vivo* network of responses of RA to JBT. The JBT protein interaction network was visualized in Cytoscape 3.6.0 software (**Figure 5B**). Each protein was represented by a node and the size of the nodes is proportional to the degree of the node. Relative pathways were analyzed according to the targets. As shown in **Figure 5C**, NF-kappa B pathways was one of the most relative pathways. More specific targets were marked with pentagram (**Supplementary 1**).

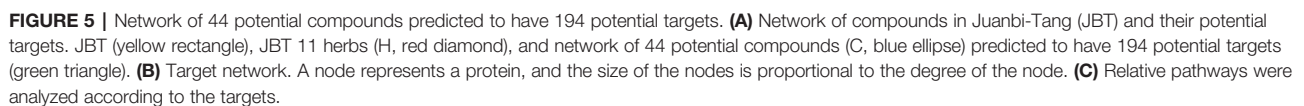
JBT Suppressed the mRNA and Protein Expression of MMP-1, IL-6, and IL-8 in TNF- α -Induced MH7A Cells

To assess the potential cytotoxicity of JBT, cell viability was evaluated by CCK-8 assay. As shown in **Figure 6A**, JBT at concentrations in the range of 0.25–2 mg/ml did not affect cell

viability after incubation for 72 h. To determine the protective effect of JBT against the expression of inflammatory cytokines, MH7A cells were incubated for 24 h with TNF- α . TNF- α significantly increased IL-6, IL-8, and MMP-1 expression at the mRNA level (**Figures 6B–D**) and the levels excreted in conditioned medium (**Figures 6E–G**). JBT significantly decreased the mRNA and protein expression of MMP-1 in TNF- α -induced MH7A cells in a dose-dependent manner, compared with that in the control group treated with TNF- α alone (**Figure 6H**). However, JBT did not show a significant effect on the mRNA expression of MMP-3 (**Supplementary 2**). Furthermore, JBT inhibited osteoclastogenesis (**Supplementary 3**).

JBT Inhibited TNF- α -Induced Activation of NF-Kappa B Pathways

To further investigate the mechanism by which JBT inhibits the production of inflammatory cytokines, we examined its effect on the



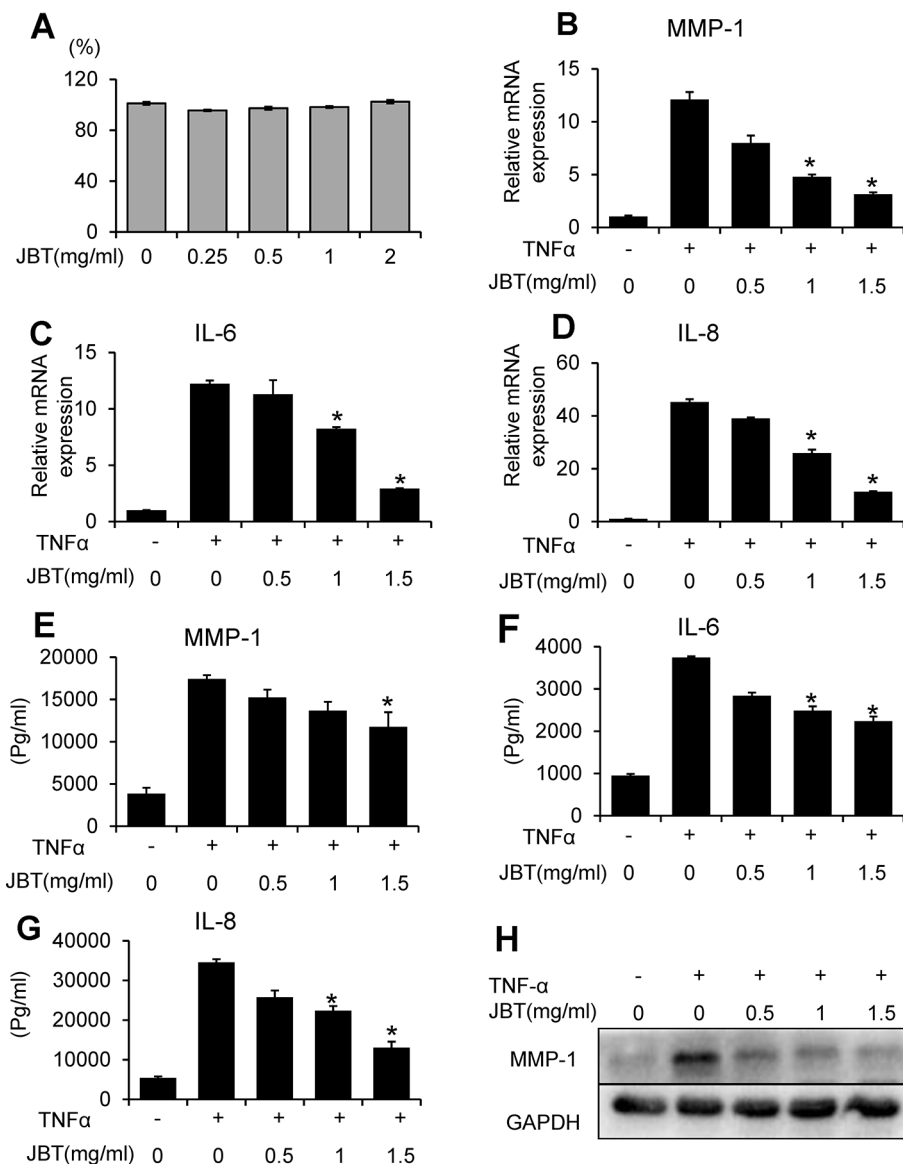


FIGURE 6 | Juanbi-Tang (JBT) suppressed the mRNA and protein expression of MMP-1, IL-6, and IL-8 in TNF- α -induced MH7A cells. **(A)** CCK-8 assay of MH7A cells after treatment with different concentrations of JBT for 0, 24, 48, and 72 h. **(B–D)** The mRNA levels of MMP-1, IL-6, and IL-8 were determined using qPCR. **(E–G)** ELISA assay of MMP-1, IL-6, and IL-8. **(H)** Western blot analysis of MMP-1. Representative images are shown from three independent experiments. Results are presented as mean \pm SEM of three independent experiments. * p < 0.05, versus group treated with TNF- α alone.

NF-kappa B-mediated pathways in TNF- α -induced MH7A cells. MH7A cells were pretreated with the indicated concentrations of JBT for 2 h, before stimulation with TNF- α (10 ng/ml) for another 30 min. Then, the protein levels and phosphorylation levels of p38, ERK, JNK, and p65 were determined. We found that the phosphorylation of p38, JNK, and p65 was markedly increased after TNF- α stimulation. JBT treatment significantly inhibited the phosphorylation of p38, JNK, p65 dose-dependently (0.5, 1, and 1.5 mg/ml, **Figures 7A–C**). We also used immunofluorescence analysis to determine the intracellular localization of p65. We pretreated MH7A cells with JBT (1.0 mg/ml) for 2 h or left them untreated, and then exposed them to TNF- α (10 ng/ml) for 0.5 h. The

immunofluorescence assay revealed that JBT significantly reduced the level of p65 in the nucleus of MH7A cells (**Figures 7D, E**).

DISCUSSION

In this study, we demonstrated that JBT could effectively inhibit joint symptoms, synovial inflammation, and joint destruction in CIA and TNF-Tg mice. We also revealed that JBT suppressed monocytes and T cells as well as the production of CCL2, CCR6, and CXCR3 ligands. *In vitro* data indicated that JBT could also profoundly inhibit the TNF- α -induced production of IL-6, IL-8,

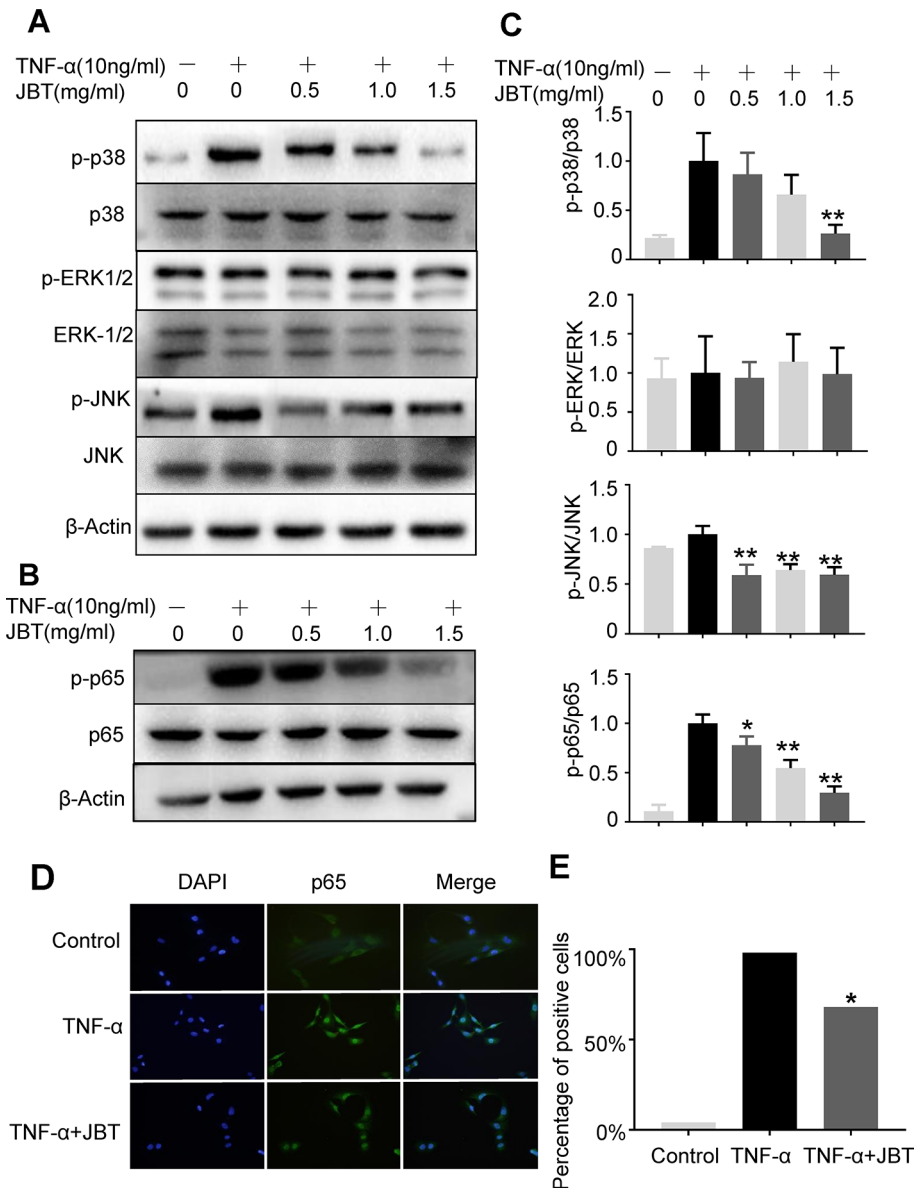


FIGURE 7 | JBT inhibited TNF α -induced activation of NF- κ B pathways. **(A–C)** The protein levels and phosphorylation levels of p38, ERK, JNK, and p65 of MH7A cells pretreated with JBT or not were determined by Western blot analysis. The total and phosphorylated levels of p38 and p65 were analyzed by Western blot analysis. Representative images are shown from three independent experiments. * $p < 0.05$, ** $p < 0.01$ versus group treated with TNF- α alone.

(D) Immunofluorescence assay of p65 in the nucleus of MH7A cells. **(E)** Assessment of the percentage of cells positive for p65 in the immunofluorescence assay.

and MMP-1 in cultured MH7A cells by downregulating p65 NF- κ B pathways, as well as probably by the downregulation of p38-MAPK pathways.

JBT was originally reported in a book from the Qing dynasty called *Yi Xue Xin Wu* ("Medical Reflections"), consisting of 11 herbs: *Notopterygii Rhizoma et Radix*, *Angelicae Pubescentis Radix*, *Radix Gentianae Macrophyllae*, *Ligusticum wallichii* (LTW), *Angelica sinensis* (ALS), *Piperis Kadsurae Caulis*, mulberry twig (MBT), *Aucklandiae radix* (ALR), frankincense (FKC), *Glycyrrhizae radix et rhizome*, and cinnamon (CNM). Primary studies have shown that JBT could be used for the

treatment of chronic lower back pain, external humeral epicondylitis, synovitis of the hip in children, ankylosing spondylitis, gout, and other bone diseases (Li, 2011; Li and Niu, 2011; Ni and Fu, 2014). It could also reduce inflammatory cytokines such as TNF- α and IL-1 in serum of model rats induced by Freund's adjuvant (Yu et al., 2015). Against this background, we adopted two animal models so as to verify the effect of JBT during the early stage of RA. One is the most widely accepted, the CIA mouse model, and the other is the TNF-Tg mice model with TNF- α overexpression, both of which showed clear joint inflammation, similar to RA, before undergoing treatment. We found that JBT significantly

reduced joint synovitis and the articular cartilage and bone defects in both animal models, thereby clarifying its efficacy *in vivo*. In other words, it was found that JBT can effectively reduce RA joint inflammation.

To clarify the pharmacological mechanism of JBT, we employed HPLC to detect its active components. We found 44 components in it, for the first time. To further analyze the mechanisms of action of these components, we then applied a network pharmacological method. Most previous studies on the mechanism of action of JBT tended to obtain the effective components based on retrieval of the associated literature from databases. For the first time, we here instead performed this based on the components detected by HPLC, which boosted the objectivity and credibility of our experimental results. Based on the network pharmacological analysis, we found that the targets of JBT components are mainly concentrated in the NF-kappa B pathway, as well as in cancer pathways, cancer proteoglycans, cancer microRNAs, viral carcinogenesis, and arachidonic acid metabolism.

Next, we conducted *in vitro* experiments for exploring the underlying mechanism. To simulate the *in vivo* environment of TNF-Tg mice and the high expression of TNF- α in the lesion area of RA, in the current study, we treated synovial cells with TNF- α (10 ng/ml) to observe the changes of inflammatory factors produced by them upon inflammatory stimulation. We found that JBT could also inhibit the TNF- α -induced production of IL-6, IL-8, and MMP-1 in synovial cells, restoring the structure of joints.

IL-6 is highly expressed in fibroblasts during the early stage of RA (Filer et al., 2017) and its inhibitor has started being used for clinical treatment (McInnes and Schett, 2017), as well as TNF- α . IL-8 also acts as a marker of synovitis (Alam et al., 2017). Among the compounds in JBT, ferulic acid was reported to have ameliorative potential for mitigating the effects of IL-6 associated with vincristine-induced painful neuropathy (Vashistha et al., 2017). Chlorogenic acid combined with chondrocytes on an alginate scaffold decreased MMP expression and improved the recovery of damaged articular cartilage (Cheng et al., 2018). Caffeic acid repressed IL-6 and TNF- α in RA-FLS by blocking the phosphorylation of I κ B and I κ B kinase (Wang et al., 2017). Moreover, sweroside inhibited IL-1 β -stimulated MMP-1, MMP-3, MMP-13, and ADAMTS-5 mRNA expression in rat articular chondrocytes by suppressing NF-kappa B and mTORC1 signaling (Zhang et al., 2019). Furthermore, ursolic acid reduced the incidence and severity of CIA-induced arthritis, accompanied by the decreased expression of TNF- α , IL-1 β , IL-6, IL-21, and IL-17 in arthritic joints (Baek et al., 2014). Osthonol was also shown to inhibit MMP-1, MMP-3, MMP-13, IL-6, and TNF- α in IL-1 β -stimulated SW982 cells, as well as NF-kappa B and MAPK pathways (Xu et al., 2018). Although much research on the ingredients of JBT has been performed, as far as we know, we are the first to find that JBT acts as an NF-kappa B inhibitor. However, further confirmation of this mechanism *via* more in-depth studies is still required. The application of inhibitors and positive controls, such as iguratimod, should also be considered in future research.

We here applied network pharmacology to identify signaling pathways associated with RA. The NF-kappa B pathway was shown

to be activated by many stimuli, including TNF- α (Wen et al., 2018). P65 participates in the classical NF-kappa B pathway. The inhibition of p65 phosphorylation was proven to suppress the pathogenesis of RA (Roman-Blas and Jimenez, 2006; Kang et al., 2018), as JBT did in this study. In the meantime, the effect inhibiting p38-MAPK was found. As a detectable component of JBT, gentiopicroside also exhibited a potent protective effect on the IL-1 β -induced inflammatory response and the release of MMPs in rat articular chondrocytes by the p38, ERK, and JNK pathways (Zhao et al., 2015). Chlorogenic acid was reported to reverse IL-1 β -induced increases in IL-6, MMP-13, and COX-2/PGE2 production in human SW1353 chondrocytes, partially *via* the p65 NF-kappa B signaling pathway (Liu et al., 2017), and to induce apoptosis to inhibit the inflammatory proliferation of IL-6-induced FLSs through modulating the activation of the JAK/STAT and NF-kappa B signaling pathways (Lou et al., 2016). Moreover, isoliquiritigenin treatment inhibited IL-1 β -induced MMP production and NF-kappa B activation both *in vitro* and *in vivo* (Zhang et al., 2018). Isoliquiritigenin was reported to suppress IL-1 β -induced apoptosis and inflammation in chondrocyte-like ATDC5 cells by inhibiting NF-kappa B and to exert chondroprotective effects on a mouse model of anterior cruciate ligament transection (Ji et al., 2017). Xanthotoxin inhibited the expression of Runx2 and MMP-13 by reducing the activation of p38-MAPK (Cao et al., 2017). In contrast to previous studies, this study involved the first time that both HPLC-Q-TOF and network pharmacology have been applied to detect the effects of this classical herbal compound and determine the mechanisms involved. However, further studies are needed to clarify the pharmacokinetics of JBT, so as to provide references for clinical indications and the optimal dose. In the process of empirical revision, there are too many vague factors in this TCM compounds, and even the proportion of the compounds themselves needs to be optimized. Therefore, we must firstly prove the effectiveness of JBT *in vitro* and *in vivo* studies. This is the foundation for all proceeding research. Therefore, we tested the active ingredients using HPLC, with the aim of finding possible targets of JBT. In this way the follow-up work could be guaranteed. In future work, we also plan to continue to conduct experiments to explore other signal pathways by network pharmacology.

In conclusion, this study indicates that JBT could markedly ameliorate synovial inflammation and joint destruction in CIA and TNF-Tg mice. The NF-kappa B pathways were found to be closely involved in the inhibitory effects.

DATA AVAILABILITY STATEMENT

The raw data supporting the conclusions of this article will be made available by the authors, without undue reservation, to any qualified researcher.

ETHICS STATEMENT

The animal study was reviewed and approved by Longhua Hospital - Animal Ethics Committee.

AUTHOR CONTRIBUTIONS

QL, HX, QS, and YW conceptualized and planned the experiments. TW and QJ performed most of the experiments and completed the original draft. TC completed the network pharmacological analysis. HY completed HPLC-Q-TOF. XL completed experiments on osteoclasts. XT and HX analyzed the data. YL and YZ raised the animals and assessed the symptoms of arthritis. CH provided guidance for target prediction. All authors were involved in the writing and critical review of the manuscript and approved its final version.

FUNDING

This work was sponsored by research grants from the National Natural Science Foundation (81822050, 81920108032, and 81673990 to QL, 81873321 to HX), Leading Medical Talents in

Shanghai (2019LJ02 to QL), Dawn Plan of Shanghai Municipal Education Commission (19SG39 to QL), Shanghai TCM Medical Center of Chronic Disease (2017ZZ01010 to YW), The Program for Innovative Research Team of the Ministry of Science and Technology of China (2015RA4002 to YW), Research Project of Shanghai Science and Technology Commission (17401971100 to QL), “Innovation Team” development projects (IRT1270 to YW), and Three Years Action to Accelerate the Development of Traditional Chinese Medicine Plan [ZY(2018-2020)-CCCX-3003 to YW].

SUPPLEMENTARY MATERIAL

The Supplementary Material for this article can be found online at: <https://www.frontiersin.org/articles/10.3389/fphar.2020.00045/full#supplementary-material>

REFERENCES

- Alam, J., Jantan, I., and Bukhari, S. N. A. (2017). Rheumatoid arthritis: recent advances on its etiology, role of cytokines and pharmacotherapy. *BioMed. Pharmacother.* 92, 615–633. doi: 10.1016/j.biopha.2017.05.055
- Baek, S. Y., Lee, J., Lee, D. G., Park, M. K., Lee, J., Kwok, S. K., et al. (2014). Ursolic acid ameliorates autoimmune arthritis via suppression of Th17 and B cell differentiation. *Acta Pharmacol. Sin.* 35 (9), 1177–1187. doi: 10.1038/aps.2014.58
- Brand, D. D., Latham, K. A., and Rosloniec, E. F. (2007). Collagen-induced arthritis. *Nat. Protoc.* 2 (5), 1269–1275. doi: 10.1038/nprot.2007.173
- Cao, Z., Bai, Y., Liu, C., Dou, C., Li, J., Xiang, J., et al. (2017). Hypertrophic differentiation of mesenchymal stem cells is suppressed by xanthotoxin via the p38MAPK/HDAC4 pathway. *Mol. Med. Rep.* 16 (3), 2740–2746. doi: 10.3892/mmr.2017.6886
- Chen, Y., Li, J., Li, Q., Wang, T., Xing, L., Xu, H., et al. (2016). Du-Huo-Ji-Sheng-Tang attenuates inflammation of TNF-Tg mice related to promoting lymphatic drainage function. *Evid. Based Complement Alternat. Med.* 2016, 7067691. doi: 10.1155/2016/7067691
- Chen, P., Niu, X., Du, Y., Zhang, S., and Xu, H. (2018). Experimental study of cheng shi juan-bi decoction in the treatment of adjuvant arthritis in rats. *J. hefei Univ. Technol. (natural Sci. edition)* 41 (03), 415–419.
- Cheng, X., Li, K., Xu, S., Li, P., Yan, Y., Wang, G., et al. (2018). Applying chlorogenic acid in an alginate scaffold of chondrocytes can improve the repair of damaged articular cartilage. *PLoS One* 13 (4), e0195326. doi: 10.1371/journal.pone.0195326
- Filer, A., Ward, L. S. C., Kembler, S., Davies, C. S., Munir, H., Rogers, R., et al. (2017). Identification of a transitional fibroblast function in very early rheumatoid arthritis. *Ann. Rheum. Dis.* 76 (12), 2105–2112. doi: 10.1136/annrheumdis-2017-211286
- Guo, R., Zhou, Q., Proulx, S. T., Wood, R., Ji, R. C., Ritchlin, C. T., et al. (2009). Inhibition of lymphangiogenesis and lymphatic drainage via vascular endothelial growth factor receptor 3 blockade increases the severity of inflammation in a mouse model of chronic inflammatory arthritis. *Arthritis Rheum.* 60 (9), 2666–2676. doi: 10.1002/art.24764
- Ji, B., Guo, W., Ma, H., Xu, B., Mu, W., Zhang, Z., et al. (2017). Isoliquiritigenin suppresses IL-1 β induced apoptosis and inflammation in chondrocyte-like ATDC5 cells by inhibiting NF- κ B and exerts chondroprotective effects on a mouse model of anterior cruciate ligament transection. *Int. J. Mol. Med.* 40 (6), 1709–1718. doi: 10.3892/ijmm.2017.3177
- Jia, Q., Wang, T., Wang, X., Xu, H., Liu, Y., Wang, Y., et al. (2019). Astragalus suppresses inflammatory responses and bone destruction in mice with collagen-induced arthritis and in human fibroblast-like Synoviocytes. *Front. Pharmacol.* 10, 94. doi: 10.3389/fphar.2019.00094
- Jiang, X., Lv, B., Li, P., Ma, X., Wang, T., Zhou, Q., et al. (2015). Bioactivity-integrated UPLC/Q-TOF-MS of Danhong injection to identify NF- κ B inhibitors and anti-inflammatory targets based on endothelial cell culture and network pharmacology. *J. Ethnopharmacol.* 174, 270–276. doi: 10.1016/j.jep.2015.08.026
- Kang, L. J., Kwon, E. S., Lee, K. M., Cho, C., Lee, J. I., Ryu, Y. B., et al. (2018). 3'-Sialyllactose as an inhibitor of p65 phosphorylation ameliorates the progression of experimental rheumatoid arthritis. *Br. J. Pharmacol.* 175, 23, 4295–4309. doi: 10.1111/bph.14486
- Keffer, J., Probert, L., Cazlaris, H., Georgopoulos, S., Kaslaris, E., Kioussis, D., et al. (1991). Transgenic mice expressing human tumour necrosis factor: a predictive genetic model of arthritis. *EMBO J.* 10 (13), 4025–4031. doi: 10.1002/j.1460-2075.1991.tb04978.x
- Korb-Pap, A., Bertrand, J., Sherwood, J., and Pap, T. (2016). Stable activation of fibroblasts in rheumatic arthritis-causes and consequences. *Rheumatol. (Oxford)* 55 (suppl 2), ii64–ii67. doi: 10.1093/rheumatology/kew347
- Li, Q., and Niu, Y. (2011). Clinical observation of juanbi decoction combined with traditional Chinese medicine fumigation and washing therapy for rheumatoid arthritis in active stage. *New Chin. Med.* 43 (09), 52–54.
- Li, P., Schwarz, E. M., O'Keefe, R. J., Ma, L., Looney, R. J., Ritchlin, C. T., et al. (2004). Systemic tumor necrosis factor alpha mediates an increase in peripheral CD11bhigh osteoclast precursors in tumor necrosis factor alpha-transgenic mice. *Arthritis Rheum.* 50 (1), 265–276. doi: 10.1002/art.11419
- Li, Z. (2011). Treatment of 62 cases of hip synovitis in children with the addition and subtraction of phlegm and blood stasis. *TCM Res.* 24 (02), 51–52.
- Liu, C. C., Zhang, Y., Dai, B. L., Ma, Y. J., Zhang, Q., Wang, Y., et al. (2017). Chlorogenic acid prevents inflammatory responses in IL1 β stimulated human SW1353 chondrocytes, a model for osteoarthritis. *Mol. Med. Rep.* 16 (2), 1369–1375. doi: 10.3892/mmr.2017.6698
- Lou, L., Zhou, J., Liu, Y., Wei, Y. L., Zhao, J., Deng, J., et al. (2016). Chlorogenic acid induces apoptosis to inhibit inflammatory proliferation of IL-6-induced fibroblast-like synoviocytes through modulating the activation of JAK/STAT and NF- κ B signaling pathways. *Exp. Ther. Med.* 11 (5), 2054–2060. doi: 10.3892/etm.2016.3136
- Luchetti, M. M., Benfaremo, D., and Gabrielli, A. (2017). Biologics in inflammatory and immunomediated arthritis. *Curr. Pharm. Biotechnol.* 18 (12), 989–1007. doi: 10.2174/1389201019666171226151852
- McInnes, I. B., and Schett, G. (2017). Pathogenetic insights from the treatment of rheumatoid arthritis. *Lancet* 389 (10086), 2328–2337. doi: 10.1016/S0140-6736(17)31472-1
- Miyazawa, K., Mori, A., and Okudaira, H. (1998). Establishment and characterization of a novel human rheumatoid fibroblast-like synoviocyte line, MH7A, immortalized with SV40 T antigen. *J. Biochem.* 124 (6), 1153–1162. doi: 10.1093/oxfordjournals.jbchem.a022233
- Ni, J., and Fu, L. (2014). Clinical observation on 36 cases of external epicondylitis of the tibia treated by removing decoction. *Zhejiang J. Tradit. Chin. Med.* 49 (11), 818.

- Niu, X., Chen, P., Du, Y., and Xu, H. (2018a). Anti-inflammatory and analgesic effects of Cheng's Decoction. *J. Anhui Univ. Tradit. Chin. Med.* 37 (04), 71–75.
- Niu, X., Chen, P., Du, Y., and Xu, H. (2018b). Effect of Cheng's Decoction on immune function in rats with adjuvant arthritis. *Pharmacol. Clin. Med.* 34 (03), 6–10.
- Ørnbjerg, L. M., Østergaard, M., Jensen, T., Hørslev-Petersen, L. M., Stengaard-Pedersen, K., Junker, P., et al. (2017). Hand bone loss in early rheumatoid arthritis during a methotrexate-based treat-to-target strategy with or without adalimumab—a substudy of the optimized treatment algorithm in early RA (OPERA) trial. *Clin. Rheumatol.* 36 (4), 781–789. doi: 10.1007/s10067-016-3489-1
- Rana, A. K., Li, Y., Dang, Q., and Yang, F. (2018). Monocytes in rheumatoid arthritis: circulating precursors of macrophages and osteoclasts and, their heterogeneity and plasticity role in RA pathogenesis. *Int. Immunopharmacol.* 65, 348–359. doi: 10.1016/j.intimp.2018.10.016
- Roman-Blas, J. A., and Jimenez, S. A. (2006). NF-kappaB as a potential therapeutic target in osteoarthritis and rheumatoid arthritis. *Osteoarthritis Cartilage* 14 (9), 839–848. doi: 10.1016/j.joca.2006.04.008
- Sun, Y., Zhao, D., Liu, Z., Sun, X., and Li, Y. (2018). Inhibitory effect of salvianolic acid on inflammatory mediators of rats with collagen-induced rheumatoid arthritis. *Exp. Ther. Med.* 16 (5), 4037–4041. doi: 10.3892/etm.2018.6696
- Vashistha, B., Sharma, A., and Jain, V. (2017). Ameliorative potential of ferulic acid in vincristine-induced painful neuropathy in rats: An evidence of behavioral and biochemical examination. *Nutr. Neurosci.* 20 (1), 60–70. doi: 10.1179/1476830514Y.0000000165
- Vos, T., Abajobir, A. A., Abate, K. H., Abbafati, C., Abbas, K. M., Abd-Allah, F., et al. (2017). Global, regional, and national incidence, prevalence, and years lived with disability for 328 diseases and injuries for 195 countries, 1990–2016: a systematic analysis for the Global Burden of Disease Study 2016. *Lancet* 390 (10100), 1211–1259. doi: 10.1016/S0140-6736(17)32154-2
- Wang, W., Sun, W., and Jin, L. (2017). Caffeic acid alleviates inflammatory response in rheumatoid arthritis fibroblast-like synoviocytes by inhibiting phosphorylation of IkappaB kinase alpha/beta and IkappaBalpha. *Int. Immunopharmacol.* 48, 61–66. doi: 10.1016/j.intimp.2017.04.025
- Wangyang, Y., Yi, L., Wang, T., Feng, Y., Liu, G., Li, D., et al. (2018). MiR-199a-3p inhibits proliferation and induces apoptosis in rheumatoid arthritis fibroblast-like synoviocytes via suppressing retinoblastoma. *Biosci. Rep.* 1, 38(6). doi: 10.1042/BSR20180982
- Wen, X., Chen, X., Liang, X., Zhao, H., Li, Y., Sun, X., et al. (2018). The small molecule NSM00191 specifically represses the TNF-alpha/NF-small ka, CyrillicB axis in foot and ankle rheumatoid arthritis. *Int. J. Biol. Sci.* 14 (12), 1732–1744. doi: 10.7150/ijbs.24232
- Xu, X., Cheng, H., Cao, J., Du, H., Meng, Q., and Guo, M. (2017). Cheng Shiqi Decoction reduces the level of prostaglandin E receptor 4 (PTGER4) in synovial tissue of adjuvant arthritis rats. *J. Mol. Immunol.* 33 (06), 736–740.
- Xu, X., Du, H., Wu, Y., Cheng, H., Cao, J., Meng, Q., et al. (2018). Cheng Shiqi Decoction reduces peripheral blood T cell cAMP levels and CD4~+/CD8 in rats with adjuvant arthritis ~+T cell ratio. *J. Cell. Mol. Immunol.* 34 (02), 110–114.
- Xu, R., Liu, Z., Hou, J., Huang, T., and Yang, M. (2018). Osthole improves collagen-induced arthritis in a rat model through inhibiting inflammation and cellular stress. *Cell Mol. Biol. Lett.* 23, 19. doi: 10.1186/s11658-018-0086-0
- Yu, Q., Cai, W., and Wang, W. (2015). Effect of phlegm soup on cytokines in rat model of rheumatoid arthritis. *Chin. Natl. Folk Med.* 24 (14), 1–2.
- Zhang, L. M., and Zhou, J. J. (2018). CYLD suppression enhances the pro-inflammatory effects and hyperproliferation of rheumatoid arthritis fibroblast-like synoviocytes by enhancing NF-kappaB activation. *Arthritis Res. Ther.* 20 (1), 219. doi: 10.1186/s13075-018-1722-9
- Zhang, L., Ma, S., Su, H., and Cheng, J. (2018). Isoliquiritigenin Inhibits IL-1beta-induced production of matrix metalloproteinase in articular chondrocytes. *Mol. Ther. Methods Clin. Dev.* 9, 153–159. doi: 10.1016/j.omtm.2018.02.006
- Zhang, R., Wang, C. M., Jiang, H. J., Tian, X. G., Li, W., Liang, W., et al. (2019). Protective effects of sweroside on IL-1beta-induced inflammation in rat articular chondrocytes through suppression of NF-kappaB and mTORC1 signaling pathway. *Inflammation* 42 (2), 496–505. doi: 10.1007/s10753-018-0906-4
- Zhao, L., Ye, J., Wu, G. T., Peng, X. J., Xia, P. F., and Ren, Y. (2015). Gentipicroside prevents interleukin-1 beta induced inflammation response in rat articular chondrocyte. *J. Ethnopharmacol.* 172, 100–107. doi: 10.1016/j.jep.2015.06.031

Conflict of Interest: The authors declare that the research was conducted in the absence of any commercial or financial relationships that could be construed as a potential conflict of interest.

Copyright © 2020 Wang, Jia, Chen, Yin, Tian, Lin, Liu, Zhao, Wang, Shi, Huang, Xu and Liang. This is an open-access article distributed under the terms of the Creative Commons Attribution License (CC BY). The use, distribution or reproduction in other forums is permitted, provided the original author(s) and the copyright owner(s) are credited and that the original publication in this journal is cited, in accordance with accepted academic practice. No use, distribution or reproduction is permitted which does not comply with these terms.



Adjunctive Chinese Herbal Products Therapy Reduces the Risk of Ischemic Stroke Among Patients With Rheumatoid Arthritis

Hsuan-Shu Shen^{1,2}, Jen-Huai Chiang^{3,4} and Nai-Huan Hsiung^{5*}

¹ Department of Chinese Medicine, Hualien Tzu Chi Hospital, Buddhist Tzu Chi Medical Foundation, Hualien, Taiwan,

² School of Post-Baccalaureate Chinese Medicine, Tzu Chi University, Hualien, Taiwan, ³ Management Office for Health Data, China Medical University Hospital, Taichung, Taiwan, ⁴ College of Medicine, China Medical University, Taichung, Taiwan,

⁵ Department of Nursing, Asia University, Taichung, Taiwan

OPEN ACCESS

Edited by:

Per-Johan Jakobsson,
Karolinska Institutet, Sweden

Reviewed by:

Runyue Huang,
Guangzhou University of Chinese
Medicine, China
Javier Echeverria,
Universidad de Santiago
de Chile, Chile

*Correspondence:

Nai-Huan Hsiung
laineyhsung@gmail.com

Specialty section:

This article was submitted to
Ethnopharmacology,
a section of the journal
Frontiers in Pharmacology

Received: 23 March 2019

Accepted: 07 February 2020

Published: 04 March 2020

Citation:

Shen H-S, Chiang J-H and Hsiung N-H
(2020) Adjunctive Chinese Herbal
Products Therapy Reduces the Risk of
Ischemic Stroke Among Patients With
Rheumatoid Arthritis.
Front. Pharmacol. 11:169.
doi: 10.3389/fphar.2020.00169

We performed a retrospective cohort study to investigate the association between the risk of ischemic stroke (IS) and the use of Chinese herbal products (CHP) in combination with western medicine (WM) among patients with rheumatoid arthritis (RA). The data were sourced from the registry for beneficiaries, inpatient and ambulatory care claims, and Registry for Catastrophic Illness from the National Health Insurance Research Database (NHIRD) in Taiwan between 1997 and 2011. Patients, who were newly diagnosed with RA between 1997 and 2010, were classified as the CHP group or non-CHP group depending on the presence of absence the adjunctive use of CHP following a diagnosis of RA. A total of 4,148 RA patients were in both the CHP and non-CHP groups after 1:1 matching. Patients in the CHP group had a significantly lower risk of IS compared to patients in the non-CHP group (adjusted hazard ratio [aHR], 0.67; 95% confidence interval [CI], 0.52–0.86). In the CHP group, patients who used CHP for more than 30 days had a lower risk of IS than their counterparts (aHR: 0.61, 95% CI: 0.40–0.91). Gui-Zhi-Shao-Yao-Zhi-Mu-Tang, Shu-Jin-Huo-Xie-Tang, and Du-Huo-Ji-Sheng-Tang might be associated with a lower risk of IS. Finally, the use of CHP in combination with WM was associated with a decreased risk of IS in patients with RA, especially among those who had used CHP for more than 30 days. A further randomized control trial is required to clarify the casual relationship between these results.

Keywords: rheumatoid arthritis, ischemic stroke, Chinese herbal products, National Health Insurance Research Database, traditional Chinese medicine

INTRODUCTION

Patients with rheumatoid arthritis (RA) are at a greater risk of ischemic stroke (IS), which may be a leading cause of mortality and can lead to severe long-term disability (Benjamin et al., 2017). According to a meta-analysis study, the risk of stroke death was elevated by 52% among patients with RA (Avina-Zubieta et al., 2008). Danish and Taiwanese studies have also demonstrated that patients with RA were shown to have a 30% higher risk of IS compared to those without RA

(Lindhardsen et al., 2012; Liou et al., 2014). Moreover, another prospective cohort study of 114,342 American women with RA found that the relative risk for IS was 1.48 (95% confidence interval [CI]:0.70–3.12) (Solomon et al., 2003). A possible mechanism might be the systemic inflammatory response in patients with RA who have elevated levels of C-reactive protein (CRP) and tumor necrosis factor- α (TNF- α). This kind of chronic inflammation underlies the accelerated atherosclerosis, and is thought to be the main pathologic process of IS (Sattar et al., 2003; Hansson, 2005).

In addition to systemic chronic inflammation in individuals with RA, certain routinely prescribed medicines also increase the risk of IS (Nadareishvili et al., 2008; Lindhardsen et al., 2014). In accordance with the recommendations of the European League Against Rheumatism (EULAR), methotrexate, a kind of Disease-modifying antirheumatic drugs (DMARDs), plus short-term corticosteroids is the first-line therapy. When the treatment target cannot be achieved by methotrexate within 6 months or unfavorable prognostic factors are present, such as high disease activity, early erosion, or high level of rheumatoid factor, a TNF-antagonist may be considered as an add-on (Smolen et al., 2017). Previous research has documented that corticosteroids and certain non-steroidal anti-inflammatory drugs (NSAIDs) might increase the risk of IS in patients with RA 1.5- to 2-fold (Roubille et al., 2015). Methotrexate and TNF-antagonists, by contrast, are associated with the reduced risk of ischemic stroke (Tam et al., 2018). However, these drugs are associated with a potential risk of infection, fatigue, and liver damage (Salliot and van der Heijde, 2009). To avoid the side effects and debilitation associated with western medical treatment, the patients resorted to using traditional herbal remedies (Efthimiou and Kukar, 2010; Michalsen, 2013).

Thus, nearly 30% of individuals with RA were also taking Chinese herbal medicine in a recent study (Huang et al., 2015). Some of commonly used polyherbal formulations or single herbs have been demonstrated anti-inflammatory action, these include Gui-Zhi-Shao-Yao-Zhi-Mu-Tang (contains *Paeonia lactiflora* Pall., *Atractylodes macrocephala* Koidz., *Anemarrhena asphodeloides* Bge., *Saposhnikovia divaricata* (Turcz.) Schischk., *Glycyrrhiza uralensis* Fisch. ex DC., *Cinnamomum cassia* (L.) J.Presl, *Ephedra sinica* Stapf, *Aconitum carmichaelii* Debx., *Zingiber officinale* Roscoe) and *Boswellia neglecta* S.Moore (Ru-Xiang) (Ammon, 2006; Daily et al., 2017). Additionally, *Tripterygium wilfordii* Hook.f, *Stephania tetrandra* S Moore, and *Zingiber officinale* Roscoe have also been reported to have potential to suppress inflammation (Kang et al., 1996; Liacini et al., 2005; Wang et al., 2013). To date, most studies have purposely analyzed the effects of Chinese herbal products (CHP) in terms of alleviating the clinical symptoms and managing the chronic inflammation of patients with rheumatoid arthritis (Soeken et al., 2003; Zhang et al., 2011; Daily et al., 2017). However, there is a lack of studies that investigated whether the use of CHP was associated with a reduced risk of IS, which is a leading cause of death, in patients with RA. This study sought to evaluate the association between the use of CHP in combination with western medicine (WM) and the risk of IS

in patients with RA by undertaking a large-scale retrospective cohort study.

MATERIALS AND METHODS

Data Source

This study used reimbursement claims data from the Taiwan National Health Insurance Program. A national health insurance (NHI) program was implemented in March 1995, which covers 22.6 million individuals out of the total population of 23.0 million in Taiwan. The NHI is an obligatory universal health insurance program, which offers comprehensive medical care coverage to 99% of the entire Taiwanese population and has contracts with 97% of the hospitals and clinics there (<http://www.nhi.gov.tw/english/index.aspx>). The National Health Insurance Research Database (NHIRD) covers every medical record including Traditional Chinese medicine treatment that is reimbursed by the NHI.

The datasets used in the study consisted of a registry for beneficiaries, inpatient, and ambulatory care claims, and the Registry for Catastrophic Illness from the NHIRD. Ambulatory care claims contain the individuals' gender, date of birth, date of visit, codes for the International Classification of Disease, Ninth Revision, and Clinical Modification (ICD-9-CM) codes for three primary diagnoses. Inpatient claims contain ICD-9-CM codes for principal diagnosis up to a total of four secondary diagnoses. The registry for Catastrophic Illness database contains data from insurers who suffer from major diseases and are granted exemption from co-payment. A disease diagnosis without valid supporting clinical findings may be considered a medical fraud by the NHI, which carries a penalty of 100-fold of the payment claimed by the treating physician or hospital. RA is a kind of major disease in Taiwan, and we can define patients with RA clearly from the Registry for Catastrophic Illness database. Because the NHIRD contains identified secondary data for research, the requirement for informed patient consent for the present study was waived off. This study was approved by the Institutional Review Board of the China Medical University (CMUH104-REC2-115). The datasets analyzed for the current study are available from the corresponding author on reasonable request.

Selection of the Study Population

This was a retrospective cohort study. We identified patients who were diagnosed with RA (ICD-9-CM: 714.0) from the Registry for Catastrophic Illness database. Patients with RA who received WM treatment during the period from 1 January 1997 to 31 December 2010 were selected as the cohort group, and follow-up to 31 December 2011. The patients also had to be over the age of 18 years at diagnosis. The exclusion criteria were as follows: 1) dropout from insurance, 2) diagnosis of stroke (ICD-9-CM: 430-438) or coronary artery disease (ICD-9-CM: 410-414) before the first diagnosis date of RA, and 3) a follow-up period of less than 180 days. Finally, a total of 20,483 RA patients were included in the study (Figure 1).

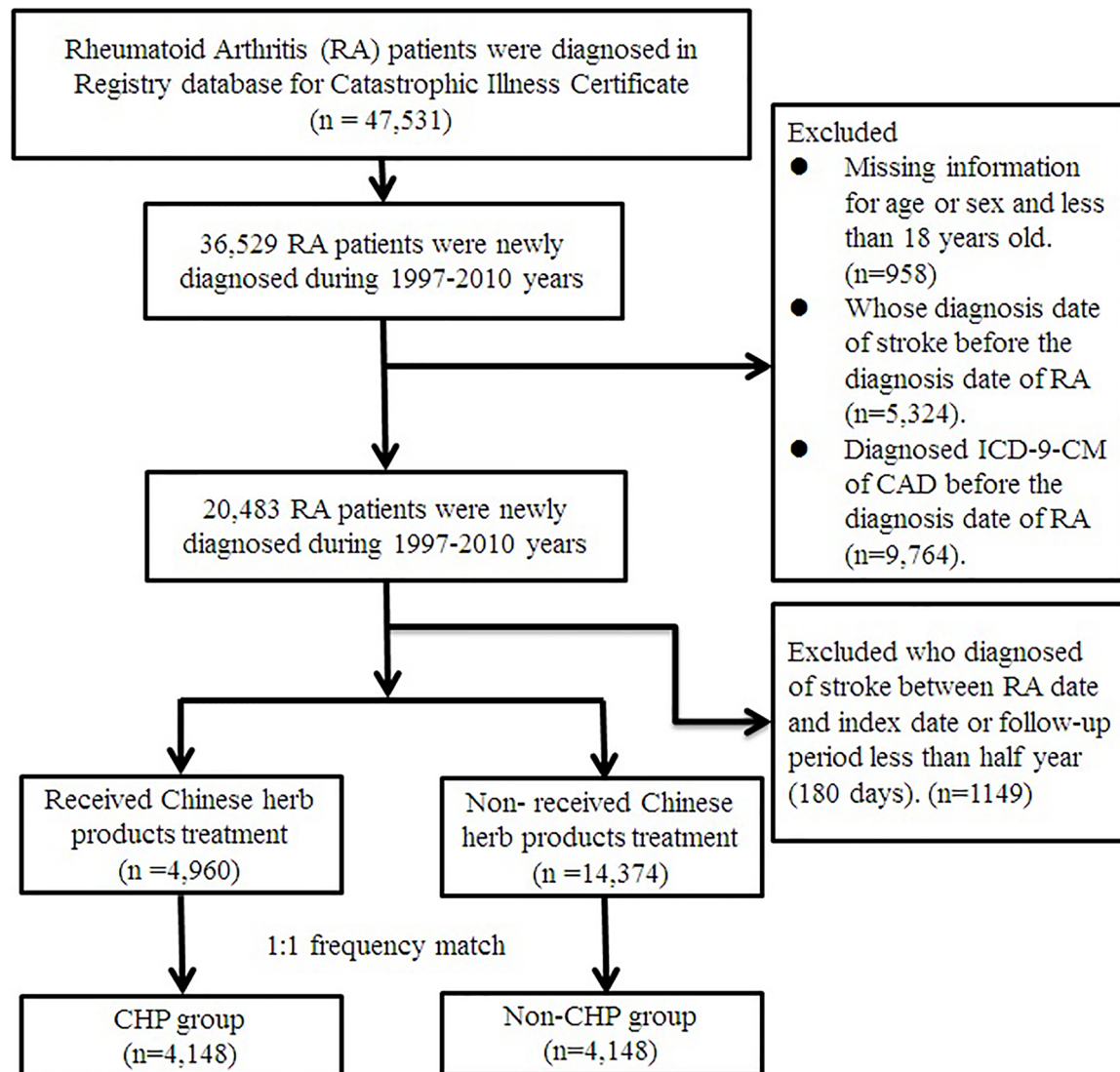


FIGURE 1 | Flowchart of patients with rheumatoid arthritis. After excluding patients not fitting inclusion criteria, CHP and non-CHP groups comprised 4,148 patients after 1:1 matching. CHP, Chinese herbal products.

The participants who had traditional Chinese Medicine outpatient visits along with CHP prescription records because of RA (ICD-9-CM code: 714.0) in combination with WM between the date of initial diagnosis of RA and the endpoint were defined as the CHP group. Those patients who only received WM because of RA were assigned to the non-CHP group. The date of the first accepted CHP after the diagnosis of RA was the index date for the CHP group. The index date of the patients in the non-CHP group was the first diagnosed date of RA. Prior to matching, there were 4,960 RA patients using CHP and 14,374 patients not using CHP. We used 1:1 frequency match by age (per 5 year-groups), gender, index year, and initial diagnosis year of RA. After frequency matching, there were 4,148 RA patients in both the CHP and non-CHP groups.

Primary Outcome

The primary outcome was IS (ICD-9-CM: 433-438) during the 14-year follow-up with at least one inpatient claim and at least three ambulatory care claims. All eligible patients were followed up from the index date to December 31, 2011, initial diagnosis date of IS, date of withdrawal from NHI or date of death, whichever occurred first.

Characteristics, Comorbidities, and Medication

The sociodemographic variables included age and gender. We identified comorbidities using ICD-9-CM from the database of outpatients and inpatients. Baseline comorbidity was defined as comorbid disease which occurred before the index date, and for which there were ambulatory care claims

for at least 3 visits or at least one inpatient claim. Based on the recommendations of the EULAR, and hypertension (ICD-9-CM: 401-405), diabetes mellitus (ICD-9-CM: 250), hyperlipidemia (ICD-9-CM: 272) were considered as the covariates (Martin-Martinez et al., 2014; Agca et al., 2017). In addition, we also included baseline comorbidities which are the established risk factors for stroke, such as chronic obstructive pulmonary disease (ICD-9-CM: 491-496), end stage renal disease (ICD-9-CM: 585), and atrial fibrillation (ICD-9-CM: 427.31) as the covariates. We also considered drugs in accordance with the recommendations of the EULAR, including NSAIDs, corticosteroids, DMARDs, and TNF-antagonist prescribed after the initial diagnosis date of RA up to the endpoint of the study (Corticosteroid: beclomethasone [ATC code: R03BA01], budesonide [ATC code: R03BA02], fluticasone [ATC code: R03BA05], ciclesonide [ATC code: R03BA08], formoterol [ATC code: R03AC13], and budesonide [ATC code: R03AK07]. DMARDs: tacrolimus [ATC code: L04AD02], mycophenolate mofetil [ATC code: L04AA06], azathioprine [ATC code: L04AX01], sulfasalazine [ATC code: A07EC01], hydroxychloroquine [ATC code: P01BA02], methotrexate [ATC code: L01BA01, L04AX03], leflunomide [ATC code: L04AA13], and cyclosporine [ATC code: L04AD01]. TNF- α antagonist: tanercept [ATC code: L04AB01], adalimumab [ATC code: L04AB04], rituximab [ATC code: L01XC02], and golimumab [ATC code: L04AB06]).

Statistical Analysis

The difference of basic characteristics and potential confounders between the two groups was assessed by absolute standardized mean difference instead of statistical testing because the difference is a property of the sample rather than an underlying population. The value of absolute standardized mean difference ≤ 0.1 indicates a negligible difference in potential confounders between the two groups. A univariate and multivariate Cox's proportional hazard model were used to estimate the hazard ratios (HRs) and 95% CI of IS for CHP use, controlling for potential confounding factors, including age, gender, diabetes mellitus, hypertension, hyperlipidemia, COPD, ESRD, atrial fibrillation, and medication. Furthermore, we performed a multivariate Cox's proportional hazard model to estimate the hazard ratios (HRs) and 95% CI of IS for the most commonly prescribed single herb and polyherbal formulations controlling for age, gender, diabetes mellitus, hypertension, hyperlipidemia, COPD, ESRD, atrial fibrillation, and medication.

The Kaplan–Meier method and log rank tests were performed to compare the cumulative incidence rate of IS among the two groups. We also performed subsequent subgroup analyses to examine the effect of cumulative numbers of days of CHP use. We stratified the patients in the CHP group into three subgroups: cumulative numbers of days of CHP use days <30 days, 30 to 180 days, and >180 days. In this study, SAS 9.4 (SAS Institute Inc., Cary, NC) was used for the statistical analysis.

RESULTS

After the frequency matching, the gender and age were similar between the CHP and non-CHP groups. The mean (standard deviation) age of the patients in the CHP and non-CHP groups was 46.60 (11.59) years and 46.67 (11.59) years, respectively. There is no difference between the two group with regard to comorbidities (all of the standardized mean difference < 0.1). However, the proportion of DMARDs and TNF-antagonist use in the CHP group was significantly higher than that in the non-CHP group. The mean (median) follow-up period of the CHP group is longer than that of the non-CHP group (4.37(4.92) years v.s. 4.81 (4.30) years, standardized mean difference = 0.108) (**Table 1**).

A total of 250 patients developed IS during follow-up; the incidence rates of IS in the CHP and non-CHP group was 4.68 per 1000 person-years and 7.00 per 1000 person-years, respectively. The Kaplan–Meier analysis demonstrated that the cumulative incidence of IS in the CHP group was significantly lower than that in the non-CHP group (log-rank test, $p = 0.0016$) (**Figure 2**). Patients in the CHP group were more likely to have a lower risk of IS (crude HR: 0.67, 95% CI: 0.52–0.86) compared to their counterparts in the non-CHP group. After multivariate adjustment, the HR for the risk of IS remained the same (aHR: 0.67, 95% CI: 0.52–0.86) (**Table 2**).

After stratification by gender, the incidence rates of IS among the female and male patients in the CHP group were 3.96 per 1000 person-years and 9.32 per 1000 person-years, respectively. Female patients in the CHP group had a significantly lower risk of IS (aHR: 0.63, 95% CI: 0.47–0.85) compared to their counterparts in the non-CHP group. However, no significant difference was observed in this respect among the male patients (aHR: 1.35, 95% CI: 0.74–2.44) between the CHP and the non-CHP groups. In the age group of 40 to 59 years, the patients in the CHP group showed a significantly lower risk of IS compared to those in the non-CHP group (**Table 2**). In addition, RA patients without DM in the CHP group were associated with a lower risk of IS (aHR: 0.74, 95% CI: 0.55–0.98) compared with those in the non-CHP group. The same results were observed regarding the other baseline comorbidities, and RA patients without any comorbidity might be associated with a 0.73 to 0.69-fold lower risk of IS. Moreover, in the stratification analysis of the medication, RA patients receiving the CHP in combination with WM treatment showed a trend of reduced risk of IS compared with those receiving WM only, with the exception of RA patients taking TNF-antagonist (**Table 2**).

Table 3 presents the results of the subgroup analysis according to the cumulative numbers of days of CHP use among patients with RA. Compared to the non-CHP group, patients who received CHP for 30 to 180 days had a significantly lower risk of IS (aHR: 0.61, 95% CI: 0.40–0.91). Moreover, patients who use CHP >180 days showed a marginal significant lower risk of IS among patients with RA (aHR: 0.62, 95% CI: 0.38–1.00).

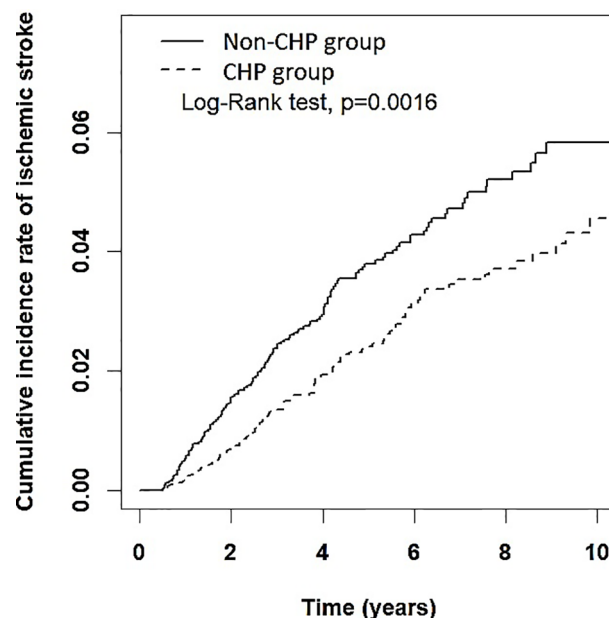
TABLE 1 | Characteristics of patients with rheumatoid arthritis classified according to the use of Chinese herbal products.

Variable	Rheumatoid Arthritis Accepted CHP				Standardized mean difference*
	Non-CHP group (n = 4148)		CHP group (n = 4148)		
	n	%	n	%	
Gender					
Female	3591	86.57	3591	86.57	0.000
Male	557	13.43	557	13.43	0.000
Age group					
18–39	1157	27.89	1157	27.89	0.000
40–59	2468	59.5	2468	59.5	0.000
≥60	523	12.61	523	12.61	0.000
Mean ± SD (years)	46.67(11.59)		46.60(11.59)		0.006
Baseline Comorbidity					
Diabetes mellitus	340	8.2	288	6.94	0.047
Hypertension	810	19.53	706	17.02	0.065
Hyperlipidemia	447	10.78	469	11.31	0.017
COPD	540	13.02	682	16.44	0.097
ESRD	49	1.18	29	0.7	0.050
Atrial fibrillation	8	0.19	6	0.14	0.012
Drug used					
NSAID	4118	99.28	4136	99.71	0.061
Corticosteroid	163	3.93	203	4.89	0.047
DMARD	3906	94.17	4058	97.83	0.19
TNF-antagonist	625	15.07	1001	24.13	0.23
Mean (median) of the follow-up period (years)	4.81 (4.30)		5.37 (4.94)		0.108
Duration between rheumatoid arthritis date and index, days (mean, median)	942(616)		931(605)		0.012

*A value of standardized mean difference ≤ 0.1 indicates a negligible difference between the two groups.

CHP, Chinese herbal products; SD, standard deviation; COPD, chronic Obstructive Pulmonary Disease; ESRD, end stage renal disease; NSAID, non-steroidal anti-inflammatory drugs; DMARD, disease-modifying antirheumatic drugs; TNF, tumor necrosis factor.

The five most commonly prescribed single herbs and polyherbal formulations are listed in **Table 4**. The most commonly used single herb was *Corydalis ambigua* Cham. & Schltdl. (Yan-Hu-Suo, $n = 954$, 22.9%), followed by *Spatholobus suberectus* Dunn (Ji-Xie-Teng, $n = 791$, 19.0%), *Cyperus rotundus* L. (Xiang-Fu, $n = 675$, 16.4%), *Morus alba* L. (Sang-Zhi, $n = 741$, 17.9%), and *Coix lacryma-jobi* L. (Yi-Yi Ren, $n = 680$, 16.39%). In addition, Gui-Zhi-Shao-Yao-Zhi-Mu-Tang ($n = 1449$, 34.9%) was the most commonly used polyherbal formulation, followed by Dang-Gui-Nian-Tong-Tang ($n = 1182$, 28.5%), Shu-Jin-Huo-Xie-Tang ($n = 991$, 23.9%), Du-Huo-Ji-Sheng-Tang ($n = 696$, 16.8%), and Jia-Wei-Xiao-Yao-San ($n = 628$, 15.1%). The association between prescribed polyherbal formulations and the risk of IS was explored using a Cox proportional hazard models. The results demonstrated that Gui-Zhi-Shao-Yao-Zhi-Mu-Tang (aHR: 0.50, 95% CI: 0.31–0.80), Shu-Jin-Huo-Xie-Tang (aHR: 0.35, 95% CI: 0.20–0.63), and Du-Huo-Ji-Sheng-Tang (aHR: 0.57, 95% CI: 0.34–0.96) were associated with a decreased risk of IS (**Table 4**).

**FIGURE 2 |** Cumulative incidence rate of ischemic stroke among patients with RA in the CHP and non-CHP group. CHP, Chinese herbal products.

DISCUSSION

This is the first nationwide retrospective cohort study designed to investigate the association between the risk of IS and the combined use of CHP in patients with RA. A total of 8,296 patients with RA were included in the study. There were 4,148 patients in each group after a 1:1 frequency match by gender, age, index year, and initial diagnosis year of RA. We observed an association between using CHP in combination with WM and a lower risk of IS among patients with RA (aHR for IS: 0.67 vs. non-CHP group). A possible reason for this is that the commonly used CHP, such as Gui-Zhi-Shao-Yao-Zhi-Mu-Tang, alleviate systemic inflammation by lowering the CRP, and erythrocyte sedimentation rate (ESR), which may decrease the progression of atherosclerosis, the main pathologic process of IS (Daily et al., 2017). Another commonly prescribed single herb, *Spatholobus suberectus* Dunn (Ji-Xie-Teng), has also been shown to suppress inflammation by decreasing TNF- α secretion (Ye et al., 2014). The findings of this study suggest that the RA patients had a decreased risk of IS which may be associated with the combined use of CHP with anti-inflammatory effects.

From the viewpoint of TCM, the etiology of RA is dampness, wind, and heat (23). In our study, Gui-Zhi-Shao-Yao-Zhi-Mu-Tang, which originated from the Synopsis of the Golden Chamber written by Zhang Zhong Jing in the Han Dynasty, was the most commonly prescribed polyherbal formulation (Bian, 2000). In TCM theory, Gui-Zhi-Shao-Yao-Zhi-Mu-Tang dispels dampness, eliminates wind, and clears heat, which is similar to the mechanism of anti-inflammatory drugs. Guo

TABLE 2 | Incidence rates, hazard ratio, and confidence intervals of ischemic stroke among rheumatoid arthritis patients with and without Chinese herbal products usage according to gender, age, comorbidities, and drug used.

Variables	Rheumatoid Arthritis						Compared with non-CHP users	
	Non-CHP group (n = 4148)			CHP group (n = 4148)			Crude HR	Adjusted HR
	Event	Person years	IR [†]	Event	Person years	IR [†]	(95%CI)	(95%CI)
Total	146	20855	7.00	104	22211	4.68	0.67(0.52–0.86)**	0.67(0.52–0.86)**
Gender								
Female	122	18184	6.71	76	19208	3.96	0.59(0.44–0.79)***	0.63(0.47–0.85)**
Male	24	2671	8.99	28	3003	9.32	1.05(0.61–1.81)	1.35(0.74–2.44)
Age group								
18–39	9	6047	1.49	7	6306	1.11	0.74(0.27–1.98)	0.73(0.26–2.01)
40–59	96	12495	7.68	56	13331	4.20	0.55(0.39–0.76)***	0.63(0.45–0.89)**
≥60	41	2313	17.73	41	2574	15.93	0.89(0.58–1.38)	0.93(0.58–1.47)
Baseline Comorbidity								
Diabetes mellitus								
No	122	19274	6.33	90	20752	4.34	0.69(0.52–0.9)**	0.74(0.55–0.98)*
Yes	24	1581	15.18	14	1459	9.60	0.63(0.33–1.22)	0.64(0.32–1.31)
Hypertension								
No	94	17151	5.48	69	18848	3.66	0.67(0.49–0.91)*	0.7(0.5–0.96)*
Yes	52	3704	14.04	35	3363	10.41	0.74(0.48–1.13)	0.81(0.51–1.27)
Hyperlipidemia								
No	123	18908	6.51	81	20062	4.04	0.62(0.47–0.82)***	0.69(0.51–0.92)*
Yes	23	1947	11.82	23	2149	10.70	0.9(0.51–1.61)	0.95(0.52–1.74)
COPD								
No	122	18498	6.60	75	18854	3.98	0.6(0.45–0.8)***	0.71(0.52–0.95)*
Yes	24	2357	10.18	29	3357	8.64	0.86(0.5–1.48)	0.85(0.48–1.49)
ESRD								
No	142	20648	6.88	101	22072	4.58	0.67(0.52–0.86)**	0.73(0.56–0.95)*
Yes	4	207	19.35	3	139	21.54	1.04(0.23–4.64)	0.84(0.09–8.05)
Atrial fibrillation								
No	146	20838	7.01	104	22187	4.69	0.67(0.52–0.86)**	0.73(0.56–0.95)*
Yes	0	17	0.00	0	24	0.00	–	–
Drug used								
NSAID								
No	1	84	11.91	0	38	0.00	–	–
Yes	145	20771	6.98	104	22173	4.69	0.67(0.52–0.87)**	0.74(0.57–0.96)*
Corticosteroid								
No	134	20009	6.70	93	21019	4.42	0.66(0.51–0.86)**	0.73(0.55–0.96)*
Yes	12	846	14.18	11	1192	9.23	0.66(0.29–1.5)	0.59(0.24–1.43)
DMARD								
No	14	1189	11.78	4	537	7.45	0.63(0.21–1.93)	0.72(0.22–2.39)
Yes	132	19666	6.71	100	21674	4.61	0.69(0.53–0.89)**	0.73(0.56–0.96)*
TNF- α antagonist								
No	138	17579	7.85	87	16746	5.20	0.66(0.51–0.87)**	0.7(0.53–0.92)*
Yes	8	3276	2.44	17	5465	3.11	1.27(0.55–2.95)	1.04(0.44–2.48)

Adjusted HR: adjusted for CHP use, age, gender, diabetes mellitus, hypertension, hyperlipidemia, COPD, ESRD, atrial fibrillation, NSAID uses, corticosteroid, DMARD, and TNF-antagonist in Cox proportional hazards regression.

HR, hazard ratio; IR, incidence rates, per 1,000 person-years; CI, confidence interval; CHP, Chinese herbal products; COPD, chronic Obstructive Pulmonary Disease; ESRD, end stage renal disease; NSAID, non-steroidal anti-inflammatory drugs; DMARD, disease-modifying antirheumatic drugs; TNF, tumor necrosis factor.

* $p < 0.05$; ** $p < 0.01$; *** $p < 0.001$.

documented that Gui-Zhi-Shao-Yao-Zhi-Mu-Tang may partially attenuate RA by reversing inflammation-immune system imbalance and regulating the signaling pathways such as those involved in the secretion of TNF- α (Guo et al., 2016). Daily et al. noted that Gui-Zhi-Shao-Yao-Zhi-Mu-Tang lowered CRP and ESR in several clinical trials (Daily et al., 2017). Moreover, single herbs in Gui-Zhi-Shao-Yao-Zhi-Mu-Tang such as *Paeonia lactiflora* Pall. (Shao-Yao) and *Anemarrhena asphodeloides* Bunge (Zhi-Mu) have an anti-inflammatory effect. Compared with patients with RA who received leflunomide alone, those who received a combination of total glucosides of peony and leflunomide showed lower levels of the CRP, ESR, and

rheumatoid factor (Feng et al., 2016). This may explain the lower risk of IS among patients with RA who received a combination of CHP and WM in the present study.

Interestingly, the study finding is that female patients in the CHP group had a significantly lower risk of IS [aHR:0.63 (95% CI: 0.47–0.85)] than those who were in the non-CHP group. However, no significant difference was observed in this respect for the in male patients. This result might be related to the patients' lifestyle, such as tobacco use, which is a well-established risk factor for stroke. According to previous surveys of Taiwanese people, the rate of smoking was higher in males than in females (Wen et al., 2005). Additionally, smoking and

TABLE 3 | Hazard Ratios and 95% confidence intervals of ischemic stroke risk associated with the cumulative numbers of days of CHP use among patients with rheumatoid arthritis.

	n	Event no. (n = 250)	Hazard Ratio(95% CI)	
			Crude	Adjusted [†]
Non-CHP group	4148	146	1(reference)	1(reference)
CHP group				
<30 days	1966	57	0.83(0.61–1.12)	0.88(0.64–1.20)
30–180 days	1380	28	0.53(0.35–0.79)**	0.61(0.40–0.91)*
>180 days	802	19	0.57(0.35–0.92)*	0.62(0.38–1.00)

Crude HR* represented relative hazard ratio;

Adjusted HR[†] represented adjusted hazard ratio: mutually adjusted for age, gender, diabetes mellitus, hypertension, hyperlipidemia, COPD, ESRD, atrial fibrillation, NSAID uses, corticosteroid, DMARD, and TNF-antagonist in Cox proportional hazard regression.

HR, hazard ratio; CI, confidence interval; CHP, Chinese herbal products; COPD, chronic Obstructive Pulmonary Disease; ESRD, end stage renal disease.

*p < 0.05, **p < 0.01.

obese male tend to engage in irregular exercise (Lin et al., 2016). This then establishes the factors for stroke that might influence this study's results (Pearson et al., 2002; Boehme et al., 2017).

Table 2 presents that there was no significant difference between the two groups in risk of IS among the RA patients with any kind of comorbidity which is the main risk factor for IS. However, a reduced risk of IS was observed in the CHP group among RA patients without any kind of comorbidity. A possible explanation for this is that the baseline comorbidities, major risk factors for IS, may reduce the efficacy of CHP and exert an influence on the risk of IS. Hypertension, diabetes, hyperlipidemia, chronic obstructive pulmonary disease, end stage renal disease, and atrial fibrillation are thought to be the independent risk factors for IS with 2- to 3-fold increased risk in stroke (Boehme et al., 2017). Possible mechanisms leading to stroke are chronic systemic inflammation (Austin et al., 2016; Chen R. et al., 2016; Jimenez et al., 2016; Nayak-Rao and Shenoy, 2017; Menet et al., 2018). Inflammation plays an important

role in the development of the atherosclerotic plaque and the main pathologic process of IS. Although several commonly prescribed CHP have anti-inflammation effects, the chronic inflammation among RA patients with any kind of comorbidity might be too severe to be reversed. Therefore, there was no association between protective effect against IS of CHP and the risk of IS among RA patients with comorbidities. In the aspect of medication, RA patients receiving CHP in combination with DMARDs had a lower risk of IS compared to those receiving WM only. However, there is no significantly lower risk of IS among RA patients receiving CHP in combination with TNF-antagonist compared to those receiving WM only. The reason might be because the systemic inflammation of RA patients receiving TNF-antagonist are too severe to be alleviated. Doctors usually prescribe TNF-antagonist to treat RA patients due to high disease activity, early joints erosion, or high level of rheumatoid factor indicate higher grade of inflammation and disease severity than those taking DMARDs

TABLE 4 | Hazard Ratios and 95% confidence intervals of ischemic stroke risk associated with the type of single herbs and polyherbal formulations used among patients with rheumatoid arthritis.

CHM prescription	Ischemic stroke		Hazard Ratio(95% CI)	
	n	No. of Event	Crude*	Adjusted [†]
Non-CHP group	4148	104	1(reference)	1(reference)
CHP group				
Single herb				
1. <i>Corydalis ambigua</i> Cham. & Schltl. (Yen-Hu-So)	954	29	0.78(0.52–1.16)	0.92(0.61–1.38)
2. <i>Spatholobus suberectus</i> Dunn (Ji-Xie-Teng)	791	22	0.69(0.44–1.08)	0.81(0.52–1.29)
3. <i>Cyperus rotundus</i> L. (Pao-Fu-Tzu)	675	18	0.70(0.43–1.14)	0.87(0.53–1.44)
4. <i>Morus alba</i> L. (Sang-Chih)	741	21	0.71(0.45–1.12)	0.84(0.52–1.33)
5. <i>Coix lacryma-jobi</i> L. (Yi-Yi Jen)	680	19	0.71(0.44–1.14)	0.84(0.51–1.36)
Polyherbal formulation				
1. Gui-Zhi-Shao-Yao-Zhi-Mu-Tang	1449	21	0.44(0.28–0.70)***	0.50(0.31–0.80)**
2. Dang-Gui-Nian-Tong-Tang	1182	35	0.61(0.42–0.89)**	0.71(0.48–1.03)
3. Shu-Jin-Huo-Xie-Tang	991	13	0.32(0.18–0.56)***	0.35(0.20–0.63)***
4. Du-Huo-Ji-Sheng-Tang	696	16	0.54(0.32–0.91)*	0.57(0.34–0.96)*
5. Jia-Wei-Xiao-Yao-San	628	18	0.72(0.44–1.17)	1.06(0.64–1.76)

Crude HR* represented relative hazard ratio; Adjusted HR[†] represented adjusted hazard ratio: mutually adjusted for CHP use, age, gender, diabetes mellitus, hypertension, hyperlipidemia, COPD, ESRD, atrial fibrillation, NSAID, corticosteroid, DMARD, and TNF-antagonist usage in Cox proportional hazard regression.

CI, confidence interval; CHP, Chinese herbal products; COPD, chronic Obstructive Pulmonary Disease; ESRD, end stage renal disease; NSAID, non-steroidal anti-inflammatory drugs; DMARD, disease-modifying antirheumatic drugs; TNF, tumor necrosis factor.

*p < 0.05, **p < 0.01, ***p < 0.001.

TABLE 5 | The function and active compounds of the top 5 commonly prescribed single herbs and the function and ingredients of the top 5 most commonly prescribed polyherbal formulations for patients with RA.

Name	Active compounds	Function	Reference				
Single herb							
Corydalis ambigua Cham. & Schltldl. (Yan-Hu-Suo)	Corynoline, Acetylcorynoline,d-corydalin, dl-tetrahydropalmatine, Protopine, Tetrahydrocoptisine, dl-tetrahydroCoptisine, d-corybulbine, Allocryptopine	Pain tolerance↑ Anti-hypertension Anti-inflammation	(Zhou et al., 2016; Zhou et al., 2019)				
Spatholobus suberectus Dunn (Ji-Xie-Teng)	Jixuetengsterol, Friedelin, Friedelinsterol, Taraxerone, β-Sitosterol, Stigmasterol, Campesterol	Anti-inflammation Anti-oxidant effects Anti-viral effects Immunomodulatory	(Fu et al., 2017; Pang et al., 2011)				
Cyperus rotundus L. (Xiang-Fu)	α-longipinane, β-selinene, Cyperene, Caryophyllene oxide	Anti-nociceptive effects Anti-inflammatory Anti-oxidant effects	(Imam and Sumi, 2014; Pirzada et al., 2015)				
Morus alba L. (Sang-Zhi)	Morin, Oxyresveratrol, Mulberrin, Mulbel- Cochromene, Cyclomulberrin, Cyclomulbel-rochromene	Anti-lipidemic, Anti-inflammation Anti-oxidant Anti-tumour activities	(Bachewal et al., 2018; Park et al., 2016; Li et al., 2015)				
Coix lacryma-jobi L. (Yi-Yi-Ren)	Coixol, Coixenolide, Myristic acid	Anti-hyperlipidemic, Anti-inflammation Anti-oxidant effects Anti-tumour activities	(Seo et al., 2000)				
Name	Ingredients	Percentage (%)	Function	Reference			
Polyherbal formulation							
Gui-Zhi-Shao-Yao-Zhi-Mu-Tang	Paeonia lactiflora Pall. (Bai-Shao)	9.6%	Morning stiffness ↓ CRP↓ RSR↓ RA factor↓	(Efthimiou and Kukar, 2010; Ye et al., 2014)			
	Atractylodes macrocephala Koidz. (Bai-Zhu)	16.1%					
	Anemarrhena asphodeloides Bge. (Zhi-Mu)	12.9%					
	Saposhnikovia divaricata (Turcz.) Schischk. (Fang-Feng)	12.9%					
	Glycyrrhiza uralensis Fisch. ex DC. (Gann-Cao)	6.5%					
	Cinnamomum cassia (L.) J.Presl (Gui-Zhi)	12.9%					
	Ephedra sinica Stapf (Ma-Huang)	6.5%					
	Aconitum camichaelii Debx. (Fu-Zi)	16.1%					
Dang-Gui-Nian-Tong-Tang	Zingiber officinale Roscoe (Sheng-Jiang)		Not available				
	Artemisia capillaris Thunb. (Yin-Chen)	10.6%					
	Notopterygium incisum K.C.Ting ex H.T.Chang (Qiang-Huo)	10.6%					
	Saposhnikovia divaricata (Turcz.) Schischk. (Fang-Feng)	6.0%					
	Actaea heracleifolia (Kom.) J.Compton (Sheng-Ma)	4.6%					
	Pueraria lobata (Willd.) Ohwi (Ge-Gen)	4.6%					
	Atractylodes lancea (Thunb.) DC. (Cang-Zhu)	6.0%					
	Atractylodes macrocephala Koidz. (Bai-Zhu)	4.6%					
	Glycyrrhiza uralensis Fisch. ex DC. (Gan-Cao)	6.0%					
	Scutellaria baicalensis Georgi (Huang-Qin)	4.6%					
	Sophora flavescens Ait. (Ku-Shen)	4.6%					
	Anemarrhena asphodeloides Bge. (Zhi-Mu)	6.0%					
	Angelica sinensis (Oliv.) Diels (Dang-Gui)	6.0%					
	Polyporus umbellatus (Pers.) Fries (Zhu-Ling)						
	Alisma plantago-aquatica subsp. orientale (Sam.) Sam. (Ze-Xie)						
	Atractylodes lancea (Thunb.) DC						
	Shu-Jin-Huo-Xie-Tang	Angelica sinensis (Oliv.) Diels (Dang-Gui)			7.2%	Interleukin 2 production ↓ Anti-hypersensitivity	(Imam and Sumi, 2014)
		Ligusticum chuanxiong Hort. (Chuan-Qiong)			3.7%		
		Paeonia lactiflora Pall. (Bai-Shao)			9.1%		
		Rehmannia glutinosa Libosch. (Di-Huang)			7.2%		
Atractylodes lancea (Thunb.) DC. (Cang-Zhu)		7.2%					
Cyathula officinalis Kuan (Niu-Xi)		7.2%					

(Continued)

TABLE 5 | Continued

Name	Ingredients	Percentage (%)	Function	Reference
Du-Huo-Ji-Sheng-Tang	<i>Citrus reticulata</i> Blanco (Chen-Pi)	7.2%	Anti-inflammation	(Kong et al., 2013)
	<i>Prunus persica</i> (L.) Batsch (Tao-Ren)	3.7%		
	<i>Clematis chinensis</i> Osbeck (Wei-Ling-Xian)	7.2%		
	<i>Stephania tetrandra</i> S. Moore (Fang-Ji)	3.7%		
	<i>Notopterygium incisum</i> K.C.Ting ex	3.7%		
	H.T.Chang (Qiang-Huo)	3.7%		
	<i>Angelica dahurica</i> (Fisch. ex Hoffm.) Benth. et	3.7%		
	Hook. (Bai-Zhi)	10.8%		
	<i>Gentiana scabra</i> Bunge (Long-Dan -Cao)	3.7%		
	<i>Zingiber officinale</i> Roscoe (Sheng-Jiang)	7.2%		
	<i>Poria cocos</i> (Schw.) Wolf (Fu-Ling)	3.7%		
	<i>Saposhnikovia divaricata</i> (Turcz.) Schischk.			
	(Fang-Feng)			
	<i>Glycyrrhiza uralensis</i> Fisch. ex DC. (Gan-Cao)			
	<i>Taxillus chinensis</i> (DC.) Danser (Sang-Ji-Sheng)	6.5%		
		9.0%		
	<i>Angelica pubescens</i> Maxim. (Du-Huo)	6.5%		
	<i>Eucommia ulmoides</i> Oliv. (Du-Zhong)	6.5%		
	<i>Cyathula officinalis</i> Kuan (Niu-Xi)	6.5%		
Jia-Wei-Xiao-Yao-San	<i>Asarum sieboldii</i> Miq. (Xi-Xin)	6.5%	Prevent bone loss Prevent atherosclerosis	(Pirzada et al., 2015)
	<i>Glycyrrhiza uralensis</i> Fisch. ex DC. (Gan-Cao)	6.5%		
	<i>Gentiana macrophylla</i> Pall. (Qin-Jiao)	6.5%		
	<i>Poria cocos</i> (Schw.) Wolf (Fu-Ling)	6.5%		
	<i>Cinnamomum cassia</i> Presl (Rou-Gui)	6.5%		
	<i>Saposhnikovia divaricata</i> (Turcz.) Schischk.	6.5%		
	(Fang-Feng)	6.5%		
	<i>Ligusticum chuanxiong</i> Hort. (Chuan-Qiong)	6.5%		
	<i>Rehmannia glutinosa</i> Libosch. (Di-Huang)	6.5%		
	<i>Paeonia lactiflora</i> Pall. (Bai-Shao)	6.5%		
	<i>Angelica sinensis</i> (Oliv.) Diels (Dang-Gui)			
	<i>Panax ginseng</i> C. A. Mey. (Ren-Shen)			
	<i>Glycyrrhiza uralensis</i> Fisch. ex DC. (Gan-Cao)	6.1%		
	<i>Paeonia lactiflora</i> Pall. (Bai-Shao)	12.1%		
	<i>Angelica sinensis</i> (Oliv.) Diels (Dang-Gui)	12.1%		
	<i>Poria cocos</i> (Schw.) Wolf (Fu-Ling)	12.1%		
	<i>Atractylodes macrocephala</i> Koidz. (Bai-Zhu)	12.1%		
	<i>Bupleurum chinense</i> DC. (Chai-Hu)	12.1%		
	<i>Mentha haplocalyx</i> Briq. (Bo-He)	6.1%		
	<i>Zingiber officinale</i> (Willd.) Rosc. (Gan-Jiang)	12.1%		
	<i>Moutan officinalis</i> (L.) Lindl. & Paxton (Mu-Dan-Pi)	7.6%		
		7.6%		
	<i>Gardenia jasminoides</i> J.Ellis (Zhi-Zi)			

only (Albrecht and Zink, 2017). Hence, the association between a lower IS risk and receiving the CHP treatment in combination with WM among severe RA patients was not significant.

In the CHP group, patients with cumulative numbers of days of CHP use between 30 and 180 days were found to have a lower risk of IS than those whose cumulative numbers of days of CHP use <30 days. A possible explanation for this is that CHP requires 30-180 days to achieve a steady effect in patients with RA. The cumulative numbers of days of CHP use was similar to the treatment duration of methotrexate recommended by the European League Against Rheumatism (Smolen et al., 2017). Moreover, the results obtained for the minimum number of days of CHP use were consistent with those of previous randomized controlled trials. Patients with RA taking *Paeonia lactiflora* Pall. (Shao-Yao) extract in combination with treatment with leflunomide and methotrexate for 24 weeks had lower CRP levels and ESR (Chen et al., 2013). Additionally, after 12 to 24

weeks of treatment with *Tripterygium wilfordii* Hook.f in combination with methotrexate, there was an improvement in the level of CRP (Lv et al., 2015). Furthermore, several randomized controlled trial about the efficacy of Gui-Zhi-Shao-Yao-Zhi-Mu-Tang with WM showed that after taking Gui-Zhi-Shao-Yao-Zhi-Mu-Tang with WM for 4-12 weeks, there was a significant decrease in ESR, RA factor, and CRP (Daily et al., 2017). The Pathological mechanisms of RA are characterized by chronic systemic inflammation, and patients using CHP for 30-180 days may achieve an improved anti-inflammatory effect in terms of reducing their risk of IS.

Another major finding of this study is that the commonly prescribed polyherbal formulations, such as Gui-Zhi-Shao-Yao-Zhi-Mu-Tang, Shu-Jin-Huo-Xie-Tang, Du-Huo-Ji-Sheng-Tang, have been found to lower the risk of IS (Table 4). A possibly explanation is that the polyherbal formulations may suppress chronic inflammation in patients with RA. The function,

ingredients, and the percentage of every single herb of the top 5 most commonly prescribed polyherbal formulations were presented in **Table 5**. Daily et al. have reported that Gui-Zhi-Shao-Yao-Zhi-Mu-Tang may lower the levels of the CRP and the ESR in patients with RA (Daily et al., 2017). Previous research has demonstrated that more than 50% of ingredients contained in Gui-Zhi-Shao-Yao-Zhi-Mu-Tang have anti-inflammatory effects with lowering the level of rheumatoid factor or suppressing the production of TNF- α or IL-6; these included *Paeonia lactiflora* Pall. (Bai-Shao), *Anemarrhena asphodeloides* Bge. (Zhi-Mu), *Saposhnikovia divaricata* (Turcz.) Schischk. (Fang-Feng) and *Zingiber officinale* Roscoe (Sheng-Jiang) (Chen et al., 2013; Kong et al., 2013; Funk et al., 2016). Although there was only a Chinese study presented that Shu-Jin-Huo-Xie-Tang may reduce the production of lymphocyte IL-2 after co-culture of the herb with lymphocyte. More than 50% of ingredients in Shu-Jin-Huo-Xie-Tang are demonstrated to have anti-RA effects, such as *Angelica sinensis* (Oliv.) Diels (Dang-Gui), *Ligusticum chuanxiong* Hort. (Chuan-Qiong), *Paeonia lactiflora* Pall. (Bai-Shao), *Atractylodes lancea* (Thunb.) DC. (Cang-Zhu), *Clematis chinensis* Osbeck (Wei-Ling-Xian), *Saposhnikovia divaricata* (Turcz.) Schischk. (Fang-Feng) and *Zingiber officinale* Roscoe (Sheng-Jiang), have been shown to suppress the expression of several inflammatory cytokines in an experimental RA model (Peng et al., 2012; Kong et al., 2013; Funk et al., 2016; Hung and Wu, 2016; Liu et al., 2016; Li et al., 2016). In addition, Du-Huo-Ji-Sheng-Tang has been claimed to mediate an anti-inflammatory effects by promoting lymphatic drainage function in TNF-Tg mice (Chen Y. et al., 2016). Certain single herbs in Du-Huo-Ji-Sheng-Tang also have an potentially anti-inflammatory effect, such as *Saposhnikovia divaricata* (Turcz.) Schischk. (Fang-Feng), these include *Paeonia lactiflora* Pall. (Shao-Yao), *Ligusticum chuanxiong* Hort. (Chuan-Qiong), and *Angelica sinensis* (Oliv.) Diels (Dang-Gui). In previous studies, *Ligusticum chuanxiong* Hort. (Chuan-Qiong) and *Angelica sinensis* (Oliv.) Diels (Dang-Gui) have been demonstrated to counteract the expression of inflammatory cytokine thereby minimize the endothelial damage, such as TNF- α and interleukins, which is a key mediator of inflammation (Kong et al., 2013; Li et al., 2016; Hung and Wu, 2016). The anti-inflammatory effects of these polyherbal formulations may be associated with a lower risk of IS among patients with RA.

This study has several strengths. First, this is a nationwide population-based study using a registry of beneficiaries, inpatient, and ambulatory care claims, and the Registry for Catastrophic Illness from the NHIRD datasets. This type of data not only prevents selection bias and recall bias related to the use of CHP but also reflects real-world practice. Second, the use of the date of first accepted CHP as the index date in the CHP group helps to avoid bias whereby patients with a longer stroke-free period of time tend to use CHP. Third, we performed a subgroup analysis based on the number of cumulative days of CHP usage. The result may provide empirical evidence pertaining to the days of CHP usage for clinical use.

Several limitations of the present study need to be considered. Data pertaining to life style, smoking, drinking, obesity, and body mass index are unavailable from the NHIRD. Similarly, data pertaining to disease activity and disease severity were unavailable, although all of them are known risk factors for IS (Dhillon and Liang, 2015). We performed a 1:1 frequency match

and used a Cox proportional hazard model to eliminate the potential effect of confounding factors. Second, NHIRD only covers CHP prescribed by licensed TCM physicians. Patients who resorted to over-the-counter use of CHP may not have been included in the study sample, which is likely to have led to an underestimation of the percentage of CHP usage. Third, safety of prescribed polyherbal formulations are not available. Certain single herbs contained in the polyherbal formulations were reported to cause adverse reactions. *Aconitum carmichaelii* Debx.(accounts for 6.5%), contained in Gui-Zhi-Shao-Yao-Zhi-Mu-Tang, might cause palpitation, hypotension, and arrhythmia due to aconitine alkaloids. *Asarum sieboldii* Miq.(accounts for 6.5%), one of the single herb in the Du-Huo-Ji-Sheng-Tang, might lead to renal failure, tubulointerstitial fibrosis, and urothelial cancer owing to aconitine alkaloids. Although, the toxic compounds of the certain single herbs might result in harmful effects, Daily and Hsieh reported that no severe adverse events and drug reactions are observed after taking Gui-Zhi-Shao-Yao-Zhi-Mu-Tang and Du-Huo-Ji-Sheng-Tang 4 to 20 weeks (Hsieh et al., 2010; Daily et al., 2017).

CONCLUSION

This study demonstrated the association between a decreased IS risk and receiving CHP treatment in combination with WM in RA patients, particularly those who used CHP for more than 30 days. Our findings suggest that Gui-Zhi-Shao-Yao-Zhi-Mu-Tang, Shu-Jin-Huo-Xie-Tang, and Du-Huo-Ji-Sheng-Tang might be associated with a lower risk of IS. A further randomized control trial is required to clarify the casual relationship between these results.

DATA AVAILABILITY STATEMENT

The datasets generated for this study are available on request to the corresponding author.

AUTHOR CONTRIBUTIONS

H-SS was responsible for the study's conception and design, reviewing and interpreting the data, and drafting the manuscript. N-HH was responsible for modifying the study design, interpreting the data, and the critical revision. J-HC contributed to the collection and analysis of the data. H-SS, N-HH, and J-HC were responsible for the final approval of the revised manuscript. All authors read and approved the final manuscript.

ACKNOWLEDGMENTS

This work was supported by grants from the Ministry of Health and Welfare, Taiwan (MOHW107-TDU-B-212-123004), China Medical University Hospital, Academia Sinica Stroke Biosignature Project (BM10701010021), MOST Clinical Trial Consortium for Stroke (MOST 106-2321-B-039-005), Tseng-Lien Lin Foundation, Taichung, Taiwan, and Katsuzo and Kiyo Aoshima Memorial Funds, Japan.

REFERENCES

- Agca, R., Heslinga, S. C., Rollefstad, S., Heslinga, M., McInnes, I. B., Peters, M. J., et al. (2017). EULAR recommendations for cardiovascular disease risk management in patients with rheumatoid arthritis and other forms of inflammatory joint disorders: 2015/2016 update. *Ann. Rheumatic Dis.* 76, 17–28. doi: 10.1136/annrheumdis-2016-209775
- Albrecht, K., and Zink, A. (2017). Poor prognostic factors guiding treatment decisions in rheumatoid arthritis patients: a review of data from randomized clinical trials and cohort studies. *Arthritis Res. Ther.* 19, 68–68. doi: 10.1186/s13075-017-1266-4(2017)
- Ammon, H. P. (2006). Boswellic acids in chronic inflammatory diseases. *Planta Med.* 72, 1100–1116. doi: 10.1055/s-2006-947227
- Austin, V., Crack, P. J., Bozinovski, S., Miller, A. A., and Vlahos, R. (2016). COPD and stroke: are systemic inflammation and oxidative stress the missing links? *Clin. Sci. (London England: 1979)* 130, 1039–1050. doi: 10.1042/cs20160043
- Avina-Zubieta, J. A., Choi, H. K., Sadatsafavi, M., Etminan, M., Esdaile, J. M., and Lacaille, D. (2008). Risk of cardiovascular mortality in patients with rheumatoid arthritis: a meta-analysis of observational studies. *Arthritis Rheum.* 59, 1690–1697. doi: 10.1002/art.24092
- Bachawal, P., Gundu, C., Yerra, V. G., Kalvala, A. K., Areti, A., Kumar, A., et al. (2018). Morin exerts neuroprotection via attenuation of ROS induced oxidative damage and neuroinflammation in experimental diabetic neuropathy. *BioFactors (Oxford England)* 44, 109–122. doi: 10.1002/biof.1397
- Benjamin, E. J., Blaha, M. J., Chiuve, S. E., Cushman, M., Das, S. R., Deo, R., et al. (2017). Heart Disease and Stroke Statistics-2017 Update: a report from the American Heart Association. *Circulation* 135, e146–e603. doi: 10.1161/cir.0000000000000485
- Bian, Y. (2000). Analysis and investigation on annotations on synopsis of Jade book of golden chamber (Jin gui yi han yao lue shu yi). *Zhonghua yi shi za zhi (Beijing China: 1980)* 30, 172–174.
- Boehme, A. K., Esenwa, C., and Elkind, M. S. (2017). Stroke Risk Factors, Genetics, and Prevention. *Circ. Res.* 120, 472–495. doi: 10.1161/circresaha.116.308398
- Chen, Z., Li, X. P., Li, Z. J., Xu, L., and Li, X. M. (2013). Reduced hepatotoxicity by total glucosides of peony in combination treatment with leflunomide and methotrexate for patients with active rheumatoid arthritis. *Int. Immunopharmacol.* 15, 474–477. doi: 10.1016/j.intimp.2013.01.021
- Chen, R., Oviagele, B., and Feng, W. (2016). Diabetes and stroke: epidemiology, pathophysiology, pharmaceuticals and outcomes. *Am. J. Med. Sci.* 351, 380–386. doi: 10.1016/j.amjms.2016.01.011
- Chen, Y., Li, J., Li, Q., Wang, T., Xing, L., Xu, H., et al. (2016). Du-Huo-Ji-Sheng-Tang attenuates inflammation of TNF-Tg mice related to promoting lymphatic drainage function. *Evidence-Based Complementary Altern. Med.: eCAM*, 2016, 7067691. doi: 10.1155/2016/7067691
- Daily, J. W., Zhang, T., Cao, S., and Park, S. (2017). Efficacy and Safety of GuiZhi-ShaoYao-ZhiMu Decoction for Treating Rheumatoid Arthritis: A Systematic Review and Meta-Analysis of Randomized Clinical Trials. *J. Altern. Complementary Med. (New York N.Y.)*. 10, 756–770 doi: 10.1089/acm.2017.0098
- Dhillon, N., and Liang, K. (2015). Prevention of stroke in rheumatoid arthritis. *Curr. Treat Options Neurol.* 17, 356. doi: 10.1007/s11940-015-0356-3
- Effthimiou, P., and Kukar, M. (2010). Complementary and alternative medicine use in rheumatoid arthritis: proposed mechanism of action and efficacy of commonly used modalities. *Rheumatol. Int.* 30, 571–586. doi: 10.1007/s00296-009-1206-y
- Feng, Z., Xu, J., He, G., Cao, M., Duan, L., Chen, L., et al. (2016). The efficacy and safety of the combination of total glucosides of Peony and Leflunomide for the treatment of rheumatoid arthritis: a systemic review and meta-analysis. *Evidence-Based Complementary Altern. Med. eCAM*. 2016, 9852793. doi: 10.1155/2016/9852793
- Fu, Y. F., Jiang, L. H., Zhao, W. D., Xi-Nan, M., Huang, S. Q., Yang, J., et al. (2017). Immunomodulatory and antioxidant effects of total flavonoids of *Spatholobus suberectus* Dunn on PCV2 infected mice. *Sci. Rep.* 7, 8676. doi: 10.1038/s41598-017-09340-9
- Funk, J. L., Frye, J. B., Oyarzo, J. N., Chen, J., Zhang, H., and Timmermann, B. N. (2016). Anti-inflammatory effects of the essential oils of ginger (*Zingiber officinale* Roscoe) in experimental rheumatoid arthritis. *PharmaNutrition* 4, 123–131. doi: 10.1016/j.phanu.2016.02.004
- Guo, Q., Mao, X., Zhang, Y., Meng, S., Xi, Y., Ding, Y., et al. (2016). Guizhi-Shaoyao-Zhimu decoction attenuates rheumatoid arthritis partially by reversing inflammation-immune system imbalance. *J. Trans. Med.* 14, 165. doi: 10.1186/s12967-016-0921-x
- Hansson, G. K. (2005). Inflammation, atherosclerosis, and coronary artery disease. *New Engl. J. Med.* 352, 1685–1695. doi: 10.1056/NEJMra043430
- Hsieh, S.-C., Lai, J. N., Chen, P. C., Chen, C. C., Chen, H. J., and Wang, J. D. (2010). Is Duhuo Jisheng Tang containing Xixin safe? A four-week safety study. *Chin. Med.* 5, 6–6. doi: 10.1186/1749-8546-5-6
- Huang, M. C., Pai, F. T., Lin, C. C., Chang, C. M., Chang, H. H., Lee, Y. C., et al. (2015). Characteristics of traditional Chinese medicine use in patients with rheumatoid arthritis in Taiwan: A nationwide population-based study. *J. Ethnopharmacol.* 176, 9–16. doi: 10.1016/j.jep.2015.10.024
- Hung, H. Y., and Wu, T. S. (2016). Recent progress on the traditional Chinese medicines that regulate the blood. *J. Food Drug Anal.* 24, 221–238. doi: 10.1016/j.jfda.2015.10.009
- Imam, M. Z., and Sumi, C. D. (2014). Evaluation of antinociceptive activity of hydromethanol extract of *Cyperus rotundus* in mice. *BMC Complementary Altern. Med.* 14, 83. doi: 10.1186/1472-6882-14-83
- Jimenez, M. C., Rexrode, K. M., Kotler, G., Everett, B. M., Glynn, R. J., Lee, I. M., et al. (2016). Association Between Markers of Inflammation and Total Stroke by Hypertensive Status Among Women. *Am. J. Hypertension* 29, 1117–1124. doi: 10.1093/ajh/hpw050
- Kang, H. S., Kim, Y. H., Lee, C. S., Lee, J. J., Choi, I., and Pyun, K. H. (1996). Anti-inflammatory effects of *Stephania tetrandra* S. Moore on interleukin-6 production and experimental inflammatory disease models. *Mediators Inflammation* 5, 280–291. doi: 10.1155/s0962935196000415
- Kong, X., Liu, C., Zhang, C., Zhao, J., Wang, J., Wan, H., et al. (2013). The suppressive effects of *Saposhnikovia divaricata* (Fangfeng) chromone extract on rheumatoid arthritis via inhibition of nuclear factor- κ B and mitogen activated protein kinases activation on collagen-induced arthritis model. *J. Ethnopharmacol.* 148, 842–850. doi: 10.1016/j.jep.2013.05.023(2013)
- Lee, S. C., Chang, S. J., and Tsai, L. Y. (2004). Effects of traditional Chinese medicines on serum lipid profiles and homocysteine in the ovariectomized rats. *Am. J. Chin. Med.* 32, 541–550. doi: 10.1142/s0192415x04002181
- Li, X., Wang, L., Gao, X., Li, G., Cao, H., Song, D., et al. (2015). Mechanisms of protective effect of *Ramulus Mori* polysaccharides on renal injury in high-fat diet/streptozotocin-induced diabetic rats. *Cell. Physiol. Biochem. Int. J. Exp. Cell. Physiol. Biochem. Pharmacol.* 37, 2125–2134. doi: 10.1159/000438570
- Li, J., Hua, Y., Ji, P., Yao, W., Zhao, H., Zhong, L., et al. (2016). Effects of volatile oils of *Angelica sinensis* on an acute inflammation rat model. *Pharmaceutical Biol.* 54, 1881–1890. doi: 10.3109/13880209.2015.1133660
- Liacini, A., Sylvester, J., and Zafarullah, M. (2005). Triptolide suppresses proinflammatory cytokine-induced matrix metalloproteinase and aggrecanase-1 gene expression in chondrocytes. *Biochem. Biophys. Res. Commun.* 327, 320–327. doi: 10.1016/j.bbrc.2004.12.020
- Lin, P. S., Hsieh, C. C., Cheng, H. S., Tseng, T. J., and Su, S. C. (2016). Association between Physical Fitness and Successful Aging in Taiwanese Older Adults. *PloS One* 11, e0150389. doi: 10.1371/journal.pone.0150389
- Lindhardsen, J., Ahlehoff, O., Gislason, G. H., Madsen, O. R., Olesen, J. B., Svendsen, J. H., et al. (2012). Risk of atrial fibrillation and stroke in rheumatoid arthritis: Danish nationwide cohort study. *BMJ (Clinical Res. ed.)* 344, e1257. doi: 10.1136/bmj.e1257
- Lindhardsen, J., Gislason, G. H., Jacobsen, S., Ahlehoff, O., Olsen, A. M., Madsen, O. R., et al. (2014). Non-steroidal anti-inflammatory drugs and risk of cardiovascular disease in patients with rheumatoid arthritis: a nationwide cohort study. *Ann. Rheumatic Dis.* 73, 1515–1521. doi: 10.1136/annrheumdis-2012-203137
- Liou, T. H., Huang, S. W., Lin, J. W., Chang, Y. S., Wu, C. W., and Lin, H. W. (2014). Risk of stroke in patients with rheumatism: a nationwide longitudinal population-based study. *Sci. Rep.* 4, 5110. doi: 10.1038/srep05110
- Liu, R., Tao, E., Yu, S., Liu, B., Dai, L., Yu, L., et al. (2016). The suppressive effects of the petroleum ether fraction from *Atractylodes lancea* (Thunb.) DC. On a Collagen-Induced Arthritis Model. *Phytother. Res.* 30, 1672–1679. doi: 10.1002/ptr.5671
- Lv, Q. W., Zhang, W., Shi, Q., Zheng, W. J., Li, X., Chen, H., et al. (2015). Comparison of *Tripterygium wilfordii* Hook F with methotrexate in the treatment of active

- rheumatoid arthritis (TRIFRA): a randomised, controlled clinical trial. *Ann. Rheumatic Dis.* 74, 1078–1086. doi: 10.1136/annrheumdis-2013-204807
- Martin-Martinez, M. A., Martin-Martinez, M. A., Gonzalez-Juanatey, C., Castaneda, S., Llorca, J., Ferraz-Amaro, I., Fernandez-Gutierrez, B., et al. (2014). Recommendations for the management of cardiovascular risk in patients with rheumatoid arthritis: scientific evidence and expert opinion. *Semin. In Arthritis Rheum.* 44, 1–8. doi: 10.1016/j.semarthrit.2014.01.002
- Menet, R., Bernard, M., and ElAli, A. (2018). Hyperlipidemia in Stroke Pathobiology and Therapy: Insights and Perspectives. *Front. In Physiol.* 9, 488. doi: 10.3389/fphys.2018.00488
- Michalsen, A. (2013). The role of complementary and alternative medicine (CAM) in rheumatology—it's time for integrative medicine. *J. Rheumatol.* 40, 547–549. doi: 10.3899/jrheum.130107
- Nadareishvili, Z., Michaud, K., Hallenbeck, J. M., and Wolfe, F. (2008). Cardiovascular, rheumatologic, and pharmacologic predictors of stroke in patients with rheumatoid arthritis: a nested, case-control study. *Arthritis Rheum.* 59, 1090–1096. doi: 10.1002/art.23935
- Nayak-Rao, S., and Shenoy, M. P. (2017). Stroke in patients with chronic kidney disease...: How do we Approach and Manage it? *Indian J. Nephrol.* 27, 167–171. doi: 10.4103/0971-4065.202405
- Pang, J., Guo, J. P., Jin, M., Chen, Z. Q., Wang, X. W., and Li, J. W. (2011). Antiviral effects of aqueous extract from *Spatholobus suberectus* Dunn. against coxsackievirus B3 in mice. *Chin. J. Integr. Med.* 17, 764–769. doi: 10.1007/s11655-011-0642-1
- Park, G. S., Kim, J. K., and Kim, J. H. (2016). Anti-inflammatory action of ethanolic extract of *Ramulus mori* on the BLT2-linked cascade. *BMB Rep.* 49, 232–237. doi: 10.5483/bmbrep.2016.49.4.002
- Pearson, T. A., Blair, S. N., Daniels, S. R., Eckel, R. H., Fair, J. M., Fortmann, S. P., et al. (2002). AHA Guidelines for primary prevention of cardiovascular disease and stroke: 2002 update: consensus panel guide to comprehensive risk reduction for adult patients without coronary or other atherosclerotic vascular diseases. American Heart Association Science Advisory and Coordinating Committee. *Circulation* 106, 388–391. doi: 10.1161/01.CIR.0000020190.45892.75
- Peng, C., Perera, P. K., Li, Y. M., Fang, W. R., Liu, L. F., and Li, F. W. (2012). Anti-inflammatory effects of *Clematis chinensis* Osbeck extract (AR-6) may be associated with NF- κ B, TNF- α , and COX-2 in collagen-induced arthritis in rat. *Rheumatol. Int.* 32, 3119–3125. doi: 10.1007/s00296-011-2083-8
- Pirzada, A. M., Ali, H. H., Naeem, M., Latif, M., Bukhari, A. H., and Tanveer, A. (2015). *Cyperus rotundus* L.: traditional uses, phytochemistry, and pharmacological activities. *J. Ethnopharmacol.* 174, 540–560. doi: 10.1016/j.jep.2015.08.012
- Roubille, C., Richer, V., Starnino, T., McCourt, C., McFarlane, A., Fleming, P., et al. (2015). The effects of tumour necrosis factor inhibitors, methotrexate, non-steroidal anti-inflammatory drugs and corticosteroids on cardiovascular events in rheumatoid arthritis, psoriasis and psoriatic arthritis: a systematic review and meta-analysis. *Ann. Rheumatic Dis.* 74, 480–489. doi: 10.1136/annrheumdis-2014-206624
- Salliot, C., and van der Heijde, D. (2009). Long-term safety of methotrexate monotherapy in patients with rheumatoid arthritis: a systematic literature research. *Ann. Rheumatic Dis.* 68, 1100–1104. doi: 10.1136/ard.2008.093690
- Sattar, N., McCarey, D. W., Capell, H., and McInnes, I. B. (2003). Explaining how “high-grade” systemic inflammation accelerates vascular risk in rheumatoid arthritis. *Circulation* 108, 2957–2963. doi: 10.1161/01.cir.0000099844.31524.05
- Seo, W. G., Pae, H. O., Chai, K. Y., Yun, Y. G., Kwon, T. H., Chung, H. T., et al. (2000). Inhibitory effects of methanol extract of seeds of Job's Tears (*Coix lachryma-jobi* L. var. *ma-yuen*) on nitric oxide and superoxide production in RAW 264.7 macrophages. *Immunopharmacol. Immunotoxicol.* 22, 545–554. doi: 10.3109/08923970009026011
- Shu, H., Arita, H., Hayashida, M., Zhang, L., An, K., Huang, W., et al. (2010). Anti-hypersensitivity effects of Shu-jing-huo-xue-tang, a Chinese herbal medicine, in CCI-neuropathic rats. *J. Ethnopharmacol.* 131, 464–470. doi: 10.1016/j.jep.2010.07.004
- Smolen, J. S., Landewe, R., Bijlsma, J., Burmester, G., Chatzidionysiou, K., Dougados, M., et al. (2017). EULAR recommendations for the management of rheumatoid arthritis with synthetic and biological disease-modifying antirheumatic drugs: 2016 update. *Ann. Rheumatic Dis.* 76, 960–977. doi: 10.1136/annrheumdis-2016-210715
- Soeken, K. L., Miller, S. A., and Ernst, E. (2003). Herbal medicines for the treatment of rheumatoid arthritis: a systematic review. *Rheumatol. (Oxford)* 42, 652–659. doi: 10.1093/rheumatology/keg183
- Solomon, D. H., Karlson, E. W., Rimm, E. B., Cannuscio, C. C., Mandl, L. A., Manson, J. E., et al. (2003). Cardiovascular morbidity and mortality in women diagnosed with rheumatoid arthritis. *Circulation* 107, 1303–1307. doi: 10.1161/01.CIR.0000054612.26458.B2
- Tam, H. W., Chen, C. M., Leong, P. Y., Chen, C. H., Li, Y. C., Wang, Y. H., et al. (2018). Methotrexate might reduce ischemic stroke in patients with rheumatoid arthritis: a population-based retrospective cohort study. *Int. J. Rheumatic Dis.* 21, 1591–1599. doi: 10.1111/1756-185x.13267
- Wang, Q., Kuang, H., Su, Y., Sun, Y., Feng, J., Guo, R., et al. (2013). Naturally derived anti-inflammatory compounds from Chinese medicinal plants. *J. Ethnopharmacol.* 146, 9–39. doi: 10.1016/j.jep.2012.12.013
- Wen, C. P., Levy, D. T., Cheng, T. Y., Hsu, C. C., and Tsai, S. P. (2005). Smoking behaviour in Taiwan, 2001. *Tob. Control* 14 Suppl 1, i51–i55. doi: 10.1136/tc.2004.008011
- Ye, H., Wu, W., Liu, Z., Xie, C., Tang, M., Li, S., et al. (2014). Bioactivity-guided isolation of anti-inflammation flavonoids from the stems of *Milletia dielsiana* Harms. *Fitoterapia* 95, 154–159. doi: 10.1016/j.fitote.2014.03.008
- Zhang, C., Jiang, M., and Lu, A. P. (2011). Evidence-based Chinese medicine for rheumatoid arthritis. *J. Tradit. Chin. Med.* 31, 152–157. doi: 10.1016/S0254-6272(11)60031-9
- Zhou, H. H., Wu, D. L., Gao, L. Y., Fang, Y., and Ge, W. H. (2016). L-Tetrahydropalmatine alleviates mechanical hyperalgesia in models of chronic inflammatory and neuropathic pain in mice. *Neuroreport* 27, 476–480. doi: 10.1097/wnr.0000000000000560
- Zhou, Z. Y., Zhao, W. R., Shi, W. T., Xiao, Y., Ma, Z. L., Xue, J. G., et al. (2019). Endothelial-dependent and independent vascular relaxation effect of tetrahydropalmatine on rat aorta. *Front. Pharmacol.* 10, 336. doi: 10.3389/fphar.2019.00336

Conflict of Interest: The authors declare that the research was conducted in the absence of any commercial or financial relationships that could be construed as a potential conflict of interest.

The handling editor and reviewer RH declared their involvement as co-editors in the Research Topic, and confirm the absence of any other collaboration.

Copyright © 2020 Shen, Chiang and Hsiung. This is an open-access article distributed under the terms of the Creative Commons Attribution License (CC BY). The use, distribution or reproduction in other forums is permitted, provided the original author(s) and the copyright owner(s) are credited and that the original publication in this journal is cited, in accordance with accepted academic practice. No use, distribution or reproduction is permitted which does not comply with these terms.



Synergistic Effects of Erzhi Pill Combined With Methotrexate on Osteoblasts Mediated *via* the Wnt1/LRP5/ β -Catenin Signaling Pathway in Collagen-Induced Arthritis Rats

Xiaoya Li^{1,2,3†}, Xiangcheng Lu^{2,4†}, Danping Fan^{2,3†}, Li Li⁵, Cheng Lu⁵, Yong Tan⁵, Ya Xia^{2,4}, Hongyan Zhao⁶, Miaoxuan Fan⁷ and Cheng Xiao^{1,2,3*}

OPEN ACCESS

Edited by:

Runyue Huang,
Guangzhou University of Chinese
Medicine, China

Reviewed by:

Priya Pusparajah,
Monash University Malaysia,
Malaysia
Jianxin Chen,
Beijing University of Chinese
Medicine, China

*Correspondence:

Cheng Xiao
xc2002812@126.com

[†]These authors have contributed
equally to this work

Specialty section:

This article was submitted to
Ethnopharmacology,
a section of the journal
Frontiers in Pharmacology

Received: 17 December 2019

Accepted: 19 February 2020

Published: 11 March 2020

Citation:

Li X, Lu X, Fan D, Li L, Lu C, Tan Y,
Xia Y, Zhao H, Fan M and Xiao C
(2020) Synergistic Effects of Erzhi Pill
Combined With Methotrexate on
Osteoblasts Mediated *via* the Wnt1/
LRP5/ β -Catenin Signaling Pathway in
Collagen-Induced Arthritis Rats.
Front. Pharmacol. 11:228.
doi: 10.3389/fphar.2020.00228

¹ Department of Emergency, China-Japan Friendship Hospital, Beijing, China, ² Institute of Clinical Medicine, China-Japan Friendship Hospital, Beijing, China, ³ Graduate School of Peking Union Medical College, Chinese Academy of Medical Sciences/Peking Union Medical College, Beijing, China, ⁴ School of Traditional Chinese Medicine, Beijing University of Chinese Medicine, Beijing, China, ⁵ Institute of Basic Research in Clinical Medicine, China Academy of Chinese Medical Sciences, Beijing, China, ⁶ Beijing Key Laboratory of Research of Chinese Medicine on Prevention and Treatment for Major Diseases, Experimental Research Center, China Academy of Chinese Medical Sciences, Beijing, China, ⁷ Beijing Institute for Drug Control, NMPA Key Laboratory for Quality Evaluation of Traditional Chinese Medicine (Traditional Chinese Patent Medicine), Beijing Key Laboratory of Analysis and Evaluation on Chinese Medicine, Beijing, China

Rheumatoid arthritis (RA) is a chronic systemic autoimmune disease characterized by chronic synovitis, bone erosion, and bone loss. Erzhi Pill (E郑), a classic Chinese patent medicine, is often used to treat osteoporosis and shows a capacity for bone metabolism regulation. Methotrexate (MTX), an essential drug for RA treatment, has been reported to inhibit generalized bone loss in RA patients. However, the combined therapeutic effects and mechanism of E郑 and MTX in RA have not been fully elucidated. The aim of this study was to investigate the synergistic effect of E郑 and MTX on RA and to explore the underlying mechanism through network pharmacological prediction and experimental verification. Chemical compounds of E郑, human target proteins of E郑 and MTX, and RA-related human genes were identified in the Encyclopedia of Traditional Chinese Medicine database, PubChem database, and NCBI database, respectively. The molecular network of E郑 and MTX in RA was generated and analyzed with Ingenuity Pathway Analysis software according to the datasets. Then, MTX monotherapy, E郑 monotherapy, and combined MTX and E郑 therapy were administered to collagen-induced arthritis rats, followed by assessment of pathological score, bone damage, bone alkaline phosphatases (BALP), and tartrate-resistant acid phosphatase (TRACP), and of gene levels related to the Wnt1/LRP5/ β -catenin pathway according to network pharmacological analysis. Finally, serum samples from MTX-, E郑- and MTX+E郑-treated rats were used to treat the rat osteoblast (OB)-like UMR-106 cell line to evaluate gene levels related to Wnt1/LRP5/ β -catenin. Network pharmacological analysis showed that the Wnt/ β -catenin signaling pathway was the top signaling pathway shared among MTX, E郑, and RA. The results from *in vivo* experiments

indicated that EZP combined with MTX reduced arthritis severity, alleviated ankle bone damage, increased BALP and decreased TRACP serum levels, and regulated the mRNA expression of Wnt1, LRP5, β -catenin, Runx2, BALP, and BGP in the ankles. *In vitro* experiments showed that EZP combined with MTX could also improve the expression of genes related to the Wnt1/LRP5/ β -catenin pathway. This study demonstrated that EZP in combination with MTX played a synergistic role in regulating OBs in RA, which was connected to the modulatory effect of EZP and MTX on the Wnt1/LRP5/ β -catenin signaling pathway.

Keywords: rheumatoid arthritis, Erzhi Pill, Methotrexate, Wnt/ β -catenin signaling pathway, Osteoblasts, synergistic effects

INTRODUCTION

Rheumatoid arthritis (RA), a clinically common and refractory disease, is pathologically characterized by chronic synovitis of the joints and disrupted bone homeostasis. In the pathological condition of RA, bone homeostasis involving bone formation mediated by osteoblasts (OBs) and bone resorption regulated by osteoclasts (OCs) is disrupted. A previous study showed that the Wnt/ β -catenin pathway plays an important role in bone development and homeostasis. It can lead to OBs commitment, proliferation, and differentiation, as well as enhancing OBs and osteocyte survival (Glass et al., 2005). Bone destruction, which occurs in RA, is regulated by receptor activator of nuclear factor- κ B (RANK) and nuclear factor-kappa beta receptor ligand (RANKL) (Jung et al., 2014). This evidence implies that RA is even more complex than initially predicted.

Erzhi Pill (EZP), a classic Chinese patent medicine consisting of *Ligustrum lucidum* Ait. and *Eclipta prostrata* L. in a one-to-one ratio, is used to clinically improve osteoporosis (OP) in China. One study showed that EZP had potential anti-OP effects by preventing the degradation of the alveolar trabecular microarchitecture and alveolar bone loss in ovariectomized rats through activation of the Wnt3a/low-density lipoprotein receptor-related protein 5 (LRP5)/ β -catenin signaling pathway (Sun et al., 2014). A study by Liang et al. found that EZP played a therapeutic role in an ovariectomized rat model by improving bone metabolism disorder, bone morphology, bone mineral density (BMD) and bone biomechanics and that the underlying mechanism was related to the Sirt1/Foxo signal (Liang et al., 2018). In addition, an *in vitro* study found that EZP-containing serum could inhibit the proliferation and differentiation of OCs from RAW264.7 cells induced by RANKL (Zhang et al., 2008). However, there are no relevant studies on the application of EZP in the treatment of RA.

Methotrexate (MTX), which is a cornerstone drug for the treatment of RA and has a clinical effective rate of approximately 60%, mainly inhibits inflammation and plays a certain role in bone protection by regulating RANK/RANKL/osteoprotegerin (OPG) (Swierkot et al., 2015; Kanagawa et al., 2016). In addition, several studies have also reported that MTX could improve the expression and activity of OB-related proteins, such as bone alkaline phosphatases (BALP), in primary human OB-like cells

(Davies et al., 2002; Davies et al., 2003). To improve its pharmaceutical effect, MTX is often combined with other drugs to treat RA. Takeuchi et al. combined AMG 162 (denosumab) with MTX in a phase II clinical trial, demonstrating an inhibitory effect on the progression of bone erosion at 12 months (Takeuchi et al., 2016). Currently, there is no drug that can be combined with MTX to improve osteogenesis for the treatment of RA. In the clinic, combinations of several drugs that interact with multiple targets in the molecular networks of a disease may achieve better efficacy than monotherapies. Thus, drug combinations can have a synergistic effect without increased toxicity (He et al., 2016).

Considering the limited therapeutic effect of MTX and the multicomponent, multitarget, and multipathway nature of the TCM formula EZP, MTX and EZP were combined, and a network pharmacological approach was applied to explore the pharmacodynamics and corresponding mechanisms of MTX combined with EZP in the treatment of RA. Animal and cell experiments were executed to verify the network pharmacological analysis results. This study may lay the foundation for an optimized combination of drugs treating RA and generate a new approach for treating RA.

MATERIALS AND METHODS

Network Pharmacology-Based Analysis of MTX, EZP, and RA

The chemical compounds of *Ligustrum lucidum* Ait. and *Eclipta prostrata* L., which constitute EZP, were found in the Encyclopedia of Traditional Chinese Medicine (ETCM) database (<http://www.ehbio.com/ETCM/>). Human protein targets of the above chemical compounds and MTX were retrieved from PubChem Compound (<https://pubchem.ncbi.nlm.nih.gov/>). Human genes related to RA were obtained from the National Center for Biotechnology Information (NCBI) Gene database (<http://www.ncbi.nlm.nih.gov/gene>), and “rheumatoid arthritis” was used as a keyword in the Gene database search.

The human target proteins and genes obtained in the first step were then uploaded to the Ingenuity Pathway Analysis (IPA) platform. The molecules imputed to the IPA platform were

termed “focus molecules.” IPA generated a set of networks based on different biofunctions. Molecules were shown as nodes, and the biological relationship between two nodes was shown as an edge (line). All edges were supported by at least one reference from a textbook, the literature, or canonical information stored in the Ingenuity Pathway Knowledge Base (IPKB). Nodes with diverse shapes represented the different functional classes of gene products.

The networks were sorted depending on the score evaluated by the IPA, representing the significance of the molecules for the network. In addition, the IPA determined the significance of the associations between the focus molecules and canonical pathways using Fisher's exact test. To study the mechanism of EZP and MTX treatment of RA, canonical pathway analysis in IPA was accomplished by using the comparison module.

Induction of Arthritis and Treatment

A total of 50 male Sprague-Dawley (SD) rats were purchased from the Research Institute of Experimental Animals, Chinese Academy of Medical Science (Animal license number: SCXK (Beijing) 2014-0013) at six weeks of age. Rats were maintained in the Experimental Animal Center of the Institute of Clinical Medical Sciences, China-Japan Friendship Hospital [Experiment Animal Center license number: SCXK (Beijing) 2016-0043]. Animals were kept in a specific pathogen-free environment with a temperature of 23°C ($\pm 2^\circ\text{C}$) and a 12-hour alternating light/dark cycle. They had free access to standard rodent chow and water. All experimental procedures were approved and directed by the Institute of Clinical Medical Sciences, China-Japan Friendship Hospital, Beijing, China (No, 180111).

After three days of acclimation, 40 rats were injected intradermally with 50 μL of emulsified mixture consisting of bovine type II collagen (Chondrex, Inc., Redmond, WA, USA) and isopycnic incomplete Freund's adjuvant (IFA, Chondrex) at the tail root. Meanwhile, the remaining 10 rats were injected with the same volume of saline. Seven days after the initial immunization, the same method was used for booster immunizations. On the day of booster immunization, the rats that had received immunizations were randomly divided into four groups and treated by gavage: the collagen-induced arthritis group (CIA) received 10 mL of purified water per kg of weight, twice per day at 9:00 AM and 3:00 PM respectively; the MTX (Shanghai Sine Pharmaceutical Co., Ltd, Shanghai, China) treatment group (MTX) received 1.5 mg of MTX per kg of weight at 3:00 PM and 10 mL of purified water per kg of weight at 9:00 AM, twice per week, and for the other day, they

received 10 mL of purified water per kg of weight, twice per day at 9:00 AM and 3:00 PM respectively; the Erzhi Pill (Yaodu Zhangshu Pharmaceutical Co., Ltd, Jiangxi, China; quality control showed in **Supplementary Material 1**) treatment group (EZP) received 1.8 g of Erzhi Pill per kg of weight, twice per day at 9:00 AM and 3:00 PM respectively; the Erzhi Pill and MTX combined group (EZP + MTX) was treated with Erzhi Pill at the same administration frequencies, dosages, and times as those of the EZP group and treated with MTX at the same administration frequencies and dosages as those of the MTX group but at 2:30 PM. In addition, the 10 unmodeled rats served as a normal control group (Control) treated with 10 mL of purified water per kg of weight, twice per day at the same time as the CIA group. The scheme of the design of the study and animal grouping are shown in **Figure 1**.

Arthritis Assessment of Hind Limbs

From the day of administration of the treatment, rats were evaluated for the degree of swelling in the hind limbs every three days. The severity of arthritis per hind leg was expressed as the arthritic index (AI) score on a scale of 0 to 4 points according to conventional criteria (Zhao et al., 2018). Briefly, 0 = no change, 1 = redness or slight swelling, 2 = mild swelling, 3 = pronounced swelling, and 4 = deformity of and inability to use limb. Any modeling rats with an AI score of 0 at the last time point were deemed a failure of modeling and were excluded in the follow-up index.

Histological Analysis of Ankle Joints

Rats were sacrificed after 28 days of treatment. The right hind ankle joints were fixed in formalin for seven days, followed by decalcification for one month. Then, the ankle joints were sectioned and stained with hematoxylin and eosin (H&E) under the guidance of a protocol. Histological score was evaluated by assessing inflammation, cartilage damage, bone damage, inflammatory cell infiltration, synovial hyperplasia, and pannus. The score was on a scale from 0 to 3 according to severity; the specific method was elaborated in an article by Zhao et al. (2018).

Micro-Computed Tomography (Micro-CT) Analysis of Ankles and Paws

Micro-CT scans of the ankles and paws were performed to assess the extent of bone damage using a Skyscan1174 Micro CT (Bruker, Belgium). The matching software N-Recon was then used for 3D image reconstruction of both ankles and paws. Finally, 3D analysis of bone volume (BV), bone surface (BS), and BS/BV were performed *via* the matching software CT-AN.

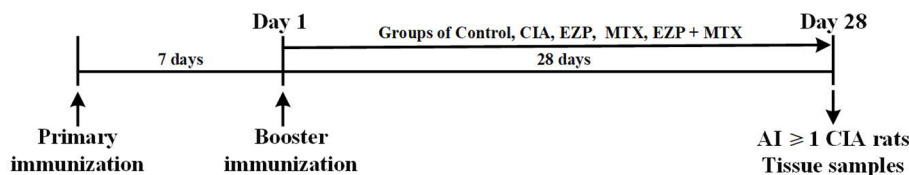


FIGURE 1 | Experimental schedule. Male SD rats were immunized twice by intradermal injection with 50 μL bovine type II collagen emulsified with IFA on 7 days before day 1 and day 1. On day 1, the rats were randomly assigned into groups CIA, EZP, MTX, and EZP + MTX and given intragastric administration for 28 days. Tissue samples of the control rats and rats with AI ≥ 1 in the model were collected at the end-point of the experiment (day 28).

Serum Bone Metabolite Assessment by Enzyme-Linked Immunosorbent Assay (ELISA)

On the last day of treatment, blood was obtained from the abdominal aorta. After centrifugation at 3000 rpm for 10 minutes at 4°C, the serum was collected and stored at -80°C. The activity and function of OCs and OBs were evaluated by the levels of tartrate-resistant acid phosphatase (TRACP) and bone alkaline phosphatases (BALP) in the serum. They were measured using ELISA according to the protocol. ELISA kits were purchased from Nanjing Jiancheng Bioengineering Institute (Nanjing, China).

Culture and Treatments of OB-Like Cells With Medicated Serum

The rat OB-like UMR-106 cell line (National Infrastructure of Cell Line Resource, China) was purchased and cultured in high-glucose Dulbecco's modified Eagle's medium (DMEM-H; HyClone, Logan, USA) containing 10% fetal bovine serum (FBS; Gibco BRL, Grand Island, NY, USA) in a constant-temperature incubator at 37°C, maintaining a moderate level of 5% CO₂ and 95% saturation humidity. When the cells became 80-90% confluent, they were digested and inoculated for serial passage. UMR-106 cells in the logarithmic growth phase were reseeded in 96- and 24-well culture plates at densities of 1×10^5 and 5×10^5 cells/well, respectively; 24 hours later, the cells were used in follow-up experiments.

Once the dosages of EZP and MTX given to the rats had reached the maximum, the rat serum collected one hour after the last gavage was considered medicated serum following inactivation and filtration. UMR-106 cells seeded in cell plates were divided into five groups: the control serology group (Control), CIA serology group (CIA), MTX serology group (MTX), EZP serology group (EZP), and MTX+EZP serology group (MTX+EZP). UMR-106 cells were treated for 48 hours with culture medium supplemented with 15% medicated serum.

Detection of OB-Like Cell Proliferation Rate via Cell Counting Kit-8 (CCK8) Assay

After 48 hours of intervention with medicated serum, the medium of UMR-106 cells was changed to DMEM-H containing 10% CCK8 (Dojindo, Japan). After reacting for 1.5 hours in the incubator, the absorbance was detected at wavelengths of 450 nm and 620 nm, and the cell proliferation rate was calculated.

Evaluation of Relative Gene Expression of Wnt1/LRP5/ β -Catenin Signaling Pathway Through Real-Time PCR

The left hindlimbs of rats were rapidly frozen with liquid nitrogen after being severed in the middle of the femur and removing the fur and muscles and then transferred to -80°C. Within a month, the bones were smashed in liquid nitrogen, and total RNA was extracted using the TRIzol reagent (Invitrogen, Carlsbad, CA, USA). Similarly, RNA was extracted from UMR-106 cells after 48 hours of intervention with medicated serum. The purity and quality of the isolated RNA were then examined

with a NanoDrop One (Thermo Fisher Scientific, Waltham, MA, USA). gDNA was eliminated with gDNA Eraser, and the RNA was reverse transcribed with the PrimeScript RT reagent Kit (TaKaRa, Tokyo, Japan). The mRNA levels of selected genes were detected using SYBR Premix Ex Taq (TliRNaseH Plus) (TaKaRa) with the Quant Studio 5 Real-Time PCR System (Thermo Fisher Scientific) according to the manufacturer's guidelines. The cycling parameters were as follows: 95°C for 15 seconds, followed by 40 cycles at 95°C for 5 seconds and 60°C for 34 seconds. The samples were analyzed in duplicate, and their relative expression levels of genes were determined by normalization to the expression level of GAPDH. The primers used are shown in **Supplementary Material 2**.

Statistical Analysis

Statistical analysis was carried out using GraphPad 8.0 software. The results were expressed as the mean \pm SEM. Differences among groups were estimated by one-way analysis of variance (ANOVA) and a posthoc Tukey's test. Differences were considered significant when $P < 0.05$.

RESULTS

Shared Signaling Pathways of MTX, EZP, and RA From Network Pharmacological Analysis

A total of 41 chemical compounds (**Supplementary Material 3**) and 1454 targets (**Supplementary Material 4**) of EZP were obtained in this study. Meanwhile, 102 targets of MTX and 1148 RA-related genes were found (**Supplementary Materials 5 and 6**). In total, 328 signaling pathways of EZP and MTX were obtained, and 374 signaling pathways of RA were acquired. Among these signaling pathways, 297 were shared by EZP, MTX, and RA. The top 14 shared signaling pathways associated with cellular immune response and cytokine signaling are shown in **Figures 2A, B**. The Wnt/ β -catenin signaling pathway was determined to be the top shared signaling pathway and the focus of further study.

EZP Combined With MTX Ameliorated the Severity of Arthritis in CIA Rats

CIA rats were used in this study to verify the therapeutic effect of EZP and MTX on RA, and treatments were continued for 28 days. As shown in **Figure 3A**, ankle swelling was severe in CIA rats, and the three treatments were able to improve joint swelling to varying degrees. EZP + MTX had the best effect, while EZP alone had the weakest effect. The dynamic swelling scores are shown in **Figure 3C** and illustrate that, among all treatments, EZP + MTX produced the best results. From day 19 of treatment, all rats in the CIA group had the maximal AI score. Compared with the CIA group, the EZP group exhibited lower AI scores beginning on the 19th day of treatment, but there was no significant difference even at the end of the observation period. Although the MTX group had the highest score in the second week, MTX was effective after day 13, and a significant reduction in joint score was observed on the 28th day after treatment ($P < 0.05$).

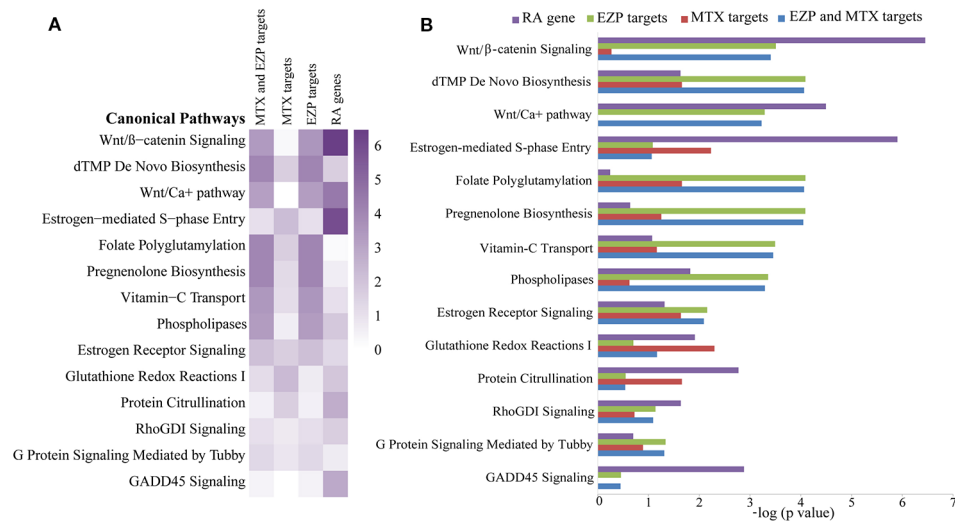


FIGURE 2 | The results of bioinformatic analysis. Signaling pathways shared among the gene molecular networks related to rheumatoid arthritis (RA) and the protein target molecular networks of EZP and MTX in the context of cytokine and cellular immune signaling, identified by using the Ingenuity Pathway Analysis (IPA) compare module. The Wnt/ β -catenin signaling pathway was the pathway focused on. **(A)** Heat map of the top 14 shared signaling pathways of EZP, MTX, and RA. **(B)** Bar graph of the top 14 shared signaling pathways of EZP, MTX, and RA.

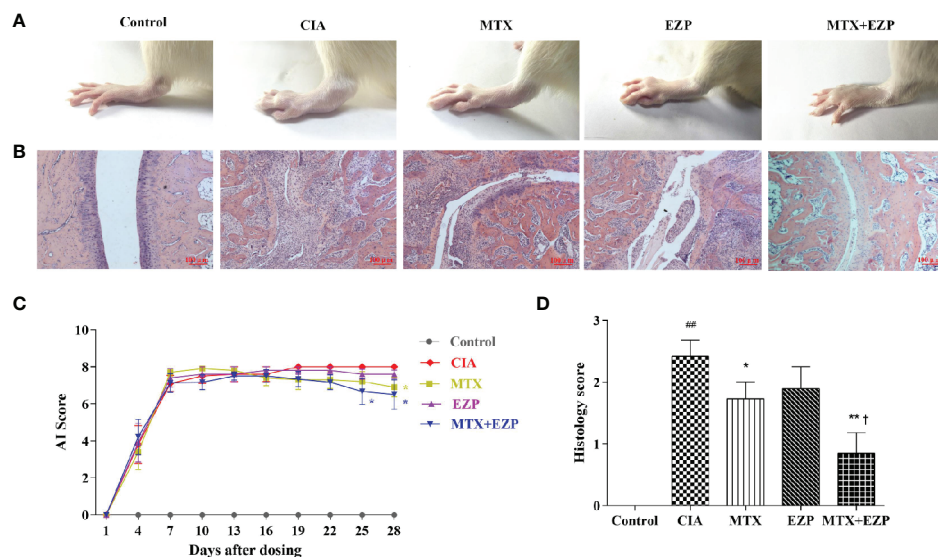


FIGURE 3 | Effects of EZP combined with MTX on arthritis severity in CIA rats. **(A)** Representative images of the ankle joints after treatment. **(B)** Representative images of ankle pathology. **(C)** AI score of each group. **(D)** Histological score of each group. $^{##}P < 0.01$ compared with the control group; $^{*}P < 0.05$, $^{**}P < 0.01$ compared with the CIA group; $^{\dagger}P < 0.05$ compared with the MTX group.

The therapeutic effects of EZP combined with MTX began to appear on the 7th day of treatment, and by the 25th day of treatment, the combination group had significantly reduced tumidness compared with the CIA group ($P < 0.05$). Although there was no significant difference between the MTX group and the EZP + MTX group, the AI score of the combined treatment group was significantly lower than that of the MTX group.

Pathological changes were shown in **Figures 3B, D**. The results suggested that the cartilage and bone were severely damaged in the CIA group, and this damage was accompanied by extensive synovial proliferation and inflammatory cell infiltration. EZP, MTX, and EZP+MTX treatments were able to reduce pathological injury to varying degrees. Histological score analysis showed that MTX and EZP + MTX prominently

inhibited the histopathological changes in the ankle joints of CIA rats ($P < 0.05$; $P < 0.01$). These findings indicated that EZP alone was not effective in CIA rats but that it could coordinate with MTX to arrest the development and progression of CIA in rats.

EZP Combined With MTX Showed Bone Protection in CIA Rats

We then evaluated the therapeutic effects of EZP and MTX on the bone injury status *via* micro-CT (**Figure 4A**). The BV, BS, and BS/BV values in inflamed ankle joints were detected to quantify the extent of the bone remodeling in the different groups. The results showed that neither MTX nor EZP alone reduced the BS value, while the group treated with the combination of MTX and EZP exhibited a reduced BS compared with the CIA group ($P < 0.05$) (**Figure 4B**). BV was decreased in the CIA group, and all of the treatments increased it ($P < 0.05$) (**Figure 4C**). When considering the combination of BS and BV, we found that bone destruction was still present in the CIA group and that MTX and MTX + EZP played roles in bone protection ($P < 0.05$; $P < 0.01$) (**Figure 4D**). Interestingly, the combination of MTX and EZP was significantly better than MTX alone ($P < 0.05$). On the one hand, the micro-CT results preliminarily verified our prediction. On the other hand, the above results also suggested that the combination of the two drugs could inhibit bone absorption or increase osteogenesis.

In addition, the levels of BALP and TRACP in the serum were detected *via* ELISA to further verify the effect of EZP combined with MTX on bone metabolism. As shown in **Figure 4E**, the levels of BALP in CIA rats declined ($P < 0.05$), suggesting that modeling decreased OBs function. The levels of BALP were increased in the MTX group and EZP + MTX group ($P < 0.05$;

$P < 0.01$), and those in the combination group were higher than those in the MTX group ($P < 0.05$), while there was no significant difference between the EZP and CIA groups. For TRACP (**Figure 4F**), CIA modeling increased the levels of TRACP in serum, and MTX, EZP, and MTX+EZP treatments could reduce these levels, but there was no difference between the EZP and MTX +EZP groups. The above results suggested that the effects of the combination of EZP and MTX were reflected in the protection of osteogenesis rather than effects on OCs.

EZP Increased the Therapeutic Effects of MTX in CIA Rats Through the Wnt/ β -Catenin Signaling Pathway

In order to further explore the molecular mechanism by which EZP enhanced the curative effects of MTX, we examined the Wnt/ β -catenin signaling pathway and several key genes associated with the differentiation and maturation of OBs: Wnt1, LRP5, β -catenin, Runx2, bone gamma-carboxyglutamic-acid-containing proteins (BGP), and BALP.

The effects of EZP and MTX on genes associated with osteogenesis in CIA joints are shown in **Figure 5**. As shown in **Figures 5A–D**, compared with that in the Control group, the gene expression of Wnt1, LRP5, β -catenin, and Runx2 in the CIA group was significantly downregulated ($P < 0.05$; $P < 0.01$); after EZP or MTX treatment alone or combined, except Runx2 in the EZP group, the gene expressions of Wnt1, LRP5, and β -catenin in the other two groups were significantly upregulated, and the combined treatment was more effective than MTX alone ($P < 0.05$; $P < 0.01$). As markers of OBs maturity, similar to the Wnt/ β -catenin signaling pathway, BALP and BGP were observed to have significantly lower gene expression in the CIA group than in

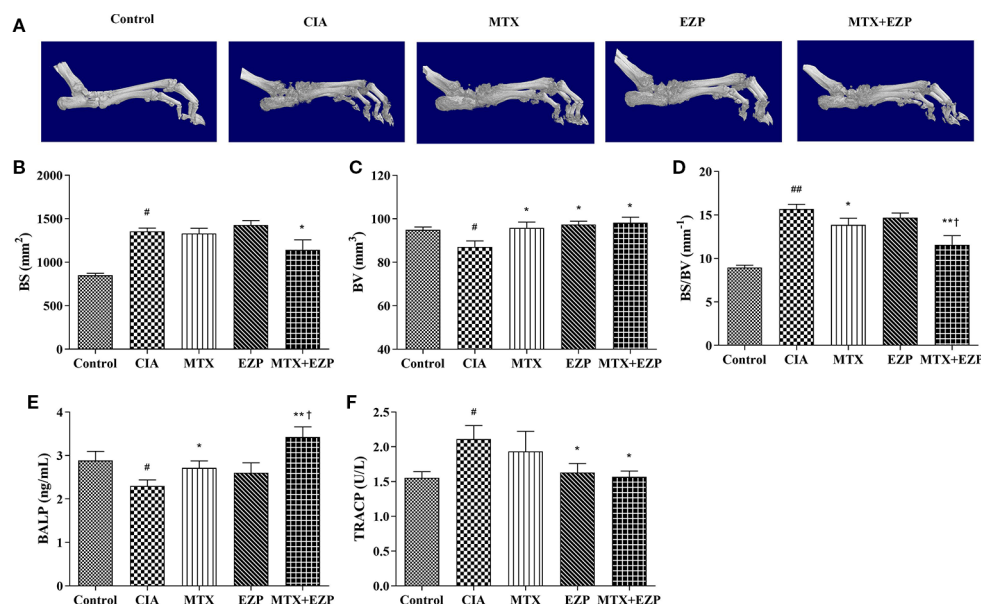


FIGURE 4 | EZP and MTX synergistically reduced bone destruction in CIA rats. **(A)** Representative micro-CT images of ankle joints after treatment. **(B–D)** Line plots representing the BS, BV, and BS/BV values of all of the groups. **(E–F)** Bar plots representing the levels of BALP and TRACP in serum. [#] $P < 0.05$, ^{##} $P < 0.01$ compared with the control group; ^{*} $P < 0.05$, ^{**} $P < 0.01$ compared with the CIA group; [†] $P < 0.05$ compared with the MTX group.

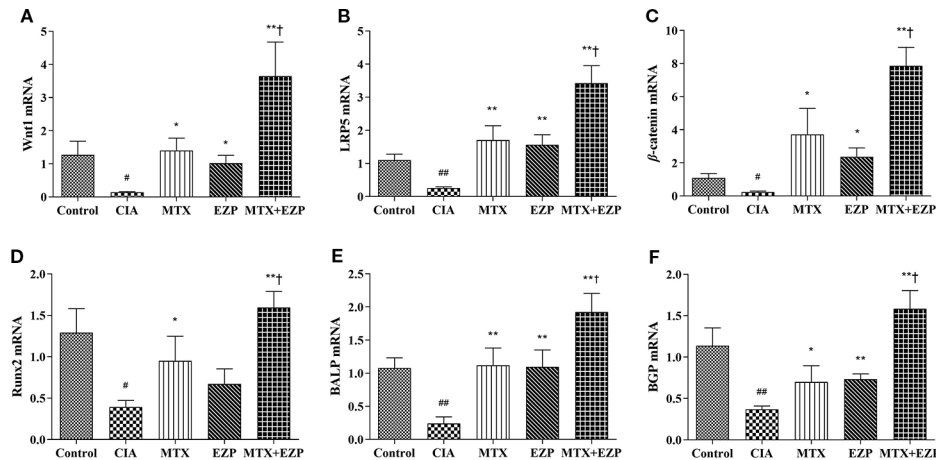


FIGURE 5 | EZP and MTX synergistically promoted the differentiation and maturation of OBs in the CIA rat model. **(A–D)** Bar plots representing the relative mRNA expression levels of molecules related to the Wnt1/LRP5/β-catenin signaling pathway in the ankle joints. **(E–F)** RT-PCR results for BALP and BGP. [#] $P < 0.05$, ^{##} $P < 0.01$ compared with the control group; ^{*} $P < 0.05$, ^{**} $P < 0.01$ compared with the CIA group; [†] $P < 0.05$ compared with the MTX group.

the Control group ($P < 0.01$); EZP, MTX, and MTX + EZP could increase the mRNA levels of both BALP and BGP to varying degrees, and the mRNA levels of BALP and BGP were increased more in the MTX + EZP group ($P < 0.05$) (Figures 5E, F). The results above showed that EZP and MTX promoted the differentiation and maturation of OBs. Moreover, EZP had a significant synergistic effect with MTX on OBs, mediated *via* the Wnt1/LRP5/β-catenin signaling pathway.

Synergistic Effects of EZP Combined With MTX on OBs Mediated *via* the Wnt1/LRP5/β-Catenin Signaling Pathway

Furthermore, we verified the results of our network pharmacology and animal experiments through cell experiments. OB-based results

(Figure 6) showed that EZP could cooperate with MTX to promote OBs proliferation, differentiation, and maturation through the Wnt1/LRP5/β-catenin signaling pathway. Figure 6A showed that serum of CIA rats inhibited the survival of OBs ($P < 0.05$) and that MTX serum and MTX + EZP serum promoted cell proliferation compared with CIA serum ($P < 0.05$); however, there was no difference between MTX serum and MTX+EZP serum treatments on cell proliferation rates ($P > 0.05$). The results for Wnt1 and LRP5 expression in OBs were similar to the results from the joints; that is, the gene expressions were reduced in the CIA group, while all treatment groups restored them, and EZP + MTX was more effective than MTX ($P < 0.05$) (Figures 6B, C). The results for BGP and Runx2 were interesting. Neither MTX nor EZP

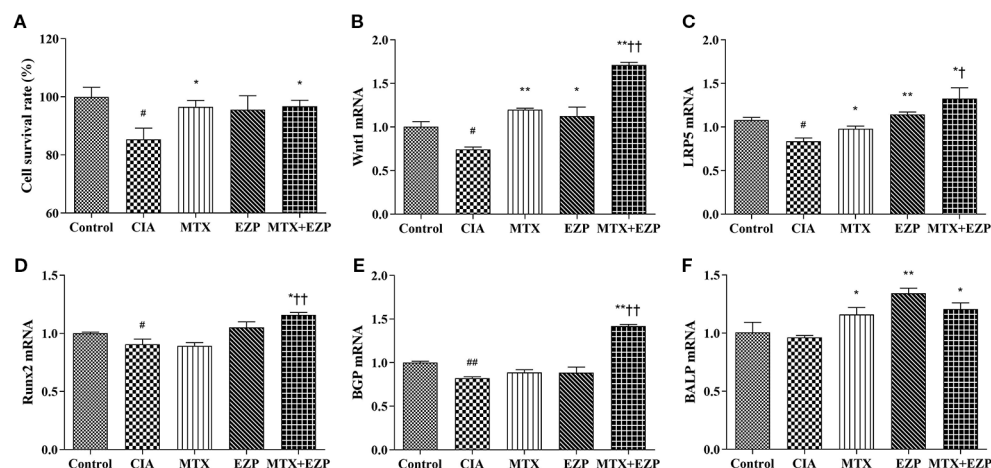


FIGURE 6 | EZP and MTX synergistically promoted the differentiation and maturation of OBs. **(A)** Bar plots of the cell proliferation rate of each group. **(B–F)** Relative mRNA expression levels in OBs. [#] $P < 0.05$, ^{##} $P < 0.01$ compared with the control group; ^{*} $P < 0.05$, ^{**} $P < 0.01$ compared with the CIA group; [†] $P < 0.05$, ^{††} $P < 0.01$ compared with the MTX group.

alone altered the CIA-induced gene expression reduction, but the combination of MTX and EZP significantly increased the mRNA levels of both molecules ($P < 0.05$; $P < 0.01$) (**Figures 6D, E**). For BALP, modeling did not seem to alter gene expression, but all three treatment groups exhibited increased BALP gene levels to varying degrees ($P < 0.05$) (**Figure 6F**). These results bear out the results of the animal experiments showing that EZP had a significant synergistic effect with MTX on OBs that was mediated *via* the Wnt1/LRP5/ β -catenin signaling pathway.

DISCUSSION

The RA management recommendations updated by the European League Against Rheumatism (EULAR) address conventional synthetic (cs) disease-modifying antirheumatic drugs (DMARDs), glucocorticoids (GC), biological (b) DMARDs, and targeted synthetic (ts) DMARDs (Smolen et al., 2017). However, the clinical use of these drugs is limited by adverse effects (Bijlsma and Buttgerit, 2016; Tarp et al., 2017; Wang et al., 2018), drug resistance (Peres et al., 2015), or high cost (Wu et al., 2014; Khilfeh et al., 2019), and none of these drugs directly target bone homeostasis. After treatment with MTX, approximately 30% of patients have no response, and 30% have side effects. Despite all this, because of its reasonable cost and remarkable curative effect, MTX has been the cornerstone drug for the treatment of RA for decades. For the purpose of increasing therapeutic effects or reducing toxicity, MTX has been used in the treatment of RA either as a single agent or in combination (Hazlewood et al., 2016).

From a clinical point of view, Chinese herbal formulas have good clinical efficacies in the treatment of RA (Huang et al., 2015), and some of them target the reestablishment of bone homeostasis in RA (Zhao et al., 2017; Zhao et al., 2018). Chinese herbal formulas have advantages that DMARDs lack, such as multiple targets, good curative effects, few adverse reactions, and low cost. EZP has exhibited a good effect in treating OP, and its effect mainly relies on bone protection (Cheng et al., 2011; Rufus et al., 2013; Sun et al., 2014). Given the unique advantages of EZP and MTX and the abilities of both agents to regulate bone homeostasis, we expect to enhance the effect of MTX by combining the two agents.

MTX combined with EZP for RA treatment involves multicomponent, multitarget, and multipathway effects from a global synergistic perspective. Traditional research methods have difficulty fully revealing the pharmacodynamics and corresponding mechanism of this combination. In recent years, along with the rapid progress in bioinformatics, network pharmacology has emerged as a holistic and efficient tool to decode the underlying mechanisms of multitarget treatments by analyzing various networks of complex and multilevel interactions (Zhang et al., 2015; Zhang et al., 2016; Zheng et al., 2016). Successful attempts to study pharmacodynamics have been achieved previously in our group by network pharmacology (Li et al., 2012; Zhao et al., 2015). In this study,

based on a network pharmacological approach, the Wnt/ β -catenin signaling pathway was the top signaling pathway shared by MTX, EZP, and RA, which meant that further study may focus on this pathway.

The CIA model is a valid experimental model for RA because the clinical changes observed are similar to those in RA patients (Alabarse et al., 2018). Furthermore, the pathological and biochemical changes in the bone and cartilage are similar to those in clinical patients (Daans et al., 2008). The basic pathological changes of RA as well CIA are chronic inflammation in the synovium, pannus formation, and progressive destruction of the articular cartilage and bone, leading to joint deformity and functional loss (Kato et al., 2015; Abasolo et al., 2019). Our ankle histological score and micro-CT results also showed that EZP cooperated with MTX to reduce cartilage and bone destruction and synovial cell and pannus proliferation, which means that EZP combined with MTX has effects on bone remodeling in RA.

Maintenance of bone homeostasis requires an exquisite balance between bone resorption by OCs and bone formation by OBs. BALP, a marker of OB differentiation and maturation from bone precursors, promotes extracellular mineralization *via* the release of inorganic phosphate (Halling et al., 2017). TRACP, a marker of OC differentiation and maturation, exerts phosphatase activity to phosphorylate osteopontin to inhibit the formation and growth of hydroxyapatite crystals (Halling et al., 2017). Our ELISA results showed that single-agent EZP had no effect on the levels of BALP but that the level of BALP increased more when EZP was combined with MTX than when MTX was used alone. The results were similar to those reported in the studies of Davies et al. (Davies et al., 2002; Davies et al., 2003). However, single-agent MTX did not decrease the levels of TRACP, and the combination of the two agents did not show an inhibitory effect on TRACP. These results suggest that EZP combined with MTX mainly acts on osteogenesis rather than osteoclasia.

For decades, studies have indicated that Wnt signaling is a critical regulator for stimulating and maintaining OB differentiation and activity in both humans and animals (Le Henaff et al., 2015; Sindhavajiva et al., 2018). When bound to an Fzd receptor complex, Wnt phosphorylates the Lrp coreceptors and recruits and coheres GSK-3 β and Axin to the ligand-receptor complex. This complex results in the accumulation of cytoplasmic β -catenin. Finally, β -catenin translocates into the nucleus and induces the expression of target genes, such as Runx2. In OB differentiation, Wnt1 (Laine et al., 2013), Wnt3a (Li et al., 2019), and Wnt5a (Wang et al., 2019) play dominant roles in activating β -catenin through the binding receptor LRP5 (Gong et al., 2001; Chang et al., 2014) with other molecules, thereby promoting the transcription of the differentiation factor Runx2 (Jiang et al., 2017). In this study, both EZP alone and MTX alone increased the gene expression of Wnt1, LRP5, and β -catenin, indicating that both agents target the Wnt1/LRP5/ β -catenin pathway. The combination of the two agents resulted in a significant additional induction of gene expression related to Wnt1/LRP5/ β -catenin signaling, including Runx2, a gene that

was not affected by the use of EZP. Furthermore, the results for BGP and BALP, two bone turnover markers, were consistent with those for the Wnt pathway. The results above preliminarily verified that the bone protection mechanism underlying the synergistic effect of EZP and MTX on RA was realized through the Wnt1/LRP5/ β -catenin signaling pathway. In addition, a previous study from Sun et al. found that the anti-OP effect of EZP occurred through Wnt3a/LRP5/ β -catenin signaling (Sun et al., 2014). We detected the gene expression of Wnt3a as well, but its level was too low for statistical analysis. The difference might be caused by the difference in bone tissues.

We further confirmed the mechanism underlying the synergistic effect of EZP and MTX on RA *in vitro* using the OB-like UMR-106 cell line. The results suggested that MTX and EZP-containing serum did not increase the proliferation rate of UMR-106 cells, indicating that the treatment of RA by EZP and MTX was not associated with promoting the proliferation of OBs. The gene expression results for the Wnt1/LRP5/ β -catenin signaling pathway finally determined that the synergistic effects of EZP combined with MTX were achieved by increasing OB differentiation *via* the Wnt1/LRP5/ β -catenin signaling pathway.

In conclusion, this study explored the anti-RA effect of EZP combined with MTX through network pharmacological analysis, a CIA rat model, and cell experiments. Our results demonstrated that EZP might exert a synergistic effect in combination with MTX to regulate OBs in RA through the Wnt1/LRP5/ β -catenin signaling pathway.

REFERENCES

- Abasolo, L., Ivorra-Cortes, J., Leon, L., Jover, J. A., Fernandez-Gutierrez, B., and Rodriguez-Rodriguez, L. (2019). Contribution of the bone and cartilage/soft tissue components of the joint damage to the level of disability in rheumatoid arthritis patients: a longitudinal study. *Clin. Rheumatol.* 38 (3), 691–700. doi: 10.1007/s10067-018-4335-4
- Alabarse, P., Lora, P. S., Silva, J., Santo, R., Freitas, E. C., de Oliveira, M. S., et al. (2018). Collagen-induced arthritis as an animal model of rheumatoid cachexia. *J. Cachexia Sarcopenia Muscle* 9 (3), 603–612. doi: 10.1002/jcsm.12280
- Bijlsma, J. W. J., and Buttgeriet, F. (2016). Adverse events of glucocorticoids during treatment of rheumatoid arthritis: lessons from cohort and registry studies. *Rheumatol. (Oxford)* 55 (suppl 2), i3–i5. doi: 10.1093/rheumatology/kew344
- Chang, M. K., Kramer, I., Keller, H., Gooi, J. H., Collett, C., Jenkins, D., et al. (2014). Reversing LRP5-dependent osteoporosis and SOST deficiency-induced sclerosing bone disorders by altering WNT signaling activity. *J. Bone Miner. Res.* 29 (1), 29–42. doi: 10.1002/jbmr.2059
- Cheng, M., Wang, Q., Fan, Y., Liu, X., Wang, L., Xie, R., et al. (2011). A traditional Chinese herbal preparation, Er-Zhi-Wan, prevent ovariectomy-induced osteoporosis in rats. *J. Ethnopharmacol.* 138 (2), 279–285. doi: 10.1016/j.jep.2011.09.030
- Daans, M., Lories, R. J., and Luyten, F. P. (2008). Dynamic activation of bone morphogenetic protein signaling in collagen-induced arthritis supports their role in joint homeostasis and disease. *Arthritis Res. Ther.* 10 (5), R115. doi: 10.1186/ar2518
- Davies, J. H., Evans, B. A., Jenney, M. E., and Gregory, J. W. (2002). In vitro effects of chemotherapeutic agents on human osteoblast-like cells. *Calcif Tissue Int.* 70 (5), 408–415. doi: 10.1007/s002230020039
- Davies, J. H., Evans, B. A., Jenney, M. E., and Gregory, J. W. (2003). Effects of chemotherapeutic agents on the function of primary human osteoblast-like cells derived from children. *J. Clin. Endocrinol. Metab.* 88 (12), 6088–6097. doi: 10.1210/jc.2003-030712

DATA AVAILABILITY STATEMENT

The datasets generated for this study are available on request to the corresponding author.

ETHICS STATEMENT

All experimental procedures were approved and directed by the Institute of Clinical Medical Sciences, China-Japan Friendship Hospital, Beijing, China (No: 180111).

AUTHOR CONTRIBUTIONS

CX, XyL, and XcL designed the conceptual framework of the study. DF and XcL designed experiments and wrote the paper. LL, CL, YT, YX, MF, and HZ performed experiments. YT, XcL, and DF analyzed the data.

SUPPLEMENTARY MATERIAL

The Supplementary Material for this article can be found online at: <https://www.frontiersin.org/articles/10.3389/fphar.2020.00228/full#supplementary-material>

- Glass, D. N., Bialek, P., Ahn, J. D., Starbuck, M., Patel, M. S., Clevers, H., et al. (2005). Canonical Wnt signaling in differentiated osteoblasts controls osteoclast differentiation. *Dev. Cell* 8 (5), 751–764. doi: 10.1016/j.devcel.2005.02.017
- Gong, Y., Slee, R. B., Fukai, N., Rawadi, G., Roman-Roman, S., Reginato, A. M., et al. (2001). LDL receptor-related protein 5 (LRP5) affects bone accrual and eye development. *Cell* 107 (4), 513–523. doi: 10.1016/s0092-8674(01)00571-2
- Halling, L. C., Ek-Rylander, B., Krumpel, M., Norgard, M., Narisawa, S., Millan, J. L., et al. (2017). Bone Alkaline Phosphatase and Tartrate-Resistant Acid Phosphatase: Potential Co-regulators of Bone Mineralization. *Calcif Tissue Int.* 101 (1), 92–101. doi: 10.1007/s00223-017-0259-2
- Hazlewood, G. S., Barnabe, C., Tomlinson, G., Marshall, D., Devoe, D., and Bombardier, C. (2016). Methotrexate monotherapy and methotrexate combination therapy with traditional and biologic disease modifying antirheumatic drugs for rheumatoid arthritis: abridged Cochrane systematic review and network meta-analysis. *BMJ* 353, i1777. doi: 10.1136/bmj.i1777
- He, B., Lu, C., Zheng, G., He, X., Wang, M., Chen, G., et al. (2016). Combination therapeutics in complex diseases. *J. Cell Mol. Med.* 20 (12), 2231–2240. doi: 10.1111/jcmm.12930
- Huang, M. C., Pai, F. T., Lin, C. C., Chang, C. M., Chang, H. H., Lee, Y. C., et al. (2015). Characteristics of traditional Chinese medicine use in patients with rheumatoid arthritis in Taiwan: a nationwide population-based study. *J. Ethnopharmacol.* 176, 9–16. doi: 10.1016/j.jep.2015.10.024
- Jiang, Z., Wang, H., Yu, K., Feng, Y., Wang, Y., Huang, T., et al. (2017). Light-Controlled BMSC Sheet-Implant Complexes with Improved Osteogenesis via an LRP5/ β -Catenin/Runx2 Regulatory Loop. *ACS Appl. Mater. Interfaces* 9 (40), 34674–34686. doi: 10.1021/acsami.7b10184
- Jung, S. M., Kim, K. W., Yang, C. W., Park, S. H., and Ju, J. H. (2014). Cytokine-mediated bone destruction in rheumatoid arthritis. *J. Immunol. Res.* 2014, 263625. doi: 10.1155/2014/263625
- Kanagawa, H., Masuyama, R., Morita, M., Sato, Y., Niki, Y., Kobayashi, T., et al. (2016). Methotrexate inhibits osteoclastogenesis by decreasing RANKL-induced calcium influx into osteoclast progenitors. *J. Bone Miner. Metab.* 34 (5), 526–531. doi: 10.1007/s00774-015-0702-2

- Kato, G., Shimizu, Y., Arai, Y., Suzuki, N., Sugamori, Y., Maeda, M., et al. (2015). The inhibitory effects of a RANKL-binding peptide on articular and periarticular bone loss in a murine model of collagen-induced arthritis: a bone histomorphometric study. *Arthritis Res. Ther.* 17 (1), 251. doi: 10.1186/s13075-015-0753-8
- Khilfeh, I., Guyette, E., Watkins, J., Danielson, D., Gross, D., and Yeung, K. (2019). Adherence, Persistence, and Expenditures for High-Cost Anti-Inflammatory Drugs in Rheumatoid Arthritis: An Exploratory Study. *J. Manage. Care Spec. Pharm.* 25 (4), 461–467. doi: 10.18553/jmcp.2019.25.4.461
- Laine, C. M., Joeng, K. S., Campeau, P. M., Kiviranta, R., Tarkkonen, K., Grover, M., et al. (2013). WNT1 mutations in early-onset osteoporosis and osteogenesis imperfecta. *N. Engl. J. Med.* 368 (19), 1809–1816. doi: 10.1056/NEJMoa1215458
- Le Henaff, C., Mansouri, R., Miodowski, D., Zarka, M., Geoffroy, V., Marty, C., et al. (2015). Increased NF-kappaB Activity and Decreased Wnt/beta-Catenin Signaling Mediate Reduced Osteoblast Differentiation and Function in DeltaF508 Cystic Fibrosis Transmembrane Conductance Regulator (CFTR) Mice. *J. Biol. Chem.* 290 (29), 18009–18017. doi: 10.1074/jbc.M115.646208
- Li, J., Lu, C., Jiang, M., Niu, X., Guo, H., Li, L., et al. (2012). Traditional chinese medicine-based network pharmacology could lead to new multicomponent drug discovery. *Evid. Based Complement Altern. Med.* 2012, 149762. doi: 10.1155/2012/149762
- Li, X., Liu, D., Li, J., Yang, S., Xu, J., Yokota, H., et al. (2019). Wnt3a involved in the mechanical loading on improvement of bone remodeling and angiogenesis in a postmenopausal osteoporosis mouse model. *FASEB J.* 33 (8), 8913–8924. doi: 10.1096/fj.201802711R
- Liang, W., Li, X., Li, G., Hu, L., Ding, S., Kang, J., et al. (2018). Sirt1/Foxo Axis Plays a Crucial Role in the Mechanisms of Therapeutic Effects of Erzhi Pill in Ovariectomized Rats. *Evid. Based Complement Altern. Med.* 2018, 9210490. doi: 10.1155/2018/9210490
- Peres, R. S., Liew, F. Y., Talbot, J., Carregaro, V., Oliveira, R. D., Almeida, S. L., et al. (2015). Low expression of CD39 on regulatory T cells as a biomarker for resistance to methotrexate therapy in rheumatoid arthritis. *Proc. Natl. Acad. Sci. U. S. A.* 112 (8), 2509–2514. doi: 10.1073/pnas.1424792112
- Rufus, P., Mohamed, N., and Shuid, A. N. (2013). Beneficial effects of traditional Chinese medicine on the treatment of osteoporosis on ovariectomized rat models. *Curr. Drug Targets* 14 (14), 1689–1693. doi: 10.2174/1389450114666131220160357
- Sindhavajiva, P. R., Sastravaha, P., Arksornnukit, M., and Pavasant, P. (2018). Intermittent compressive force induces human mandibular-derived osteoblast differentiation via WNT/beta-catenin signaling. *J. Cell Biochem.* 119 (4), 3474–3485. doi: 10.1002/jcb.26519
- Smolen, J. S., Landewe, R., Bijlsma, J., Burmester, G., Chatzidionysiou, K., Dougados, M., et al. (2017). EULAR recommendations for the management of rheumatoid arthritis with synthetic and biological disease-modifying antirheumatic drugs: 2016 update. *Ann. Rheum. Dis.* 76 (6), 960–977. doi: 10.1136/annrheumdis-2016-210715
- Sun, W., Wang, Y. Q., Yan, Q., Lu, R., and Shi, B. (2014). Effects of Er-Zhi-Wan on microarchitecture and regulation of Wnt/beta-catenin signaling pathway in alveolar bone of ovariectomized rats. *J. Huazhong Univ. Sci. Technol. Med. Sci.* 34 (1), 114–119. doi: 10.1007/s11596-014-1241-0
- Swierkot, J., Gruszecka, K., Matuszewska, A., and Wiland, P. (2015). Assessment of the Effect of Methotrexate Therapy on Bone Metabolism in Patients with Rheumatoid Arthritis. *Arch. Immunol. Ther. Exp. (Warsz)* 63 (5), 397–404. doi: 10.1007/s00005-015-0338-x
- Takeuchi, T., Tanaka, Y., Ishiguro, N., Yamanaka, H., Yoneda, T., Ohira, T., et al. (2016). Effect of denosumab on Japanese patients with rheumatoid arthritis: a dose-response study of AMG 162 (Denosumab) in patients with Rheumatoid arthritis on methotrexate to Validate inhibitory effect on bone Erosion (DRIVE)-a 12-month, multicentre, randomised, double-blind, placebo-controlled, phase II clinical trial. *Ann. Rheum. Dis.* 75 (6), 983–990. doi: 10.1136/annrheumdis-2015-208052
- Tarp, S., Eric, F. D., Boers, M., Luta, G., Bliddal, H., Tarp, U., et al. (2017). Risk of serious adverse effects of biological and targeted drugs in patients with rheumatoid arthritis: a systematic review meta-analysis. *Rheumatol. (Oxford)* 56 (3), 417–425. doi: 10.1093/rheumatology/kew442
- Wang, W., Zhou, H., and Liu, L. (2018). Side effects of methotrexate therapy for rheumatoid arthritis: A systematic review. *Eur. J. Med. Chem.* 158, 502–516. doi: 10.1016/j.ejmech.2018.09.027
- Wang, Q., Wang, C. H., and Meng, Y. (2019). microRNA-1297 promotes the progression of osteoporosis through regulation of osteogenesis of bone marrow mesenchymal stem cells by targeting WNT5A. *Eur. Rev. Med. Pharmacol. Sci.* 23 (11), 4541–4550. doi: 10.26355/eurrev_201906_18029
- Wu, N., Lee, Y. C., Shah, N., and Harrison, D. J. (2014). Cost of biologics per treated patient across immune-mediated inflammatory disease indications in a pharmacy benefit management setting: a retrospective cohort study. *Clin. Ther.* 36 (8), 1231–1241. doi: 10.1016/j.clinthera.2014.06.014
- Zhang, H., Xing, W. W., Li, Y. S., Zhu, Z., Wu, J. Z., Zhang, Q. Y., et al. (2008). Effects of a traditional Chinese herbal preparation on osteoblasts and osteoclasts. *Maturitas* 61 (4), 334–339. doi: 10.1016/j.maturitas.2008.09.023
- Zhang, Y. Q., Wang, S. S., Zhu, W. L., Ma, Y., Zhang, F. B., Liang, R. X., et al. (2015). Deciphering the pharmacological mechanism of the Chinese formula huanglian-jie-du decoction in the treatment of ischemic stroke using a systems biology-based strategy. *Acta Pharmacol. Sin.* 36 (6), 724–733. doi: 10.1038/aps.2014.124
- Zhang, W., Bai, Y., Wang, Y., and Xiao, W. (2016). Polypharmacology in Drug Discovery: A Review from Systems Pharmacology Perspective. *Curr. Pharm. Des.* 22 (21), 3171–3181. doi: 10.2174/1381612822666160224142812
- Zhao, N., Li, J., Li, L., Niu, X. Y., Jiang, M., He, X. J., et al. (2015). Molecular network-based analysis of guizhi-shaoyao-zhimu decoction, a TCM herbal formula, for treatment of diabetic peripheral neuropathy. *Acta Pharmacol. Sin.* 36 (6), 716–723. doi: 10.1038/aps.2015.15
- Zhao, H., Xu, H., Qiao, S., Lu, C., Wang, G., Liu, M., et al. (2017). Boldine isolated from Litsea cubeba inhibits bone resorption by suppressing the osteoclast differentiation in collagen-induced arthritis. *Int. Immunopharmacol.* 51, 114–123. doi: 10.1016/j.intimp.2017.08.013
- Zhao, H., Xu, H., Zuo, Z., Wang, G., Liu, M., Guo, M., et al. (2018). Yi Shen Juan Bi Pill Ameliorates Bone Loss and Destruction Induced by Arthritis Through Modulating the Balance of Cytokines Released by Different Subpopulations of T Cells. *Front. Pharmacol.* 9, 262. doi: 10.3389/fphar.2018.00262
- Zheng, C., Qiu, M., Xu, X., Ye, H., Zhang, Q., Li, Y., et al. (2016). Understanding the diverse functions of Huatan Tongluo Fang on rheumatoid arthritis from a pharmacological perspective. *Exp. Ther. Med.* 12 (1), 87–94. doi: 10.3892/etm.2016.3329

Conflict of Interest: The authors declare that the research was conducted in the absence of any commercial or financial relationships that could be construed as a potential conflict of interest.

The reviewer JC declared a shared affiliation, with no collaboration, with the authors, XL, YX, to the handling editor at time of review.

Copyright © 2020 Li, Lu, Fan, Li, Lu, Tan, Xia, Zhao, Fan and Xiao. This is an open-access article distributed under the terms of the Creative Commons Attribution License (CC BY). The use, distribution or reproduction in other forums is permitted, provided the original author(s) and the copyright owner(s) are credited and that the original publication in this journal is cited, in accordance with accepted academic practice. No use, distribution or reproduction is permitted which does not comply with these terms.



OPEN ACCESS

Edited by:

Per-Johan Jakobsson,
Karolinska Institutet, Sweden

Reviewed by:

Kai Xiao,
Second Military Medical University,
China
Amit Krishna De,
Indian Science Congress Association
(ISCA), India

***Correspondence:**

Yu Huang
Hy1973@gzucm.edu.cn

Specialty section:

This article was submitted to
Ethnopharmacology,
a section of the journal
Frontiers in Pharmacology

Received: 16 November 2019

Accepted: 30 March 2020

Published: 24 April 2020

Citation:

Chen G, Ye Y, Cheng M, Tao Y,
Zhang K, Huang Q, Deng J, Yao D,
Lu C and Huang Y (2020) Quercetin
Combined With Human Umbilical Cord
Mesenchymal Stem Cells Regulated
Tumour Necrosis Factor- α /Interferon- γ -Stimulated Peripheral Blood
Mononuclear Cells via Activation of
Toll-Like Receptor 3 Signalling.
Front. Pharmacol. 11:499.
doi: 10.3389/fphar.2020.00499

Quercetin Combined With Human Umbilical Cord Mesenchymal Stem Cells Regulated Tumour Necrosis Factor- α /Interferon- γ -Stimulated Peripheral Blood Mononuclear Cells via Activation of Toll-Like Receptor 3 Signalling

Guiling Chen^{1,2,3}, Yang Ye⁴, Ming Cheng⁴, Yi Tao⁴, Kejun Zhang^{1,2,3}, Qiong Huang⁴,
Jingwen Deng^{1,3,5}, Danni Yao^{1,3,5}, Chuanjian Lu^{1,3,5} and Yu Huang^{1,2,3*}

¹ Second Affiliated Hospital, Guangzhou University of Chinese Medicine, Guangzhou, China, ² Department of National Institute of Stem Cell Clinical Research, Guangdong Provincial Hospital of Chinese Medicine, Guangzhou, China, ³ Guangdong Provincial Academy of Chinese Medical Sciences, Guangzhou, China, ⁴ Department of Shanghai Zhangjiang Biobank, National Engineering Centre for Biochip at Shanghai, Shanghai, China, ⁵ Department of Dermatology, Guangdong Provincial Hospital of Chinese Medicine, Guangzhou, China

The beneficial effect of quercetin in rheumatic diseases is unclear. Studies have already confirmed that human umbilical cord mesenchymal stem cells (hUCMSCs) alleviate some symptoms of rheumatoid arthritis (RA) by their immunosuppressive capacities. This study explored whether there are additive effects of quercetin and hUCMSCs on peripheral blood mononuclear cells (PBMCs) under simulated rheumatic conditions. hUCMSCs were pretreated with quercetin (10 μ M) before coculture with TNF- α /IFN- γ -stimulated PBMCs at a ratio of 1:1 for 3 days. PBMC proliferation was inhibited, and the proportion of Th17 cells was shifted. These effects may be related to the effect of quercetin on functional molecules in hUCMSCs, including nitric oxide (NO), indoleamine 2,3-dioxygenase (IDO), interleukin 6 (IL-6) and Toll-like receptor-3 (TLR-3) and the Akt/I κ B pathways. These results suggest that quercetin effectively promoted the immunoregulatory effect of hUCMSCs by inhibiting the Akt/I κ B pathway, activating the Toll-like receptor-3 pathway, and regulating downstream cytokines.

Keywords: rheumatoid arthritis, quercetin, human umbilical cord mesenchymal stem cell, Toll-like receptor 3, interleukin 6, indoleamine 2,3-dioxygenase

INTRODUCTION

Rheumatoid arthritis (RA) is a long-term autoimmune disorder involving multiple systems. RA is characterized by the destruction of cartilage and bone by inflammatory cytokines, such as tumour necrosis factor- α (TNF- α) and interferon- γ (IFN- γ) (McInnes and Schett, 2011; Lubberts, 2015), and involves the complex interaction of T helper 1 cells (Th1 cells), Th17 cells, Th2 cells, immunoregulatory cells (such as Treg cells) and monocytes/macrophages. Compared to therapeutic agents and disease-modifying antirheumatic drugs (DMARDs), biological agents, such as TNF inhibitors, are efficacious and safe for the management of arthritis. Mesenchymal stem cells (MSCs), which are multipotent progenitor cells, are emerging as a promising biological agent for treating immune diseases. MSCs can be isolated from bone marrow (BM), umbilical cord, placenta, and adipose tissue, and these cells have the ability to differentiate into various other mesodermal cell lineages, including chondrocytes, adipocytes, and osteoblasts. Another property of MSCs is their anti-inflammatory and immunosuppressive effects. A large number of preclinical studies (Alunno et al., 2015; Yang et al., 2016; Zhang et al., 2017) and clinical studies (Dahbour and Jamali, 2017; Riordan et al., 2018; Zhang et al., 2018) have shown that MSCs considerably alleviate symptoms of autoimmune diseases. Compared with stem cells from other sources, umbilical cord mesenchymal stem cells possess advantages, including rapid, non-invasive harvest procedures, easy expansion *in vitro*, and ethical access; additionally, umbilical cord mesenchymal stem cells exhibit robust immunosuppressive functions (Jin et al., 2013; Wang et al., 2016).

The flavonoid quercetin is widely distributed in plants, foods, and beverages and is an active ingredient that is abundant in traditional Chinese medicines, such as Huangqi Guizhi Wuwu tang. It is a classic formula for treating autoimmune diseases with clinical efficacy that is based on decades of clinical observation and clinical practice. The formula is composed of 5 herbs: *Astragalus mongholicus* Bge (Huangqi), *Cassia twig* (Guizhi), *Paeonia lactiflora* Pall. (Shaoyao), *Zingiber officinale* Roscoe (Shengjiang), and *Ziziphus jujuba* Mill. (Dazao). Pang et al. conducted a meta-analysis of sixteen randomized controlled trials with a total of 1,173 patients suffering diabetic peripheral neuropathy. The results revealed that Huangqi Guizhi Wuwu tang had significant therapeutic efficacy in treating peripheral diabetic neuropathy (Pang et al., 2016). Previous studies have shown that quercetin has various biological actions, such as antioxidative and anti-inflammatory effects (Chen et al., 2018), including inhibiting inflammatory cytokines, such as ROS, IFN- γ , TNF- α , and IL-2 (Meng et al., 2018). Quercetin suppresses the secretion of inflammatory cytokines by regulating transcription factors (NF- κ B) (Chen et al., 2005; Potapovich et al., 2011).

We hypothesized that quercetin has an anti-inflammatory effect and an additive effect when combined with UCMSCs, and this study aimed to investigate the mechanism by which quercetin and UCMSCs affect TNF- α and IFN- γ -stimulated PBMCs and explain the effect of quercetin and UCMSC

treatment on clinical symptoms and disease activity in patients with RA.

MATERIALS AND METHODS

Isolation and Culture of UCMSCs

Human umbilical cords ($n = 3$) were isolated from tissue obtained after full-term, healthy births. The mothers had been informed beforehand and consented to donate. In brief, the vein and artery of the UC were removed to retain Wharton's jelly. Wharton's jelly was cut into small pieces ($1\text{--}2\text{ mm}^3$) and placed into 100 mm tissue culture dishes (NUNC, Thermo Fisher Scientific, USA). A total of 10 ml complete culture medium containing MEM- α (HyClone, USA) supplemented with 5% serum substitute (UltraGRO Advanced, HELIOS, USA) was added to the tissue culture dishes and incubated at 37°C in a 5% carbon dioxide incubator for 7 to 8 days. The medium was changed every 3 to 4 days. After 7 to 8 days, the tissue pieces were removed, and the cells that had attached to the tissue culture dishes were cultured. After another 7 to 8 days, the cells reached 50% to 60% confluence and were passaged into a T175 culture flask at a density of $2 \times 10^6/\text{cm}^2$. Each flask contained 25 ml of MEM- α supplemented with 5% serum substitute (UltraGRO Advanced, HELIOS, USA) and maintained at 37°C in a 5% carbon dioxide incubator. UCMSCs were further passaged when they reached 90% confluence. All UCMSCs used in this study were used within passages 3–5. This study was approved by the Ethics Committee at Guangdong Provincial Hospital of Chinese Medicine and was conducted in accordance with the 1989 Declaration of Helsinki.

UCMSC Characterization

UCMSCs (1×10^6 per tube) were phenotypically characterized by flow cytometry (FACS Aria II, BD Biosciences, USA) using the following antibodies: CD105-PerCy, CD90-FITC, CD44-PE, CD73-FITC, and a negative MSC cocktail (CD45/CD34/CD11b/CD19/HLA-DR) (BD Biosciences, USA). A total of 20,000 events were recorded for each sample, and the data were analysed using FlowJo software (BD Biosciences, USA). In addition, UCMSCs were functionally characterized by multipotent differentiation to adipocytes, osteocytes, and chondrocytes using differentiation and staining kits (Biological Industries, Israel). Briefly, 6×10^4 cells/well were seeded in 24-well plates for adipogenic or osteogenic differentiation assays, and 1×10^5 cells/well were seeded in 96-well U-bottom culture plates for chondrogenic differentiation assays using complete culture medium. All plates were placed in a 5% carbon dioxide incubator at 37°C for 24 to 48 h, and when the cells were 80% to 90% confluent, the medium was changed to differentiation medium (05-330-1-1B, 05-331-1-01 & 05-332-1-15 for adipogenesis; 05-442-1 for osteogenesis; 05-220-1B & D for chondrogenesis). Then, the cells were incubated for 10 to 21 days, and the differentiation medium was changed every 3 to 4 days. Oil red O staining, Alizarin red staining, and Alcian blue staining were used to evaluate adipogenesis, osteogenesis, and chondrogenesis.

Cell Viability Measurement

The effect of quercetin (HPLC≥98%, China National Analytical Centre, Guangzhou (NACC)) on UCMSC viability was assessed by measuring the absorbance of 3-(4,5-dimethylthiazol-2-yl)-2,5-diphenyl tetrazolium bromide (MTT) dye in the cells. For this, 2×10^3 UCMSCs were cultured in 96-well culture plates and then treated with quercetin (0, 1.25 μ M, 2.5 μ M, 5 μ M, 10 μ M, and 20 μ M) for 3 days. Subsequently, 10 μ l of MTT (5 mg/ml) was added to each well, and the plates were incubated at 37°C for 4 h. Then, the MTT and medium were discarded and replaced with DMSO, and the plates were incubated for 10 min. The optical density was read on a PerkinElmer VICTOR X5 (PerkinElmer, USA) with a monochromatic microplate reader at a wavelength of 570 nm.

Isolation and Activation of PBMCs

PBMCs were isolated from the blood of healthy volunteers by centrifugation using Lymphoprep (Axis-Shield, Norway) and washed three times with PBS. Isolated PBMCs were then activated with 20 ng/ml TNF- α and 50 ng/ml IFN- γ (PeproTech, USA) and used in coculture experiments.

Immunosuppression Assays

To test the effect of UCMSCs in combination with quercetin on PBMC proliferation, 5×10^5 UCMSCs were cocultured for 3 days in 6-well plates with carboxyfluorescein succinimidyl ester CFSE-labeled (Beyotime, China) PBMCs (1:1 ratio) that were activated with TNF- α and IFN- γ ; quercetin (10 μ M) was added to the UCMSCs 2 h before coculture of the UCMSCs with the PBMCs. On the third day, the PBMCs were collected, and PBMC proliferation was analysed by flow cytometry.

The presence of Th1, Th2, and Th17 cells was determined by measuring IFN- γ -FITC, IL-4-PE, and IL-17-PE cells using flow cytometry. UCMSCs (5×10^5) were cultured in 6-well plates with 20 ng/ml TNF- α , 50 ng/ml IFN- γ , and 15 ng/ml brefeldin A (added 3 h after TNF- α and IFN- γ) (all from PeproTech, USA) and then cocultured with 5×10^5 UCMSCs (1:1 ratio) that were treated or without 10 μ M quercetin for 72 h at 37°C. After incubation with FITC-conjugated anti-human CD3 and PE-Cyanine7-CD4 antibodies (eBioscience, USA), the cells were fixed and permeabilized and further incubated with FITC-conjugated anti-human IFN- γ (eBioscience, USA), phycoerythrin (PE)-conjugated anti-human IL-4 (eBioscience, USA), and PE-conjugated anti-human IL-17 (eBioscience, USA) antibodies. The cells were then resuspended in PBS and subjected to flow cytometric analysis.

Cytokine Examination

The levels of the cytokines IL-6 and IL-10 in the supernatant were evaluated by enzyme-linked immunosorbent assay (ELISA) using kits purchased from DAKWE (Shenzhen, China). Tests were performed according to the manufacturer's recommended protocols. Each cytokine standard and sample was run in duplicate.

Nitrite Measurement

Nitrite released into the medium was used as a measure of NO production. Nitrite determination was performed using Griess reagent (Invitrogen, Thermo Fisher Scientific, USA) according to the manufacturer protocols.

qRT-PCR

Total RNA from UCMSCs was extracted in the presence or absence of PBMCs and/or quercetin with a FastPure Cell/Tissue total RNA isolation kit (Vazyme, China). RNA concentration and purity were estimated by optical density measurement. RNA isolation was followed by DNase digestion. Total RNA (1 μ g) was reverse transcribed to cDNA with a HiScript III RT SuperMix for qPCR kit (Vazyme, China) at 37°C for 15 min and 85°C for 5 s. Quantitative PCR was performed using ChamQ Universal SYBR qPCR master mix (Vazyme, Q711-02) and an Applied Biosystems QuantStudio 3 Detection System according to the manufacturer's recommendations (Thermo Fisher Scientific, USA). Specific primers for IDO were designed using Primer3 software (Table 1). Expression levels of the transcripts were normalized to the housekeeping gene glyceraldehyde-3-phosphate dehydrogenase (GAPDH). For quantification, the values are expressed as the relative mRNA level of a specific gene as determined using the $2^{-\Delta\Delta C_t}$ method.

Western Blot Analysis

UCMSCs were washed with PBS once and then collected. Subsequently, the cells were lysed in RIPA buffer (Beyotime Biotechnology, China) at 4°C for 30 min. Then, the mixture was centrifuged at 16,000 rcf for 20 min. The lysates were incubated at 95°C for 5 min, separated by 10% SDS-PAGE (Beyotime Biotechnology, China) and transferred to a polyvinylidene difluoride (PVDF) membrane (Millipore, USA). Each PVDF membrane was blocked in TBST with 5% nonfat milk or BSA with gentle shaking for 60 min and then incubated with their respective primary monoclonal antibodies (1:1000; diluted in primary antibody solutions, purchased from Beyotime Biotechnology) against p-I κ B (2859), p-AKT (4060), AKT (4691), Toll-like receptor 3 (6961), and GAPDH (5174) (Cell Signalling Technology, USA) overnight at 4°C. Then, each PVDF membrane was incubated with 1:5000 horseradish peroxidase-conjugated secondary antibody (BA1054) (BOSTER, China) in TBST with 5% nonfat milk or BSA for 1 h. Finally, the membranes were visualized by enhanced chemiluminescence staining. The intensities of the bands were quantified with a computerized densitometer.

TABLE 1 | Primer sequences and access numbers of study genes.

Gene Name	Forward Primer (5' to 3')	Reverse Primer (5' to 3')
GAPDH	ACAACTTTGGTATCGTGGAAGG	GCCATCACGCCACAGTTTC
IDO	TCTCAGACACACAAGTCACAGC	AGAGTTGGCAGTAAGGAACAGCA

Statistical Analysis

Statistical analysis was performed using SPSS 13.0. The data are expressed as the means \pm SEM. One-way ANOVA was used to analyse the data. Significance was set at $P < 0.05$.

RESULTS

Isolation and Characterization of UCMSCs

UCMSCs were grown from the tissue for 5 to 7 days, and single cell-derived clones gradually reached confluence with a whirlpool-like arrangement. When cells were 50% to 60% confluent in 100 mm culture dishes, the cells were passaged into a T175 culture flask at a density of $2 \times 10^6/\text{cm}^2$. The cells were digested and passaged into another T175 culture flask when they reached 80% to 90% confluence.

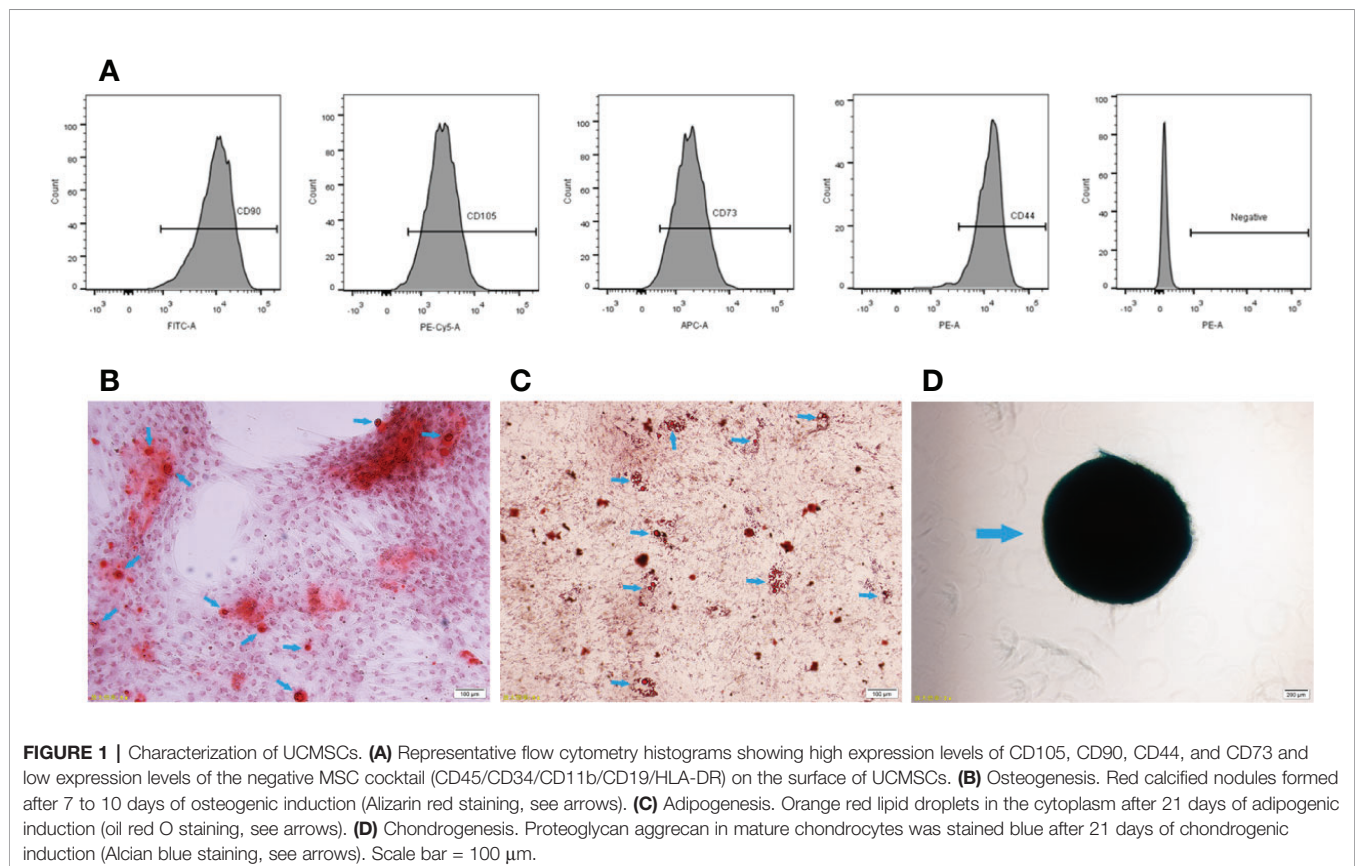
Cultured UCMSCs that were isolated from human umbilical cords showed the capacity for differentiation into osteoblasts, adipocytes, and chondrocytes after culture in differentiation medium for 10 to 21 days. The formation of lipid droplets in mature adipocytes and mineralized calcified nodules in osteoblasts and chondrocyte clusters were observed. Calcified nodules in osteoblasts were stained red using Alizarin red (**Figure 1B**), lipid droplets in mature adipocytes were stained orange using oil red O (**Figure 1C**), and the proteoglycan

aggrecan in chondrocytes was stained blue using Alcian blue (**Figure 1D**).

In addition, UCMSCs presented a typical MSC immunophenotype, with positive expression of CD105 ($97.57\% \pm 0.67\%$), CD73 ($97.83\% \pm 0.51\%$), CD44 ($95.37\% \pm 1.13\%$), and CD90 ($99\% \pm 0.7\%$), and the cells lacked CD34, CD45, and HLA-DR (total $0.1\% \pm 0.1\%$) markers (**Figure 1A**).

Quercetin Did Not Influence UCMSC Viability, Morphology, Phenotype or Cell Cycle

The effect of quercetin on the basic properties of UCMSCs, including viability, morphology, surface marker expression, and cell cycle, was evaluated. No changes were observed in UCMSC viability in an MTT assay after 3 days of culture in complete medium or with 1.25 μM , 2.5 μM , 5 μM , and 10 μM quercetin (**Figure 2B**). In addition, 20 μM quercetin inhibited UCMSC viability, and a dose of 10 μM quercetin was used in the subsequent study. Regarding morphology and phenotype, UCMSCs treated with 10 μM quercetin and untreated UCMSCs shared similar shapes (**Figure 2A**) and the same surface markers, and the cells were positive for CD44, CD73, CD90, and CD105 and negative for CD34, CD45, CD19, CD11b, and HLA-DR (data not shown). Both of them had analogous proportions of cells in the G1, S, and G2/M phases of the cell cycle (**Figure 2C**).



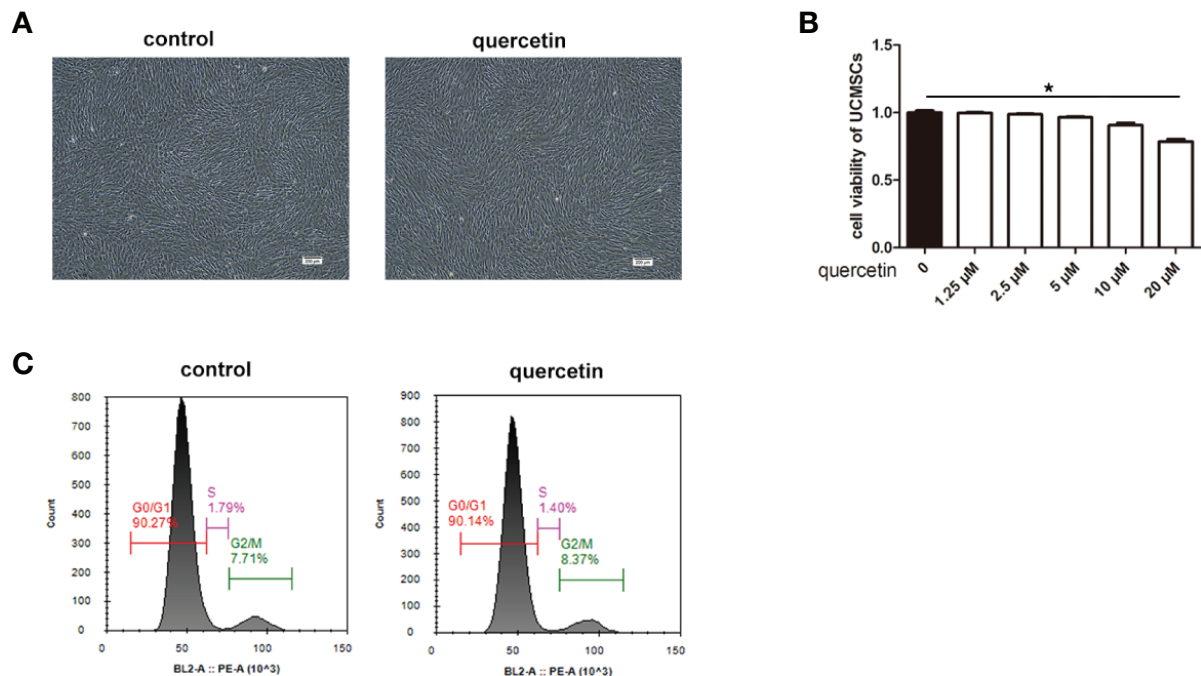


FIGURE 2 | Morphology, viability, phenotype, and cell cycle of UCMSCs. Untreated UCMSCs and UCMSCs that were pretreated with 10 μ M quercetin were cultured for 3 days. **(A)** Morphology (100 \times). Untreated UCMSCs and UCMSCs that were pretreated with 10 μ M quercetin shared the same morphology. **(B)** UCMSC viability was examined by MTT assay. Quercetin at 20 μ M influenced UCMSC viability. * $P < 0.05$, mean \pm SEM, $n=5$. **(C)** The proportion of cells in the G1, S, and G2/M phases of the cell cycle in untreated UCMSCs and UCMSCs that were pretreated with 10 μ M quercetin. No significant differences were detected. Representative examples are shown.

Quercetin Enhanced UCMSC Immunosuppression of PBMCs

The inhibitory effects of UCMSCs on PBMC proliferation were evaluated, and the difference between UCMSCs with and without quercetin treatment was compared. CFSE-labeled PBMCs were collected and detected by FACS on the third day after coculture with TNF- α /IFN- γ -activated UCMSCs that were treated with or without 10 μ M quercetin. The data showed that the proportion of divided PBMCs in the stimulated group (sPBMCs) reached $84.74\% \pm 1.85\%$ (M2), while the proportion of unstimulated PBMCs (nPBMCs) was $7.42\% \pm 1.6\%$ (M2). UCMSCs significantly inhibited the proliferation of PBMCs in the coculture system, showing $78.05\% \pm 1.41\%$ (M2) divided cells, and quercetin ($66.45\% \pm 2.88\%$ (M2)) enhanced the effect. As shown in **Figure 3A**, when UCMSCs were treated with quercetin before coculture, the division rates of PBMCs after TNF- α /IFN- γ activation decreased significantly. Th17 subsets in PBMCs were evaluated by counting the CD4⁺IL-17⁺ cells using flow cytometry. The proliferation of CD4⁺IL-17⁺ cells was promoted in stimulated PBMCs but inhibited in activated PBMCs that were cocultured with UCMSCs compared to stimulated PBMCs, and the addition of quercetin to the coculture system had a combined inhibitory effect on CD4⁺IL-17⁺ cell proliferation (**Figure 3B**).

These results indicated that the suppressive effects of UCMSCs on PBMC proliferation were augmented by quercetin treatment.

Quercetin Promoted UCMSCs to Express TLR-3 and Suppressed AKT or I κ B

To explore the mechanism by which quercetin and UCMSCs suppressed PBMC proliferation, the expression of TLR-3, AKT, and I κ B was assessed in untreated UCMSCs, as well as in UCMSCs that were treated with 10 μ M quercetin or/and activated PBMCs for 3 days. TLR-3 is linked to MSC immunosuppressive capacity, promoting MSCs to secrete cytokines that inhibit the inflammatory response. AKT or I κ B are signals that are relevant to inflammatory reactions. The data showed that UCMSCs overexpressed TLR-3 when cocultured with activated PBMCs, and quercetin enhanced this effect. As shown in **Figure 4A**, UCMSCs alone expressed low levels of TLR-3. When cocultured with activated PBMCs, UCMSCs showed increased expression of TLR-3, and when UCMSCs were pretreated with quercetin in the coculture system, TLR-3 expression was higher. p-AKT and p-I κ B expression was increased in UCMSCs that were cocultured with stimulated PBMCs, and quercetin decreased p-AKT and p-I κ B expression (**Figures 4A–D**) show the quantification of the TLR-3, p-AKT and p-I κ B.

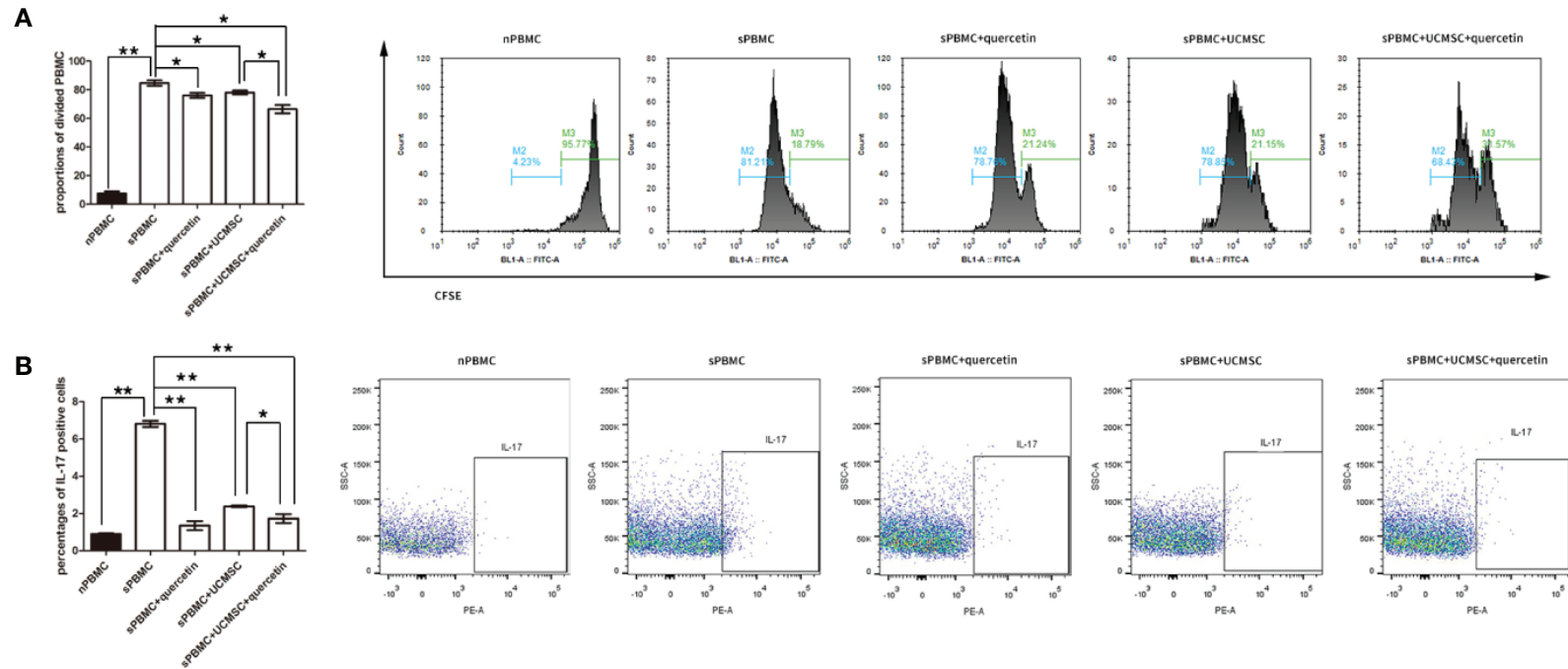


FIGURE 3 | Quercetin enhanced UCMSC immunomodulation. UCMSCs were cocultured with TNF- α /IFN- γ -activated PBMCs (1:1 ratio) for 3 days. **(A)** CFSE-labeled PBMCs were cocultured with UCMSCs that were treated with or without quercetin for 3 days, and PBMC proliferation was determined by the proportions of attenuated CFSE-fluorescent cells (divided cells). Both UCMSCs and quercetin suppressed PBMC division, and UCMSCs and quercetin acted on PBMCs additively; they had a combined inhibitory effect on PBMC division. Mean \pm SEM, $n = 3$, * $P < 0.05$, ** $P < 0.01$. **(B)** Th17 cells were measured by IL-17-positive cells from purified CD4⁺ T cells. Quercetin and UCMSCs alone or in combination inhibited the proliferation of Th17 cells, and quercetin enhanced the suppressive effect of UCMSCs when UCMSCs were pretreated before coculture. Mean \pm SEM, $n = 3$, * $P < 0.05$, ** $P < 0.01$.

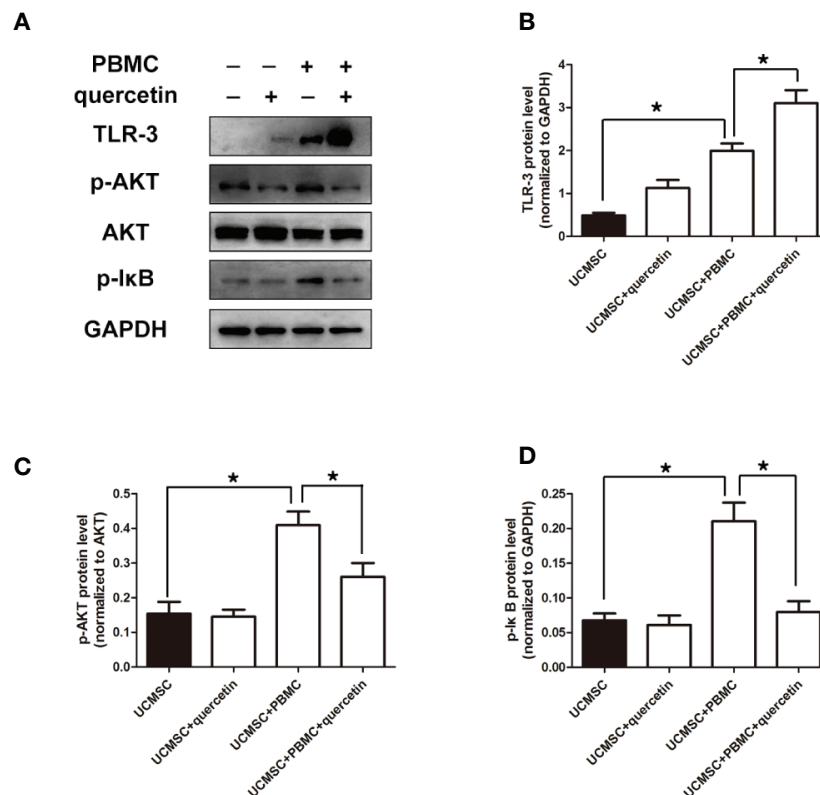


FIGURE 4 | Changes in signaling pathways in UCMSCs. UCMSCs were cocultured with TNF- α /IFN- γ -activated PBMCs (1:1 ratio) in the presence or absence of quercetin for 3 days. **(A)** Expression of TLR-3 and AKT/I κ B was assessed by Western blotting. Quercetin induced TLR-3 expression and inhibited AKT/I κ B expression in UCMSCs. **(B–D)** The bar graphs show the quantification of the indicated proteins. Mean \pm SEM, $n = 3$. * $P < 0.05$.

Quercetin Promoted UCMSCs to Produce the Anti-Inflammatory Factors IL-6, NO, and IDO in Response to Activated PBMCs

Furthermore, the levels of the anti-inflammatory factors IL-6, NO, and IDO, which are linked to TLR-3 signaling, were assessed in UCMSCs that were pretreated with or without 10- μ M quercetin and co-cultured with activated PBMCs for 3 days. As shown in **Figures 5A, B**, IL-6 and NO were increased in the supernatant of UCMSCs in the coculture system, and 10 μ M quercetin enhanced the effect, with higher levels of IL-6 and NO. Consistently, IDO transcripts were significantly increased in UCMSCs that were treated with activated PBMCs. Quercetin increased the level of IDO transcripts in UCMSCs in the coculture system (**Figure 5C**). IL-10 expression was not affected by quercetin or activated PBMCs (data not shown).

DISCUSSION

Rheumatoid arthritis is a systemic inflammatory autoimmune disease that is characterized by synovitis. Infiltrated T cells (Th1 cells, Th17 cells, and Th2 cells), resident macrophages,

and Treg cells and the overproduction of inflammatory factors (such as TNF- α , IFN- γ , IL-6, and IL-17) have been extensively studied to explain the mechanism. Their cross-interaction causes complex inflammatory cascades all lead to persistent synovial inflammation, and associated damage to articular cartilage and underlying bone.

MSCs are emerging as a new type of immunosuppressant in multiple autoimmune diseases. Biological agents are non-dependent, non-resistant, and have no side effects that are increasingly favoured by clinical researchers. How to improve the immunosuppressive effect of MSCs is currently a concern. Quercetin, a traditional Chinese medicine monomer, has anti-inflammatory and antioxidant effects. A few studies have focused on its anti-inflammatory effects on autoimmune diseases (Milenkovic et al., 2010; Wang et al., 2013; Javadi et al., 2017).

Consistent with other studies (Allanore et al., 2001; Kim et al., 2007; Xiong et al., 2014), this study used TNF- α /IFN- γ to mimic the *in vitro* condition of RA, which promoted PBMC proliferation and amplified Th17 subsets. Quercetin and UCMSCs were then administered to stimulate the PBMCs. The results showed that quercetin and UCMSCs both inhibited the inflammatory response. They had an additive effect on activated

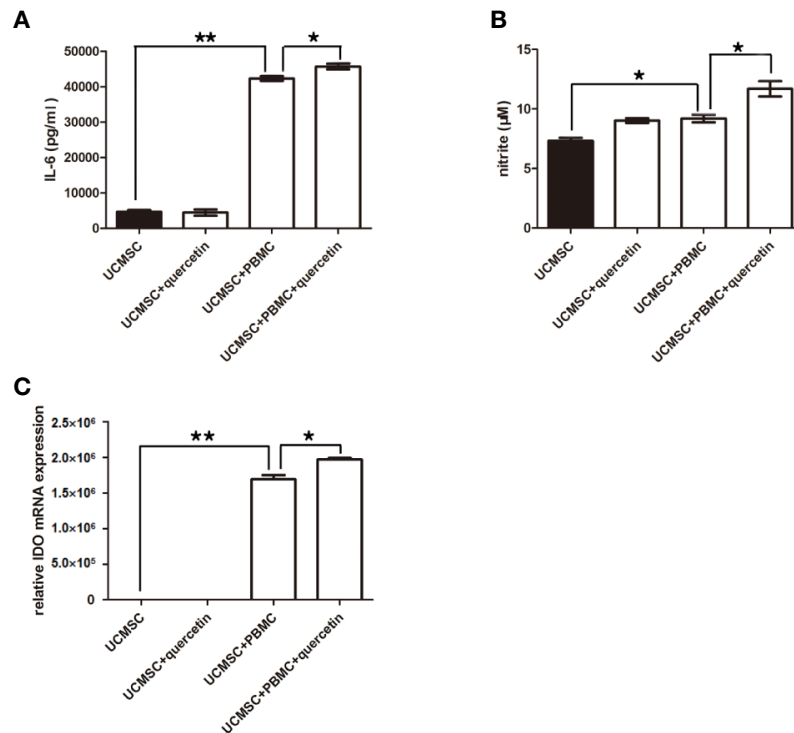


FIGURE 5 | Changes in anti-inflammatory molecules in UCMSCs. TNF- α /IFN- γ -activated PBMCs (1:1 ratio) in the presence or absence of quercetin for 3 days. The anti-inflammatory molecules IL-6 (A), NO (B), and IDO (C) were determined by ELISA, Griess assay and RT-PCR. UCMSCs overexpressed IL-6, NO, and IDO in the coculture system with PBMCs. Quercetin enhanced the effect. Mean \pm SEM, $n = 3$. * $P < 0.05$, ** $P < 0.01$.

PBMCs. Notably, quercetin alone did not affect the proliferation, phenotype, or cell cycle of UCMSCs.

Furthermore, the results demonstrated that quercetin downregulated p-AKT/p-I κ B expression and upregulated TLR-3 on UCMSCs and induced high levels of IL-6, IDO, and NO, which may explain some of the mechanisms by which UCMSCs suppress PBMC responses. Activation of the AKT/I κ B pathway is involved in the inflammatory response in many studies (Burris et al., 2014; Ye et al., 2017; Harikrishnan and Jantan, 2018), and the findings of this study are consistent with these observations. TNF- α /IFN- γ stimulated PBMCs to activate p-AKT/p-I κ B in cocultured UCMSCs; however, quercetin reversed these effects. TLR-3 is capable of polarizing MSCs towards an anti-inflammatory phenotype with enhanced immunosuppressive capacity (Opitz et al., 2009; Waterman et al., 2010; Cassano et al., 2018). According to the data, quercetin treatment of UCMSCs induced TLR-3 signaling and boosted the capacity of these cells to control PBMC inflammatory reactions. Quercetin alone has a direct suppressive effect. Poly(I:C) (a TLR-3 agonist) interacts with TLR-3 and prominently induces IL-6, IL-10, IL-11, LIF, VEGF, SDF1, and PGE2 (Mastri et al., 2012; Kim et al., 2018) in MSCs, which suggests that expression of the anti-inflammatory factors IDO, NO, and IL-6 by UCMSCs may be regulated by TLR-3.

Collectively, this study confirmed that UCMSCs combined with 10 μ M quercetin ameliorated proliferation of TNF- α /IFN- γ -activated PBMCs by inducing TLR-3 signaling, providing an

understanding of the mechanism by which quercetin potentiates UCMSCs and induces anti-inflammatory proteins in UCMSCs. This work may provide new ideas for the treatment of rheumatoid arthritis in the clinic.

DATA AVAILABILITY STATEMENT

The data generated for this study can be found in NCBI using the accession number NM_002164 (version NM_002164.6).

ETHICS STATEMENT

The studies involving human participants were reviewed and approved by the ethics committee of Guangdong Provincial Hospital of Chinese Medicine. The patients/participants provided their written informed consent to participate in this study.

AUTHOR CONTRIBUTIONS

GC designed and conducted the study. KZ and QH conducted part of the study. YY, MC, and YT analyzed the data and interpreted the results. JD and DY polished the manuscript. CL provided the technical support and advices for the study. YH

supervised the study. All authors contributed to the review and the approval of the final manuscript.

FUNDING

This study was approved by grants from Special Funding for TCM Science and Technology Research of Guangdong

Provincial Hospital of Chinese Medicine (project number: No.CMR-20170220-1001) and received grant from Special Funding for TCM Science and Technology Research of Guangdong Provincial Hospital of Chinese Medicine (project number: YN2016QJ02), the Traditional Chinese Medicine Bureau Foundation of Guangdong Province (project number: No.20183005).

REFERENCES

- Allanore, Y., Borderie, D., Hilliquin, P., Hernvann, A., Levacher, M., Lemarchal, H., et al. (2001). Low levels of nitric oxide (NO) in systemic sclerosis: inducible NO synthase production is decreased in cultured peripheral blood monocyte/macrophage cells. *Rheumatol. (Oxford)* 40 (10), 1089–1096. doi: 10.1093/rheumatology/40.10.1089
- Alunno, A., Montanucci, P., Bistoni, O., Basta, G., Caterbi, S., Pescara, T., et al. (2015). In vitro immunomodulatory effects of microencapsulated umbilical cord Wharton jelly-derived mesenchymal stem cells in primary Sjogren's syndrome. *Rheumatol. (Oxford)* 54 (1), 163–168. doi: 10.1093/rheumatology/keu292
- Burris, R. L., Ng, H. P., and Nagarajan, S. (2014). Soy protein inhibits inflammation-induced VCAM-1 and inflammatory cytokine induction by inhibiting the NF-kappaB and AKT signaling pathway in apolipoprotein E-deficient mice. *Eur. J. Nutr.* 53 (1), 135–148. doi: 10.1007/s00394-013-0509-7
- Cassano, J. M., Schnabel, L. V., Goodale, M. B., and Fortier, L. A. (2018). The immunomodulatory function of equine MSCs is enhanced by priming through an inflammatory microenvironment or TLR3 ligand. *Vet. Immunol. Immunopathol.* 195, 33–39. doi: 10.1016/j.vetimm.2017.10.003
- Chen, J. C., Ho, F. M., Pei-Dawn Lee, C., Chen, C. P., Jeng, K. C., Hsu, H. B., et al. (2005). Inhibition of iNOS gene expression by quercetin is mediated by the inhibition of IkappaB kinase, nuclear factor-kappa B and STAT1, and depends on heme oxygenase-1 induction in mouse BV-2 microglia. *Eur. J. Pharmacol.* 521 (1–3), 9–20. doi: 10.1016/j.ejphar.2005.08.005
- Chen, Z., Yuan, Q., Xu, G., Chen, H., Lei, H., and Su, J. (2018). Effects of Quercetin on Proliferation and H(2)O(2)-Induced Apoptosis of Intestinal Porcine Enterocyte Cells. *Molecules* 23 (8), 1–25. doi: 10.3390/molecules23082012
- Dahbour, S., and Jamali, F. (2017). Mesenchymal stem cells and conditioned media in the treatment of multiple sclerosis patients: Clinical, ophthalmological and radiological assessments of safety and efficacy. *CNS Neurosci. Ther.* 23 (11), 866–874. doi: 10.1111/cns.12759
- Harikrishnan, H., and Jantan, I. (2018). Anti-Inflammatory Effects of Hypophyllanthin and Niranthin Through Downregulation of NF-kappaB/ MAPKs/PI3K-Akt Signaling Pathways. *Inflammation* 41 (3), 984–995. doi: 10.1007/s10753-018-0752-4
- Javadi, F., Ahmadzadeh, A., Egtesadi, S., Aryaeian, N., Zabihiyeganeh, M., Rahimi Foroushani, A., et al. (2017). The Effect of Quercetin on Inflammatory Factors and Clinical Symptoms in Women with Rheumatoid Arthritis: A Double-Blind, Randomized Controlled Trial. *J. Am. Coll. Nutr.* 36 (1), 9–15. doi: 10.1080/07315724.2016.1140093
- Jin, H. J., Bae, Y. K., Kim, M., Kwon, S. J., Jeon, H. B., Choi, S. J., et al. (2013). Comparative analysis of human mesenchymal stem cells from bone marrow, adipose tissue, and umbilical cord blood as sources of cell therapy. *Int. J. Mol. Sci.* 14 (9), 17986–18001. doi: 10.3390/ijms140917986
- Kim, H. A., Kim, S., Chang, S. H., Hwang, H. J., and Choi, Y. N. (2007). Anti-arthritis effect of ginsenoside Rb1 on collagen induced arthritis in mice. *Int. Immunopharmacol.* 7 (10), 1286–1291. doi: 10.1016/j.intimp.2007.05.006
- Kim, D. S., Lee, W. H., Lee, M. W., Park, H. J., Jang, I. K., Lee, J. W., et al. (2018). Involvement of TLR3-Dependent PGES Expression in Immunosuppression by Human Bone Marrow Mesenchymal Stem Cells. *Stem Cell Rev. Rep.* 14 (2), 286–293. doi: 10.1007/s12015-017-9793-6
- Lubberts, E. (2015). Role of T lymphocytes in the development of rheumatoid arthritis. Implications for treatment. *Curr. Pharm. Des.* 21 (2), 142–146. doi: 10.2174/1381612820666140825122247
- Mastri, M., Shah, Z., McLaughlin, T., Greene, C. J., Baum, L., Suzuki, G., et al. (2012). Activation of Toll-like receptor 3 amplifies mesenchymal stem cell trophic factors and enhances therapeutic potency. *Am. J. Physiol. Cell Physiol.* 303 (10), C1021–C1033. doi: 10.1152/ajpcell.00191.2012
- McInnes, I. B., and Schett, G. (2011). The pathogenesis of rheumatoid arthritis. *N Engl. J. Med.* 365 (23), 2205–2219. doi: 10.1056/NEJMra1004965
- Meng, L. Q., Yang, F. Y., Wang, M. S., Shi, B. K., Chen, D. X., Chen, D., et al. (2018). Quercetin protects against chronic prostatitis in rat model through NF-kappaB and MAPK signaling pathways. *Prostate* 78 (11), 790–800. doi: 10.1002/pros.23536
- Milenkovic, M., Arsenovic-Ranin, N., Stojic-Vukanic, Z., Bufan, B., Vucicevic, D., and Jancic, I. (2010). Quercetin ameliorates experimental autoimmune myocarditis in rats. *J. Pharm. Pharm. Sci.* 13 (3), 311–319. doi: 10.18433/J3VS3S
- Opitz, C. A., Litzenburger, U. M., Lutz, C., Lanz, T. V., Tritschler, I., Koppel, A., et al. (2009). Toll-like receptor engagement enhances the immunosuppressive properties of human bone marrow-derived mesenchymal stem cells by inducing indoleamine-2,3-dioxygenase-1 via interferon-beta and protein kinase R. *Stem Cells* 27 (4), 909–919. doi: 10.1002/stem.7
- Pang, B., Zhao, T. Y., Zhao, L. H., Wan, F., Ye, R., Zhou, Q., et al. (2016). Huangqi Guizhi Wuwu Decoction for treating diabetic peripheral neuropathy: a meta-analysis of 16 randomized controlled trials. *Neural Regener. Res.* 11 (8), 1347–1358. doi: 10.4103/1673-5374.189202
- Potapovich, A. I., Lulli, D., Fidanza, P., Kostyuk, V. A., De Luca, C., Pastore, S., et al. (2011). Plant polyphenols differentially modulate inflammatory responses of human keratinocytes by interfering with activation of transcription factors NFkappaB and AhR and EGFR-ERK pathway. *Toxicol. Appl. Pharmacol.* 255 (2), 138–149. doi: 10.1016/j.taap.2011.06.007
- Riordan, N. H., Morales, I., Fernandez, G., Allen, N., Fearnott, N. E., Leckrone, M. E., et al. (2018). Clinical feasibility of umbilical cord tissue-derived mesenchymal stem cells in the treatment of multiple sclerosis. *J. Transl. Med.* 16 (1), 57. doi: 10.1186/s12967-018-1433-7
- Wang, W., Wang, C., Ding, X. Q., Pan, Y., Gu, T. T., Wang, M. X., et al. (2013). Quercetin and allopurinol reduce liver thioredoxin-interacting protein to alleviate inflammation and lipid accumulation in diabetic rats. *Br. J. Pharmacol.* 169 (6), 1352–1371. doi: 10.1111/bph.12226
- Wang, Q., Yang, Q., Wang, Z., Tong, H., Ma, L., Zhang, Y., et al. (2016). Comparative analysis of human mesenchymal stem cells from fetal-bone marrow, adipose tissue, and Warton's jelly as sources of cell immunomodulatory therapy. *Hum. Vaccin Immunother.* 12 (1), 85–96. doi: 10.1080/21645515.2015.1030549
- Waterman, R. S., Tomchuck, S. L., Henkle, S. L., and Betancourt, A. M. (2010). A new mesenchymal stem cell (MSC) paradigm: polarization into a pro-inflammatory MSC1 or an immunosuppressive MSC2 phenotype. *PLoS One* 5 (4), e10088. doi: 10.1371/journal.pone.0010088
- Xiong, Y. S., Cheng, Y., Lin, Q. S., Wu, A. L., Yu, J., Li, C., et al. (2014). Increased expression of Siglec-1 on peripheral blood monocytes and its role in mononuclear cell reactivity to autoantigen in rheumatoid arthritis. *Rheumatol. (Oxford)* 53 (2), 250–259. doi: 10.1093/rheumatology/ket342
- Yang, H., Sun, J., Wang, F., Li, Y., Bi, J., and Qu, T. (2016). Umbilical cord-derived mesenchymal stem cells reversed the suppressive deficiency of T regulatory cells from peripheral blood of patients with multiple sclerosis in a co-culture - a preliminary study. *Oncotarget* 7 (45), 72537–72545. doi: 10.18632/oncotarget.12345

- Ye, J., Piao, H., Jiang, J., Jin, G., Zheng, M., Yang, J., et al. (2017). Polydatin inhibits mast cell-mediated allergic inflammation by targeting PI3K/Akt, MAPK, NF-kappaB and Nrf2/HO-1 pathways. *Sci. Rep.* 7 (1), 11895. doi: 10.1038/s41598-017-12252-3
- Zhang, Z., Feng, R., Niu, L., Huang, S., Deng, W., Shi, B., et al. (2017). Human Umbilical Cord Mesenchymal Stem Cells Inhibit T Follicular Helper Cell Expansion Through the Activation of iNOS in Lupus-Prone B6.MRL-Fas(lpr) Mice. *Cell Transplant.* 26 (6), 1031–1042. doi: 10.3727/096368917X694660
- Zhang, J., Lv, S., Liu, X., Song, B., and Shi, L. (2018). Umbilical Cord Mesenchymal Stem Cell Treatment for Crohn's Disease: A Randomized Controlled Clinical Trial. *Gut Liver* 12 (1), 73–78. doi: 10.5009/gnl17035

Conflict of Interest: The authors declare that the research was conducted in the absence of any commercial or financial relationships that could be construed as a potential conflict of interest.

Copyright © 2020 Chen, Ye, Cheng, Tao, Zhang, Huang, Deng, Yao, Lu and Huang. This is an open-access article distributed under the terms of the Creative Commons Attribution License (CC BY). The use, distribution or reproduction in other forums is permitted, provided the original author(s) and the copyright owner(s) are credited and that the original publication in this journal is cited, in accordance with accepted academic practice. No use, distribution or reproduction is permitted which does not comply with these terms.



OPEN ACCESS

Edited by:

Runyue Huang,
Guangzhou University of Chinese
Medicine, China

Reviewed by:

Yi Zhao,
Sichuan University, China
Hailong Wang,
China Academy of Chinese Medical
Sciences, China
Kayo Masuko,
Sanno Medical Center, Japan
Guangxing Chen,
First Affiliated Hospital of Guangzhou
University of Chinese Medicine, China

***Correspondence:**

Yingsong Wu
wg@smu.edu.cn
Ligang Jie
Jieligang@hotmail.com

Specialty section:

This article was submitted to
Ethnopharmacology,
a section of the journal
Frontiers in Pharmacology

Received: 05 February 2020

Accepted: 14 April 2020

Published: 15 May 2020

Citation:

Du H, Wang Y, Zeng Y, Huang X, Liu D,
Ye L, Li Y, Chen X, Liu T, Li H, Wu J,
Yu Q, Wu Y and Jie L (2020)
Tanshinone IIA Suppresses
Proliferation and Inflammatory
Cytokine Production of Synovial
Fibroblasts from Rheumatoid Arthritis
Patients Induced by TNF- α and
Attenuates the Inflammatory
Response in AIA Mice.
Front. Pharmacol. 11:568.
doi: 10.3389/fphar.2020.00568

Tanshinone IIA Suppresses Proliferation and Inflammatory Cytokine Production of Synovial Fibroblasts from Rheumatoid Arthritis Patients Induced by TNF- α and Attenuates the Inflammatory Response in AIA Mice

Hongyan Du¹, Yuechun Wang^{2,3}, Yongchang Zeng¹, Xiaoming Huang¹, Dingfei Liu¹, Lulan Ye¹, Yang Li¹, Xiaochen Chen^{1,3}, Tiancai Liu¹, Hongwei Li¹, Jing Wu², Qinghong Yu², Yingsong Wu^{1*} and Ligang Jie^{2*}

¹ School of Laboratory Medicine and Biotechnology, Southern Medical University, Guangzhou, China, ² Department of Rheumatology and Clinical Immunology, Zhujiang Hospital, Southern Medical University, Guangzhou, China, ³ School of Chinese Medicine, Southern Medical University, Guangzhou, China

Rheumatoid arthritis (RA) is a chronic and progressive autoimmune disease in which activated RA fibroblast-like synoviocytes (RA-FLSs) are one of the main factors responsible for inducing morbidity. Previous reports have shown that RA-FLSs have proliferative features similar to cancer cells, in addition to causing cartilage erosion that eventually causes joint damage. Thus, new therapeutic strategies and drugs that can effectively contain the abnormal hyperplasia of RA-FLSs and restrain RA development are necessary for the treatment of RA. Tanshinone IIA (Tan IIA), one of the main phytochemicals isolated from *Salvia miltiorrhiza* Bunge, is capable of promoting RA-FLS apoptosis and inhibiting arthritis in an AIA mouse model. In addition, RA patients treated at our clinic with Tan IIA showed significant improvements in their clinical symptoms. However, the details of the molecular mechanism by which Tan IIA effects RA are unknown. To clarify this mechanism, we evaluated the antiproliferative and inhibitory effects of proinflammatory factor production caused by Tan IIA to RA-FLSs. We demonstrated that Tan IIA can restrict the proliferation, migration, and invasion of RA-FLSs in a time- and dose-dependent manner. Moreover, Tan IIA effectively suppressed the increase in mRNA expression of some matrix metalloproteinases and proinflammatory factors induced by TNF- α in RA-FLSs, resulting in inflammatory reactivity inhibition and blocking the destruction of the knee joint. Through the integration of network pharmacology analyses with the experimental data obtained, it is revealed that the effects of Tan IIA on RA can be attributed to its influence on different signaling

pathways, including MAPK, AKT/mTOR, HIF-1, and NF- κ B. Taken together, these data suggest that the compound Tan IIA has great therapeutic potential for RA treatment.

Keywords: Tan IIA, suppress, RA-FLSs, AIA, MAPK, AKT/mTOR, HIF-1 α

INTRODUCTION

Rheumatoid arthritis (RA) is a chronic and systemic autoimmune disease characterized by deformity and joint dysfunction (Smolen et al., 2016). Although the pathogenesis and etiology of RA have not been fully explained, fibroblast-like synoviocytes (FLSs) are considered to be crucial in the development of synovial hyperplasia and the progressive joint destruction in RA patients (Huber et al., 2006; Lefevre et al., 2009). Recent evidence indicates that activated RA-FLSs display biological characteristics similar to tumor cells, such as aggressive proliferation, migration, and invasion. Remarkably, these features are conducive to causing damage to articular cartilage and bone (Bustamante et al., 2017; Wang Z. et al., 2019; Wang and Zhao, 2019). Therefore, the inactivation of RA-FLSs has been pointed to as a potential therapeutic strategy for the treatment of RA.

Many natural ingredients from herbal medicine have been found to be pharmaceutically effective against RA. *Salvia miltiorrhiza* Bunge, a famous herbal medicine, has been widely used to treat cardiovascular diseases in China. Tanshinone IIA (Tan IIA) is the main phytochemical isolated from *S. miltiorrhiza* and is the main contributor to its beneficial cardiovascular effect. Besides, several studies have revealed other medicinal effects of Tan IIA, including anti-tumor, anti-proliferation, and anti-inflammatory effects in various cancers, such as non-small-cell lung cancer, liver cancer, cervical cancer, colorectal cancer, and gastric cancer (Sui et al., 2017; Zhang et al., 2018; Liu et al., 2019; Wang R. et al., 2019; Zhang et al., 2019). Additionally, there are also reports that Tan IIA can be used to treat arthritis (Jia et al., 2017; Zhang et al., 2017).

RA patients have an increased mortality rate due to cardiovascular events. The increase in inflammation associated with RA is the main mechanism that leads to an increase in the cardiovascular mortality rate. These data may suggest that aggressive treatment of inflammation may decrease cardiovascular risk in patients with RA. Tan IIA has been shown to have anti-inflammatory and immunomodulatory effects on atherosclerosis (Chen and Xu, 2014). Recent studies pointed out that Tan IIA can be used in antiatherosclerosis treatment targeting immune cells, antigens, cytokines, and cell signaling pathways (Ren et al., 2019). In this context, the anti-inflammatory and immunomodulatory effects of Tan IIA could be used in the treatment of rheumatoid arthritis also. In fact, patients with RA treated at our clinic with compound *Salvia* injection, in which Tan IIA is one of the main ingredients, showed significant improvements in their clinical symptoms (Jie et al., 2002; Jie et al., 2010).

All of the above indicate that Tan IIA is safe and could be a potential clinical medicine, but further research on the

mechanism is needed to provide a basis for clinical use. In particular, for RA patients with cardiovascular disease or related risk factors, Tan IIA may be a better choice than the alternatives. In recent years, several studies have focused on the effect and the mechanism of tanshinone in the treatment of RA. Our previous studies demonstrated that Tan IIA induced apoptosis of RA-FLSs by blocking the cell cycle in the G2/M phase and regulating a mitochondrial pathway. In addition, other studies have shown that Tan IIA and a derivate, sodium tanshinone IIA sulfonate, inhibited proliferation, migration, invasion, and inflammation in RA-FLSs and attenuated RA progression in collagen-induced arthritis (CIA) mice (Tang et al., 2019; Wang Z. et al., 2019). However, the details of the molecular mechanisms that result in the effect of Tan IIA on RA have not yet been discovered due to its various effects and targets. Therefore, in this study, several approaches (an AIA animal model for *in vivo* experiments, RA-FLS strain construction for *in vitro* evaluation, and network pharmacology and signaling pathway analyses) were applied to further investigate the effects and therapeutic use of Tan IIA in RA.

MATERIALS AND METHODS

Animals

Male C57BL/6 mice at the age of 10–12 weeks were obtained from the Lab Animal Center of Southern Medicine University. The experiment was approved by the Southern Medical University Ethics Committee for Animal Laboratory Research. All animal experimentation procedures were in accordance with the Ethical Guide for Institutional Animal Care and Use of Laboratory Animals of the National Institutes of Health. The mice were fed in the suitable environment according to previously described conditions (Du et al., 2019).

AIA Induction and Tan IIA Treatments

Eighteen male C57BL/6 mice, about 20 g in body weight each, were divided into three groups randomly: the normal group, AIA model group, and AIA model with Tan IIA treatment group. The protocol for inducing the AIA model was as previously described (Atkinson and Nansen, 2017; Dong et al., 2019; Du et al., 2019; Grötsch et al., 2019), adjusted on some points. The experimental timeline for AIA is shown in **Figure 1**. Briefly, mixtures (1:1/ volume ratio) of 5% bovine serum albumin (BSA, Sigma, USA) and Freund's complete adjuvant (CFA) (Sigma-Aldrich, USA) were made by emulsification. On day 0, the mice immunizations were performed by subcutaneously injecting 100 μ L of emulgator into the knee joint space under general anesthesia. Mice were injected with 20 μ L of emulgator in which Freund's incomplete adjuvant (IFA) (Sigma-Aldrich, USA) was substituted for CFA

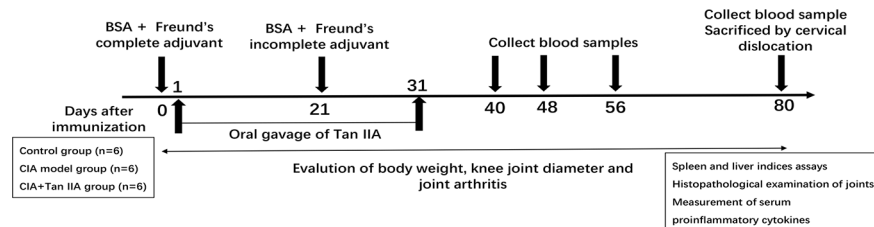


FIGURE 1 | Study design of the AIA experiment. Male C57BL/6 mice aged 10–12 weeks were immunized at each side of the knee articular cavity on day 0, and second immunizations were performed on day 21. From day 2 to day 31 after immunization, mice were administered with oral gavage Tan IIA once a day consecutively, as described in the Materials and Methods. Body weight and knee joint diameter were measured every 5 days. Blood samples for proinflammatory cytokine analysis were collected on days 40, 48, 56, and 80. The mice were euthanized at day 80, and bone, spleen, liver, and serum samples were collected. Histopathological analysis was performed on the bones of knee joints. Spleen and liver indices were calculated by weighing spleen and liver. Serum samples were subjected to ELISA assay.

on day 21. From day 2 to day 31 after immunization, mice were intragastrically administrated with 100 μ L Tan IIA (30mg/kg, Selleck, Shanghai, China) every single day. The normal and AIA model groups were given an equal volume of 1% sodium carboxymethyl cellulose suspension i.g. simultaneously. Body weight and mediolateral knee joint diameter were monitored by experimenters blinded to the experimental design every 5 days (Frey et al., 2018; Dong et al., 2019; Du et al., 2019).

Measurement of Serum Proinflammatory Cytokine Concentration

On days 40, 48, 56, and 80 after immunization, 200–300 μ L blood samples were gathered from the eyeballs of mice and 100–200 μ L serum samples were separated by centrifuge and stored at -80°C for analysis. The ELISA detections of IL-6, IL-17, and TNF- α were carried on with ELISA kits (Jiangsu Meimian Industrial Co., Ltd, Jiangsu, China) according to the manufacturer's instructions (Gou et al., 2018; Du et al., 2019; Li et al., 2019).

Measurement of Spleen and Liver Indices

On day 80 after immunization, all the mice were sacrificed by cervical dislocation. The liver and spleen indices were determined by the ratio of spleen and liver wet weight to mouse body weight (g/g), respectively. They were expressed as organ index = organ wet weight (g)/animal body weight (g) \times 100% (Hu et al., 2005; Gou et al., 2018; Du et al., 2019).

Histopathological Evaluation of Joints

Hind limbs with knee articular were removed from mice and fixed in Roles-Bio[®] Universal Tissue Fixative (Roles-Bio, Guangzhou Routh Biotechnology Co., Ltd.). Subsequently, the tissues were decalcified with Roles-Bio[®] Quick Decalcifying Solution (Roles-Bio, Guangzhou Routh Biotechnology Co., Ltd.) and embedded in paraffin. About 5- μ m-thick paraffin sections were made and stained with hematoxylin and eosin (H&E) (Gou et al., 2018; Du et al., 2019). The HE results were graded in a blinded manner according to previous research (Du et al., 2019; Grötsch et al., 2019). The scoring standard was as follows: 1=mild, 2=moderate, and 3=severe.

Cells Isolation and Culture

The synovial tissues were removed from the knee joints of active RA patients who were undergoing synovectomy with arthroscopy. The detailed data from the patients, of whom 2 were males and 4 females, were shown in **Table S1**. RA patients selected for our research conformed to the American College of Rheumatology revised criteria of the diagnosis of RA (Arnett et al., 1988) and provided informed consent. Moreover, our experiments were in accordance with the guidelines formulated by the Medical Ethics Committee of Zhujiang Hospital, Southern Medical University, and were performed according to the recommendations of the Declaration of Helsinki. The primary synoviocytes (RA-FLSs) were isolated from the harvested synovial tissue and cultured according to our previously published research (Du et al., 2019). After being subcultured, the three to six passage RA-FLSs were used for the subsequent experiments. All reagents for culturing cells were purchased from Gibco[®] (Thermo Fisher Scientific, MA, USA).

Cell Viability Assay

RA-FLSs were placed in a 96-well plate and treated with Tan IIA ($\text{C}_{19}\text{H}_{18}\text{O}_3$, $\geq 98\%$ HPLC, CAS:568-72-9, Selleck) at various concentrations (0 μM , 2.5 μM , 5 μM , 10 μM , 20 μM) and TNF- α (20 ng/mL). The cell viability assay was carried out with a Cell Counting Kit (CCK-8) (KeyGEN BioTECH) according to the manufacturer's instructions. The absorbance was measured at 450 nm with a microplate reader.

Cell Migration and Invasion Assay

RA-FLS migration and invasion assays were performed in a Boyden chamber with 6.5-mm-diameter inserts containing 8- μm pores (Costar, New York, NY, USA) or coated with Matrigel basement membrane matrix (BD Biosciences, Oxford, UK) in a 24-well plate. Briefly, after being treated with various concentrations of Tan IIA for 24 h respectively, 4×10^3 /200 μL RA-FLSs suspended in serum-free DMEM medium were added into the upper chamber, and 500 μL DMEM media with 10% FBS were placed in the lower well as a chemoattractant. Following incubation, the cells that had migrated through the filter were fixed and stained with 0.1% crystal violet. The cells

were quantified by counting the stained cells with a microscope. The mean number of cells per 5–6 random fields was calculated for each assay (Du et al., 2019; Wu et al., 2019).

Wound Healing Assay

RA-FLSs were planted into a 12-well culture dish on the first day. On the next day, a pipette tip was used to make a scratch, and deciduous cells were washed away with PBS twice. After being treated with various concentrations of Tan IIA for 48 h, the wound areas were photographed with a microscope and the extent of wound closure was calculated with Image J software. The data are shown as the mean \pm SD of three independent experiments.

RNA Isolation and Real-Time PCR Assay

Real-time PCR was performed for analyzing the expression of some cytokines and MMPs in RA-FLSs treated with Tan IIA according to previous descriptions (Jie et al., 2015; Du et al., 2019). Total RNAs in RA-FLSs treated with or without TNF- α (20ng/mL) and Tan IIA were isolated by TRIzol (Invitrogen, U.S.A.) and reverse transcribed into cDNA using the Prime Script RT Reagent kit (Takara Biotechnology, Dalian, China), adopting the manufacturer's protocol. According to the manufacturer's instructions, PCR quantification for cytokines and MMP mRNA with an SYBR Premix Ex TaqTM kit (Takara Biotechnology, Dalian, China) was carried out in an ABI 7500 type PCR instrument (Applied Biosystems Inc., Foster City, CA, USA). DdH₂O containing no template was set as negative control. All of the primers were synthesized by IGE Biotech. Co., Ltd (Guangzhou, China) and are listed in **Table S2**. All experiments were performed in triplicate and repeated three times independently. To quantify the relative expression of each gene, the $\Delta\Delta C_t$ method ($\Delta\Delta C_t = \Delta C_{t_{\text{sample}}} - \Delta C_{t_{\text{control}}}$) was used to indicate the ratio of the expression of the target gene in the model group to that of the control group (Du et al., 2019; Wu et al., 2019).

Western Blot Assay

After treatment with TNF- α (20ng/mL) or/and 10 μ M and 20 μ M Tan IIA for 24 h, RA-FLSs were collected and total protein was extracted using RIPA lysis buffer and phosphatase inhibitors (Beyotime Biotechnology, Nantong, China) on ice. The proteins from RA-FLSs were obtained by separating supernatants and debris *via* centrifugation at 12,000 rpm for 20 min at 4°C. The Pierce® BCA Protein Assay Kit (Thermo Scientific, USA) was used to determine the protein concentration. The levels of protein were adjusted to 0.5–1 μ g/ μ L and detected by automated electrophoresis western analysis assay (ProteinSimple, Biotechne, San Jose CA, United States) as described previously (Baradaran-Heravi et al., 2016). According to the user manual, all procedures were performed using the manufacturer's reagents. Briefly, 8 μ L diluted protein lysate was mixed with 2 μ L of 5 \times fluorescent master mix and heated at 95°C for 5 min. Various ingredients, including the sample (about 1 μ g), blocking reagent, wash buffer, primary antibodies, secondary antibodies, and chemiluminescent substrate were allotted into the designated wells in a manufacturer-provided microplate. The plate was loaded into the instrument, and protein

was drawn into individual capillaries on a 25-capillary cassette provided by the manufacturer (Jess/Wes Separation 12-230 kDa 8 \times 25 Capillary Cartridges kit). Protein separation and immunodetection were automatically performed on the individual capillaries using the default settings. The data were analyzed with inbuilt Compass software (ProteinSimple, Biotechne, United States). The truncated and target protein peak intensities (area under the curve) were normalized to that of the vinculin peak, used as a loading control. Primary antibodies included AKT, mTOR, p70S6K, 4E-BP1, p38 MAPK, p44/42 MAPK (Erk1/2), JNK, NF κ B p65, I κ B α , and HIF-1 α and their corresponding phosphorylation antibodies, Phospho-Akt (Ser473), Phospho-p70 S6 Kinase (Thr389), Phospho-4E-BP1 (Ser65), Phospho-p38 MAPK(Thr180/Tyr182), Phospho-p44/42 MAPK (Erk1/2) (Thr202/Tyr204), Phospho-JNK (Thr183/Tyr185), p-NF κ B p65(Ser 536), and p-I κ B α /B(Ser176/180), which were all purchased from Cell Signaling Technology, USA. GAPDH antibodies used as a reference standard for quantification were purchased from Bioworld Technology Inc.

Measurements of Cytokine Levels by ELISA

To determine the effect of Tan IIA on cytokine production, ELISA experiments were performed using human enzyme-linked immunosorbent assay (ELISA) kits (Jiangsu Meimian Industrial Co., Ltd, Jiangsu, China) according to the manufacturer's instructions. For example, RA-FLSs were seeded into six-well plates and treated with TNF- α (20ng/mL) or/and 10 μ M and 20 μ M Tan IIA for 48 h. The culture supernatants were collected, and the level of IL-6 release from the RA-FLSs was detected as previously described (Jie et al., 2015; Du et al., 2019). The other cytokine assays were carried out using the same method. All experiments were performed in triplicate and replicated 3 times.

Search for Potential Tan IIA Targets in RA by Network Pharmacology

Firstly, data preparation was carried out by searching for Rheumatoid Arthritis-related genes at the National Biotechnology Center (<https://www.ncbi.nlm.nih.gov>). Additionally, the chemical structure, molecular weight, 2D structure, 3D structure, chemical number, and physicochemical properties of Tan IIA had to be confirmed. The target genes of Tan IIA were obtained by PharmMapper (<http://www.lilab-ecust.cn/pharmmapper/>). Next, a drug–target–disease interaction network was constructed. A Venn diagram was constructed based on the functions of the human genes related to rheumatoid arthritis and the potential Tan IIA targets, and the intersection target genes were obtained. Moreover, a protein–protein interaction network (PPI) was constructed on-line by STRING (<https://string-db.org/cgi/input.pl>). Finally, biological process and pathway analysis was performed. According to the function of human genes related to rheumatoid arthritis and potential Tan IIA targets, the Bioconductor database was used to perform Gene Ontology (GO) Enrichment and Kyoto Encyclopedia of Genes and Genomes (KEGG) pathway enrichment analysis of target genes through R (R 3.6.1 for Windows). The target genes were screened with $P < 0.05$ set as

the critical value of significant functions and pathways, and the main signaling pathways and biological processes involved in the pharmacological effects of Tan IIA in treating rheumatoid arthritis were obtained.

Statistical Analysis

Data from multiple experiments are presented as the mean \pm standard deviation (SD). Statistical software was used for all data analysis. The statistical difference comparisons (P-values) between two groups were calculated using Student's t-test, and P-values between more than three groups were calculated using one-way analysis of variance (ANOVA) with GraphPad Prism 8.0. Two-sided $p < 0.05$ was considered statistically significant. The number of replicates and/or total number of animals are shown in figure legends or within the figures.

RESULTS

Tan IIA Attenuates the Inflammatory Response in Mice With AIA

Tan IIA Suppresses Weight Loss and Knee Joint Swelling in AIA Mice

All of the mice from different groups could access food and water freely during the whole study period. To clarify the effect of Tan IIA on AIA model mice, the mean changes in body weight of mice were monitored every 5 days from day 0 to day 80. As shown in **Figure 2A**, the mean body weight change of mice from the AIA group significantly decreased compared with the change in the normal group at the 25th day after immunization. Nevertheless, compared with the normal group, the mean body weight change of mice from the group treated with Tan IIA (30mg/kg) *via* gavage had declined little at that time. There was significant difference between the Tan IIA treatment group and the AIA model group.

Synchronously, the effect of Tan IIA on arthritis severity, as characterized by measurements of the knee joint diameters, were assessed every 5 days. As shown in **Figure 2B**, the mean value of the diameters of knee joints in AIA mice increased obviously compared to the normal group from the 20th day after immunization because of obvious swelling. Moreover, the increase was rapid from the 25th to the 40th day, when the mean diameter reached a peak value. After the 40th day, it gradually reduced. The values of the mean diameter for AIA mice were significantly different from those of the normal control group during the whole process. However, the mean diameter of knee joints in the mice with Tan IIA treatment was lower than that of AIA mice from the 25th to the 60th day.

Tan IIA Reduces Spleen and Liver Indices of AIA Mice

The spleen and liver indices from mice in different groups were assessed to evaluate the effect of Tan IIA on the main immune organs. The spleen and liver indices of mice in the AIA model group was obviously raised compared with those of the normal

group (**Figure 2C**). Nevertheless, the spleen and liver indices for the Tan IIA treatment group were significantly lower than those of the AIA group.

Tan IIA Improves the Pathohistological Characters of Knee Joints and Arthritis Severity in AIA Mice

To study how Tan IIA affected the pathohistological features of AIA mice, histological examinations of tissue sections were performed. The knee joints from all mice were removed at the 80th day after euthanization and were then stained with H&E to make pathohistological sections. Clear and complete histological architecture was seen through microscopic observation of the knee joints from the normal control group. However, the knee joints of the AIA model group had abnormal histological architecture, characterized by synovial tissue hyperplasia and massive inflammatory cell infiltration, accompanied by epithelial cell degradation and angiogenesis (microvessel density increase). Compared with the AIA group, the abnormalities of the histological architectures of knee joints from the Tan IIA treatment group were milder, with less synovial hyperplasia, inflammatory cell infiltration, and synovial tissue erosion (**Figure 2D**). Additionally, as shown in **Figure 2E**, the pathohistological score exhibited similar differential tendencies in the three experimental groups, which suggested that Tan IIA did attenuate the inflammatory response in mice from the AIA group and had good anti-arthritis effect.

Tan IIA Restrains Proinflammatory Cytokine Expression in AIA Mice

On days 40, 48, 56, and 80 after immunization, the expressions of IL-6, IL-17, and TNF- α in serum from AIA mice with and without Tan IIA treatment were examined by ELISA to explore how Tan IIA affected the proinflammatory cytokines. In the case of IL-6, its expression in serum from AIA mice was significantly higher than in serum from the normal control group on the 40th, 48th, and 56th day. Moreover, it was obviously increased compared to in mice treated with Tan IIA on days 40 and 48. However, on days 56 and 80, there was no obvious difference between them. Similar trends on days 40, 48, and 56 were observed in IL-17 and TNF- α expression in the three groups. Although there was a difference between the expression levels in normal mice and AIA mice on day 80, no differences in IL-17 and TNF- α were witnessed between the Tan IIA treatment group and the AIA group (**Figure 2F**). All the data indicated that Tan IIA (30mg/kg) could suppress production of the proinflammatory cytokines IL-6, IL-17, and TNF- α in serum of AIA mice.

Tan IIA Suppresses the Migration and Invasion of RA-FLSs

Primary RA-FLSs were separated from synovial tissue from clinical samples. Transwell experiments were performed using the transwell Boyden chamber with or without Matrigel matrix to evaluate the effect of Tan IIA on the migration and invasion of RA-FLSs *in vitro*. Treatment with 10 μ M or 20 μ M Tan IIA profoundly reduced both the migratory and the

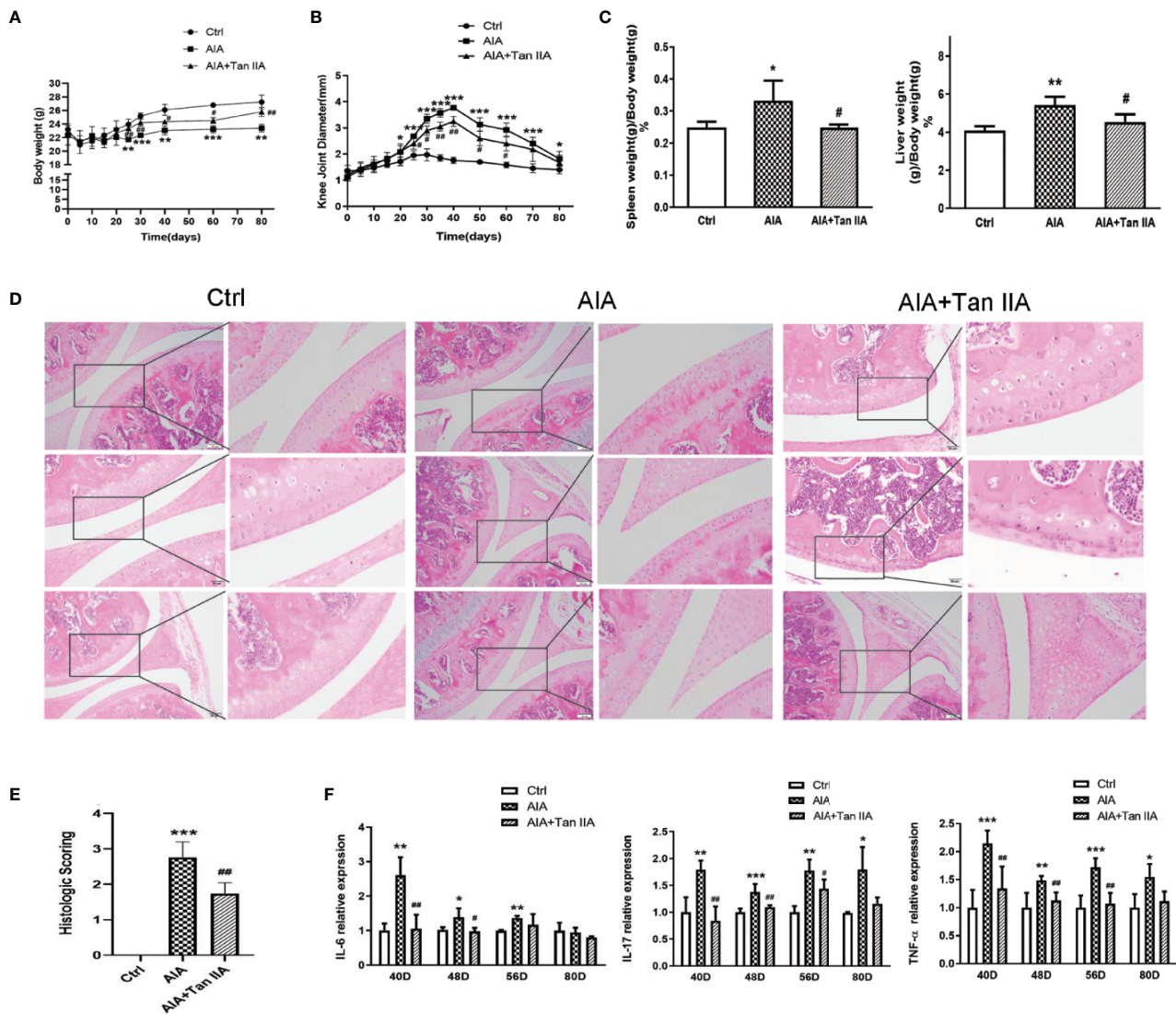


FIGURE 2 | Tan IIA ameliorates arthritis severity in mice with AIA. **(A)** The effect of Tan IIA on mean change in the body weight of mice after immunization (from day 0 to day 80), monitored every 5 days. **(B)** The effect of Tan IIA on mean change in knee joint diameter after immunization (from day 0 to day 80), monitored every 5 days. **(C)** The effect of Tan IIA on the spleen and liver indices of mice with AIA and control. Data are shown as spleen weight (g)/body weight (g) $\times 100\%$. **(D)** The effect of Tan IIA on the pathohistological features of knee joints in mice with AIA. Photomicrographs of knee joint sections stained with H&E (original magnification 200 \times). **(E)** The scores for inflammatory severity. **(F)** The effect of Tan IIA on IL-6, IL-17, and TNF- α expression in serum of mice with AIA and control on days 40, 48, 56, and 80 after immunization. All of the data are expressed as means \pm S.D. $n=6$, * $P < 0.05$, ** $P < 0.01$, *** $P < 0.001$ vs. the control group, # $P < 0.05$, ## $P < 0.01$, vs. the AIA model group.

invasion ability of RA-FLSs comparing with control, as presented in **Figures 3A, B**. This result was further confirmed by wound closure assay, the results of which are shown in **Figure 3C**. After 48 h, the control group cells had almost recovered from the scratch. The cells treated with Tan IIA had inhibited wound healing. Although 5 μ M Tan IIA did not significantly interfere with the capacity of RA-FLSs to migrate from one side of the wound to the other, higher concentrations Tan IIA (10 and 20 μ M) did restrain the cell migration into the wounded area, as presented in **Figure 3C**.

All of the data indicated the Tan IIA could block the migration and invasion of RA-FLSs *in vitro*.

Tan IIA Inhibits the Viability of RA-FLSs Activated by TNF- α

As is well known, TNF- α is one of the important pro-inflammatory cytokines conducive to RA-FLS survival and progressive arthritis in RA pathology (Bottini and Firestein, 2013; Bustamante et al., 2017). To discover the effect of Tan IIA on the viability of RA-FLSs induced by TNF- α , the effect of

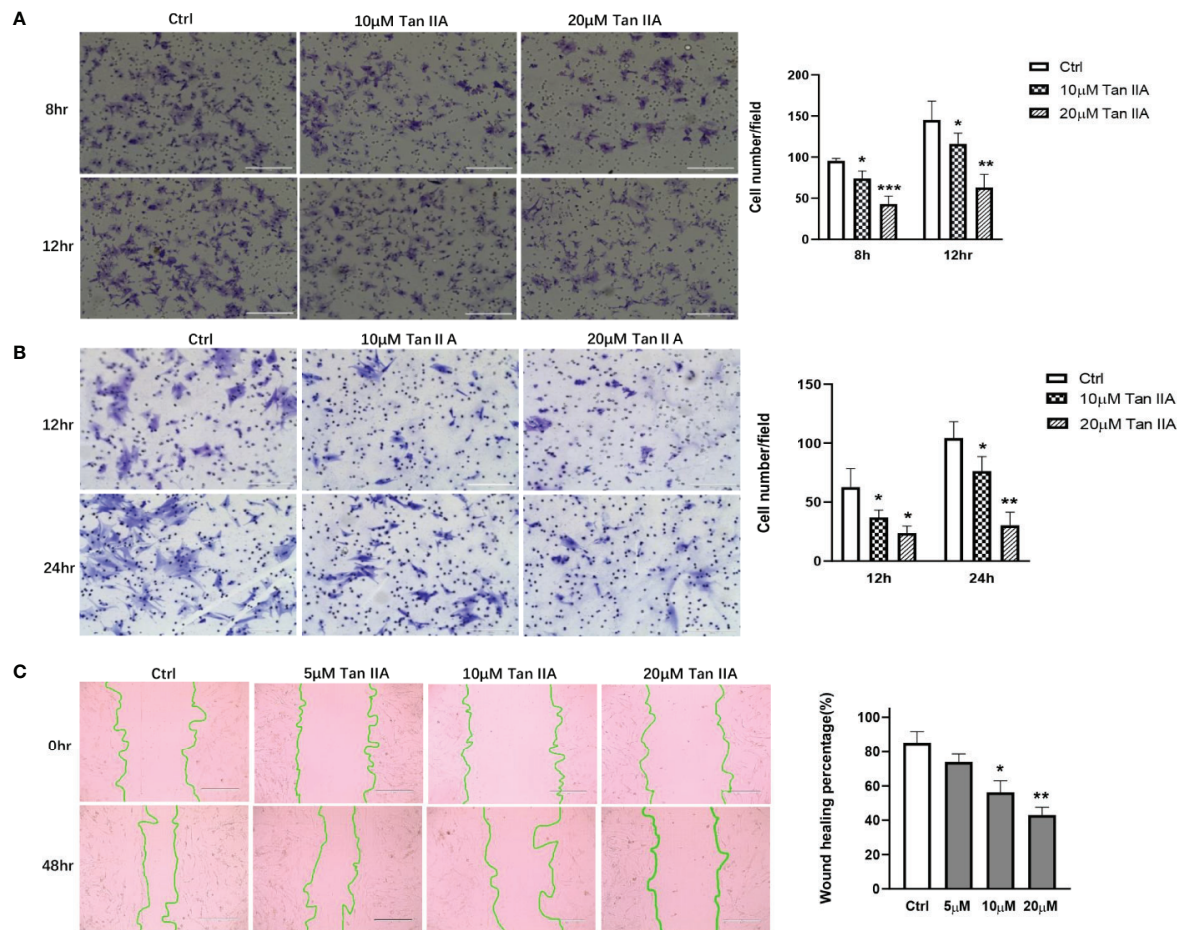


FIGURE 3 | Tan IIA suppresses the migration and invasion of RA-FLSs. **(A)** The effect of Tan IIA on migration was detected with transwell Boyden chamber after 8 and 12 h. The images are representative of migration or invasion through the membrane after staining. Original magnification 200 \times (left panel). Cell numbers/field are presented as the mean \pm SD of eight independent fields (right panel). **(B)** The effect of Tan IIA on invasion was detected with a transwell Boyden chamber coated with a Matrigel basement membrane matrix after 12 and 24 h. The images are representative of migration or invasion through the membrane after staining. Original magnification 200 \times (left panel). Cell numbers/field are presented as the mean \pm SD of eight independent fields (right panel). **(C)** The effect of Tan IIA on wound healing was detected with cell scratch assay. After 48 h, the wound area was photographed using a microscope. Original magnification 100 \times (left panel). The extent of wound closure is presented as the percentage by which the original scratch width had decreased at each measured time point. The values are the mean \pm SEM from at least 3 independent experiments (right panel). * $P < 0.05$, ** $P < 0.01$, *** $P < 0.001$ vs. 0 μ M (Ctrl).

Tan IIA with a series of concentrations (0, 2.5, 5, 10, and 20 μ M) on the viability of RA-FLSs activated with TNF- α was measured. A concentration of 20 ng/mL TNF- α obviously promoted the viability of RA-FLSs (**Figure 4A**). Tan IIA had almost no effect on cell viability induced by TNF- α after 24 h treatment (data not shown), while higher concentrations Tan IIA (10 and 20 μ M) showed a dose-dependent inhibition in cell viability induced by TNF- α after 48 h treatment (**Figure 4A**).

Tan IIA Suppresses the Pro-inflammatory Cytokine and MMP Expression Stimulated by TNF- α

Accumulating evidence has pointed out that, during the development of RA, certain pro-inflammatory cytokines and

matrix metalloproteinases (MMPs) in particular contribute to the pathogenic factors for proliferation, migration, and invasion of RA-FLSs and even erosion of cartilago articularis (Bottini and Firestein, 2013; Bustamante et al., 2017). To explore the role of Tan IIA on the expression of key pro-inflammatory cytokines induced by TNF- α , the mRNA expression levels of *IL-6*, *IL-8*, *IL-17*, and *IL-1 β* stimulated by TNF- α in RA-FLSs treated with 10 μ M and 20 μ M Tan IIA for 24 h were assessed with qPCR. As presented in **Figure 4B**, although TNF- α (20ng/mL) did upregulate, to a greater or lesser extent, the mRNA levels of *IL-6*, *IL-1 β* , and *IL-8* in RA-FLSs, 20 μ M Tan IIA inhibited the *IL-6*, *IL-1 β* , and *IL-8* mRNA upregulation stimulated by 20-ng/mL TNF- α , while 10 μ M Tan IIA had no obvious effect except for on *IL-1 β* . Unexpectedly, neither Tan IIA treatment nor TNF-

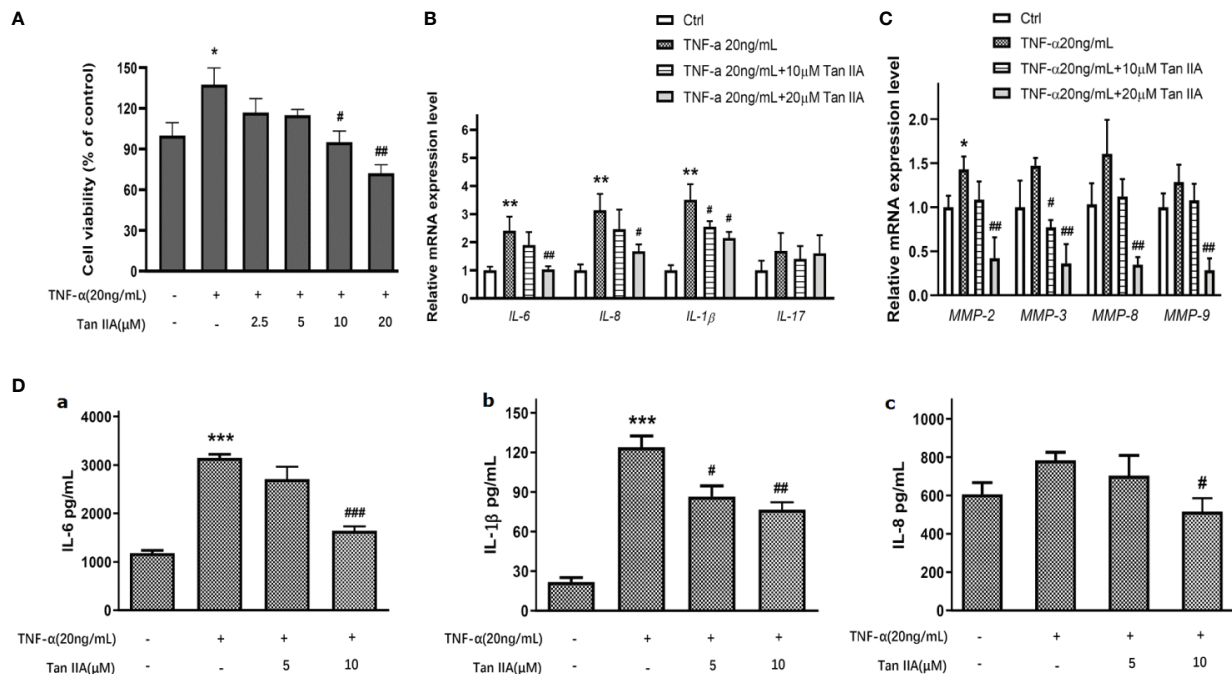


FIGURE 4 | The effect of Tan IIA on producing pro-inflammatory cytokines and MMPs in RA-FLSs. **(A)** The effect of 0, 2.5, 5, 10, and 20 μM Tan IIA on cell viability induced by TNF-α (20 ng/mL). **(B)** The effect of 10 μM and 20 μM Tan IIA on relative mRNA expression of pro-inflammatory cytokines induced by TNF-α (20 ng/mL) normalized with β-actin in RA-FLSs. **(C)** The effect of 10 μM and 20 μM Tan IIA on relative mRNA expression of MMP-2, MMP-3, MMP-8, and MMP-9 induced by TNF-α (20 ng/mL) compared to β-actin in RA-FLSs. **(D)** The effect of Tan IIA on pro-inflammatory cytokines release induced by TNF-α in RA-FLSs. a. The effect of 10 μM and 20 μM Tan IIA on IL-6 release induced by TNF-α (20 ng/mL). b. The effect of 10 μM and 20 μM Tan IIA on IL-1β release induced by TNF-α (20 ng/mL). c. The effect of 10 μM and 20 μM Tan IIA on IL-8 release induced by TNF-α (20 ng/mL). The values are the mean ± SEM from at least 3 independent experiments. **P* < 0.05, ***P* < 0.01, ****P* < 0.001 vs. Ctrl (0 μM Tan IIA and 0 ng/mL TNF-α). #*P* < 0.05, ##*P* < 0.01, ###*P* < 0.001 vs. group treated with TNF-α (20 ng/mL).

α stimulation profoundly changed *IL-17* mRNA expression. Additionally, as shown in **Figure 4C**, only an increase in *MMP-2* mRNA expression was induced by TNF-α (20 ng/mL), and *MMP-3* mRNA expression was decreased by 10 μM Tan IIA treatment. However, the mRNA expressions of *MMP-2*, *MMP-3*, *MMP-8*, and *MMP-9* dropped significantly after 20-μM Tan IIA treatment, which suggested that Tan IIA significantly blocked upregulation in mRNA expression of *MMP-2*, *MMP-3*, *MMP-8*, and *MMP-9* stimulated by TNF-α in RA-FLSs.

In addition, the effect of Tan IIA on the release of some pro-inflammatory cytokines stimulated by TNF-α, as well as on the mRNA level, was also investigated. After being treated with Tan IIA (10 μM and 20 μM) for 48 h, ELISA assays for IL-6, IL-1β, and IL-8 were performed in cell culture supernatant. As indicated in **Figure 4D**, 20-ng/mL TNF-α significantly increased IL-6 and IL-1β production in RA-FLSs, but Tan IIA treatment could suppress the increase, as shown in **Figures 4D-a** and **4D-b**. Of interest, stimulation with 20-ng/mL TNF-α did not arouse profound upregulation of IL-8, but 20 μM Tan IIA indeed downregulated IL-8 release (**Figure 4D-c**). There was no detectable IL-17 in the ELISA assay because there was less expression in cell culture supernatants. In short, the results suggest that Tan IIA may be helpful for reducing the

production and release of some MMPs and pro-inflammatory cytokines from RA-FLSs.

Potential Targets for Tan IIA in RA Found by Database Search Tools

To uncover potential targets for Tan IIA in RA, we searched the NCBI database and obtained 1147 human genes associated with rheumatoid arthritis. At the same time, we found 297 target genes involved in Tan IIA from the PubChem and PharmMapper databases. A Venn diagram was made with R (R 3.6.1 for Windows) based on the 297 drug targets of Tan IIA and 1147 gene targets of rheumatoid arthritis (**Figure 5A**). We found 31 common targets, which were designated as the key targets of Tanshinone IIA in the treatment of RA. The common targets were then imported into STRING to build the PPI network (**Figure 5B**). This network consists of 71 nodes. The size of the node in the figure indicates the magnitude of the Degree value. The higher the Degree value, the larger the node. We predicted that the proteins BCL2L1, MAPK14, CTNBN1, TP53, EIF4EBP1, HIF1a, HMGB, and mTOR would be potential direct targets of Tan IIA in the treatment of rheumatoid arthritis.

Meanwhile, considering the common targets of RA and Tan IIA, 43 biological processes (*P* < 0.05) were screened by

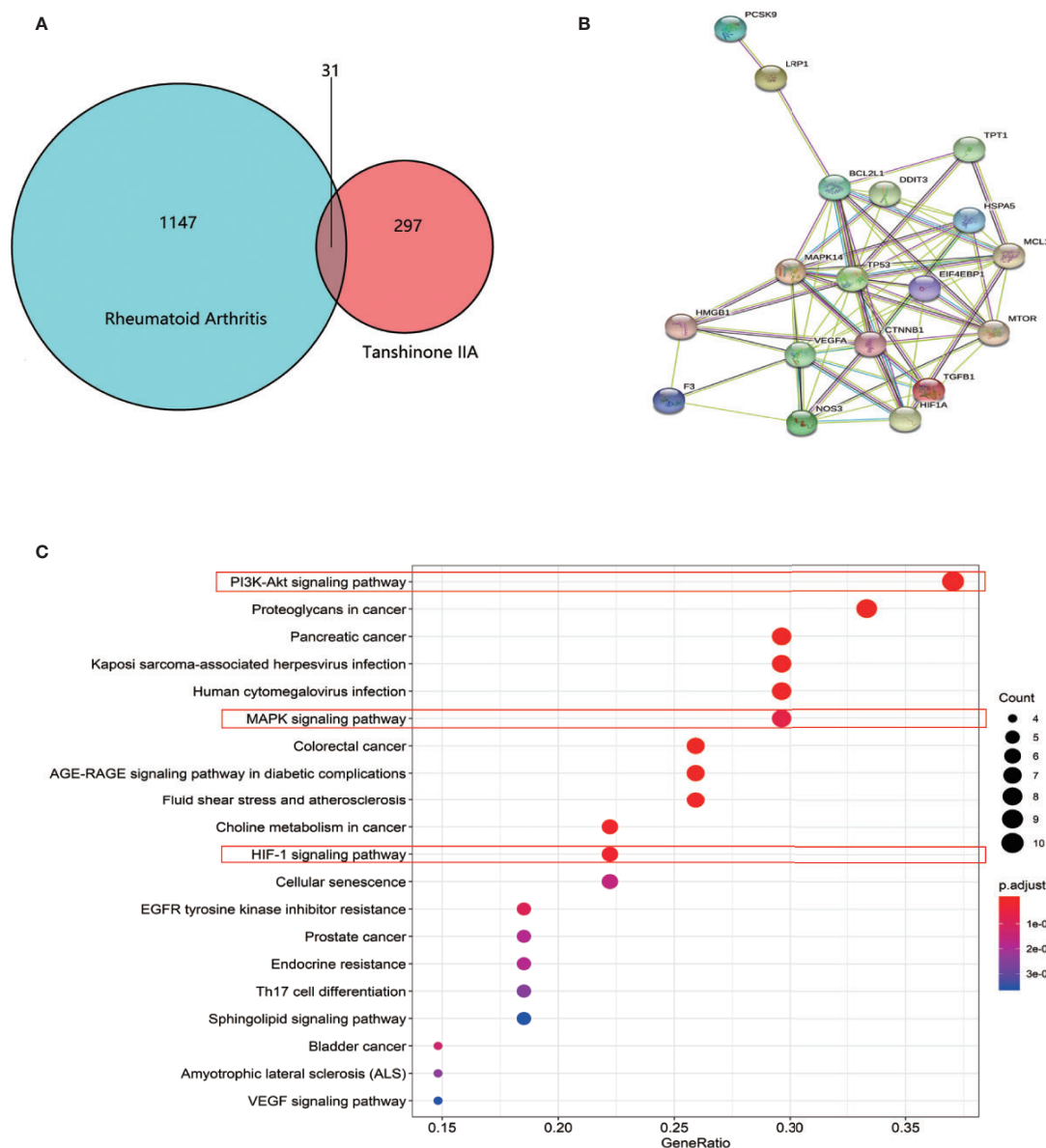


FIGURE 5 | Enrichment analysis of Tan IIA against rheumatoid arthritis: **(A)** Venn diagram revealing the overlapping target genes of Tan IIA against rheumatoid arthritis. **(B)** Protein interaction network of the overlapping target genes of Tan IIA against rheumatoid arthritis. Each network node represents all the proteins produced by a single, protein-coding gene locus, and the edge represents protein-protein associations. **(C)** KEGG enrichment and network analysis of RA target genes. Top 20 functionally enriched biological processes with corresponding adjusted p -values, displayed in a dot plot. The color scale indicates the different thresholds of adjusted p -values, and the sizes of the dots represented the gene count of each term.

GO, including protein heterodimerization activity, growth factor activity, receptor regulator activity, disordered domain-specific binding, ribonucleoprotein complex binding, receptor ligand activity, etc. Next, we performed functional enrichment analysis using the KEGG database to clarify the functions of these target genes and signaling pathways. It is of note that the data show that the potential target genes found were functionally related with various

signal transduction pathways, including the PI3K-Akt signaling pathway, proteoglycans in cancer, pancreatic cancer; Kaposi sarcoma-associated herpesvirus infection, human cytomegalovirus infection, the MAPK signaling pathway, choline metabolism in cancer, and the hypoxia-inducible factor (HIF-1) signaling pathway (**Figure 5C**). In general, Tan IIA may participate in these pathways, and this could ultimately affect the progression of the disease.

Tan IIA Affects the Activation of RA-FLSs Induced by TNF- α Through Modulation of the MAPK, Akt/mTOR, and HIF-1 Pathways

Combining the results from GO and KEGG with our preliminary research data, we speculated that Tan IIA probably affected RA through the PI3K-Akt, MAPK, and HIF-1 signaling pathways. We detected the main protein expressions and phosphorylation levels of the MAPK signaling pathway, including of p38MAPK, JNK, and ERK, to further verify our supposition as to the effect of Tan IIA on MAPK. After treatment with 20 ng/mL TNF- α and Tan IIA (10 and 20 μ M) for 24 h, the RA-FLSs were collected, and the expression and phosphorylation levels of p38MAPK, JNK, and ERK were evaluated by Western blot analysis. As presented in **Figure 6A**, enhanced p38MAPK and JNK phosphorylation activations in RA-FLSs were observed to be induced by TNF- α compared with the control without TNF- α stimulation. Also, Tan IIA efficiently inhibited TNF- α -induced phosphorylation of p38MAPK and JNK. Intriguingly, Tan IIA had less influence on the ERK phosphorylation level. The fact that Tan IIA strongly reduced p38MAPK and JNK activity may contribute to controlling abnormal synovial hyperplasia in the articular cavity.

Moreover, the phosphorylation levels of the Akt/mTOR signaling pathway and its downstream molecules, p70 ribosomal S6 kinase (p70S6K) and eukaryotic translation initiation factor 4E-binding protein 1 (4E-BP1), in RA-FLSs were evaluated with Western blot to explore the effect of Tan IIA on the mTOR pathway. From **Figure 6B**, it can be seen that Tan IIA indeed inhibited the phosphorylation activation of Akt and mTOR stimulated by 20-ng/mL TNF- α . Meanwhile, the increased phosphorylation of p70S6K and 4E-BP1 triggered by TNF- α was also inhibited by Tan IIA treatment in a concentration-dependent manner, suggesting that Tan IIA suppressed the Akt/mTOR/p70S6K and 4E-BP1 signaling pathway in RA-FLSs.

Additionally, according to the results of GO and KEGG analysis, the HIF-1 pathway is a potential target for Tan IIA. The molecular mechanism of hypoxia sensitivity involves oxygen sensing hydroxylases, prolyl-hydroxylases, orchestrating two main transcription factors related to the induction of inflammation and angiogenesis, namely nuclear factor- κ B (NF κ B) and HIF-1 (D'Ignazio and Rocha, 2016; Fearon et al., 2016). Therefore, we detected the effect of Tan IIA on the HIF-1 α and NF κ B expression variation in RA-FLSs. Similarly, Tan IIA suppressed the phosphorylation level of NF κ B p65 and upstream

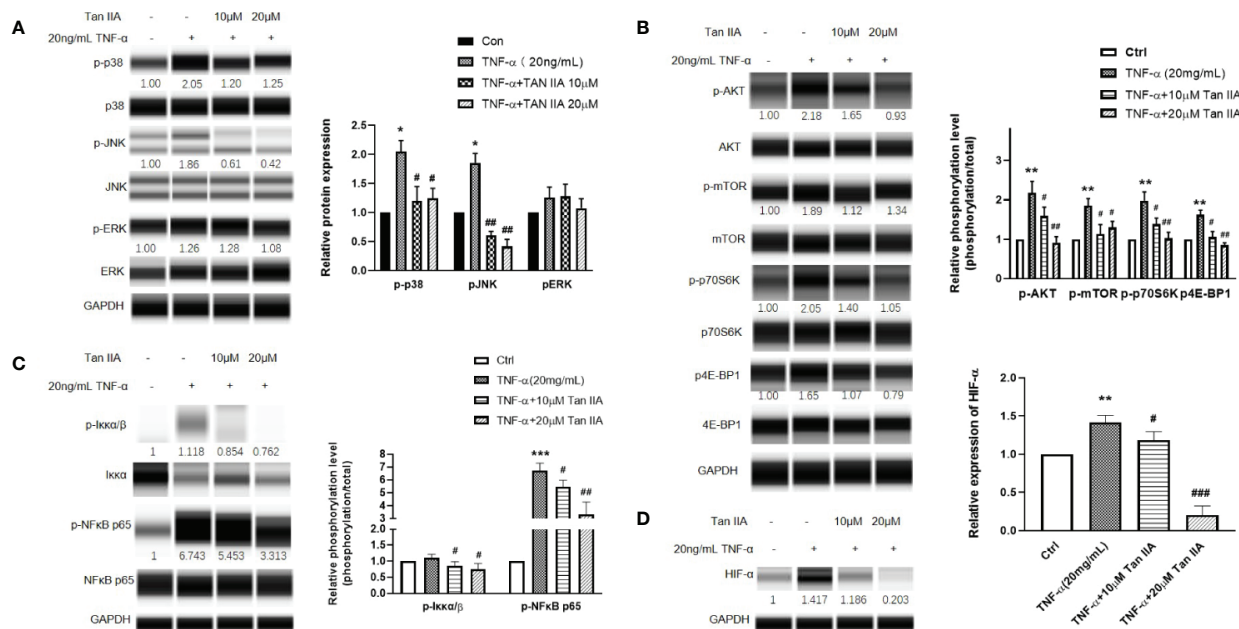


FIGURE 6 | The effect of Tan IIA on the intracellular phosphorylated activation of the MAPK and Akt/mTOR pathway induced by TNF- α in RA-FLSs. RA-FLSs were treated with TNF- α (20ng/mL) or/and Tan IIA (10 and 20 μ M) for 24 h. **(A)** Western blot analysis was conducted to assess the expression and phosphorylation levels of p38MAPK, JNK, ERK, and FAK. Representative images of immune blot (left panel) and densitometric quantification phosphorylation/total of p38MAPK, JNK, and ERK expression (right panel). **(B)** Western blot analysis was conducted to assess the expression and phosphorylation levels of AKT, mTOR, p70S6K, and 4E-BP1. Representative images of immune blot (left panel) and densitometric quantification phosphorylation/total of AKT, mTOR, p70S6K, and 4E-BP1 expression (right panel). **(C)** Western blot analysis was conducted to assess the expression and phosphorylation levels of I κ B α and NF κ B p65. Representative images of immune blot (left panel) and densitometric quantification phosphorylation/total of I κ B α and NF κ B p65 expression (right panel). **(D)** Western blot analysis was conducted to assess the expression level of HIF-1 α . Representative images of immune blot (left panel) and densitometric quantification of HIF-1 α expression (right panel). Densitometry analysis from three independent experiments was used to quantitate the protein expression. * P < 0.05, ** P < 0.01, *** P < 0.001 vs. Ctrl (0 μ M Tan IIA), # P < 0.05, ## P < 0.01, ### P < 0.001 vs. group treated by TNF- α (20 ng/mL).

IKK α (Figure 5C) and the HIF-1 α expression (Figure 5D) stimulated by TNF- α , which indicated that Tan IIA could participate in regulating the response of synovial tissues to hypoxia. Altogether, the regulation of the biological characteristics of RA-FLSs by Tan IIA is dependent on impeding not only intracellular phosphorylation activation of the MAPK and Akt/mTOR pathways but the expression and activation of HIF-1 α and NF κ B.

DISCUSSION

RA is a chronic autoimmune disease with a hyperplastic, aggressive, and invasive phenotype that causes the formation of pannus angiogenesis, inflammation, cartilage degradation, and subsequent bone erosion (Smolen et al., 2016). RA-FLSs play a leading role in the pathogenesis of inflammatory arthritis due to their tumor-like features of proliferation, migration, and invasion (Karami et al., 2019). In this context, RA-FLSs stand out as a potential target for RA treatment (de Oliveira et al., 2019). Currently, the main RA treatment strategies in clinical practice are chemical drugs, including non-steroidal anti-inflammatory drugs (NSAIDs), disease-modifying anti-rheumatic drugs (DMARDs), and glucocorticoids (Conigliaro et al., 2019). Nevertheless, these treatments are usually associated with adverse reactions, such as cardiovascular and gastrointestinal bleeding risk, liver and kidney toxicity, growth inhibition, infection, and risk of tumors (Yamamoto et al., 2011; Rubbert-Roth and Petereit, 2012; Xue et al., 2016; Nissen, 2017; Wang et al., 2018). In recent years, progress in research on the pathogenesis of RA has resulted in the development of new anti-rheumatic drugs, such as biological agents and small-molecule targeted signaling pathway inhibitors. These new drugs have greatly improved the chronic inflammatory state and quality of life of RA patients (Conigliaro et al., 2019). However, clinical data show that only less than 50% of RA patients can benefit from these new drugs. Unfortunately, more than 30% of patients still suffer from unsatisfactory disease control, and it is not possible to effectively control disease activities in more than 20% of RA patients. In such cases, the bone destruction process cannot be blocked or delayed, even after the clinical use of these recent drugs (Ranganath et al., 2015; Smolen et al., 2016; Conigliaro et al., 2019).

Recently, herbal medicines have received a large amount of scientific attention for their remarkable healing effects and for having fewer side effects than synthetic drugs. The therapeutic effects of Tan IIA, a compound isolated from *Salvia miltiorrhiza* Bunge (*Salviae miltiorrhizae*), includes pro-apoptotic, anti-tumor, and anti-inflammatory activities. Additionally, Tang et al. showed that Tan IIA injections could inhibit the inflammatory response in PBMCs of RA patients by decreasing TNF- α and IL-6 levels (Tang et al., 2019). Therefore, the application of Tan IIA in the treatment of RA is feasible in terms of therapeutic effect. To highlight the potential of Tan IIA for RA treatment, we first used an AIA mouse model to verify its therapeutic effects. The AIA model has been widely used to clarify the pathogenesis of RA and to explore potential therapeutic targets, including the validation of the therapeutic

effects of new drugs (Sardar and Andersson, 2016; Atkinson and Nansen, 2017; Dong et al., 2019; Du et al., 2019). Our experiments showed that AIA mice treated with Tan IIA showed decreased histologic scores and attenuated synovial inflammation. The level of the inflammatory cytokines, including IL-6, IL-17, and TNF- α , measured after 40 days of treatment was significantly higher in the AIA model group than in the normal group. However, the level of inflammatory cytokines was significantly lower in AIA mice treated with Tan IIA than in the AIA model group. The data obtained using the AIA model showed that Tan IIA not only reduced the swelling of the knee joint caused by inflammation but also inhibited the expression of pro-inflammatory factors and improved pathological manifestations in AIA mice. These data corroborate our initial hypothesis that Tan IIA has therapeutic potential for RA treatment. To date, few *in vivo* studies on the effects of Tan IIA in RA treatment have been conducted, and no detailed related mechanisms had previously been discovered.

To discover the mechanisms involved in the effects of Tan IIA on RA, we constructed primary RA-FLS strains from samples of synovial tissue from RA patients. We demonstrated that Tan IIA can inhibit the tumor-like proliferation characteristics of RA-FLSs in clinically safe concentrations. According to our data, although Tan IIA does not have a remarkable effect on the vitality of RA-FLSs after 24-h treatment, it can prevent TNF- α -stimulated cell proliferation in a dose-dependent manner after 48 h of treatment. In addition, previous reports suggested that high concentrations Tan IIA can promote RA-FLS apoptosis (Jie et al., 2014; Li et al., 2018), probably by upregulating lncRNA GAS5 (Li et al., 2018). However, we found in our experiments that RA-FLSs do not undergo apoptosis when treated with up to 20 μ M of Tan IIA, while cell apoptosis may accrue at concentrations of Tan IIA above 40 μ M. Therefore, we speculate that the effect of Tan IIA on RA-FLSs is different for higher and lower concentrations of Tan IIA, although further studies are needed to elucidate this issue. Moreover, Tan IIA could restrict the migration and invasion of RA-FLSs, which would be better for suppressing the tumor-like properties of RA-FLSs and reducing the damage to distal cartilage.

The RA pathogenesis states that RA-FLSs usually secrete pro-inflammatory factors and chemokines, including TNF- α , IL-6, IL-8, IL-17, and IL-1 β , to recruit and activate various immune cells. These immune cells, in turn, secrete cytokines to activate RA-FLSs, contributing to cartilage damage and joint destruction (Bartok and Firestein, 2010; Bottini and Firestein, 2013). TNF- α is one of the most important inflammatory cytokines in the joint cavity of RA patients and is commonly used as an activator of RA-FLSs *in vitro* to simulate the inflammatory microenvironment (Shi et al., 2018; Du et al., 2019; Wang Z. et al., 2019; Wu et al., 2019). We found that 20 ng/mL of exogenous TNF- α can stimulate RA-FLSs and produce a similar effect. It is worth mentioning that 10 or 20 μ M of Tan IIA inhibited the increased mRNA expression of IL-6, IL-1 β , and IL-8 induced by 20-ng/mL TNF- α . Moreover, only 1 μ M of sodium tanshinone IIA sulfonate, a Tan IIA derivative, can decrease IL-6 and IL-1 β mRNA expression (Wang Z. et al.,

2019). Taken together, these data suggest that Tan IIA acts as an anti-inflammatory in RA by inhibiting the production of pro-inflammatory cytokines, despite the different worked concentrations of Tan IIA or its derivative. Remarkably, Tan IIA did not inhibit TNF- α -induced IL-17 mRNA expression, a result that was similar to those of our previous research on 3'-Diindolylmethane (DIM) (Du et al., 2019). This may be related to the individual differences of the patients or may indicate that IL-17 production is not related to TNF- α stimulation, and, therefore, it is regulated by other mechanisms. From the ELISA results, we observed that, although there was no increase in TNF- α -induced IL-8, 20 μ M of Tan IIA suppressed the release of IL-8 by RA-FLSs. Moreover, we also found that Tan IIA inhibited the tendency of IL-1 β increase induced by TNF- α , although the basal expression of IL-1 β in the blank control group was difficult to detect because it was low.

Previous studies suggested that the expression of MMPs in fibroblasts of synovial joints is responsible for the degradation of synovial collagen in several inflammatory diseases, including RA (Agere et al., 2017). More than fifteen synovial MMPs are expressed in the synovial joints from RA patients, and they fall into three main categories: collagenase, gelatinase, and matrix metalloproteinase (Konttinen et al., 1999). We found that 20 μ M of Tan IIA prevented TNF- α -induced mRNA expression of MMP-8 collagenase, MMP-2 and MMP-9 gelatinases, and MMP-3 matrix metalloproteinase. However, we were unable to detect these MMPs at the protein level in the culture supernatant, similar to previous studies (Du et al., 2019). Despite the absence of bands in Western blot and gelatinase analyzes, our data suggest that these MMPs did indeed play an important role in the invasion and migration of RA-FLSs. In addition, we demonstrated that Tan IIA decreased the expression of MMPs in RA-FLSs.

Tan IIA has been reported to affect the proliferation, invasion, and migration of tumor cells through different signaling pathways (Zhang et al., 2018; Liao et al., 2019; Xue et al., 2019). However, such reports left the specific molecular mechanism of Tan IIA in RA-FLSs unknown. We performed network pharmacology analyzes and found some potential pathways for Tan IIA action in the treatment of RA. The integration of the network pharmacology analyses with the experimental *in vitro*-obtained data reveals that Tan IIA can affect three different pathways: MAPK, AKT/mTOR, HIF-1, and NF- κ B.

The mitogen-activated protein kinases (MAPK) family is widely conserved among eukaryotes and is responsible for the phosphorylation and dephosphorylation of several key proteins involved in regulatory mechanisms of different cells (Tong et al., 2014). Extracellular signal-regulated kinase (ERK), c-Jun N-terminal kinase (JNK), and P38MAP kinase (p38) are the main members of the MAPK family. These proteins are the main intracellular responders embedded in a highly active signaling flow that is involved in the activation of RA-FLSs (Müller-Ladner et al., 2007; Tong et al., 2014; Bustamante et al., 2017). Several compounds, including sodium tanshinone IIA sulfonate, DIM, and triptolide, have been shown to inhibit MAPK signaling

pathway activation by preventing the phosphorylation of p38, JNK, and ERK. Thus, these compounds are able to inhibit the proliferation, metastasis, and invasion of RA-FLSs (Yang et al., 2016; Du et al., 2019; Wang Z. et al., 2019). Our data showed that Tan IIA played an inhibitory role in TNF- α -stimulated p38 and JNK phosphorylation in RA-FLSs but had no significant effect on ERK. Therefore, we suggest that the effect of Tan IIA on proliferation, migration, and invasion in RA-FLSs is mainly mediated by inactivation of p38 and JNK proteins. There is near-consensus that the expression and activation of p38 and JNK in the synovial tissue of RA patients modulate the growth, apoptosis, and differentiation of RA-FLSs. Thus, inflammation and cartilage damage is triggered in the joint cavity of RA patients (Yang et al., 2016; Bustamante et al., 2017).

The PI3K/AKT signaling pathway is involved in the pathogenesis of inflammation (Malemud, 2015), and, therefore, understanding its regulation would be of great benefit for the control of RA (Laragione and Gulko, 2010; Jia et al., 2015). mTOR complex 1 (mTORC1) lies downstream of the PI3K/Akt pathway. The activation of the downstream signaling through AKT-mediated mTORC1 phosphorylation promotes anabolic processes and limits catabolic processes involved in cell growth, proliferation, and metabolism (Liu et al., 2006; Laplante and Sabatini, 2009). Moreover, previous reports have shown that activation of the PI3K/AKT/mTOR pathway appears to be the critical driver of proliferation and anti-apoptosis responses and is a typical feature of inflamed synovial tissue in RA (Garcia et al., 2010). Cytokines, especially TNF- α , in RA-FLS lead to the activation of the PI3K/AKT/mTOR pathway, thereby promoting cell migration and invasion (Karonitsch et al., 2018). Moreover, S6K1 and 4E-BP1 are the two best-characterized mTORC1 substrates, whereby mTORC1 plays the role of an mRNA to protein translator (Wendel et al., 2004). In our data, we found direct evidence that Tan IIA can influence the AKT/mTOR pathway. We showed that Tan IIA blocks activation by TNF- α -stimulated phosphorylation of AKT/mTOR and downstream p70S6K and 4E-BP1. Therefore, these data indicate that Tan IIA has antiproliferative activity and highlight that Tan IIA can be used independently or in combination with other drugs to improve clinical symptoms in RA patients. On the other hand, numerous studies have revealed that autophagy and autophagy-related proteins also participate in the pathogenesis and progress of RA. Furthermore, the mTOR pathway is also involved in autophagy in RA (Li et al., 2017; Wu and Adamopoulos, 2017). Further studies are needed to assess whether Tan IIA can regulate RA-FLS autophagy *via* the AKT/mTOR pathway.

Insufficient oxygen supply appears in the damaged articular cavity in RA pathology and is accompanied by metabolic disorders and pannus hyperplasia, resulting in a hypoxic microenvironment (Fearon et al., 2016; Quiñonez-Flores et al., 2016; Veale et al., 2017). The transcription factors NF- κ B and HIFs, in addition to the relevant enzymes, oxygen-sensitive and prolyl hydroxylases, are responsible for responding to the hypoxia signal in the hypoxic microenvironment. In particular, NF- κ B and HIFs play key roles in several disorders, including

induction of inflammation and angiogenesis and rheumatoid arthritis (Szade et al., 2015; D'Ignazio and Rocha, 2016). Our analysis showed that the HIF-1 pathway may be a potential target for Tan IIA in RA. Based on previous data, we chose NF- κ B p65 and HIF-1 α as targets to assess their changes in response to hypoxia to highlight the effect of Tan IIA on hypoxia pathways. Our data showed that Tan IIA can actually inhibit HIF-1 α expression and TNF- α -stimulated NF κ B p65 phosphorylation. Moreover, Tan IIA can also decrease LPS-induced p65 protein expression in PBMCs of RA patients (Tang et al., 2019). Therefore, it can be concluded that Tan IIA may affect RA by suppressing HIF-1 α and NF- κ B p65 to alleviate damage from hypoxia and the release of proinflammatory cytokines. Nevertheless, the regulatory mechanism of HIF-1 α and NF- κ B p65 needs further study to be fully revealed.

In conclusion, our data reveal a specific role of Tan IIA on TNF-dependent arthritogenesis. We identified that Tan IIA can inhibit the proliferation, migration, and invasion of RA-FLSs and suppress the release of proinflammatory cytokines and MMPs. We also showed that Tan IIA achieves these effects by affecting the MAPK, AKT/mTOR, HIF-1, and NF- κ B signaling pathways. Finally, we present *in vivo* evidence that Tan IIA is able to improve arthritis severity in AIA mice. Therefore, this study highlights the therapeutic role of Tan IIA in the treatment of RA and shows its potential to improve the quality of life of RA patients.

DATA AVAILABILITY STATEMENT

The raw data supporting the conclusions of this manuscript will be made available by the authors, without undue reservation, to any qualified researcher.

ETHICS STATEMENT

Our study was authorized by the Medical Ethics Committee of Zhujiang Hospital, Southern Medical University. All patients voluntarily signed an informed consent form. All of the animal experiments were conducted with the approval of the Southern

Medical University Ethics Committee for Animal Laboratory Research. Animal care and handling procedures abided by the guidelines of ethical regulations for institutional animal care used in the Southern Medical University.

AUTHOR CONTRIBUTIONS

Design of the entire study: HD, YiW, and LJ. Experimental studies: HD, YZ, XH, DL, LY, and JW. Network pharmacology analysis: YuW. Animal model construction: YL and XC. Experimental data analysis and statistics: HD, HL, and LJ. Writing and revising the manuscript: HD, QY, YiW, and LJ. All authors read and approved the final manuscript.

FUNDING

This work was supported by grants from the National Natural Science Foundation of China (81601397, 81771727, 81102688, and 81401920), the Natural Science Foundation of Guangdong Province (2016A030313624), the Program of Guangdong Innovation and Entrepreneurship training for college students (201812121108), and the Scientific Enlightenment Project of Southern Medical University.

ACKNOWLEDGMENTS

Additionally, we thank Ningchao Du, Wei Wang, Quanbao Wu, Yuefan Chen, Qiong Li, and Yuting Chen for technical assistance during the experiments.

SUPPLEMENTARY MATERIAL

The Supplementary Material for this article can be found online at: <https://www.frontiersin.org/articles/10.3389/fphar.2020.00568/full#supplementary-material>

REFERENCES

- Agere, S. A., Akhtar, N., Watson, J. M., and Ahmed, S. (2017). RANTES/CCL5 Induces Collagen Degradation by Activating MMP-1 and MMP-13 Expression in Human Rheumatoid Arthritis Synovial Fibroblasts. *Front. Immunol.* 8, 1341. doi: 10.3389/fimmu.2017.01341
- Arnett, F. C., Edworthy, S. M., Bloch, D. A., McShane, D. J., Fries, J. F., Cooper, N. S., et al. (1988). The American Rheumatism Association 1987 revised criteria for the classification of rheumatoid arthritis. *Arthritis Rheum.* 31 (3), 315–324. doi: 10.1002/art.1780310302
- Atkinson, S. M., and Nansen, A. (2017). Pharmacological Value of Murine Delayed-type Hypersensitivity Arthritis: A Robust Mouse Model of Rheumatoid Arthritis in C57BL/6 Mice. *Basic Clin. Pharmacol. Toxicol.* 120 (2), 108–114. doi: 10.1111/bcpt.12657
- Baradaran-Heravi, A., Balgi, A. D., Zimmerman, C., Choi, K., Shidmoosavee, F. S., Tan, J. S., et al. (2016). Novel small molecules potentiate premature termination codon readthrough by aminoglycosides. *Nucleic Acids Res.* 44 (14), 6583–6598. doi: 10.1093/nar/gkw638
- Bartok, B., and Firestein, G. S. (2010). Fibroblast-like synoviocytes: key effector cells in rheumatoid arthritis. *Immunol. Rev.* 233 (1), 233–255. doi: 10.1111/j.0105-2896.2009.00859.x
- Bottini, N., and Firestein, G. S. (2013). Duality of fibroblast-like synoviocytes in RA: passive responders and imprinted aggressors. *Nat. Rev. Rheumatol.* 9 (1), 24–33. doi: 10.1038/nrrheum.2012.190
- Bustamante, M. F., Garcia-Carbonell, R., Whisenant, K. D., and Guma, M. (2017). Fibroblast-like synovocyte metabolism in the pathogenesis of rheumatoid arthritis. *Arthritis Res. Ther.* 19 (1), 110. doi: 10.1186/s13075-017-1303-3
- Chen, Z., and Xu, H. (2014). Anti-Inflammatory and Immunomodulatory Mechanism of Tanshinone IIA for Atherosclerosis. *Evid Based Complement Alternat Med.* 2014, 267976. doi: 10.1155/2014/267976
- Conigliaro, P., Triggianese, P., De Martino, E., Fonti, G. L., Chimenti, M. S., Sunzini, F., et al. (2019). Challenges in the treatment of Rheumatoid Arthritis. *Autoimmun Rev.* 18 (7), 706–713. doi: 10.1016/j.autrev.2019.05.007

- D'Ignazio, L., and Rocha, S. (2016). Hypoxia Induced NF-kappaB. *Cells* 5, 1. doi: 10.3390/cells5010010
- de Oliveira, P. G., Farinon, M., Sanchez-Lopez, E., Miyamoto, S., and Guma, M. (2019). Fibroblast-Like Synoviocytes Glucose Metabolism as a Therapeutic Target in Rheumatoid Arthritis. *Front. Immunol.* 10, 1743. doi: 10.3389/fimmu.2019.01743
- Dong, L., Wu, J., Chen, K., Xie, J., Wang, Y., Li, D., et al. (2019). Mannan-Binding Lectin Attenuates Inflammatory Arthritis Through the Suppression of Osteoclastogenesis. *Front. Immunol.* 10, 1239. doi: 10.3389/fimmu.2019.01239
- Du, H., Zhang, X., Zeng, Y., Huang, X., Chen, H., Wang, S., et al. (2019). A Novel Phytochemical, DIM, Inhibits Proliferation, Migration, Invasion and TNF- α Induced Inflammatory Cytokine Production of Synovial Fibroblasts From Rheumatoid Arthritis Patients by Targeting MAPK and AKT/mTOR Signal Pathway. *Front. Immunol.* 10, 1620. doi: 10.3389/fimmu.2019.01620
- Fearon, U., Canavan, M., Canavan, M., Biniecka, M., and Veale, D. J. (2016). Hypoxia, mitochondrial dysfunction and synovial invasiveness in rheumatoid arthritis. *Nat. Rev. Rheumatol.* 12 (7), 385–397. doi: 10.1038/nrrheum.2016.69
- Frey, O., Hükel, M., Gajda, M., Petrow, P. K., and Bräuer, R. (2018). Induction of chronic destructive arthritis in SCID mice by arthritogenic fibroblast-like synoviocytes derived from mice with antigen-induced arthritis. *Arthritis Res. Ther.* 20 (1), 261. doi: 10.1186/s13075-018-1720-y
- Garcia, S., Liz, M., Gómez-Reino, J. J., and Conde, C. (2010). Akt activity protects rheumatoid synovial fibroblasts from Fas-induced apoptosis by inhibition of Bid cleavage. *Arthritis Res. Ther.* 12 (1), R33. doi: 10.1186/ar2941
- Gou, K. J., Zeng, R., Ren, X. D., Dou, Q. L., Yang, Q. B., Dong, Y., et al. (2018). Anti-rheumatoid arthritis effects in adjuvant-induced arthritis in rats and molecular docking studies of Polygonum orientale L. extracts. *Immunol. Lett.* 201, 59–69. doi: 10.1016/j.imlet.2018.11.009
- Grötsch, B., Bozec, A., and Schett, G. (2019). In Vivo Models of Rheumatoid Arthritis. *Methods Mol. Biol.* 1914, 269–280. doi: 10.1007/978-1-4939-8997-3_14
- Hu, F., Hepburn, H. R., Li, Y., Chen, M., Radloff, S. E., and Daya, S. (2005). Effects of ethanol and water extracts of propolis (bee glue) on acute inflammatory animal models. *J. Ethnopharmacol.* 100 (3), 276–283. doi: 10.1016/j.jep.2005.02.044
- Huber, L. C., Distler, O., Tarner, I., Gay, R. E., Gay, S., and Pap, T. (2006). Synovial fibroblasts: key players in rheumatoid arthritis. *Rheumatol. (Oxford)* 45 (6), 669–675. doi: 10.1093/rheumatology/kel065
- Jia, Q., Cheng, W., Yue, Y., Hu, Y., Zhang, J., Pan, X., et al. (2015). Cucurbitacin E inhibits TNF-alpha-induced inflammatory cytokine production in human synovial cell MH7A cells via suppression of PI3K/Akt/NF-kappaB pathways. *Int. Immunopharmacol.* 29 (2), 884–890. doi: 10.1016/j.intimp.2015.08.026
- Jia, P. T., Zhang, X. L., Zuo, H. N., Lu, X., and Li, L. (2017). Articular cartilage degradation is prevented by tanshinone IIA through inhibiting apoptosis and the expression of inflammatory cytokines. *Mol. Med. Rep.* 16 (5), 6285–6289. doi: 10.3892/mmr.2017.7340
- Jie, L., Huang, Q., Shen, Y., and Zhu, X. (2002). The curative effect evaluation of salvia miltiorrhiza on RA. *Chin. J. Clin. Rehabil.* 6 (14), 2301.
- Jie, L., Huang, Q., Shen, Y., Sun, W., Wei, S., and Xu, W. (2010). Clinical observation of compound salvia injection in patients with active RA. *Liaoning J. Tradit. Chin. Med.* 37 (10), 1945–1948.
- Jie, L., Du, H., Huang, Q., Wei, S., Huang, R., and Sun, W. (2014). Tanshinone IIA induces apoptosis in fibroblast-like synoviocytes in rheumatoid arthritis via blockade of the cell cycle in the G2/M phase and a mitochondrial pathway. *Biol. Pharm. Bull.* 37 (8), 1366–1372. doi: 10.1248/bpb.b14-00301
- Jie, L. G., Huang, R. Y., Sun, W. F., Wei, S., Chu, Y. L., Huang, Q. C., et al. (2015). Role of cysteine-rich angiogenic inducer 61 in fibroblast-like synovial cell proliferation and invasion in rheumatoid arthritis. *Mol. Med. Rep.* 11 (2), 917–923. doi: 10.3892/mmr.2014.2770
- Karami, J., Aslani, S., Tahmasebi, M. N., Mousavi, M. J., Sharafat, V. A., Jamshidi, A., et al. (2020). Epigenetics in rheumatoid arthritis; fibroblast-like synoviocytes as an emerging paradigm in the pathogenesis of the disease. *Immunol. Cell Biol.* 98 (3), 171–186. doi: 10.1111/imcb.12311
- Karonitsch, T., Kandasamy, R. K., Kartnig, F., Herdy, B., Dalwigk, K., Niederreiter, B., et al. (2018). mTOR Senses Environmental Cues to Shape the Fibroblast-like Synovial Cell Response to Inflammation. *Cell Rep.* 23 (7), 2157–2167. doi: 10.1016/j.celrep.2018.04.044
- Kontinen, Y. T., Ainola, M., Valleala, H., Ma, J., Ida, H., Mandelin, J., et al. (1999). Analysis of 16 different matrix metalloproteinases (MMP-1 to MMP-20) in the synovial membrane: different profiles in trauma and rheumatoid arthritis. *Ann. Rheum. Dis.* 58 (11), 691–697. doi: 10.1136/ard.58.11.691
- Laplanche, M., and Sabatini, D. M. (2009). mTOR signaling at a glance. *J. Cell Sci.* 122 (Pt 20), 3589–3594. doi: 10.1242/jcs.051011
- Laragione, T., and Gulko, P. S. (2010). mTOR regulates the invasive properties of synovial fibroblasts in rheumatoid arthritis. *Mol. Med.* 16 (9–10), 352–358. doi: 10.2119/molmed.2010.00049
- Lefevre, S., Knedla, A., Tennie, C., Kampmann, A., Wunrau, C., Dinser, R., et al. (2009). Synovial fibroblasts spread rheumatoid arthritis to unaffected joints. *Nat. Med.* 15 (12), 1414–1420. doi: 10.1038/nm.2050
- Li, S., Chen, J. W., Xie, X., Tian, J., Deng, C., Wang, J., et al. (2017). Autophagy inhibitor regulates apoptosis and proliferation of synovial fibroblasts through the inhibition of PI3K/AKT pathway in collagen-induced arthritis rat model. *Am. J. Transl. Res.* 9 (5), 2065–2076. doi: 10.1136/annrheumdis-2017-eular.2044
- Li, G., Liu, Y., Meng, F., Xia, Z., Wu, X., Fang, Y., et al. (2018). Tanshinone IIA promotes the apoptosis of fibroblast-like synoviocytes in rheumatoid arthritis by up-regulating lncRNA GAS5. *Biosci. Rep.* 38, 5. doi: 10.1042/BSR20180626
- Li, Y., Niu, S. X., Xi, D. L., Zhao, S. Q., Sun, J., Jiang, Y., et al. (2019). Differences in Lipopolysaccharides-Induced Inflammatory Response Between Mouse Embryonic Fibroblasts and Bone Marrow-Derived Macrophages. *J. Interferon Cytokine Res.* 39 (6), 375–382. doi: 10.1089/jir.2018.0167
- Liao, X. Z., Gao, Y., Huang, S., Chen, Z. Z., Sun, L. L., Liu, J. H., et al. (2019). Tanshinone IIA combined with cisplatin synergistically inhibits non-small-cell lung cancer in vitro and in vivo via down-regulating the phosphatidylinositol 3-kinase/Akt signalling pathway. *Phytother. Res.* 33 (9), 2298–2309. doi: 10.1002/ptr.6392
- Liu, L., Li, F., Cardelli, J. A., Martin, K. A., Blenis, J., and Huang, S. (2006). Rapamycin inhibits cell motility by suppression of mTOR-mediated S6K1 and 4E-BP1 pathways. *Oncogene* 25 (53), 7029–7040. doi: 10.1038/sj.onc.1209691
- Liu, Z., Zhu, W., Kong, X., Chen, X., Sun, X., Zhang, W., et al. (2019). Tanshinone IIA inhibits glucose metabolism leading to apoptosis in cervical cancer. *Oncol. Rep.* 42 (5), 1893–1903. doi: 10.3892/or.2019.7294
- Malemud, C. J. (2015). The PI3K/Akt/PTEN/mTOR pathway: a fruitful target for inducing cell death in rheumatoid arthritis? *Future Med. Chem.* 7 (9), 1137–1147. doi: 10.4155/fmc.15.55
- Müller-Ladner, U., Ospelt, C., Gay, S., Distler, O., and Pap, T. (2007). Cells of the synovium in rheumatoid arthritis. Synovial fibroblasts. *Arthritis Res. Ther.* 9 (6), 223. doi: 10.1186/ar2337
- Nissen, S. E. (2017). Cardiovascular Safety of Celecoxib, Naproxen, or Ibuprofen for Arthritis. *N. Engl. J. Med.* 376 (14), 1390. doi: 10.1056/NEJMc1702534
- Quiñonez-Flores, C. M., González-Chávez, S. A., and Pacheco-Tena, C. (2016). Hypoxia and its implications in rheumatoid arthritis. *J. BioMed. Sci.* 23 (1), 62. doi: 10.1186/s12929-016-0281-0
- Ranganath, V. K., Motamedi, K., Haavardsholm, E. A., Maranian, P., Elashoff, D., McQueen, F., et al. (2015). Comprehensive appraisal of magnetic resonance imaging findings in sustained rheumatoid arthritis remission: a substudy. *Arthritis Care Res. (Hoboken)* 67 (7), 929–939. doi: 10.1002/acr.22541
- Ren, J., Fu, L., Nile, S. H., Zhang, J., and Kai, G. (2019). Salvia miltiorrhiza in Treating Cardiovascular Diseases: A Review on Its Pharmacological and Clinical Applications. *Front. Pharmacol.* 10, 753. doi: 10.3389/fphar.2019.00753
- Rubbert-Roth, A., and Peteret, H. F. (2012). [Nervous system side effects of disease modifying treatments of rheumatoid arthritis]. *Z. Rheumatol.* 71 (7), 572–582. doi: 10.1007/s00393-012-0959-y
- Sardar, S., and Andersson, A. (2016). Old and new therapeutics for Rheumatoid Arthritis: in vivo models and drug development. *Immunopharmacol. Immunotoxicol.* 38 (1), 2–13. doi: 10.3109/08923973.2015.1125917
- Shi, M., Wang, J., Xiao, Y., Wang, C., Qiu, Q., Lao, M., et al. (2018). Glycogen Metabolism and Rheumatoid Arthritis: The Role of Glycogen Synthase 1 in Regulation of Synovial Inflammation via Blocking AMP-Activated Protein Kinase Activation. *Front. Immunol.* 9, 1714. doi: 10.3389/fimmu.2018.01714
- Smolen, J. S., Aletaha, D., and McInnes, I. B. (2016). Rheumatoid arthritis. *Lancet* 388 (10055), 2023–2038. doi: 10.1016/S0140-6736(16)30173-8
- Sui, H., Zhao, J., Zhou, L., Wen, H., Deng, W., Li, C., et al. (2017). Tanshinone IIA inhibits beta-catenin/VEGF-mediated angiogenesis by targeting TGF-beta1 in

- normoxic and HIF-1 α in hypoxic microenvironments in human colorectal cancer. *Cancer Lett.* 403, 86–97. doi: 10.1016/j.canlet.2017.05.013
- Szade, A., Grochot-Przeczek, A., Florczyk, U., Jozkowicz, A., and Dulak, J. (2015). Cellular and molecular mechanisms of inflammation-induced angiogenesis. *IUBMB Life* 67 (3), 145–159. doi: 10.1002/iub.1358
- Tang, J., Zhou, S., Zhou, F., and Wen, X. (2019). Inhibitory effect of tanshinone IIA on inflammatory response in rheumatoid arthritis through regulating beta-arrestin 2. *Exp. Ther. Med.* 17 (5), 3299–3306. doi: 10.3892/etm.2019.7371
- Tong, B., Wan, B., Wei, Z., Wang, T., Zhao, P., Dou, Y., et al. (2014). Role of cathepsin B in regulating migration and invasion of fibroblast-like synoviocytes into inflamed tissue from patients with rheumatoid arthritis. *Clin. Exp. Immunol.* 177 (3), 586–597. doi: 10.1111/cei.12357
- Veale, D. J., Orr, C., and Fearon, U. (2017). Cellular and molecular perspectives in rheumatoid arthritis. *Semin. Immunopathol.* 39 (4), 343–354. doi: 10.1007/s00281-017-0633-1
- Wang, J., and Zhao, Q. (2019). Kaempferitin inhibits proliferation, induces apoptosis, and ameliorates inflammation in human rheumatoid arthritis fibroblast-like synoviocytes. *Phytother. Res.* 33 (6), 1726–1735. doi: 10.1002/ptr.6364
- Wang, W., Zhou, H., and Liu, L. (2018). Side effects of methotrexate therapy for rheumatoid arthritis: A systematic review. *Eur. J. Med. Chem.* 158, 502–516. doi: 10.1016/j.ejmech.2018.09.027
- Wang, R., Luo, Z., Zhang, H., and Wang, T. (2019). Tanshinone IIA Reverses Gefitinib-Resistance In Human Non-Small-Cell Lung Cancer Via Regulation Of VEGFR/Akt Pathway. *Onco. Targets Ther.* 12, 9355–9365. doi: 10.2147/OTT.S221228
- Wang, Z., Li, J., Zhang, J., and Xie, X. (2019). Sodium tanshinone IIA sulfonate inhibits proliferation, migration, invasion and inflammation in rheumatoid arthritis fibroblast-like synoviocytes. *Int. Immunopharmacol.* 73, 370–378. doi: 10.1016/j.intimp.2019.05.023
- Wendel, H. G., De Stanchina, E., Fridman, J. S., Malina, A., Ray, S., Kogan, S., et al. (2004). Survival signalling by Akt and eIF4E in oncogenesis and cancer therapy. *Nature* 428 (6980), 332–337. doi: 10.1038/nature02369
- Wu, D. J., and Adamopoulos, I. E. (2017). Autophagy and autoimmunity. *Clin. Immunol.* 176, 55–62. doi: 10.1016/j.clim.2017.01.007
- Wu, J., Li, Q., Jin, L., Qu, Y., Liang, B. B., Zhu, X. T., et al. (2019). Kirenel Inhibits the Function and Inflammation of Fibroblast-like Synoviocytes in Rheumatoid Arthritis in vitro and in vivo. *Front. Immunol.* 10, 1304. doi: 10.3389/fimmu.2019.01304
- Xue, Y., Cohen, J. M., Wright, N. A., and Merola, J. F. (2016). Skin Signs of Rheumatoid Arthritis and its Therapy-Induced Cutaneous Side Effects. *Am. J. Clin. Dermatol.* 17 (2), 147–162. doi: 10.1007/s40257-015-0167-z
- Xue, J., Jin, X., Wan, X., Yin, X., Fang, M., Liu, T., et al. (2019). Effects and Mechanism of Tanshinone II A in Proliferation, Apoptosis, and Migration of Human Colon Cancer Cells. *Med. Sci. Monit.* 25, 4793–4800. doi: 10.12659/MSM.914446
- Yamamoto, K., Mimori, T., Shinohara, S., Hirabayashi, Y., and Nakachi, S. (2011). [Discussion meeting on treatment of rheumatoid arthritis with biologics and their side effects]. *Nihon Naika Gakkai Zasshi* 100 (10), 2998–3017. doi: 10.2169/naika.100.2998
- Yang, Y., Ye, Y., Qiu, Q., Xiao, Y., Huang, M., Shi, M., et al. (2016). Triptolide inhibits the migration and invasion of rheumatoid fibroblast-like synoviocytes by blocking the activation of the JNK MAPK pathway. *Int. Immunopharmacol.* 41, 8–16. doi: 10.1016/j.intimp.2016.10.005
- Zhang, S., Huang, G., Yuan, K., Zhu, Q., Sheng, H., Yu, R., et al. (2017). Tanshinone IIA ameliorates chronic arthritis in mice by modulating neutrophil activities. *Clin. Exp. Immunol.* 190 (1), 29–39. doi: 10.1111/cei.12993
- Zhang, Y., Guo, S., Fang, J., Peng, B., Zhang, Y., and Cao, T. (2018). Tanshinone IIA inhibits cell proliferation and tumor growth by downregulating STAT3 in human gastric cancer. *Exp. Ther. Med.* 16 (4), 2931–2937. doi: 10.3892/etm.2018.6562
- Zhang, L., Lin, W., Chen, X., Wei, G., Zhu, H., and Xing, S. (2019). Tanshinone IIA reverses EGF- and TGF- β 1-mediated epithelial-mesenchymal transition in HepG2 cells via the PI3K/Akt/ERK signaling pathway. *Oncol. Lett.* 18 (6), 6554–6562. doi: 10.3892/ol.2019.11032

Conflict of Interest: The authors declare that the research was conducted in the absence of any commercial or financial relationships that could be construed as a potential conflict of interest.

Copyright © 2020 Du, Wang, Zeng, Huang, Liu, Ye, Li, Chen, Liu, Li, Wu, Yu, Wu and Jie. This is an open-access article distributed under the terms of the Creative Commons Attribution License (CC BY). The use, distribution or reproduction in other forums is permitted, provided the original author(s) and the copyright owner(s) are credited and that the original publication in this journal is cited, in accordance with accepted academic practice. No use, distribution or reproduction is permitted which does not comply with these terms.



Uncovering the Complexity Mechanism of Different Formulas Treatment for Rheumatoid Arthritis Based on a Novel Network Pharmacology Model

Ke-xin Wang^{1,2†}, Yao Gao^{1,2†}, Cheng Lu³, Yao Li², Bo-ya Zhou⁴, Xue-mei Qin¹, Guan-hua Du^{1,5}, Li Gao^{1*}, Dao-gang Guan^{6,7*} and Ai-ping Lu^{2*}

OPEN ACCESS

Edited by:

Per-Johan Jakobsson,
Karolinska Institutet (KI), Sweden

Reviewed by:

Mingze Qin,
Shenyang Pharmaceutical University,
China
Qiong Wang,
Southwest Medical University, China

*Correspondence:

Li Gao
gaoli87@sxu.edu.cn
Dao-gang Guan
guandg0929@hotmail.com
Ai-ping Lu
aipinglu@hkbu.edu.hk

[†]These authors have contributed
equally to this work

Specialty section:

This article was submitted to
Ethnopharmacology,
a section of the journal
Frontiers in Pharmacology

Received: 13 November 2019

Accepted: 25 June 2020

Published: 10 July 2020

Citation:

Wang K-x, Gao Y, Lu C, Li Y,
Zhou B-y, Qin X-m, Du G-h, Gao L,
Guan D-g and Lu A-p (2020)
Uncovering the Complexity
Mechanism of Different Formulas
Treatment for Rheumatoid Arthritis
Based on a Novel Network
Pharmacology Model.
Front. Pharmacol. 11:1035.
doi: 10.3389/fphar.2020.01035

¹ Modern Research Center for Traditional Chinese Medicine, Shanxi University, Taiyuan, China, ² Institute of Integrated Biomedicine and Translational Science, Hong Kong Baptist University, Hong Kong, Hong Kong, ³ Institute of Basic Research in Clinical Medicine, China Academy of Chinese Medical Sciences, Beijing, China, ⁴ Department of Ultrasound, Eighth Affiliated Hospital of Sun Yat-sen University, Guangzhou, China, ⁵ Institute of Materia Medica, Chinese Academy of Medical Sciences & Peking Union Medical College, Beijing, China, ⁶ Department of Biochemistry and Molecular Biology, School of Basic Medical Sciences, Southern Medical University, Guangzhou, China, ⁷ Guangdong Key Laboratory of Single Cell Technology and Application, Southern Medical University, Guangzhou, China

Traditional Chinese medicine (TCM) with the characteristics of “multi-component-multi-target-multi-pathway” has obvious advantages in the prevention and treatment of complex diseases, especially in the aspects of “treating the same disease with different treatments”. However, there are still some problems such as unclear substance basis and molecular mechanism of the effectiveness of formula. Network pharmacology is a new strategy based on system biology and poly-pharmacology, which could observe the intervention of drugs on disease networks at systematical and comprehensive level, and especially suitable for study of complex TCM systems. Rheumatoid arthritis (RA) is a chronic inflammatory autoimmune disease, causing articular and extra articular dysfunctions among patients, it could lead to irreversible joint damage or disability if left untreated. TCM formulas, Danggui-Sini-decoction (DSD), Guizhi-Fuzi-decoction (GFD), and Huangqi-Guizhi-Wuwu-Decoction (HGWD), et al., have been found successful in controlling RA in clinical applications. Here, a network pharmacology-based approach was established. With this model, key gene network motif with significant (KNMS) of three formulas were predicted, and the molecular mechanism of different formula in the treatment of rheumatoid arthritis (RA) was inferred based on these KNMSs. The results show that the KNMSs predicted by the model kept a high consistency with the corresponding C-T network in coverage of RA pathogenic genes, coverage of functional pathways and cumulative contribution of key nodes, which confirmed the reliability and accuracy of our proposed KNMS prediction strategy. All validated KNMSs of each RA therapy-related formula were employed to decode the mechanisms of different formulas treat the same disease. Finally, the key components in KNMSs of each formula were evaluated by *in vitro* experiments. Our proposed KNMS prediction and validation

strategy provides methodological reference for interpreting the optimization of core components group and inference of molecular mechanism of formula in the treatment of complex diseases in TCM.

Keywords: Traditional Chinese medicine (TCM), rheumatoid arthritis, key gene network motif with significant (KNMS), mechanisms, network pharmacology

INTRODUCTION

Rheumatoid Arthritis (RA) is a chronic systemic autoimmune disease with symmetric inflammation of aggressive multiple joints (Sodhi et al., 2015). As the most common inflammatory rheumatic disease, the prevalence of RA is about 0.5%-1.0% in the world (Saraux et al., 2006). The inflammatory cell infiltration of synovium, pannus formation, and the progressive destruction of articular cartilage and bone destruction are the main pathological properties of RA (Brzustewicz and Bryl, 2015). The data from epidemiological investigations shows that about 90% of RA patients developed bone erosions within 2 years, eventually leading to joint deformities or even disability (Cecilia et al., 2013). Therefore, RA brings great impact on the quality of life of patients and also imposes a heavy burden on families and society.

Traditional Chinese medicine (TCM) has the advantages of definite curative effect, safety and few side effects in the treatment of rheumatoid arthritis and has attracted more and more attention in the prevention and treatment of rheumatoid arthritis. TCM usually treats RA and other complex diseases in the form of formulas, which has theoretical advantages and rich clinical experience. In the study of RA therapy-related formulas, increasing evidence confirmed that different formulas can treat RA, which coincide with the theoretical concept of “treating the same disease with different treatments” in TCM (Fu et al., 2014). Such as Danggui-Sini-decoction (DSD) (Bang et al., 2017), Guizhi-Fuzi-decoction (GFD) (Peng et al., 2013), and Huangqi-Guizhi Wuwu-Decoction (HGWD) (Wang et al., 2010) etc., have been found successful in controlling RA in TCM clinics. Previous pharmacological studies have shown that DSD exert positive effects and good anti-inflammatory function which might protect collagen-induced arthritis rats from bone and cartilage destruction (Cheng et al., 2017). It has been reported that GFD could substantially inhibit the activities of interleukin-6 and tumor necrosis factor- α in the serum of adjuvant-induced arthritis rats, as well as inhibit the formation of synovitis and pannus, and has obvious therapeutic effect on rheumatoid arthritis (He and Gu, 2008; Xia and Song, 2011). In addition, some pharmacological experimental studies have found that HGWD could promote the apoptosis of synovial cells in rheumatoid arthritis rats with abnormal hyperfunction (Liu et al., 2017), and reduce the degree of foot swelling in adjuvant arthritis rats, affect the arthritis index of rats, and play a role in treating rheumatoid arthritis (Shi et al., 2006).

In these formulas, DSD consists of 7 herbs: *Angelica sinensis* (Oliv.) Diels (Danggui, 12 g), *Cinnamomum cassia* (L.) J. Presl

(*Cinnamomi ramulus*, Guizhi, 9 g), *Paeonia lactiflora* Pall. (Baishao, 9 g), *Asarum sieboldii* Miq. (Xixin, 3 g), *Glycyrrhiza uralensis* Fisch. ex DC. (Gancao, 6 g), *Tetrapanax papyrifer* (Hook.) K. Koch (Medulla tetrapanacis, Tongcao, 6 g), *Ziziphus jujuba* Mill. (Jujubae fructus, Dazao, 8). GFD consists of 5 herbs: *Cinnamomum cassia* (L.) J. Presl (*Cinnamomi ramulus*, Guizhi, 12 g), *Aconitum carmichaeli* Debeaux (*Aconiti lateralis radix praeparata*, Fuzi, 15 g), *Zingiber officinale* Roscoe (Shengjiang, 9 g), *Glycyrrhiza uralensis* Fisch. ex DC. (Gancao, 6 g), *Ziziphus jujuba* Mill. (Jujubae fructus, Dazao, 12). HGWD consists of 5 herbs: *Astragalus mongholicus* Bunge (Huangqi, 15 g), *Paeonia lactiflora* Pall. (Baishao, 12 g), *Cinnamomum cassia* (L.) J. Presl (*Cinnamomi ramulus*, Gui zhi, 12 g), *Zingiber officinale* Roscoe (Shengjiang, 25 g), *Ziziphus jujuba* Mill. (Jujubae fructus, Dazao, 4). These traditional formulas are recorded in the Chinese pharmacopoeia (National Pharmacopoeia Commission, 2015). However, the molecular mechanism of these different formulas in treating rheumatoid arthritis under the concept of “treating the same disease with different treatments” is still unclear. How to develop new methods to detect the key component groups of different formulas for treating rheumatoid arthritis and speculate the possible mechanism not only provides the benefit therapy strategy for the precise treatment of RA, but also provides methodological reference for the analysis of the mechanism of treating the same disease with different treatments in TCM.

Network pharmacology has been widely used in the research of treating the same diseases with different formulas. For example, Gao et al. used network pharmacology to decode the mechanisms of Xiaoyao powder and Kaixin powder in treating depression; Liu et al. clarified the molecular mechanism of Sini San and Suanzaoren Tang in treating insomnia based on network pharmacology, etc (Yao et al., 2018; Liu et al., 2019). With the in-depth intersection of systems biology, poly-pharmacology, bioinformatics and other technologies, and the continuous improvement of the accuracy, reliability, and integrity of data resources, the research ideas and technical means of network pharmacology will be better applied to the mechanism research of formulas in TCM and provide more innovation in methodology for the molecular level research of TCM.

In this study, network pharmacology model was applied to analyze the key gene network motif with significant (KNMS) of different formulas in the treatment of RA. Coverage of RA pathogenic genes, coverage of functional pathways and cumulative contribution of key nodes were employed to evaluate the accuracy and reliability of KNMSs, and then the validated KNMSs were used to infer the common potential

mechanism of different formulas in the treatment of RA. In summary, the proposed network pharmacology strategy aims to identify major mechanism and related pharmacological effects of different treatments in treating RA through specific KNMSs, which may offer a new network-based method for evaluating and selecting suitable treatment strategies of complex diseases in TCM.

MATERIALS AND METHODS

Flowchart

This phenomenon that different formulas treat the same diseases is widely used in TCM clinical applications. However, there is lack of systematic method to decode the mechanisms of treat the same disease with different treatments. In this study, we designed a network pharmacology model to decode the common and specific potential mechanisms of 3 formulas in the treatment of RA, which may provide a methodological reference for different formulas treat the same disease. The workflow is illustrated in **Figure 1** and described as follows: 1) the components of DSD, GFD and HGWD were collected from TCMSP, TCMID, and TCM@Taiwan; 2) ADME based methods were used to identify the main active components; 3) the main active components from three formulas and their predicted targets were used to construct the component-target (C-T) networks; 4) The KNMSs were detected from integrated C-T and target-target interaction networks; 5) the KNMSs were validated by the coverage of RA

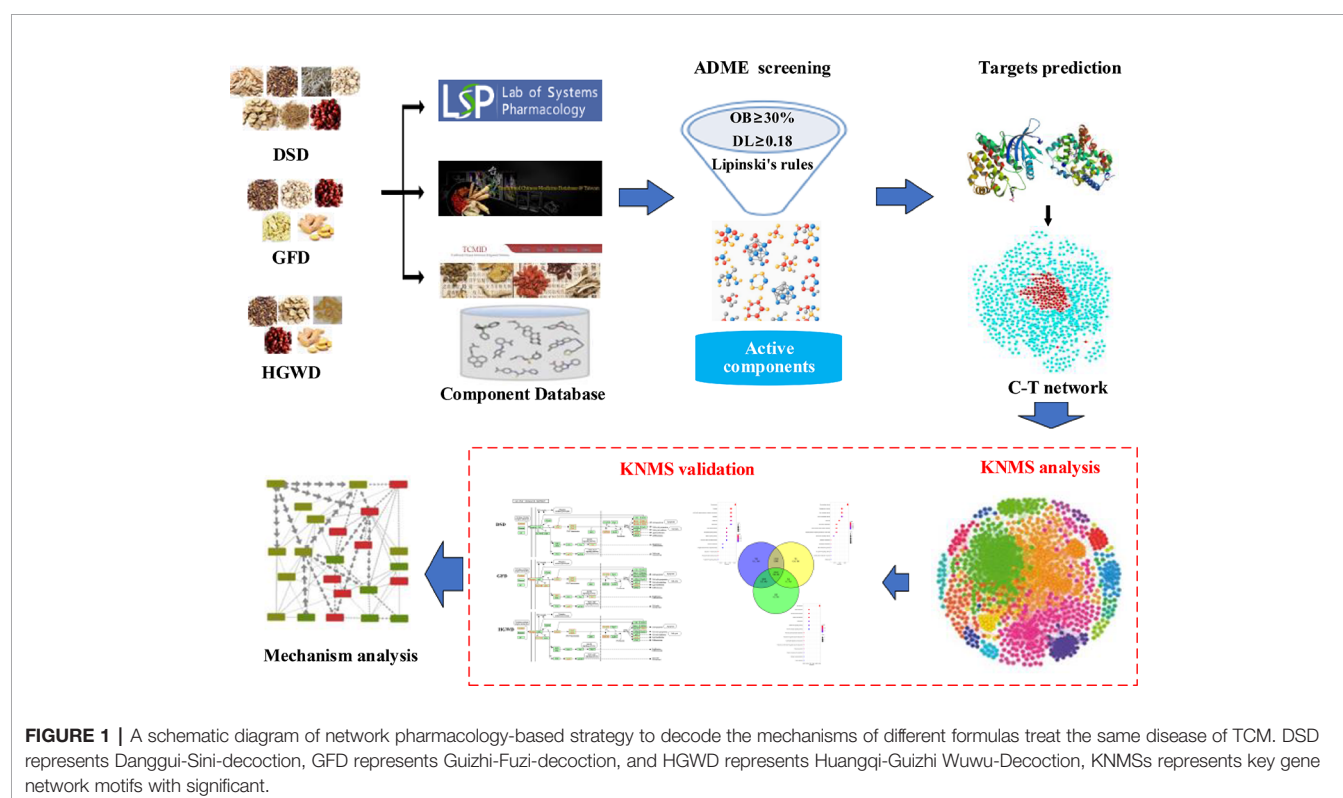
pathogenic genes, coverage of functional pathways and cumulative contribution of key nodes; 6) Finally, all validated KNMSs were employed to decode the underlying mechanism of different formulas treat the same disease.

Component Identification

All chemical components of Danggui-Sini-decoction (DSD), Guizhi-Fuzi-decoction (GFD), and Huangqi-Guizhi Wuwu-Decoction (HGWD) were collected from Traditional Chinese Medicine Systems Pharmacology (TCMSP) Database (Ru et al., 2014) (<http://lsp.nwsuaf.edu.cn/tcmsp.php>), Traditional Chinese Medicine integrated database (Xue et al., 2013) (TCMID, <http://www.megabionet.org/tcmid/>), and TCM@Taiwan (Chen, 2012) (<http://tcm.cmu.edu.tw/zh-tw>). The chemical identification and concentration of the herbs in DSD, GFD, and HGWD were collected from the previous reports. All chemical structures were prepared and converted into canonical SMILES using Open Babel Toolkit (version 2.4.1). The targets of DSD, GFD, and HGWD were predicted by using Similarity Ensemble Approach SEA (Keiser et al., 2007) (<http://sea.bkslab.org/>) and Swiss Target Prediction (David et al., 2014) (<http://www.swisstargetprediction.ch/>).

ADME Screening

Components that meet the Lipinski's rules of five usually have better pharmacokinetic properties, higher bioavailability during metabolism in the body, and are therefore more likely to be drug candidates (Lipinski et al., 2012; Damião et al., 2014). Oral bioavailability (OB) refers to the extent and rate of active



components release from the herbs into the systemic circulation and is an important indicator for evaluating the intrinsic quality of the component (Xu et al., 2012). Drug-like (DL) indicate the characteristics that an ideal drug should have and was a comprehensive reflection of the physical and chemical properties and structural characteristics exhibited by successful drugs (Tao et al., 2013). In this study, active components from DSD, GFD, and HGWD were mainly filtered by integrating Lipinski's rules, oral bioavailability (OB), and drug-likeness (DL). The detail of Lipinski's rules includes molecular weight lower than 500 Da, number of donor hydrogen bonds less than 5, number of acceptor hydrogen bonds less than 10, the $\log P$ lower than 5 and over -2, and meets only the criteria of 10 or fewer rotatable bonds. Besides, oral bioavailability (OB), and drug-likeness (DL) also were employed to screen the active components. The components with OB values higher than 30% and DL values higher than 0.14 were retained for further investigation (Wang et al., 2018).

Networks Construction

The component-target (C-T) networks of three formulas were constructed by using Cytoscape software (Version 3.7.0) (Lopes et al., 2010). The topological parameters of networks were analyzed using Cytoscape plugin NetworkAnalyzer (Jong et al., 2003).

Detection of Key Gene Network Motif With Significant (KNMS)

The exploration of motif structures in networks is an important issue in many domains and disciplines. To find key gene network motifs with significant (KNMS) of 3 formulas in the treatment of RA, a mathematical algorithm was designed and described as follows:

To take advantage of the motif structure of the network, m motif codebooks, and one index codebook are used to describe the random walker's movements within and between motifs, respectively. Motif codebook i has one codeword for each node $\alpha \in i$ and one exit codeword. The codeword lengths are derived from the frequencies at which the random walker visits each of the nodes in the motif, $p_{\alpha \in i}$, and exits the motif, $q_{i \leftarrow}$. We use $p_{i \cup}$ to denote the sum of these frequencies, the total use of codewords in motif i , and P^i to denote the normalized probability distribution. Similarly, the index codebook has codewords for motif entries. The codeword lengths are derived from the set of frequencies at which the random walker enters each motif, $q_{i \leftarrow}$. We use q_{\leftarrow} to denote the sum of these frequencies, the total use of codewords to move into motifs, and Q to denote the normalized probability distribution. We want to express average length of codewords from the index codebook and the motif codebooks weighted by their rates of use. Therefore, the map equation is

$$L(M) = q_{\leftarrow} H(Q) + \sum_{i=1}^m p_{i \cup} H(p_i)$$

Below we explain the terms of the map equation in detail and we provide examples with Huffman codes for illustration.

$L(M)$ represents the per-step description length for motif partition M . That is, for motif partition M of n nodes into m

motifs, the lower bound of the average length of the code describing a step of the random walker.

$$q_{\leftarrow} = \sum_{i=1}^m q_{i \leftarrow}$$

The rate at which the index codebook is used. The per-step use rate of the index codebook is given by the total probability that the random walker enters any of them motifs. This variable represents the proportion of all codes representing motif names in the codes. Where $q_{i \leftarrow}$ is probability of jumping out of Motif i .

$$H(Q) = -\sum_{i=1}^m (q_{i \leftarrow} / q_{\leftarrow}) \log(q_{i \leftarrow} / q_{\leftarrow})$$

This variable represents the average byte length required to encode motif names. The frequency-weighted average length of codewords in the index codebook. The entropy of the relative rates to use the motif codebooks measures the smallest average codeword length that is theoretically possible. The heights of individual blocks under *Index codebook* correspond to the relative rates and the codeword lengths approximately correspond to the negative logarithm of the rates in base 2.

$$p_{i \cup} = \sum_{\alpha \in i} p_{\alpha} + q_{i \leftarrow}$$

This variable represents the coding proportion of all nodes (including jump-out nodes) belonging to motif i in the coding. The rate at which the motif codebook i is used, which is given by the total probability that any node in the motif is visited, plus the probability that the random walker exits the motif and the exit codeword is used.

$$H(p^i) = -(q_{i \leftarrow} / p_{i \cup}) \log(q_{i \leftarrow} / p_{i \cup}) - \sum_{\alpha \in i} (p_{\alpha} / p_{i \cup}) \log(p_{\alpha} / p_{i \cup})$$

This variable represents the average byte length required to encode all nodes in motif i . The frequency-weighted average length of codewords in motif codebook i . The entropy of the relative rates at which the random walker exits motif i and visits each node in motif i measures the smallest average codeword length that is theoretically possible. The heights of individual blocks under motif codebooks correspond to the relative rates and the codeword lengths approximately correspond to the negative logarithm of the rates in base 2.

Contribution Coefficient Calculation

The contribution coefficient (CC) represents the network contribution of KNMSs in 3 formulas. R value was used to determine the importance of the components by the following mathematical model:

$$R = \frac{d_c - d_c(\min)}{d_{c,\max} - d_c(\min)}$$

$$CC(i) = \frac{\sum_i^n R_i}{\sum_j^n R_j} \times 100\%$$

where d_c represents the degree of each component, which is calculated by Cytoscape. R is an indicator to evaluate the importance of the component.

Where n is the number of components from different KNMSs of DSD, GFD, and HGWD, respectively; m is the number of components from C-T network of DSD, GFD, and HGWD, respectively; R_i represents the indicator of each component in KNMSs of DSD, GFD, and HGWD, and R_j represents the indicator of each component in C-T network of DSD, GFD, and HGWD.

KEGG Pathway

To analyze the main function of the KNMSs, the pathway data were obtained from the Kyoto Encyclopedia of Genes and Genomes (KEGG) database (Draghici et al., 2007) for KEGG pathway enrichment analyses. P-values were set at 0.05 as the cut-off criterion. The results of analysis were annotated by Pathview (Luo and Brouwer, 2013) in the R Bioconductor package (<https://www.bioconductor.org/>).

Experimental Validation

Materials

Isoliquiritigenin, isorhamnetin and quercetin ($\geq 98\%$ purity by HPLC) was obtained from Chengdu Pufei De Biotech Co., Ltd (Chengdu, China). Fetal bovine serum (FBS) and Dulbecco's modified Eagle's medium (DMEM) were purchased from Gibco (Grand Island, USA). Lipopolysaccharide (LPS) was purchased from Sigma-Aldrich Co., Ltd (St Louis, USA).

Cell Culture and Treatment

RAW264.7 cells were obtained from the cell bank of the Chinese Academy of Sciences (Shanghai, China). The cells were cultured in DMEM with 10% FBS, and incubated at 37°C under $5\% \text{CO}_2$. When RAW264.7 cells reached 80% confluency, the cells were treated with isoliquiritigenin, isorhamnetin and quercetin for 2 h, then the cells were treated with LPS ($1 \mu\text{g/ml}$) for 24 h.

Cell Viability Assay

MTT assay was utilized to measure cell viability. RAW264.7 cells (6×10^4 per/well) were seeded in 96-well plates. After 24 h incubation, RAW264.7 cells were treated with 1, 5, 10, 20, 40, and $80 \mu\text{M}$ isoliquiritigenin, isorhamnetin and quercetin for 24 h. Ten μl of MTT were added to reach a final concentration of 0.5 mg/ml , and incubated for a further 4 h. The absorbance was measured at 570 nm with a microplate reader (BioTek, USA).

Measurement of NO

Griess reagent was utilized to detect the level of NO in the culture supernatant of RAW264.7 cells. After incubation with isoliquiritigenin, isorhamnetin and quercetin for 2 h and LPS ($1 \mu\text{g/ml}$) for 24 h, the culture supernatant was collected and mixed with Griess reagent for NO assay. The absorbance was measured at 540 nm using a microplate reader.

Statistical Analysis

To compare the importance of motifs in three formulas, SPSS22.0 was used for statistical analysis. One-way analysis of variance followed by a Dunnett post-hoc test was used to

compare more than two groups. Obtained p-values were corrected by Benjamini-Hochberg false discovery rate (FDR). Results were considered as statistically significant if the p-value was < 0.05 .

RESULTS

Chemical Analysis

Chemical analysis plays important roles in the study of substances basis and mechanism of herbs in the formulas. By searching from the literature, we collected the information on specific chemical identification and concentration of the herbs in DSD, GFD and HGWD, respectively. The detail information was shown in **Table 1** and **Table S1**. The results suggest that chemical components of herbs and the concentration of identified components provide an experiment-aided chemical space for search of active components. This will provide valuable reference for the further analysis.

Active Components in DSD, GFD, and HGWD

By a comprehensive search of the TCMSP, TCMID, and TCM@Taiwan database, 812 components from seven herbs in DSD, 640 components from five herbs in GFD, and 459 components from five herbs in HGWD were obtained. A TCM formula usually contains large number of components, and ADME screening approaches are always used to select active components. After ADME screening, 124 active components in DSD, 120 active components in GFD, and 48 active components in HGWD were passed the combined filtering criteria which integrated by Lipinski's rule, OB, and DL (**Table 2**). For further analysis of these active components, 31 common components in three formulas and 93, 89, and 17 unique components in DSD, GFD, and HGWD were found (**Figure 2**). These results indicate that three formulas might exert roles in treating RA by affecting the common components and specific components.

C-T Network Construction

To facilitate analysis of the complex relationships between active components and their targets of three formulas, component-target networks were constructed by using Cytoscape (**Figures S1–S3**). The results revealed that the DSD network consisted of 124 active components, 846 target proteins, and 3758 interactions; the GFD network contained 120 active components, 821 target proteins, and 3759 interactions; the HGWD network consisted of 48 active components, 612 target proteins, and 1373 interactions.

We further analyzed the topology parameters of these C-T networks using NetworkAnalyzer and found that the average degree of components and targets in DSD were 30.31 and 5.20; the average degree of components and targets in GFD were 31.33 and 5.36; the average degree of components and targets in HGWD were 28.6 and 2.43. These results indicate that there exist interactions between one component and multiple targets

TABLE 1 | The information on chemical analysis of the herbs from the literature in DSD, GFD, and HGWD.

Herb	Method	Component	Concentration	Formula	Ref.
<i>Angelica sinensis</i> (Oliv.) Diels (Danggui)	HPLC	Ferulic acid	0.36 mg/g	DSD	Xie et al., 2007
		Coniferylferulate	6.11 mg/g		
		Z-ligustilide	4.34 mg/g		
		E-ligustilide	0.23 mg/g		
		Z-3-butylidenephthalide	0.20 mg/g		
<i>Cinnamomum cassia</i> (L.) J. Presl (Cinnamomi ramulus, Guizhi)	UHPLC	E-3-butylidenephthalide	0.08 mg/g	DSD, GFD, HGWD	Liang et al., 2011
		Protocatechuic acid	0.11 mg/g		
		Coumarin	0.84 mg/g		
		Cinnamic alcohol	0.04 mg/g		
		Cinnamic acid	0.68 mg/g		
<i>Paeonia lactiflora</i> Pall. (Baishao)	HPLC	Cinnamaldehyde	9.93 mg/g	DSD, HGWD	Li et al., 2011
		Gallic acid	2.33 mg/g		
		Hydroxyl-paeoniflorin	1.89 mg/g		
		Catechin	0.03 mg/g		
		Albiflorin	4.44 mg/g		
		Paeoniflorin	4.81 mg/g		
		Benzoic acid	0.03 mg/g		
		1, 2, 3, 4, 6 -pentagalloylglucose	4.80 mg/g		
		Benzoyl -paeoniflorin	0.11 mg/g		
		Paeonol	0.07 mg/g		
<i>Asarum sieboldii</i> Miq. (Xixin)	HPLC	Aristolochic acid A	0.009 mg/g	DSD	Gao et al., 2005
<i>Glycyrrhiza uralensis</i> Fisch. ex DC. (Gancao)	HPLC	Glycyrrhizin	97.49 mg/g	DSD, GFD	Chen et al., 2009
		Liquiritin	102.83 mg/g		
<i>Tetrapanax papyrifer</i> (Hook.) K.Koch (Medulla tetrapanacis, Tongcao)	RP- HPLC	Lsoliquritigenin	98.30 mg/g	DSD	Gao et al., 2007
		Calceolar ioside B	0.86 mg/g		
<i>Ziziphus jujuba</i> Mill. (Jujubae fructus (Dazao)	HPLC	Rutin	0.21 mg/g	DSD, GFD, HGWD	Wang et al., 2013
		Quercetin	0.008 mg/g		
		Isorhamnetin	0.17 mg/g		
		aconitine	0.28 mg/g		
<i>Aconitum carmichaeli</i> Debeaux (Aconiti lateralis radix praeparata, Fuzi)	HPLC	hypaconitine	0.70 mg/g	GFD	Sun et al., 2009
		mesaconitine	1.04 mg/g		
		benzoylaconine	0.009 mg/g		
		benzoylhypaconine	0.007 mg/g		
		benzoylmesaconin	0.07 mg/g		
<i>Zingiber officinale</i> Roscoe (Shengjiang)	HPLC	6-Gingerol	16.62 mg/g	GFD, HGWD	Zhang et al., 2009
		6-Shogaol	4.92 mg/g		
<i>Astragalus mongholicus</i> Bunge (Huangqi)	HPLC	Campanulin	0.42 mg/g	HGWD	Li et al., 2015
		Formononetin	0.02 mg/g		

in three formulas, and also exist phenomenon that different components act on the same target, which is in line with the characteristics of multi-component and multi-target mediated synergistic effect of TCM, and also reflects the complexity of the mechanism of TCM.

KNMSs Predication and Validation

KNMSs Predication

These C-T networks are complex and huge. How to quickly extract important information from these complex networks is the key step to decode underlying molecular mechanism. Here, we introduced the infomap algorithm in the network pharmacology model for the first time based on the random walk theory combined with Huffman-encoding. The algorithm performs to optimize the discovery of KNMSs in C-T network heuristically by using a reasonable global metric. 7, 10, and 10 KNMSs were predicted in DSD, GFD, and HGWD, respectively (p value < 0.05) (Figures 3–5). The detail information of network KNMSs were shown in Table S2.

KNMSs Validation

In order to validate whether predicted KNMSs in each formula can represent corresponding full C-T networks in treating RA. Three strategies were used to verify the accuracy and reliability and of KNMSs. The first strategy was used to see whether the number of RA pathogenic genes in KNMSs are close to the number of RA pathogenic genes in CT network. The coverage was defined as the percentage of the number of pathogenic genes in KNMSs to the number of pathogenic genes in C-T network. High coverage indicated that KNMSs could retain most formula-targeted RA pathogenic genes that included in the corresponding C-T network. The second strategy was designed to see whether the gene enrichment pathways in KNMSs covers the gene enrichment pathways in C-T network as much as possible. High coverage indicated that KNMSs could cover most genes enriched pathways of the corresponding C-T network. The third strategy was employed to calculate the percentage of cumulative contribution of important nodes in KNMSs to that of nodes in C-T network. High percentage means KNMSs can retain the

TABLE 2 | Components in DSD, GFD, and HGWD for further analysis after ADME screening.

ID	Component	MW	Logp	HDON	HACC	RBN	OB	DL	Source
DSD1	(+)-catechin	290.29	1.02	5	6	1	54.83	0.24	Baishao
DSD2	(3S,5R,8R,9R,10S,14S)-3,17-dihydroxy-4,4,8,10,14-pentamethyl-2,3,5,6,7,9-hexahydro-1H-cyclopenta[a]phenanthrene-15,16-dione	358.52	3.52	2	4	0	43.56	0.53	Baishao
DSD3	11alpha,12alpha-epoxy-3beta-23-dihydroxy-30-norolean-20-en-28,12beta-olide	470.71	3.82	2	5	1	64.77	0.38	Baishao
DSD4	albiflorin_qt	318.35	0.53	2	6	4	66.64	0.33	Baishao
DSD5	kaempferol	286.25	1.23	4	6	1	41.88	0.24	Baishao
DSD6	Lactiflorin	462.49	0.31	3	10	5	49.12	0.8	Baishao
DSD7	paeoniflorgenone	318.35	0.86	1	6	4	87.59	0.37	Baishao
DSD8	paeoniflorin_qt	318.35	0.69	2	6	4	68.18	0.4	Baishao
DSD9	(-)-catechin	290.29	1.02	5	6	1	49.68	0.24	Dazao
DSD10	(S)-Coclaurine	285.37	2.2	3	4	3	42.35	0.24	Dazao
DSD11	21302-79-4	486.76	4.53	3	5	3	73.52	0.77	Dazao
DSD12	berberine	336.39	3.75	0	4	2	36.86	0.78	Dazao
DSD13	coumestrol	268.23	2.43	2	5	0	32.49	0.34	Dazao
DSD14	Fumarine	353.4	1.95	0	6	0	59.26	0.83	Dazao
DSD15	Jujubasaponin V_qt	472.78	4.61	2	4	2	36.99	0.63	Dazao
DSD16	jujuboside A_qt	472.78	3.8	2	4	1	36.67	0.62	Dazao
DSD17	Jujuboside C_qt	472.78	3.8	2	4	1	40.26	0.62	Dazao
DSD18	malkangunin	432.56	2.72	2	7	6	57.71	0.63	Dazao
DSD19	Mauritine D	342.46	1.11	2	6	2	89.13	0.45	Dazao
DSD20	Moupinamide	313.38	2.46	3	5	6	86.71	0.26	Dazao
DSD21	Nuciferin	295.41	3.38	0	3	2	34.43	0.4	Dazao
DSD22	quercetin	302.25	1.07	5	7	1	46.43	0.28	Dazao
DSD23	Ruvoside_qt	390.57	1.42	3	5	2	36.12	0.76	Dazao
DSD24	Spiradine A	311.46	1.29	1	3	0	113.52	0.61	Dazao
DSD25	stepharine	297.38	1.76	1	4	2	31.55	0.33	Dazao
DSD26	Stepholidine	327.41	2.26	2	5	2	33.11	0.54	Dazao
DSD27	Ziziphin_qt	472.78	3.8	2	4	1	66.95	0.62	Dazao
DSD28	zizyphus saponin I_qt	472.78	3.8	2	4	1	32.69	0.62	Dazao
DSD29	2,6-di(phenyl)thiopyran-4-thione	280.43	4.39	0	0	2	69.13	0.15	Danggui
DSD30	(-)-Medicocarpin	432.46	1.26	4	9	4	40.99	0.95	Gancao
DSD31	(2R)-7-hydroxy-2-(4-hydroxyphenyl)chroman-4-one	256.27	2.79	2	4	1	71.12	0.18	Gancao
DSD32	(2S)-6-(2,4-dihydroxyphenyl)-2-(2-hydroxypropan-2-yl)-4-methoxy-2,3-dihydrofuro[3,2-g]chromen-7-one	384.41	2.61	3	7	3	60.25	0.63	Gancao
DSD33	(2S)-7-hydroxy-2-(4-hydroxyphenyl)-8-(3-methylbut-2-enyl)chroman-4-one	324.4	3.62	2	4	3	36.57	0.32	Gancao
DSD34	(E)-1-(2,4-dihydroxyphenyl)-3-(2,2-dimethylchromen-6-yl)prop-2-en-1-one	322.38	4.46	2	4	3	39.62	0.35	Gancao
DSD35	(E)-3-[3,4-dihydroxy-5-(3-methylbut-2-enyl)phenyl]-1-(2,4-dihydroxyphenyl)prop-2-en-1-one	340.4	3.47	4	5	5	46.27	0.31	Gancao
DSD36	1,3-dihydroxy-8,9-dimethoxy-6-benzofurano[3,2-c]chromenone	328.29	2.74	2	7	2	62.9	0.53	Gancao
DSD37	1,3-dihydroxy-9-methoxy-6-benzofurano[3,2-c]chromenone	298.26	2.48	2	6	1	48.14	0.43	Gancao
DSD38	18α-hydroxyglycyrrhetic acid	486.76	4.54	3	5	1	41.16	0.71	Gancao
DSD39	1-Methoxyphaseollidin	354.43	3.66	2	5	3	69.98	0.64	Gancao
DSD40	2-(3,4-dihydroxyphenyl)-5,7-dihydroxy-6-(3-methylbut-2-enyl)chromone	354.38	2.99	4	6	3	44.15	0.41	Gancao
DSD41	2-[(3R)-8,8-dimethyl-3,4-dihydro-2H-pyrano[6,5-f]chromen-3-yl]-5-methoxyphenol	338.43	4.35	1	4	2	36.21	0.52	Gancao
DSD42	3-(2,4-dihydroxyphenyl)-8-(1,1-dimethylprop-2-enyl)-7-hydroxy-5-methoxy-coumarin	368.41	3.92	3	6	4	59.62	0.43	Gancao
DSD43	3-(3,4-dihydroxyphenyl)-5,7-dihydroxy-8-(3-methylbut-2-enyl)chromone	354.38	3.02	4	6	3	66.37	0.41	Gancao

(Continued)

TABLE 2 | Continued

ID	Component	MW	Logp	HDON	HACC	RBN	OB	DL	Source
DSD44	3'-Hydroxy-4'-O-Methylglabridin	354.43	3.76	2	5	2	43.71	0.57	Gancao
DSD45	3'-Methoxyglabridin	354.43	3.76	2	5	2	46.16	0.57	Gancao
DSD46	5,7-dihydroxy-3-(4-methoxyphenyl)-8-(3-methylbut-2-enyl)chromone	352.41	3.29	2	5	4	30.49	0.41	Gancao
DSD47	6-prenylated eriodictyol	356.4	2.99	4	6	3	39.22	0.41	Gancao
DSD48	7,2',4'-trihydroxy-5-methoxy-3-aryl coumarin	300.28	2.51	3	6	2	83.71	0.27	Gancao
DSD49	7-Acetoxy-2-methylisoflavone	294.32	3.41	0	4	3	38.92	0.26	Gancao
DSD50	7-Methoxy-2-methyl isoflavone	266.31	3.48	0	3	2	42.56	0.2	Gancao
DSD51	8-(6-hydroxy-2-benzofuranyl)-2,2-dimethyl-5-chromenol	308.35	4.27	2	4	1	58.44	0.38	Gancao
DSD52	8-prenylated eriodictyol	356.4	2.99	4	6	3	53.79	0.4	Gancao
DSD53	Calycosin	284.28	2.82	2	5	2	47.75	0.24	Gancao
DSD54	dehydroglyasperins C	340.4	3.11	4	5	3	53.82	0.37	Gancao
DSD55	DFV	256.27	2.79	2	4	1	32.76	0.18	Gancao
DSD56	echinatin	270.3	3.41	2	4	4	66.58	0.17	Gancao
DSD57	Eurycarpin A	338.38	3.29	3	5	3	43.28	0.37	Gancao
DSD58	formononetin	268.28	3.01	1	4	2	69.67	0.21	Gancao
DSD59	Gancaonin A	352.41	3.34	2	5	4	51.08	0.4	Gancao
DSD60	Gancaonin B	368.41	3.14	3	6	4	48.79	0.45	Gancao
DSD61	Gancaonin G	352.41	3.25	2	5	4	60.44	0.39	Gancao
DSD62	Gancaonin H	420.49	3.99	3	6	3	50.1	0.78	Gancao
DSD63	Glabranin	324.4	3.59	2	4	3	52.9	0.31	Gancao
DSD64	Glabrene	322.38	3.68	2	4	1	46.27	0.44	Gancao
DSD65	Glabridin	324.4	3.81	2	4	1	53.25	0.47	Gancao
DSD66	Glabrone	336.36	3.78	2	5	1	52.51	0.5	Gancao
DSD67	Glepidotin A	338.38	2.88	3	5	3	44.72	0.35	Gancao
DSD68	Glepidotin B	340.4	2.88	3	5	3	64.46	0.34	Gancao
DSD69	glyasperin B	370.43	3.14	3	6	4	65.22	0.44	Gancao
DSD70	Glyasperin C	356.45	3.53	3	5	4	45.56	0.4	Gancao
DSD71	glyasperin F	354.38	3.52	3	6	1	75.84	0.54	Gancao
DSD72	Glyasperins M	368.41	3.57	2	6	2	72.67	0.59	Gancao
DSD73	Glycyrin	382.44	3.78	2	6	5	52.61	0.47	Gancao
DSD74	Glycyrol	366.39	4.06	2	6	3	90.78	0.67	Gancao
DSD75	Glycyrrhiza flavonol A	370.38	2.18	4	7	1	41.28	0.6	Gancao
DSD76	Glypallichalcone	284.33	3.8	1	4	5	61.6	0.19	Gancao
DSD77	Glyzaglabrin	298.26	2.32	2	6	1	61.07	0.35	Gancao
DSD78	HMO	268.28	2.92	1	4	2	38.37	0.21	Gancao
DSD79	Inermine	284.28	2.19	1	5	0	75.18	0.54	Gancao
DSD80	Inflacoumarin A	322.38	4.36	2	4	3	39.71	0.33	Gancao
DSD81	Isoglycyrol	366.39	4.15	1	6	1	44.7	0.84	Gancao
DSD82	Isolicoiflavanol	354.38	2.92	4	6	3	45.17	0.42	Gancao
DSD83	isoliquiritigenin	256.27	3.04	3	4	3	85.32	0.15	Gancao
DSD84	isorhamnetin	316.28	1.31	4	7	2	49.6	0.31	Gancao
DSD85	Isotrifoliol	298.26	2.54	2	6	1	31.94	0.42	Gancao
DSD86	Jaranol	314.31	2.8	2	6	3	50.83	0.29	Gancao
DSD87	kanzonols W	336.36	3.97	2	5	1	50.48	0.52	Gancao
DSD88	Licoagrocarpin	338.43	3.94	1	4	3	58.81	0.58	Gancao
DSD89	Licoagroisoflavone	336.36	2.95	2	5	2	57.28	0.49	Gancao
DSD90	licochalcone a	338.43	4.74	2	4	6	40.79	0.29	Gancao
DSD91	Licochalcone B	286.3	3.17	3	5	4	76.76	0.19	Gancao
DSD92	licochalcone G	354.43	4.21	3	5	6	49.25	0.32	Gancao
DSD93	Licocoumarone	340.4	4.1	3	5	4	33.21	0.36	Gancao
DSD94	licoisoflavanone	354.38	3.54	3	6	1	52.47	0.54	Gancao
DSD95	Licoisoflavone	354.38	2.99	4	6	3	41.61	0.42	Gancao
DSD96	Licoisoflavone B	352.36	3.54	3	6	1	38.93	0.55	Gancao
DSD97	licopyranocoumarin	384.41	2.47	3	7	3	80.36	0.65	Gancao
DSD98	Licoricone	382.44	3.08	2	6	5	63.58	0.47	Gancao
DSD99	liquiritin	418.43	0.43	5	9	4	65.69	0.74	Gancao
DSD100	Lupiwighteone	338.38	3.23	3	5	3	51.64	0.37	Gancao
DSD101	Medicarpin	270.3	3.07	1	4	1	49.22	0.34	Gancao
DSD102	naringenin	272.27	2.47	3	5	1	59.29	0.21	Gancao
DSD103	Odoratin	314.31	2.81	2	6	3	49.95	0.3	Gancao

(Continued)

TABLE 2 | Continued

ID	Component	MW	Logp	HDON	HACC	RBN	OB	DL	Source
DSD104	Phaseol	336.36	4.59	2	5	2	78.77	0.58	Gancao
DSD105	Phaseolinisoflavan	324.4	3.77	2	4	1	32.01	0.45	Gancao
DSD106	Pinocebrin	256.27	2.85	2	4	1	64.72	0.18	Gancao
DSD107	Quercetin der.	330.31	2.55	3	7	3	46.45	0.33	Gancao
DSD108	Semilicoisoflavone B	352.36	3.55	3	6	1	48.78	0.55	Gancao
DSD109	shinpterocarpin	322.38	4.13	1	4	0	80.3	0.73	Gancao
DSD110	Sigmoidin-B	356.4	3.02	4	6	3	34.88	0.41	Gancao
DSD111	Vestitol	272.32	2.89	2	4	2	74.66	0.21	Gancao
DSD112	ent-Epicatechin	290.29	2.83	5	6	1	48.96	0.24	Guizhi
DSD113	beta-sitosterol	414.79	3.2	1	1	6	36.91	0.75	Guizhi
DSD114	sitosterol	414.79	2.71	1	1	6	36.91	0.75	Guizhi
DSD115	(-)-taxifolin	304.27	1.66	5	7	1	60.51	0.27	Guizhi
DSD116	DMEP	282.32	1.93	0	6	10	55.66	0.15	Guizhi
DSD117	paryriogenin A	466.72	4.62	1	4	1	41.41	0.76	Tongcao
DSD118	(3S)-7-hydroxy-3-(2,3,4-trimethoxyphenyl)chroman-4-one	330.36	1.59	1	6	4	48.23	0.33	Xixin
DSD119	[(1S)-3-[(E)-but-2-enyl]-2-methyl-4-oxo-1-cyclopent-2-enyl] (1R,3R)-3-[(E)-3-methoxy-2-methyl-3-oxoprop-1-enyl]-2,2-dimethylcyclopropane-1-carboxylate	360.49	4.18	0	5	8	62.52	0.31	Xixin
DSD120	4,9-dimethoxy-1-vinyl-5b-carboline	254.31	2.96	0	3	3	65.3	0.19	Xixin
DSD121	Carbine	326.43	0.53	2	5	0	37.06	0.83	Xixin
DSD122	Cryptopin	369.45	2.38	0	6	2	78.74	0.72	Xixin
DSD123	sesamin	354.38	2.25	0	6	2	56.55	0.83	Xixin
DSD124	ZINC05223929	354.38	2.25	0	6	2	31.57	0.83	Xixin
GFD1	(-)-catechin	290.29	1.02	5	6	1	49.68	0.24	Dazao
GFD2	(+)-catechin	290.29	1.02	5	6	1	54.83	0.24	Dazao
GFD3	(S)-Coclaurine	285.37	2.2	3	4	3	42.35	0.24	Dazao
GFD4	21302-79-4	486.76	4.53	3	5	3	73.52	0.77	Dazao
GFD5	berberine	336.39	3.75	0	4	2	36.86	0.78	Dazao
GFD6	coumestrol	268.23	2.43	2	5	0	32.49	0.34	Dazao
GFD7	Fumarine	353.4	1.95	0	6	0	59.26	0.83	Dazao
GFD8	Jujubasaponin V_qt	472.78	4.61	2	4	2	36.99	0.63	Dazao
GFD9	jujuboside A_qt	472.78	3.8	2	4	1	36.67	0.62	Dazao
GFD10	Jujuboside C_qt	472.78	3.8	2	4	1	40.26	0.62	Dazao
GFD11	malkangunin	432.56	2.72	2	7	6	57.71	0.63	Dazao
GFD12	Mauritine D	342.46	1.11	2	6	2	89.13	0.45	Dazao
GFD13	Moupinamide	313.38	2.46	3	5	6	86.71	0.26	Dazao
GFD14	Nuciferin	295.41	3.38	0	3	2	34.43	0.4	Dazao
GFD15	quercetin	302.25	1.07	5	7	1	46.43	0.28	Dazao
GFD16	Ruvoside_qt	390.57	1.42	3	5	2	36.12	0.76	Dazao
GFD17	Spiradine A	311.46	1.29	1	3	0	113.52	0.61	Dazao
GFD18	stepharine	297.38	1.76	1	4	2	31.55	0.33	Dazao
GFD19	Stepholidine	327.41	2.26	2	5	2	33.11	0.54	Dazao
GFD20	Ziziphin_qt	472.78	3.8	2	4	1	66.95	0.62	Dazao
GFD21	zizyphus saponin I_qt	472.78	3.8	2	4	1	32.69	0.62	Dazao
GFD22	(-)-Medicocarpin	432.46	1.26	4	9	4	40.99	0.95	Gancao
GFD23	(2R)-7-hydroxy-2-(4-hydroxyphenyl)chroman-4-one	256.27	2.79	2	4	1	71.12	0.18	Gancao
GFD24	(2S)-6-(2,4-dihydroxyphenyl)-2-(2-hydroxypropan-2-yl)-4-methoxy-2,3-dihydrofuro[3,2-g]chromen-7-one	384.41	2.61	3	7	3	60.25	0.63	Gancao
GFD25	(2S)-7-hydroxy-2-(4-hydroxyphenyl)-8-(3-methylbut-2-enyl)chroman-4-one	324.4	3.62	2	4	3	36.57	0.32	Gancao
GFD26	(E)-1-(2,4-dihydroxyphenyl)-3-(2,2-dimethylchromen-6-yl)prop-2-en-1-one	322.38	4.46	2	4	3	39.62	0.35	Gancao
GFD27	(E)-3-[3,4-dihydroxy-5-(3-methylbut-2-enyl)phenyl]-1-(2,4-dihydroxyphenyl)prop-2-en-1-one	340.4	3.47	4	5	5	46.27	0.31	Gancao
GFD28	1,3-dihydroxy-8,9-dimethoxy-6-benzofurano[3,2-c]chromenone	328.29	2.74	2	7	2	62.9	0.53	Gancao

(Continued)

TABLE 2 | Continued

ID	Component	MW	Logp	HDON	HACC	RBN	OB	DL	Source
GFD29	1,3-dihydroxy-9-methoxy-6-benzofurano[3,2-c]chromenone	298.26	2.48	2	6	1	48.14	0.43	Gancao
GFD30	18 α -hydroxyglycyrrhetic acid	486.76	4.54	3	5	1	41.16	0.71	Gancao
GFD31	1-Methoxyphaseollidin	354.43	3.66	2	5	3	69.98	0.64	Gancao
GFD32	2-(3,4-dihydroxyphenyl)-5,7-dihydroxy-6-(3-methylbut-2-enyl)chromone	354.38	2.99	4	6	3	44.15	0.41	Gancao
GFD33	2-[(3R)-8,8-dimethyl-3,4-dihydro-2H-pyrano[6,5-f]chromen-3-yl]-5-methoxyphenol	338.43	4.35	1	4	2	36.21	0.52	Gancao
GFD34	3-(2,4-dihydroxyphenyl)-8-(1,1-dimethylprop-2-enyl)-7-hydroxy-5-methoxy-coumarin	368.41	3.92	3	6	4	59.62	0.43	Gancao
GFD35	3-(3,4-dihydroxyphenyl)-5,7-dihydroxy-8-(3-methylbut-2-enyl)chromone	354.38	3.02	4	6	3	66.37	0.41	Gancao
GFD36	3'-Hydroxy-4'-O-Methylglabridin	354.43	3.76	2	5	2	43.71	0.57	Gancao
GFD37	3'-Methoxyglabridin	354.43	3.76	2	5	2	46.16	0.57	Gancao
GFD38	5,7-dihydroxy-3-(4-methoxyphenyl)-8-(3-methylbut-2-enyl)chromone	352.41	3.29	2	5	4	30.49	0.41	Gancao
GFD39	6-prenylated eriodictyol	356.4	2.99	4	6	3	39.22	0.41	Gancao
GFD40	7,2',4'-trihydroxy-5-methoxy-3-aryl coumarin	300.28	2.51	3	6	2	83.71	0.27	Gancao
GFD41	7-Acetoxy-2-methylisoflavone	294.32	3.41	0	4	3	38.92	0.26	Gancao
GFD42	7-Methoxy-2-methyl isoflavone	266.31	3.48	0	3	2	42.56	0.2	Gancao
GFD43	8-(6-hydroxy-2-benzofuranyl)-2,2-dimethyl-5-chromenol	308.35	4.27	2	4	1	58.44	0.38	Gancao
GFD44	8-prenylated eriodictyol	356.4	2.99	4	6	3	53.79	0.4	Gancao
GFD45	Calycosin	284.28	2.82	2	5	2	47.75	0.24	Gancao
GFD46	dehydroglyasperins C	340.4	3.11	4	5	3	53.82	0.37	Gancao
GFD47	DFV	256.27	2.79	2	4	1	32.76	0.18	Gancao
GFD48	echinatin	270.3	3.41	2	4	4	66.58	0.17	Gancao
GFD49	Eurycarpin A	338.38	3.29	3	5	3	43.28	0.37	Gancao
GFD50	formononetin	268.28	3.01	1	4	2	69.67	0.21	Gancao
GFD51	Gancaonin A	352.41	3.34	2	5	4	51.08	0.4	Gancao
GFD52	Gancaonin B	368.41	3.14	3	6	4	48.79	0.45	Gancao
GFD53	Gancaonin G	352.41	3.25	2	5	4	60.44	0.39	Gancao
GFD54	Gancaonin H	420.49	3.99	3	6	3	50.1	0.78	Gancao
GFD55	Glabranin	324.4	3.59	2	4	3	52.9	0.31	Gancao
GFD56	Glabrene	322.38	3.68	2	4	1	46.27	0.44	Gancao
GFD57	Glabridin	324.4	3.81	2	4	1	53.25	0.47	Gancao
GFD58	Glabrone	336.36	3.78	2	5	1	52.51	0.5	Gancao
GFD59	Glepidotin A	338.38	2.88	3	5	3	44.72	0.35	Gancao
GFD60	Glepidotin B	340.4	2.88	3	5	3	64.46	0.34	Gancao
GFD61	glyasperin B	370.43	3.14	3	6	4	65.22	0.44	Gancao
GFD62	Glyasperin C	356.45	3.53	3	5	4	45.56	0.4	Gancao
GFD63	glyasperin F	354.38	3.52	3	6	1	75.84	0.54	Gancao
GFD64	Glyasperins M	368.41	3.57	2	6	2	72.67	0.59	Gancao
GFD65	Glycyrin	382.44	3.78	2	6	5	52.61	0.47	Gancao
GFD66	Glycyrol	366.39	4.06	2	6	3	90.78	0.67	Gancao
GFD67	Glycyrrhiza flavonol A	370.38	2.18	4	7	1	41.28	0.6	Gancao
GFD68	Glypallichalcone	284.33	3.8	1	4	5	61.6	0.19	Gancao
GFD69	Glyzaglabrin	298.26	2.32	2	6	1	61.07	0.35	Gancao
GFD70	HMO	268.28	2.92	1	4	2	38.37	0.21	Gancao
GFD71	Inermine	284.28	2.19	1	5	0	75.18	0.54	Gancao
GFD72	Inflacoumarin A	322.38	4.36	2	4	3	39.71	0.33	Gancao
GFD73	Isoglycyrol	366.39	4.15	1	6	1	44.7	0.84	Gancao
GFD74	Isolicoflavonol	354.38	2.92	4	6	3	45.17	0.42	Gancao
GFD75	isoliquritigenin	256.27	3.04	3	4	3	85.32	0.15	Gancao
GFD76	isorhamnetin	316.28	1.31	4	7	2	49.6	0.31	Gancao
GFD77	Isotrifoliol	298.26	2.54	2	6	1	31.94	0.42	Gancao
GFD78	Jaranol	314.31	2.8	2	6	3	50.83	0.29	Gancao
GFD79	kaempferol	286.25	1.23	4	6	1	41.88	0.24	Gancao
GFD80	kanzonols W	336.36	3.97	2	5	1	50.48	0.52	Gancao
GFD81	Licoagrocarpin	338.43	3.94	1	4	3	58.81	0.58	Gancao

(Continued)

TABLE 2 | Continued

ID	Component	MW	Logp	HDON	HACC	RBN	OB	DL	Source
GFD82	Licoagrosiflavone	336.36	2.95	2	5	2	57.28	0.49	Gancao
GFD83	llicoalcone a	338.43	4.74	2	4	6	40.79	0.29	Gancao
GFD84	Licoalcone B	286.3	3.17	3	5	4	76.76	0.19	Gancao
GFD85	llicoalcone G	354.43	4.21	3	5	6	49.25	0.32	Gancao
GFD86	Licocoumarone	340.4	4.1	3	5	4	33.21	0.36	Gancao
GFD87	llicoiflavanone	354.38	3.54	3	6	1	52.47	0.54	Gancao
GFD88	Licoiflavone	354.38	2.99	4	6	3	41.61	0.42	Gancao
GFD89	Licoiflavone B	352.36	3.54	3	6	1	38.93	0.55	Gancao
GFD90	licopyranocoumarin	384.41	2.47	3	7	3	80.36	0.65	Gancao
GFD91	Licoricone	382.44	3.08	2	6	5	63.58	0.47	Gancao
GFD92	liquiritin	418.43	0.43	5	9	4	65.69	0.74	Gancao
GFD93	Lupiwighteone	338.38	3.23	3	5	3	51.64	0.37	Gancao
GFD94	Medicarpin	270.3	3.07	1	4	1	49.22	0.34	Gancao
GFD95	naringenin	272.27	2.47	3	5	1	59.29	0.21	Gancao
GFD96	Odoratin	314.31	2.81	2	6	3	49.95	0.3	Gancao
GFD97	Phaseol	336.36	4.59	2	5	2	78.77	0.58	Gancao
GFD98	Phaseolinisoflavan	324.4	3.77	2	4	1	32.01	0.45	Gancao
GFD99	Pinocembrin	256.27	2.85	2	4	1	64.72	0.18	Gancao
GFD100	Quercetin der.	330.31	2.55	3	7	3	46.45	0.33	Gancao
GFD101	Semilicoisoflavone B	352.36	3.55	3	6	1	48.78	0.55	Gancao
GFD102	shinpterocarpin	322.38	4.13	1	4	0	80.3	0.73	Gancao
GFD103	Sigmoidin-B	356.4	3.02	4	6	3	34.88	0.41	Gancao
GFD104	Vestitol	272.32	2.89	2	4	2	74.66	0.21	Gancao
GFD105	ent-Epicatechin	290.29	2.83	5	6	1	48.96	0.24	Guizhi
GFD106	beta-sitosterol	414.79	3.2	1	1	6	36.91	0.75	Guizhi
GFD107	sitosterol	414.79	2.71	1	1	6	36.91	0.75	Guizhi
GFD108	(-)-taxifolin	304.27	1.66	5	7	1	60.51	0.27	Guizhi
GFD109	DMEP	282.32	1.93	0	6	10	55.66	0.15	Guizhi
GFD110	6-gingerol	294.43	3.45	2	4	10	35.64	0.16	Shengjiang
GFD111	6-shogaol	276.41	4.95	1	3	9	31	0.14	Shengjiang
GFD112	(R)-Norcoclaurine	271.34	1.73	4	4	2	82.54	0.21	Fuzi
GFD113	6-Demethyldesoline	453.64	-0.53	4	8	5	51.87	0.66	Fuzi
GFD114	benzoylnapelline	463.67	2.9	2	5	4	34.06	0.53	Fuzi
GFD115	Deltoin	328.39	2.95	0	5	4	46.69	0.37	Fuzi
GFD116	Deoxyandrographolide	334.5	2.71	2	4	4	56.3	0.31	Fuzi
GFD117	ignavine	449.59	0.72	3	6	3	84.08	0.25	Fuzi
GFD118	isotalatizidine	407.61	0.41	3	6	4	50.82	0.73	Fuzi
GFD119	karakoline	377.58	0.8	3	5	2	51.73	0.73	Fuzi
GFD120	Karanjin	292.3	3.42	0	4	2	69.56	0.34	Fuzi
HGWD1	(+)-catechin	290.29	1.02	5	6	1	54.83	0.24	Baishao
HGWD2	(3S,5R,8R,9R,10S,14S)-3,17-dihydroxy-4,4,8,10,14-pentamethyl-2,3,5,6,7,9-hexahydro-1H-cyclopenta[a]phenanthrene-15,16-dione	358.52	3.52	2	4	0	43.56	0.53	Baishao
HGWD3	11alpha,12alpha-epoxy-3beta-23-dihydroxy-30-norolean-20-en-28,12beta-olide	470.71	3.82	2	5	1	64.77	0.38	Baishao
HGWD4	albiflorin_qt	318.35	0.53	2	6	4	66.64	0.33	Baishao
HGWD5	kaempferol	286.25	1.23	4	6	1	41.88	0.24	Baishao
HGWD6	Lactiflorin	462.49	0.31	3	10	5	49.12	0.8	Baishao
HGWD7	paeoniflorgenone	318.35	0.86	1	6	4	87.59	0.37	Baishao
HGWD8	paeoniflorin_qt	318.35	0.69	2	6	4	68.18	0.4	Baishao
HGWD9	(-)-catechin	290.29	1.02	5	6	1	49.68	0.24	Dazao
HGWD10	(S)-Coclaurine	285.37	2.2	3	4	3	42.35	0.24	Dazao
HGWD11	21302-79-4	486.76	4.53	3	5	3	73.52	0.77	Dazao
HGWD12	berberine	336.39	3.75	0	4	2	36.86	0.78	Dazao
HGWD13	coumestrol	268.23	2.43	2	5	0	32.49	0.34	Dazao
HGWD14	Fumarine	353.4	1.95	0	6	0	59.26	0.83	Dazao
HGWD15	Jujubasaponin V_qt	472.78	4.61	2	4	2	36.99	0.63	Dazao
HGWD16	jujuboside A_qt	472.78	3.8	2	4	1	36.67	0.62	Dazao
HGWD17	Jujuboside C_qt	472.78	3.8	2	4	1	40.26	0.62	Dazao
HGWD18	malkangunin	432.56	2.72	2	7	6	57.71	0.63	Dazao
HGWD19	Mauritine D	342.46	1.11	2	6	2	89.13	0.45	Dazao

(Continued)

TABLE 2 | Continued

ID	Component	MW	Logp	HDON	HACC	RBN	OB	DL	Source
HGWD20	Moupinamide	313.38	2.46	3	5	6	86.71	0.26	Dazao
HGWD21	Nuciferin	295.41	3.38	0	3	2	34.43	0.4	Dazao
HGWD22	quercetin	302.25	1.07	5	7	1	46.43	0.28	Dazao
HGWD23	Ruvoside_qt	390.57	1.42	3	5	2	36.12	0.76	Dazao
HGWD24	Spiradine A	311.46	1.29	1	3	0	113.52	0.61	Dazao
HGWD25	stepharine	297.38	1.76	1	4	2	31.55	0.33	Dazao
HGWD26	Stepholidine	327.41	2.26	2	5	2	33.11	0.54	Dazao
HGWD27	Ziziphin_qt	472.78	3.8	2	4	1	66.95	0.62	Dazao
HGWD28	zizyphus saponin l_qt	472.78	3.8	2	4	1	32.69	0.62	Dazao
HGWD29	ent-Epicatechin	290.29	2.83	5	6	1	48.96	0.24	Guizhi
HGWD30	beta-sitosterol	414.79	3.2	1	1	6	36.91	0.75	Guizhi
HGWD31	sitosterol	414.79	2.71	1	1	6	36.91	0.75	Guizhi
HGWD32	(-)-taxifolin	304.27	1.66	5	7	1	60.51	0.27	Guizhi
HGWD33	DMEP	282.32	1.93	0	6	10	55.66	0.15	Guizhi
HGWD34	6-gingerol	294.43	3.45	2	4	10	35.64	0.16	Shengjiang
HGWD35	6-shogaol	276.41	4.95	1	3	9	31	0.14	Shengjiang
HGWD36	(6aR, 11aR)-9,10-dimethoxy-6a, 11a-dihydro-6H-benzofurano[3,2-c]chromen-3-ol	300.33	2.88	1	5	2	64.26	0.42	Huangqi
HGWD37	1,7-Dihydroxy-3,9-dimethoxy pterocarpene	314.31	2.85	2	6	2	39.05	0.48	Huangqi
HGWD38	3,9-di-O-methylisissolin	314.36	3.28	0	5	3	53.74	0.48	Huangqi
HGWD39	7-O-methylisomucronulatol	316.38	2.85	1	5	4	74.69	0.3	Huangqi
HGWD40	Bifendate	418.38	1.75	0	10	7	31.1	0.67	Huangqi
HGWD41	Calycosin	284.28	2.82	2	5	2	47.75	0.24	Huangqi
HGWD42	formononetin	268.28	3.01	1	4	2	69.67	0.21	Huangqi
HGWD43	isoflavanone	316.33	2.76	2	6	3	109.99	0.3	Huangqi
HGWD44	isorhamnetin	316.28	1.31	4	7	2	49.6	0.31	Huangqi
HGWD45	Jaranol	314.31	2.8	2	6	3	50.83	0.29	Huangqi
HGWD46	9,10-dimethoxypterocarpan-3-O-β-D-glucoside	462.49	1.18	4	10	5	36.74	0.92	Huangqi
HGWD47	(Z)-1-(2,4-dihydroxyphenyl)-3-(4-hydroxyphenyl)prop-2-en-1-one	256.27	3.04	3	4	3	87.51	0.15	Huangqi
HGWD48	(3R)-3-(2-hydroxy-3,4-dimethoxyphenyl)chroman-7-ol	302.35	2.76	2	5	3	67.67	0.26	Huangqi

important nodes in the corresponding C-T network. The detail results are as follows:

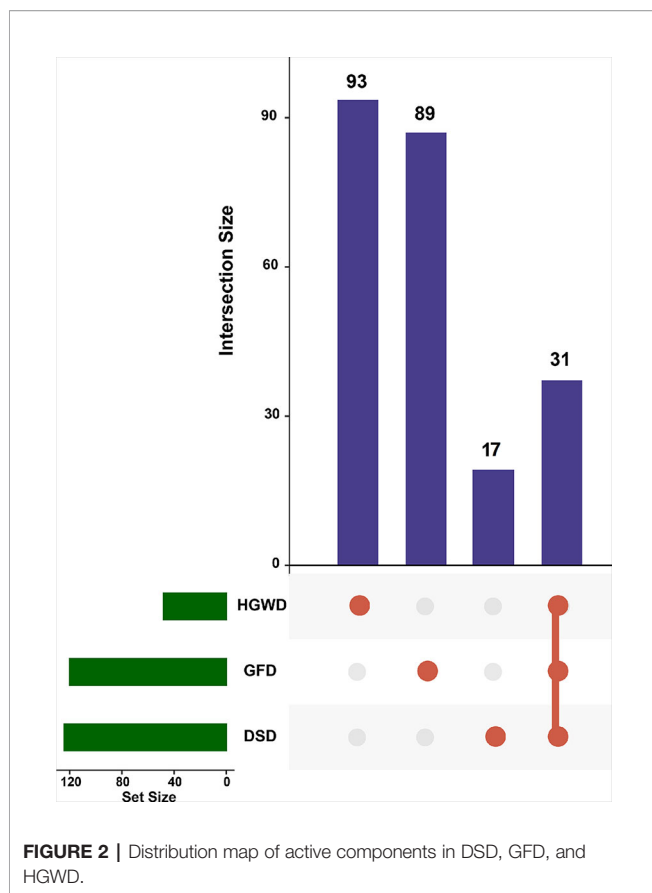
Validated the Number and Coverage of Pathogenic Genes in KNMSs

To assess whether the number of RA pathogenic genes in KNMSs are close to the number of RA pathogenic genes in corresponding C-T network. The known pathogenic genes of RA reported by published literature and databases were collected, and the pathogenic genes confirmed by more than 5 literatures were selected for further analysis (**Table S3**). We found that the C-T network of DSD, GFD, and HGWD contains 50, 52, and 39 pathogenic genes, respectively. While the KNMSs of DSD, GFD, and HGWD contains 39, 40, and 30 pathogenic genes. The number of pathogenic genes in KNMSs compared to that in C-T network of DSD, GFD, and HGWD reached 78%, 76.9%, and 76.9%, which confirmed that the predicted KNMSs with high coverage of pathogenic genes (**Figures 6A–C**). These results demonstrate that KNMSs have a high coincidence degree with C-T network in the number and coverage of pathogenic genes, it also indicated that our proposed KNMS detection model can

maximize the coincidence degree of pathogenic genes in the C-T network of formulas.

Validated the Genes Enriched Pathways in KNMSs

An additional metric for evaluating the importance of the inferred motifs is determined by their functional coherence, which can be accessed *via* their related genes enrichment pathways from KEGG (Kanehisa and Goto, 2000). Here, we used this method to detect whether KNMSs found in each formula can represent their full C-T networks at functional level. Our analysis shown that genes enriched pathways of KNMSs in DSD accounts for 85.8% of genes enriched pathways of the full C-T network in DSD; genes enriched pathways of KNMSs in GFD accounts for 86.6% genes enriched pathways of the full C-T network in GFD; genes enriched pathways of KNMSs in HGWD accounts for 81.9% genes enriched pathways of the full C-T network in HGWD (**Figures 7A, B**). It was encouraged that the gene enriched pathways involved in KNMSs of 3 formulas are highly compatible with gene enriched pathways of their C-T networks. This result confirmed that KNMSs have a high



coincidence degree with C-T network at the gene functional level and also suggested that our proposed KNMS detection model can maximize the retention of functional pathways in the formulas of TCM.

Validated the Cumulative Contribution of Important Nodes in KNMSs

The degree of nodes is a key topological parameter that characterizes the influence of nodes in a network (Lv et al., 2014). Here, a mathematical model was established to evaluate the importance of KNMSs in each formula based on the degree of nodes. According to the calculation results, each KNMS was assigned a CC value. The detailed information was shown in **Figure 8** and **Table S4**. The sum of CC of 7, 10, and 10 KNMSs in each formula reached 80.44%, 79.88%, and 70.76% of that in C-T networks of DSD, GFD, and HGWD, respectively. The results confirmed that KNMSs have a high coincidence degree with C-T network on the topological structure and also indicated that our proposed KNMS detection model could maximize the coverage of important network topological structures compared with C-T network in each formula.

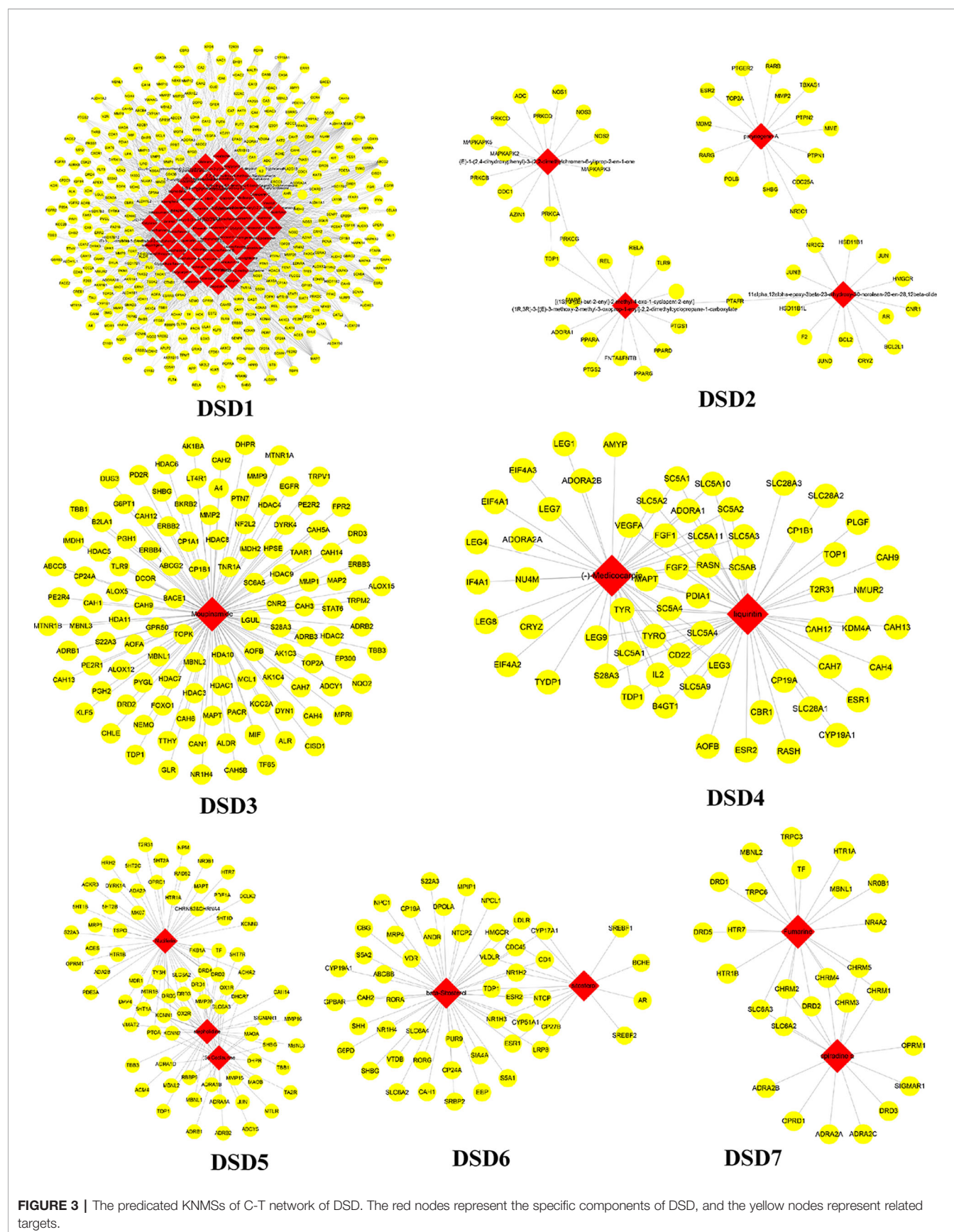
Potential Mechanisms Analysis of Different Formulas Treats the Same Disease

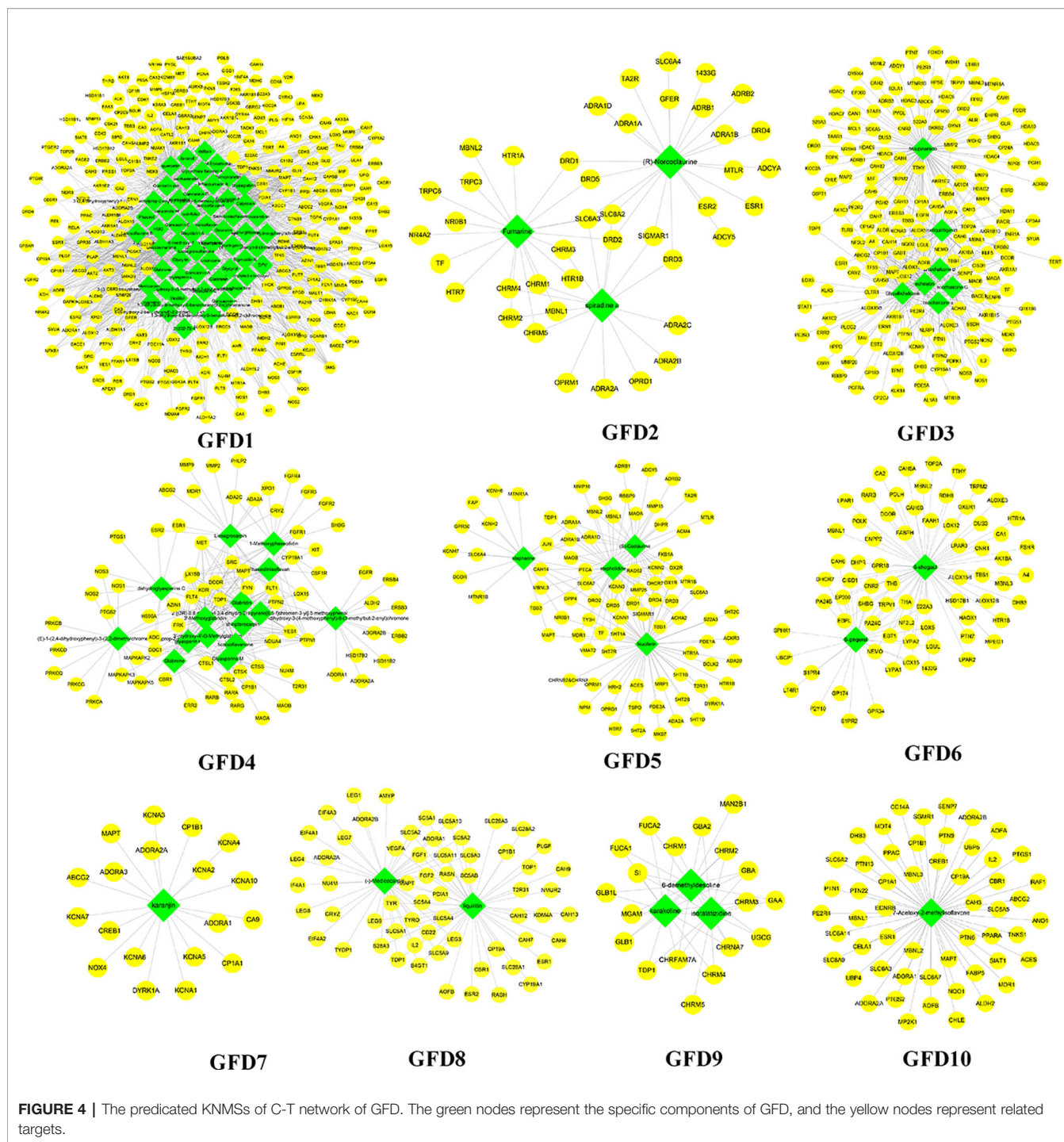
In order to reveal the potential mechanism of KNMSs in different formula for treating rheumatoid arthritis, pathway enrichment

analysis of KNMS-related genes in each formula were performed. In the DSD, genes in total 7 KNMSs were enriched in 165 pathways, genes in two KNMSs, DSD1, and DSD2 were enriched in 158 pathways, accounting for 95.8% of that in 7 KNMSs. The arthritis-related signaling pathways corresponding to DSD1 and DSD2 were partially complementary, for example, genes in DSD1 were mainly enriched in JAK-STAT signaling pathway and AMPK signaling pathway, genes in DSD2 mainly enriched in NF-kappa B signaling pathway, p53 signaling pathway and Wnt signaling pathway. In GFD, we total got 10 KNMSs. Genes in these 10 KNMSs were enriched in 151 pathways. Four of 10 KNMSs, GFD1, GFD3, GFD4, and GFD5 related genes are enriched in 144 pathways, accounting for 95.4% of enrichment pathways in 10 KNMSs of GFD. Moreover, some of their corresponding arthritis-related signaling pathways are complementary. For example, GFD1 mainly includes TNF signaling pathway, IL-17 signaling pathway and AMPK signaling pathway, and GFD3 mainly includes Inflammatory mediator regulation of TRP channels and GnRH signaling pathway. In HGWD, genes in 10 predicted KNMSs were enriched in 110 pathways, genes in HGWD4 and HGWD5, HGWD6, and HGWD8 covered 102 pathways, accounting for 92.7% of all KNMSs gene enrichment pathways. Consistent with DSD and GFD results, some of their corresponding arthritis-related signal pathways were also complementary. For example, HGWD4 mainly includes TNF signaling pathway, Hedgehog signaling pathway and IL-17 signaling pathway, HGWD5 mainly includes VEGF signaling pathway, NF-kappa B signaling pathway and mTOR signaling pathway, HGWD6 mainly includes cAMP signaling pathway and cGMP-PKG signaling pathway (**Figure 9**, **Table S5**). These results show that KNMSs in different formulas have distinct roles and synergistic effects in the treatment of rheumatoid arthritis.

In order to further explore the potential mechanism of the three formulas in treating RA, besides the difference analysis of each KNMS in different formulas, KEGG enrichment analysis of all KNMSs in each formula were also implemented and found that 3 formulas play the therapeutic effect on RA through the following five common pathways: Rap1 signaling pathway, cAMP signaling pathway, MAPK signaling pathway, EGFR Tyrosine Kinase Inhibitor Resistance, Calcium signaling pathway and Neuroactive ligand-receptor interaction. Except the common pathways, we found that the three formulas can play the role of treating RA through their specific pathways (**Figure 10**). For example, DSD can play the role of treating RA by regulating VEGF signaling pathway. GFD can play a role in treating RA by regulating HIF-1 signaling pathway. HGWD can play a role in treating RA by regulating PI3K-Akt signaling pathway. These results indicate that 3 formulas can play the role of treating RA through different and common pathways, which may act as the essence of different formulas treat the same disease.

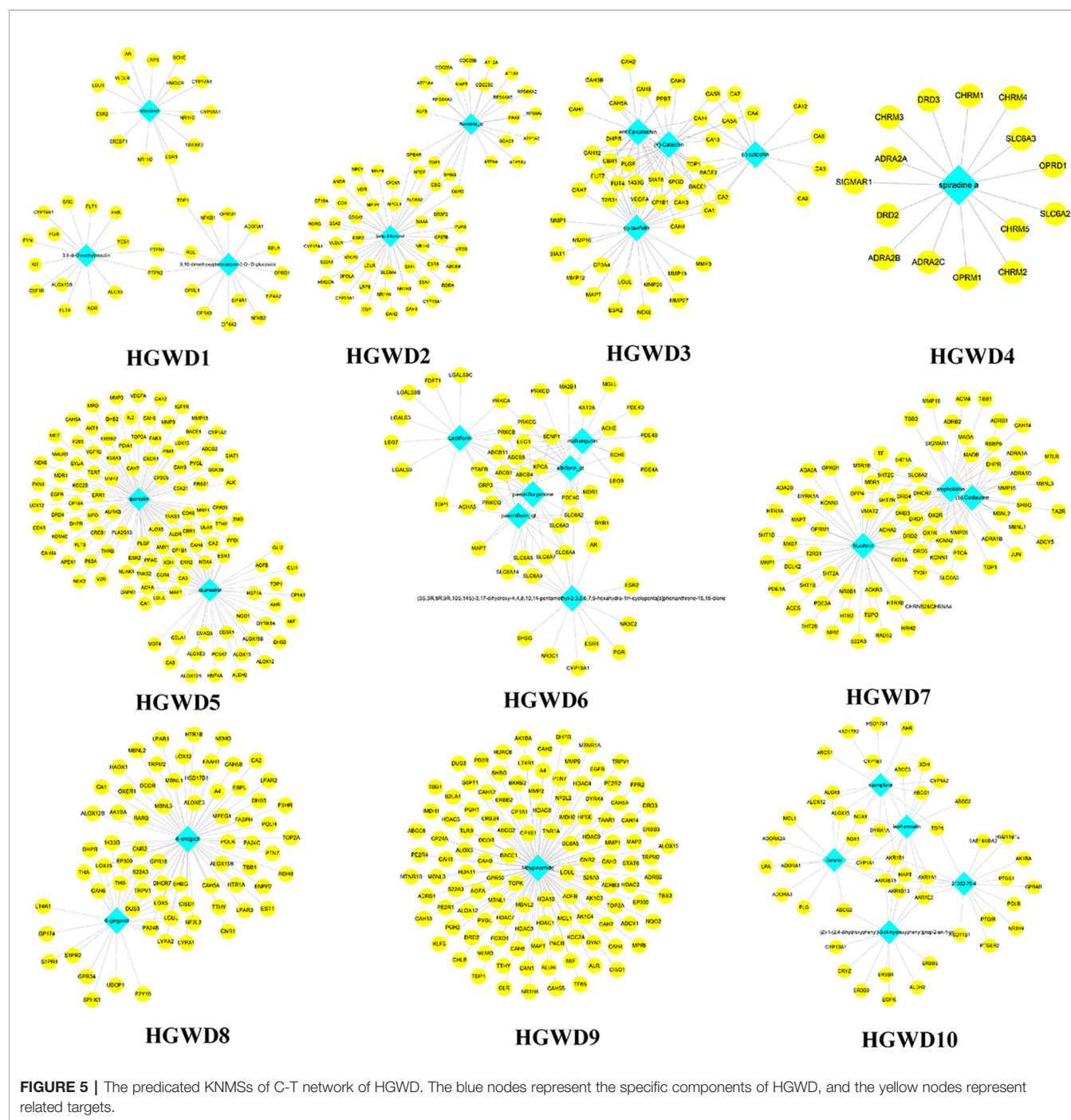
Through PubMed literature search, we found that among the common pathways, MAPK signaling pathway and cAMP signaling pathway have the most correlation records with rheumatoid arthritis. We selected MAPK signaling pathway





and cAMP signaling pathway which were reported closely related to inflammation to illustrate the mechanism of different formulas treat the same disease in detail. Firstly, a comprehensive inflammatory pathway was constructed by integrating the two pathways. And then, the genes in KNMSs of three formulas were mapped to the comprehensive inflammatory pathway (Figure 11). Results show that genes in the KNMSs of DSD mainly distributed in the downstream of

the comprehensive inflammatory pathway, such as MAPK14, MAPK8, and JUND; Genes in the KNMSs of GFD mainly distributed in the downstream of the comprehensive inflammatory pathway, such as AKT3, RAF1, and TAOK3; while genes in the KNMSs of HGWD distributed both in the upstream and downstream of the comprehensive inflammatory pathway, such as CSF1R, ADCYAP1R1, CHRM1, NFKB1, MAPT, and JUN. The results suggest that different formulas



play therapeutic roles through targeting different genes in the comprehensive inflammatory pathway.

Experimental Validation *In Vitro*

Effects of isoliquiritigenin, isorhamnetin and quercetin with different concentrations on cell viabilities of RAW264.7 cells were detected by MTT assay. Compared with control group, 1, 5, 10, and 20 μM isoliquiritigenin, isorhamnetin, and quercetin had no effects on RAW264.7 cells viabilities (**Figures 12A–C**).

Therefore, four concentrations were used (1, 5, 10, and 20 μM) for subsequent experiments.

NO is a regulator of information transmission between cells and has the function of mediating cellular immune and inflammatory reactions. In order to further evaluate the results obtained by the network pharmacology model, the key components in KNMSs of each formula were selected for experimental validation. Isoliquiritigenin from motif 1 (DSD1) of DSD, isorhamnetin from motif 1 (GFD1) of GFD, and

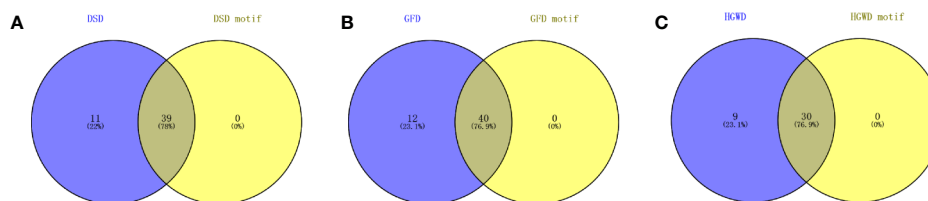


FIGURE 6 | The number of overlap pathogenic genes between C-T network and KNMSs in DSD, GFD and HGWD (A–C). (A–C) use venn diagram to visualize the overlap number between C-T network and KNMSs in DSD, GFD, and HGWD, respectively.

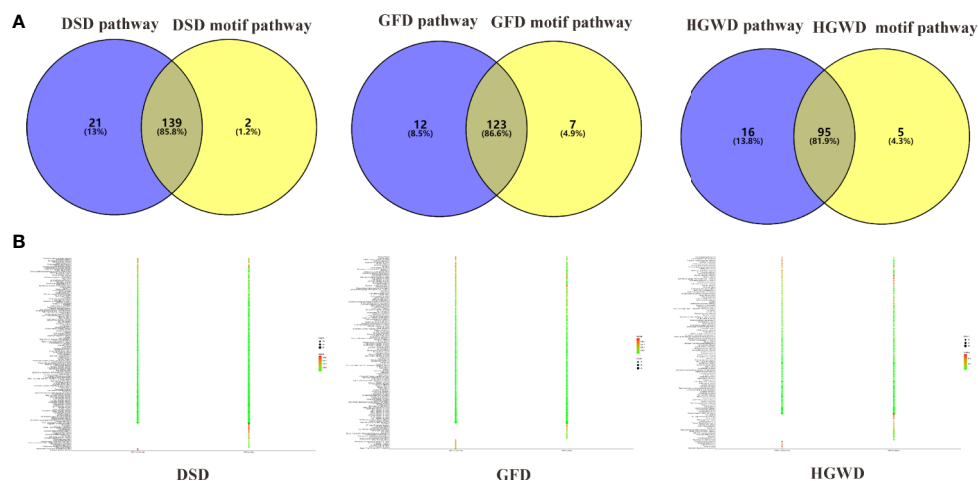


FIGURE 7 | The functional similarity analysis between C-T network and KNMSs in DSD, GFD, and HGWD, respectively. (A, B) represent the functional similarity visualized by venn diagram and bubble diagram, respectively.

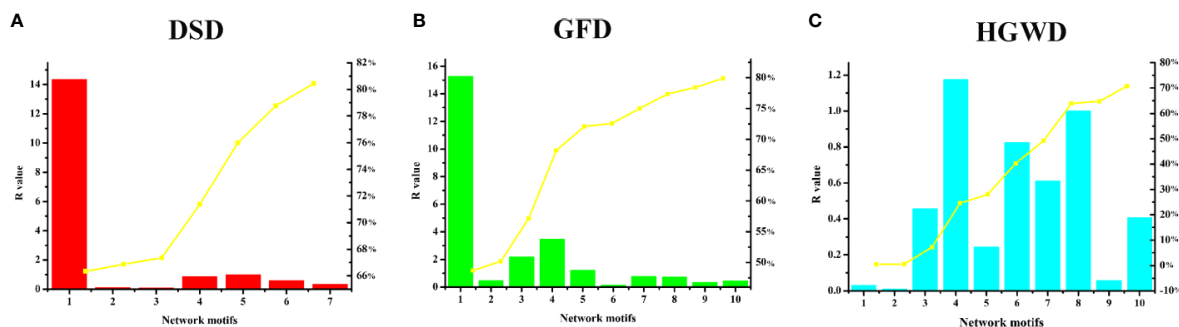


FIGURE 8 | The contribution coefficient of network topological between C-T network and KNMSs in DSD, GFD and HGWD (A–C). (A–C) use bar diagram to visualize the cumulative contribution rate between C-T network and KNMSs in DSD, GFD and HGWD, respectively.

quercetin from motif 5 (HGWD5) of HGWD were chose to detect potential anti-inflammatory effects using LPS induced RAW264.7 cells. Compared with control group, the NO level was significantly increased by 275.34% in the culture medium of LPS treated cells, however, isoliquiritigenin (10 and 20 μ M)

markedly decreased the extracellular NO levels by 107.94% and 151.04%, isorhamnetin (10 and 20 μ M) markedly decreased the extracellular NO levels by 81.59% and 137.94%, quercetin (5, 10 and 20 μ M) markedly decreased the extracellular NO levels by 56.68%, 106.57% and 174.59%, respectively, in a concentration-

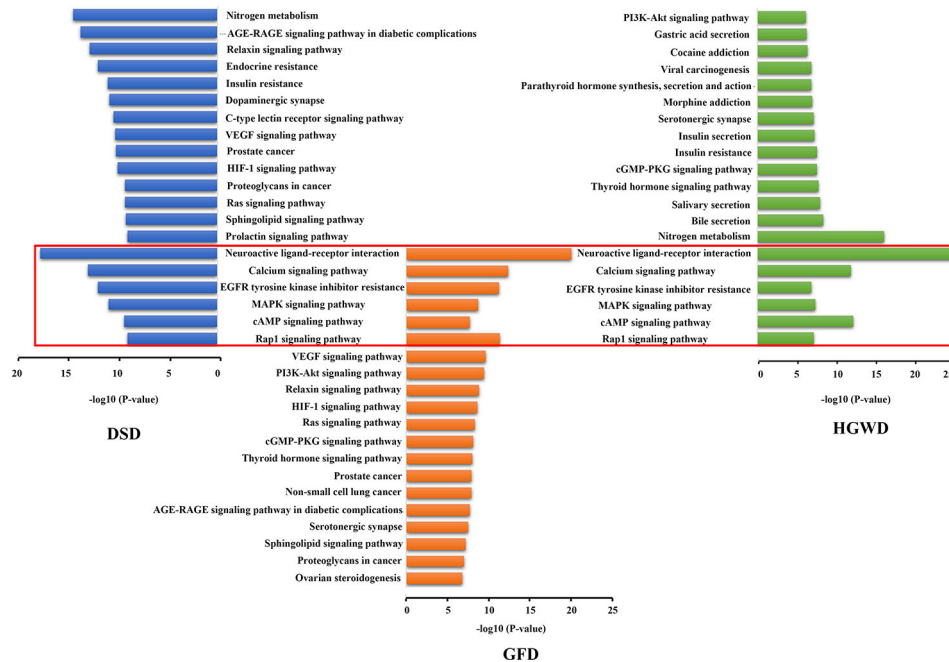


FIGURE 9 | The enrichment pathway map of KNMSs in the C-T network of DSD, GFD, and HGWD.

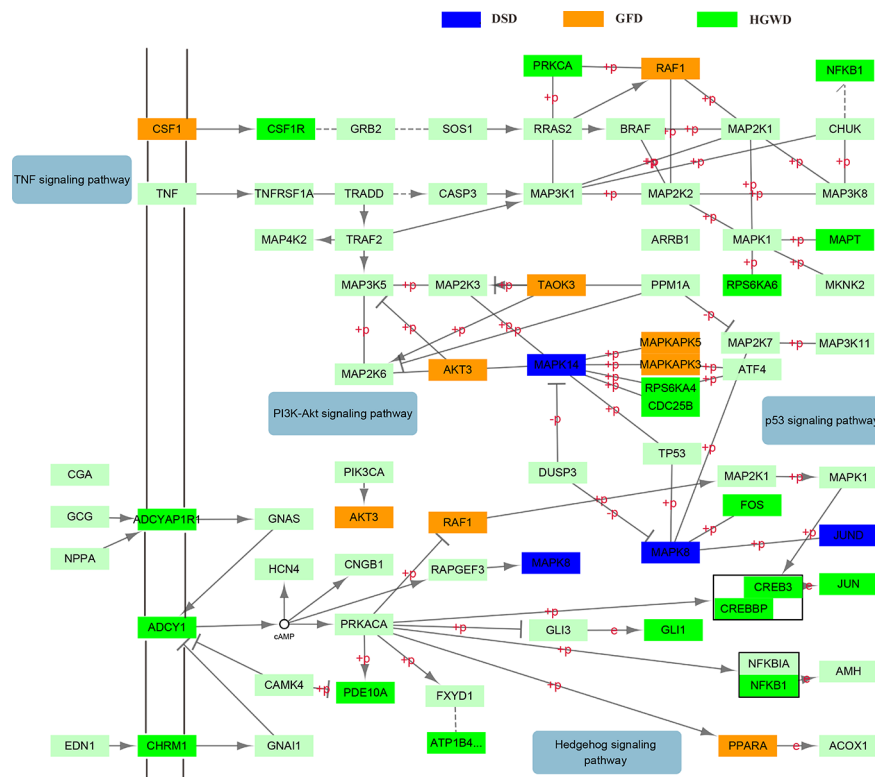
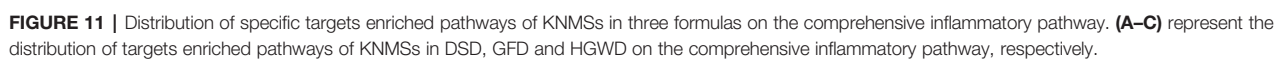


FIGURE 10 | Gene enrichment analysis of all KNMSs from DSD, GFD, and HGWD, respectively.



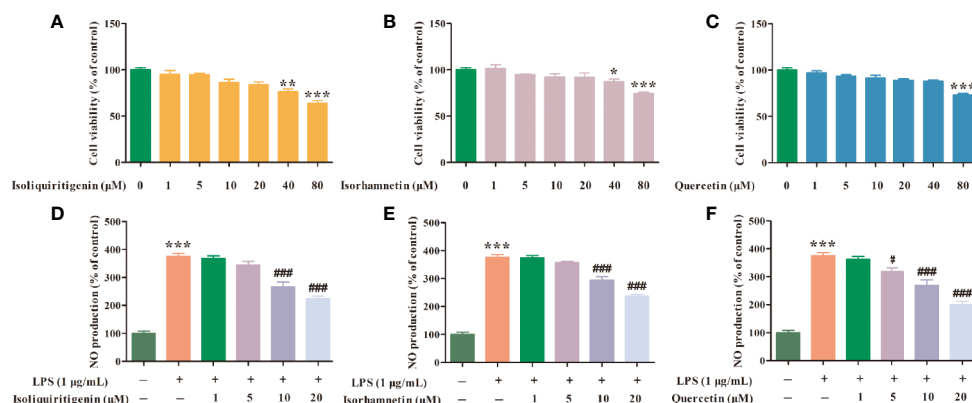


FIGURE 12 | Effects of isoliquiritigenin (A, D), isorhamnetin (B, E), and quercetin (C, F) on cell viabilities and NO of LPS induced RAW264.7 cells. * $p < 0.05$, ** $p < 0.01$, *** $p < 0.001$ compared with control group. # $p < 0.05$, ### $p < 0.001$ compared with the LPS group.

dependent manner (Figures 12D–F). Our results demonstrated that isoliquiritigenin, isorhamnetin, and quercetin inhibited NO production in LPS induced RAW264.7 cells.

DISCUSSION

The therapeutic effect of current synthetic agents in treating RA is not satisfactory and most of them have undesirable side effects. In China, some classical formulas have a long history of clinical application to treat RA and have shown significant curative effects. However, TCM formulas is a multi-component and multi-target agent from the molecular perspective (Corson and Crews, 2007; Bo et al., 2013). Based on the characteristics of complex components and unclear targets of TCM formula, the development of novel methods became an urgent issue needed to be solved.

TCM network pharmacology emerging recently has become a flourishing field in TCM modern studies along with the rapid progress of bioinformatics (Guo et al., 2017; Gao et al., 2018; Wang et al., 2018). So, using the method, combined with the rich experience of TCM treatment, could hopefully decode the underlying mechanism of TCM formula in the treatment of complex disease with the characteristic of “multi-targets, multi-component”. Network pharmacology approach could help us search for putative active components and targets of herbs based on widely existing databases and shows the network of drug-targets by a visual way (Gao et al., 2016). Moreover, it abstracts the interaction between drugs and target genes into a network model and investigates the effects of drugs on biological networks from a holistic perspective. It can help us to further understand potential action mechanisms of TCM within the context of interactions at the system level. However, in the decode process of complex networks, there are still exist redundancies and noises in current network pharmacology study.

In order to solve this problem, we introduced the infomap algorithm based on huffman encoding and the random walk

theory for the first time. The algorithm performs to optimize the discovery of motif in C-T network heuristically by using a reasonable global metric. The results of optimized KNMSs are used to analyze the mechanism of different formulas for the treatment of RA. During this process the contribution coefficient model was used to validate the predicted KNMSs, which confirm the accuracy and reliability of our proposed strategy.

In this study, 230 active components of three formulas were found in total after ADME screening, 31 of these components are common to the three formulas, and 93, 89, and 17 components are specific to each formula. It suggested that the three formulas play therapeutic effect on rheumatoid arthritis through both common and specific components. In order to analyze the key component groups and mechanisms of the three formulas in the treatment of rheumatoid arthritis, we used target prediction tools to predict the targets of active components in different formulas and construct C-T networks. The degree distribution in the C-T network shows that the same components could act on different targets, and different components could also act on the same targets, which fully reflects the multi-component and multi-target complexity of TCM in treating complex diseases.

In order to quickly extract important information from complex C-T networks, motif prediction and validation strategy were used to rapidly discover the KNMSs of different formulas in the treatment of RA by using multidimensional data. More and more evidences show that network motif is an effective method to extract functional units and find core elements in complex networks. Radicchi et al. has confirmed that network motif offers an effective and manageable approach for characterizing rapidly the main functional unit of disease progression (Radicchi et al., 2004). Yang has reported that identifying overlapping motifs is crucial for understanding the structure as well as the function of real-world networks (Yang and Leskovec, 2012). Cai et al. indicate that uncovering motif structures of a complex network can help us to understand how the network play functions (Cai et al., 2014). Utilizing the network motif prediction model, 7, 10, and 10 KNMSs

($p < 0.05$) were predicted in DSD, GFD and HGWD, respectively.

Coverage of RA pathogenic genes, coverage of functional pathways and cumulative contribution of key nodes were employed to evaluate the accuracy and reliability of KNMSs. The verification results show that KNMSs has a high coincidence degree with C-T network at the pathogenic genes, gene functional and topological structure level. It suggests that our proposed KNMS detection model can maximize the retention of functional pathways, the coverage of network topological structure and the coincidence degree of pathogenic genes in the formulas of TCM.

Through the analysis of KNMSs gene enrichment pathways in different formulas, we found that the percentage of gene enrichment pathways of different KNMSs is distinct compare to the gene enrichment pathways of all KNMSs in each formula. In DSD, gene enrichment pathways of DSD1, DSD2 account for more than 95% of gene enrichment pathways of 7 KNMSs. In GFD, the gene enrichment pathways of 4 KNMSs, GFD1, GFD3, GFD4, and GFD5 account for 95.4% of gene enrichment pathways of 10 KNMSs. In HGWD, the gene enrichment pathways of 4 KNMSs, HGWD4, HGWD5, HGWD6, and HGWD8 account for 92.7% of gene enrichment pathways of 10 KNMSs. These KNMSs in each formula play different roles by targeting on common and complementary inflammation-related signaling pathways. These complementary inflammatory signaling pathways include: DSD1 specifically related JAK-STAT signaling pathway and AMPK signaling pathway, DSD2 specifically related NF-kappa B signaling pathway, p53 signaling pathway and Wnt signaling pathway. GFD1 specifically related TNF signaling pathway, IL-17 signaling pathway, GFD3 specifically related Inflammatory mediator regulation of TRP channels and GnRH signaling pathway, HGWD4 specifically related TNF signaling pathway, Hedgehog signaling pathway, HGWD5 specifically related VEGF signaling pathway and mTOR signaling pathway, HGWD6 specifically related cAMP signaling pathway and cGMP-PKG signaling pathway. These results indicate that KNMSs in different formulas have distinct roles and synergistic effects in the treatment of rheumatoid arthritis.

In addition to the difference analysis of each KNMS in different formulas, KEGG enrichment analysis of all KNMSs in each formula were also implemented and revealed that 3 formulas exert the therapeutic effect of RA through common pathway, such as MAPK signaling pathway, cAMP signal pathway etc. or specific pathway, such as VEGF signaling pathway, HIF-1 signaling pathway, PI3K-Akt signaling pathway etc. Among them, MAPK signaling pathway plays an important role in the pathological process of RA (Schett and Zwerina, 2008). Its over-activation is closely related to inflammatory hyperplasia of synovial tissue and destruction of articular cartilage tissue. As an inducible transcription factor, MAPK regulates the expression of many genes and has been considered as a promising target for the treatment of RA (Rubbert-Roth, 2012). Studies have shown that collagen-induced arthritis rats administrated with MAPK signal transduction pathway inhibitor have significant differences in inhibiting synovitis, bone destruction and articular cartilage destruction compared with the group without signal pathway inhibitor (Adelheid et al., 2014). cAMP signal pathway is an important

signal pathway for peripheral blood lymphocytes of RA patients. The study found that the cAMP level in peripheral blood lymphocytes (PBL) of RA patients increased, and its proliferation response was significantly lower than that of PBL in normal patients. It was also found that the abnormal activation of adenylate cyclase in RA patients was related to the low function of Gi protein (Dai and Wei, 2003). The formation of RA neovascularization depends on the expression of various angiogenic factors, especially VEGF and its receptor in RA (Mi-La et al., 2006). It has been confirmed that VEGF expression is upregulated in synovial macrophages and fibroblasts of RA patients, and VEGF expression is positively correlated with RA disease activity and joint destruction (Kanbe et al., 2015). The articular cavity of RA is anoxic microenvironment. Recent studies have shown that the increased expression of HIF-1 in synovium of RA joint is closely related to the occurrence and development of RA (Xu et al., 2010). PI3K-AKT signal pathway is an important intracellular signal transduction pathway, which is closely related to abnormal apoptosis of RA fibroblast-like synovial cells (RAFLS) (Smith and Walker, 2004). Inhibition of abnormally activated PI3K-AKT signaling pathway or expression of anti-apoptotic molecules can induce apoptosis in RAFLS and have therapeutic effect on RA (Liu and Pope, 2003).

Besides the function analysis, we also analysis and validated the key components in KNMSs of each formula. In DSD, the results suggested that the key component isoliquiritigenin from motif 1 (DSD1) exert effect on treatment of RA possibly through acting on MAPK signaling pathway. Studies have shown that isoliquiritigenin suppresses RANKL-induced osteoclastogenesis and inflammatory bone loss *via* RANK-TRAF6, MAPK, I κ B α /NF- κ B, and AP-1 signaling pathways (Zhu et al., 2012). In GFD, the results suggested that the key component isorhamnetin from motif 1 (GFD1) treats RA possibly through acting on TNF signaling pathway. Published reports confirmed that isorhamnetin play intervening roles in the development and progression of RA *via* anti-inflammatory and anti-oxidative activities. Previous studies have suggested that isorhamnetin attenuates collagen-induced arthritis *via* modulating the levels of cytokines TNF- α , IL-1 β , and IL-6 etc. in the joint tissue homogenate of mice (Wang and Zhong, 2015). In HGWD, the results suggested that the key component quercetin from motif 5 (HGWD5) has therapeutic effect on RA possibly through acting on PI3K-Akt signaling pathway. This also verified by previous studies, which found that the mechanisms responsible for the quercetin-induced apoptosis of FLS from patients with RA are associated with the inhibition of PI3K/AKT pathway activation (Pan et al., 2016). Cellular experiments were applied to prove the reliability of the network pharmacology model through verifying the protective effects of key components in KNMSs of three formulas on the inflammation of mice RAW264.7 cells induced by LPS. In addition, in order to better evaluate the reliability of our proposed network pharmacology model, *in vivo* study will be conducted in our future research.

To summarize, a network pharmacology-based approach was established to extract core components group and decode the mechanisms of different formulas treat the same disease of TCM. Additionally, our proposed KNMS prediction and validation

strategy provides methodological reference for optimization of core components group and interpretation of the molecular mechanism in the treatment of complex diseases using TCM.

DATA AVAILABILITY STATEMENT

The raw data supporting the conclusions of this article will be made available by the authors, without undue reservation, to any qualified researcher.

AUTHOR CONTRIBUTIONS

A-PL, D-GG, and LG provided the concept and designed the study. K-XW and YG conducted the analyses. K-XW and D-GG wrote the manuscript. K-XW, YG, CL, YL and B-YZ participated in data analysis. X-MQ, G-HD, and A-PL provided oversight. A-PL, D-GG, and LG contributed to revising and proof-reading the manuscript. All authors contributed to the article and approved the submitted version.

REFERENCES

- Adelheid, K., Makiyeh, T. A., Erdal, C., Roland, A., Josef, S., and Georg, S. (2014). Differential tissue expression and activation of p38 MAPK alpha, beta, gamma, and delta isoforms in rheumatoid arthritis. *Arthritis Rheum.* 54 (9), 2745–2756. doi: 10.1002/art.22080
- Bang, C., Hua, Z., Fang, W., Wu, J., Liu, X., Tang, C., et al. (2017). Metabolomics analysis of Danggui Sini decoction on treatment of collagen-induced arthritis in rats. *J. Chromatogr. B. Anal. Technol. Biomed. Life Sci.* 1061–1062, 282–291. doi: 10.1016/j.jchromb.2017.07.043
- Bo, Z., Xu, W., and Shao, L. (2013). An Integrative Platform of TCM Network Pharmacology and Its Application on a Herbal Formula, Qing-Luo-Yin. *Evidence-Based Complementary Altern. Med.* 2013 (343), 1–12. doi: 10.1155/2013/456747
- Brzustewicz, E., and Bryl, E. (2015). The role of cytokines in the pathogenesis of rheumatoid arthritis – Practical and potential application of cytokines as biomarkers and targets of personalized therapy. *Cytokine* 76 (2), 527–536. doi: 10.1016/j.cyt.2015.08.260
- Cai, Q., Ma, L., and Gong, M. (2014). A survey on network community detection based on evolutionary computation. *Int. J. Bio-Inspired Comput.* 8 (2), 167–256. doi: 10.1504/IJBIC.2016.076329
- Cecilia, O., Sara, W., Henrik, K. L., Marie, H., Karlson, E. W., Lars, A., et al. (2013). Parity and the risk of developing rheumatoid arthritis: results from the Swedish Epidemiological Investigation of Rheumatoid Arthritis study. *Ann. Rheum. Dis.* 73 (4), 752–755. doi: 10.1136/annrheumdis-2013-203567
- Chen, Y. C. (2012). TCM Database@Taiwan: The World's Largest Traditional Chinese Medicine Database for Drug Screening In Silico. *PLoS One* 6 (1), e15939. doi: 10.1371/journal.pone.0015939
- Chen, Y. H., Zhao, X. X., and Wang, W. Q. (2009). Simultaneous determination of glycyrrhizin, liquiritin and isoliquiritigenin in licorice by hplc. *Chin. J. Inf. Tradit. Chin. Med.* 16 (8), 52–58. doi: 10.3969/j.issn.1005-5304.2009.08.024
- Cheng, B., Zheng, H., Wu, F., Wu, J. X., Liu, X. W., Tang, C. L., et al. (2017). Metabolomics analysis of Danggui Sini decoction on treatment of collagen-induced arthritis in rats. *J. Chromatogr. B.* 1061–1062, 282–291. doi: 10.1016/j.jchromb.2017.07.043
- Corson, T. W., and Crews, C. M. (2007). Molecular understanding and modern application of traditional medicines: triumphs and trials. *Cell* 130 (5), 769–774. doi: 10.1016/j.cell.2007.08.021
- Dai, M., and Wei, W. (2003). Research progress of signal transduction mechanism of synovocytes with rheumatoid arthritis. *Chin. Pharmacol. Bull.* 19 (5), 481–485. doi: 10.3321/j.issn:1001-1978.2003.05.001

FUNDING

This study is financially supported by the Startup fund from Southern Medical University (grant No. G619280010), the Natural Science Foundation Council of China (grant No. 31501080), Hong Kong Baptist University Strategic Development Fund [grant No. SDF13-1209-P01, SDF15-0324-P02(b) and SDF19-0402-P02], the Key Laboratory of Effective Substances Research and Utilization in TCM of Shanxi Province (No. 201705D111008-21), Hong Kong Baptist University Interdisciplinary Research Matching Scheme (grant No. RC/IRCs/17-18/04), the General Research Fund of Hong Kong Research Grants Council (grant No. 12101018, 12100719, 12102518).

SUPPLEMENTARY MATERIAL

The Supplementary Material for this article can be found online at: <https://www.frontiersin.org/articles/10.3389/fphar.2020.01035/full#supplementary-material>

- Damião, M. C., Pasqualoto, K. F., Polli, M. C., and Parise, F. R. (2014). To be drug or prodrug: structure-property exploratory approach regarding oral bioavailability. *Journal of pharmacy & pharmaceutical sciences : a publication of the Canadian Society for Pharmaceutical Sciences, Société. Can. Des. Sci. Pharm.* 17 (4), 532–540. doi: 10.18433/J3BS4H
- David, G., Aurélien, G., Matthias, W., Antoine, D., Olivier, M., and Vincent, Z. (2014). SwissTargetPrediction: a web server for target prediction of bioactive small molecules. *Nucleic Acids Res.* 42, 32–38. doi: 10.1093/nar/gku293
- Draghici, S., Khatri, P., Tarca, A. L., Amin, K., Done, A., Voichita, C., et al. (2007). A systems biology approach for pathway level analysis. *Genome Res.* 17 (10), 1537–1545. doi: 10.1101/gr.6202607
- Fu, S., Yi, W., Ai, J., Bah, A. J., and Gao, X. (2014). GW25-e3314 Clinical application of “treating different diseases with the same method” - Xuefu Zhuyu Capsule (a traditional Chinese patent medicine) for blood stasis syndrome. *J. Am. Coll. Cardiol.* 64 (16), C208–C209. doi: 10.1016/j.jacc.2014.06.970
- Gao, J., Li, W., and Wei, F. (2005). Quantitative analysis of aristolochic acid in *asarum sieboldii* by hplc. *Chin. Pharm. J.* 40 (20), 1579–1589. doi: 10.3321/j.issn:1001-2494.2005.20.019
- Gao, H. M., Wang, Z. M., Qu, L., Fu, X. T., and Li, L. (2007). Determination of calceolariside b in *caulis akebiae* by rp-hplc. *China J. Chin. Mater. Med.* 32 (6), 476–478. doi: 10.3321/j.issn:1001-5302.2007.06.004
- Gao, L., Wang, X., Niu, Y., Duan, D., Yang, X., Hao, J., et al. (2016). Molecular targets of Chinese herbs: a clinical study of hepatoma based on network pharmacology. *Sci. Rep.* 6 (24944), 24944. doi: 10.1038/srep24944
- Gao, L., Wang, K., Zhou, Y., Fang, J., Qin, X., and Du, G. (2018). Uncovering the anticancer mechanism of Compound Kushen Injection against HCC by integrating quantitative analysis, network analysis and experimental validation. *Sci. Rep.* 8 (1), 624. doi: 10.1038/s41598-017-18325-7
- Guo, Q., Zheng, K., Fan, D., Zhao, Y., Li, L., Bian, Y., et al. (2017). Wu-Tou Decoction in Rheumatoid Arthritis: Integrating Network Pharmacology and In Vivo Pharmacological Evaluation. *Front. Pharmacol.* 8, 230. doi: 10.3389/fphar.2017.00230
- He, J. Y., and Gu, S. (2008). Effects of Guizhi Fuzi Tang on TNF- α in rheumatoid arthritis rats. *J. Pract. Tradit. Chin. Internal Med.* 22 (12), 48–49. doi: 10.13729/j.issn.1671-7813.2008.12.058
- Jong, H. D., Geiselman, J., Hernandez, C., and Page, M. (2003). Genetic Network Analyzer: qualitative simulation of genetic regulatory networks. *Bioinformatics* 19 (3), 336–344. doi: 10.1093/bioinformatics/btf851
- Kanbe, K., Chiba, J., Inoue, Y., Taguchi, M., and Yabuki, A. (2015). SAT0019 SDF-1/CXCR4 is associated with the Disease Activity and Bone and Joint

- Destruction in Patients with Rheumatoid Arthritis Treated with Golimumab. *Mod. Rheumatol.* 74 (Suppl 2), 1–15. doi: 10.3109/14397595.2015.1054088
- Kanehisa, M., and Goto, S. (2000). KEGG: kyoto encyclopedia of genes and genomes. *Nucleic Acids Res.* 27 (1), 29–34. doi: 10.1093/nar/28.1.27
- Keiser, M. J., Roth, B. L., Armbruster, B. N., Ernsberger, P., Irwin, J. J., and Shoichet, B. K. (2007). Relating protein pharmacology by ligand chemistry. *Nat. Biotechnol.* 25 (2), 197–206. doi: 10.1038/nbt1284
- Li, T. T., Shu, Z. H., Yu, L., Hao, W. J., and Fu, X. Y. (2015). Hplc/dad fingerprints and determination of main flavones in radix astragali from different origins. *Chin. J. Hosp. Pharmacy.* 35 (13), 1182–1187. doi: 10.13286/j.cnki.chinhosppharmacyj.2015.13.05
- Li, W. M., Zhao, Y. R., Yang, Y. Y., Zhang, Z. Q., Lai, J. Y., and Zhuang, L. (2011). Rp-hplc with uv switch determination of 9 components in white peony root pieces. *Chin. J. Pharm. Anal. Volume* 31 (12), 2208–2212. doi: 10.1631/jzus.B1000135
- Liang, K., Cui, S., Zhang, Q., Bi, K., Qin, Z., and Jia, Y. (2011). Uplc simultaneous determination of five active components in cinnamomi ramulus. *China J. Chin. Mater. Med.* 36 (23), 3298–3301. doi: 10.4268/cjcm20112317
- Lipinski, C. A., Lombardo, F., Dominy, B. W., and Feeney, P. J. (2012). Experimental and computational approaches to estimate solubility and permeability in drug discovery and development settings 1. *Adv. Drug Delivery Rev.* 64 (1–3), 4–17. doi: 10.1016/j.addr.2012.09.019
- Liu, H., and Pope, R. M. (2003). The role of apoptosis in rheumatoid arthritis. *Curr. Opin. Pharmacol.* 3 (3), 317–322. doi: 10.1016/S1471-4892(03)00037-7
- Liu, J. W., Wang, Y. H., Li, Y. Y., Zhang, Y. G., Zhao, L., Zhang, R. N., et al. (2017). Effect of Huangqi Guizhi Wuwutong on Joint Synovial Cell Apoptosis in CIA Rat Models. *Chin. J. Exp. Tradit. Med. Formulae.* 23 (14), 171–176. doi: 10.13422/j.cnki.syfjx.2017140171
- Liu, M., Wu, F., Zhang, W., Wang, X., Ma, J., Dai, N., et al. (2019). Molecular mechanism of Sini San and Suanzaoren Tang in treatment of insomnia based on network pharmacology: a comparative study. *J. Beijing Univ. Tradit. Chin. Med.* 42 (01), 48–55. doi: 10.3969/j.issn.1006-2157.2019.01.008
- Lopes, C. T., Franz, M., Kazi, F., Donaldson, S. L., Morris, Q., and Bader, G. D. (2010). Cytoscape Web: an interactive web-based network browser. *Bioinformatics* 26 (18), 2347–2348. doi: 10.1093/bioinformatics/btq430
- Luo, W., and Brouwer, C. (2013). Pathview: an R/Bioconductor package for pathway-based data integration and visualization. *Bioinformatics* 29 (14), 1830–1831. doi: 10.1093/bioinformatics/btt285
- Li, T. T., Shu, Z. H., Yu, L., Hao, W. J., and Fu, X. Y. (2015). Hplc/dad fingerprints and determination of main flavones in radix astragali from different origins. *Chin. J. Hosp. Pharmacy.* 35 (13), 1182–1187. doi: 10.13286/j.cnki.chinhosppharmacyj.2015.13.05
- Lv, Y. N., Li, S. X., Zhai, K. F., Kou, J. P., and Yu, B. Y. (2014). Network pharmacology-based prediction and verification of the molecular targets and pathways for schisandrin against cerebrovascular disease. *Chin. J. Nat. Med.* 12 (4), 251–258. doi: 10.1016/s1875-5364(14)60051-0
- Mi-La, C., Young Ok, J., Young-Mi, M., So-Youn, M., Chong-Hyeon, Y., Sang-Heon, L., et al. (2006). Interleukin-18 induces the production of vascular endothelial growth factor (VEGF) in rheumatoid arthritis synovial fibroblasts via AP-1-dependent pathways. *Immunol. Lett.* 103 (2), 159–166. doi: 10.1016/j.imlet.2005.10.020
- National Pharmacopoeia Commission. *Pharmacopoeia of the People's Republic of China: a 2015 edition [S]*. (2015) Beijing: China Pharmaceutical Science and Technology Press.
- Pan, F., Zhu, L., Lv, H., and Pei, C. (2016). Quercetin promotes the apoptosis of fibroblast-like synoviocytes in rheumatoid arthritis by upregulating lncRNA MALAT1. *Int. J. Mol. Med.* 38 (5), 1507–1514. doi: 10.3892/ijmm.2016.2755
- Peng, D. P., Tang, X. H., and Yan, Y. M. (2013). Effects of Guizhi Fuzi Decoction on tumor necrosis factor in rheumatoid arthritis. *Chin. J. Basic Med. Tradit. Chin. Med.* 19 (10), 1136–1138.
- Radicchi, F., Castellano, C., Cecconi, F., Loreto, V., and Parisi, D. (2004). Defining and identifying communities in networks. *Proc. Natl. Acad. Sci. U. States America* 101 (9), 2658–2663. doi: 10.1073/pnas.0400054101
- Ru, J., Peng, L., Wang, J., Wei, Z., Li, B., Chao, H., et al. (2014). TCMSP: a database of systems pharmacology for drug discovery from herbal medicines. *J. Cheminf.* 6 (1), 13. doi: 10.1186/1758-2946-6-13
- Rubbert-Roth, A. (2012). [New kinase inhibitors]. *Z. Für Rheumatol.* 71 (6), 479–484. doi: 10.1007/s00393-011-0880-9
- Sarau, A., Devauchelle-Pensec, V., Engerran, L., and Flipo, R. M. (2006). Most rheumatologists are conservative in active rheumatoid arthritis despite methotrexate therapy: results of the PRISME survey. *J. Rheumatol.* 33 (7), 1258–1265. doi: 10.1016/j.jbspin.2005.12.011
- Schett, G., and Zwerina, J. (2008). The p38 mitogen-activated protein kinase (MAPK) pathway in rheumatoid arthritis. *Ann. Rheum. Dis.* 67 (7), 909–916. doi: 10.1136/ard.2007.074278
- Shi, X. G., Zhu, W., Huang, Z. S., Zhao, Z. D., and Wang, Z. W. (2006). Effects of Huangqi Guizhi Wuwu decoction (黄芪桂枝五物汤) on rats with adjuvant arthritis. *Pharmacol. Clinics Chin. Mater. Med.* 22 (34), 3–5. doi: 10.1111/j.1745-7254.2006.00347.x
- Smith, M. D., and Walker, J. G. (2004). Apoptosis a relevant therapeutic target in rheumatoid arthritis? *Rheumatology* 43 (4), 405–407. doi: 10.1093/rheumatology/keh084
- Sodhi, A., Naik, S., Pai, A., and Anuradha, A. (2015). Rheumatoid arthritis affecting temporomandibular joint. *Contemp. Clin. Dent.* 6 (1), 124–127. doi: 10.4103/0976-237X.149308
- Sun, L., Zhou, H. Y., Zhao, R. H., You, C., and Chang, Q. (2009). Determination of six kinds of monoester- and diester-alkaloids in radix aconitii lateralis praeparata by hplc. *Chin. Tradit. Herbal Drugs* 40 (1), 131–134. doi: 10.3321/j.issn:0253-2670.2009.01.039
- Tao, W., Xu, X., Wang, X., Li, B., Wang, Y., Li, Y., et al. (2013). Network pharmacology-based prediction of the active ingredients and potential targets of Chinese herbal Radix Curcumae formula for application to cardiovascular disease. *J. Ethnopharmacol.* 145 (1), 1–10. doi: 10.1016/j.jep.2012.09.051
- Wang, X., and Zhong, W. (2015). Isorhamnetin attenuates collagen-induced arthritis via modulating cytokines and oxidative stress in mice. *Int. J. Clin. Exp. Med.* 8 (9), 16536–16542.
- Wang, C., Ren, Q., Chen, X. T., Song, Z. Q., Ning, Z. C., Gan, J. H., et al. (2018). System Pharmacology-Based Strategy to Decode the Synergistic Mechanism of Zhi-zhu Wan for Functional Dyspepsia. *Front. Pharmacol.* 9, 841. doi: 10.3389/fphar.2018.00841
- Wang, W. P., Shi, S. M., Liu, J., and Zhang, Q. Q. (2010). Treatment of 31 cases of rheumatoid arthritis of qi-blood deficiency by internal and external administration of modified “Huangqi Guizhi Wuwu Decoction”. *Shanghai J. Tradit. Chin. Med.* 44 (5), 43–45. doi: 10.16305/j.1007-1334.2010.05.014
- Wang, Y. J., Li, J., and Zhang, H. R. (2013). Simultaneous determination of rutin, quercetin and isorhamnetin in zizyphus jujuba cv. jun by hplc. *Food Res. Dev.* 34 (6), 83–88. doi: 10.3969/j.issn.1005-6521.2013.06.023
- Xia, S. U., and Song, G. U. (2011). Experimentall Effect of Guizhi Fuzi Decoction on Levels of Interleukin 6 in Adjuvant-Induced Arthritis Rats. *J. liaoning Univ. Tradit. Chin. Med.* 13 (6), 250–255. doi: 10.13194/j.jlunivtcm.2011.06.252.sux.091
- Xie, J.-J., Yu, Y., Wang, Y.-T., and Li, S.-P. (2007). Simultaneous hplc determination of 6 components in angelica sinensis. *Chin. J. Pharm. Anal.* 27 (9), 1314–1317. doi: 10.16155/j.0254-1793.2007.09.008
- Xu, Y. D., Song, X. M., Jin, H. T., and Zhang, S. J. (2010). Expression of HIF-1 α and VEGF in synovium of knee joint in adjuvant-induce-arthritis rat. *Chin. J. Immunol.* 4 (26), 360–362. doi: 10.3969/j.issn.1000-484X.2010.04.016
- Xu, X., Zhang, W., Huang, C., Li, Y., Yu, H., Wang, Y., et al. (2012). A novel chemometric method for the prediction of human oral bioavailability. *Int. J. Mol. Sci.* 13 (6), 6964–6982. doi: 10.3390/ijms13066964
- Xue, R., Fang, Z., Zhang, M., Yi, Z., Wen, C., and Shi, T. (2013). TCMID: Traditional Chinese Medicine integrative database for herb molecular mechanism analysis. *Nucleic Acids Res.* 41, D1089. doi: 10.1093/nar/gks1100
- Yang, J., and Leskovec, J. (2012). “Community-Affiliation Graph Model for Overlapping Network Community Detection” in *IEEE International Conference on Data Mining*. 1170–1175. doi: 10.1109/ICDM.2012.139
- Yao, G., Dan, W. U., Jun-Sheng, T., Yu-Zhi, Z., Xiao-Xia, G., and Xue-Mei, Q. (2018). Mechanism of network pharmacology of Xiaoyao Powder and Kaixin Powder in treating depression with “Same disease with different treatments”. *Chin. Tradit. Herbal Drugs* 49 (15), 3483–3492. doi: 10.7501/j.issn.0253-2670.2018.15.004
- Zhang, K. W., Song, S., Cui, X. B., and Xu, Z. Y. (2009). Determination of 6-gingerol and 6-shogaol in ginger of different districts in china. *Chin. Pharm. J.* 44 (22), 1692–1694.
- Zhu, L., Wei, H., Wu, Y., Yang, S., Xiao, L., Zhang, J., et al. (2012). Licorice isoliquiritigenin suppresses RANKL-induced osteoclastogenesis in vitro and

prevents inflammatory bone loss in vivo. *Int. J. Biochem. Cell Biol.* 44 (7), 1139–1152. doi: 10.1016/j.biocel.2012.04.003

Conflict of Interest: The authors declare that the research was conducted in the absence of any commercial or financial relationships that could be construed as a potential conflict of interest.

Copyright © 2020 Wang, Gao, Lu, Li, Zhou, Qin, Du, Gao, Guan and Lu. This is an open-access article distributed under the terms of the Creative Commons Attribution License (CC BY). The use, distribution or reproduction in other forums is permitted, provided the original author(s) and the copyright owner(s) are credited and that the original publication in this journal is cited, in accordance with accepted academic practice. No use, distribution or reproduction is permitted which does not comply with these terms.



Potential Advantages of Bioactive Compounds Extracted From Traditional Chinese Medicine to Inhibit Bone Destructions in Rheumatoid Arthritis

Yingjie Shi^{1,2}, Haiyang Shu^{2,3}, Xinyu Wang^{2,4}, Hanxiao Zhao^{2,3}, Cheng Lu², Aiping Lu^{1,5*} and Xiaojuan He^{2*}

¹ Shanghai Innovation Center of TCM Health Service, Shanghai University of Traditional Chinese Medicine, Shanghai, China, ² Institute of Basic Research in Clinical Medicine, China Academy of Chinese Medical Sciences, Beijing, China, ³ The Second Clinical Medical College, Guangzhou University of Chinese Medicine, Guangzhou, China, ⁴ College of Medicine, Southwest Jiaotong University, Chengdu, China, ⁵ School of Chinese Medicine, Law Sau Fai Institute for Advancing Translational Medicine in Bone and Joint Diseases, Hong Kong Baptist University, Hong Kong, Hong Kong

OPEN ACCESS

Edited by:

Alejandro Urzua,
University of Santiago, Chile

Reviewed by:

Shijun Xu,
Chengdu University of Traditional
Chinese Medicine, China
Jianxin Chen,
Beijing University of Chinese
Medicine, China

*Correspondence:

Aiping Lu
aipinglu@hkbu.edu.hk
Xiaojuan He
hxj19@126.com

Specialty section:

This article was submitted to
Ethnopharmacology,
a section of the journal
Frontiers in Pharmacology

Received: 14 May 2020

Accepted: 16 September 2020

Published: 07 October 2020

Citation:

Shi Y, Shu H, Wang X, Zhao H, Lu C,
Lu A and He X (2020) Potential
Advantages of Bioactive Compounds
Extracted From Traditional Chinese
Medicine to Inhibit Bone Destructions
in Rheumatoid Arthritis.
Front. Pharmacol. 11:561962.
doi: 10.3389/fphar.2020.561962

Bone destruction is an important pathological feature of rheumatoid arthritis (RA), which finally leads to the serious decline of life quality in RA patients. Bone metabolism imbalance is the principal factor of bone destruction in RA, which is manifested by excessive osteoclast-mediated bone resorption and inadequate osteoblast-mediated bone formation. Although current drugs alleviate the process of bone destruction to a certain extent, there are still many deficiencies. Recent studies have shown that traditional Chinese medicine (TCM) could effectively suppress bone destruction of RA. Some bioactive compounds from TCM have shown good effect on inhibiting osteoclast differentiation and promoting osteoblast proliferation. This article reviews the research progress of bioactive compounds extracted from TCM in inhibiting bone destruction of RA, so as to provide references for further clinical and scientific research.

Keywords: bone destruction, rheumatoid arthritis, traditional Chinese medicine, bioactive compounds, bone metabolism

INTRODUCTION

Rheumatoid arthritis (RA) is a erosive autoimmune condition with lingering course (Smolen et al., 2016). Bone destruction is one of the most typical pathological features in the early RA patients, more than 10% of patients will occur pathological manifestation 8 weeks after onset (Panagopoulos and Lambrou, 2018). Current drugs for the treatment of RA are mainly non-steroidal anti-inflammatory drugs (NSAIDs), disease modifying anti-rheumatic drugs (DMARDs), hormones, biological agents and so on. Although these drugs alleviate the process of bone destruction to a certain extent, the long-term use is easy to produce side effects. Therefore, further scientific research on the treatment of bone destruction is still urgently needed. As is known to all, traditional Chinese medicine (TCM) has been used to treat RA for centuries and shown good efficacy (Guo Q. et al.,

2017; Zhang Q. et al., 2019; Zhao H. et al., 2018). Recently, accumulating evidence have indicated that bioactive compounds extracted from TCM can effectively inhibit osteoclast differentiation as well as promote osteoblast proliferation, and may be used as potential therapeutically drugs. Therefore, this paper aims to review the potential therapeutic effect and targets of some representative bioactive compounds extracted from TCM, in order to provide reference for future research and development.

BONE METABOLISM IMBALANCE IS THE KEY TO BONE DESTRUCTION IN RA

Bone is a metabolically active organ that keeps alive through continuous renewal in the process of bone remodeling. Bone remodeling depends on the balance between bone formation and bone resorption that maintains the homeostasis of bone reconstruction (Lian, 2015). Bone destruction in RA mainly lies in excessive bone absorption and insufficient bone reconstruction. Osteoclasts play an important role in bone resorption; they are derived from monocyte/macrophage-lineage hematopoietic precursor cells which are stimulated by macrophage colony stimulating factor (M-CSF) and receptor activator of nuclear factor- κ B ligand (RANKL) (Fujiwara et al., 2016). Mature osteoclasts can express proteins including integrin, artrate resistant acid phosphatase (TRAP), calcitonin receptor (CTR), cathepsin K (CTSK), and matrix metalloproteinase (MMP) at the bone surfaces that are infiltrated by synovial cells (Zhu et al., 2020a). Osteoclast differentiation is a complex multistep process, and its molecular mechanism mainly involves the regulation of inflammation mediators, transcription factors, and signal pathways. Inflammatory mediators including tumor necrosis factor- α (TNF- α), interleukin-1 beta (IL-1 β), interleukin-6 (IL-6), interleukin-8 (IL-8), and interleukin-17 (IL-17), prostaglandin E2 (PGE2), inducible nitric oxide synthase (iNOS), etc., can promote the augment of RANKL and M-CSF after binding to the receptors on osteoclasts, so as to aggravate bone resorption in RA. Simultaneously, the initiation of osteoclast differentiation in the process of bone destruction in RA also needs the regulation of transcription factors including nuclear factor of activated T cells (NFATc1), cellular oncogene fos (c-fos), cellular oncogene jun (c-Jun) (Zhu et al., 2020a). These cytokines mediate the regulation of osteoclasts on bone destruction in RA through multiple signal pathways. For instance, TNF- α and other pro-inflammatory cytokines secreted by synoviocytes and T cells in RA promote osteoclast differentiation by activating nuclear factor kappa-B (NF- κ B), mitogen-activated protein kinase (MAPK), Janus kinase/signal transducer and activator (JAK/STAT), hypoxia inducible factor-1 α (HIF-1 α), phosphatidylinositol-3 kinase/protein-serine-threonine kinase (PI3K/AKT), Toll-like receptor (TLR), etc. In-depth understanding of the pathological process of osteoclasts in RA, monitoring and interfering with the cytokines and signal pathways that promote osteoclast

activation can provide a new target for the treatment of bone destruction in RA.

The occurrence of bone destruction in RA is not only the reason of the enhancement of bone resorption mediated by osteoclasts, but also due to the limited bone formation (bone repair) mediated by osteoblasts (Gravallese, 2017). Osteoblasts participate in osteoclasts regulation by expressing RANKL and OPG (Corrado et al., 2017). Bone marrow mesenchymal stem cells (BMSCs) are the main source of osteoblasts, BMSCs is a kind of stem cells with the potential of self-proliferation and multi-directional differentiation, which can differentiate into bone, cartilage, muscle, and other tissues under the action of different environments and stimulating factors (Komori, 2010). Because of the stimulation of cytokines such as insulin-like growth factor 1 (IGF-1) and transforming growth factor- β (TGF- β), BMSCs differentiate into osteoblast progenitor cells under the regulation of transcription factors such as Runt-related transcription factor 2 (Runx2) and bone morphogenetic protein-2 (BMP-2) (Blair et al., 2017; Komori, 2019). Subsequently, osteoblasts form osteoid, and mature osteoblasts highly express calcification-related proteins, which are mainly osteocalcin (OCN), bone morphogenetic protein-2 (BMP-2), and osteopontin (OPN) (Blair et al., 2017; Halling Linder et al., 2017; Komori, 2019). At the same time, Wnt/ β -catenin, BMP/Smad, and Notch signaling pathways will act on osteoblast differentiation and maturation. Sclerostin and dickkopf-related protein 1 (Dkk-1) are the Wnt/ β -catenin signaling pathway inhibitors which prevent low-density lipoprotein receptor-related protein 5/6 (LRP 5/6) from binding to downstream signal receptor. Studies have found the expression of Wnt/ β -catenin signal pathway inhibitors in osteoblasts of patients with RA was increased, which inhibited the activity of osteoblasts and promoted osteoblast apoptosis, and TNF- α and IL-1 played a promoting role (Miao et al., 2013). BMP/Smad signaling pathway can promote the formulation of osteoblasts by regulating all aspects of osteoblast cycle and has a synergistic effect with Wnt/ β -catenin signaling pathway (Dejaeger et al., 2017). Miyazono et al. found that both osteoblast development and osteoblast function in BMP2/4 knockout mice were defective, and the number of osteoblasts decreased, all of which might be caused by the down-regulation of Runx2 and Osx (Miyazono et al., 2010). Verschueren et al. have proved that the total amount of phosphorylated Smad1 and Smad5 in synovium of patients with RA increased significantly compared with the control group (Verschueren et al., 2009). Many kinds of cytokines and signal pathways are interlaced with each other, and the correlation is complicated in bone metabolism. Therefore, it is the key to treat bone destruction in RA by regulating the balance between osteoclasts and osteoblasts.

EXISTING CHEMICAL AND BIOLOGICAL DRUGS FOR TREATING BONE DESTRUCTION IN RA

Once bone destruction occurs, it means that its pathological changes enter an irreversible phase, so delaying or even blocking

bone destruction has become one of the main strategies for the treatment of RA. The treatment guidelines recommend the use of methotrexate (MTX) or biological disease modifying anti-rheumatic drugs (bDMARDs) first when bone destruction is found (Singh et al., 2016; Smolen et al., 2017). Conventional synthetic disease modifying anti-rheumatic drugs (csDMARDs) is regarded as the cornerstone in the treatment of RA, and it is also a first-line drug recognized by domestic and foreign guidelines (Singh et al., 2016; Smolen et al., 2017). This type of drug can effectively control the development of the disease, improve the clinical symptoms of RA and prevent the continued destruction of joint structure, but the therapeutic effect is relatively slow and it is not effective in all patients with RA (Schett et al., 2016). Glucocorticoids have strong anti-inflammatory and immuno-suppressive effects, short-acting hormones are used in the treatment of acute stage of RA (Güler-Yüksel et al., 2018). low-dose glucocorticoid can quickly relieve joint swelling and prevent joint bone destruction (Tada et al., 2016). However, unreasonable long-term use of glucocorticoids can lead to a decrease in bone mineral density and an increase in the risk of fractures (Zerbini et al., 2017; Güler-Yüksel et al., 2018). The emergence of bDMARDs can be said to be a breakthrough in the treatment of bone destruction in RA and bDMARDs have clear targeting in the treatment of bone destruction (Aletaha and Smolen, 2018). The main function of it is to antagonize the activities of T cells, B cells, osteoclasts, cytokines, and some small molecules, which delay bone destruction (Ho et al., 2019). Although the bDMARDs can correct the abnormal bone metabolism of patients to a certain extent, and improve their imaging examination and serum bone metabolism indexes, high costs reduce the dose, or frequency of bDMARDs (Burmester and Pope, 2017). In addition, they are not suitable for the complex conditions of all patients because of the single target (Zampeli et al., 2015). In summary, the current clinical application of drugs cannot adequately prevent the bone destruction in all RA patients. Due to the complexity of the bone destruction mechanism in RA, we need to explore multi-target drugs with reliable efficacy and little side effects.

EFFECT OF BIOACTIVE COMPOUNDS ON BONE DESTRUCTION IN RA

TCM in the treatment of rheumatism has a history of thousands of years, especially the single TCM and its bioactive compounds, which is more popular in recent years, the therapeutic effect of TCM on bone destruction has gradually become a new research hotspot (Shen et al., 2019). A large number of experimental studies have been carried out, which directly or indirectly verified the role of TCM in inhibiting bone destruction in RA from different perspectives. These studies have shown that bioactive compounds extracted from TCM could down-regulate bone destruction promoting factors and up-regulate bone protective factors (Cai X. et al., 2018). Due to its diversified action ways and targets, TCM may have potential advantage in restraining RA bone destruction. Therefore, in this

review, we elaborated the potential mechanisms of bioactive compounds extracted from TCM in the treatment of bone destruction in RA and divide them into alkaloids, saponins, flavonoids, and so on.

Alkaloids

Alkaloids generally represent a highly diverse group of compounds containing cyclic structures with at least one basic nitrogen atom, which exist widely in medicinal plants, such as *Coptis chinensis* Franch., *Sinomenium acutum* (Thunb.) Rehder & E.H. Wilson, *Conioselinum anthriscoides* 'Chuanxiong', *Ephedra sinica* Stapf, etc (Bednarz et al., 2019). In recent years, it has been found that alkaloids have many pharmacological activities, such as anti-inflammatory, analgesic and immunoregulation (Bach and Lee, 2019). The bone-protective alkaloids include sinomenine (SIN), tetrandrine (TET), norisoboldine (NOR), berberine, magnoflorine, ligustrazine, etc. The repair effect of SIN, TET, NOR on bone destruction in RA has been confirmed.

SIN is a kind of bioactive compound extracted from the medicinal rhizome of *Sinomenium acutum* (Thunb.) Rehder & E.H. Wilson, which has been used in the treatment of various diseases for hundreds of years. SIN is one of the strongest histamine-releasing agents, and has been proved to have anti-inflammatory, immunosuppressive, analgesic, antihypertensive, and anti-arrhythmic effects (Sun et al., 2010). In China and Japan, several SIN preparations have been used for RA in clinical practice, such as Zhengqing Fengtongning sustained-release tablets, SIN hydrochloride injection (Liu et al., 2016). The pharmacological basis of SIN in the treatment of RA lies in its anti-inflammatory, analgesic and immunosuppressive effects. Wei-Wei Liu et al. systematically evaluated the efficacy and safety of SIN in treating RA by searching the Pubmed, Cochrane Library, and other databases electronically, and including sixteen randomized controlled trials (RCTs) involving 1,500 subjects; the results of this meta-analysis indicated that SIN had better clinical efficacy and relatively fewer adverse events in the treatment of RA when compared to MTX (Liu et al., 2016). Initially, the effect of SIN on RA is the inhibition of synovitis. Related studies have confirmed that SIN exerted an effect on anti-inflammatory and immunomodulatory activities in the treatment of synovitis in RA by inhibiting pro-inflammatory cytokines, inhibiting synovial cells proliferation and T cell activation, and regulating monocyte/macrophage subsets (Zhao et al., 2007; Zhang et al., 2015; Liu et al., 2016). In addition, the preponderance of SIN in the treatment of bone destruction in RA are gradually emerging with the deepening of basic research. On one hand, SIN can indirectly inhibit bone destruction in RA by inhibiting the secretion of pro-inflammatory cytokines. on the other hand, it can directly inhibit osteoclast-mediated bone resorption (Bao et al., 2017; Liu et al., 2018). NFATc1 is one of the important transcription factors that induce osteoclast differentiation, and it can induce the formation of osteoclast specific genes such as TRAP, CTR and CTSK (Li H. et al., 2018). Recent studies have shown that NFATc1 is mainly activated through NF- κ B and Ca²⁺ signaling pathways (Bendickova et al., 2017). Long-gang He et al. found

that SIN inhibited the expression and transcriptional activity of NFATc1 mRNA during the differentiation of human peripheral blood mononuclear cells into osteoclasts induced by lipopolysaccharide (LPS), and the main mechanism was to inhibit the activation of NF- κ B and reduce the level of Ca^{2+} in cells (He et al., 2016). In addition, SIN also reduced the breast cancer cells induced bone destruction by inhibiting the protein activity of NFATc1 (Zhang et al., 2019b). The OPG/RANKL ratio plays a decisive role in osteoclast differentiation. SIN regulated OPG/RANKL ratio induced by PGE2 and reduced the amount of TRAP-positive multinucleated osteoclasts which differentiated from RAW264.7 cells (Zhou B. et al., 2017). Another study showed that SIN obviously reduced the activation of caspase-3 and the phosphorylation of p38 (p-p38), and JNK (p-JNK) in RANKL-stimulated RAW264.7 cells, but has no effect on ERK1/2 phosphorylation (He et al., 2014; Li X. et al., 2013). Xiaojuan Li et al. confirmed that SIN prevented the reduction of tissue mineral density (TMD), bone mineral density (BMD), trabecular number (Tb. N), trabecular thickness (Tb. Th), as well as the activity of TRACP5b and ALP in RA rat model induced by M. tuberculosis H37Ra (Mt) (Li X. et al., 2013). The inhibitory effect of SIN on bone resorption was also confirmed in collagen-induced arthritis (CIA) rats that SIN reduced the level of MMP-3 and MMP-13 in serum and RANKL protein expression in the synovium (Sun et al., 2014). Obviously, SIN has a good prospect and application potential in the field of clinical treatment of bone destruction in RA. However, current researches of SIN were mainly focused on its inhibitory effect on bone resorption, its effect on bone formation in RA is still unknown and needs further research. Meanwhile, the adverse effects caused by SIN through histamine release, such as allergic reactions and gastrointestinal reactions, have severely impeded the further clinical application of SIN. For people with allergic constitution, SIN should be taken in small doses and the use of SIN should be cautious; and it is suggested to avoid taking high-fat and high-protein diets during administration. For digestive tract reactions, appropriate preparation forms should be selected to alter the irritation and instability of SIN. Hence, further studies are urgently needed to explore the possibilities of decreasing the clinical adverse effects of SIN.

Besides SIN, other alkaloids also have the effect on bone destruction in RA. As a potential ligand of aryl hydrocarbon receptor (AhR), TET markedly inhibited the differentiation of RAW264.7 cells and bone marrow-derived macrophages (BMMs) into osteoclasts through AhR/c-Src/c-Cbl signal pathway. Moreover, bone mineral density (BMD) and trabecular bone (Tb) of bone parameters increased in CIA rats significantly after continuous administration of TET (Yuan et al., 2016; Jia et al., 2018; Jia Y. et al., 2019). NOR is the main isoquinoline alkaloid that inhibited the differentiation of osteoclasts *via* MAPK/NF- κ B/c-fos/NFATc1, HIF, and p38/ERK/AKT/AP-1 signal pathway, and it also significantly reduced the number of TRAP-positive multinucleated osteoclasts in the joints of CIA rats as well as the levels of RANKL, IL-6, PGE2, and MMP-13 in serum of AIA rats independently of its anti-inflammatory effect, but the results

also showed that NOR could not reduce the levels of OPG and MMP-1 (Luo et al., 2010; Wei et al., 2013a; Wei et al., 2013b; Wei et al., 2015). All these experimental evidences have been summarized in **Table 1**.

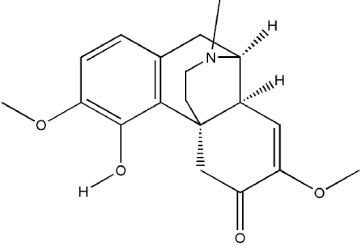
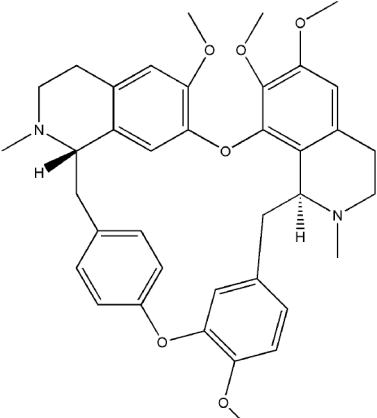
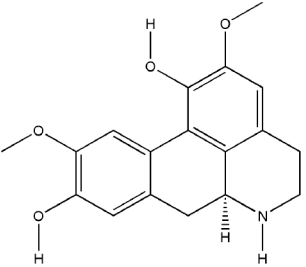
Berberine, magnoflorine, ligustrazine, and other alkaloids have been confirmed to inhibit the bone resorption or promote the bone formation *in vitro*, but whether they have any effect on bone destruction in RA is still unknown and needs to be verified *in vivo* (Wang et al., 2016; Wang et al., 2017; Cai Z. et al., 2018; Dinesh and Rasool, 2018). Collectively, most of the alkaloids play a role in relieving bone destruction by inhibiting the formation, differentiation and maturation of osteoclasts, and their biological activities may be related to their special structure which need to be explored by more related researches. The major challenges associated with alkaloid researches are the poor water solubility and low bioavailability which will limit their oral administration. Low bioavailability may be resolved by using semisynthetic and biochemical transformation approach. Most of the alkaloids have different biological characteristics, and biosynthesis of these agents is also varied. Therefore, it is indeed a daunting task to indicate the common mechanisms of action for alkaloids, because compounds exhibit differential cellular and molecular mechanisms even within a particular structural class. Hence, more studies *in vitro* and *in vivo* are needed to verify the effects of alkaloids agents on bone destruction in RA.

Saponins

Saponins are linked by hydrophobic sapogenins and hydrophilic glycosyl groups through glycosides which the main components are triterpenes or spiral steranes. They have the activities of anti-inflammatory and improving body immunity (Zhao Y. et al., 2018). Saponins' bone protection is also very prominent, triterpenoid saponins such as asperosaponin VI (ASA VI), ginsenoside Rg1, notoginsenoside R1, glycyrrhizin, and steroidal saponins such as dioscin, all of them are bone-protective saponins. The repair effect of ASA VI, ginsenoside Rg1 on bone destruction in RA has been confirmed.

ASA VI is the main bioactive compound of *Dipsacus japonicus* Miq., which has a wide range of pharmacological effects. Its pharmacological activities in neuroprotection, prevention of osteoporosis, anti-apoptosis, analgesia, etc. that have attracted the attention of the majority of scholars, and has high research and development value (Ke et al., 2016). Liu et al. demonstrated ASA VI inhibited osteoclast differentiation to protect bone tissue, it reduced the levels of TNF- α and IL-1 β in serum of CIA mice, and significantly reduced the expression of TRAP, CTSK, MMP-9 and β 3-integrin involved in bone resorption, in addition, the formation of F-actin ring induced by RANKL in BMMs significantly inhibited, as well as the phosphorylation levels of AKT, JNK, and p38 (Liu et al., 2019). ASA VI not only inhibited osteoclast differentiation, but also promoted osteoblast differentiation. ASA VI induced osteoblast maturation and differentiation, and then increase bone formation in MC3T3-E1 and primary osteoblastic cells *via* increasing BMP-2 synthesis, and activating p38 and ERK1/2 (Niu et al., 2011). Ding et al. demonstrated ASA VI enhanced the

TABLE 1 | Effects and mechanisms of alkaloids on bone destruction in rheumatoid arthritis (RA).

Bioactivecompounds	Source	Chemical structure	Targets	Functions	References
Sinomenine	<i>Sinomenium acutum</i> (Thunb.) Rehder & E.H. Wilson		Down-regulated: GM-CSF, IL-1, IL-12, TNF- α , IL-6, RANKL, NFATc1, TRAP, MMP-9, CTSK, TLR4/TRAFF6, Ca ²⁺ , p38MAPK-NF- κ B pathway Up-regulated: OPG	inhibit osteoclast differentiation	(Liu et al., 2018) (Zhou B. et al., 2017) (Yuan et al., 2018) (He et al., 2016)
Tetrandrine	<i>Stephania tetrandra</i> S. Moore		Down-regulated: NF- κ B-p65, NFATc1, IFN- γ , IL-17A, Syk-PLC γ 2 signaling pathway Up-regulated: IL-10, AhR nuclear translocation	inhibit osteoclast differentiation	(Jia et al., 2018) (Yuan et al., 2016) (Jia Y. et al., 2019)
Norisoboldine	<i>Lindera aggregata</i> (Sims) Kosterm.		Down-regulated: RANKL, IL-6, PGE2, MMP-13, TRAF6-TAK1, p38/ERK/AKT/AP-1, MAPKs/NF- κ B/c-Fos/NFATc1, HIF signal pathway	inhibit osteoclast differentiation	(Wei et al., 2013a) (Wei et al., 2013b) (Wei et al., 2015)

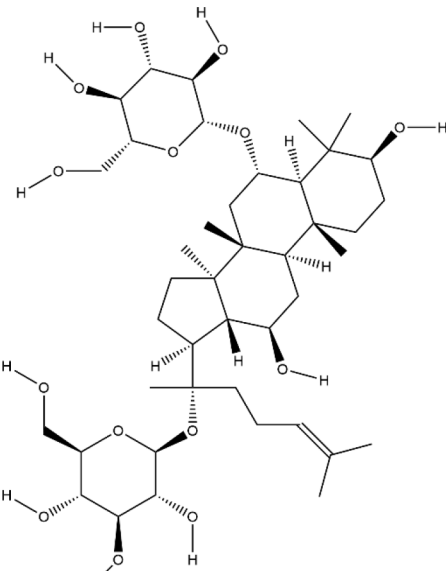
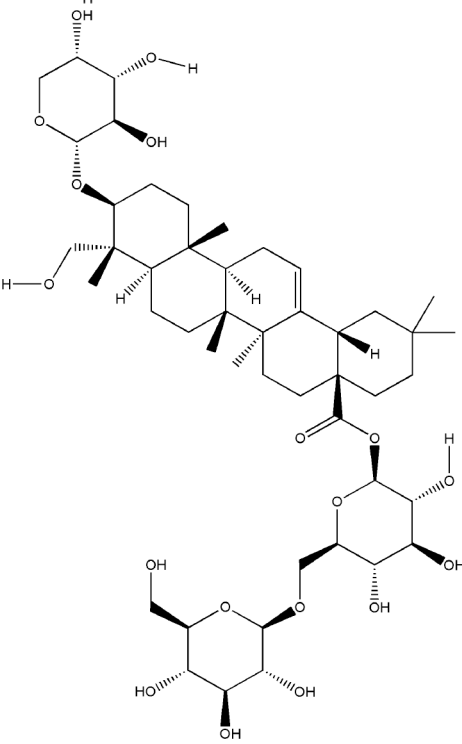
ALP activity of adipose-derived stem cells (ADSCs), promoted matrix mineralization, and up-regulated the phosphorylation of bone-related proteins OCN, Runx2, and Smad2/3, which promoted the osteogenic differentiation of ADSCs (Ding et al., 2019). Although the pharmacological action of ASA VI has a wide application prospect, its development and popularization are greatly limited by its poor bioavailability. It is suggested that it can be further improved through preparation technologies such as nano-drug delivery system, sustained and controlled release drug delivery system and so on.

Ginsenoside Rg1 effectively controlled the bone damage in CIA mice, which was mainly manifested by significant decrease in the number of osteoclasts in the interphalangeal joint and ankle joint, and the expression of TRAP, CTSK, MMP and calcitonin receptor (CTR) induced by RANKL was inhibited (Gu et al., 2014). This bone-protective effect was also effective in AIA rats, after intraperitoneal injection of ginsenoside Rg1 for 14 days, the levels of TNF- α and IL-6 in the blood of AIA rats were significantly decreased. In addition, Rg1 increased the expression of peroxisome proliferators-activated receptors-gamma (PPAR-

γ) protein and inhibited NF- κ B nuclear translocation in RAW264.7 cells stimulated by lipopolysaccharide (LPS) (Zhang et al., 2017). All these experimental evidences have been summarized in **Table 2**.

In vitro studies, it has been proven that notoginsenoside R1, glycyrrhizin, dioscin, and other saponins can inhibit the osteoclasts' differentiation or promote the osteoblasts' differentiation, but their effect on bone destruction in RA requires the verification of relevant animal experiments (Li Z. et al., 2018; Qu et al., 2014; Wang et al., 2015). Based on the above findings, we can find that most of the saponins (mainly triterpenoid saponins) play a role in bone resorption or bone formation. However, it is not known whether triterpenoid saponins and steroidal saponins have different pharmacological effects on bone-protection, whether the bone protection of steroidal saponins is affected by the structural changes of liver microsomes. Therefore, a large number of related experiments are still needed. Similarly, because of the structural diversity and complexity of saponins, the acquisition of many saponins is still a difficult task, which greatly limits the further exploration of

TABLE 2 | Effects and mechanisms of saponins on bone destruction in rheumatoid arthritis (RA).

Bioactivecompounds	source	Chemical structure	Targets	Functions	References
Ginsenoside Rg1	<i>Panax ginseng</i> C. A. Mey		Down-regulated: NF- κ B p65, MAPK, JNK, ERK1/2, P38, TNF- α , IL-6 Up-regulated: PPAR- γ	inhibit osteoclast differentiation and maturation	(Gu et al., 2014) (Zhang et al., 2017)
Asperosaponin VI	<i>Dipsacus japonicus</i> Miq.		Down-regulated: NFATc1, c-Fos, TNF- α , IL-6, IL-1 β , NF- κ B, MAPKs, AKT pathway Up-regulated: OCN, Runx2, Smad2/3 phosphorylation	inhibit osteoclast formation; promote osteogenic differentiation	(Liu et al., 2019) (Ding et al., 2019)

saponins' pharmacological activity and mechanism. In addition, the bioavailability of most saponins is low after oral administration, which also brings difficulties to the research of new drugs based on active natural saponins.

Flavonoids

Flavonoids generally refer to a series of bioactive compounds formed by the connection of two benzene rings with phenolic hydroxyl groups (A and B rings) through the central three

carbon atoms. They have the effects of anti-inflammation, anti-oxidation, scavenging free radicals and so on (Wen et al., 2017). The bioactive compounds of flavonoids for protecting effect on bone by acting on osteoclasts or osteoblasts include kaempferol (KP), quercetin, icariin, poncirin, baicalin, silibinin, etc. The repair effect of KP, quercetin, icariin on bone destruction in RA has been confirmed.

KP is a natural flavonol-type flavonoid, which is present in the rhizomes of the ginger plant *Kaempferia galanga* L.

According to literature reports, previous studies have shown that KP has many pharmacological effects, such as anticancer, anti-inflammatory, antioxidant, antibacterial, antiviral, immunosuppressive, etc (Calderón-Montañón et al., 2011; Jia Z. et al., 2019). KP is the basis of the quality control standard of Duanteng Yimutang preparation for clinical treatment of RA, the mechanism and molecular target of KP in the treatment of RA can provide more theoretical support and basis for its clinical application. The effect of KP on synovitis is shown that it inhibited proliferation, induced apoptosis, and ameliorated inflammation in fibroblast-like synoviocytes by suppressing the NF- κ B and AKT/mTOR pathways or targeting on the fibroblast growth factor receptor 3 (FGFR3)-ribosomal S6 kinase 2 (RSK2) signaling axis (Wang J. et al., 2019). In addition to its inhibitory effect on synovitis, KP also showed bone-protecting effect in the treatment of RA. KP's bone-protective function in RA is to inhibit pro-inflammatory cytokines indirectly, it also can directly act on osteoclast-mediated bone resorption or osteoblast-mediated bone formation. Alice Wattel et al. explored the effect of KP on bone resorption for the first time, they found KP directly induced apoptosis of mature osteoclasts in the highly purified rabbit osteoclasts, and its estrogenic effect could be involved in the inhibition of bone resorption (Wattel et al., 2003). KP inhibited RANKL-induced expression of c-fos, c-RANK and CTR in RAW264.7 cells, however, TNF- α -stimulated intracellular ROS production was unaltered by KP (Pang et al., 2006). KP inhibited IL-1 β -stimulated, RANKL-mediated the expression of NFATc1, phosphorylation of ERK 1/2, p38 and JNK MAP kinases in bone marrow cells (Lee et al., 2014). Autophagy has pivotal roles in maintaining bone metabolic balance. Sequestosome 1 (p62/SQSTM1) is an important bridge protein that becomes incorporated into autophagosomes in RANKL-induced autophagy and osteoclastogenesis (Rea et al., 2013). Kim et al. found KP inhibited autophagy and promoted apoptotic cell death in RAW 264.7 cells by the degradation of p62/SQSTM1. KP's main manifestation of inhibiting osteoclastogenesis was to abrogate the formation of TRAP-positive multinucleated cells induced by RANKL in this *in vitro* experiment (Kim C. J. et al., 2018). There are studies that showed the direct effects of KP on osteoblastic cells or osteoblastic precursor cells by different mechanisms. KP's estrogenic effect acted on osteoblast differentiation, KP induced the activity of osteoblast differentiation biomarkers including ALP, OCN, osterix, Runx2 by estrogen receptor activation in rat primary osteoblasts (Guo et al., 2012). Interestingly, KP-mediated autophagy promotes osteoblast differentiation and bone mineralization. Kim et al. found KP increased the expression of the autophagy-related factors beclin-1, p62/SQSTM1, and the expression of osteoblast-related factors Runx2, osterix, BMP-2, and collagen I also decreased with dose dependent under the concentration of 10 μ M in MC3T3-E1 cells (Kim et al., 2016). With further insights into the mechanism of bone-protective action of KP, Yang Wang et al. found KP's regulation of Wnt/ β -catenin pathway was to up-regulate the microRNA-101 in MC3T3-E1 cells (Wang Y. et al., 2019). The effect of KP on bone destruction

in RA has also been confirmed *in vivo*. After intragastric administration of KP, the effect of synovitis on the invasion of surrounding bone and the level of MMP were suppressed in CIA model (Pan et al., 2018). Furthermore, KP inhibited the progressive structural destruction of RA joints by blocking the bFGF/FGFR3/RSK2 signaling axis in CIA model, the mainly manifest was shown as decreased the levels of osteoclast specific genes TRAP, CTR, CTSK, c-jun, and p50 (Lee et al., 2018). Though KP's poor bioavailability represents a significant obstacle, the use of KP-based nanoparticles has brought more hope on chemoprevention strategies. While KP shows potential for improving bone destruction by the alterations of osteoclast or osteoblast related protein genes or RNAs, but most of the research conducted on KP resistance to bone destruction potency was *in vitro*, making it difficult to draw a final conclusion on its usefulness, *in vivo* studies and clinical trials are scarce so far, thus stressing the need for more in-depth experiments.

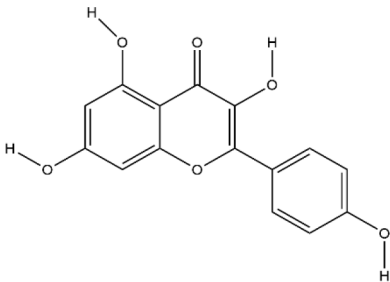
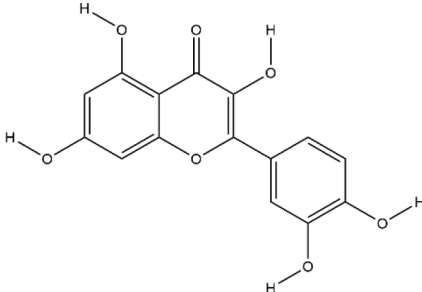
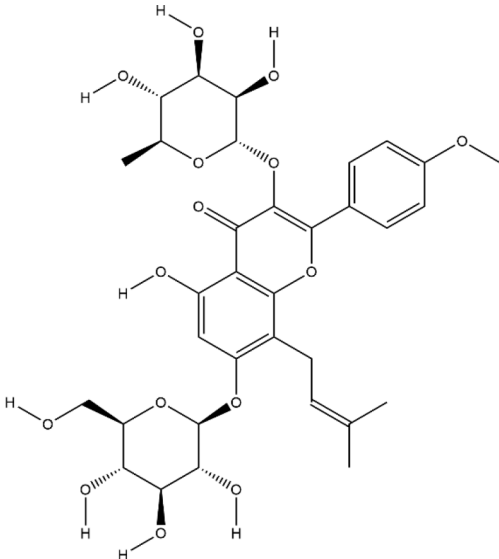
Quercetin and icariin are two other flavonoids with the effect of treating bone destruction in RA. Quercetin not only inhibited the expression of osteoclast-specific genes TRAP, CTSK, NFATc1 *in vitro*, and the plasma level of MMP-3, MMP-9 in CIA mice, but also up-regulated the mRNA and protein expression of osteoblast-specific genes Osx, Runx2, ALP and OCN (Guo C. et al., 2017; Haleagrahara et al., 2018; Kim H. R. et al., 2019). Icariin blocked osteoclast generation by inhibiting the expression of TRAF6 in the early stage of osteoclast formation and the activation of ERK1/2 and NF- κ B. In addition, the decrease of F-actin ring formation revealed that bone resorption capacity of mature osteoclasts was inhibited by Icariin. Moreover, Icariin's inhibitory effect on bone resorption in RA has also been confirmed in CIA model (Chi et al., 2014; Kim B. et al., 2018; Xu et al., 2019). All these experimental evidences have been summarized in **Table 3**.

Poncirin, baicalin, silibinin, and other flavonoids have been shown significant effects on osteoclasts or osteoblasts (Kim et al., 2009; Lu et al., 2017; Chun et al., 2020). But whether they can repair bone destruction in RA is not verified which need a large number of relevant animal experiments. Actually, most of the flavonoids play a role in bone resorption or bone formation by different signal transduction mechanisms. Autophagy may be involved in, but still need conduct appropriate animal experiments. The difference between protective autophagy and inhibitory autophagy induced by flavonoids may be related to the type, mode and dose of flavonoids, as well as the type and the state of the cell lines. Moreover, most flavonoids have low cytotoxicity to normal cells at normal dose, and are safer than traditional cytotoxic drugs, so they have strong potential for clinical application.

Terpenoids

Terpenoids, a kind of compounds with isoprene unit (C5 unit) as the basic structural unit in the molecular framework, have anti-inflammatory, immunoregulatory and other pharmacological activities (Guesmi et al., 2017). The bioactive compounds of terpenoids for protecting effect on bone include triptolide (TP), celastrol, artesunate, parthenolide, andrographolide (AP), etc.

TABLE 3 | Effects and mechanisms of flavonoids on bone destruction in rheumatoid arthritis (RA).

Bioactive compounds	Source	Chemical structure	Targets	Functions	References
Kaempferol	<i>Kaempferia galanga</i> L.		Down-regulated: MMP-1, MMP-3, COX-2, PGE2, ERK-1/2, p38, JNK, NF- κ B, TRAP, CTR, MAPKs, c-Fos, NFATc1, CTSK, c-Jun Up-regulated: collagen I, Runx2, Osx, BMP-2, ATG5, beclin-1, LC3	inhibit osteoclast differentiation; promote osteoblast differentiation	(Yoon et al., 2013) (Lee et al., 2018) (Lee et al., 2014) (Kim et al., 2016)
Quercetin	<i>Sophora japonica</i> L.		Down-regulated: TNF- α , IL-1 β , MCP-1, IL-17, ERK, I κ B α , TRAP, CTSK, DC-STAMP, NFATc1, OC-STAMP, caspase3 Up-regulated: Wnt/ β -catenin signaling pathway	inhibit osteoclast differentiation; promote osteoblast differentiation and inhibit osteoblast apoptosis	(Kim et al., 2019) (Guo C. et al., 2017)
Icariin	<i>Epimedium brevicornu</i> Maxim.		Down-regulated: TRAF6, ERK phosphorylation, NF- κ B, MAPK signaling pathway	inhibit osteoclast formation and differentiation	(Kim B. et al., 2018) (Xu et al., 2019) (Hsieh et al., 2011)

The repair effect of TP, celastrol, artesunate on bone destruction in RA has been confirmed.

TP (a diterpene triepoxide in chemical structure), extracted from *Tripterygium wilfordii* Hook.f., is a kind of natural product with various biological activities. It attracted worldwide attention in the 1960s because of its pharmacological effects in a variety of diseases such as RA, no small cell lung cancer, and refractory nephrotic syndrome (Yuan et al., 2019). TP has been considered as a promising anti-RA drug which has definite effects including immunosuppression, anti-inflammatory reaction, inducing apoptosis, inhibiting angiogenesis (Li et al., 2014). Tripterygium wilfordii tablets, Tripterygium wilfordii glycosides tablets, and Tripterygium hypoglaucum hutch tablets which take triptolide as the quality control standard are

available in clinic (Law et al., 2011). The pharmacological effect of TP on synovitis is the focus of researchers to explore the mechanism of triptolide in the treatment of RA at the very start. TP treated synovitis in RA by regulating immune-related cells (such as T cells, macrophages, dendritic cells), immune-related inflammatory mediators and immune-related angiogenesis (Chan et al., 1999; Zhu et al., 2005; Kong et al., 2013). With the research developed, researchers found that delaying or even blocking bone destruction is another primary mechanism of TP in the treatment of RA. Zhu et al. systematically evaluated the effect of Tripterygium wilfordii glycosides tablets in the treatment of RA by searching the Pubmed, Web of Science, Cochrane Library and other databases, three RCTs were employed which involved a total of 223 subjects, and the

results indicated that *Tripterygium wilfordii* glycosides tablets had a good effect on regulating the modified Sharp score (mTSS), tender joint erosions (JE) and joint space narrowing (JSN), and the effect is better than the positive drugs MTX and sulfasalazine, which reflected the advantages of TP in the treatment of bone destruction in RA (Zhu G. Z. et al., 2019). As a typical anti-inflammatory drug, TP indirectly treated bone destruction in RA by inhibiting the levels of pro-inflammatory cytokines such as TNF- α and IL-1 β and promoting the secretion of IL-10 and TGF- β 1 derived from T cells (Xu et al., 2016). RANK-RANKL signaling activates a variety of downstream signaling pathways required for osteoclast development. TP suppressed RANKL-induced NF- κ B activation in osteoclast precursor cells by inhibiting I κ B α kinase activation, I κ B α phosphorylation, and I κ B α degradation effectively, and osteoclast formation induced by tumor cells was inhibited (Park, 2014). Spleen cells are also one of the main sources of osteoclast precursors, low-dose TP promoted the apoptosis of osteoclast precursors by inhibiting the overexpression of cellular inhibitor of apoptosis protein 2 (cIAP2) in fresh spleen cells induced by M-CSF (Wang et al., 2018). AKT-MDM2-induced cell death might contribute to the osteoclastogenesis suppression. Cui et al. found TP suppressed NFATc1 overexpression and AKT phosphorylation when PI3K-AKT-NFATc1 pathway was activated induced by RANKL in BMMCs or RAW264.7 cells (Cui et al., 2020). The therapeutic effect of TP on bone destruction in RA has been confirmed *in vivo*, TP improved bone destruction of TNF-Tg mice by decreasing the levels of pro-inflammatory cytokines, promoting the apoptosis of osteoclast precursors and inhibiting the generation of osteoclast (Wang et al., 2018). The result of Micro CT showed that TP significantly increased joint bone density, bone volume fraction and trabecular thickness of CIA mice, reduced trabecular separation of inflammatory joints through inhibiting the expression of RANKL and increasing the expression of OPG (Liu et al., 2013). Although TP has already been proved to have potential advantages in the treatment of bone destruction in RA *in vitro* and *in vivo*, its precise molecular targets that responsible for the potent biological activity have not been fully identified yet. At the same time, the side effects of TP are to block its clinical application to a great extent, development of efficient TP-targeted delivery system is an available strategy to realize targeted delivery of TP with reduced toxicity.

Celastrrol and artesunate are two other terpenoids with the effect of treating bone destruction in RA. Celastrrol played an inhibitory effect against the formation and function of osteoclasts by regulating the ratio of RANKL/OPG and the expression of transcription factors in osteoclasts induced by RANKL, the main mechanisms involved the phosphorylation of NF- κ B and MAPK (Nanjundaiah et al., 2012; Gan et al., 2015; Cascao et al., 2017). Artesunate down-regulated the expression of osteoclast-specific genes TRAP, CTSK, c-fos, and NFATc, as well as the expression of MMP-9 protein in CIA model hind paw by inhibiting the ERK and JNK phosphorylation (Li Y. et al., 2013; Wei et al., 2018). All these experimental evidences have been summarized in **Table 4**.

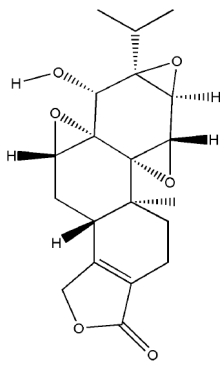
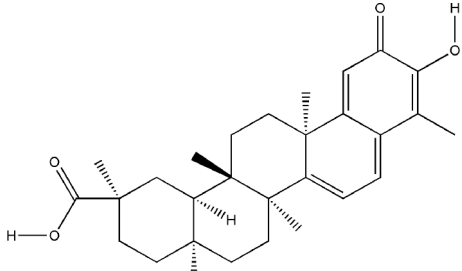
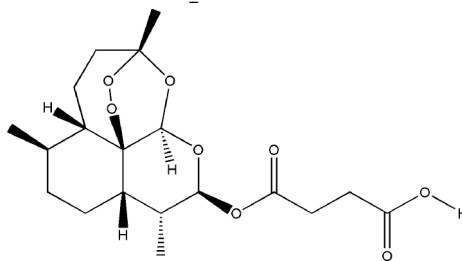
Parthenolide, AP and other terpenoids exerting an effect on osteoclasts or osteoblasts has been found *in vitro* (Kim et al., 2014; Qu et al., 2014; Zhang et al., 2014; Li et al., 2016). But whether they have any effect on bone destruction in RA is unknown, it is critical to verified terpenoids' pharmacological action of bone protection *in vivo*. Terpenoids are expected to become the main drugs for the treatment of bone destruction in RA with its significant pharmacological effects, low toxicity and side effects, but the efforts to further improve terpenoids' efficacy are limited because of the unclear structure-activity relationship. Therefore, it is necessary to explore new technical measures to definite the structure-activity relationship.

Phenols

Phenols is a kind of bioactive compound, and its hydroxyl group is directly connected to benzene ring or other aromatic ring. Phenols has strong effects of anti-oxidation, anti-atherosclerosis, anti-infection, anti-tumor, and anti-osteoporosis (Zenkov et al., 2016). The bioactive compounds of terpenoids for protecting effect on bone by acting on osteoclasts or osteoblasts including resveratrol (RES), ferulic acid (FA), curcumin, gastrodin, paeonol, etc. The repair effect of RES, FA on bone destruction in RA has been confirmed.

RES, extracted from *Reynoutria japonica* Houtt., is a naturally occurring polyphenolic compound containing stilbene structure. It has reported that RES has positive effects on health and increase life span (Baur and Sinclair, 2006). RES mainly functioned on the centrum restraint, heart sturdiness, inflammation diminishing, and anti-cancer (Ko et al., 2017; Wahab et al., 2017). At present, the role of RES in the treatment of RA is particularly remarkable because of its unique anti-inflammatory and immunosuppressive pharmacological effects. RES treated RA by enhancing the apoptosis of fibroblast-like synoviocytes, inhibiting angiogenesis, etc, the mechanism of its inhibition of synovitis included the regulation of NF- κ B, MAPK-p38, JAK/STAT, PI3K/AKT, etc signaling pathways (Yang et al., 2017; Yang et al., 2018; Zhang et al., 2019a). As a natural phytoestrogen, RES acts as an estrogen receptor agonist which obviously promotes bone growth under normal bone growth environment and protects bone under weightlessness and diseases (Baur and Sinclair, 2006). The dosage forms of RES used for RCT to investigate the effects of RES on bone in type 2 diabetic patients or metabolic syndrome (MetS) include RES tablets and RES capsules, these clinical trials further confirmed the protective effect of RES on bone (Ornstrup et al., 2014; Bo et al., 2018). RES is reported to impact bone destruction by increasing osteoblast differentiation and function *in vitro*. RES at non-toxic concentrations dose-dependently inhibited RANKL-induced osteoclast differentiation and induced osteoclast apoptosis by inhibition of ROS generation (He et al., 2010). RES improved the oxidative stress state of RAW264.7 cells, thus inhibited the mRNA expression of osteoclast specific enzyme MMP-9, TRAP, CTSK, this was the first time to confirm that RES promoted resistance to oxidative damage and restrained

TABLE 4 | Effects and mechanisms of terpenoids on bone destruction in rheumatoid arthritis (RA).

Bioactive compounds	Source	Chemical structure	Targets	Functions	References
Triptolide	<i>Tripterygium wilfordii</i> <i>Hook.f.</i>		Down-regulated: IL-1 α , IL-1 β , TNF- α , cIAP2, RANKL Up-regulated: IL-10, TGF- β 1, OPG	promote the apoptosis of osteoclast and inhibit osteoclast differentiation	(Wang et al., 2018) (Wang S. et al., 2019) (Liu et al., 2013) (Xu et al., 2016)
Celastrrol	<i>Tripterygium wilfordii</i> <i>Hook.f.</i>		Down-regulated: IL-6, IL-1 β , NF- κ B, 90 β protein, c-Fos, c-Jun, NFATc1, TRAP, CTSK, CTR, MMP-9, RANKL, GM-CSF, M-CSF, OPN, IGF-1, MMP-9	inhibit osteoclast differentiation and function	(Astry et al., 2015) (Cascao et al., 2017) (Gan et al., 2015) (Nanjundaiah et al., 2012)
Artesunate	<i>Artemisia annua</i> L.		Down-regulated: MMP-9, TNF- α , IL-1 β , IL-17, ERK, JNK, TRAP, CTSK, c-Fos, NFATc1	inhibit osteoclast differentiation	(Li Y. et al., 2013) (Wei et al., 2018)

osteoclastogenesis by inhibiting the PI3K/AKT signaling pathway at the molecular level (Feng et al., 2018). The role of RES in promoting osteoblast differentiation may be more prominent. RES suppressed OCN synthesis in osteoblasts induced by stimulating factors (triiodothyronine or BMP-4) *via* the activation of SIRT1 or the amplification of p38 MAP kinase activity (Kuroyanagi et al., 2015; Fujita et al., 2017). Although RES indirectly promoted osteoblast differentiation by inhibiting inflammation, RES promoted the increase of ALP and OPG in BMSCs induced by LPS, but did not decrease the levels of IL-6 and IL-8, the result indicated RES's effect on osteoblasts could be independent of inflammation. Meanwhile, the Wnt/ β -catenin and ERK/MAPK signaling pathways also participated in the mechanism of RES's bone-protection (Ornstrup et al., 2016; Zhao X. E. et al., 2018). Silent information regulator 2 homologue 1 (SIRT1) is a positive regulator of the master osteoblast transcription factor, RES reduced the decrease of OCN, OPN, and RUNX2 expression in MC3T3-E1 cells induced by LPS, and the main possible mechanism was to regulate mitochondrial function of osteoblasts by increasing the expression of SIRT1 (Ma et al., 2018). Yaqiong Yu et al. found a new mechanism of

RES promoting osteoblast differentiation under the same result, the activation of AMP-activated protein kinase (AMPK) phosphorylation and inhibitor of suppressor of cytokine signaling 1 (SOCS1) were important signal events that RES inhibited LPS-induced MMP-2 production in MC3T3-E1 cells (Yu et al., 2018). The potential protective effects of RES on bone destruction in RA has been confirmed *in vivo*, RES significantly improved the narrowing of joint space, and the expression level of MMP1 and MMP13 in the synovial tissue was significantly reduced in CIA rats (Hao et al., 2017). Similarly, the expressions of MAPK, Src kinase, STAT3, and Wnt5a in the CIA model joint tissue also participated in the repairing effect of RES on bone destruction in RA (Oz et al., 2019). More and more experimental studies have emphasized the immunomodulatory and osteoprotective effects of RES *in vivo* and *in vitro*. Although these studies have produced exciting results, we still faced with some problems such as poor water solubility and low bioavailability. Therefore, various strategies are being implemented, including the development of RES-related preparations (nanoparticles, liposomes, micelles and phospholipid complexes, etc.) to improve their bioavailability. In addition, several other methods have been used

to improve its bioavailability, including changing the route of administration of resveratrol and blocking the metabolic pathway through treatment with other drugs. In fact, since RES has multiple intracellular targets, additional data are needed to determine the results of interactions or synergies between other polyphenols.

FA has the functions of anti-inflammatory, anti-oxidation, inhibiting platelet aggregation, improving microcirculation, and so on (Zheng et al., 2019; Perez-Ternero et al., 2017). Zhu et al. found FA significantly alleviated joint swelling and reversed the increase of C-reactive protein (CRP) and rheumatoid factor (RF) in CFA rats, its protective mechanism on joints is mainly to reduce the secretion of TNF- α and increase the secretion of TGF- β by inhibiting JAK/STAT pathway (Zhu et al., 2020b). Sagar et al. found that FA inhibited the expression of DC-STAMP which is necessary for the differentiation and maturation of osteoclasts, as well as inhibited RANKL-induced upregulation of MMP-9 and CTSK. In addition, it induced mature osteoclast apoptosis through the caspase-3 pathway (Sagar et al., 2016). Scanning electron microscopy and TRAP staining analysis showed that FA significantly inhibited the osteoclast differentiation induced by RANKL, it inhibited the formation of mature osteoclasts by inhibiting the expression of NFATc1 and c-fos, it further inhibited the bone resorption activity of mature osteoclasts by inhibiting the expression of TRAP, MMP-9, and CTSK (Doss et al., 2018). All these experimental evidences have been summarized in **Table 5**.

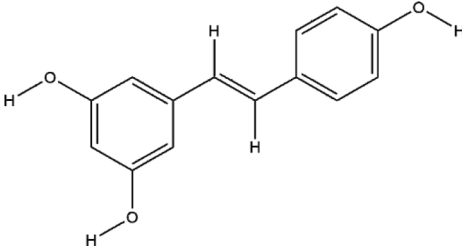
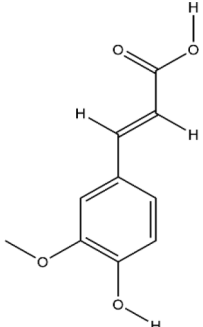
In vitro studies, it has been found that curcumin, gastrodin, paeonol and other phenols can also inhibit bone resorption or promote bone formation (Zhou F. et al., 2017; Li et al., 2019; Wang Q. et al., 2019). However, we need more experiments *in vivo* to explore their effects on bone destruction in RA. Phenols has good antioxidant activity because of the high reactivity of

hydroxyl substitution and the ability to engulf free radicals. It is known that oxidative stress can improve the activity of osteoclasts, whether phenols' antioxidant properties are closely related to its pharmacological effects on osteoclasts or osteoblasts needs to be further studied.

CONCLUSION AND FURTHER PERSPECTIVES

Bone destruction in RA is difficult to cure, and the disability rate is high, which is a serious threat to human health. Therefore, it is particularly important to find more effective and reliable treatment methods and means. TCM in the treatment of RA has a long history, the research of TCM in the treatment of bone destruction in RA has made rapid progress, which shows that TCM has strong advantages and characteristics in the treatment of bone destruction in RA. These bioactive compounds extracted from TCM display anti-bone destructive activity *in vitro* and *in vivo*, and they have shown very good results from different aspects. The potential of bioactive compounds extracted from TCM to provide or inspire the development of anti-bone destruction bioactive drugs is, therefore, really quite evident. However, the biological tests about these compounds and test results are different, mainly due to the different extraction protocols, compounds purity and intervention projects (including doses, animal, or cell models, test methods, and so on). Even compounds with the same purity in the study may have different test results and will make people doubt the authenticity of these tests. Therefore, it has become necessary to use some advanced and interdisciplinary technology and methodology unify extraction protocols and purity

TABLE 5 | Effects and mechanisms of phenols on bone destruction in rheumatoid arthritis (RA).

Bioactive compounds	Source	Chemical structure	Targets	Functions	References
Resveratrol	<i>Reynoutria japonica</i> <i>Houtt.</i>		Down-regulated: ROS, MMP-9, TRAP, CTSK, PI3K/AKT, MAPK signaling pathway Up-regulated: ALP, OPG, OCN, OPN, RUNX2, Wnt/ β -catenin signaling pathway	inhibit osteoclast differentiation; promote osteoblast differentiation	(He et al., 2010) (Feng et al., 2018) (Zhao X. E. et al., 2018). (Ma et al., 2018). (Hao et al., 2017)
Ferulic acid	<i>Ferula assa-foetida</i> L.		Down-regulated: TNF- α , JAK2, MMP-9, CTSK, NFATc1, c-Fos, TRAP, NF- κ B signaling pathway Up-regulated: TGF- β , caspase-3	inhibit osteoclast differentiation and mature	(Zhu L. et al., 2019) (Sagar et al., 2016) (Doss et al., 2018)

identification standard. Furthermore, the studies on compounds are only in the early stage, most of them are focused on *in vitro* experiments. Hence, additional investigation into pharmacokinetics with animal models and clinical studies are necessary. In addition, proper dosage needs to be considered to prevent the potential toxicity when developing these compounds into clinically viable drugs. Similar compounds can treat bone destruction of RA through different signal transduction mechanisms. Whether these mechanisms are interrelated, and whether compounds with the same or similar structures have similar pharmacological effects on osteoclasts or osteoblasts remain to be further verified. Combinations of different compounds that regulate bone destruction in RA through different mechanisms may have synergistic or cumulative effects. This also needs to be further verified.

It is hoped that this review can highlight the importance of bioactive compounds extracted from TCM in the treatment of bone destruction in RA and provide a new direction for future researchers. In the future, we need advanced technology to separate more bioactive compounds from TCM for the

treatment of bone destruction in RA, and further explore the exact molecular mechanism and therapeutic targets of the bioactive compounds, which will be helpful for the treatment of bone destruction in the early stage, preventing disability and enhancing the quality of patients' life.

AUTHOR CONTRIBUTIONS

YS wrote the manuscript. HS, XW, and HZ contributed to the literature research for the manuscript. CL revised the manuscript. AL and XH revised and approved the manuscript. All authors contributed to the article and approved the submitted version.

FUNDING

This work was supported by the National Key R&D Program of China (2018YFC1705205).

REFERENCES

- Aletaha, D., and Smolen, J. S. (2018). Diagnosis and Management of Rheumatoid Arthritis: A Review. *Jama* 320, 1360–1372. doi: 10.1001/jama.2018.13103
- Astry, B., Venkatesha, S. H., Laurence, A., Christensen-Quick, A., Garzino-Demo, A., Frieman, M. B., et al. (2015). Celastrol, a Chinese herbal compound, controls autoimmune inflammation by altering the balance of pathogenic and regulatory T cells in the target organ. *Clin. Immunol.* 157, 228–238. doi: 10.1016/j.clim.2015.01.011
- Bach, D. H., and Lee, S. K. (2019). The Potential Impacts of Tylophora Alkaloids and their Derivatives in Modulating Inflammation, Viral Infections, and Cancer. *Curr. Med. Chem.* 26, 4709–4725. doi: 10.2174/0929867325666180726123339
- Bao, B. H., Kang, A., Zhao, Y., Shen, Q., Li, J. S., Di, L. Q., et al. (2017). A selective HPLC-MS/MS method for quantification of SND-117 in rat plasma and its application to a pharmacokinetic study. *J. Chromatogr. B. Analyt. Technol. Biomed. Life Sci.* 1052, 60–65. doi: 10.1016/j.jchromb.2017.03.008
- Baur, J. A., and Sinclair, D. A. (2006). Therapeutic potential of resveratrol: the in vivo evidence. *Nat. Rev. Drug Discovery* 5, 493–506. doi: 10.1038/nrd2060
- Bednarz, H., Roloff, N., and Niehaus, K. (2019). Mass Spectrometry Imaging of the Spatial and Temporal Localization of Alkaloids in Nightshades. *J. Agric. Food Chem.* 67, 13470–13477. doi: 10.1021/acs.jafc.9b01155
- Bendickova, K., Tidu, F., and Fric, J. (2017). Calcineurin-NFAT signalling in myeloid leucocytes: new prospects and pitfalls in immunosuppressive therapy. *EMBO Mol. Med.* 9, 990–999. doi: 10.15252/emmm.201707698
- Blair, H. C., Larrouette, Q. C., Li, Y., Lin, H., Beer-Stoltz, D., Liu, L., et al. (2017). Osteoblast Differentiation and Bone Matrix Formation In Vivo and In Vitro. *Tissue Eng. Part B. Rev.* 23, 268–280. doi: 10.1089/ten.TEB.2016.0454
- Bo, S., Gambino, R., Ponzio, V., Cioffi, I., Goitre, L., Evangelista, A., et al. (2018). Effects of resveratrol on bone health in type 2 diabetic patients. A double-blind randomized-controlled trial. *Nutr. Diabetes* 8, 51. doi: 10.1038/s41387-018-0059-4
- Burmester, G. R., and Pope, J. E. (2017). Novel treatment strategies in rheumatoid arthritis. *Lancet* 389, 2338–2348. doi: 10.1016/s0140-6736(17)31491-5
- Cai, X., Chen, X. M., Xia, X., Bao, K., Wang, R. R., Peng, J. H., et al. (2018). The Bone-Protecting Efficiency of Chinese Medicines Compared With Western Medicines in Rheumatoid Arthritis: A Systematic Review and Meta-Analysis of Comparative Studies. *Front. Pharmacol.* 9:914–914. doi: 10.3389/fphar.2018.00914
- Cai, Z., Feng, Y., Li, C., Yang, K., Sun, T., Xu, L., et al. (2018). Magnoflorine with hyaluronic acid gel promotes subchondral bone regeneration and attenuates cartilage degeneration in early osteoarthritis. *Bone* 116, 266–278. doi: 10.1016/j.bone.2018.08.015
- Calderón-Montaña, J. M., Burgos-Morón, E., Pérez-Guerrero, C., and López-Lázaro, M. (2011). A review on the dietary flavonoid kaempferol. *Mini Rev. Med. Chem.* 11, 298–344. doi: 10.2174/138955711795305335
- Cascao, R., Vidal, B., Jalmari Finnilä, M. A., Lopes, I. P., Teixeira, R. L., Saarakkala, S., et al. (2017). Effect of celastrol on bone structure and mechanics in arthritic rats. *RMD Open* 3, e000438. doi: 10.1136/rmdopen-2017-000438
- Chan, M. A., Kohlmeier, J. E., Branden, M., Jung, M., and Benedict, S. H. (1999). Triptolide is more effective in preventing T cell proliferation and interferon-gamma production than is FK506. *Phytother. Res.* 13, 464–467. doi: 10.1002/(sici)1099-1573(199909)13:6<464::aid-ptr483>3.0.co;2-4
- Chi, L., Gao, W., Shu, X., and Lu, X. (2014). A natural flavonoid glucoside, icariin, regulates Th17 and alleviates rheumatoid arthritis in a murine model. *Mediators Inflamm.* 2014:392062. doi: 10.1155/2014/392062
- Chun, K. H., Jin, H. C., Kang, K. S., Chang, T. S., and Hwang, G. S. (2020). Poncirin Inhibits Osteoclast Differentiation and Bone Loss through Down-Regulation of NFATc1 In Vitro and In Vivo. *Biomol. Ther. (Seoul)* 28, 337–343. doi: 10.4062/biomolther.2018.216
- Corrado, A., Maruotti, N., and Cantatore, F. P. (2017). Osteoblast Role in Rheumatic Diseases. *Int. J. Mol. Sci.* 18, 1272. doi: 10.3390/ijms18061272
- Cui, J., Li, X., Wang, S., Su, Y., Chen, X., Cao, L., et al. (2020). Triptolide prevents bone loss via suppressing osteoclastogenesis through inhibiting PI3K-AKT-NFATc1 pathway. *J. Cell Mol. Med.* 24, 6149–6161. doi: 10.1111/jcmm.15229
- Dejaeger, M., Böhm, A. M., Dirckx, N., Devriese, J., Nefyodova, E., Cardoen, R., et al. (2017). Integrin-Linked Kinase Regulates Bone Formation by Controlling Cytoskeletal Organization and Modulating BMP and Wnt Signaling in Osteoprogenitors. *J. Bone Miner. Res.* 32, 2087–2102. doi: 10.1002/jbmr.3190
- Dinesh, P., and Rasool, M. (2018). Berberine inhibits IL-21/IL-21R mediated inflammatory proliferation of fibroblast-like synoviocytes through the attenuation of PI3K/Akt signaling pathway and ameliorates IL-21 mediated osteoclastogenesis. *Cytokine* 106, 54–66. doi: 10.1016/j.cyto.2018.03.005
- Ding, X., Li, W., Chen, D., Zhang, C., Wang, L., Zhang, H., et al. (2019). Asperosaponin VI stimulates osteogenic differentiation of rat adipose-derived stem cells. *Regener. Ther.* 11, 17–24. doi: 10.1016/j.reth.2019.03.007
- Doss, H. M., Samarpita, S., Ganesan, R., and Rasool, M. (2018). Ferulic acid, a dietary polyphenol suppresses osteoclast differentiation and bone erosion via the inhibition of RANKL dependent NF-kappaB signalling pathway. *Life Sci.* 207, 284–295. doi: 10.1016/j.lfs.2018.06.013
- Feng, Y. L., Jiang, X. T., Ma, F. F., Han, J., and Tang, X. L. (2018). Resveratrol prevents osteoporosis by upregulating FoxO1 transcriptional activity. *Int. J. Mol. Med.* 41, 202–212. doi: 10.3892/ijmm.2017.3208

- Fujita, K., Tokuda, H., Kainuma, S., Kuroyanagi, G., Yamamoto, N., Matsushima-Nishiwaki, R., et al. (2017). Resveratrol suppresses thyroid hormone-induced osteocalcin synthesis in osteoblasts. *Mol. Med. Rep.* 16, 2881–2886. doi: 10.3892/mmr.2017.6872
- Fujiwara, T., Zhou, J., Ye, S., and Zhao, H. (2016). RNA-binding protein Musashi2 induced by RANKL is critical for osteoclast survival. *Cell Death Dis.* 7, e2300. doi: 10.1038/cddis.2016.213
- Gan, K., Xu, L., Feng, X., Zhang, Q., Wang, F., Zhang, M., et al. (2015). Celastrol attenuates bone erosion in collagen-Induced arthritis mice and inhibits osteoclast differentiation and function in RANKL-induced RAW264.7. *Int. Immunopharmacol.* 24, 239–246. doi: 10.1016/j.intimp.2014.12.012
- Gravallese, E. M. (2017). Bone Wasn't Built in a Day: Destruction and Formation of Bone in the Rheumatic Diseases. *Trans. Am. Clin. Climatol. Assoc.* 128, 24–43.
- Gu, Y., Fan, W., and Yin, G. (2014). The study of mechanisms of protective effect of Rg1 against arthritis by inhibiting osteoclast differentiation and maturation in CIA mice. *Mediators Inflamm.* 2014, 305071. doi: 10.1155/2014/305071
- Guesmi, F., Prasad, S., Tyagi, A. K., and Landoulsi, A. (2017). Antiinflammatory and anticancer effects of terpenes from oily fractions of *Teucrium alopecurus*, blocker of IkappaBalpha kinase, through downregulation of NF-kappaB activation, potentiation of apoptosis and suppression of NF-kappaB-regulated gene expression. *BioMed. Pharmacother.* 95, 1876–1885. doi: 10.1016/j.biopha.2017.09.115
- Güler-Yüksel, M., Hoes, J. N., Bultink, I. E. M., and Lems, W. F. (2018). Glucocorticoids, Inflammation and Bone. *Calcif. Tissue Int.* 102, 592–606. doi: 10.1007/s00223-017-0335-7
- Guo, C., Yang, R. J., Jang, K., Zhou, X. L., and Liu, Y. Z. (2017). Protective Effects of Pretreatment with Quercetin Against Lipopolysaccharide-Induced Apoptosis and the Inhibition of Osteoblast Differentiation via the MAPK and Wnt/beta-Catenin Pathways in MC3T3-E1 Cells. *Cell Physiol. Biochem.* 43, 1547–1561. doi: 10.1159/000481978
- Guo, A. J., Choi, R. C., Zheng, K. Y., Chen, V. P., Dong, T. T., Wang, Z. T., et al. (2012). Kaempferol as a flavonoid induces osteoblastic differentiation via estrogen receptor signaling. *Chin. Med.* 7:10. doi: 10.1186/1749-8546-7-10
- Guo, Q., Zheng, K., Fan, D., Zhao, Y., Li, L., Bian, Y., et al. (2017). Wu-Tou Decoction in Rheumatoid Arthritis: Integrating Network Pharmacology and In Vivo Pharmacological Evaluation. *Front. Pharmacol.* 8, 230. doi: 10.3389/fphar.2017.00230
- Haleagrahara, N., Hodgson, K., Miranda-Hernandez, S., Hughes, S., Kulur, A. B., and Ketheesan, N. (2018). Flavonoid quercetin-methotrexate combination inhibits inflammatory mediators and matrix metalloproteinase expression, providing protection to joints in collagen-induced arthritis. *Inflammopharmacology* 26, 1219–1232. doi: 10.1007/s10787-018-0464-2
- Halling Linder, C., Ek-Rylander, B., Krumpel, M., Norgård, M., Narisawa, S., Millán, J. L., et al. (2017). Bone Alkaline Phosphatase and Tartrate-Resistant Acid Phosphatase: Potential Co-regulators of Bone Mineralization. *Calcif. Tissue Int.* 101, 92–101. doi: 10.1007/s00223-017-0259-2
- Hao, L., Wan, Y., Xiao, J., Tang, Q., Deng, H., and Chen, L. (2017). A study of Sirt1 regulation and the effect of resveratrol on synovial cell invasion and associated joint destruction in rheumatoid arthritis. *Mol. Med. Rep.* 16, 5099–5106. doi: 10.3892/mmr.2017.7299
- He, X., Andersson, G., Lindgren, U., and Li, Y. (2010). Resveratrol prevents RANKL-induced osteoclast differentiation of murine osteoclast progenitor RAW 264.7 cells through inhibition of ROS production. *Biochem. Biophys. Res. Commun.* 401, 356–362. doi: 10.1016/j.bbrc.2010.09.053
- He, L. G., Li, X. L., Zeng, X. Z., Duan, H., Wang, S., Lei, L. S., et al. (2014). Sinomenine induces apoptosis in RAW 264.7 cell-derived osteoclasts in vitro via caspase-3 activation. *Acta Pharmacol. Sin.* 35, 203–210. doi: 10.1038/aps.2013.139
- He, L., Duan, H., Li, X., Wang, S., Zhang, Y., Lei, L., et al. (2016). Sinomenine down-regulates TLR4/TRAFF6 expression and attenuates lipopolysaccharide-induced osteoclastogenesis and osteolysis. *Eur. J. Pharmacol.* 779, 66–79. doi: 10.1016/j.ejphar.2016.03.014
- Ho, C. T. K., Mok, C. C., Cheung, T. T., Kwok, K. Y., and Yip, R. M. L. (2019). Management of rheumatoid arthritis: 2019 updated consensus recommendations from the Hong Kong Society of Rheumatology. *Clin. Rheumatol.* 38, 3331–3350. doi: 10.1007/s10067-019-04761-5
- Hsieh, T. P., Sheu, S. Y., Sun, J. S., and Chen, M. H. (2011). Icaritin inhibits osteoclast differentiation and bone resorption by suppression of MAPKs/NF-kappaB regulated HIF-1alpha and PGE(2) synthesis. *Phytomedicine* 18, 176–185. doi: 10.1016/j.phymed.2010.04.003
- Jia, Y., Miao, Y., Yue, M., Shu, M., Wei, Z., and Dai, Y. (2018). Tetrandrine attenuates the bone erosion in collagen-induced arthritis rats by inhibiting osteoclastogenesis via spleen tyrosine kinase. *FASEB J.* 32, 3398–3410. doi: 10.1096/fj.201701148RR
- Jia, Y., Tao, Y., Lv, C., Xia, Y., Wei, Z., and Dai, Y. (2019). Tetrandrine enhances the ubiquitination and degradation of Syk through an AhR-c-src-c-Cbl pathway and consequently inhibits osteoclastogenesis and bone destruction in arthritis. *Cell Death Dis.* 10:38. doi: 10.1038/s41419-018-1286-2
- Jia, Z., Chen, A., Wang, C., He, M., Xu, J., Fu, H., et al. (2019). Amelioration effects of Kaempferol on immune response following chronic intermittent cold-stress. *Res. Vet. Sci.* 125, 390–396. doi: 10.1016/j.rvsc.2019.08.012
- Ke, K., Li, Q., Wang, X., Xie, Z., Wang, Y., Shi, J., et al. (2016). Asperosaponin VI promotes bone marrow stromal cell osteogenic differentiation through the PI3K/AKT signaling pathway in an osteoporosis model. *Sci. Rep.* 6, 35233. doi: 10.1038/srep35233
- Kim, B., Lee, K. Y., and Park, B. (2018). Icaritin abrogates osteoclast formation through the regulation of the RANKL-mediated TRAF6/NF-kappaB/ERK signaling pathway in Raw264.7 cells. *Phytomedicine* 51, 181–190. doi: 10.1016/j.phymed.2018.06.020
- Kim, C. J., Shin, S. H., Kim, B. J., Kim, C. H., Kim, J. H., Kang, H. M., et al. (2018). The Effects of Kaempferol-Inhibited Autophagy on Osteoclast Formation. *Int. J. Mol. Sci.* 19, 125. doi: 10.3390/ijms19010125
- Kim, J. H., Kim, K., Jin, H. M., Song, I., Youn, B. U., Lee, J., et al. (2009). Silibinin inhibits osteoclast differentiation mediated by TNF family members. *Mol. Cells* 28, 201–207. doi: 10.1007/s10059-009-0123-y
- Kim, J. Y., Cheon, Y. H., Yoon, K. H., Lee, M. S., and Oh, J. (2014). Parthenolide inhibits osteoclast differentiation and bone resorbing activity by down-regulation of NFATc1 induction and c-Fos stability, during RANKL-mediated osteoclastogenesis. *BMB Rep.* 47, 451–456. doi: 10.5483/bmbrep.2014.47.8.206
- Kim, I. R., Kim, S. E., Baek, H. S., Kim, B. J., Kim, C. H., Chung, I. K., et al. (2016). The role of kaempferol-induced autophagy on differentiation and mineralization of osteoblastic MC3T3-E1 cells. *BMC Complement Altern. Med.* 16, 333. doi: 10.1186/s12906-016-1320-9
- Kim, H. R., Kim, B. M., Won, J. Y., Lee, K. A., Ko, H. M., Kang, Y. S., et al. (2019). Quercetin, a Plant Polyphenol, Has Potential for the Prevention of Bone Destruction in Rheumatoid Arthritis. *J. Med. Food.* 22, 152–161. doi: 10.1089/jmf.2018.4259
- Ko, J. H., Sethi, G., Um, J. Y., Shanmugam, M. K., Arfuso, F., Kumar, A. P., et al. (2017). The Role of Resveratrol in Cancer Therapy. *Int. J. Mol. Sci.* 18, 2589. doi: 10.3390/ijms18122589
- Komori, T. (2010). Regulation of osteoblast differentiation by Runx2. *Adv. Exp. Med. Biol.* 658, 43–49. doi: 10.1007/978-1-4419-1050-9_5
- Komori, T. (2019). Regulation of Proliferation, Differentiation and Functions of Osteoblasts by Runx2. *Int. J. Mol. Sci.* 20, 1694. doi: 10.3390/ijms20071694
- Kong, X., Zhang, Y., Liu, C., Guo, W., Li, X., Su, X., et al. (2013). Anti-angiogenic effect of triptolide in rheumatoid arthritis by targeting angiogenic cascade. *PloS One* 8, e77513. doi: 10.1371/journal.pone.0077513
- Kuroyanagi, G., Tokuda, H., Yamamoto, N., Matsushima-Nishiwaki, R., Mizutani, J., Kozawa, O., et al. (2015). Resveratrol amplifies BMP-4-stimulated osteoprotegerin synthesis via p38 MAP kinase in osteoblasts. *Mol. Med. Rep.* 12, 3849–3854. doi: 10.3892/mmr.2015.3877
- Law, S. K., Simmons, M. P., Techen, N., Khan, I. A., He, M. F., Shaw, P. C., et al. (2011). Molecular analyses of the Chinese herb Leigongteng (*Tripterygium wilfordii* Hook.f.). *Phytochemistry* 72, 21–26. doi: 10.1016/j.phytochem.2010.10.015
- Lee, W. S., Lee, E. G., Sung, M. S., and Yoo, W. H. (2014). Kaempferol inhibits IL-1 β -stimulated, RANKL-mediated osteoclastogenesis via downregulation of MAPKs, c-Fos, and NFATc1. *Inflammation* 37, 1221–1230. doi: 10.1007/s10753-014-9849-6
- Lee, C. J., Moon, S. J., Jeong, J. H., Lee, S., Lee, M. H., Yoo, S. M., et al. (2018). Kaempferol targeting on the fibroblast growth factor receptor 3-ribosomal S6 kinase 2 signaling axis prevents the development of rheumatoid arthritis. *Cell Death Dis.* 9, 401. doi: 10.1038/s41419-018-0433-0
- Li, X. J., Jiang, Z. Z., and Zhang, L. Y. (2014). Triptolide: progress on research in pharmacodynamics and toxicology. *J. Ethnopharmacol.* 155, 67–79. doi: 10.1016/j.jep.2014.06.006

- Li, B., Hu, R. Y., Sun, L., Luo, R., Lu, K. H., and Tian, X. B. (2016). Potential role of andrographolide in the proliferation of osteoblasts mediated by the ERK signaling pathway. *BioMed. Pharmacother.* 83, 1335–1344. doi: 10.1016/j.biopha.2016.07.033
- Li, J., Li, Y., Pan, S., Zhang, L., He, L., and Niu, Y. (2019). Paeonol attenuates ligation-induced periodontitis in rats by inhibiting osteoclastogenesis via regulating Nrf2/NF- κ B/NFATc1 signaling pathway. *Biochimie* 156, 129–137. doi: 10.1016/j.biochi.2018.09.004
- Li, H., Wang, J., Sun, Q., Chen, G., Sun, S., Ma, X., et al. (2018). Jatrorrhizine Hydrochloride Suppresses RANKL-Induced Osteoclastogenesis and Protects against Wear Particle-Induced Osteolysis. *Int. J. Mol. Sci.* 19, 3698. doi: 10.3390/ijms19113698
- Li, X., He, L., Hu, Y., Duan, H., Li, X., Tan, S., et al. (2013). Sinomenine suppresses osteoclast formation and Mycobacterium tuberculosis H37Ra-induced bone loss by modulating RANKL signaling pathways. *PLoS One* 8, e74274. doi: 10.1371/journal.pone.0074274
- Li, Y., Wang, S., Wang, Y., Zhou, C., Chen, G., Shen, W., et al. (2013). Inhibitory effect of the antimalarial agent artemunate on collagen-induced arthritis in rats through nuclear factor kappa B and mitogen-activated protein kinase signaling pathway. *Transl. Res.* 161, 89–98. doi: 10.1016/j.trsl.2012.06.001
- Li, Z., Chen, C., Zhu, X., Li, Y., Yu, R., and Xu, W. (2018). Glycyrrhizin Suppresses RANKL-Induced Osteoclastogenesis and Oxidative Stress Through Inhibiting NF- κ B and MAPK and Activating AMPK/Nrf2. *Calcif. Tissue Int.* 103, 324–337. doi: 10.1007/s00223-018-0425-1
- Lian, J. B. (2015). Epigenetic pathways regulating bone homeostasis. *Bone* 81, 731–732. doi: 10.1016/j.bone.2015.05.036
- Liu, C., Zhang, Y., Kong, X., Zhu, L., Pang, J., Xu, Y., et al. (2013). Triptolide Prevents Bone Destruction in the Collagen-Induced Arthritis Model of Rheumatoid Arthritis by Targeting RANKL/RANK/OPG Signal Pathway. *Evid. Based. Complement Alternat. Med.* 2013:626038. doi: 10.1155/2013/626038
- Liu, W., Qian, X., Ji, W., Lu, Y., Wei, G., and Wang, Y. (2016). Effects and safety of Sinomenine in treatment of rheumatoid arthritis contrast to methotrexate: a systematic review and Meta-analysis. *J. Tradit. Chin. Med.* 36, 564–577. doi: 10.1016/s0254-6272(16)30075-9
- Liu, W., Zhang, Y., Zhu, W., Ma, C., Ruan, J., Long, H., et al. (2018). Sinomenine Inhibits the Progression of Rheumatoid Arthritis by Regulating the Secretion of Inflammatory Cytokines and Monocyte/Macrophage Subsets. *Front. Immunol.* 9:2228. doi: 10.3389/fimmu.2018.02228
- Liu, K., Liu, Y., Xu, Y., Nandakumar, K. S., Tan, H., He, C., et al. (2019). Asperosaponin VI protects against bone destructions in collagen induced arthritis by inhibiting osteoclastogenesis. *Phytomedicine* 63, 153006. doi: 10.1016/j.phymed.2019.153006
- Lu, L., Rao, L., Jia, H., Chen, J., Lu, X., Yang, G., et al. (2017). Baicalin positively regulates osteoclast function by activating MAPK/Mitf signalling. *J. Cell Mol. Med.* 21, 1361–1372. doi: 10.1111/jcmm.13066
- Luo, Y., Liu, M., Xia, Y., Dai, Y., Chou, G., and Wang, Z. (2010). Therapeutic effect of norisoboldine, an alkaloid isolated from *Radix Linderae*, on collagen-induced arthritis in mice. *Phytomedicine* 17, 726–731. doi: 10.1016/j.phymed.2010.01.013
- Ma, J., Wang, Z., Zhao, J., Miao, W., Ye, T., and Chen, A. (2018). Resveratrol Attenuates Lipopolysaccharides (LPS)-Induced Inhibition of Osteoblast Differentiation in MC3T3-E1 Cells. *Med. Sci. Monit.* 24, 2045–2052. doi: 10.12659/msm.905703
- Miao, C. G., Yang, Y. Y., He, X., Li, X. F., Huang, C., Huang, Y., et al. (2013). Wnt signaling pathway in rheumatoid arthritis, with special emphasis on the different roles in synovial inflammation and bone remodeling. *Cell Signal.* 25, 2069–2078. doi: 10.1016/j.cellsig.2013.04.002
- Miyazono, K., Kamiya, Y., and Morikawa, M. (2010). Bone morphogenetic protein receptors and signal transduction. *J. Biochem.* 147, 35–51. doi: 10.1093/jb/mvp148
- Nanjundiah, S. M., Venkatesha, S. H., Yu, H., Tong, L., Stains, J. P., and Moudgil, K. D. (2012). Celastrol and its bioactive celastrol protect against bone damage in autoimmune arthritis by modulating osteoimmune cross-talk. *J. Biol. Chem.* 287, 22216–22226. doi: 10.1074/jbc.M112.356816
- Niu, Y., Li, Y., Huang, H., Kong, X., Zhang, R., Liu, L., et al. (2011). A saponin component from *Dipsacus asper* wall, induces osteoblast differentiation through bone morphogenetic protein-2/p38 and extracellular signal-regulated kinase 1/2 pathway. *Phytother. Res.* 25, 1700–1706. doi: 10.1002/ptr.3414
- Ornstrup, M. J., Harsløf, T., Kjær, T. N., Langdahl, B. L., and Pedersen, S. B. (2014). Resveratrol increases bone mineral density and bone alkaline phosphatase in obese men: a randomized placebo-controlled trial. *J. Clin. Endocrinol. Metab.* 99, 4720–4729. doi: 10.1210/jc.2014-2799
- Ornstrup, M. J., Harsløf, T., Sørensen, L., Stenkjær, L., Langdahl, B. L., and Pedersen, S. B. (2016). Resveratrol Increases Osteoblast Differentiation In Vitro Independently of Inflammation. *Calcif. Tissue Int.* 99, 155–163. doi: 10.1007/s00223-016-0130-x
- Oz, B., Yildirim, A., Yolbas, S., Celik, Z. B., Etem, E. O., Deniz, G., et al. (2019). Resveratrol inhibits Src tyrosine kinase, STAT3, and Wnt signaling pathway in collagen induced arthritis model. *Biofactors* 45, 69–74. doi: 10.1002/biof.1463
- Pan, D., Li, N., Liu, Y., Xu, Q., Liu, Q., You, Y., et al. (2018). Kaempferol inhibits the migration and invasion of rheumatoid arthritis fibroblast-like synoviocytes by blocking activation of the MAPK pathway. *Int. Immunopharmacol.* 55, 174–182. doi: 10.1016/j.intimp.2017.12.011
- Panagopoulos, P. K., and Lambrou, G. I. (2018). Bone erosions in rheumatoid arthritis: recent developments in pathogenesis and therapeutic implications. *J. Musculoskelet. Neuronal Interact.* 18, 304–319.
- Pang, J. L., Ricupero, D. A., Huang, S., Fatma, N., Singh, D. P., Romero, J. R., et al. (2006). Differential activity of kaempferol and quercetin in attenuating tumor necrosis factor receptor family signaling in bone cells. *Biochem. Pharmacol.* 71, 818–826. doi: 10.1016/j.bcp.2005.12.023
- Park, B. (2014). Triptolide, a diterpene, inhibits osteoclastogenesis, induced by RANKL signaling and human cancer cells. *Biochimie* 105, 129–136. doi: 10.1016/j.biochi.2014.07.003
- Perez-Ternero, C., Werner, C. M., Nickel, A. G., Herrera, M. D., Motilva, M. J., Bohm, M., et al. (2017). Ferulic acid, a bioactive component of rice bran, improves oxidative stress and mitochondrial biogenesis and dynamics in mice and in human mononuclear cells. *J. Nutr. Biochem.* 48, 51–61. doi: 10.1016/j.jnutbio.2017.06.011
- Qu, X., Zhai, Z., Liu, X., Li, H., Ouyang, Z., Wu, C., et al. (2014). Dioscin inhibits osteoclast differentiation and bone resorption through down-regulating the Akt signaling cascades. *Biochem. Biophys. Res. Commun.* 443, 658–665. doi: 10.1016/j.bbrc.2013.12.029
- Rea, S. L., Walsh, J. P., Layfield, R., Ratajczak, T., and Xu, J. (2013). New insights into the role of sequestosome 1/p62 mutant proteins in the pathogenesis of Paget's disease of bone. *Endocr. Rev.* 34, 501–524. doi: 10.1210/er.2012-1034
- Sagar, T., Rantla, M., Kruger, M. C., Coetzee, M., and Deepak, V. (2016). Ferulic acid impairs osteoclast fusion and exacerbates survival of mature osteoclasts. *Cytotechnology* 68, 1963–1972. doi: 10.1007/s10616-016-0009-8
- Schett, G., Emery, P., Tanaka, Y., Burmester, G., Pisetsky, D. S., Naredo, E., et al. (2016). Tapering biologic and conventional DMARD therapy in rheumatoid arthritis: current evidence and future directions. *Ann. Rheum. Dis.* 75, 1428–1437. doi: 10.1136/annrheumdis-2016-209201
- Shen, W., Guan, Y. Y., Wu, R. M., Liu, L. X., Li, H. D., Bao, W. L., et al. (2019). Protective effects of Wang-Bi tablet on bone destruction in collagen-induced arthritis by regulating osteoclast-osteoblast functions. *J. Ethnopharmacol.* 238:111861. doi: 10.1016/j.jep.2019.111861
- Singh, J. A., Saag, K. G., Bridges, S. L. Jr., Akl, E. A., Bannuru, R. R., Sullivan, M. C., et al. (2016). 2015 American College of Rheumatology Guideline for the Treatment of Rheumatoid Arthritis. *Arthritis Care Res. (Hoboken)* 68, 1–25. doi: 10.1002/acr.22783
- Smolen, J. S., Aletaha, D., and McInnes, I. B. (2016). Rheumatoid arthritis. *Lancet* 388, 2023–2038. doi: 10.1016/s0140-6736(16)30173-8
- Smolen, J. S., Landewe, R., Bijlsma, J., Burmester, G., Chatzidionysiou, K., Dougados, M., et al. (2017). EULAR recommendations for the management of rheumatoid arthritis with synthetic and biological disease-modifying antirheumatic drugs: 2016 update. *Ann. Rheum. Dis.* 76, 960–977. doi: 10.1136/annrheumdis-2016-210715
- Sun, S., Wang, Y., and Zhou, Y. (2010). [Research progress on immunosuppressive activity of monomers extracted from Chinese medicine]. *Zhongguo Zhong Yao Za Zhi* 35, 393–396.
- Sun, Y., Yao, Y., and Ding, C. Z. (2014). A combination of sinomenine and methotrexate reduces joint damage of collagen induced arthritis in rats by modulating osteoclast-related cytokines. *Int. Immunopharmacol.* 18, 135–141. doi: 10.1016/j.intimp.2013.11.014

- Tada, M., Inui, K., Sugioka, Y., Mamoto, K., Okano, T., Koike, T., et al. (2016). Reducing glucocorticoid dosage improves serum osteocalcin in patients with rheumatoid arthritis—results from the TOMORROW study. *Osteoporos. Int.* 27, 729–735. doi: 10.1007/s00198-015-3291-y
- Verschueren, P. C., Lories, R. J., Daans, M., Théate, I., Durez, P., Westhovens, R., et al. (2009). Detection, identification and in vivo treatment responsiveness of bone morphogenetic protein (BMP)-activated cell populations in the synovium of patients with rheumatoid arthritis. *Ann. Rheum. Dis.* 68, 117–123. doi: 10.1136/ard.2007.080127
- Wahab, A., Gao, K., Jia, C., Zhang, F., Tian, G., Murtaza, G., et al. (2017). Significance of Resveratrol in Clinical Management of Chronic Diseases. *Molecules* 22, 1329. doi: 10.3390/molecules22081329
- Wang, J., and Zhao, Q. (2019). Kaempferitrin inhibits proliferation, induces apoptosis, and ameliorates inflammation in human rheumatoid arthritis fibroblast-like synoviocytes. *Phytother. Res.* 33, 1726–1735. doi: 10.1002/ptr.6364
- Wang, T., Wan, D., Shao, L., Dai, J., and Jiang, C. (2015). Notoginsenoside R1 stimulates osteogenic function in primary osteoblasts via estrogen receptor signaling. *Biochem. Biophys. Res. Commun.* 466, 232–239. doi: 10.1016/j.bbrc.2015.09.014
- Wang, J., Qu, T. B., Chu, L. S., Li, L., Ren, C. C., Sun, S. Q., et al. (2016). [Ligustrazine Promoted the Migration of Bone Marrow Mesenchymal Stem Cells by Up-regulating MMP-2 and MMP-9 Expressions]. *Zhongguo Zhong Xi Yi Jie He Za Zhi* 36, 718–723.
- Wang, X., He, X., Zhang, C. F., Guo, C. R., Wang, C. Z., and Yuan, C. S. (2017). Anti-arthritis effect of berberine on adjuvant-induced rheumatoid arthritis in rats. *BioMed. Pharmacother.* 89, 887–893. doi: 10.1016/j.biopha.2017.02.099
- Wang, S., Zuo, S., Liu, Z., Ji, X., Yao, Z., and Wang, X. (2018). Study on the efficacy and mechanism of triptolide on treating TNF transgenic mice with rheumatoid arthritis. *BioMed. Pharmacother.* 106, 813–820. doi: 10.1016/j.biopha.2018.07.021
- Wang, Q., Ye, C., Sun, S., Li, R., Shi, X., Wang, S., et al. (2019). Curcumin attenuates collagen-induced rat arthritis via anti-inflammatory and apoptotic effects. *Int. Immunopharmacol.* 72, 292–300. doi: 10.1016/j.intimp.2019.04.027
- Wang, S., Liu, Z., Wang, J., Wang, Y., Liu, J., Ji, X., et al. (2019). The triptolide-induced apoptosis of osteoclast precursor by degradation of cIAP2 and treatment of rheumatoid arthritis of TNF-transgenic mice. *Phytother. Res.* 33, 342–349. doi: 10.1002/ptr.6224
- Wang, Y., Chen, H., and Zhang, H. (2019). Kaempferol promotes proliferation, migration and differentiation of MC3T3-E1 cells via up-regulation of microRNA-101. *Artif. Cells Nanomed. Biotechnol.* 47, 1050–1056. doi: 10.1080/21691401.2019.1591428
- Wattel, A., Kamel, S., Mentaverri, R., Lorget, F., Prouillet, C., Petit, J. P., et al. (2003). Potent inhibitory effect of naturally occurring flavonoids quercetin and kaempferol on in vitro osteoclastic bone resorption. *Biochem. Pharmacol.* 65, 35–42. doi: 10.1016/s0006-2952(02)01445-4
- Wei, Z. F., Jiao, X. L., Wang, T., Lu, Q., Xia, Y. F., Wang, Z. T., et al. (2013a). Norisoboldine alleviates joint destruction in rats with adjuvant-induced arthritis by reducing RANKL, IL-6, PGE(2), and MMP-13 expression. *Acta Pharmacol. Sin.* 34, 403–413. doi: 10.1038/aps.2012.187
- Wei, Z. F., Tong, B., Xia, Y. F., Lu, Q., Chou, G. X., Wang, Z. T., et al. (2013b). Norisoboldine suppresses osteoclast differentiation through preventing the accumulation of TRAF6-TAK1 complexes and activation of MAPKs/NF-kappaB/c-Fos/NFATc1 Pathways. *PloS One* 8, e59171. doi: 10.1371/journal.pone.0059171
- Wei, Z. F., Lv, Q., Xia, Y., Yue, M. F., Shi, C., Xia, Y. F., et al. (2015). Norisoboldine, an Anti-Arthritis Alkaloid Isolated from Radix Linderae, Attenuates Osteoclast Differentiation and Inflammatory Bone Erosion in an Aryl Hydrocarbon Receptor-Dependent Manner. *Int. J. Biol. Sci.* 11, 1113–1126. doi: 10.7150/ijbs.12152
- Wei, C. M., Liu, Q., Song, F. M., Lin, X. X., Su, Y. J., Xu, J., et al. (2018). Artesunate inhibits RANKL-induced osteoclastogenesis and bone resorption in vitro and prevents LPS-induced bone loss in vivo. *J. Cell Physiol.* 233, 476–485. doi: 10.1002/jcp.25907
- Wen, L., Zhao, Y., Jiang, Y., Yu, L., Zeng, X., Yang, J., et al. (2017). Identification of a flavonoid C-glycoside as potent antioxidant. *Free Radic. Biol. Med.* 110, 92–101. doi: 10.1016/j.freeradbiomed.2017.05.027
- Xu, H., Zhao, H., Lu, C., Qiu, Q., Wang, G., Huang, J., et al. (2016). Triptolide Inhibits Osteoclast Differentiation and Bone Resorption In Vitro via Enhancing the Production of IL-10 and TGF-beta1 by Regulatory T Cells. *Mediators Inflamm.* 2016:8048170. doi: 10.1155/2016/8048170
- Xu, Q., Chen, G., Liu, X., Dai, M., and Zhang, B. (2019). Icarin inhibits RANKL-induced osteoclastogenesis via modulation of the NF-kappaB and MAPK signaling pathways. *Biochem. Biophys. Res. Commun.* 508, 902–906. doi: 10.1016/j.bbrc.2018.11.201
- Yang, C. M., Chen, Y. W., Chi, P. L., Lin, C. C., and Hsiao, L. D. (2017). Resveratrol inhibits BK-induced COX-2 transcription by suppressing acetylation of AP-1 and NF-kB in human rheumatoid arthritis synovial fibroblasts. *Biochem. Pharmacol.* 132, 77–91. doi: 10.1016/j.bcp.2017.03.003
- Yang, G., Chang, C. C., Yang, Y., Yuan, L., Xu, L., Ho, C. T., et al. (2018). Resveratrol Alleviates Rheumatoid Arthritis via Reducing ROS and Inflammation, Inhibiting MAPK Signaling Pathways, and Suppressing Angiogenesis. *J. Agric. Food Chem.* 66, 12953–12960. doi: 10.1021/acs.jafc.8b05047
- Yoon, H. Y., Lee, E. G., Lee, H., Cho, I. J., Choi, Y. J., Sung, M. S., et al. (2013). Kaempferol inhibits IL-1beta-induced proliferation of rheumatoid arthritis synovial fibroblasts and the production of COX-2, PGE2 and MMPs. *Int. J. Mol. Med.* 32, 971–977. doi: 10.3892/ijmm.2013.1468
- Yu, Y., Li, X., Mi, J., Qu, L., Yang, D., Guo, J., et al. (2018). Resveratrol Suppresses Matrix Metalloproteinase-2 Activation Induced by Lipopolysaccharide in Mouse Osteoblasts via Interactions with AMP-Activated Protein Kinase and Suppressor of Cytokine Signaling 1. *Molecules* 23, 2327. doi: 10.3390/molecules23092327
- Yuan, X., Tong, B., Dou, Y., Wu, X., Wei, Z., and Dai, Y. (2016). Tetrandrine ameliorates collagen-induced arthritis in mice by restoring the balance between Th17 and Treg cells via the aryl hydrocarbon receptor. *Biochem. Pharmacol.* 101, 87–99. doi: 10.1016/j.bcp.2015.11.025
- Yuan, Y., Zhang, Y., He, X., and Fan, S. (2018). Protective Effects of Sinomenine on CFA-Induced Inflammatory Pain in Rats. *Med. Sci. Monit.* 24, 2018–2024. doi: 10.12659/msm.906726
- Yuan, K., Li, X., Lu, Q., Zhu, Q., Jiang, H., Wang, T., et al. (2019). Application and Mechanisms of Triptolide in the Treatment of Inflammatory Diseases-A Review. *Front. Pharmacol.* 10:1469:1469. doi: 10.3389/fphar.2019.01469
- Zampeli, E., Vlachoyiannopoulos, P. G., and Tzioufas, A. G. (2015). Treatment of rheumatoid arthritis: Unraveling the conundrum. *J. Autoimmun.* 65, 1–18. doi: 10.1016/j.jaut.2015.10.003
- Zenkov, N. K., Chechushkov, A. V., Kozhin, P. M., Kandalintseva, N. V., Martinovich, G. G., and Menshchikova, E. B. (2016). Plant Phenols and Autophagy. *Biochem. (Mosc)* 81, 297–314. doi: 10.1134/s0006297916040015
- Zerbini, C. A. F., Clark, P., Mendez-Sanchez, L., Pereira, R. M. R., Messina, O. D., Una, C. R., et al. (2017). Biologic therapies and bone loss in rheumatoid arthritis. *Osteoporos. Int.* 28, 429–446. doi: 10.1007/s00198-016-3769-2
- Zhang, C., Peng, J., Wu, S., Jin, Y., Xia, F., Wang, C., et al. (2014). Dioscin promotes osteoblastic proliferation and differentiation via Lrp5 and ER pathway in mouse and human osteoblast-like cell lines. *J. BioMed. Sci.* 21, 30. doi: 10.1186/1423-0127-21-30
- Zhang, H. C., Liu, M. X., Wang, E. P., Lin, Z., Lv, G. F., and Chen, X. (2015). Effect of sinomenine on the expression of rheumatoid arthritis fibroblast-like synoviocytes MyD88 and TRAF6. *Genet. Mol. Res.* 14, 18928–18935. doi: 10.4238/2015.December.28.41
- Zhang, L., Zhu, M., Li, M., Du, Y., Du, S., Huang, Y., et al. (2017). Ginsenoside Rg1 attenuates adjuvant-induced arthritis in rats via modulation of PPAR-gamma/NF-kappaB signal pathway. *Oncotarget* 8, 55384–55393. doi: 10.18632/oncotarget.19526
- Zhang, Q., Peng, W., Wei, S., Wei, D., Li, R., Liu, J., et al. (2019). Guizhi-Shaoyao-Zhimu decoction possesses anti-arthritis effects on type II collagen-induced arthritis in rats via suppression of inflammatory reactions, inhibition of invasion & migration and induction of apoptosis in synovial fibroblasts. *BioMed. Pharmacother.* 118:109367. doi: 10.1016/j.biopha.2019.109367
- Zhang, Y., Wang, G., Wang, T., Cao, W., Zhang, L., and Chen, X. (2019a). Nrf2-Keap1 pathway-mediated effects of resveratrol on oxidative stress and apoptosis in hydrogen peroxide-treated rheumatoid arthritis fibroblast-like synoviocytes. *Ann. N. Y. Acad. Sci.* 1457, 166–178. doi: 10.1111/nyas.14196
- Zhang, Y., Zou, B., Tan, Y., Su, J., Wang, Y., Xu, J., et al. (2019b). Sinomenine inhibits osteolysis in breast cancer by reducing IL-8/CXCR1 and c-Fos/NFATc1 signaling. *Pharmacol. Res.* 142, 140–150. doi: 10.1016/j.phrs.2019.02.015

- Zhao, Y., Li, J., Yu, K., Liu, Y., and Chen, X. (2007). Sinomenine inhibits maturation of monocyte-derived dendritic cells through blocking activation of NF-kappa B. *Int. Immunopharmacol.* 7, 637–645. doi: 10.1016/j.intimp.2007.01.007
- Zhao, H., Xu, H., Zuo, Z., Wang, G., Liu, M., Guo, M., et al. (2018). Yi Shen Juan Bi Pill Ameliorates Bone Loss and Destruction Induced by Arthritis Through Modulating the Balance of Cytokines Released by Different Subpopulations of T Cells. *Front. Pharmacol.* 9:262:262. doi: 10.3389/fphar.2018.00262
- Zhao, X. E., Yang, Z., Zhang, H., Yao, G., Liu, J., Wei, Q., et al. (2018). Resveratrol Promotes Osteogenic Differentiation of Canine Bone Marrow Mesenchymal Stem Cells Through Wnt/Beta-Catenin Signaling Pathway. *Cell Reprog.* 20, 371–381. doi: 10.1089/cell.2018.0032
- Zhao, Y., Sun, X., Yu, X., Gao, R., and Yin, L. (2018). Saponins from Panax notoginseng leaves improve the symptoms of aplastic anemia and aberrant immunity in mice. *BioMed. Pharmacother.* 102, 959–965. doi: 10.1016/j.biopha.2018.03.175
- Zheng, X., Cheng, Y., Chen, Y., Yue, Y., Li, Y., Xia, S., et al. (2019). Ferulic Acid Improves Depressive-Like Behavior in Prenatally-Stressed Offspring Rats via Anti-Inflammatory Activity and HPA Axis. *Int. J. Mol. Sci.* 20, 493. doi: 10.3390/ijms20030493
- Zhou, B., Lu, X., Tang, Z., Liu, D., Zhou, Y., Zeng, P., et al. (2017). Influence of sinomenine upon mesenchymal stem cells in osteoclastogenesis. *BioMed. Pharmacother.* 90, 835–841. doi: 10.1016/j.biopha.2017.03.084
- Zhou, F., Shen, Y., Liu, B., Chen, X., Wan, L., and Peng, D. (2017). Gastrodin inhibits osteoclastogenesis via down-regulating the NFATc1 signaling pathway and stimulates osseointegration in vitro. *Biochem. Biophys. Res. Commun.* 484, 820–826. doi: 10.1016/j.bbrc.2017.01.179
- Zhu, K. J., Shen, Q. Y., Cheng, H., Mao, X. H., Lao, L. M., and Hao, G. L. (2005). Triptolide affects the differentiation, maturation and function of human dendritic cells. *Int. Immunopharmacol.* 5, 1415–1426. doi: 10.1016/j.intimp.2005.03.020
- Zhu, L., Tang, Y., Li, X. Y., Keller, E. T., Yang, J., Cho, J. S., et al. (2020a). Osteoclast-mediated bone resorption is controlled by a compensatory network of secreted and membrane-tethered metalloproteinases. *Sci. Transl. Med.* 12, 6143. doi: 10.1126/scitranslmed.aaw6143
- Zhu, L., Zhang, Z., Xia, N., Zhang, W., Wei, Y., Huang, J., et al. (2020b). Anti-arthritic activity of ferulic acid in complete Freund's adjuvant (CFA)-induced arthritis in rats: JAK2 inhibition. *Inflammopharmacology* 28, 463–473. doi: 10.1007/s10787-019-00642-0
- Zhu, G. Z., Han, X. C., Wang, H. Z., Yang, Y. Z., Gao, Y., and Wang, H. L. (2019). [Effect of Tripterygium Glycosides Tablets in treating rheumatoid arthritis: a systematic review and Meta-analysis]. *Zhongguo Zhong Yao Za Zhi* 44, 3358–3364. doi: 10.19540/j.cnki.cjcmm.20190305.004
- Zhu, L., Zhang, Z., Xia, N., Zhang, W., Wei, Y., Huang, J., et al. (2019). Anti-arthritic activity of ferulic acid in complete Freund's adjuvant (CFA)-induced arthritis in rats: JAK2 inhibition. *Inflammopharmacology* 28 (2), 463–473. doi: 10.1007/s10787-019-00642-0

Conflict of Interest: The authors declare that the research was conducted in the absence of any commercial or financial relationships that could be construed as a potential conflict of interest.

Copyright © 2020 Shi, Shu, Wang, Zhao, Lu, Lu and He. This is an open-access article distributed under the terms of the Creative Commons Attribution License (CC BY). The use, distribution or reproduction in other forums is permitted, provided the original author(s) and the copyright owner(s) are credited and that the original publication in this journal is cited, in accordance with accepted academic practice. No use, distribution or reproduction is permitted which does not comply with these terms.



Computational Prediction of Antiangiogenesis Synergistic Mechanisms of Total Saponins of *Panax japonicus* Against Rheumatoid Arthritis

Xiang Guo^{1†}, Jinyu Ji^{1†}, Goutham Sanker Jose Kumar Sreena¹, Xiaoqiang Hou², Yanan Luo¹, Xianyun Fu¹, Zhigang Mei^{3*} and Zhitao Feng^{1,2*}

¹Third-Grade Pharmacological Laboratory on Chinese Medicine Approved by State Administration of Traditional Chinese Medicine, Medical College of China Three Gorges University, Yichang, China, ²Institute of Rheumatology, the First College of Clinical Medical Sciences, China Three Gorges University, Yichang, China, ³Key Laboratory of Hunan Province for Integrated Traditional Chinese and Western Medicine on Prevention and Treatment of Cardio-Cerebral Diseases, Hunan University of Chinese Medicine, Changsha, China

OPEN ACCESS

Edited by:

Per-Johan Jakobsson,
Karolinska Institutet (KI), Sweden

Reviewed by:

Maria Luisa Del Moral,
University of Jaén, Spain
Paul F. Seke Etet,
Université de Ngaoundéré, Cameroon

*Correspondence:

Zhitao Feng
zhitao.feng@ctgu.edu.cn
Zhigang Mei
meizhigang@hnucm.edu.cn

[†]These authors have contributed
equally to this work.

Specialty section:

This article was submitted to
Ethnopharmacology,
a section of the journal
Frontiers in Pharmacology.

Received: 27 May 2020

Accepted: 21 September 2020

Published: 29 October 2020

Citation:

Guo X, Ji J, Jose Kumar Sreena GS, Hou X, Luo Y, Fu X, Mei Z and Feng Z (2020) Computational Prediction of Antiangiogenesis Synergistic Mechanisms of Total Saponins of *Panax japonicus* Against Rheumatoid Arthritis. *Front. Pharmacol.* 11:566129. doi: 10.3389/fphar.2020.566129

Objective: To investigate the anti-angiogenesis mechanisms and key targets of total saponins of *Panax japonicus* (TSPJ) in the treatment of rheumatoid arthritis (RA).

Methods: RStudio3.6.1 software was used to obtain differentially expressed genes (DEGs) by analyzing the differences in gene expression in the synovial tissue of RA and to predict the potential targets of active compounds from TSPJ by the PharmMapper and SwissTargetPrediction databases. We evaluated the overlapping genes by intersectional analysis of DEGs and drug targets. Based on the overlapping genes, we used Cytoscape 3.7.2 software to construct a protein–protein interactions (PPI) network and applied Kyoto Encyclopedia of Genes and Genomes (KEGG) analysis to determine the mechanisms of the treatment. Finally, the correlations with angiogenesis-related genes were explored. Collagen-induced arthritis (CIA) model was established and treated with different doses of TSPJ. The manifestations of CIA were determined by evaluation of arthritis index and histology score. Serum levels of vascular endothelial growth factor (VEGF) and the hypoxia-inducible factor 1 (HIF-1) were tested by ELISA. The mRNA levels of IL-1 β and IL-17A were detected by real time-quantitative PCR.

Results: Altogether, 2670 DEGs were obtained by differential analysis, and 371 drug targets were predicted for four active components (Araloside A, Chikusetsusaponin IVa, Ginsenoside Rg2, and Ginsenoside Ro). A total of 52 overlapping genes were included in the PPI network and the KEGG analysis. However, only 41 genes in the PPI network had protein interactions. The results of the KEGG enrichment analysis were all related to angiogenesis, including VEGF and HIF-1 signaling pathways. Seven genes with negative correlations and 16 genes with positive correlations were obtained by correlational analysis of DEGs in the VEGF and HIF-1 signaling pathways. SRC proto-oncogene, nonreceptor tyrosine kinase (SRC), and the signal transducer and activator of transcription 3 (STAT 3)

had a higher value of degree and showed a significant correlation in the pathways; they were regarded as key targets. Compared with the model group, TSPJ significantly relieved the symptoms and decreased the expression of VEGFA, HIF-1 α , IL-1 β , and IL-17A in serum or spleens of CIA mice.

Conclusion: In the current study, we found that antiangiogenesis is one of the effective strategies of TSPJ against RA; SRC and STAT 3 may be the key targets of TSPJ acting on the VEGF and HIF-1 signaling pathways, which will provide new insight into the treatment of RA by inhibiting inflammation and angiogenesis.

Keywords: *Panax japonicus*, saponins, rheumatoid arthritis, angiogenesis, network pharmacology

INTRODUCTION

Rheumatoid arthritis (RA) is a chronic inflammatory autoimmune disease affected by both genetic and environmental factors (Croia et al., 2019). Approximately 0.5–1% of the world's population suffers from RA, and many patients have symptoms of joint damage or even disability (Smolen et al., 2016; Aletaha and Smolen, 2018). When synovitis occurs, macrophages and fibroblasts in synovial tissue are induced to secrete angiogenic factors, leading to an abnormal increase of synovial vessels. A large number of inflammatory cells enter the joint through newly formed blood vessels, causing synovitis and synovial hyperplasia. Increased angiogenesis leads to the permanence of RA (Elshabrawy et al., 2015; Leblond et al., 2017; Lu et al., 2017; Chen et al., 2018). Eventually, these mechanisms destroy the joint and lead to deformity. It is worth noting that the treatment of RA with vascular targeted therapy has gradually entered the clinic (Leblond et al., 2017).

Recently, many people have become interested in research into traditional Chinese medicine (TCM) because it plays an important role in the treatment of difficult and complicated diseases (Yuan et al., 2017). The study of Chinese herbal medicine, with the identification of the main components of herbals and the molecular mechanisms of their curative effects, has become a hot research topic. Currently, TCM is increasingly being used in clinical treatment or for developing new treatment methods (Wang et al., 2018). *Panax japonicus* (T.Nees) C.A.Mey is a kind of Chinese herbal medicine that belongs to the *Panax* genus, which is widely grown in the southwest of China. Studies have shown that *Panax japonicus* (T.Nees) C.A.Mey has analgesic, anti-inflammatory, antioxidant, and joint swelling-relieving properties (Yang et al., 2014; Yang et al., 2018). Saponins are the main components of *Panax japonicus* (T.Nees) C.A.Mey. Total saponins of *Panax japonicus* (TSPJ) are extracted from *Panax japonicus* (T.Nees) C.A.Mey and are widely used to treat RA. Its main ingredients include Araloside A, Chikusetsusaponin IVa, Ginsenoside Rg2, and Ginsenoside Ro (Yu-min et al., 2019) (**Supplementary Figure S1 and Table S1**). Ding et al. have confirmed that Araloside A has an anti-inflammatory effect in the treatment of RA (Ding

et al., 2019). Chikusetsusaponin IVa and Ginsenoside Ro exhibit antiangiogenic effects (Zheng et al., 2019). In the treatment of RA, TSPJ can inhibit synovial hyperplasia and reduce capillary permeability (Guo et al., 2019). Yuan et al. found that TSPJ could reduce the degree of foot swelling (Ding et al., 2008) and downregulate the serum levels of TNF- α and IL-1 β in CIA rats (Ding et al., 2009). Related studies have shown that TSPJ can inhibit angiogenesis during tumor therapy (Yongui, 2011). However, no previous studies have shown whether TSPJ can be used as a targeted drug against angiogenesis in RA.

With the development of biomedical big data research, the network pharmacology approach and data mining in bioinformatics is being applied to help study the potential mechanism of different actions of drugs in organisms (Boezio et al., 2017) and has been proven to effectively reveal the regulation principles of small molecules of TCM (Zhang R.-z. et al., 2017). There is a large quantity of biological data in the public database, among which there is much valuable information that has not yet been highlighted. Bioinformatic methods are widely used to extract productive data because of their advantages of being quick and inexpensive (Ramharack and Soliman, 2018). By constructing an interaction network of disease-related proteins of TCM components, network pharmacology can identify the key targets in the network, and study the interactions among the drugs, targets, and pathways (Yuan et al., 2017; Sidders et al., 2018). In this study, we first identified differentially expressed genes (DEGs) of RA related to angiogenesis by bioinformatics analysis. After predicting potential targets for the active compounds of TSPJ, we used a network pharmacology approach to identify the possible antiangiogenic mechanism of the main components of TSPJ in RA therapy. Because CIA model has many similar pathological and immunological characteristics to human RA, many animal experiments have used CIA mice as RA models (Choudhary et al., 2018). We successfully established CIA model and verified partly of our computational prediction results (**Supplementary Figures S2–S5**). The findings of this study deepen our understanding of the therapeutic mechanism of TSPJ and provide a new therapeutic idea in the antiangiogenic treatment of RA. The flow diagram of this study is shown in **Figure 1**.

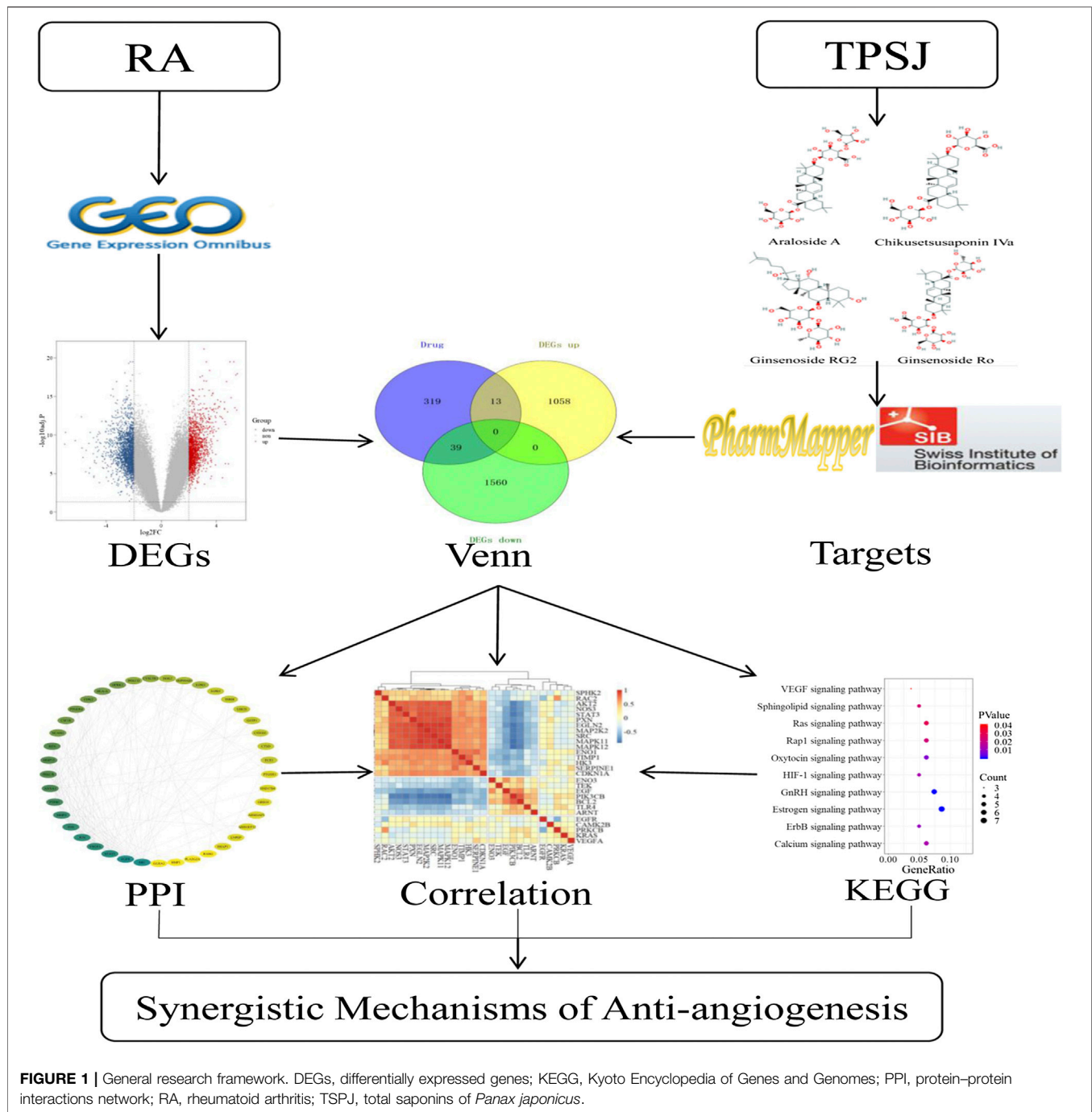


FIGURE 1 | General research framework. DEGs, differentially expressed genes; KEGG, Kyoto Encyclopedia of Genes and Genomes; PPI, protein-protein interactions network; RA, rheumatoid arthritis; TSPJ, total saponins of *Panax japonicus*.

METHODS

Data Collection and Preprocessing

The Gene Expression Omnibus (GEO) database (<https://www.ncbi.nlm.nih.gov/geo/>), a public functional genomics database built and maintained by the National Center for Biotechnology Information (NCBI), collects microarray, next-generation sequencing, and other forms of high-throughput functional genomic data. Persistent synovitis and joint destruction are the main characteristics of RA (Scott et al., 2010). In our

study, we mainly studied the difference in synovial tissue expression between RA patients and healthy individuals. Microarray raw data were downloaded from the GEO database by searching with the keywords: “rheumatoid arthritis,” “synovial tissue,” and “*Homo sapiens*.” All the above data sets were merged according to the same probe name by RStudio3.6.1 software to build the gene expression data matrix. The gene expression data matrix was normalized using the “Limma” R package. In the end, the gene expression matrix of synovial tissue was obtained.

PubChem (<https://pubchem.ncbi.nlm.nih.gov/>) is an open-access database that contains chemical structures, molecular formulas and patents, and article identifiers of drugs (Sayers et al., 2020). The chemical structures of the main components of TSPJ were searched in the PubChem database. Based on the chemical structure models, drug targets were predicted via the PharmMapper database (<http://www.lilab-ecust.cn/pharmmapper/>) and the SwissTargetPrediction database (<http://www.swisstargetprediction.ch/>).

Differentially Expressed Genes' Screening

The “Limma” R package is commonly used for variance analysis. First, RStudio3.6.1 software was used to read the gene expression matrix of synovial tissue. All samples were divided into two groups (healthy control and the RA group). Second, the “Limma” package was adopted to identify the DEGs between the healthy control and the RA group. The results also included fold change (FC) and the p values to reflect the degree of gene differences. p values were adjusted for multiple test correction using the Hochberg and Benjamini test. Finally, $|\log_2FC| > 2$ and $\text{adj.}p < 0.05$ were used as the cutoff criteria to identify DEGs.

Network Pharmacology

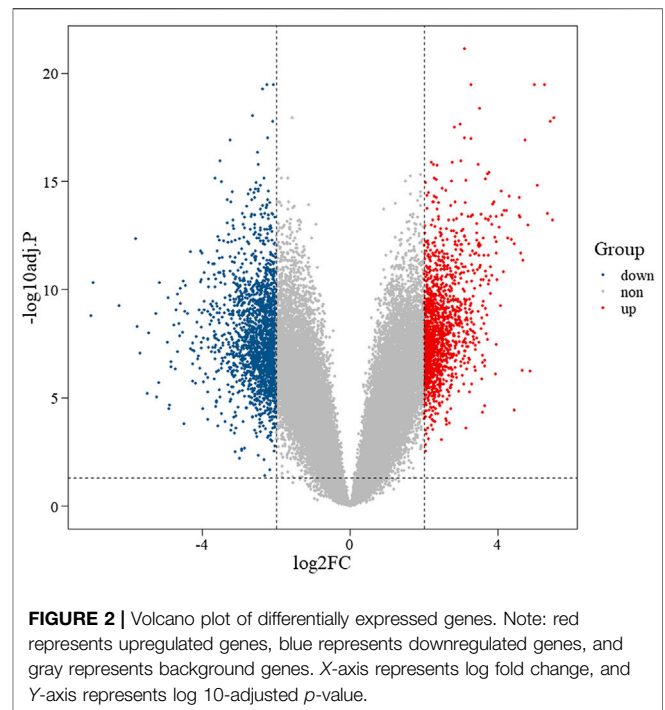
The UniProt database (<http://www.uniprot.org/>) provides high-quality annotation for proteins (The UniProt Consortium, 2017). The UniProt database was utilized for retrieving drug prediction targets information and screening out targets for the “*Homo sapiens*” species. The overlapping targets between the drug targets and the DEGs were identified, and input into the STRING database (<https://string-db.org/>) to retrieve the protein–protein interactions (PPI). Cytoscape3.7.2 software was used to import the data to construct and visualize the PPI network. We used the “Network Analyzer” plugin to analyze the network to obtain network-related parameters.

Pathway Enrichment Analysis

The DAVID database (<https://david.ncifcrf.gov/>) is commonly used for annotation, visualization, and integrated discovery (Dennis et al., 2003). To illustrate the possible mechanism of drug action in the treatment of RA, the overlapping targets were adopted for the Kyoto Encyclopedia of Genes and Genomes (KEGG) enrichment analysis by the DAVID database with the “*Homo sapiens*” setting. Finally, the signaling pathway with $p < 0.05$ was selected for the next study.

Correlation Analysis

Significant signaling pathways were acquired by KEGG enrichment analysis. To learn more about the synergistic mechanisms of these pathways, we performed correlation analysis and identified negative and positive genes in the related pathways. First, we downloaded all targets in these signaling pathways from the KEGG (<https://www.kegg.jp/>) database. Second, the overlapping genes between the DEGs and pathways were identified by intersection analysis. Finally, the roles of these overlapping genes in the pathway were determined by correlation analysis.



RESULTS

Gene Expression Matrix

After a systematic review, we found two gene expression data sets that met our requirements. The gene expression data sets GSE48780 and GSE77298 were downloaded from the GEO database (**Supplementary Table S2**). These data sets are based on the GPL570 platform (Affymetrix Human Genome U133 Plus 2.0 Array). We used the “dplyr” R package to merge the data sets to construct the gene expression matrix of synovial tissue. This matrix contained seven healthy samples and 99 RA samples.

Differentially Expressed Genes

We compared two groups of data in the gene expression matrix, and subsequently we obtained 2,670 DEGs ($\text{adj.}p < 0.05$, $|\log_2FC| > 2$), including 1,071 upregulated ($\text{adj.}p < 0.05$, $\log_2FC > 2$) and 1,599 downregulated ($\text{adj.}p < 0.05$, $\log_2FC < -2$) DEGs. Meanwhile, the volcano plot was used to display both the DEGs and the background genes (**Figure 2**).

Identification of the Overlapping Targets

A total of four active ingredients were identified from TSPJ, including Araloside A, Chikusetsusaponin IVa, Ginsenoside Rg2, and Ginsenoside Ro. The targets of the four main ingredients (**Figure 3A**) of TSPJ were predicted by using the PharmMapper database and SwissTargetPrediction database. We obtained 157 Araloside A targets, 157 Chikusetsusaponin IVa targets, 163 Ginsenoside Rg2 targets, and 127 Ginsenoside Ro targets. Then, 371 drug targets were attained by using the UniProt database to screen and remove repetition. Subsequently, the drug targets and DEGs were set as a background list to get the overlapping targets using Venn diagrams. As shown in the Venn

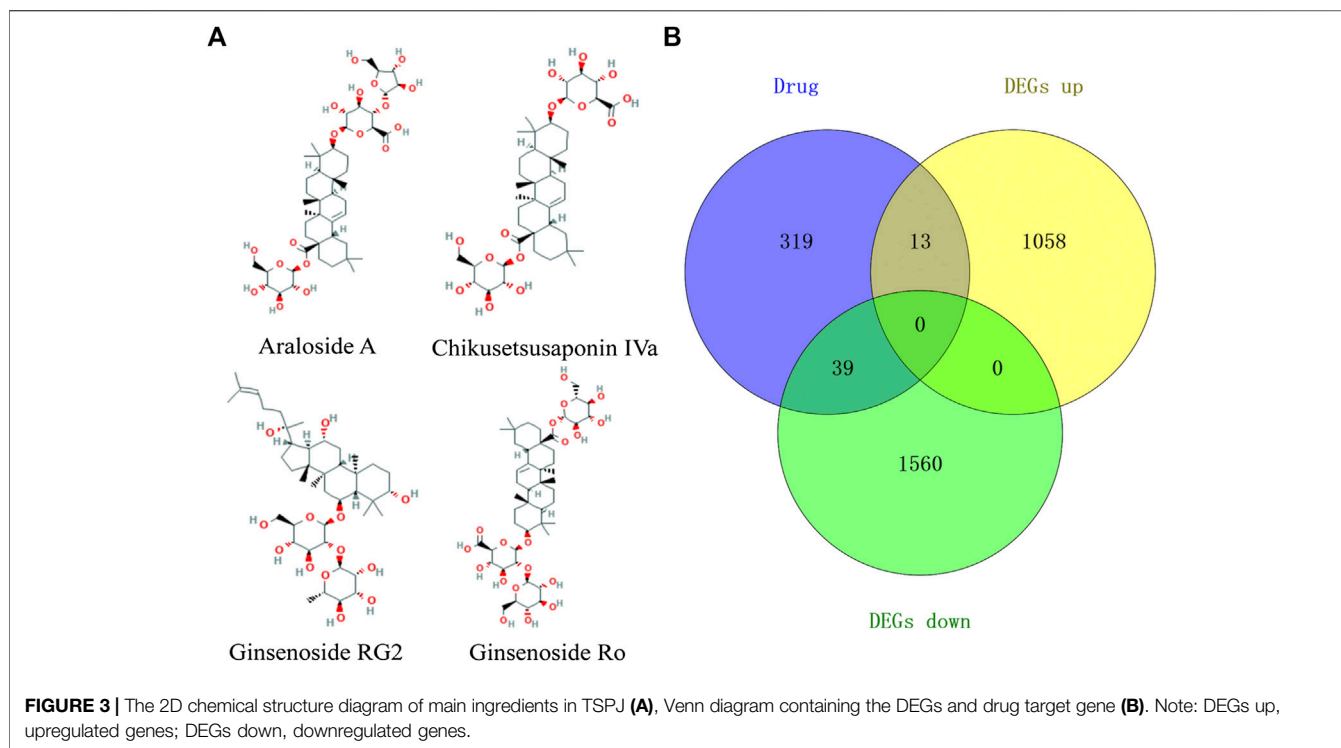


diagram (Figure 3B), 52 overlapping targets could be tested in further research.

Protein–Protein Interactions Network

According to the related data in the STRING databases, the PPI relationships of the overlapping targets were obtained. Using the Cytoscape3.7.2 software, we constructed the PPI network of the overlapping targets. In the network (Figure 4), nodes represent targets and edges represent interaction relationships existing between two targets. The value of degree indicates the connectivity of the node in the network. The higher the value of the node, the more important the node is in the network. We found a total of 41 nodes and 124 edges in this PPI network after applying the “Network Analyzer” plugin. According to the node degree, some hub targets were identified among the network. The top 10 (degree ≥ 7) targets in the network are SRC proto-oncogene, nonreceptor tyrosine kinase, epidermal growth factor receptor, signal transducer and activator of transcription 3, vascular endothelial growth factor A, jun proto-oncogene, AP-1 transcription factor subunit, Fos proto-oncogene, AP-1 transcription factor subunit, matrix metalloproteinase 2, protein tyrosine phosphatase receptor type C, annexin A1, protein kinase C beta, matrix metalloproteinase 13, and renin.

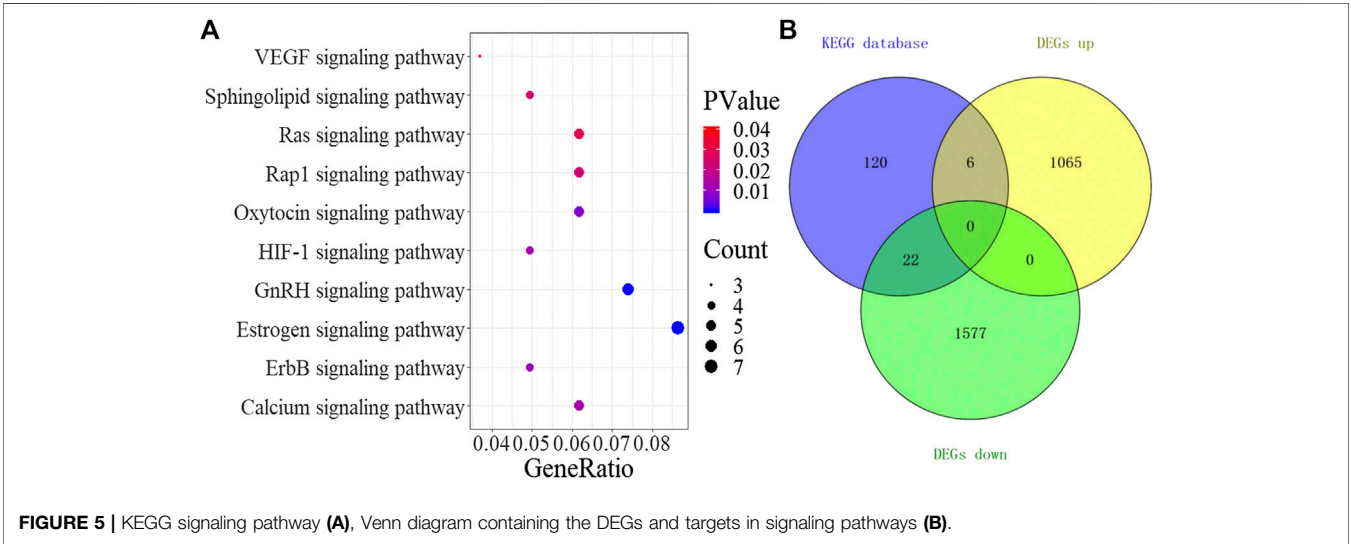
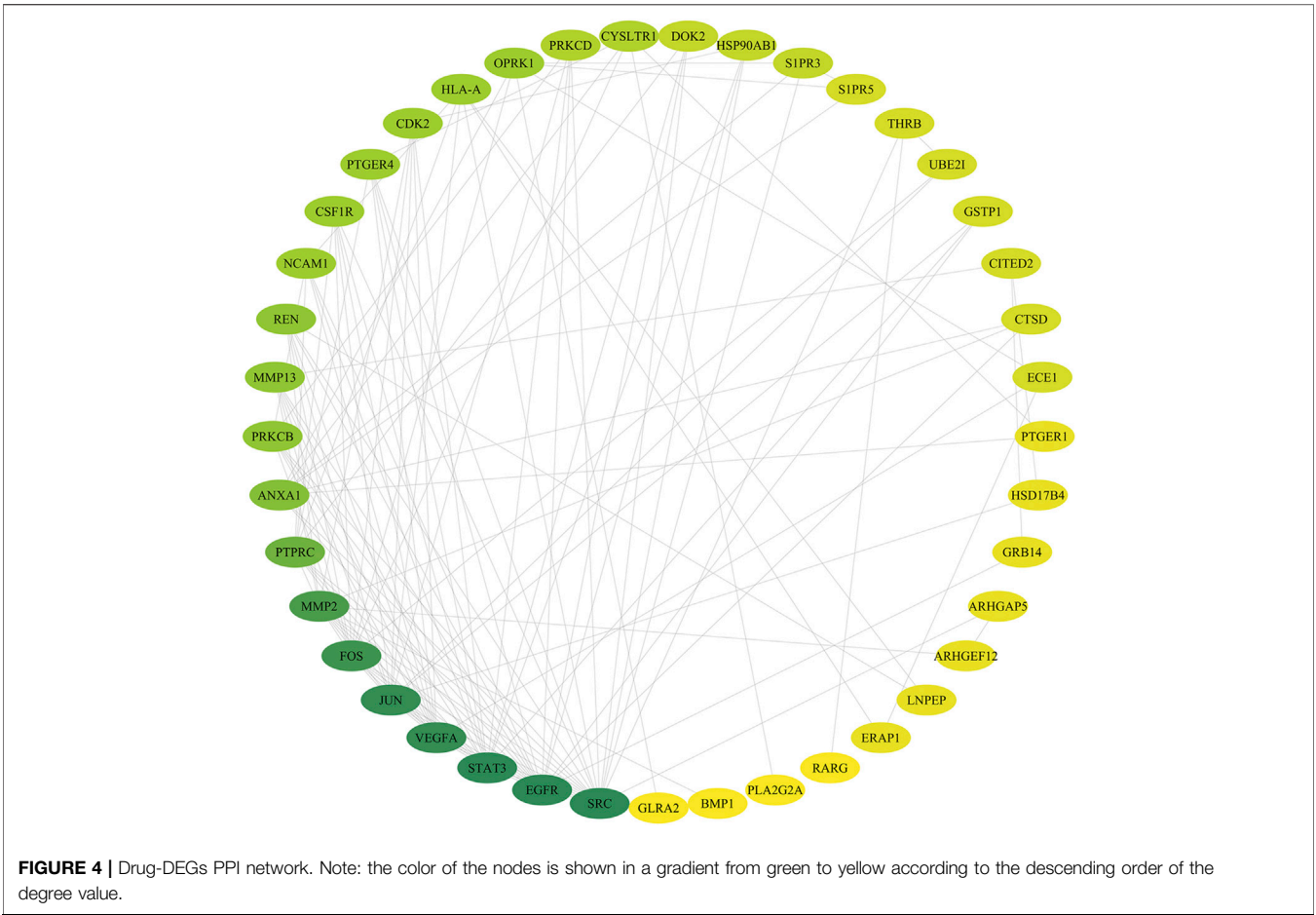
Signaling Pathway

A total of 10 significant signaling pathways ($p < 0.05$) were obtained by KEGG analysis of the 52 drug and DEGs overlapping targets in the DAVID database. The results of pathway enrichment analysis (Figure 5A) included VEGF, sphingolipid, Ras, Rap1, oxytocin, HIF-1, GnRH, estrogen, ErbB, and calcium signaling pathways. Through the analysis of

the pathways, we found that all 10 signaling pathways were related to angiogenesis. Antiangiogenesis may be one of the effective mechanisms of TSPJ in the treatment of RA. Recent studies showed that the VEGF (Elaimy and Mercurio, 2018; Apte et al., 2019) and the HIF-1 signaling pathways (Wang et al., 2016; Serocki et al., 2018) were classic angiogenesis signaling pathways. Next, we downloaded all the genes in the two classic signaling pathways (the VEGF signaling pathway and the HIF-1 signaling pathway) from the KEGG database, and 148 genes were obtained after filtering and deleting the duplicates. Intersection analysis between the 148 genes in the signaling pathways and the DEGs identified 28 genes related to angiogenesis, including six upregulated and 22 downregulated DEGs (Figure 5B). Five out of the top 10 targets (SRC proto-oncogene, nonreceptor tyrosine kinase, epidermal growth factor receptor, signal transducer and activator of transcription 3, vascular endothelial growth factor A, and protein kinase C beta) in the PPI network were also in the same two pathways, and they may play an important role in the mechanism underlying the anti-angiogenesis effect of TSPJ.

Correlation Analysis

To analyze the synergistic mechanisms of the antiangiogenesis effect, we performed a correlation analysis for DEGs in the pathways and calculated the correlation coefficient between the expression of each gene and the others. According to the results of the correlation analysis, the genes with a correlation coefficient greater than 0.5 are defined as positive correlation genes to promote each other, and those with correlation coefficients less than -0.5 are negative correlation genes that inhibit each other. The results of the correlation analysis are shown as a heat



map (Figure 6A) by the “Pheatmap” R package. By clustering the results of the correlation analysis, the genes in the red region indicate a positive correlation, the blue region indicates a negative correlation, and the yellow region indicates that the correlation is not significant; seven negative and 16 positive correlation genes were found. We mapped these genes into signaling pathways

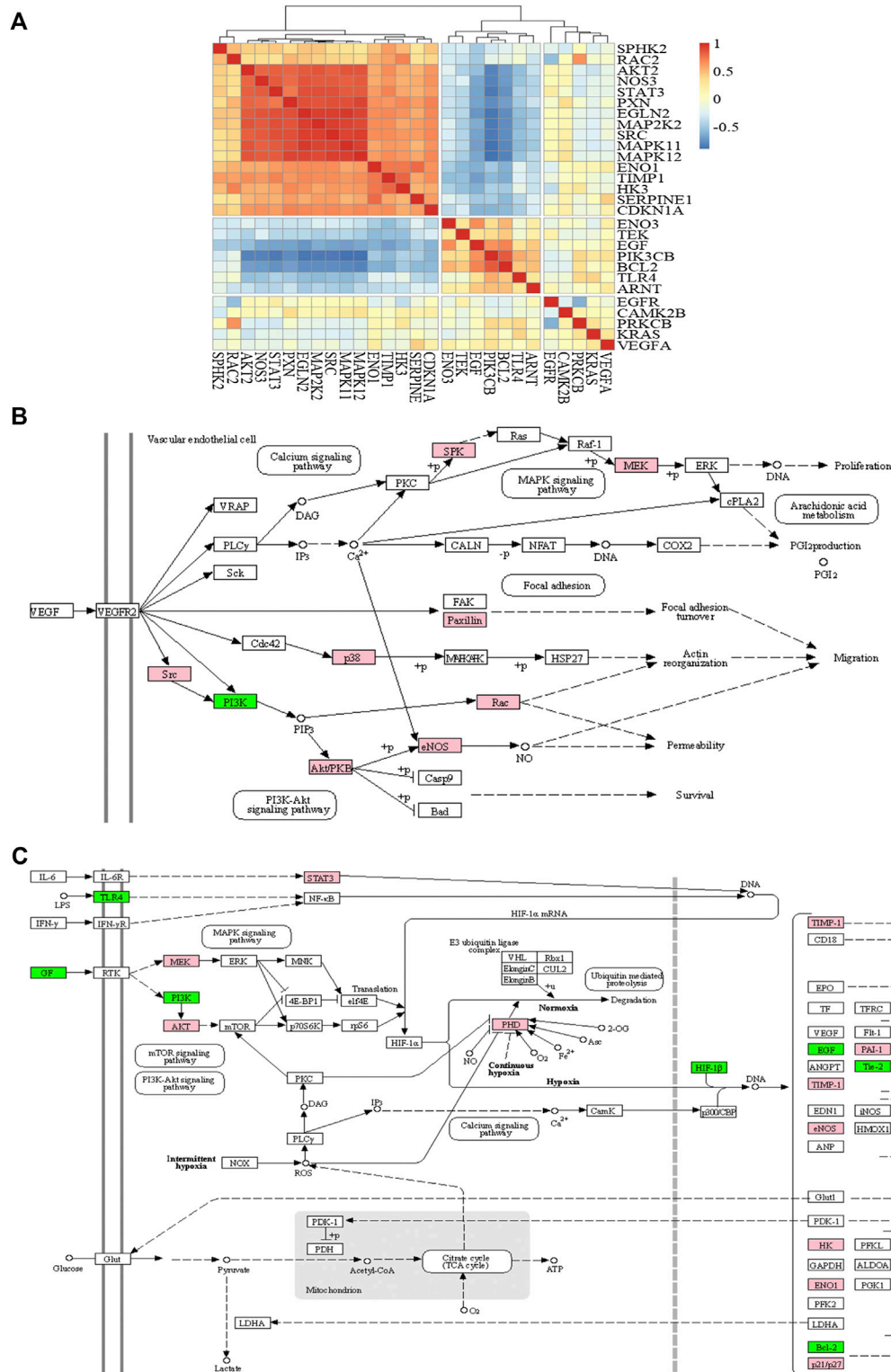


FIGURE 6 | The heat map of correlation analysis **(A)**, VEGF signaling pathway **(B)**, and HIF-1 signaling pathway **(C)**. Note: red or pink represents positive correlation and blue or green represents negative correlation.

(Figures 6B,C) by the KEGG database. As shown in the figures, nine genes (sphingosine kinase 2, mitogen-activated protein kinase kinase 2, paxillin, Mitogen-activated protein kinase 11, Mitogen-activated protein kinase 12, SRC proto-oncogene, nonreceptor tyrosine kinase, Ras-related C3 botulinum toxin substrate 2, AKT serine/threonine kinase 2, and nitric oxide synthase 3) showed positive correlations and promoted each other's expression. PIK3CB is the only suppressed gene in the VEGF signaling pathway. However, in the HIF-1 signaling pathway, seven genes (epidermal growth factor, phosphatidylinositol 4,5-bisphosphate 3-kinase catalytic subunit beta, enolase 3, BCL2 apoptosis regulator, Toll-like receptor 4, aryl hydrocarbon receptor nuclear translocator, and TEK receptor tyrosine kinase) showed negative correlations, and 11 genes (signal transducer and activator of transcription 3, mitogen-activated protein kinase kinase 2, AKT serine/threonine kinase 2, egl-9 family hypoxia inducible factor 2, TIMP metalloproteinase inhibitor 1, serpin family E member 1, nitric oxide synthase 3, hexokinase 3, enolase 1, and cyclin-dependent kinase inhibitor 1A) had positive correlations.

DISCUSSION

In this study, 52 overlapping genes were found based on 2670 DEGs and 371 drug targets. In addition, the pathways of the KEGG analysis were all involved in angiogenesis, especially the HIF-1 α and VEGF signaling pathways. Two key genes in the PPI network were also in these two pathways. Moreover, we successfully established CIA model and verified partly of our computational prediction results. These results suggested that TSPJ could inhibit angiogenesis by targeting the HIF-1 α or the VEGF signaling pathway through multitargets such as SRC and STAT 3, effectively treating RA.

Angiogenesis is one of the main features of RA, and it often occurs in the early stage of inflammation (Lu et al., 2017; Li Y. et al., 2018). RA synovial macrophages and fibroblasts produce growth factors, cytokines, and chemokines after inflammatory stimulation or hypoxia (Bartok and Firestein, 2010; Konisti et al., 2012). These include the production of HIF-1 α after hypoxia and the most famous angiogenic stimulator VEGF (Świdrowska-Jaros and Smolewska, 2018). New angiogenesis aggravates the inflammation and then promotes synovial neovascularization. There is a positive feedback loop between the two (Leblond et al., 2017). Inhibition of angiogenesis has become a new choice for the treatment of RA in recent years (Jia et al., 2018). However, many drugs targeting RA angiogenesis are still under research and development (Alaarg et al., 2017; Feng and Chen, 2018), including Chinese medicine compounds or monomers. For example, sinomenine inhibits angiogenesis through the HIF-1 α -VEGF-ANG-1 axis (Feng et al., 2019). *Tripterygium wilfordii*, Hook f. indirectly suppresses VEGF by inhibiting TNF- α (Zhang W. et al., 2017). It has previously been reported that some components of TSPJ have an antiangiogenic effect in tumors; however, the mechanism of the antiangiogenesis effect of TSPJ in the treatment of RA was not clear. Because of the

multicomponent combination therapy, it is difficult to identify the specific interactions between the components and a single target. Network pharmacology is consistent with the overall concept and can help to predict the targets and identify the mechanisms of TCM (Lee et al., 2019; Zhang et al., 2019). We use the methods of network pharmacology and bioinformatics analysis to further understand the possible mechanism underlying the antiangiogenic effect of TSPJ.

In this study, four active components (Araloside A, Chikusetsusaponin IVa, Ginsenoside Rg2, and Ginsenoside Ro) of TSPJ and the 371 potential targets of TSPJ were predicted. DEGs in RA synovium were obtained by difference analysis and could be involved in the pathogenesis of RA. Acting on these DEGs may be very helpful for the targeted therapy of RA. The pathways containing these DEGs may also be important targets for the treatment of RA. The results of the intersection analysis showed that 52 of the targets may be related. The protein interactions of the 52 overlapping genes were obtained from the STRING database and network visualized by Cytoscape3.7.2 software. The top 10 genes' (SRC proto-oncogene, nonreceptor tyrosine kinase, epidermal growth factor receptor, signal transducer and activator of transcription 3, vascular endothelial growth factor A, jun proto-oncogene, AP-1 transcription factor subunit, Fos proto-oncogene, AP-1 transcription factor subunit, matrix metalloproteinase 2, protein tyrosine phosphatase receptor type C, annexin A1, protein kinase C beta, matrix metalloproteinase 13, and renin) degree values were not less than seven according to the network visualization analysis. A high degree value indicates that these genes play a key role in the regulatory network of RA proteins in responding to TSPJ therapy. Similarly, the important pathways of TSPJ in the treatment of RA were found by the KEGG analysis of overlapping genes. To our surprise, the 10 signaling pathways were all related to angiogenesis, and the top four genes (SRC proto-oncogene, nonreceptor tyrosine kinase, epidermal growth factor receptor, signal transducer and activator of transcription 3, and vascular endothelial growth factor A) in the PPI network are all involved in the VEGF and HIF-1 signaling pathways. We supposed that TSPJ might treat RA by inhibiting angiogenesis.

The VEGF and HIF-1 signaling pathways are two important pathways of angiogenesis. VEGF-A induces endothelial cell proliferation, migration, and survival by activating VEGFR2 and its downstream signal transduction pathway, thus promoting new angiogenesis (Karaman et al., 2018). Synovial inflammation and hyperplasia consume much oxygen, leaving the tissue in a state of local hypoxia. When hypoxia occurs, activation of the HIF-1 signal pathway leads to an increase in the expression of angiogenesis-related factors such as VEGF (Li Y. et al., 2018; Fallah and Rini, 2019). To further identify the synergistic mechanism of the TSPJ against angiogenesis, we analyzed the correlation of DEGs in the VEGF and HIF-1 signaling pathways. Seven genes showed a negative correlation, and 16 showed a positive correlation. The difference in correlation reflects the competition or mutual promotion among these genes (Xuan et al., 2019). Meanwhile, we found only two genes (SRC and STAT 3) with higher degree values in angiogenesis-related pathways according to the results of

the correlation analysis. STAT 3 is a marker of angiogenesis that interacts with SRC (Sp et al., 2017). Li et al. and L. Claesson-Welsh et al. have shown that the activation of SRC phosphorylation promotes angiogenesis (Claesson-Welsh and Welsh, 2013; Li P. et al., 2018). In addition, the results showed that the degree value of STAT 3 in the PPI network is higher than that of other DEGs in the HIF-1 signaling pathway. Studies have shown that STAT 3 is a potential therapeutic target of RA (Oike et al., 2017). STAT 3 directly regulates VEGF, and blocking STAT 3 can effectively inhibit angiogenesis (Wei et al., 2003; Xu et al., 2005). Therefore, we propose that when SRC and STAT 3 are inhibited by TSPJ, the genes positively related to SRC and STAT 3 are also suppressed, and thus reduce angiogenesis.

To further verify the prediction results above, we successfully established CIA mice model. The data showed that TSPJ could significantly reduce the arthritis index of CIA mice. This indicated that TSPJ can effectively relieve the symptoms of CIA mice. The results of H&E staining and histology score of knee joint sections showed that TSPJ inhibited articular cartilage destruction, synovial hyperplasia, and inflammatory cell infiltration in a dose-dependent manner. In addition, TSPJ could reduce the expression of HIF-1 α and VEGFA in serum. This is consistent with our prediction that TSPJ may act as an antiangiogenic by regulating the VEGF or the HIF-1 signaling pathway. Results also showed that TSPJ could decrease the expression of IL-1 β and IL-17A in spleen (Supplementary Figures S2–S5). The above results indicated that TSPJ application might improve joint inflammation, vascular proliferation, and bone erosion.

CONCLUSION

The current study demonstrated that TSPJ may regulate the VEGF or HIF-1 signaling pathways by inhibiting two targets,

STAT 3 and SRC, thus inhibiting inflammation and angiogenesis, which will provide a new strategy for the treatment of RA.

DATA AVAILABILITY STATEMENT

All data sets presented in this study are included in the article/Supplementary Material.

AUTHOR CONTRIBUTIONS

ZF and ZM conceived and designed the experiments; XG, JJ, XF, and YL analyzed the data; XH provided information support; ZF and XG drafted the manuscript; and ZF, GJ, and ZM amended the final manuscript.

FUNDING

This project was supported by grants from the National Natural Science Foundation of China (No. 81703783) and the Hubei Provincial Natural Science Foundation (No. 2017CFB126).

ACKNOWLEDGMENTS

Special thanks to GJ for English language editing.

SUPPLEMENTARY MATERIAL

The Supplementary Material for this article can be found online at: <https://www.frontiersin.org/articles/10.3389/fphar.2020.566129/full#supplementary-material>

REFERENCES

- Alaarg, A., Pérez-Medina, C., Metselaar, J. M., Nahrendorf, M., Fayad, Z. A., Storm, G., et al. (2017). Applying nanomedicine in maladaptive inflammation and angiogenesis. *Adv. Drug Deliv. Rev.* 119, 143–158. doi:10.1016/j.addr.2017.05.009
- Aletaha, D., and Smolen, J. S. (2018). Diagnosis and management of rheumatoid arthritis. *JAMA* 320 (13), 1360–1372. doi:10.1001/jama.2018.13103
- Apte, R. S., Chen, D. S., and Ferrara, N. (2019). VEGF in signaling and disease: beyond discovery and development. *Cell* 176 (6), 1248–1264. doi:10.1016/j.cell.2019.01.02
- Bartok, B., and Firestein, G. S. (2010). Fibroblast-like synoviocytes: key effector cells in rheumatoid arthritis. *Immunol. Rev.* 233 (1), 233–255. doi:10.1111/j.0105-2896.2009.00859.x
- Boezio, B., Audouze, K., Ducrot, P., and Taboureaux, O. (2017). Network-based approaches in pharmacology. *Molecular informatics* 36 (10), 1700048. doi:10.1002/minf.201700048
- Chen, Z., Wang, H., Xia, Y., Yan, F., and Lu, Y. (2018). Therapeutic potential of mesenchymal cell-derived miRNA-150-5p-expressing exosomes in rheumatoid arthritis mediated by the modulation of MMP14 and VEGF. *J. Immunol.* 201 (8), 2472–2482. doi:10.4049/jimmunol.1800304
- Choudhary, N., Bhatt, L., and Prabhavalkar, K. (2018). Experimental animal models for rheumatoid arthritis. *Immunopharmacol. Immunotoxicol.* 40 (3), 193–200. doi:10.1080/08923973.2018.1434793
- Claesson-Welsh, L., and Welsh, M. (2013). VEGFA and tumour angiogenesis. *J. Intern. Med.* 273 (2), 114–127. doi:10.1111/joim.12019
- Croia, C., Bursi, R., Suter, D., Petrelli, F., Alunno, A., and Puxeddu, I. (2019). One year in review 2019: pathogenesis of rheumatoid arthritis. *Clin. Exp. Rheumatol.* 37 (3), 347–357.
- Dennis, G., Jr., Sherman, B. T., Hosack, D. A., Yang, J., Gao, W., Lane, H. C., et al. (2003). DAVID: database for annotation, visualization, and integrated discovery. *Genome Biol.* 4 (5), P3. doi:10.1186/gb-2003-4-5-p3
- Ding, Y., Keming, L., and Changcheng, Z. (2008). Study on the anti-inflammatory effect of total saponins of *Panax japonicus*. *Hubei J. Tradit. Chin. Med.* 4, 7–8. doi:10.3969/j.issn.1000-0704.2008.04.003
- Ding, Y., Qi, Y., and Changcheng, Z. (2009). Effect of total saponins of *Panax japonicus* on expression of serum TNF- α and IL-1 β in rheumatoid arthritis rats. *Shandong Med. J.* 19, 4–6. doi:10.3969/j.issn.1002-266X.2009.19.002
- Ding, Y., Zhao, Q., and Wang, L. (2019). Pro-apoptotic and anti-inflammatory effects of araloside A on human rheumatoid arthritis fibroblast-like synoviocytes. *Chem. Biol. Interact.* 306, 131–137. doi:10.1016/j.cbi.2019.04.025
- Elaimy, A. L., and Mercurio, A. M. (2018). Convergence of VEGF and YAP/TAZ signaling: implications for angiogenesis and cancer biology. *Sci. Signal.* 11 (552), eaau1165. doi:10.1126/scisignal.aau1165
- Elshabrawy, H. A., Chen, Z., Volin, M. V., Ravella, S., Virupannavar, S., and Shahrara, S. (2015). The pathogenic role of angiogenesis in rheumatoid arthritis. *Angiogenesis* 18 (4), 433–448. doi:10.1007/s10456-015-9477-2
- Fallah, J., and Rini, B. I. (2019). HIF inhibitors: status of current clinical development. *Curr. Oncol. Rep.* 21 (1), 6. doi:10.1007/s11912-019-0752-z

- Feng, X., and Chen, Y. (2018). Drug delivery targets and systems for targeted treatment of rheumatoid arthritis. *J. Drug Target.* 26 (10), 845–857. doi:10.1080/1061186x.2018.1433680
- Feng, Z.-t., Yang, T., Hou, X.-q., Wu, H.-y., Feng, J.-t., Ou, B.-j., et al. (2019). Sinomenine mitigates collagen-induced arthritis mice by inhibiting angiogenesis. *Biomed. Pharmacother.* 113, 108759. doi:10.1016/j.biopha.2019.108759
- Guo, Z., Feng, Z., Zhang, H., Yan, L., Liang, M., Mei, Z., et al. (2019). Research progress of bamboo ginseng and its preparations in the treatment of rheumatoid arthritis. *J. Chin. Med. Mater.* 42 (4), 941–944. doi:10.13863/j.issn1001-4454.2019.04.050
- Jia, W., Wu, W., Yang, D., Xiao, C., Huang, M., Long, F., et al. (2018). GATA4 regulates angiogenesis and persistence of inflammation in rheumatoid arthritis. *Cell Death Dis.* 9 (5), 503. doi:10.1038/s41419-018-0570-5
- Karaman, S., Leppänen, V.-M., and Alitalo, K. (2018). Vascular endothelial growth factor signaling in development and disease. *Development* 145 (14), dev151019. doi:10.1242/dev.151019
- Konisti, S., Kiriakidis, S., and Paleolog, E. M. (2012). Hypoxia—a key regulator of angiogenesis and inflammation in rheumatoid arthritis. *Nat. Rev. Rheumatol.* 8 (3), 153–162. doi:10.1038/nrrheum.2011.205
- Leblond, A., Allanore, Y., and Avouac, J. (2017). Targeting synovial neoangiogenesis in rheumatoid arthritis. *Autoimmun. Rev.* 16 (6), 594–601. doi:10.1016/j.autrev.2017.04.005
- Lee, W.-Y., Lee, C.-Y., Kim, Y.-S., and Kim, C.-E. (2019). The methodological trends of traditional herbal medicine employing network pharmacology. *Biomolecules* 9 (8), 362. doi:10.3390/biom9080362
- Li, P., Chen, D., Cui, Y., Zhang, W., Weng, J., Yu, L., et al. (2018). Src plays an important role in AGE-induced endothelial cell proliferation, migration, and tubulogenesis. *Front. Physiol.* 9, 765. doi:10.3389/fphys.2018.00765
- Li, Y., Liu, Y., Wang, C., Xia, W.-R., Zheng, J.-Y., Yang, J., et al. (2018). Succinate induces synovial angiogenesis in rheumatoid arthritis through metabolic remodeling and HIF-1 α /VEGF axis. *Free Radic. Biol. Med.* 126, 1–14. doi:10.1016/j.freeradbiomed.2018.07.009
- Lu, Y., Yu, S. S., Zong, M., Fan, S. S., Lu, T. B., Gong, R. H., et al. (2017). Glucose-6-Phosphate isomerase (G6PI) mediates hypoxia-induced angiogenesis in rheumatoid arthritis. *Sci. Rep.* 7, 40274. doi:10.1038/srep40274
- Oike, T., Sato, Y., Kobayashi, T., Miyamoto, K., Nakamura, S., Kaneko, Y., et al. (2017). Stat3 as a potential therapeutic target for rheumatoid arthritis. *Sci. Rep.* 7 (1), 10965. doi:10.1038/s41598-017-11233-w
- Ramharack, P., and Soliman, M. E. S. (2018). Bioinformatics-based tools in drug discovery: the cartography from single gene to integrative biological networks. *Drug Discov. Today* 23 (9), 1658–1665. doi:10.1016/j.drudis.2018.05.041
- Sayers, E. W., Beck, J., Brister, J. R., Bolton, E. E., Canese, K., Comeau, D. C., et al. (2020). Database resources of the National Center for Biotechnology Information. *Nucleic Acids Res.* 48 (D1), D9–D16. doi:10.1093/nar/gkz899
- Scott, D. L., Wolfe, F., and Huizinga, T. W. (2010). Rheumatoid arthritis. *Lancet* 376 (9746), 1094–1108. doi:10.1016/s0140-6736(10)60826-4
- Serocki, M., Bartoszewska, S., Janaszak-Jasiecka, A., Ochocka, R. J., Collawn, J. F., and Bartoszewski, R. (2018). miRNAs regulate the HIF switch during hypoxia: a novel therapeutic target. *Angiogenesis* 21 (2), 183–202. doi:10.1007/s10456-018-9600-2
- Sidders, B., Karlsson, A., Kitching, L., Torella, R., Karila, P., and Phelan, A. (2018). Network-based drug discovery: coupling network pharmacology with phenotypic screening for neuronal excitability. *J. Mol. Biol.* 430 (18 Pt A), 3005–3015. doi:10.1016/j.jmb.2018.07.016
- Smolen, J. S., Aletaha, D., and McInnes, I. B. (2016). Rheumatoid arthritis. *Lancet* 388 (10055), 2023–2038. doi:10.1016/s0140-6736(16)30173-8
- Sp, N., Kang, D., Joong, Y., Park, J., Kim, W., Lee, H., et al. (2017). Nobiletin inhibits angiogenesis by regulating src/FAK/STAT3-mediated signaling through PXN in ER⁺ breast cancer cells. *Int. J. Mol. Sci.* 18 (5), 935. doi:10.3390/ijms18050935
- Świdrowska-Jaros, J., and Smolewska, E. (2018). A fresh look at angiogenesis in juvenile idiopathic arthritis. *Cent. Eur. J. Immunol.* 43 (3), 325–330. doi:10.5114/ceji.2018.80052
- The UniProt Consortium (2017). UniProt: the universal protein knowledgebase. *Nucleic Acids Res.* 45 (D1), D158–D169. doi:10.1093/nar/gkw1099
- Wang, J., Wong, Y. K., and Liao, F. (2018). What has traditional Chinese medicine delivered for modern medicine? *Expert. Rev. Mol. Med.* 20, e4. doi:10.1017/erm.2018.3
- Wang, L.-H., Jiang, X.-R., Yang, J.-Y., Bao, X.-F., Chen, J.-L., Liu, X., et al. (2016). SYP-5, a novel HIF-1 inhibitor, suppresses tumor cells invasion and angiogenesis. *Eur. J. Pharmacol.* 791, 560–568. doi:10.1016/j.ejphar.2016.09.027
- Wei, D., Le, X., Zheng, L., Wang, L., Frey, J. A., Gao, A. C., et al. (2003). Stat3 activation regulates the expression of vascular endothelial growth factor and human pancreatic cancer angiogenesis and metastasis. *Oncogene* 22 (3), 319–329. doi:10.1038/sj.onc.1206122
- Xu, Q., Briggs, J., Park, S., Niu, G., Kortylewski, M., Zhang, S., et al. (2005). Targeting Stat3 blocks both HIF-1 and VEGF expression induced by multiple oncogenic growth signaling pathways. *Oncogene* 24 (36), 5552–5560. doi:10.1038/sj.onc.1208719
- Xuan, C., Gao, Y., Jin, M., Xu, S., Wang, L., Wang, Y., et al. (2019). Bioinformatic analysis of Cacybp-associated proteins using human glioma databases. *IUBMB Life* 71 (7), 827–834. doi:10.1002/iub.1999
- Yang, B. R., Yuen, S. C., Fan, G. Y., Cong, W. H., Leung, S. W., and Lee, S. M. (2018). Identification of certain *Panax* species to be potential substitutes for *Panax notoginseng* in hemostatic treatments. *Pharmacol. Res.* 134, 1–15. doi:10.1016/j.phrs.2018.05.005
- Yang, X., Wang, R., Zhang, S., Zhu, W., Tang, J., Liu, J., et al. (2014). Polysaccharides from *Panax japonicus* C.A. Meyer and their antioxidant activities. *Carbohydr. Polym.* 101, 386–391. doi:10.1016/j.carbpol.2013.09.038
- Yongui, L. (2011). The mechanistic approach of Saponins from *Panax japonicus* for treatment of alcohol-induced hepatic injury. Dissertation. Hangzhou, China: Zhejiang University.
- Yuan, H., Ma, Q., Cui, H., Liu, G., Zhao, X., Li, W., et al. (2017). How can synergism of traditional medicines benefit from network pharmacology? *Molecules* 22 (7), 1135. doi:10.3390/molecules22071135
- Yu-min, H., Ke, A., Chun-xi, H., Chang-cheng, Z., Ding, Y., and San-jin, C. (2019). Triterpene saponins in *Panax japonicus* and their 13C-NMR spectroscopic characteristics. *China J. Chin. Mater. Med.* 44 (02), 249–260. doi:10.19540/j.cnki.cjcmm.20181101.016
- Zhang, R.-z., Yu, S.-j., Bai, H., and Ning, K. (2017). TCM-Mesh: the database and analytical system for network pharmacology analysis for TCM preparations. *Sci. Rep.* 7 (1), 2821. doi:10.1038/s41598-017-03039-7
- Zhang, W., Li, F., and Gao, W. (2017). *Tripterygium wilfordii* inhibiting angiogenesis for rheumatoid arthritis treatment. *J. Natl. Med. Assoc.* 109 (2), 142–148. doi:10.1016/j.jnma.2017.02.007
- Zhang, R., Zhu, X., Bai, H., and Ning, K. (2019). Network pharmacology databases for traditional Chinese medicine: review and assessment. *Front. Pharmacol.* 10, 123. doi:10.3389/fphar.2019.00123
- Zheng, S.-W., Xiao, S.-Y., Wang, J., Hou, W., and Wang, Y.-P. (2019). Inhibitory effects of Ginsenoside Ro on the growth of B16F10 melanoma via its metabolites. *Molecules* 24 (16), 2985. doi:10.3390/molecules24162985

Conflict of Interest: The authors declare that the research was conducted in the absence of any commercial or financial relationships that could be construed as a potential conflict of interest.

Copyright © 2020 Guo, Ji, Jose Kumar Sreena, Hou, Luo, Fu, Mei and Feng. This is an open-access article distributed under the terms of the Creative Commons Attribution License (CC BY). The use, distribution or reproduction in other forums is permitted, provided the original author(s) and the copyright owner(s) are credited and that the original publication in this journal is cited, in accordance with accepted academic practice. No use, distribution or reproduction is permitted which does not comply with these terms.



Chinese Medicine Formula PSORI-CM02 Alleviates Psoriatic Dermatitis via M-MDSCs and Th17 Crosstalk

Jingwen Deng^{1,2}, Siyi Tan³, Ruonan Liu⁴, Wanlin Yu⁵, Haiming Chen¹, Nan Tang⁶, Ling Han^{1,2*} and Chuanjian Lu^{1,2*}

¹The Second Affiliated Hospital of Guangzhou University of Chinese Medicine, Guangzhou, China, ²Guangdong Provincial Key Laboratory of Clinical Research on Traditional Chinese Medicine Syndrome, Guangdong Provincial Hospital of Chinese Medicine, Guangzhou, China, ³Guangzhou Panyu Central Hospital, Guangzhou, China, ⁴Department of Physiology, Medical College, Jinan University, Guangzhou, China, ⁵Central Laboratory, Guangdong Provincial Hospital of Chinese Medicine, Guangzhou, China, ⁶Guangzhou Red Cross Hospital, Medical College, Jinan University, Guangzhou, China

OPEN ACCESS

Edited by:

Xiaojuan He,
China Academy of Chinese Medical
Sciences, China

Reviewed by:

Ying Chi Song,
China Medical University, Taiwan
Xiaojuan Li,
Southern Medical University, China

*Correspondence:

Ling Han
linghan36@163.com
Chuanjian Lu
lcj@gzucm.edu.cn

Specialty section:

This article was submitted to
Ethnopharmacology,
a section of the journal
Frontiers in Pharmacology

Received: 18 May 2020

Accepted: 24 November 2020

Published: 18 January 2021

Citation:

Deng J, Tan S, Liu R, Yu W, Chen H,
Tang N, Han L and Lu C (2021)
Chinese Medicine Formula PSORI-
CM02 Alleviates Psoriatic Dermatitis
via M-MDSCs and Th17 Crosstalk.
Front. Pharmacol. 11:563433.
doi: 10.3389/fphar.2020.563433

Psoriasis is a chronic inflammatory skin disease that is associated with multiple coexisting conditions. Extensive literature suggests that psoriasis is a T-cell-mediated condition, and its pathogenesis is related to dysfunction of the immune system. Myeloid-derived suppressor cells (MDSCs) are a group of heterogeneous myeloid cells that have suppressive effects on T cells. MDSCs are present at very low levels in healthy individuals but can substantially expand in tumours or inflammatory conditions. PSORI-CM02, a Chinese medical formula designed based on the Chinese medicine theory (*Blood Stasis*), has been prescribed extensively for psoriasis therapy and shows a stable clinical effect and safety. This study discusses the mechanisms of MDSCs involved in disease development and therapeutic progress. Our data provides evidence that monocytic myeloid-derived suppressor cells (M-MDSCs) play a role in IMQ-induced psoriatic dermatitis. Functional characterization and correlation analysis indicated that MDSCs are positively correlated with Th17 cells. PSORI-CM02 alleviated IMQ-induced psoriatic dermatitis and suppressed the proliferation of Th17 cells via M-MDSC-induced Arg1 upregulation, suggesting M-MDSCs could be a novel therapeutic target for psoriasis, and PSORI-CM02 exerted its effects via the perturbation of M-MDSCs and Th17 cell crosstalk.

Keywords: Chinese medicine, PSORI-CM02, Th17, MDSCs, psoriasis

INTRODUCTION

Psoriasis is a common skin disease caused by both autoimmune dysfunction and genetic burden. The worldwide prevalence of psoriasis is estimated at approximately 2%, and the prevalence is in a diverse range according to regions (Parisi et al., 2013). Patients with psoriasis have been reported to suffer from elevated rates of various psychopathologies, including depression, anxiety, sexual dysfunction, poor self-esteem, and even suicidal ideation (Kimball et al., 2005; Kimball et al., 2012).

In the past decade, breakthroughs in the understanding of the pathogenesis of psoriasis have developed from its histopathologic accelerated cell proliferation of keratinocytes to the pathogenesis of chronic inflammatory with a dominant IL-23/Th17 axis (Zheng et al., 2007; Ogawa et al., 2018). The crosstalk within neutrophils, dendritic cells, T cells, and the cytokines released from immune cells are the central pathogenesis of psoriasis progress (Boehncke and Schon, 2015).

However, we still lack a holistic knowledge of the role of the myeloid cell-derived immune system in psoriasis. Myeloid-derived suppressor cells (MDSCs) are a heterogeneous population of activated myeloid precursors and relatively immature myeloid cells that are associated with various pathological immune environments (Brandau et al., 2013; Ost et al., 2016). Most studies have divided MDSCs into two major subsets: monocytic myeloid-derived suppressor cells (M-MDSCs) and polymorphonuclear or granulocytic myeloid-derived suppressor cells (PMN-MDSCs or G-MDSCs). PMN-MDSCs are similar to neutrophils, whereas M-MDSCs share many morphological and phenotypic characteristics of monocytes (Gabrilovich and Nagaraj, 2009; Gabrilovich, 2017).

Recent studies have indicated that the MDSC population increases in patients with psoriasis (Cao et al., 2016; Soler et al., 2016). But we still know little about the perturbations of MDSCs in the immune system of psoriasis patients and its immune response in the psoriatic therapeutic progress. To explore how the different subpopulation of MDSCs in psoriasis patients mediate psoriasis development, we detected the expansion of MDSCs and its subpopulation PMN-MDSCs and M-MDSCs in imiquimod (IMQ)-induced murine psoriatic dermatitis. The results showed that the MDSCs and their subpopulations were also different between psoriatic dermatitis mice and the controls.

Recently, series of clinical trials and systematic reviews have reported that Chinese medicine is effective in treating psoriasis (May et al., 2012; Deng et al., 2013; 2014; Zhang et al., 2014). Yinxieling (PSORI-CM) formula is a Chinese herbal medicine compound preparation with 10 ingredients (*Angelica sinensis* (Oliv.) Diels, *Paeonia lactiflora* Pall., *Chloranthus spicatus* (Thunb.) Makino, *Prunus mume* (Siebold) Siebold and Zucc., *Rehmannia glutinosa* (Gaertn.) DC., *Ligusticum striatum* DC., *Lithospermum erythrorhizon* Siebold and Zucc., *Curcuma zedoaria* (Christm.) Roscoe, *Smilax glabra* Roxb., *Glycyrrhiza glabra* L.) for psoriasis. This medicine was developed by a well-known Chinese Medicine dermatologist National Medical Master Guo-wei Xuan and formulated according to traditional Chinese medicine theory. The clinical practice in these 20 years showed that PSORI-CM formula has been prescribed extensively for psoriasis therapy and has shown a stable curative effect on not only relieving symptoms of psoriasis but also reducing the relapse rate (Cz and Liu, 2006; Han et al., 2011). To expand the application of Yinxieling, an optimized formula PSORI-CM02 was developed, composed of only five ingredients (*Curcuma longa* L., *Paeonia lactiflora* Pall., *Smilax glabra* Roxb., *Prunus mume* (Siebold) Siebold and Zucc. and *Sarcandra glabra* (Thunb.) Nakai) from the original Yinxieling. In the theory of Traditional Chinese medicine, psoriasis is generally associated with three syndromes: *blood stasis*, *blood heat*, and *blood dryness*. In the acute stage of the pathogenesis of psoriasis, *blood heat* is mainly obstructed on the surface of the lesion. In the chronic stage, *qi* and *blood* deficiency lead to *dryness*, which obstructs the normal nourishment in the skin, as well as *blood stasis*, which prohibits blood flow smoothly in the skin (Lu et al., 2012). Therefore, the therapeutic principle of psoriasis is to activate blood circulation and remove blood stasis.

In PSORI-CM02 formula, *Curcuma longa* L. and *Paeonia lactiflora* Pall. help to activate blood circulation, while *Smilax glabra* Roxb., *Prunus mume* (Siebold) Siebold and Zucc. and *Sarcandra glabra* (Thunb.) Nakai play the roles of removing *blood stasis*. These five ingredients in PSORI-CM02 were found to have positive correlations with pharmacodynamic indicators by using computer systematic pharmacological methods and laboratory experiments (Gu et al., 2018). However, previous studies of PSORI-CM02 are mostly focused on the role of the adaptive immune system in psoriasis. One of our previous studies showed that PSORI-CM02 suppressed allograft rejection by reducing the proliferation of T cells (Lu et al., 2018), implying that the mechanism of T-cell suppression needed to be investigated.

The IMQ-induced mouse model for psoriasisform dermatitis is one of the most widely used mouse models in recent research studies on psoriasis, as psoriasis mediated by the IL-23/Th17 axis can be triggered by this TLR7 agonist (van der Fits et al., 2009). Considering there are many effective components characterized by inducing multitarget effects in Chinese Medicine, whether the myeloid cell is also a target of PSORI-CM02 or not is still uncertain. Therefore, based on the observation of MDSCs and their subpopulation in IMQ-induced murine psoriatic dermatitis, we investigated the effect of PSORI-CM02 on MDSCs in the psoriatic mouse model.

Currently, various immunosuppressive and promoting functions of MDSCs on diseases have been reported in the literature. In this study, we performed the functional analysis of murine MDSCs in psoriatic dermatitis. We also discussed the association of MDSCs with T-help cells in psoriasis and the Chinese medicine formula PSORI-CM02 effects on their crosstalk. We aimed at providing suggestions for the contemporary biological characterization of MDSCs and the mechanism of Chinese medicine on psoriasis.

MATERIALS AND METHODS

Reagents and Antibodies

Reagents were purchased as follows: liberase TM (5401119001) was purchased from Roche, DNase I (D4263-1VL) was purchased from Sigma-Aldrich. Cell Staining Buffer (554656), BD GolgiPlug™ (brefeldin A, 550583), RBC Lysing Buffer (10X concentrate), Ms CD11b FITC (561688), Ms Gr1 PE (553128), Ms LY-6G PE (561104), Ms Ly-6C PerCP-Cy™5.5 (560525), Ms CD16/CD32 PURE (553142) and mouse Th1-Th2-Th17 CBA KIT (560485) was purchased from BD (United States), Ms Arg1 (A1exF5) APC (17-3697-80) antibody was purchased from Invitrogen, Arg1 ELISA Kit, TGF-beta1 ELISA Kit, iNOS ELISA Kit, IL-17A ELISA Kit were purchased from Cusabio (China). Mouse CD4⁺ T cell isolation kit II (130-095-248) were purchased from Miltenyi Biotec. Fetal bovine serum (FBS) and High-glucose Dulbecco's modified Eagle's medium (DMEM) were purchased from Gibco (United States). Trizol reagent was purchased from Life (United States). RNeasy fibrous tissue mini kit was purchased from Qiagen (Germany), Ms CD45.2 PerCP, Ms CD4 eFluor 660, Ms IL-17A FITC, Ms

IL-22 APC, First Strand cDNA Synthesis Kit was purchased from and FastStart Universal SYBR Green Master Mix were purchased from Thermo (United States). RIPA Buffer was purchased from Cell Signaling Technology (United States). Imiquimod cream was obtained from Ming Xin Pharmaceutical Co. LTD. (China), Vaseline® pure petroleum jelly was purchased from Unilever (United Kingdom), methotrexate (MTX) was purchased from the Shanghai Pharmaceutical Group Co. Ltd. (China), PSORI-CM02 was obtained from the Chinese Medicine Hospital of Guangdong Province (China).

BD FACSAria™ III (BD Biosciences, United States), ABI7500 Real-Time PCR System (ABI, United States), NanoDrop 2000C Spectrophotometer (Thermo Scientific, United States), microscope (Olympus, Japan) and VICTOR™ X5 (PerkinElmer, United States) were used for the analysis.

IMQ-Induced Psoriatic Dermatitis in Mice

BALB/c mice with an equal sex ratio at 6–8 weeks of age with an average weight of 16–18 g were purchased and transferred from Guangdong Medical Laboratory Animal Center (Guangdong, China). All of the mice were settled in a specific pathogen-free (SPF) animal facility with unlimited access to food and water and a 12-h daylight, 12-h night cycle. Mice in the IMQ group received a topical dose of 60 mg imiquimod cream on the shaved back skin (2 × 3 cm) once per day for seven consecutive days, and mice in the control group received Vaseline® as vehicle controls.

A modified Psoriasis Area Severity Index (PASI) score for measuring the inflammation of psoriatic dermatitis was recorded every day before painting of the cream. Erythema, scaling and thickening of back skin were measured based on 0–4 scales (0, none; 1, slight; 2, moderate; 3, marked; and 4, very marked). Bodyweight was measured daily. At day-8 morning, all mice were anaesthetised with a ketamine/acepromazine mixture (ketamine 100 mg/kg, acepromazine 5 mg/kg) and then weighed, PASI was recorded, and the digital photo was taken. Then, the mice were sacrificed. Skin tissues were collected and processed for flow cytometric analysis. The skin sample was also reserved for histological analysis and gene expression analysis.

Treatment of Mice

The mice were housed in a stable SPF environment for one week after purchase. For the experiments, they were allocated randomly to different groups.

PSORI-CM02 group: 60 mg imiquimod cream painted on the shaved back skin daily, PSORI-CM02 decoction (5 ml/kg) was administered orally twice per day. The treatment of PRORI-CM02 began one week before the IMQ painting and lasted 14 consecutive days. Considering the ethical statement of Institutional Animal Care and Use Committee of Guangdong Provincial Academy of Chinese Medical Sciences, as all of our previous multiple-dose studies indicated that the treatment with PSORI-CM02 decoction dose with 2.94 g/kg to the mice was the most effective (Chen et al., 2017; Wu et al., 2019; Yue et al., 2019; Li

et al., 2020), we prepared the PSORI-CM02 decoction dose only with 2.94 g/kg in this study to reduce and refine the use of animals in research.

MTX group: 60 mg imiquimod cream painted on the shaved back skin daily, MTX 0.65 mg/kg was administered orally twice per day.

Model group: 60 mg imiquimod cream painted on the shaved back skin daily, saline was administered orally twice per day.

Control group: Vaseline® painted on the shaved back skin daily, saline was administered orally twice per day.

Preparation of PSORI-CM02

All the herbs of the PSORI-CM02 formula were pharmacopeia-grade and purchased from the Department of Pharmacy, Guangdong Provincial Hospital of Chinese Medicine. Five herbs are used in the PSORI-CM02 formula: *Curcuma longa* L., *Paeonia lactiflora* Pall., *Smilax glabra* Roxb., *Prunus mume* (Siebold) Siebold and Zucc. and *Sarcandra glabra* (Thunb.) Nakai, with a weight ratio of 2:3:5:2:5. The types of specimens used in this study were deposited in the herbarium in the School of Chinese Materia Medica, Guangzhou University of Chinese Medicine (GUCM).

Water extracts were then concentrated and dried with a rotary evaporator under vacuum. The PSORI-CM02 decoctions were prepared using the following procedures: herbs were marinated in a pot with filtered water for half an hour. Then, the pot was heated and kept boiling for 15 mins. Then, decocting was done for 30 mins with a small fire. The herbs were decocted twice. The two decoctions were mixed, filtered using a 75-µm filter and stored in a refrigerator at 4 °C. A chromatographic fingerprint for quality control and quantitative analysis of the PSORI-CM02 decoction was performed and reported in our previous study (Supplementary Figure S1; Table S1) (Chen et al., 2017; Wu et al., 2019). All procedures followed the procedures of the China Pharmacopoeia (2010 Edition).

Single-Cell Preparation From Skin

The skin samples from the mice were cut from the shaved back region. Skin samples were chopped into small pieces with scissors and digested with 2 ml of liberase TM (2.5 mg/ml) containing 0.1% DNase I for 90 min at 37 °C. The cell suspensions were filtered with 40 µm of cell strainer and washed twice with 5 ml of PBS 1% FBS.

Drainage from the lymph nodes was obtained from the abdomens of the mice and ground by the frosted surface of the glass slides. The cell suspensions were filtered with 40 µm of cell strainer and washed with 2 ml of PBS 1% FBS.

Flow Cytometric Analysis

Immune phenotype characterization of the skin sample was performed by flow cytometry with a 12-colour setup, based on the surface staining and intracellular staining method. A 3-h stimulation of 10⁶ cells/ml suspension at 37 °C with PMA (25 ng/ml)/ionomycin (1 mg/ml) in the presence of Brefeldin-A (10 mg/ml) was performed. Before the staining, the cells were

resuspended in 10^6 cells/100 μ L per well in a 96-well plate with 2 μ g/ml of anti-CD16/CD32 diluted in PBS 1% FBS and incubated at 4 °C for 15 mins to block non-specific binding to Fc receptors. After the preparation, cells were incubated in the dark at 4 °C for 30 mins for surface staining with the following antibodies: Ms CD11b FITC, Ms Gr1 PE, Ms LY-6G PE, Ms Ly-6C PerCP-CyTM5.5. The cells for intracellular staining were also surface stained with the following antibodies: Ms CD45.2 PerCP, Ms CD4 eFluor 660. Intracellular staining was performed for the cells with the following antibodies: Ms IL-17A FITC, Ms IL-22 APC, Ms Arg1 APC. The stained cells were analysed by flow cytometer BD FACSaria III. Data were analysed by using FlowJo software (Version.10.0.8, Tree Star Ashland, OR). The results were represented as the percentage of positive cell populations.

Skin Biopsy Histological Analysis

The skin biopsies extracted from the mice were fixed in fresh 4% (w/v) formaldehyde solution for 24 h and then embedded in paraffin. After paraffin embedding, the slides were stained with haematoxylin and eosin (H&E).

Real-Time Quantitative PCR (RT-qPCR)

Skin biopsies were stored under liquid nitrogen. On the day of the RT-qPCR assay, the biopsies were allowed to thaw, and 30 mg of tissue was homogenized with the aid of a homogenizer in ice-cold Trizol reagent. mRNA was obtained from the back-skin biopsy of all mice with the RNeasy fibrous tissue mini-kit. cDNA was synthesized using the Thermo First Strand cDNA Synthesis Kit. For the qPCR reaction, complementary DNA (cDNA) was amplified with FastStart Universal SYBR Green Master Mix. Quantitative research detection of target nucleic acid sequences was then performed on the ViiA seven Real-Time PCR System.

All target genes were normalized with housekeeping gene GAPDH expression in parallel as the internal control. The relative expression of target genes was calculated by the $2^{-\Delta\Delta CT}$ method.

Cytometric Bead Array (CBA) Analysis

Skin biopsies were lysed with Radio-Immunoprecipitation Assay (RIPA) lysis buffer. Th1/Th2/Th17 cytokine (IL-2, IL-4, IL-6, IL-10, IL-17A, TNF and IFN- γ) secretion in the skin and the serum of mice were detected by cytometric bead array, a flow cytometric bead-based technology for multiplexed assay, by using the mouse Th1-Th2-Th17 CBA kit according to the manufacturer's technical guidelines and protocols (Morgan et al., 2004). Data were acquired through flow cytometry BD FACSariaTM III. FCAP Array software (V4.0, BD Biosciences) was used to calculate the cytokine levels.

Enzyme-Linked Immunosorbent Assay (ELISA)

Skin biopsies from the shaved back region were stored under liquid nitrogen. On the day of the ELISA assay, the biopsies were thawed, and 20–50 mg of wet tissue was homogenized with the

aid of a homogenizer in ice-cold PBS. The homogenates were centrifuged for 20 mins at 10,000 \times g to remove debris and insoluble material, and aliquots of the supernatants were assayed by ELISA. Skin tissue Arg1, TGF β 1, iNOS, IL-13, and IL-22 levels were measured using the commercial ELISA kits according to the manufacturer's instructions. The 96-well plates were detected using VICTORTM X multilabel reader at a wavelength of 450 nm.

Cell Isolation

Whole blood was obtained from the inferior vena cava of anaesthetised mice and then collected by lepirudin tubes from the anaesthetised mice. Red Blood Cell (RBC) Lysis Buffer was used to remove the red blood cells from the blood samples. The CD4⁺ T cells were isolated from the sample with CD4⁺ T cell isolation kit II according to the manufacturer's instruction. To assess the purity, cells were stained with anti-CD4-eFluor 660 antibody and analysed by flow cytometry. The purity of CD4⁺ T cells reached 97% and was acceptable for the coculture.

MDSCs were isolated from the remaining cells by flow cytometric sorting. For flow cytometric sorting, 1×10^7 cells/mL suspension cells were stained with anti-CD11b-FITC, anti-Ly6G-PE and anti-Ly6C -PerCP-CyTM5.5 antibodies for 30 mins on ice in the staining buffer. After the cells were washed twice with PBS, the cells were then sorted with BD FACSariaTM III.

CD4⁺ T Cells and MDSCs Coculture

M-MDSC (1×10^6) or PMN-MDSC were plated at 1×10^6 cells per well in a 6-well culture plate in RPMI 1640 medium. CD4⁺ T cells were added to MDSC in the Transwell system. Then, CD4⁺ T cells were activated with anti-CD3/anti-CD28. The coculture system was incubated at 37 °C in a humidified incubator and 5% CO₂ atmosphere for 24 h. Then, the culture supernatant was collected for the enzyme-linked immunosorbent assay.

Statistical Analysis

All data were described as the mean with standard deviation (SD). Differences between two groups were analysed with unpaired Student's *t*-test (two-tailed, assuming equal variance). Correlation analysis was performed with the Spearman method. Correlation heatmap was plotted by R (Version 3.6.0). All statistical analyses were performed and presented using GraphPad Prism software (version 6.0 for windows). Statistically significant difference was indicated when $p < 0.05$.

RESULTS

MDSCs Were Elevated in IMQ-Induced Psoriatic Dermatitis

To explore the role of MDSCs in psoriasis, a mouse model with skin inflammation was induced by IMQ to mimic psoriasis (Figure 1A). H&E stained sections of the back skin of mice treated with 5% IMQ cream showed the

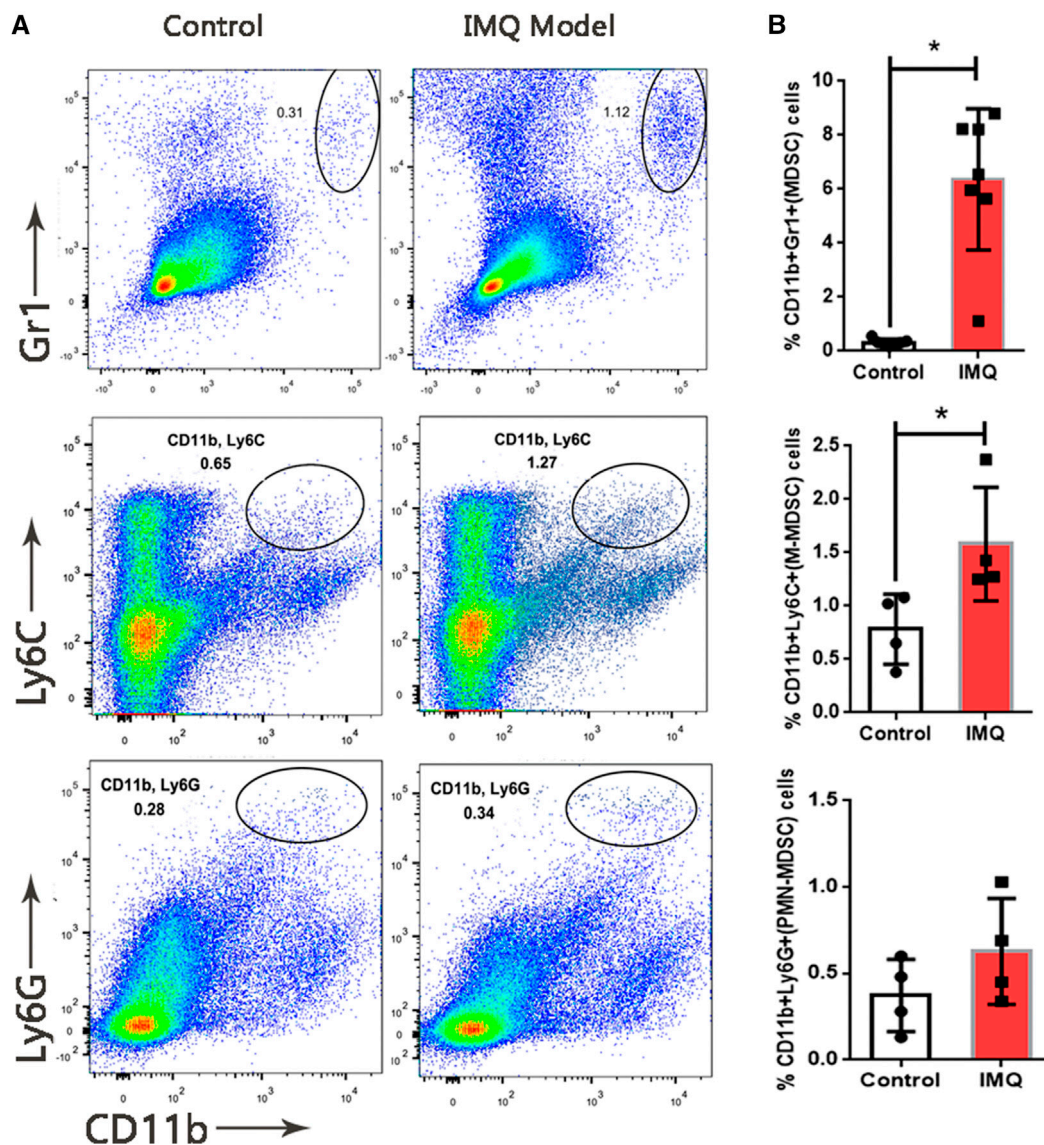


FIGURE 1 | Expansion of MDSCs in IMQ-induced psoriatic dermatitis. **(A)** Flow cytometry analysis of MDSCs (CD11b⁺ Gr1⁺), M-MDSC (CD11b⁺ Ly6C⁺) and PMN-MDSC (CD11b⁺ Ly6G⁺) in skin samples. First row: MDSCs (CD11b⁺ Gr1⁺), second row: M-MDSC (CD11b⁺ Ly6C⁺), third row: PMN-MDSC (CD11b⁺ Ly6G⁺). First column: sample from control group, second column: sample from model (IMQ) group. **(B)** Percentages of MDSCs, M-MDSC and PMN-MDSC in live cells of skin tissue. Seven mice per group in MDSC analysis, four mice per group in M-MDSC and PMN-MDSC analysis; **p* < 0.05, ***p* < 0.01.

epidermal thickening due to hyperkeratosis, parakeratosis, neovascularization and infiltration of immune cells in dermis and epidermis (**Figure 1B**). To determine the dysfunction of MDSCs and its subpopulations in psoriatic dermatitis, we measured the MDSCs marker levels of CD11b, Gr1, Ly-6G and Ly-6C in mouse skin samples by using flow cytometry (**Figures 2A,B**). The percentages (%) of MDSCs (CD11b⁺ Gr1⁺) and M-MDSCs (CD11b⁺ Ly-6C⁺) among total cells significantly increased in the skin samples of IMQ mice. These results suggested that the MDSCs, especially M-MDSCs, were involved in the pathological mechanism of IMQ-induced psoriatic dermatitis.

PSORI-CM02 Alleviated IMQ-Induced Psoriatic Dermatitis

Mice in different groups showed different effects on the skin inflammatory symptoms such as the erythema, thickness and scales. Comparing to the model group, dermatitis in the MTX group and the PSORI-CM02 group was alleviated significantly (**Figure 1A**). H&E stained sections of the back skin of mice in different groups presented a consistency with skin inflammatory symptoms. Hyperkeratosis, parakeratosis, neovascularization and infiltration of immune cells into the dermis and epidermis in the MTX group and PSORI-CM02 group were lighter than those parameters in the model group (**Figure 1B**).

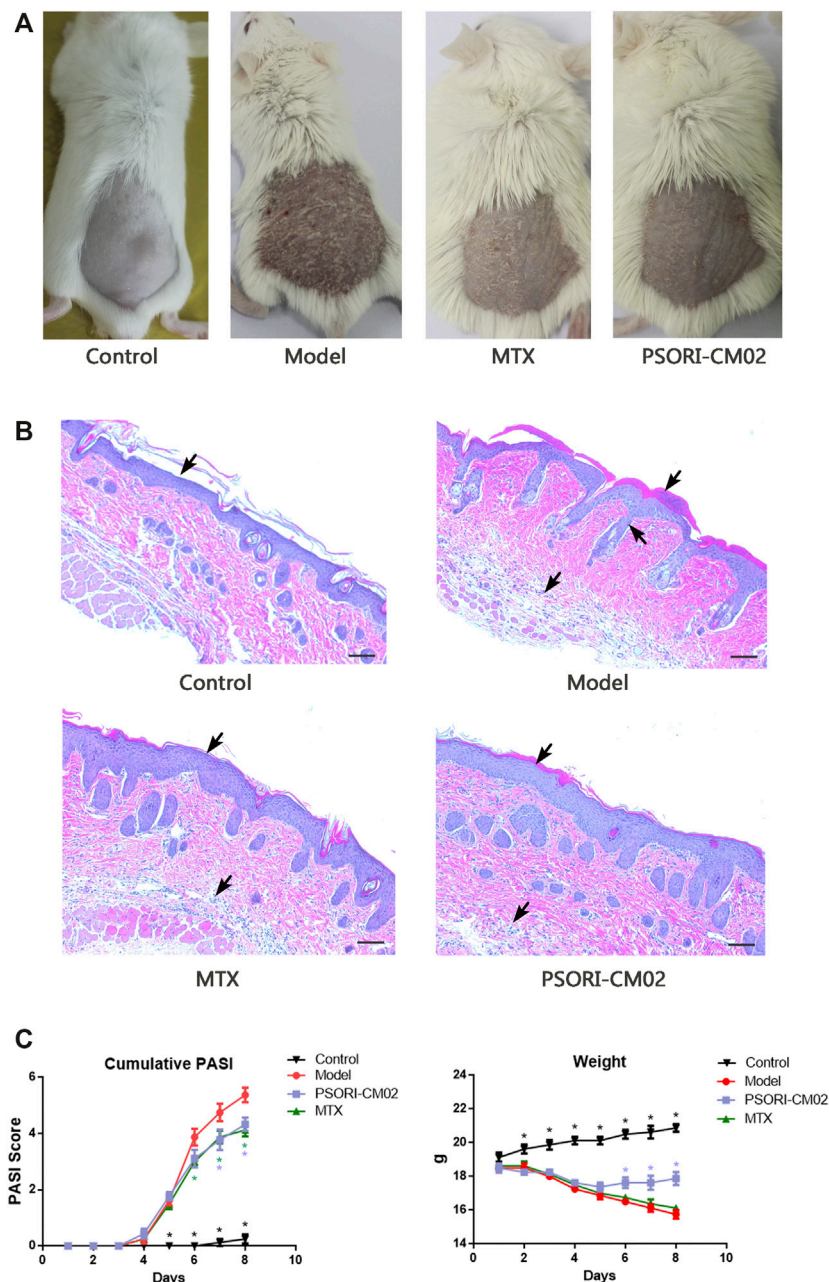


FIGURE 2 | Different treatment caused different effects on IMQ-induced psoriatic dermatitis. **(A)** Skin inflammatory symptoms in different groups. **(B)** H&E stained sections of back skin of mice in different groups. Psoriasis-specific hyperkeratosis, parakeratosis, neovascularization and infiltration of immune cells in dermis and epidermis were labeled by arrows. **(C)** Accumulative PASI score based on the erythema, induration, desquamation and percentage of affected area during the dermatitis progress. $n = 8$ mice per group **(D)** Weight loss during the treatments challenged. $n = 8$ mice per group.

The accumulative PASI score of the model group at day 7 was 5.38 ± 1.18 , whereas the score was 4.13 ± 0.64 in the MTX group and 4.33 ± 0.71 in the PSORI-CM02 group (Figure 1C). Body weights were recorded daily, showing the difference between the PSORI-CM02 group and other groups of those challenged with IMQ. PSORI-CM02 treatment alleviated IMQ-caused weight loss (Figure 1D).

PSORI-CM02 Reduced M-MDSCs in Psoriatic Dermatitis Tissue and Lymph Nodes

To determine whether PSORI-CM02 treatment was affected via MDSCs, we evaluated the M-MDSC and PMN-MDSC levels in skin and lymph node samples of different groups by flow cytometric analysis (Figures 3A,B). The results showed that the percentages of M-MDSCs differed among the groups. In

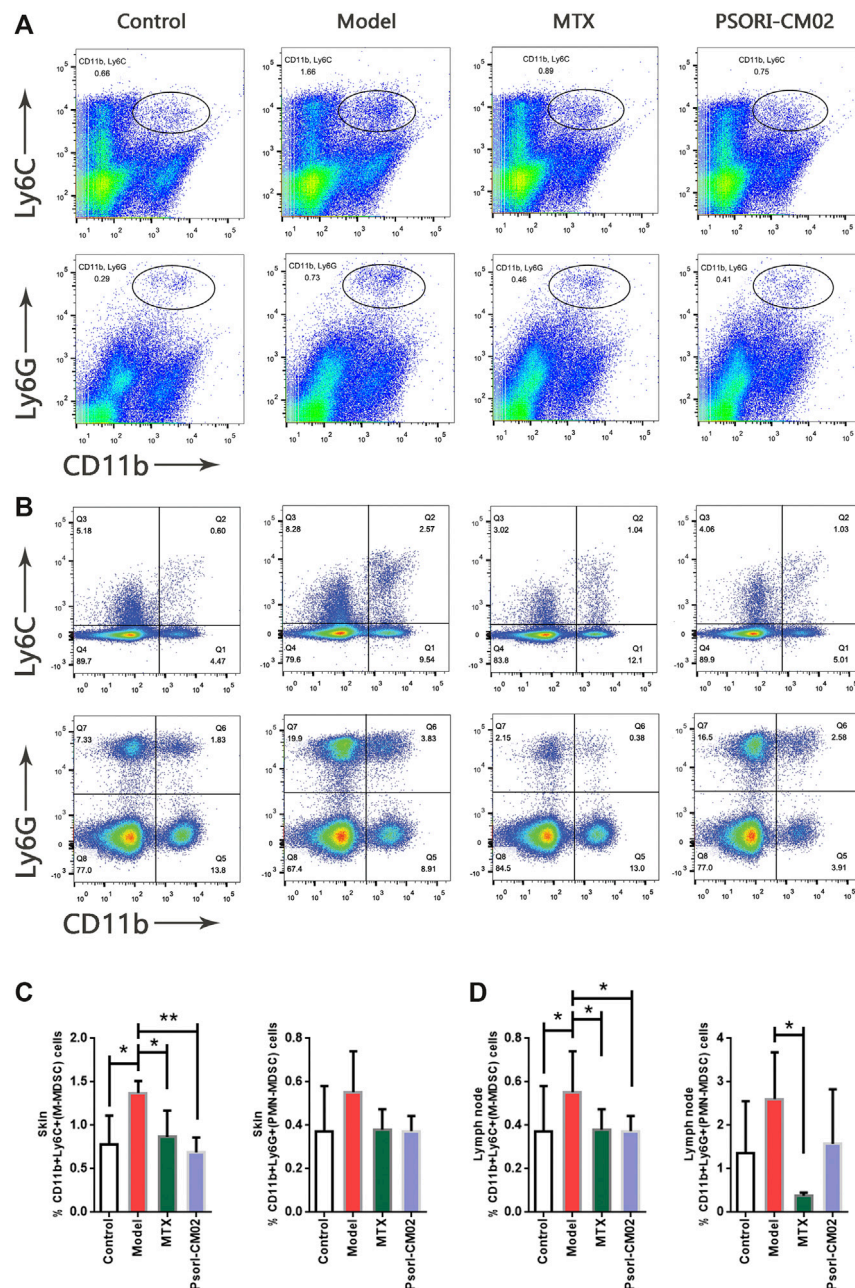
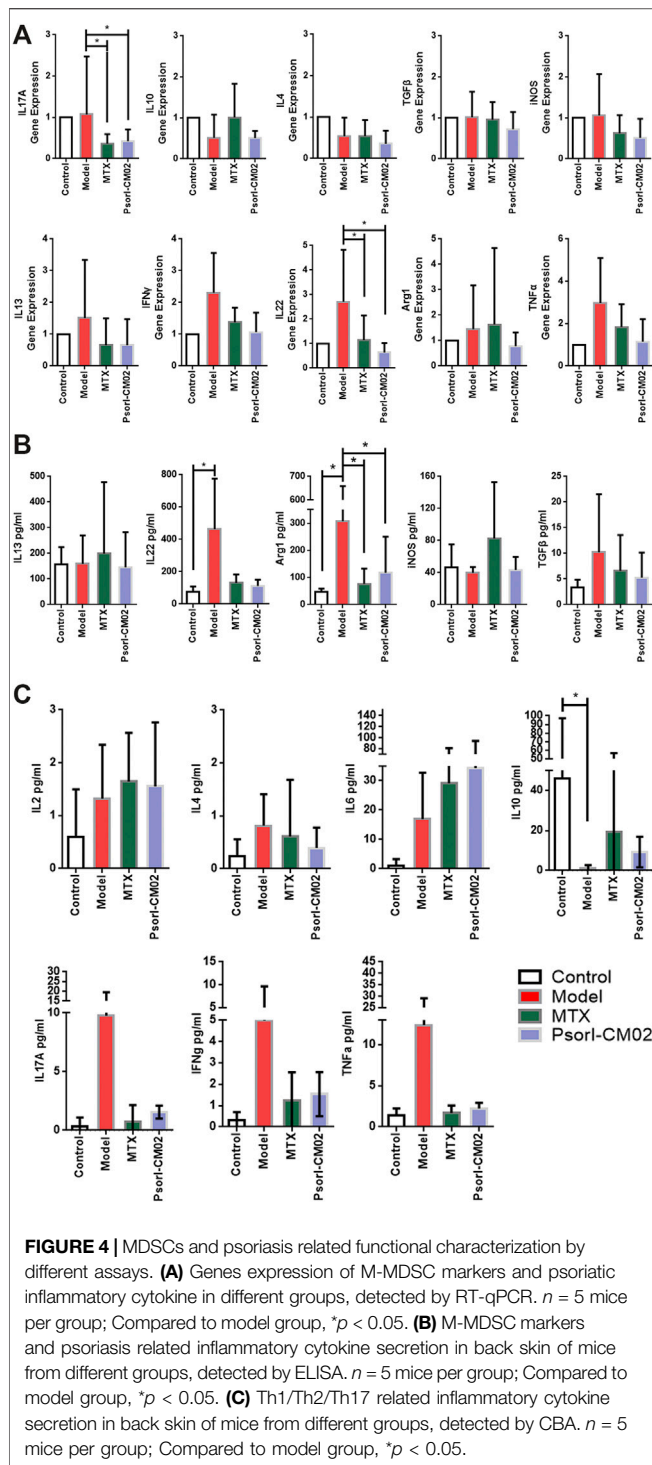


FIGURE 3 | Treatment effects on M-MDSC and PMN-MDSC. **(A)** Flow cytometric analysis on M-MDSC and PMN-MDSC levels in skin samples of different groups. First row: M-MDSC (CD11b⁺ Ly6C⁺), second row: PMN-MDSC (CD11b⁺ Ly6G⁺). **(B)** Flow cytometric analysis on M-MDSC and PMN-MDSC levels in lymph nodes of different groups. First row: M-MDSC (CD11b⁺ Ly6C⁺), second row: PMN-MDSC (CD11b⁺ Ly6G⁺). **(C)** Percentages of M-MDSC and PMN-MDSC in live cells of skin samples of different groups. *n* = 4 mice per group; **p* < 0.05, ***p* < 0.01. **(D)** Percentages of M-MDSC and PMN-MDSC in live cells of lymph nodes of different groups. *n* = 4 mice per group; **p* < 0.05.

the PSORI-CM02 group and the MTX group, the percentage of M-MDSCs was lower than in the model group, not only in skins but also in lymph nodes (**Figure 3C**). No differences were observed in the PMN-MDSCs in skins from different groups.

However, in lymph nodes, MTX can reduce the cell ratio of PMN-MDSCs (**Figure 3D**). These results were consistent with the conclusion in **Figure 2** that M-MDSCs but not PMN-MDSCs played a role in psoriatic dermatitis.



PSORI-CM02 Reduced the Inflammatory Infiltrate in Psoriatic Dermatitis Tissue

To analyse the mechanism of PSORI-CM02 treatment effected on the psoriatic immune environment, we evaluated the M-MDSC markers (Arg1, TGF β 1, iNOS, IL-10, and IL-13) and psoriatic inflammatory cytokines (Th1/Th2/Th17 cytokines) in skin samples of different groups by CBA, ELISA and RT-qPCR.

The results acquired from different assays are concisely illustrated in **Figure 4**.

As expected, at the transcript level, the psoriatic inflammatory cytokines IL-17 and IL-22 increased in the model group and decreased notably after MTX and PSORI-CM02 (**Figure 4A**). At the protein level, Arg1, IL-10 and IL-22 were significantly different between model group and control. Only Arg1 changed significantly after treatments (**Figures 4B,C**).

Given that IL-17 and IL-22 positively related to psoriatic dermatitis at the mRNA level but not at the protein level detected by CBA, we examined the IL-17 $^{+}$ CD4 $^{+}$ T cells and IL-22 $^{+}$ CD4 $^{+}$ T cells in the skin by flow cytometric analysis (**Figure 5A**). The results showed that the percentages of IL-17 $^{+}$ CD4 $^{+}$ T cells and IL-22 $^{+}$ CD4 $^{+}$ T cells differed among the groups. Compared to the control, they were both higher in the model group. MTX and PSORI-CM02 reduced the percentages of IL-17 $^{+}$ CD4 $^{+}$ T cells and IL-22 $^{+}$ CD4 $^{+}$ T cells (**Figure 5B**). These results indicated that PSORI-CM02 reduced IL-17 and IL-22 mainly to control the inflammatory infiltrate in psoriatic dermatitis.

Relationship of MDSCs and Psoriatic Inflammatory Cytokines

The above results showed that PSORI-CM02 reduced both M-MDSCs and inflammatory cytokines IL-17 and IL-22. However, the evidence for the relationship of MDSCs and psoriatic inflammatory cytokines *in vivo* was still lacking. To clarify that point, we performed a correlation analysis on MDSC levels and inflammatory cytokines. The heatmap depicts the full-scale statistical analysis using all samples (**Figure 6A**), revealing a very strong correlation between M-MDSCs and IL-17 $^{+}$ CD4 $^{+}$ T cells, the same as the IL-22 $^{+}$ CD4 $^{+}$ T cells. PMN-MDSC was positively correlated to IL-17 $^{+}$ CD4 $^{+}$ T cells as well (**Figure 6B**).

Psoriatic MDSCs Promoted Th17 Cell Differentiation via Arg1

We screened the gene expression and protein abundance of MDSCs and psoriasis-related molecules (**Figure 4**). The correlation of MDSCs and Th17 was confirmed (**Figure 6**). Only Arg1, IL-17, and IL-22 were positive in the above assays. We then assessed the effect of MDSCs on anti-CD3/CD28-activated CD4 $^{+}$ T cells in the coculture system. After the CD4 T cells and MDSCs coculture, the secretions of Arg1 by M-MDSC or PMN-MDSC obtained from IMQ mice were higher than the secretions from normal mice, suggesting that the effect of MDSC subpopulations is mediated by their secretion of Arg-1. In addition, M-MDSC obtained from IMQ mice can significantly promote the secretion of IL-17A by CD4 $^{+}$ T cells (**Figure 7A**), implying that M-MDSC from IMQ mice was much more potent in Th17 cell polarisation via Arg1. When we compared the secretions of Arg1 by M-MDSC and PMN-MDSC from different treatments, we found that both MTX and PSORI-CM02 could significantly reduce the production

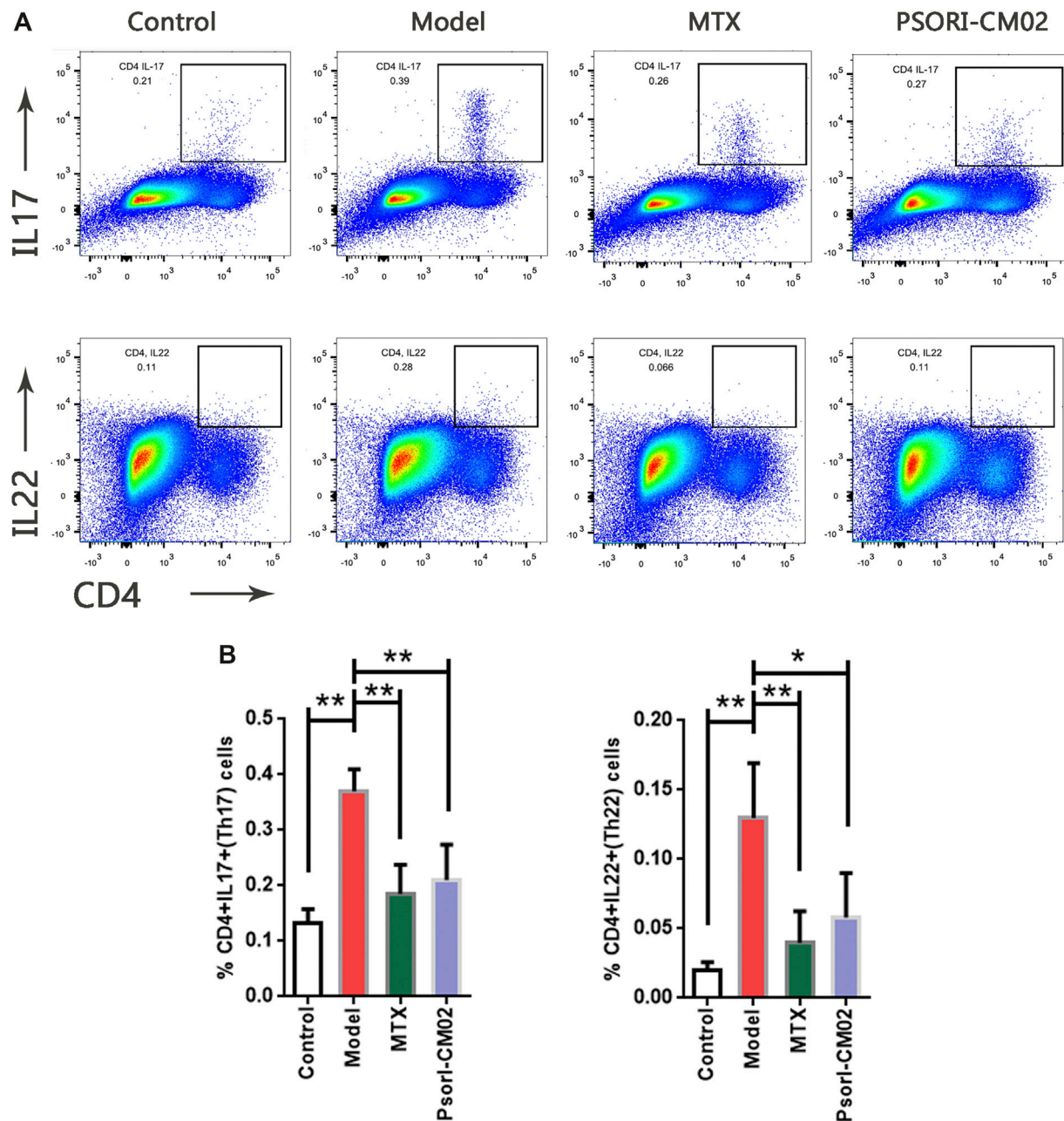


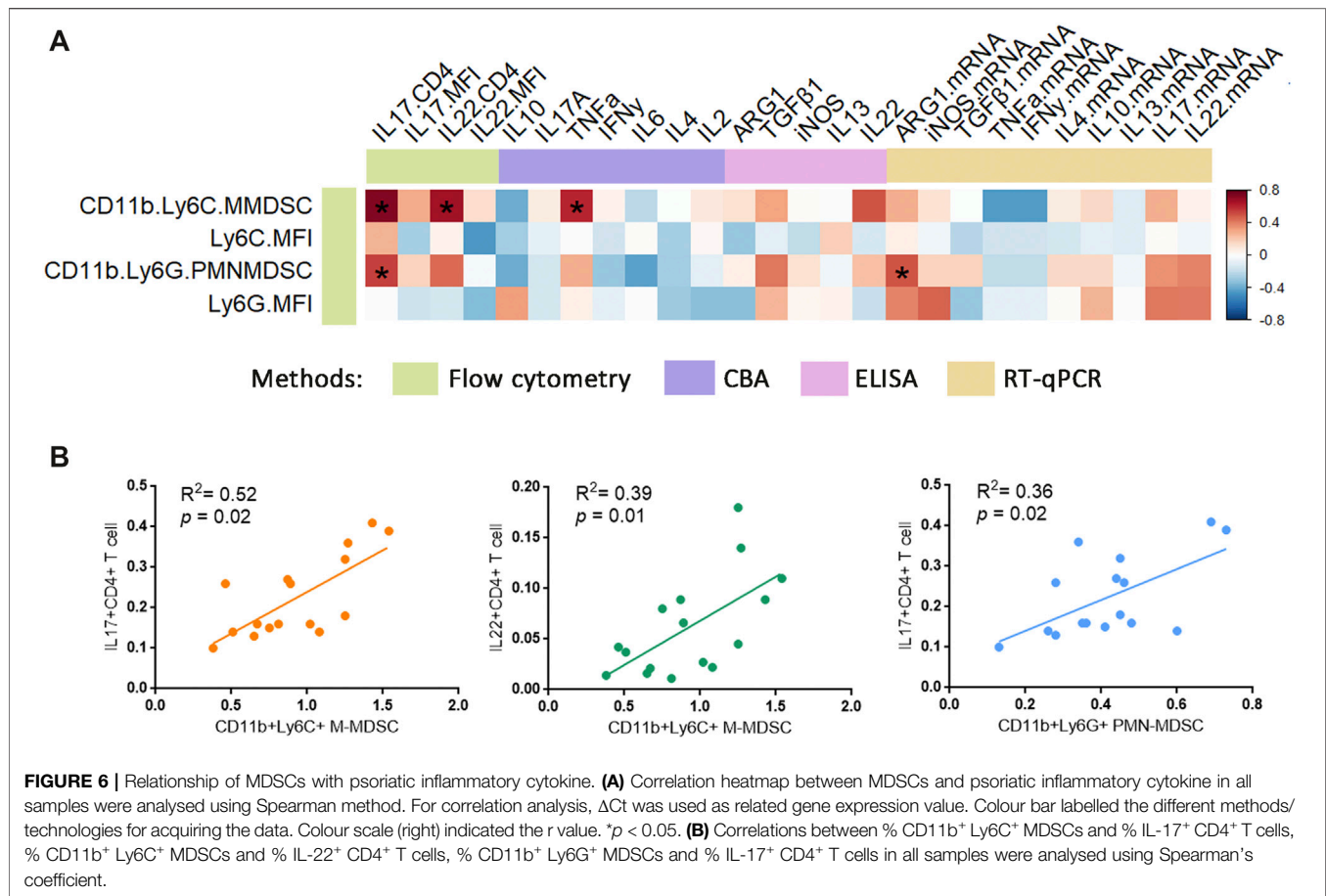
FIGURE 5 | Expansion of IL-17⁺ CD4⁺ T cells and IL-22⁺ CD4⁺ T cells in live cells of back skin of mice from different groups. **(A)** Flow cytometric analysis on IL-17⁺ CD4⁺ T cells and IL-22⁺ CD4⁺ T cells in live cells of back skin of mice from different groups. First row: IL-17⁺ CD4⁺ T cells, second row: IL-22⁺ CD4⁺ T cells. **(B)** Percentages of IL-17⁺ CD4⁺ T cells and IL-22⁺ CD4⁺ T cells in live cells of back skin of mice from different groups. *n* = 4 mice per group; **p* < 0.05, ***p* < 0.01.

of Arg1 from M-MDSC but not from PMN-MDSC (Figures 7B,C).

DISCUSSION

Psoriasis is a chronic inflammatory disease characterized by erythema, with thickening and scaling of the skin. Its histopathologic change in the epidemic is abnormal

proliferation and differentiation of keratinocyte (Boehncke, 2015; Boehncke and Schon, 2015). However, the cause of this histopathologic change remains unknown. Accumulating evidence indicates that psoriasis is a T-cell-mediated disease (Gottlieb et al., 1995). The IL-23/Th17 pathway plays a pivotal role in the progress of psoriasis (Hawkes et al., 2017). The Th17 cell is the key factor in the inflammatory infiltrate, whereas the development of Th17 is maintained by IL-23, which is secreted mainly by monocytes and dendritic cells. With the dendritic cell



activation, lymphocytes, neutrophils and monocytes migrate into the skin. Th17 cells produce inflammatory cytokines, including IL-17 and IL-22. IL-17 and IL-22 lead to hyperkeratosis and parakeratosis. TNF α production is induced indirectly by IL-17 and IL-22, which accelerates the inflammatory infiltrate. (Zheng et al., 2007; Ogawa et al., 2018). In clinical practice, biologics targeting these cytokines showed credible efficacy on psoriasis, which proved the importance of the role of the IL-23/Th17 axis in the aetiology of psoriasis.

Recently, the important biological role of MDSCs has been investigated. MDSCs are a cluster of heterogeneous cells that present immunosuppressive to T cell and NK cell function (Gabrilovich and Nagaraj, 2009; Dar et al., 2020). The absence of MDSCs caused T cell proliferation, whereas the accumulation of MDSCs was associated with *tuberculosis* (TB) progress and severity (Knaul et al., 2014; Tsiganov et al., 2014). Myeloid-derived cells have been indicated as an essential factor in the immune system, particularly in cancer immunotherapy. Two subtypes of MDSCs have clear roles that have been established in murine: CD11b⁺Ly6G⁺Ly6C⁺ monocytic MDSCs (M-MDSCs) and CD11b⁺Ly6G⁺Ly6C⁻ polymorphonuclear or granulocytic myeloid-derived suppressor cells (PMN-MDSCs or G-MDSCs) (Wu and Chiang, 2019). Generally, PMN-MDSCs make up the majority of the population of MDSCs. Both M-MDSCs and PMN-MDSCs

have strong immunosuppressive activity, which has been indicated to contribute to immunosuppression in the tumour microenvironment and allergic inflammation (Gabrilovich and Nagaraj, 2009). Meanwhile, both PMN-MDSCs and M-MDSCs can reverse from being immunosuppressive to immunostimulatory. The proportion of subpopulations of MDSCs is highly variable (Ben-Meir et al., 2018). In response to different conditions or environments, M-MDSCs can directionally differentiate into dendritic cells or macrophages, while PMN-MDSCs consist of myeloid progenitors that differentiate into granulocytes (Kumar et al., 2016).

In recent years, CD14⁺HLA-DR⁻/low M-MDSCs have been reported to suppress T-cell activation (Lauret Marie Joseph et al., 2020). In psoriatic patient PBMC, M-MDSCs was increased, compared to the healthy control (Soler et al., 2016; Sun et al., 2020). *In vivo* and *in vitro* assays demonstrated that Treg cells induced by M-MDSCs in the PBMC of a psoriasis patient presented suppressive functionality reduction. These results suggest that M-MDSCs increased in psoriasis with the impaired suppressive function of effector T-cell expansion. Our present study also proved that MDSCs, especially M-MDSCs, were elevated in IMQ-induced psoriatic dermatitis and lymph nodes.

As Th17 has been found to increase in psoriatic dermatitis, it would be interesting to understand how MDSCs interact

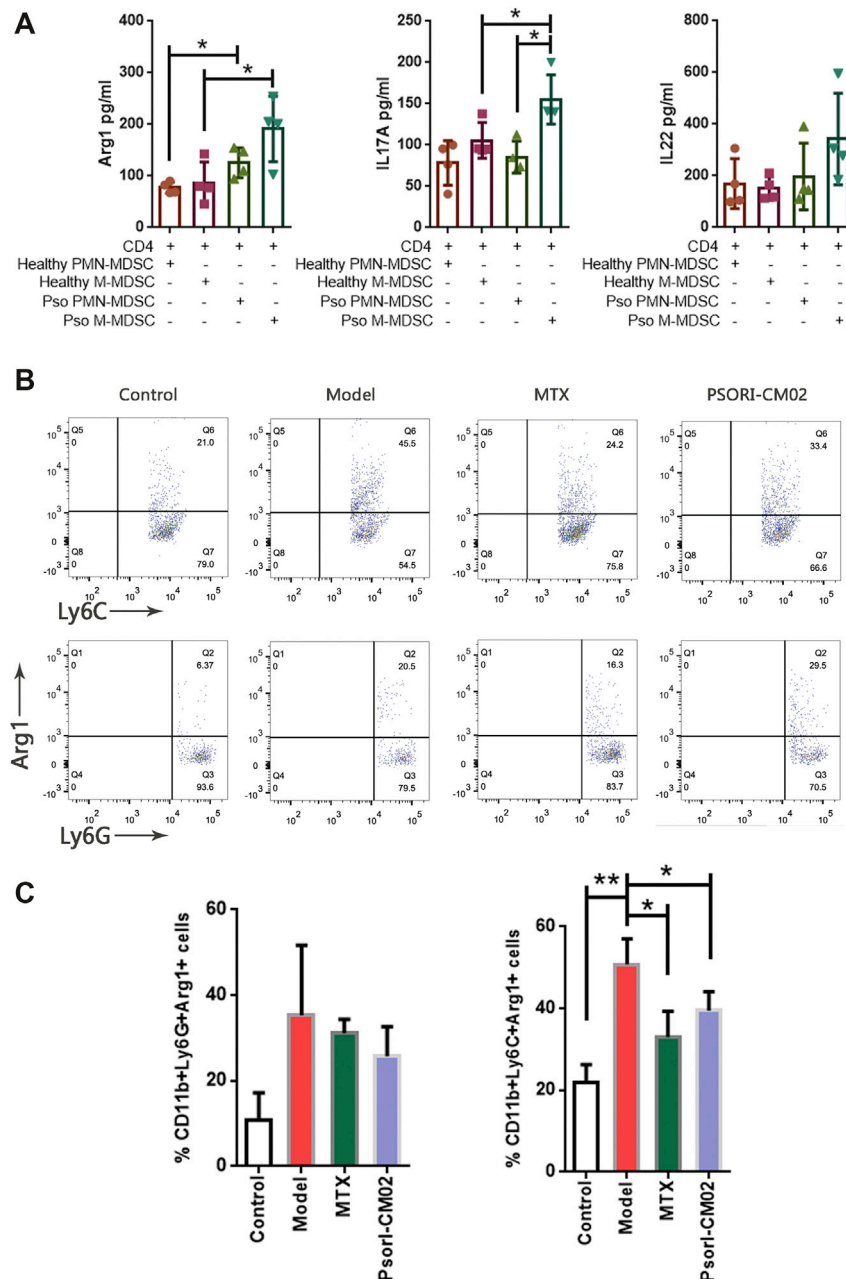


FIGURE 7 | MDSCs induced Th17 differentiation. **(A)** The expression of Arg1, IL-17A and IL-22 in the co-culture supernatant. * $p < 0.05$. **(B)** Flow cytometric analysis on Arg1+ M-MDSC and Arg1+ PMN-MDSC in skin samples of different groups. First row: Arg1+ M-MDSC cells, second row: Arg1+ PMN-MDSC T cells. **(C)** Percentages of Arg1+ M-MDSC and Arg1+ PMN-MDSC in different groups. $n = 3$ in control group and $n = 4$ in other groups; * $p < 0.05$, ** $p < 0.01$.

with T cells in the immune environment of psoriasis. The functions of MDSCs in suppressing T cells, including producing inducible arginase-1 (Arg1) and inducible nitric oxide synthase (iNOS), which lead to the nitration of T cell receptors and chemokines that are essential for T cell migration, induce T cell apoptosis (Gabrilovich et al., 2012). IL-10 and TGF- β 1 are produced, inhibiting immune effector cell proliferation and functions (Umansky et al., 2017). We therefore checked all these molecules in the

present study. However, only Arg1 was significantly different between IMQ-induced psoriatic dermatitis and control, and Arg1 was reduced after treatment. The dynamic changes in Arg1 for different groups strongly suggested that M-MDSC was involved in the pathogenesis of psoriasis. However, the functional characterisation presented that most of the marker molecules of MDSCs showed negative results. The relationship between MDSCs and Th17 cells was confirmed by the correlation analysis. Both

M-MDSCs and PMN-MDSCs were positively correlated to IL-17⁺CD4⁺ T cells, while M-MDSCs were also associated with IL-22⁺CD4⁺ T cells.

PSORI-CM02 is the Chinese medicine formula formulated based on the Chinese medicine theory (Blood Stasis). As a compound formula, PSORI-CM02 exerts its effects via the combination of the five herbal components. According to our prior published results, PSORI-CM02 can alleviate psoriatic dermatitis induced by IMQ in mice, by increasing the regulatory T cell level (Chen et al., 2017), inducing autophagy to promote the apoptosis of keratinocytes (Yue et al., 2019), and regulating the infiltration and polarisation of macrophages (Li et al., 2020). We found that PSORI-CM02 alleviated IMQ-induced psoriatic dermatitis and suppressed proliferation of M-MDSCs and Th17 cells. Interestingly, M-MDSCs-induced Arg1 is confirmed to cause the suppression of T cell by depletion of the semi-essential amino acid L-arginine (Bogdan, 2011). MDSCs are reported to induce the suppressive activity of Th17 cells through the upregulation of Arg1 (Wu et al., 2016). In our study, the correlation analysis indicated that MDSCs and Th17 cells had a strong relationship with each other, suggesting the existence of crosstalk between MDSCs and Th17 cells in dermatitis. This crosstalk was involved in the therapeutic progress of PSORI-CM02. However, the positive correlation does not mean that the change in MDSCs or Th17 is the cause of the change in the levels of the other variable. To establish the relationship between MDSC and Th17 and the regulatory effects of PSORI-CM02 in the psoriatic dermatitis model, we assessed the *in vitro* coculture assay and found that M-MDSC from IMQ mice was much more potent in Th17 cell polarisation via Arg1. *In vivo* experiment indicated that PSORI-CM02 could significantly reduce the production of Arg1 from M-MDSC, which implied that PSORI-CM02 suppressed proliferation of Th17 cells by targeted M-MDSC-induced Arg1.

CONCLUSION

Taken together, our data provided evidence that the percentage of CD11b⁺ Ly6C⁺ M-MDSCs was elevated in IMQ-induced psoriatic dermatitis. Chinese medicine formula PSORI-CM02 alleviated IMQ-induced psoriatic dermatitis and suppressed proliferation of M-MDSCs and Th17 cells. Moreover, our

study also determined that M-MDSCs were positively associated with Th17 cell. Psoriatic MDSCs promoted Th17 cell differentiation via Arg1, suggesting that PSORI-CM02 exerted its effects on suppressing Th17 cells by targeted M-MDSC-induced Arg1.

DATA AVAILABILITY STATEMENT

The raw data supporting the conclusions of this article will be made available by the authors, without undue reservation.

ETHICS STATEMENT

The animal study was reviewed and approved by Institutional Animal Care and Use Committee of Guangdong Provincial Academy of Chinese Medical Sciences.

AUTHOR CONTRIBUTIONS

CL and LH designed the study and revised the manuscript. JD, RL, WY, HC, YX, ST and NT performed the experiments, JD conducted the data analysis and drafted the manuscript. All authors have read and approved the final manuscript.

FUNDING

This study was supported by the National Natural Science Foundation of China (No. 81603619), Science and Technology Planning Project of Guangdong Province (No. 2017B030314166 and 2020B1111100006); Natural Science Foundation of Guangdong Province (No. 2020A1515010607) and Special Funding for TCM Science and Technology Research of Guangdong Provincial Hospital of Chinese Medicine (No. YN2019QL12 and YN2018RBA02).

SUPPLEMENTARY MATERIAL

The Supplementary Material for this article can be found online at: <https://www.frontiersin.org/articles/10.3389/fphar.2020.563433/full#supplementary-material>.

REFERENCES

- Ben-Meir, K., Twaik, N., and Baniyash, M. (2018). Plasticity and biological diversity of myeloid derived suppressor cells. *Curr. Opin. Immunol.* 51, 154–161. doi:10.1016/j.coi.2018.03.015
- Boehncke, W. H., and Schön, M. P. (2015). Psoriasis. *Lancet* 386 (9997), 983–994. doi:10.1016/S0140-6736(14)61909-7
- Boehncke, W. H. (2015). Etiology and pathogenesis of psoriasis. *Rheum. Dis. Clin. N. Am.* 41 (4), 665–675. doi:10.1016/j.rdc.2015.07.013
- Bogdan, C. (2011). Regulation of lymphocytes by nitric oxide. *Methods Mol. Biol.* 677, 375–393. doi:10.1007/978-1-60761-869-0_24

- Brandau, S., Moses, K., and Lang, S. (2013). The kinship of neutrophils and granulocytic myeloid-derived suppressor cells in cancer: cousins, siblings or twins? *Semin. Canc. Biol.* 23 (3), 171–182. doi:10.1016/j.semcancer.2013.02.007
- Cao, L. Y., Chung, J. S., Teshima, T., Feigenbaum, L., Cruz, P. D., Jacobe, H. T., et al. (2016). Myeloid-derived suppressor cells in psoriasis are an expanded population exhibiting diverse T-cell-suppressor mechanisms. *J. Invest. Dermatol.* 136 (9), 1801–1810. doi:10.1016/j.jid.2016.02.816
- Chen, H., Liu, H., Lu, C., Wang, M., Li, X., Zhao, H., et al. (2017). PSORI-CM02 formula increases CD4⁺ Foxp3⁺ regulatory T cell frequency and ameliorates imiquimod-induced psoriasis in mice. *Front. Immunol.* 8, 1767. doi:10.3389/fimmu.2017.01767
- Cz, L. X. W., and Liu, F. N. (2006). Effect of Yinxieling on PCNA expression and apoptosis of keratinocyte. *Trad. Chin Drug Res Clin Pharmacol.* 17, 329–331.

- Dar, A. A., Patil, R. S., Pradhan, T. N., Chaukar, D. A., D'Cruz, A. K., and Chiplunkar, S. V. (2020). Myeloid-derived suppressor cells impede T cell functionality and promote Th17 differentiation in oral squamous cell carcinoma. *Cancer Immunol. Immunother.* 69 (6), 1071–1086. doi:10.1007/s00262-020-02523-w
- Deng, S., May, B. H., Zhang, A. L., Lu, C., and Xue, C. C. (2013). Plant extracts for the topical management of psoriasis: a systematic review and meta-analysis. *Br. J. Dermatol.* 169 (4), 769–782. doi:10.1111/bjd.12557
- Deng, S., May, B. H., Zhang, A. L., Lu, C., and Xue, C. C. (2014). Topical herbal formulae in the management of psoriasis: systematic review with meta-analysis of clinical studies and investigation of the pharmacological actions of the main herbs. *Phytother. Res.* 28 (4), 480–497. doi:10.1002/ptr.5028
- Gabrilovich, D. I., and Nagaraj, S. (2009). Myeloid-derived suppressor cells as regulators of the immune system. *Nat. Rev. Immunol.* 9 (3), 162–174. doi:10.1038/nri2506
- Gabrilovich, D. I., Ostrand-Rosenberg, S., and Bronte, V. (2012). Coordinated regulation of myeloid cells by tumours. *Nat. Rev. Immunol.* 12 (4), 253–268. doi:10.1038/nri3175
- Gabrilovich, D. I. (2017). Myeloid-derived suppressor cells. *Cancer Immunol. Res.* 5 (1), 3–8. doi:10.1158/2326-6066.CIR-16-0297
- Gottlieb, S. L., Gilleaudeau, P., Johnson, R., Estes, L., Woodworth, T. G., Gottlieb, A. B., et al. (1995). Response of psoriasis to a lymphocyte-selective toxin (DAB389IL-2) suggests a primary immune, but not keratinocyte, pathogenic basis. *Nat. Med.* 1 (5), 442–447. doi:10.1038/nm0595-442
- Gu, J., Li, L., Wang, D., Zhu, W., Han, L., Zhao, R., et al. (2018). Deciphering metabonomics biomarkers-targets interactions for psoriasis vulgaris by network pharmacology. *Ann. Med.* 50 (4), 323–332. doi:10.1080/07853890.2018.1453169
- Han, L., Peng, Y., Zhao, R. Z., Feng, B., and Lu, C. J. (2011). Effect of yinxieling on proliferation of HaCaT. *J. Guangzhou Univ. TCM.* 28, 159–162.
- Hawkes, J. E., Chan, T. C., and Krueger, J. G. (2017). Psoriasis pathogenesis and the development of novel targeted immune therapies. *J. Allergy Clin. Immunol.* 140 (3), 645–653. doi:10.1016/j.jaci.2017.07.004
- Kimball, A. B., Jacobson, C., Weiss, S., Vreeland, M. G., and Wu, Y. (2005). The psychosocial burden of psoriasis. *Am. J. Clin. Dermatol.* 6 (6), 383–392. doi:10.2165/00128071-200506060-00005
- Kimball, A. B., Wu, E. Q., Guérin, A., Yu, A. P., Tsaneva, M., Gupta, S. R., et al. (2012). Risks of developing psychiatric disorders in pediatric patients with psoriasis. *J. Am. Acad. Dermatol.* 67 (4), 651–652. doi:10.1016/j.jaad.2011.11.948
- Knall, J. K., Jörg, S., Oberbeck-Mueller, D., Heinemann, E., Scheuermann, L., Brinkmann, V., et al. (2014). Lung-residing myeloid-derived suppressors display dual functionality in murine pulmonary tuberculosis. *Am. J. Respir. Crit. Care Med.* 190 (9), 1053–1066. doi:10.1164/rccm.201405-0828OC
- Kumar, V., Patel, S., Tcyganov, E., and Gabrilovich, D. I. (2016). The nature of myeloid-derived suppressor cells in the tumor microenvironment. *Trends Immunol.* 37 (3), 208–220. doi:10.1016/j.it.2016.01.004
- Lauret Marie Joseph, E., Laheurte, C., Jary, M., Boullerot, L., Asgarov, K., Gravelin, E., et al. (2020). Immunoregulation and clinical implications of ANGPT2/TIE2(+) M-MDSC signature in non-small cell lung cancer. *Cancer Immunol. Res.* 8 (2), 268–279. doi:10.1158/2326-6066.CIR-19-0326
- Li, L., Zhang, H. Y., Zhong, X. Q., Lu, Y., Wei, J., Li, L., et al. (2020). PSORI-CM02 formula alleviates imiquimod-induced psoriasis via affecting macrophage infiltration and polarization. *Life Sci.* 243, 117231. doi:10.1016/j.lfs.2019.117231
- Lu, C. J., Yu, J. J., and Deng, J. W. (2012). Disease-syndrome combination clinical study of psoriasis: present status, advantages, and prospects. *Chin. J. Integr. Med.* 18 (3), 166–171. doi:10.1007/s11655-012-1006-1
- Lu, C., Liu, H., Jin, X., Chen, Y., Liang, C. L., Qiu, F., et al. (2018). Herbal components of a novel formula PSORI-CM02 interdependently suppress allograft rejection and induce CD8⁺CD122⁺PD-1⁺ regulatory T cells. *Front. Pharmacol.* 9, 88. doi:10.3389/fphar.2018.00088
- May, B. H., Zhang, A. L., Zhou, W., Lu, C. J., Deng, S., and Xue, C. C. (2012). Oral herbal medicines for psoriasis: a review of clinical studies. *Chin. J. Integr. Med.* 18 (3), 172–178. doi:10.1007/s11655-012-1008-z
- Morgan, E., Varro, R., Sepulveda, H., Ember, J. A., Appgar, J., Wilson, J., et al. (2004). Cytometric bead array: a multiplexed assay platform with applications in various areas of biology. *Clin. Immunol.* 110 (3), 252–266. doi:10.1016/j.clim.2003.11.017
- Ogawa, E., Sato, Y., Minagawa, A., and Okuyama, R. (2018). Pathogenesis of psoriasis and development of treatment. *J. Dermatol.* 45 (3), 264–272. doi:10.1111/1346-8138.14139
- Ost, M., Singh, A., Peschel, A., Mehling, R., Rieber, N., and Hartl, D. (2016). Myeloid-derived suppressor cells in bacterial infections. *Front. Cell. Infect. Microbiol.* 6, 37. doi:10.3389/fcimb.2016.00037
- Parisi, R., Symmons, D. P., Griffiths, C. E., and Ashcroft, D. M. Identification and Management of Psoriasis and Associated Comorbidities (IMPACT) Project Team (2013). Identification, Management of, Global epidemiology of psoriasis: a systematic review of incidence and prevalence. *J. Invest. Dermatol.* 133 (2), 377–385. doi:10.1038/jid.2012.339
- Soler, D. C., Young, A. B., Fiessinger, L., Galimberti, F., Debanne, S., Groft, S., et al. (2016). Increased, but functionally impaired, CD14(+) HLA-DR(–/low) myeloid-derived suppressor cells in psoriasis: a mechanism of dysregulated T cells. *J. Invest. Dermatol.* 136 (4), 798–808. doi:10.1016/j.jid.2015.12.036
- Sun, S., Wei, Y., Zeng, X., Yuan, Y., Wang, N., An, C., et al. (2020). Circulating CD14(+)HLA-DR(–/low) myeloid-derived suppressor cells as potential biomarkers for the identification of psoriasis TCM blood-heat syndrome and blood-stasis syndrome. *Evid. Based Complement Alternat. Med.* 2020, 4582459. doi:10.1155/2020/4582459
- Tsiganov, E. N., Verbina, E. M., Radaeva, T. V., Sosunov, V. V., Kosmiadi, G. A., Nikitina, I. Y., et al. (2014). Gr-1dimCD11b+ immature myeloid-derived suppressor cells but not neutrophils are markers of lethal tuberculosis infection in mice. *J. Immunol.* 192 (10), 4718–4727. doi:10.4049/jimmunol.1301365
- Umansky, V., Blattner, C., Fleming, V., Hu, X., Gebhardt, C., Altevogt, P., et al. (2017). Myeloid-derived suppressor cells and tumor escape from immune surveillance. *Semin. Immunopathol.* 39 (3), 295–305. doi:10.1007/s00281-016-0597-6
- van der Fits, L., Mourits, S., Voerman, J. S., Kant, M., Boon, L., Laman, J. D., et al. (2009). Imiquimod-induced psoriasis-like skin inflammation in mice is mediated via the IL-23/IL-17 axis. *J. Immunol.* 182 (9), 5836–5845. doi:10.4049/jimmunol.0802999
- Wu, D. H., Zhang, M. M., Li, N., Li, X., Cai, Q. W., Yu, W. L., et al. (2019). PSORI-CM02 alleviates IMQ-induced mouse dermatitis via differentially regulating pro- and anti-inflammatory cytokines targeting of Th2 specific transcript factor GATA3. *Biomed. Pharmacother.* 110, 265–274. doi:10.1016/j.biopha.2018.11.092
- Wu, H., Zhen, Y., Ma, Z., Li, H., Yu, J., Xu, Z. G., et al. (2016). Arginase-1-dependent promotion of TH17 differentiation and disease progression by MDSCs in systemic lupus erythematosus. *Sci. Transl. Med.* 23; 8 (331), 331ra40. doi:10.1126/scitranslmed.aae0482
- Wu, S. Y., and Chiang, C. S. (2019). Distinct role of CD11b(+)Ly6G(–)Ly6C(–) myeloid-derived cells on the progression of the primary tumor and therapy-associated recurrent brain tumor. *Cells.* 9 (1), 51. doi:10.3390/cells9010051
- Yue, L., Ailin, W., Jinwei, Z., Leng, L., Jianan, W., Li, L., et al. (2019). PSORI-CM02 ameliorates psoriasis *in vivo* and *in vitro* by inducing autophagy via inhibition of the PI3K/Akt/mTOR pathway. *Phytomedicine.* 64, 153054. doi:10.1016/j.phymed.2019.153054
- Zhang, C. S., Yu, J. J., Parker, S., Zhang, A. L., May, B., Lu, C., et al. (2014). Oral Chinese herbal medicine combined with pharmacotherapy for psoriasis vulgaris: a systematic review. *Int. J. Dermatol.* 53 (11), 1305–1318. doi:10.1111/ijd.12607
- Zheng, Y., Danilenko, D. M., Valdez, P., Kasman, I., Eastham-Anderson, J., Wu, J., et al. (2007). Interleukin-22, a T(H)17 cytokine, mediates IL-23-induced dermal inflammation and acanthosis. *Nature.* 445, 648. doi:10.1038/nature05505

Conflict of Interest: The authors declare that the research was conducted in the absence of any commercial or financial relationships that could be construed as a potential conflict of interest.

Copyright © 2021 Deng, Tan, Liu, Yu, Chen, Tang, Han and Lu. This is an open-access article distributed under the terms of the Creative Commons Attribution License (CC BY). The use, distribution or reproduction in other forums is permitted, provided the original author(s) and the copyright owner(s) are credited and that the original publication in this journal is cited, in accordance with accepted academic practice. No use, distribution or reproduction is permitted which does not comply with these terms.

Advantages of publishing in Frontiers



OPEN ACCESS

Articles are free to read
for greatest visibility
and readership



FAST PUBLICATION

Around 90 days
from submission
to decision



HIGH QUALITY PEER-REVIEW

Rigorous, collaborative,
and constructive
peer-review



TRANSPARENT PEER-REVIEW

Editors and reviewers
acknowledged by name
on published articles

Frontiers

Avenue du Tribunal-Fédéral 34
1005 Lausanne | Switzerland

Visit us: www.frontiersin.org

Contact us: frontiersin.org/about/contact



REPRODUCIBILITY OF RESEARCH

Support open data
and methods to enhance
research reproducibility



DIGITAL PUBLISHING

Articles designed
for optimal readership
across devices



FOLLOW US

@frontiersin



IMPACT METRICS

Advanced article metrics
track visibility across
digital media



EXTENSIVE PROMOTION

Marketing
and promotion
of impactful research



LOOP RESEARCH NETWORK

Our network
increases your
article's readership